

ROZPRAWA
DOKTORSKA

**INSTYTUT CHEMII ORGANICZNEJ
POLSKIEJ AKADEMII NAUK**



A-21-6
K-c-125
K-c-123
K-g-180

Porfiryny jako efektywne katalizatory fotoredoks w reakcjach tworzenia wiązań C-C

mgr Katarzyna Rybicka-Jasińska

Monotematyczny cykl publikacji z komentarzem przedstawiony
Radzie Naukowej Instytutu Chemii Organicznej Polskiej Akademii Nauk
w celu uzyskania stopnia doktora

Promotor: prof. dr hab. Dorota Gryko

Biblioteka Instytutu Chemii Organicznej PAN

O-B.399/18



WARSZAWA 2018



B. Org. 399/18

Don't try

Charles Bukowski

*Pragnę serdecznie podziękować **prof. Dorocie Gryko** za powierzone mi zaufanie oraz wsparcie na każdym etapie pracy.*

Specjalne podziękowania należą się również:

Obecnym i byłym członkom najlepszego na świecie Zespołu XV za wspianą atmosferę pracy, a w szczególności Lolo, Agnieszce, Misiowi, Asi, Łukaszowi, Aleksandrze P., Oli W., Maksymilianowi, Dominiczce, Uszki, Orłowi, Pięknemu Michałowi oraz Sabince i Maćkowi

Rodzicom

Mężowi

Praca doktorska wykonana w ramach projektów:



NARODOWE CENTRUM NAUKI

„Porfiryny jako nowe, inspirowane naturą katalizatory fotoredoks”

realizowanego w ramach grantu **PRELUDIUM**

Narodowego Centrum Nauki

Numer grantu: UMO-2016/21/N/ST5/03353

„Porfiryny jako efektywne katalizatory fotoredoks w reakcjach tworzenia wiązań C-C”

realizowanego w ramach programu **ETIUDA**

Narodowego Centrum Nauki

Numer grantu: UMO-2017/24/T/ST5/00032

SPIS TREŚCI

1. Spis publikacji wchodzących w skład rozprawy doktorskiej	8
2. Spis wybranych wystąpień konferencyjnych	9
3. Spis publikacji niewchodzących w skład rozprawy doktorskiej	10
4. Przewodnik po rozprawie doktorskiej	11
4.1. Założenia i cel pracy	11
4.2. Fotochemiczna funkcjonalizacja aldehydów katalizowana kompleksem rutenu	14
4.3. Fotochemiczna funkcjonalizacja aldehydów katalizowana porfirynami	16
4.4. Fotochemiczna funkcjonalizacja ketonów katalizowana porfirynami	18
4.5. Fotochemiczna funkcjonalizacja związków heterocyklicznych	21
4.6. Podsumowanie	24
5. Streszczenie w języku polskim	25
6. Streszczenie w języku angielskim / Abstract in English	26
7. Publikacje przeglądowe	27
8. Publikacje oryginalne	48
9. Oświadczenia autorów publikacji	282

1. Spis publikacji wchodzących w skład rozprawy doktorskiej

Publikacje przeglądowe:

[R1] **K. Rybicka-Jasińska**, Ł. W. Ciszewski, D. T. Gryko, D. Gryko
J. Porphyrins Phthalocyanines **2016**, 20, 76-95:
C–C bond forming reactions catalyzed by chiral metalloporphyrins

Publikacje oryginalne:

[P1] **K. Rybicka-Jasińska**, Ł. W. Ciszewski, D. Gryko
Adv. Synth. Catal. **2016**, 358, 1671-1678:
Photocatalytic Reaction of Diazo Compounds with Aldehydes

[P2] **K. Rybicka-Jasińska**, W. Shan, K. Zawada, K. M. Kadish, D. Gryko
J. Am. Chem. Soc. **2016**, 138, 15451-15458:
Porphyrins as Photoredox Catalysts: Experimental and Theoretical Studies

[P3] **K. Rybicka-Jasińska**, K. Orłowska, M. Karczewski, K. Zawada, D. Gryko
Eur. J. Org. Chem. DOI: 10.1002/ejoc.201800542:
Why Cyclopropanation is not involved in Photoinduced α -Alkylation of Ketones with Diazo Compounds?

[P4] **K. Rybicka-Jasińska**, B. König, D. Gryko
Eur. J. Org. Chem. **2017**, 2104-2107:
Porphyrin-Catalyzed Photochemical C–H Arylation of Heteroarenes

2. Spis wybranych wystąpień konferencyjnych

Wyniki przedstawione w niniejszej pracy zostały zaprezentowane na konferencjach:

1. *The Polish-German Conference on Organic Chemistry*, Warszawa, Polska, 2016:
Prezentacja ustna: *Photocatalytic Reaction of Diazo compounds with Aldehydes*
2. *Postępy w syntezie związków nieracemicznych*, Łądek Zdrój, Polska, 2017:
Prezentacja ustna: *Związki diazoorganiczne jako źródło rodników w fotochemicznej funkcjonalizacji aldehydów*
3. *IX Kopernikańskie Seminarium Doktoranckie*, Toruń, Polska, 2015:
Prezentacja posterowa: *Kataliza enaminowa – enancjoselektywna metoda funkcjonalizacji aldehydów*
4. *231ST Electrochemical Chemical Society Meeting*, Nowy Orlean, USA, 2016:
Prezentacja posterowa: *Porphyrins As Photoredox Catalysts In Efficient C-C Bond Formation;*
Nagroda w panelu *Porphyrins, Phthalocyanines and Supramolecular Assemblies: Nanocarbons*
5. *YoungChem 2017*, Lublin, Polska, 2017:
Prezentacja posterowa: *Porphyrins As Photoredox Catalysts In Efficient C-C Bond Formation;*
Nagroda publiczności

3. Spis publikacji niewchodzących w skład rozprawy doktorskiej

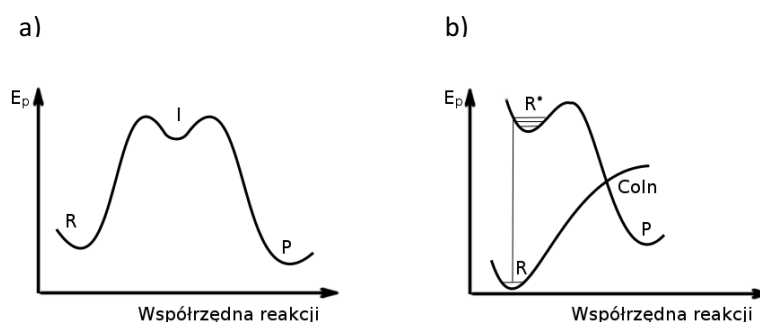
Prace oryginalne:

1. D. J. Walaszek, K. Maximova, **K. Rybicka-Jasińska**, A. Lipke, D. Gryko
J. Porphyrins Phthalocyanines **2014**, *18*, 493-505:
Synthesis of chiral porphyrins and their use in photochemical oxidation of carbonyl compounds
2. D. J. Walaszek, **K. Rybicka-Jasińska**, S. Smoleń, M. Karczewski, D. Gryko
Adv. Synth. and Catal. **2015**, *357*, 2061-2070:
Mechanistic Insights into Enantioselective C-H Photooxygenation of Aldehydes via Enamine Catalysis
3. A. A. Ptaszyńska, M. Trytek, G. Borsuk, K. Buczek, **K. Rybicka-Jasińska**,
D. Gryko
Scientific Reports **2018**, DOI: 10.1038/s41598-018-23678-8:
Porphyrins inactivate Nosema spp. microsporidia

4. Przewodnik po rozprawie doktorskiej

4.1. Założenia i cel pracy

Poszukiwanie nowych metod pozwalających na efektywne, niskokosztowe i przyjazne środowisku tworzenie wiązań C-C pozostaje jednym z najważniejszych zadań współczesnej syntezy organicznej. Dobrym podejściem do tego problemu jest wykorzystanie szybko rozwijającej się w ostatnich latach fotokatalizy. Reakcje fotochemiczne są nie tylko tańsze i bezpieczniejsze dla środowiska, ale często pozwalają na otrzymywanie związków organicznych, niemożliwych do syntezy innymi metodami.¹ Absorpcja fotonów przez cząsteczkę powoduje jej przejście do stanów wzbudzonych elektronowo, zatem w reakcjach fotochemicznych substratami są cząsteczki wysokoenergetyczne, w przeciwieństwie do reakcji aktywowanych termicznie (Rysunek 1).



Rysunek 1. Profil energetyczny a) aktywacji termicznej b) aktywacji fotochemicznej²

Użycie barwników jako fotokatalizatorów zdolnych absorbować światło widzialne pozwala na zastosowanie tej metodologii w reakcjach z udziałem cząsteczek nieabsorbujących fal elektromagnetycznych w zakresie widzialnym (380-780 nm). Najczęściej jako katalizatory fotoredoks stosowane są kompleksy rutenu i irydu, które są kosztowne i często toksyczne, dlatego też próbuje się wykorzystywać tańsze, łatwiejsze do modyfikacji i bardziej przyjazne środowisku barwniki organiczne. Spośród wielu znanych współczesnej chemii barwników organicznych na szczególne wyróżnienie zasługują porfirynoidy, związki określane mianem „pigmentów życia”. Są one bowiem odpowiedzialne za najważniejsze procesy życiowe: a) transport tlenu we krwi (hem), b) transport elektronu w łańcuchu oddechowym (hemoproteina – cytochrom, c) fotosynteza (chlorofil). W tym ostatnim procesie następuje konwersja energii świetlnej w chemiczną, która jest możliwa dzięki szczególnym właściwościom fotochemicznym chlorofilu. Te same właściwości decydują również o tym, że porfiryny powinny być dobrymi fotokatalizatorami w transformacjach organicznych. *Porfiryny z ich 18 π -elektronowym*

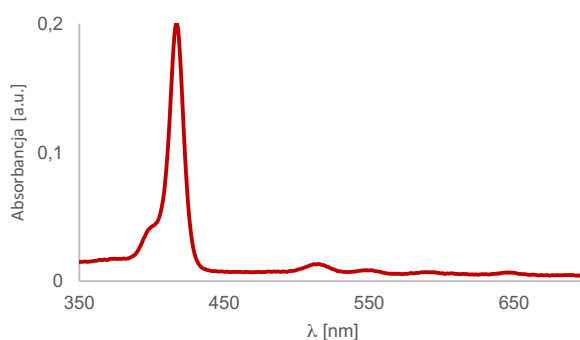
¹ M. Fintecave *Angew. Chem. Int. Ed.* **2015**, *54*, 6946.

² B. König, *Chemical Photocatalysis*, **2013**, De Gruyter.

pierścieniem makrocyklicznym są idealnym materiałem do badań, ponieważ absorbują światło widzialne, posiadają wysoką kwantową wydajność fluorescencji oraz relatywnie długie czasy życia w stanie wzbudzonym.

Głównym celem moich badań było wykorzystanie porfiryn jako nowych, inspirowanych naturą katalizatorów fotoredoks w reakcjach tworzenia wiązań C-C.

Porfiryny są związkami barwnymi, absorbują światło oraz spełniają regułę aromatyczności Hückla. Ich barwa związana jest z obecnością sprzężonych elektronów π , stąd posiadają one bardzo charakterystyczne widmo UV-Vis. W widmie tym wyróżnia się dwa ważne regiony absorpcji: bliski ultrafiolet (pasmo Soreta: ~ 420 nm) i region widzialny (cztery słabsze pasma Q: $\sim 518, 553, 592$ and 648 nm) (Rysunek 2). Zmiany w strukturze i symetrii porfiryny mają wpływ na proces absorpcji, a w związku z tym również na przebieg widma.



Rysunek 2. Typowy przebieg widma UV-Vis porfiryny

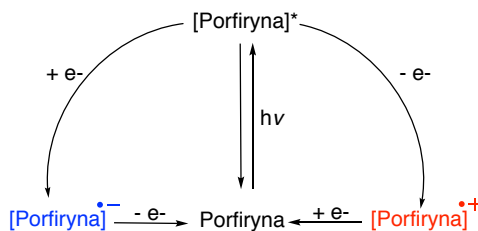
Po zaabsorbowaniu światła widzialnego i przejściu do stanu wzbudzonego porfiryny mogą zostać użyte jako katalizatory działające na zasadzie transferu energii lub elektronu. Są one znanymi fotosensybilizatorami stosowanymi do generowania tlenu singletowego. Wytworzony w ten sposób tlen singletowy jest silnym utleniaczem, który dalej może uczestniczyć w reakcji cykloaddycji czy reakcji enowej.³ Porfiryny w stanie wzbudzonym mogą również zostać stopniowo utlenione lub zredukowane do odpowiednich π -kationorodników oraz π -anionorodników,⁴ zatem w stanie wzbudzonym mogą być zarówno utleniaczami jak i reduktorami (Schemat 1). Do 2016 roku idea ta była wykorzystywana tylko w pracach nad sztuczną fotosyntezą, w terapii fotodynamicznej czy polimeryzacji,⁵ brak było jednak doniesień na temat użycia porfiryn jako katalizatorów

³ M. C. DeRosa, R. J. Crutchley, *Coordination Chemistry Reviews* **2002**, 233, 351.

⁴ (a) T. Lazarides, I. V. Sazanovich, A. J. Simaan, M. C. Kafentazi, M. Delor, Y. Mekmouche, B. Faure, M. Reglier, J. A. Weinstein, A. G. Coutsolelos, T. Tron *J. Am. Chem. Soc.* **2013**, 135, 3095. (b) C. Inisan, J. – Y. Saillard, R. Guillard, A. Tabard, Y. Le Mest *New J. Chem.* **1998**, 22, 823.

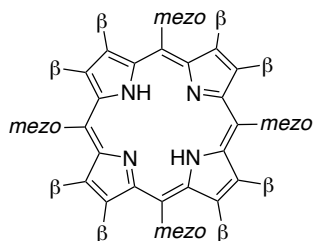
⁵ (a) H. Imahori, Y. Mori, Y. Matano *J. Photochem. Photobiol. C* **2003**, 4, 51. D. Guest, T. A. Moore, A. (b) L. Moore *Acc. Chem. Res.* **2009**, 42, 1890. (c) S. Fukuzumi *Bull. Chem. Soc. Jpn.* **2006**, 79, 177.

fotoredoks w syntezie organicznej.⁶



Schemat 1. Proces transferu energii i elektronu

Wartości potencjałów, przy których zachodzą opisane procesy zależą od wielu czynników, m.in. struktury porfiryny, obecności grup elektrono-donorowych i -akceptorowych na zewnątrz pierścienia makrocyklicznego w pozycjach *mezo* i β (Rysunek 3).⁷ Poprzez zastosowanie odpowiednich podstawników można zmieniać wartości potencjałów elektrochemicznych, zwiększając przy tym użyteczność porfiryn w katalizowaniu reakcji fotochemicznych.



Rysunek 3. Struktura porfiryny z zaznaczonymi pozycjami w pierścieniu makrocyklicznym

W reakcjach nieindukowanych światłem, porfiryny a raczej ich kompleksy z metalami, są powszechnie używane jako katalizatory reakcji cyklopropanowania, epoksydacji, C-H insercji, cykloaddycji, utleniania i innych.⁸ W reakcjach tych działają one głównie na zasadzie transferu karbenu, a więc to metal skoordynowany we wnętrzu makrocyklicznego pierścienia porfiryny jest odpowiedzialny za jej właściwości katalityczne.

Obecny stan wiedzy na temat enancjoselektywnych reakcji tworzenia wiązań C-C katalizowanych kompleksami porfiryn został zebrany w formie artykułu przeglądowego i opublikowany na łamach czasopisma *Journal of Porphyrins and Phthalocyanines*:

⁶ N. R. Romero, D. A. Nicewicz *Chem. Rev.* **2016**, *116*, 10075.

⁷ (a) K. M. Kadish, M. M. Morrison *Bioinorg. Chem.* **1977**, *7*, 107. (b) K. M. Kadish, E. Van Caemelbecke *J. Solid State Electrochem.* **2003**, *7*, 254. (c) R. F. X. Williams, P. Hambright *Bioinorg. Chem.* **1978**, *9*, 537. (d) Y. Cui, L. Zeng, Y. Fang, Y., J. Zhu, C. H. Devillers, D. Lucas, N. Desbois, C. P. Gros, K. M. Kadish *ChemElectroChem* **2016**, *3*, 228. (e) Y. -J. Tu, H. C. Cheng, I. Chao, C.-R. Cho, R.-J. Cheng, Y. O. Su *J. Phys. Chem. A* **2012**, *116*, 1632 (f) Y. Fang, P. Bhyrappa, Z. Ou, K. M. Kadish *Chem. - Eur. J.* **2014**, *20*, 524. (g) K. M. Kadish, M. M. Morrison *J. Am. Chem. Soc.* **1976**, *98*, 3326.

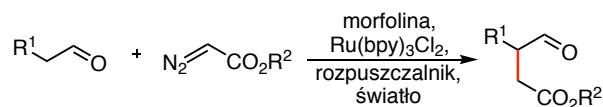
⁸ K. M. Kadish, K. M. Smith, R. Guilard *Handbook of porphyrin science. Vol.21: Catalysis*, Singapore, World Scientific Pub. Co., **2012**.

[R1] **K. Rybicka-Jasińska**, Ł. W. Ciszewski, D. T. Gryko, D. Gryko *J. Porphyrins Phthalocyanines* **2016**, *20*, 76-95: C–C bond forming reactions catalyzed by chiral metalloporphyrins

4.2. Fotochemiczna funkcjonalizacja aldehydów katalizowana kompleksami rutenu

W ostatnich latach kataliza fotoredoks cieszy się coraz większym zainteresowaniem,⁹ zastosowano ją między innymi do selektywnej funkcjonalizacji związków karbonylowych. We wczesnych pracach z tej tematyki opisano fotoindukowane metody modyfikacji aldehydów (trifluorometylowanie,¹⁰ benzylowanie,¹¹ alkiłowanie¹²) w pozycji α . Metodologia ta jest jednak ograniczona do użycia aktywnych bromków, ubogich w elektrony olefin lub polifluorowanych związków organicznych jako czynników alkiłujących. **W związku z tym postanowiłam rozszerzyć znaną już metodologię podwójnej katalizy i wykorzystać związki diazoorganiczne jako źródło rodników w fotokatalitycznej reakcji funkcjonalizacji aldehydów.**

W początkowym etapie badań odkryłam, że indukowana światłem reakcja aldehydu z diazoocetanem etylu w obecności Ru(bpy)₃Cl₂ - katalizatora fotoredoks i morfoliny – organokatalizatora prowadzi do aldehydu sfunkcjonalizowanego w pozycji α (Schemat 2).



Schemat 2. Funkcjonalizacja aldehydów w pozycji α

Zoptymalizowałam warunki reakcji, w tym aminę, rozpuszczalnik, czas i temperaturę prowadzenia reakcji, rodzaj i natężenie światła oraz zastosowanie różnych dodatków. W optymalnych warunkach sprawdziłam zakres stosowalności i ograniczenia badanej reakcji (Schemat 3). Fotochemiczna reakcja C-H alkiłowania różnych aldehydów dawała

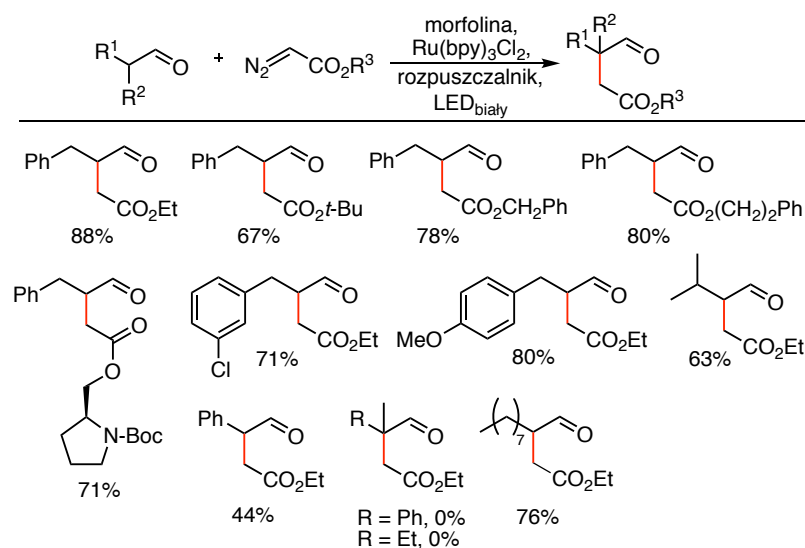
⁹ (a) C. K. Prier, D. A. Rankic, D. W. C. MacMillan, *Chem. Rev.* **2013**, *113*, 5322-5363. (b) K. L. Skubi, T. R. Blum, T. P. Yoon, *Chem. Rev.* **2016**, *116*, 10035-10074. (c) J. W. Tucker, C. R. J. Stephenson, *J. Org. Chem.* **2012**, *77*, 1617-1622. (d) J. J. Douglas, M. J. Sevrin, C. R. J. Stephenson, *Org. Process Res. Dev.* **2016**, *20*, 1134-1147. (e) D. Staveness, I. B. Bosque, C. R. J. Stephenson, *Acc. Chem. Res.* **2016**, *49*, 2295-2306. (f) K. Teegardin, J. I. Day, J. Chan, J. Weaver, *Org. Process Res. Dev.* **2016**, *20*, 1156-1163. (g) D. A. Nicewicz, T. M. Nguyen, *ACS Catal.* **2014**, *4*, 355-360. (h) M. H. Shaw, J. Twilton, D. W. C. MacMillan, *J. Org. Chem.*, **2016**, *81*, 6898-6926. (i) J. Twilton, C. C. Le, P. Zhang, M. H. Shaw, R. W. Evans, D. W. C. MacMillan, *Nature Reviews Chemistry* **2017**, *1*, 0052. (j) Y.-Q. Zou, F. M. Hörmann, T. Bach, *Chem. Soc. Rev.* **2018**, DOI: 10.1039/C7CS00509A.

¹⁰ D. A. Nagib, M. E. Scott, D. W. C. MacMillan, *J. Am. Chem. Soc.* **2009**, *131*, 10875-10877.

¹¹ H.-W. Shih, M. N. Vander Wal, R. L. Grange, D. W. C. MacMillan, *J. Am. Chem. Soc.* **2010**, *132*, 13600-13603.

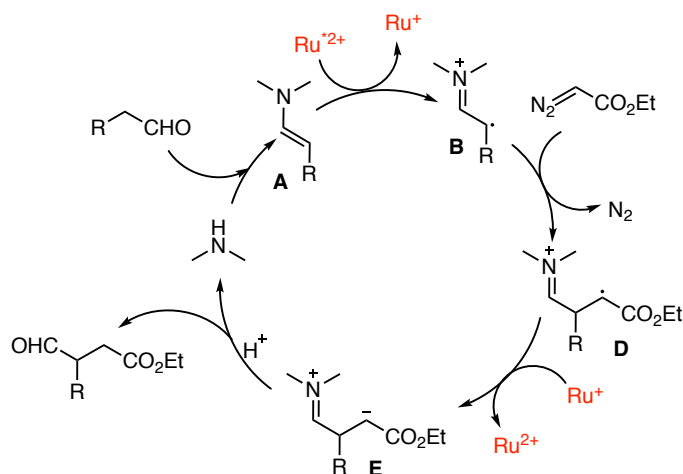
¹² D. A. Nicewicz, D. W. C. MacMillan, *Science* **2008**, *322*, 77-80.

oczekiwane produkty z dobrymi wydajnościami, niestety w podanych warunkach aldehydy posiadające podstawniki w pozycji α były niereaktywne. Diazoestry z różnymi grupami estrowymi reagowały równie dobrze jak modelowy diazoocetan etylu.



Schemat 3. Indukowana światłem reakcja funkcjonalizacji aldehydów – badanie zakresu stosowalności reakcji

W kolejnym etapie badań przeprowadziłam eksperymenty mające na celu wyjaśnienie mechanizmu badanej reakcji (Schemat 4). W pierwszym etapie tworzy się enamina, której obecność w mieszaninie reakcyjnej potwierdziłam metodą spektroskopii magnetycznego rezonansu jądrowego (NMR) oraz spektrometrii mas (MS). W oparciu eksperymenty wykonane spektroskopią elektronowego rezonansu paramagnetycznego (EPR) oraz eksperymentu z dodatkiem pułapki rodnikowej (TEMPO) udowodniłam, że reakcja jest rodnikowa. Ponadto analiza wyników eksperymentu Sterna-Volmera wykazała, że enamina, w porównaniu do innych składników mieszaniny reakcyjnej, silnie wygasza luminescencję kompleksu rutenowego.



Schemat 4. Proponowany mechanizm reakcji

Podsumowując wykazałam, że diazo związki mogą być stosowane jako odczynniki

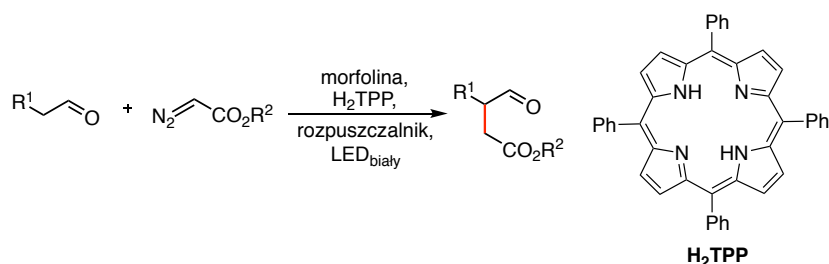
alkilujące. Zoptymalizowałam warunki reakcji α -funkcjonalizacji aldehydów, a następnie zbadalam zakres i ograniczenia metody oraz zaproponowałam mechanizm opisanej reakcji.

Wyniki opisane w tym podrozdziale zostały opublikowane w artykule naukowym:

[P1] **K. Rybicka-Jasińska**, Ł. W. Ciszewski, D. Gryko *Adv. Synth. Catal.* **2016**, *358*, 1671-1678: *Photocatalytic Reaction of Diazo Compounds with Aldehydes*

4.3. Fotochemiczna funkcyjnalizacja aldehydów katalizowana porfirynami

Niska toksyczność, możliwość łatwej funkcyjnalizacji struktury porfiryny i w związku z tym łatwa zmiana jej potencjałów fotoredoks, stosunkowo długi czas życia w stanie wzbudzonym oraz wysoka kwantowa wydajność fluorescencji sprawia, że porfiryny powinny być efektywnymi katalizatorami fotoredoks. Co ciekawe, do 2016 roku w literaturze nie było przykładów użycia porfiryn jako katalizatorów fotoredoks w syntezie organicznej. Z tego względu zdecydowałam się przetestować je w odkrytej przeze mnie fotoindukowanej reakcji aldehydów ze związkami diazoorganicznymi (Schemat 5). Warunki reakcji, w tym struktura katalizatora, aminy, rozpuszczalnik, rodzaj oraz natężenie światła, zostały przeze mnie zoptymalizowane.



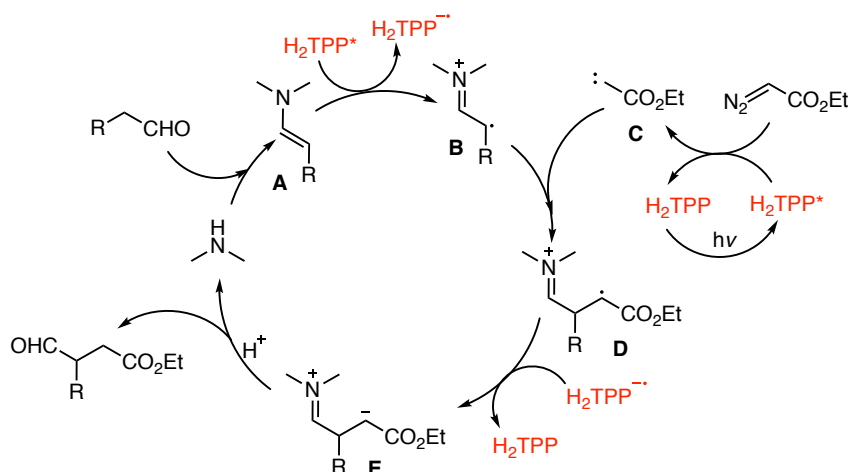
Schemat 5. Funkcyjnalizacja aldehydów w pozycji α katalizowane porfiryną H_2TPP

W optymalnych warunkach sprawdziłam zakres stosowalności i ograniczenia badanej reakcji. Reakcja C-H alkilowania różnych aldehydów dawała oczekiwane produkty z dobrymi wydajnościami i były one takie same lub nieco wyższe od tych otrzymanych w reakcji katalizowanej kompleksem rutenem. Najbardziej wymagającym i jednocześnie najciekawszym okazało się zbadanie i zaproponowanie mechanizmu reakcji, w której porfiryna pełniła rolę katalizatora fotoredoks. W pierwszym etapie sprawdziłam właściwości elektrochemiczne porfiryn – z punktu widzenia katalizy fotoredoks istotne są nie tylko wartości potencjałów redoks w stanie podstawowym, ale również te w stanie wzbudzonym. W przybliżeniu, wartości potencjałów w stanie wzbudzonym są związane z potencjałem w stanie podstawowym i spektroskopową energią zero-zero (E_{00}), obliczyłam je z danych uzyskanych z woltamperometrii cyklicznej i spektroskopii UV-Vis (Tabela 1).

Tabela 1. Potencjały redukcji dla porfiryn w stanie wzbudzonym

Fotoutlenianie	Fotoredukcja
$E_{ox}^*[Por^{+}/Por^*] = E_{ox}[Por^{+}/Por] - E_{0,0}$	$E_{red}^*[Por^*/Por^{\bullet-}] = E_{red}[Por/Por^{\bullet-}] + E_{0,0}$
Stan singletowy (S)	Stan Singletowy (S)
$E_{ox}^*[TPP^{+}/TPP^*] = 1.03\text{ V} - 1.94\text{ V} = -\mathbf{0.91\text{ V}}$	$E_{red}^*[TPP^*/TPP^{\bullet-}] = -1.03\text{ V} + 1.94\text{ V} = \mathbf{0.91\text{ V}}$
$E_{ox}^*[ZnTPP^{+}/ZnTPP^*] = 0.86\text{ V} - 2.04\text{ V} = -\mathbf{1.18\text{ V}}$	$E_{red}^*[ZnTPP^*/ZnTPP^{\bullet-}] = -1.32\text{ V} + 2.04\text{ V} = \mathbf{0.79\text{ V}}$
Stan tripletowy (T)	Stan tripletowy (T)
$E_{ox}^*[TPP^{+}/TPP^*] = 1.03\text{ V} - 1.45\text{ V} = -\mathbf{0.42\text{ V}}$	$E_{red}^*[TPP^*/TPP^{\bullet-}] = -1.03\text{ V} + 1.45\text{ V} = \mathbf{0.42\text{ V}}$
$E_{ox}^*[ZnTPP^{+}/ZnTPP^*] = 0.86\text{ V} - 1.59\text{ V} = -\mathbf{0.73\text{ V}}$	$E_{red}^*[ZnTPP^*/ZnTPP^{\bullet-}] = -1.32\text{ V} + 1.59\text{ V} = \mathbf{0.27\text{ V}}$

Obliczone potencjały redukcji w stanie wzbudzonym dla H₂TPP i jej cynkowego kompleksu są nieco niższe, ale bardzo podobne do tych obliczonych dla Ru(bpy)₃Cl₂ (0.67 V) i eozyiny Y (0.83 V), mimo to okazały się one wystarczająco wysokie, aby porfiryra mogła pełnić rolę efektywnego fotoutleniacza w badanej reakcji. Proponowany mechanizm reakcji aldehydów ze związkami diazoorganicznymi w warunkach katalizy porfiryryną zakłada współistnienie dwóch cykli katalitycznych, w których każdy ze składników mieszaniny reakcyjnej (amina, fotokatalizator, światło) pełni istotną rolę. Zakładam, że porfiryra pełni podwójną rolę: fotosensybilizatora i katalizatora fotoredoks. Pod wpływem naświetlania katalizator (H₂TPP) przechodzi ze stanu podstawowego w stan wzbudzony. Na drodze fotosensybilizacji generowany jest karben w stanie tripletowym z jednoczesną ekstruzją azotu, ponieważ wiadomo, że porfiryny są znanymi tripletowymi fotosensybilizatorami, a ponadto obecność dirodnika **C** została potwierdzona w eksperymencie Sterna-Volmera oraz w eksperymencie z dodatkiem pułapki rodnikowej (TEMPO). W drugim cyklu katalitycznym aldehyd reaguje z II-rzędową aminą tworząc enaminę (**A**), której obecność w środowisku reakcji udowodniono metodą spektroskopii rezonansu magnetycznego (NMR) i spektrometrii mas (MS). Następnie jest ona utleniana przez porfiryrynę (H₂TPP*) w stanie wzbudzonym do kationorodnika **B**, o czym świadczy wynik eksperymentu Sterna-Volmera. Obecność tego rodnika potwierdziłam również metodami spektroskopii NMR i EPR oraz spektrometrii mas (MS). Powstały kationorodnik **B** reaguje z dirodnikiem **C** dając kationorodnik **D**, który po następczej redukcji i hydrolizie prowadzi do produktu – aldehydu sfunkcjonalizowanego w pozycji α (Schemat 6).



Schemat 6. Proponowany mechanizm reakcji

Podsumowując, opisane przeze mnie badania wykazują, że porfiryny mogą pełnić funkcję efektywnych katalizatorów fotoredoks i dzięki temu odkryciu można je dopisać do listy barwników już istniejących i wykorzystywanych w katalizie fotoredoks. W związku z tym, że porfiryny są łatwe do syntezy, a ich właściwości optyczne i elektrochemiczne mogą być łatwo dostosowywane do potrzeb reakcji, są one obiecującymi na katalizatorami fotoredoks.

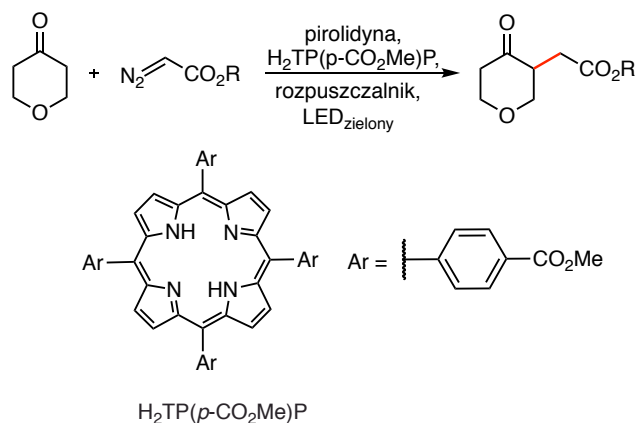
Wyniki opisane w tym podrozdziale zostały opublikowane w artykule naukowym:

[P2] **K. Rybicka-Jasińska**, W. Shan, K. Zawada, K. M. Kadish, D. Gryko *J. Am. Chem. Soc.* **2016**, *138*, 15451-15458: *Porphyrins as Photoredox Catalysts: Experimental and Theoretical Studies*

4.4. Fotochemiczna funkcjonalizacja ketonów katalizowana porfirynami

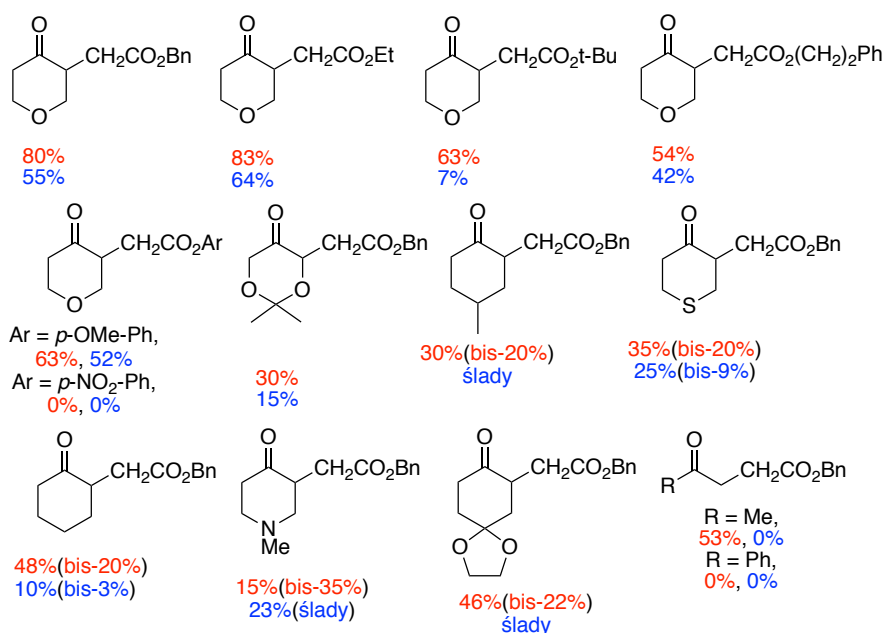
Następnie sprawdziłam czy katalizatory porfirynowe można wykorzystać również w alkilowaniu mniej reaktywnych ketonów. Zastosowanie takich samych warunków reakcji jak w przypadku alkilowania aldehydów, prowadziło jedynie do odzyskania substratów. Biorąc pod uwagę fakt, że reaktywność enamin wzrasta w kierunku: morforlina > piperidyna > aminy acykliczne > pirolidyna,¹³ a ketony są związkami mniej reaktywnymi od aldehydów, postanowiłam zastosować inny organokatalizator. Użycie pirolidyny jako organokatalizatora oraz porfiryny jako katalizatora fotoredoks pozwoliło na otrzymanie produktu α -alkilowania z zadawalającą wydajnością (Schemat 7).

¹³ P. M. Pihko, I. Majander, A. Erkkilä, *Asymmetric Organocatalysis*, (Ed.: B. List), 1st edn., Springer, **2010**, pp 145-200.



Schemat 7. Funkcjonalizacja ketonów w pozycji α

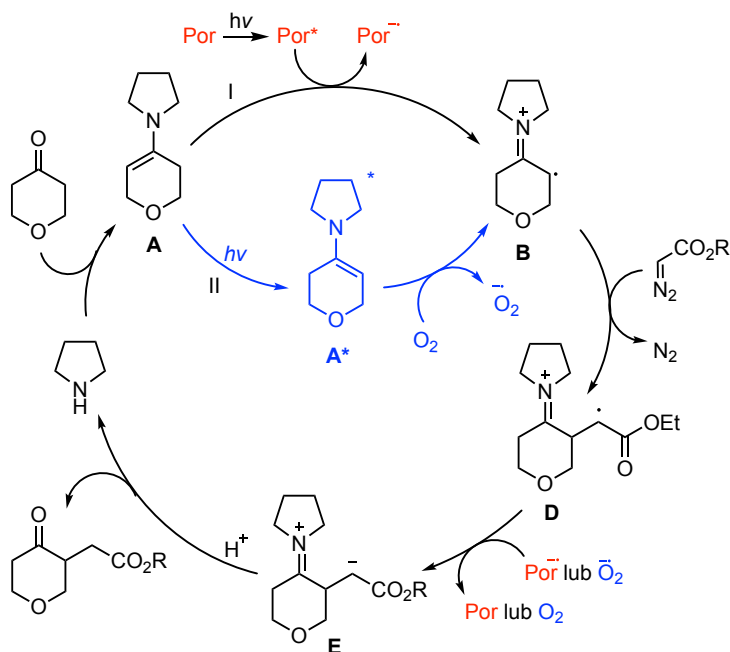
Warunki reakcji, w tym struktura katalizatora, amina, rozpuszczalnik oraz światło, zostały przeze mnie zoptymalizowane. W opracowanych warunkach sprawdziłam zakres stosowalności i ograniczenia badanej reakcji. Katalizowana porfiryńą reakcja C-H alkirowania różnych ketonów cyklicznych dawała oczekiwane produkty z dobrymi wydajnościami (Rysunek 4).



Rysunek 4. Zakres stosowalności i ograniczenia α -alkirowania ketonów diazoestrami¹⁴

Badania wstępne wykazały, że zarówno światło, jak i amina są konieczne do przeprowadzenia reakcji. Co ciekawe, produkt powstawał również w reakcji bez katalizatora porfiryńowego chociaż z niższą wydajnością. To niespodziewane odkrycie spowodowało, że należało zaproponować nie jeden, a dwa mechanizmy reakcji zachodzących w obecności katalizatora i bez jego dodatku.

¹⁴ Wydajności: **kolor czerwony** – z porfiryńą, **kolor niebieski** – bez dodatku porfiryńy.



Schemat 8. Proponowany mechanizm reakcji alkilowania ketonów

W obu reakcjach (I oraz II) początkowo keton reaguje z aminą tworząc enaminę (**A**) (wykryta metodą spektroskopii rezonansu magnetycznego (NMR) i spektrometrii mas (MS)). Następnie zostaje ona utleniona przez porfiryne ($E_{red}^*[\text{Por}^*/\text{Por}^{\bullet-}] = 1.03 \text{ V vs SCE}$, DMSO) w stanie wzbudzonym do kationorodnika **B**. W reakcji bez dodatku porfiryne, w środowisku reakcji wytworzona enamina **A** absorbuje światło i przechodzi ze stanu podstawowego do wzbudzonego i jako taka zostaje utleniona tlenem (ta droga (II) możliwa jest tylko dla ketonów, które z piperolidyną tworzą enaminy zdolne do absorpcji światła w zakresie widzialnym – potwierdzone badaniami postępu reakcji metodą UV-Vis oraz tworzenia się enamin w czasie). Obecność kationorodnika **B** została potwierdzona metodą spektroskopii EPR oraz eksperymentów z dodatkiem pułapki rodnikowej (TEMPO). Następnie powstały w ten sposób kationorodnik **B** reaguje z diazoesztem dając kationorodnik **D**, który po następczej redukcji i hydrolizie daje produkt – keton sfunkcjonalizowany w pozycji α (Schemat 8).

Należy wziąć pod uwagę fakt, że wytworzona in situ enamina może ulegać cyklopropanowaniu z następczym otwarciem pierścienia.¹⁵ Jednakże w oparciu o wyniki eksperymentów NMR w czasie, zastosowanie typowych dla cyklopropanowania substratów w opracowanych warunkach oraz obliczeń kwantowo-mechanicznych wykluczyłam taką możliwość w przebiegu reakcji.

¹⁵ (a) M. E. Kuehne, J. C. King *J. Org. Chem.* **1973**, *38*, 304. (b) A. Pereira, Y. Champouret, C. Martin, E. Alvarez, M. Etienne, T. R. Belderrain, P. J. Perez, P. J.; *Chem. Eur. J.* **2015**, *21*, 9769. (c) S. Muthusamy, P. Srinivasan *Tetrahedron Lett.* **2006**, *47*, 6297.

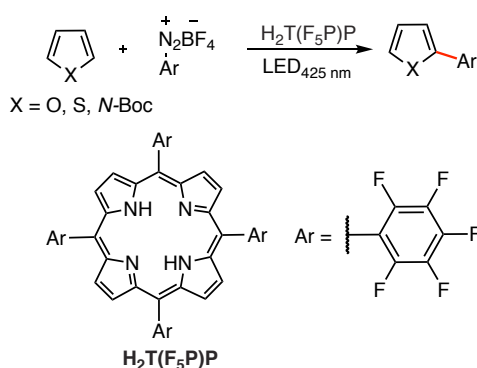
Podsumowując, udowodniłam, że porfiryny w postaci wolnych zasad mogą pełnić rolę katalizatorów fotoredoks również w reakcji alkilowania ketonów diazoestrami. Reakcja zachodzi poprzez indukowany światłem transfer elektronu pomiędzy porfiryką w stanie wzbudzonym a wytworzoną *in situ* enaminą. Odkryta przeze mnie reakcja została zoptymalizowana, zbadalam jej zakres stosowalnosci oraz ograniczenia i zaproponowalam mechanizm reakcji.

Wyniki opisane w tym podrozdziale zostaly opublikowane w artykule naukowym:

[P3] K. Rybicka-Jasińska, K. Orłowska, M. Karczewski, K. Zawada, D. Gryko *Eur. J. Org. Chem.* DOI: 10.1002/ejoc.201800542: *Why Cyclopropanation is not involved in Photoinduced α -Alkylation of Ketones with Diazo Compounds?*

4.5. Fotochemiczna funkcjonalizacja związków heterocyklicznych

Alkilowanie aldehydów i ketonów katalizowane porfirykami sa przykladami reakcji, w ktorych porfiryka pelni role fotoutleniacza, skoro porfiryki latwo tworza rowniez kationorodniki, naturalnym zadaniem stalo sie przetestowanie katalizatorow porfirykowych w reakcji, w ktorej moga one pelnic role fotoreduktora. W literaturze znana byla reakcja typu Meerweina – arylowania związkow heterocyklicznych solami diazoniowymi w warunkach katalizy Eozyną Y, ktora w stanie wzbudzonym redukuje sol diazoniowa do rodnika.¹⁶ W związku z tym postanowilam, ze wykorzystam te reakcje do przebadania wlasciwosci fotoredukcyjnych porfiryki (Schemat 8).¹⁷



Schemat 9. Arylowanie heteroarenow solami diazoniowymi katalizowane porfiryką

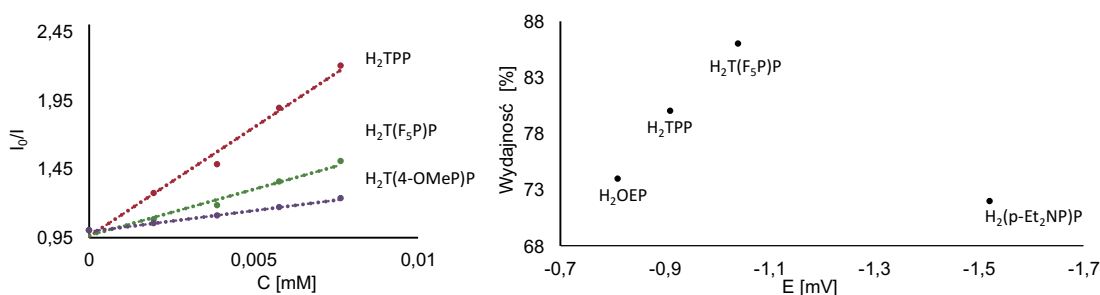
Warunki reakcji soli diazoniowej z furanem poddalam optymalizacji (porfiryka, rodzaj swiatla, rozpuszczalniki, czas prowadzenia reakcji oraz ilosc reagentow). W toku badan

¹⁶ D. P. Hari, P. Schroll, B. König *J. Am. Chem. Soc.* **2012**, *134*, 2958.

¹⁷ (a) D. Kalyani, K. B. McMurtrey, S. R. Neufeldt, M. S. Sanford, *J. Am. Chem. Soc.* **2011**, *133*, 18566. (b) P. Hari, P. Schroll, B. König, *J. Am. Chem. Soc.* **2012**, *134*, 2958. (c) D. P. Hari, B. König, *Angew. Chem. Int. Ed.* **2013**, *52*, 4734. (d) M. Majek, A. J. von Wangelin, *Chem. Commun.* **2013**, *49*, 5507.

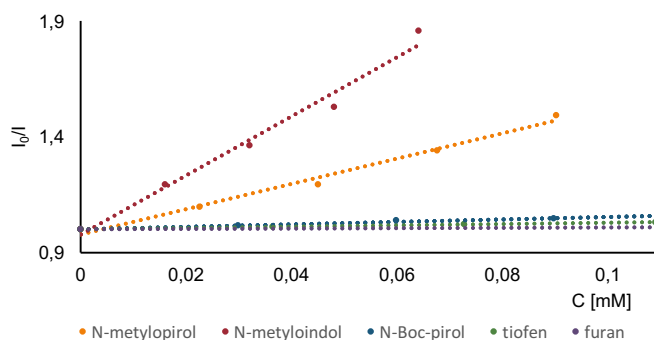
przebadalam katalizatory porfiryne z różnymi grupami aryłowymi przy makrocyklicznym pierścieniu, stąd posiadające różne potencjały elektrochemiczne.

Okazało się, że najlepszy rezultat w reakcji arylowania uzyskałam w przypadku ubogiej w elektrony ($H_2T(F_5P)P$). Eksperyment Sterna-Volmera wykazał, że sól diazoniowa wygasa luminescencję wszystkich badanych porfiryn, jednakże dla każdej z różną wartością stałej wygaszania. Największą stałą wygaszania zaobserwowałam dla H_2TPP , która dawała produkt reakcji z nieznacznie mniejszą wydajnością (80%) niż ta w przypadku dla $H_2T(F_5P)P$ (86%). Korelacje wartości stałych wygaszenia luminescencji i potencjałów utlenienia badanych porfiryn wyraźnie pokazały, że w reakcji arylowania heteroarenow solami diazoniowymi istnieje optymalna wartość stałej wygaszenia luminescencji oraz optymalny potencjał redoks w stanie wzbudzonym (Rysunek 5).



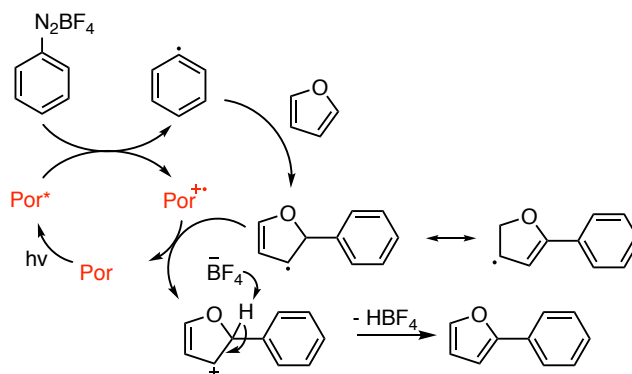
Rysunek 5. Katalizatory porfiryne badane w arylowaniu heteroarenow solami diazoniowymi

Następnie zbadalam zakres stosowalności reakcji. Przebadalam sole diazoniowe z podstawnikami elektronoakceptorowymi (Br, Cl, I, NO_2) i elektronodonorowymi (OMe, Me). Sole z podstawnikami elektronodonorowymi są w tej reakcji mniej reaktywne od tych z podstawnikami elektronoakceptorowymi. Fotochemiczne arylowanie katalizowane porfiryne można przeprowadzić efektywnie również dla tiofenu, *N*-Boc-pirolu i kumaryny. Niestety, *N*-metylopirol i *N*-metyloindol nie ulegał reakcji w podanych warunkach. Na wyjaśnienie tego zaskakującego braku reaktywności tych związków pozwoliły odpowiedzieć eksperymenty Sterna-Volmera. Wykazały one, że wydajność tworzonego produktu w reakcji arylowania zależy od stałej wygaszenia luminescencji katalizatora porfiryne (Rysunek 4). Prawdopodobnie katalizator porfiryne reaguje szybciej z *N*-metylopirolem czy *N*-metyloindolem niż solą diazoniową, co uniemożliwia tworzenie się rodnika arylowego z soli diazoniowej.



Rysunek 4. Eksperyment Sterna-Volmera dla różnych substratów w arylowaniu heteroarenow

Mając do dyspozycji optymalne warunki reakcji postanowiłam wykonać eksperymenty mające na celu zbadanie mechanizmu reakcji. Proponowany mechanizm reakcji zakłada, że porfiryne w stanie wzbudzonej redukuje sól diazoniową do rodnika arylowego. Następnie rodnik ten reaguje z furanem, dając po kolejnych przekształceniach produkt reakcji arylowania (Schemat 9). W trakcie prowadzonych badań, wykonałam między innymi eksperyment z dodatkiem pułapki rodników – TEMPO, w ten sposób potwierdziłam obecność rodnika arylowego w mieszaninie reakcyjnej.



Schemat 9. Proponowany mechanizm reakcji arylowanie heteroarenow solami diazoniowmi

Podsumowując, udowodniłam, że porfiryny w postaci wolnych zasad mogą pełnić rolę katalizatorów fotoredoks w bezpośrednim C-H arylowaniu heteroarenow. Reakcja zachodzi w wyniku indukowanego światłem transferu elektronu pomiędzy porfiryne w stanie wzbudzonej a solą diazoniową, a więc porfiryne w tym przypadku jest fotoreduktorem. Ponadto zoptymalizowałam warunki reakcji i zbadalam jej zakres stosowalności oraz zaproponowalam mechanizm reakcji.

Wyniki opisane w tym podrozdziale zostały opublikowane w artykule naukowym:

[P4] **K. Rybicka-Jasińska**, B. König, D. Gryko *Eur. J. Org. Chem.* **2017**, 2104-2107:
Porphyrin-Catalyzed Photochemical C–H Arylation of Heteroarenes

4.6. Podsumowanie

Podsumowując, prowadzone przeze mnie badania doprowadziły do pierwszego zastosowania porfiryn w postaci wolnych zasad jako katalizatorów fotoredoks w reakcjach tworzenia wiązań C-C.

Za moje największe osiągnięcia badawcze uważam:

1. **Odkrycie i udowodnienie, że porfiryny mogą pełnić rolę fotoutleniaczy (w reakcji alkilowania aldehydów i ketonów) oraz fotoreduktorów (w reakcji arylowania heteroarenów);**
2. **Odkrycie nowej reakcji α -alkilowania aldehydów katalizowanej zarówno kompleksami rutenu, jak i porfirynami;**
3. **Odkrycie nowej reakcji α -alkilowania ketonów katalizowanej porfirynami oraz udowodnienie, że ścieżka reakcji nie prowadzi przez produkt pośredni – cyklopropan.**

Badania przedstawione w niniejszej rozprawie stanowią zwartą całość i jasno demonstrują użyteczność porfiryn jako katalizatorów fotoredoks i ich wykorzystanie w syntezie organicznej.

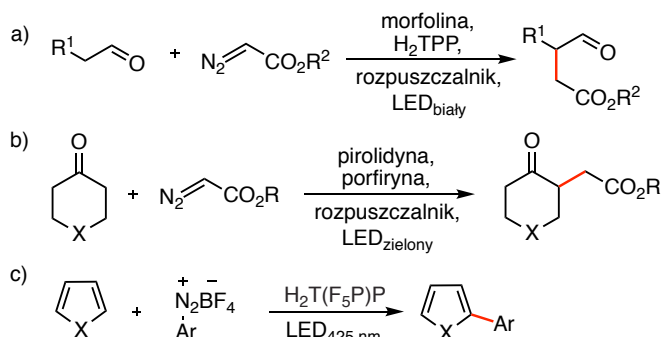
Nie jest to jednak koniec, a początek odkrywania właściwości katalitycznych porfiryn, a w związku z tym nowych reakcji, które mogą być przez nie katalizowane.

5. Streszczenie w języku polskim

Badania przedstawione w niniejszej rozprawie zakładają opracowanie i wykorzystanie nowych, organicznych katalizatorów fotoredoks. W reakcjach fotochemicznych, absorpcja fotonów przez cząsteczkę powoduje jej przejście do stanów wzbudzonych elektronowo, w związku z tym, w reakcji substratami są cząsteczki wysokoenergetyczne, w przeciwieństwie do reakcji aktywowanych termicznie. Ponadto, zastosowanie barwników jako fotokatalizatorów zdolnych absorbować światło widzialne pozwala na zastosowanie tej metodologii w reakcjach z udziałem cząsteczek nieabsorbujących fal elektromagnetycznych w zakresie widzialnym. Większość reakcji fotochemicznych przebiega poprzez transfer protonu (tworząc rodniki) lub transfer elektronu (tworząc jono-rodniki), z których oba prowadzą do aktywacji wiązań C-H. Porfiryny z ich 18π -elektronowym pierścieniem makrocyklicznym są idealnym materiałem do badań, ponieważ absorbują światło widzialne, posiadają wysoką kwantową wydajność fluorescencji oraz relatywnie długie czasy życia w stanie wzbudzonym. Po absorpcji światła mogą one zostać utlenione lub zredukowane do kationo- lub anionorodników, zatem w stanie wzbudzonym mogą pełnić rolę utleniaczy lub reduktorów. Do 2016 roku brak było przykładów użycia porfiryn jako katalizatorów fotoredoks w syntezie organicznej.

Celem moich badań było wykorzystanie porfiryn jako nowych, inspirowanych naturą katalizatorów fotoredoks w fotochemicznych reakcjach tworzenia wiązań C-C.

Przeprowadzone przeze mnie badania wykazały, że porfiryny mogą pełnić funkcję katalizatorów fotoredoks. W indukowanej światłem widzialnym reakcji aldehydów i ketonów z diazoestrami działały jako fotoutleniacze (Schemat 1a,b), a w fotochemicznej reakcji arylowania związków heterocyklicznych – jako fotoreduktory (Schemat 1b).



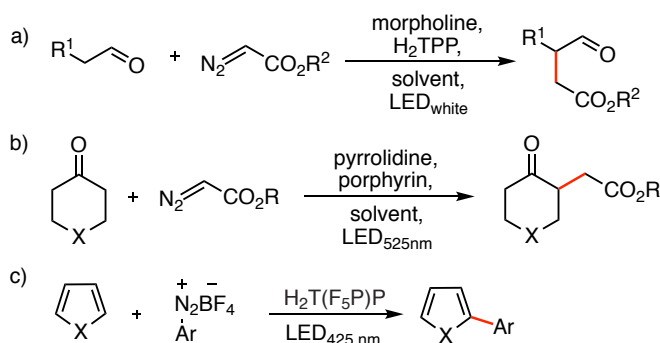
Schemat 1. Indukowane światłem reakcje tworzenia wiązań C-C katalizowane porfirynami

6. Streszczenie w języku angielskim/Abstract in English

The following dissertation focuses on the development of new organic, photoredox catalysts. I envisaged that porphyrins with their 18 π -electron aromatic macrocycle are perfectly suited for this role because they a) absorb visible-light, b) have high absorption coefficient, c) exhibit a small singlet-triplet splitting, d) have high quantum yield for intersystem crossing, e) and possess longer lifetime of the triplet state in comparison to the singlet state, not to mention straightforward synthesis. After light absorption porphyrins are excited to the triplet state and at this state they are able to transfer energy (photosensitization) or electrons (photoredox catalysis). These properties have been broadly used in the generation of singlet oxygen, conversion of solar energy, and in water splitting but before 2016 there were no example describing their use in C-C bond forming reactions through the porphyrin ring oxidation and reduction to ion radicals.

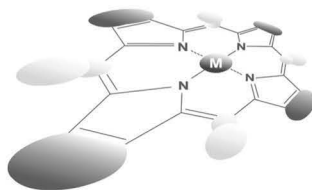
The main goal of my research was to establish a solid background for porphyrin's as photoredox catalysts that can be utilized in C-C bond forming reactions.

Herein, I demonstrate a successful application of these compounds as efficient photoredox catalysts for C-C bond forming reactions involving the reductive or oxidative quenching. Employing dual catalytic system – photocatalysis merged with enamine-iminium catalysis alkylation of aldehydes and ketones at the α position was accomplished (reductive quenching) (Scheme 1a, b). I have also found that porphyrins are also effective in catalyzing light-induced direct arylation of heteroarenes and cumarins with diazonium salts (oxidative quenching) (Scheme 1c).



Scheme 1. Porphyrins as photoredox catalysts in C-C bond forming reactions

7. Publikacje przeglądowe



C–C bond forming reactions catalyzed by chiral metalloporphyrins

Katarzyna Rybicka-Jasińska^a, Łukasz W. Ciszewski^{a,b}, Daniel T. Gryko^{*a} and Dorota Gryko^{*a}

^aInstitute of Organic Chemistry Polish Academy of Sciences, Kasprzaka 44/52, 01-224 Warsaw, Poland

^bDepartment of Chemistry, Warsaw University of Technology, Noakowskiego 3, 00-664 Warsaw, Poland

Dedicated to Professor Kevin M. Smith on the occasion of his 70th birthday

Received 14 December 2015

Accepted 5 January 2016

ABSTRACT: Porphyrins are abundant in nature facilitating many enzymatic reactions by being present in the active sites of many enzymes. Consequently, over the years, a number of chiral metalloporphyrins have been synthesized and have proved efficient in catalyzing C–C bond forming reactions. Herein, we review the synthesis of chiral metalloporphyrins and their catalytic activity in cyclopropanation, cyclopropanation, and C–H insertion reactions.

KEYWORDS: chiral porphyrins, cyclopropanation, C–H insertion, cyclopropanation.

J. Porphyrins Phthalocyanines 2016, 20:76-95. Downloaded from www.worldscientific.com by 188.146.97.147 on 04/22/18. For personal use only.

[Faint, illegible text from the main body of the article, likely bleed-through from the reverse side of the page.]

[Faint text at the bottom of the page, possibly a reference or a note.]

Scheme 1. General reaction catalyzed by metalloporphyrins.



Table 1

Entry	Substrate	Yield (%)	Enantiomeric excess (%)
1	1	85	92
2	2	78	88
3	3	90	95

Reaction conditions: $\text{Mg}(\text{TPP})_2$ (10 mol%), R-X (1.2 equiv), CH_2Cl_2 , 0°C , 12 h.

1: $\text{R} = \text{H}$, $\text{X} = \text{Br}$; 2: $\text{R} = \text{H}$, $\text{X} = \text{I}$; 3: $\text{R} = \text{Me}$, $\text{X} = \text{Br}$.

the reaction of $\text{R}_2\text{C}=\text{CH}_2$ with $\text{R}'\text{X}$ to form $\text{R}_2\text{CH}-\text{CH}_2\text{R}'$ is a well-known reaction, but had been

achieved only by using a chiral metal complex as a catalyst. The reaction of $\text{R}_2\text{C}=\text{CH}_2$ with $\text{R}'\text{X}$ to form $\text{R}_2\text{CH}-\text{CH}_2\text{R}'$ is a well-known reaction, but had been

8. Publikacje oryginalne

Photocatalytic Reaction of Diazo Compounds with Aldehydes

K. Rybicka-Jasińska,^a Ł. W. Ciszewski,^{a,b} and D. Gryko^{a,*}

^a Institute of Organic Chemistry, Polish Academy of Sciences, Kasprzaka 44/52, 01-224 Warsaw, Poland

E-mail: dorota.gryko@icho.edu.pl

^b Department of Chemistry, Warsaw University of Technology, Noakowskiego 3, 00-664 Warsaw, Poland

Received: January 20, 2016; Revised: March 2, 2016; Published online: April 27, 2016



Supporting information for this article is available on the WWW under <http://dx.doi.org/10.1002/adsc.201600084>.

Abstract: Photocatalytic reactions of diazoacetates with aldehydes led to α -alkylated carbonyl compounds instead of the expected cyclopropane derivatives. The reaction requires a dual catalytic system – photocatalysis merged with enamine-iminium catalysis. NMR, EPR, UV/Vis, and ESI-MS analyses pro-

vided sufficient data to corroborate the proposed radical mechanism – enamine catalysis merged with photocatalysis.

Keywords: aldehydes; diazo compounds; organocatalysis; photocatalysis; radicals

Advanced 
**Synthesis &
Catalysis**

Supporting Information

Supporting Information (SI)
for
Photocatalytic reaction of diazo compounds with aldehydes

K. Rybicka-Jasińska^[a], Ł. W. Ciszewski^{[a],[b]} and D. Gryko^{*[a]}

[a] prof. D. Gryko, K. Rybicka-Jasińska, Ł. W. Ciszewski
Institute of Organic Chemistry, Polish Academy of Science
Kasprzaka 44/52, 01-224 Warsaw (Poland)
E-mail: dorota.gryko@icho.edu.pl

[b] Ł. W. Ciszewski
Department of Chemistry
Warsaw University of Technology
Noakowskiego 3, 00- 664 Warsaw (Poland)

Table of Contents

1. General information	S3
2. General synthetic procedures	S3
3. Scope and limitations	S4
4. Mechanistic considerations	S8
4.1. Proposed mechanism	S8
4.2. EPR studies	S8
4.3. Experiment with deuterated reagents	S11
4.4. NMR studies	S12
4.5. Mass spectrometry studies	S15
4.6. Verification of cyclopropane-intermediate mechanism	S22
4.7. Stern–Volmer quenching experiments	S24
4.6. UV-Vis measurement	S25
5. ¹ H and ¹³ C NMR spectra	S28
a) Ethyl 3-benzyl-4-oxobutanoate (10)	S28
b) Ethyl 3-formyl-4-(4-methoxyphenyl)butanoate (22)	S29
c) Ethyl 3-formylundecanoate (23)	S30
d) Ethyl 4-oxo-3-phenylbutanoate (24)	S31
e) Ethyl 3-(3-chlorobenzyl)-4-oxobutanoate (25)	S32
f) Ethyl 2-formyl-3-methylbutanoate (26)	S33
g) <i>tert</i> -Butyl 3-benzyl-4-oxobutanoate (29)	S34
h) Benzyl 3-benzyl-4-oxobutanoate (30)	S35
i) 3-Phenylpropyl 3-benzyl-4-oxobutanoate (31)	S36
j) (2 <i>S</i>)- <i>tert</i> -Butyl-2-(((3-benzyl-4-oxobutanoyl)oxy)methyl)pyrrolidine-1-carboxylate (32) (CD ₃ Cl, rt)	S37
k) (2 <i>S</i>)- <i>tert</i> -Butyl-2-(((3-benzyl-4-oxobutanoyl)oxy)methyl)pyrrolidine-1-carboxylate (32) (DMSO- <i>d</i> ₆ , 80 °C)	S38
6. Emission spectra measurements	S39
7. The photoreactor	S40

1. General Information

All solvents and chemicals used in the syntheses were of reagent grade and were used without further purification. High resolution ESI mass spectra were recorded on a Mariner and SYNAPT spectrometer. ^1H and ^{13}C NMR spectra were recorded at rt on Bruker 400 and Varian 600 MHz instruments with TMS as an internal standard. EPR spectrum was recorded on Magnettech MS200 spectrometer. Thin layer chromatography (TLC) was performed using Merck Silica Gel GF254, 0.20 mm thickness. GC measurements were made on Gas Chromatograph Perkin Elmer Clarus 500. Aldehydes were purified by flash column chromatography (hexane: AcOEt) if necessary.

Photo-induced reactions were performed using a homemade photoreactor equipped with four LED light bulbs (1200 Lm; warm light).

2. General synthetic procedures

General procedure for α -functionalization of aldehydes:

Photocatalyst (2 mol%) was placed in a reaction tube and dissolved in DMSO and buffer pH = 4 (mixture 9:1, 10 mL). Then an aldehyde (1 mmol), morpholine (0.4 equiv., 0.4 mmol), LiBF_4 (20 mol%) and EDA (1 equiv., 1 mmol) were added into the reaction tube. The reaction mixture was stirred at 39 °C under irradiation (4xLED, 1200 lumens) for 5 h. After that, the light was turned off; the reaction mixture was diluted with AcOEt, and extracted with 1N HCl. The aqueous phase was separated and then extracted with AcOEt three times. Combined organic phases were washed with NaHCO_3 , brine and dried over Na_2SO_4 , filtered and concentrated. The crude product was purified by flash chromatography using silica gel (hexanes/AcOEt) to afford the corresponding product.

3. Scope and limitations

Ethyl 3-benzyl-4-oxobutanoate (10) (194 mg, 88%)

^1H NMR (CDCl_3 , 500 MHz) δ 9.79 (s, 1H, CHO), 7.31-7.17 (m, 5H, Ph), 4.11 (q, $J = 7.1$ Hz, 2H COCH_2CH_3), 3.14-3.08 (m, 2H, CH_2), 2.77-2.71 (m, 1H, CH), 2.65 (dd, $J(\text{H,H}) = 7.6$ Hz, 1H, CH), 1.40 (dd, $J = 4.8$ Hz, 1H, CH), 1.23 (t, $J = 7.0$ Hz, 3H, COCH_2CH_3).

^{13}C NMR (CDCl_3 , 100 MHz) δ 202.2, 171.6, 137.7, 129.0, 128.6, 126.7, 60.7, 49.2, 34.6, 32.7, 14.1. IR (cm^{-1}): 3029, 2982, 2934, 2725, 1733 (CO), 1496, 1454 (CHO), 1375, 1199, 1161, 1031, 750, 702.

HRMS ESI calcd. for $\text{C}_{13}\text{H}_{16}\text{O}_3$ $[\text{M}+\text{Na}]^+$ 243.0997, found: 243.0993.

Elemental analysis calcd (%) for $\text{C}_{13}\text{H}_{16}\text{O}_3$: C 70.89, H, 7.32, found: C 70.74, H, 7.40.

Ethyl 3-formyl-4-(4-methoxyphenyl)butanoate (22) (200 mg, 80%)

^1H NMR (CDCl_3 , 500 MHz) δ 9.78 (s, 1H, CHO), 7.09-7.07 (m, 2H, Ph), 6.84-6.83 (m, 2H, Ph), 4.10 (q, $J = 7.0$ Hz, 2H, COCH_2CH_3), 3.78 (s, 3H, OCH_3), 3.08-3.01 (m, 2H, CH_2), 2.71-2.60 (m, 2H, CH_2), 2.40 dd, $J = 5.5$ Hz, (1H, CH), 1.23 (t, $J = 7.0$ Hz, 3H, COCH_2CH_3).

^{13}C NMR (CDCl_3 , 100 MHz) δ 202.5, 171.7, 158.3, 129.9, 129.5, 114.0, 60.7, 55.2, 49.4, 33.7, 32.6, 14.1.

IR (cm^{-1}): 2982, 2958, 2935, 2837, 1731 (CO), 1612, 1514 (CHO), 1249 (OCH_3), 1179, 1034, 838.

HRMS ESI calcd. for $\text{C}_{14}\text{H}_{18}\text{O}_4$ $[\text{M}+\text{Na}]^+$ 273.11032, found: 273.1102

Elemental analysis calcd (%) for $\text{C}_{14}\text{H}_{18}\text{O}_4$: C 67.18, H 7.25, found: C 67.24, H 7.10.

Ethyl 3-formylundecanoate (23) (184mg, 76%)

^1H NMR (CDCl_3 , 400 MHz) δ 9.71 (s, 1H, CHO), 4.15 (q, $J = 4$ Hz, 2H, COCH_2CH_3), 2.83-2.79 (m, 1H, CH), 2.70-2.64 (m, 1H, CH), 3.39 (dd, $J = 4$ Hz, 1H, CH), 1.72-1.68 (m, 1H, CH), 1.49-1.43 (m, 1H, CH), 1.35- 1.23 (m, 15H, CH_2), 0.87 (t, $J = 4$ Hz, 3H, CH_3).

^{13}C NMR (CDCl_3 , 100 MHz) δ 202.9, 171.9, 60.7, 47.7, 33.1, 31.8, 29.5, 29.3, 29.1, 28.6, 26.7, 22.6, 14.1, 14.0.

IR (cm^{-1}): 2927, 2856, 1737 (CO), 1466 (CHO), 1374, 1185, 1032, 723. HRMS ESI calcd. for $\text{C}_{14}\text{H}_{26}\text{O}_3$ $[\text{M}+\text{Na}]^+$ 265.1780, found: 265.1779.

Elemental analysis calcd (%) for $\text{C}_{14}\text{H}_{26}\text{O}_3$: C 69.38, H 10.81, found: C 69.30, H 10.85.

Ethyl 4-oxo-3-phenylbutanoate (24)¹ (103 mg, 44%)

¹H NMR (CDCl₃, 400 MHz) δ 9.70 (s, 1H, CHO), 7.40-7.32 (m, 3H, Ph), 7.21-7.19 (m, 2H, Ph), 4.17-4.10 (m, 3H, COCH₂CH₃, CH), 3.14 (dd, *J* = 8.0 Hz, 1H, CH), 2.61 (dd, *J* = 8 Hz, 1H, CH), 1.22 (t, *J* = 8 Hz, 3H, COCH₂CH₃).

¹³C NMR (CDCl₃, 100 MHz) δ 198.5, 171.5, 134.8, 129.2, 128.8, 128.0, 60.7, 54.6, 34.6, 14.0.

Ethyl 3-(3-chlorobenzyl)-4-oxobutanoate (25) (180 mg, 71%).

¹H NMR (CDCl₃, 400 MHz) δ 9.78 (s, 1H, CHO), 7.26-7.18 (m, 3H, Ph), 7.07-7.06 (m, 1H, Ph), 4.12 (q, *J* = 7.2 Hz, 2H, COCH₂CH₃), 3.12-3.07 (m, 2H, CH₂), 2.74-2.69 (m, 1H, CH), 2.65 (dd, *J* = 7.1 Hz, 1H, CH), 2.40 (dd, *J* = 5.1 Hz, 1H, CH), 1.24 (t, *J* = 7.1 Hz, 3H, COCH₂CH₃).

¹³C NMR (CDCl₃, 100 MHz) δ 201.7, 171.4, 139.9, 134.5, 129.9, 129.1, 127.2, 127.0, 60.9, 49.0, 34.1, 32.7, 14.1.

IR (cm⁻¹): 2982, 2934, 1730 (CO), 1598, 1574, 1476, 1374 (CHO), 1198, 1157, 1027, 878, 783, 703, 684, 443.

HRMS ESI calcd. for C₁₃H₁₅ClO₃ [M+CH₃OH+Na]⁺ 309.0870, found: 309.0867. Elemental analysis calcd (%) for C₁₃H₁₅ClO₃: C 61.30, H, 5.94, Cl 13.9, found: C 61.27, H 5.91, Cl 13.86.

Ethyl 2-formyl-3-methylbutanoate (26)² (117 mg, 63%).

¹H NMR (CDCl₃, 400 MHz) δ 9.74 (s, 1H, CHO), 4.12 (q, *J* = 8.0 Hz, 2H, COCH₂CH₃), 2.81-2.64 (m, 2H, CH), 2.42-2.28 (ddd, *J* = 4.0 Hz, 1H, CH), 2.19-2.01 (m, 1H, CH), 1.25-1.21 (td, *J* = 8.0 Hz, *J* = 4Hz, 3H, COCH₂CH₃), 1.01-0.92 (m, 6H, 2xCH₃).

¹³C NMR (CDCl₃, 100 MHz) δ 203.3, 179.8, 172.2, 60.7, 60.6, 53.5, 47.2, 32.6, 29.8, 27.7, 20.1, 19.9, 19.3, 19.1, 14.0, 14.0.; residual peaks from AcOEt, hexane and CH₂Cl₂ – product is very volatile and difficult to dry.

¹ L. Carman, L. D. Kwart, T. Hulicky, *Synth. Commun.*, **1986**, *16*, 169-182.

² P. Deslongchamps, A. Bélanger, D. J. F. Berney, H.-J. Borschberg, R. Brousseau, A. Doutheau, R. Durand, H. Katayama, R. Lapalme, D. M. Leturc, C.-C. Liao, F. N. MacLachlan, J.-P. Maffrand, F. Marazza, R. Martino, C. Moreau, L. Ruest, L. Saint-Laurent, R. Saintonge, P. Soucy, *Can. J. Chem.*, **1990**, *68*, 127-152.

tert-Butyl 3-benzyl-4-oxobutanoate (29) (166 mg, 67%).

^1H NMR (CDCl_3 , 500 MHz) δ 9.78 (s, 1H, CHO), 7.30-7.16 (m, 5H, Ph), 3.10-3.04 (m, 2H, CH_2), 2.74-2.2.72 (m, 1H, CH), 2.56 (dd, J = 7.6 Hz, 1H, CH), 2.35 (dd, J = 5.1 Hz, 1H, CH), 1.42 (s, 9H, *t*-Bu).

^{13}C NMR (CDCl_3 , 125 MHz) δ 202.5, 170.8, 137.9, 129.0, 128.6, 126.6, 81.1, 49.4, 34.5, 34.1, 28.0.

IR (cm^{-1}): 2979, 2931, 1728 (CO), 1455, 1368 (CHO), 1255, 1150, 751, 701.

HRMS ESI calcd. for $\text{C}_{15}\text{H}_{20}\text{O}_3$ [$\text{M}+\text{CH}_3\text{OH}+\text{Na}$] $^+$ 303.1572, found: 303.1562.

Elemental analysis calcd (%) for $\text{C}_{15}\text{H}_{20}\text{O}_3$: C 72.55; H 8.12, found: C 72.31, H 8.29.

Benzyl 3-benzyl-4-oxobutanoate (30) (219 mg, 78%)

^1H NMR (CDCl_3 , 500 MHz) δ 9.79 (s, 1H, CHO), 7.36-7.28 (m, 6H, Ph), 7.27-7.22 (m, 2H, Ph), 7.15-7.13 (m, 2H, Ph), 5.08 (s, 2H, CH_2Ph), 3.14-3.07 (m, 2H, CH_2), 2.76-2.67 (m, 2H, CH_2), 2.42 (dd, J = 4.0 Hz, 1H, CH).

^{13}C NMR (CDCl_3 , 125 MHz) δ 202.1, 171.5, 137.5, 135.5, 129.0, 128.7, 128.5, 128.3, 128.2, 126.7, 66.6, 49.2, 34.5, 32.6.

IR (cm^{-1}): 3087, 3063, 3030, 2925, 2828, 2724, 1732 (CO), 1496, 1455, 1383 (CHO), 1352, 1189, 1160, 748, 700, 491

HRMS ESI calcd. for $\text{C}_{18}\text{H}_{18}\text{O}_3$ [$\text{M}+\text{CH}_3\text{OH}+\text{Na}$] $^+$ 337.1416 found: 337.1413.

Elemental analysis calcd (%) for $\text{C}_{18}\text{H}_{18}\text{O}_3$: C 76.57, H 6.43, found: C 76.48, H 6.24.

3-Phenylpropyl 3-benzyl-4-oxobutanoate (31) (248 mg, 80%).

^1H NMR (CDCl_3 , 500 MHz) δ 9.79 (s, 1H, CHO), 7.31-7.25 (m, 5H, Ph), 7.19-7.16 (m, 5H, Ph), 4.06 (td, J = 4.0 Hz, 2H, CH_2), 3.12-3.10 (m, 2H, CH_2), 2.75 (d, J = 4.0 Hz, 1H, CH), 2.68-2.62 (m, 3H, CH_2+CH), 2.39 (dd, J = 4.0 Hz, 1H, CH), 1.95-1.91 (m, 2H, CH_2).

^{13}C NMR (CDCl_3 , 125 MHz) δ 202.2, 171.7, 141.0, 137.6, 129.0, 128.7, 128.4, 128.3, 126.7, 126.0, 64.2, 49.2, 34.6, 32.6, 32.1, 30.1.

IR (cm^{-1}): 3085, 3061, 3027, 2952, 2925, 2858, 1731 (CO), 1603, 1496, 1453 (CHO), 1192, 1163, 1030, 748, 701, 492.

HRMS ESI calcd. for $\text{C}_{20}\text{H}_{22}\text{O}_3$ [$\text{M}+\text{Na}$] $^+$ 333.1467, found: 333.1461.

Elemental analysis calcd (%) for $\text{C}_{20}\text{H}_{22}\text{O}_3$: C 77.39, H 7.14, found: C, 77.36, H 7.01.

(2S)-tert-Butyl-2-(((3-benzyl-4-oxobutanoyl)oxy)methyl)pyrrolidine-1-carboxylate (32)

(266 mg, 71%).

^1H NMR (CDCl_3 , 600 MHz) δ 9.78 (s, 1H, CHO), 7.33-7.30 (m, 2H, Ph), 7.27 (m, 1H, Ph), 7.19-7.17 (m, 2H, Ph), 4.17-3.99 (m, 3H, CH_2 , CH), 3.34-3.32 (m, 2H, CH_2), 3.16-3.09 (m, 2H, CH_2), 2.79-2.72 (m, 1H, CH), 2.69-2.61 (m, 1H, CH), 2.40 (dd, $J = 6\text{Hz}$, 1H, CH), 2.01-1.70 (m, 4H, $2\times\text{CH}_2$), 1.46 (s, 9H, *t*-Bu).

^{13}C NMR (CDCl_3 , 150 MHz) δ 202.1, 171.5, 154.4, 137.5, 129.9, 128.7, 126.7, 79.7, 79.3, 64.9, 55.4, 49.1, 46.4, 34.5, 32.5, 28.7, 28.4, 27.8, 23.7, 22.9.

^1H NMR ($(\text{CD}_3)_2\text{SO}$, 80 °C, 500 MHz) δ 9.70 (s, 1H, CHO), 7.31-7.27 (m, 2H, Ph), 7.23-7.18 (m, 3H, Ph), 4.11-4.06 (m, 1H, CH), 4.05-3.99 (m, 1H, CH), 3.92-3.86 (m, 1H, CH), 3.33-3.27 (m, 1H, CH), 3.10-3.02 (m, 3H, CH_2+CH), 2.80-2.73 (m, 1H, CH), 2.63-2.57 (dd, $J = 6\text{ Hz}$, 1H, CH), 2.49-2.41 (m, 1H, CH), 1.97-1.68 (m, 4H, $2\times\text{CH}_2$), 1.41 (s, 9H, *t*-Bu).

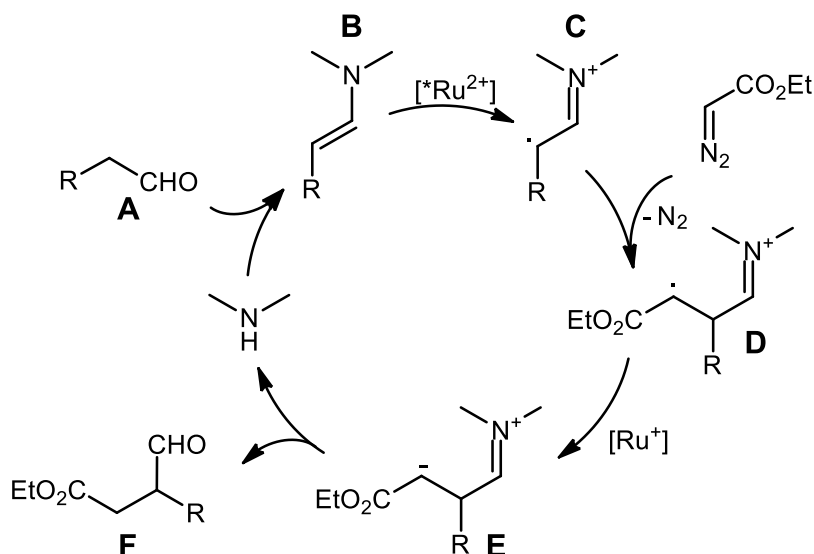
^{13}C NMR ($(\text{CD}_3)_2\text{SO}$, 80 °C, 125 MHz) δ 203.1, 171.4, 171.4, 154.0, 138.7, 129.3, 128.7, 126.7, 79.0, 64.9, 55.7, 55.7, 49.1, 46.7, 40.8, 40.7, 40.5, 40.3, 40.2, 40.0, 39.8, 34.2, 32.8, 28.6, 28.5, 28.3, 23.3. IR (cm^{-1}): 2975, 2932, 2880, 1736 (CO), 1693 (CO), 1394 (CHO), 1366, 1167, 1109, 702.

HRMS ESI calcd. for $\text{C}_{20}\text{H}_{22}\text{O}_3$ [$\text{M}+\text{CH}_3\text{OH}+\text{Na}$] $^+$ 430.2206, found: 430,2208.

Elemental analysis calcd (%) for $\text{C}_{21}\text{H}_{29}\text{NO}_5$: C 67.18, H 7.79, N 3.73, found: C,67.22, H 7.72, N 3.69.

4. Mechanistic considerations:

4.1. Proposed Mechanism



B – confirmed by NMR and MS experiment – see pp. S12-S14 and S15-S22.

C – confirmed by EPR experiment – see pp. S8-S10.

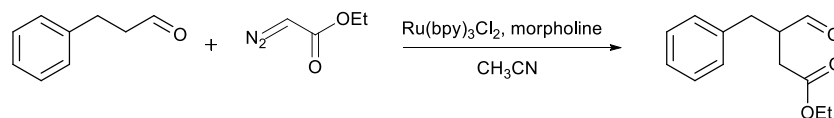
D – confirmed EPR and MS experiment – see pp. S8-S10 and S15-S22.

E – confirmed in experiment with D_2O NMR – see pp. S11.

4.2. EPR spectroscopy

Carbenes with triplet ground state exhibit characteristic EPR spectra which can be used to confirm their presence. Therefore, the reaction of 3-phenylpropanal with EDA was studied using EPR spectroscopy. As the concentration of free radicals in the reaction mixture was too low to be detected directly by EPR spectroscopy, the spin trapping experiment was performed by adding phenyl-*N-t*-butyl-nitron (PBN) as a spin trap to the reaction mixture (Chart 1). In the control experiment EDA was irradiated with LED light in the presence $Ru(bpy)_3Cl_2$. Weak signal was observed, which is understandable since triplet carbenes easily undergo intersystem crossing, confirming the formation of carbene in the triplet ground state. Additionally, the same experiment was performed for 3-phenylpropanal and morpholine. The characteristic signal corroborates the presence of the assumed cation-radical. This intermediate formed upon the enamine reduction with $*Ru^{2+}$. Finally, the EPR

spectrum was measured for the reaction mixture after 10 min. The formation of 'spin adducts' was ascertained thus supporting the radical mechanism. On these bases, we concluded that the C-H insertion at the α -position involves radicals.



Reaction conditions: 3-phenylpropanal (1 equiv., 1 mmol), ethyl diazoacetate (1 equiv., 1 mmol) morpholine (0.4 equiv., 0.4 mmol), Ru(bpy)₃Cl₂ (2 mol%), CH₃CN. After 10 min. of stirring under irradiation (4xLED) *N-tert*-Butyl- α -phenylnitrone (spin trap) was added and EPR spectra (9.3 GHz) was recorded.

spin trap: *N-tert*-butyl- α -phenylnitrone;
 central magnetic field: 333 mT;
 sweep width: 7,9 mT;
 modulation amplitude: 0,06 mT;
 microwave strength: 6,3 mW;
 sweep time: 30 s;
 number of scans: 16

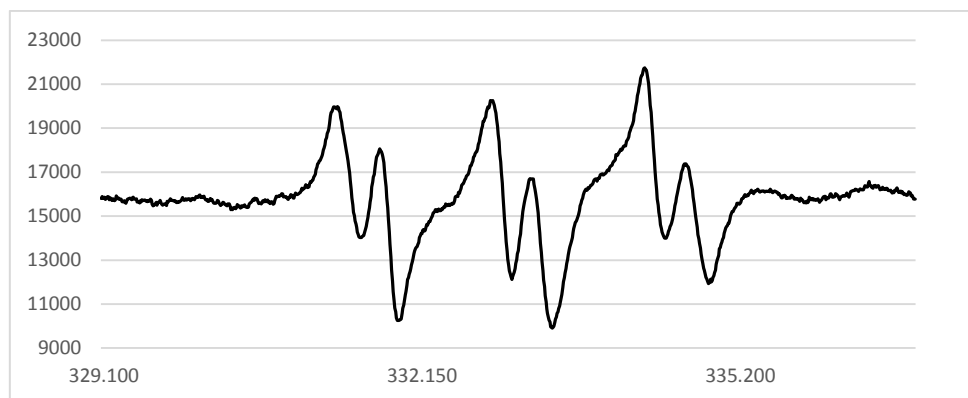


Chart 1. EPR spectra of the reaction mixture.

EPR data suggests that two radicals are present.

Control EPR experiments of a background's reactions were performed:

1. Ru(bpy)₃Cl₂ in CH₃CN was stirred under light irradiation (4xLED) for 10 minutes and then *N-tert-butyl-α-phenylnitron*e (spin trap) was added followed by EPR spectra (9.3 GHz) recording. No signals corresponding to radicals were detected.
2. Ru(bpy)₃Cl₂ with EDA in CH₃CN was stirred under light irradiation (4xLED) for 10 minutes and then *N-tert-butyl-α-phenylnitron*e (spin trap) was added followed by measurement EPR spectra (9.3 GHz). Weak signals were detected suggesting the formation of a radical.
3. Ru(bpy)₃Cl₂ with aldehyde and morpholine in CH₃CN was stirred under light irradiation (4xLED) for 10 minutes after that *N-tert-Butyl-α-phenylnitron*e (spin trap) was added followed by measurement EPR spectra (9.3 GHz). Strong signals were detected suggesting the presence of radical.

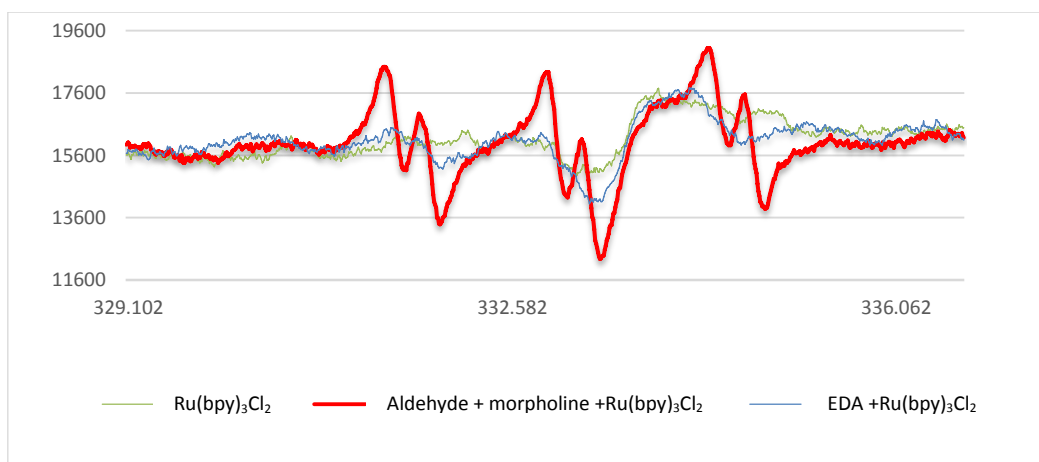


Chart 2. EPR spectra of background's reaction.

4.3 Experiment with deuterated reagents (D₂O)

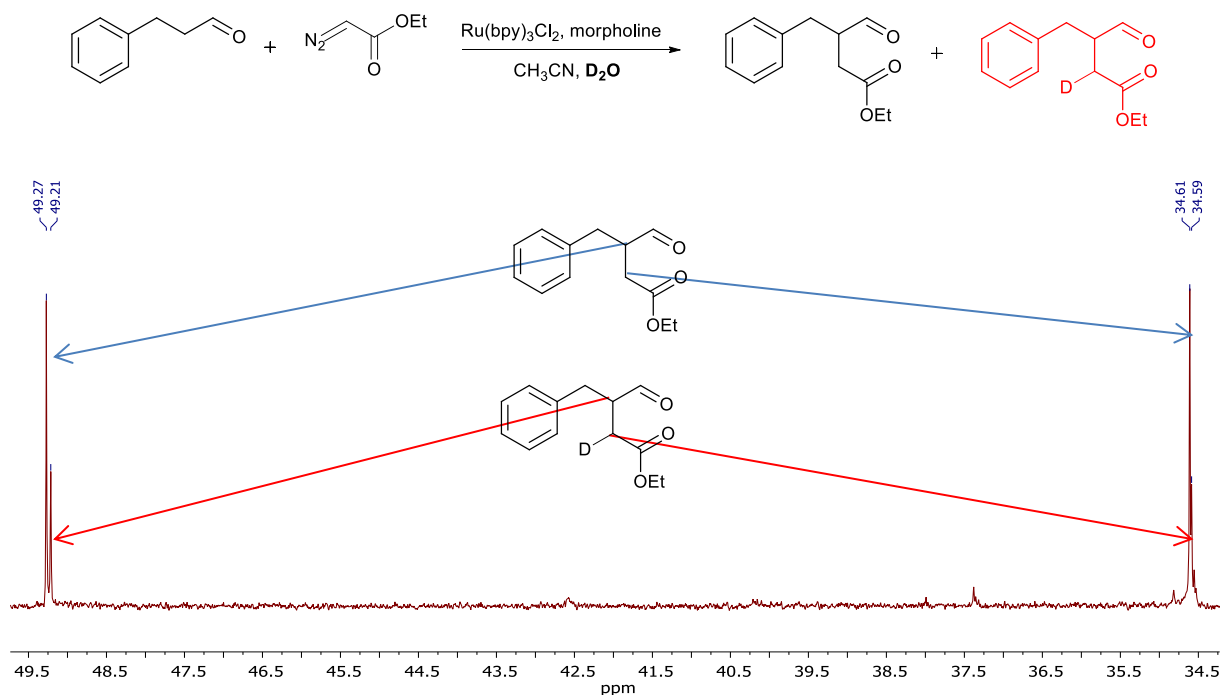
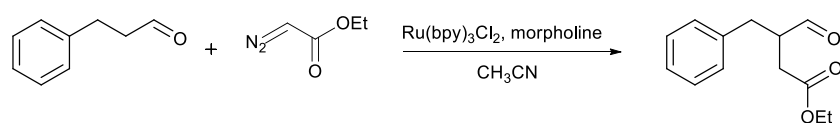


Chart 1. ¹³C NMR spectra : 1) product of reaction without D₂O, 2) product of a reaction with D₂O

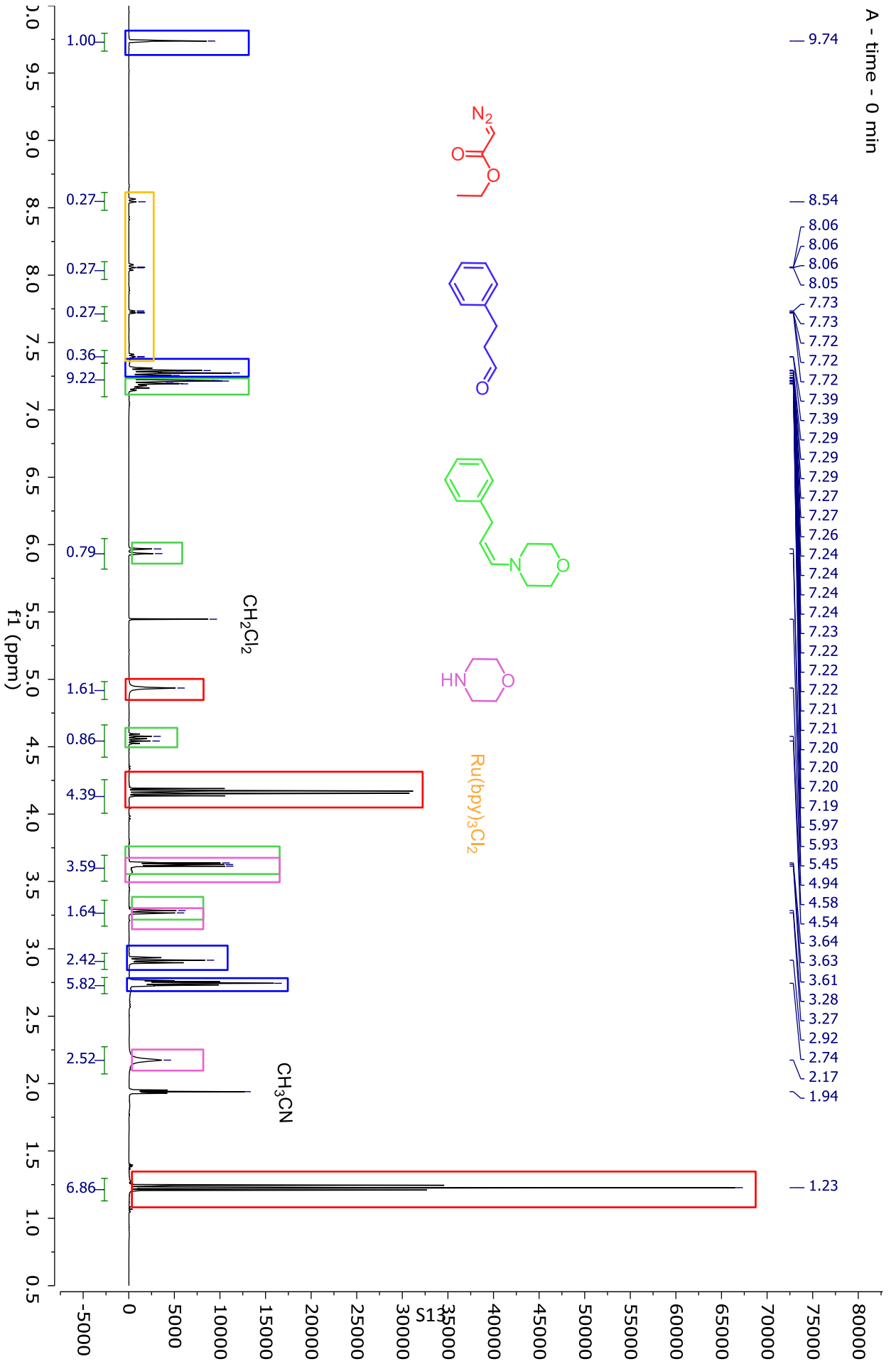
To prove the hypothesis of the external proton incorporation in the α-position to the ester group, the experiment with D₂O was performed. ¹H and ¹³C NMR spectra suggested that after the reaction in the presence of D₂O, a mixture of deuterated and undeuterated product formed. In ¹³C NMR spectrum two pairs of signals 49.27, 49.21 and 34.61 and 34.59 suggested the presence of the deuterated product. In ¹H NMR spectrum signals corresponding to the deuterated product were too weak to judge about ratio of products.

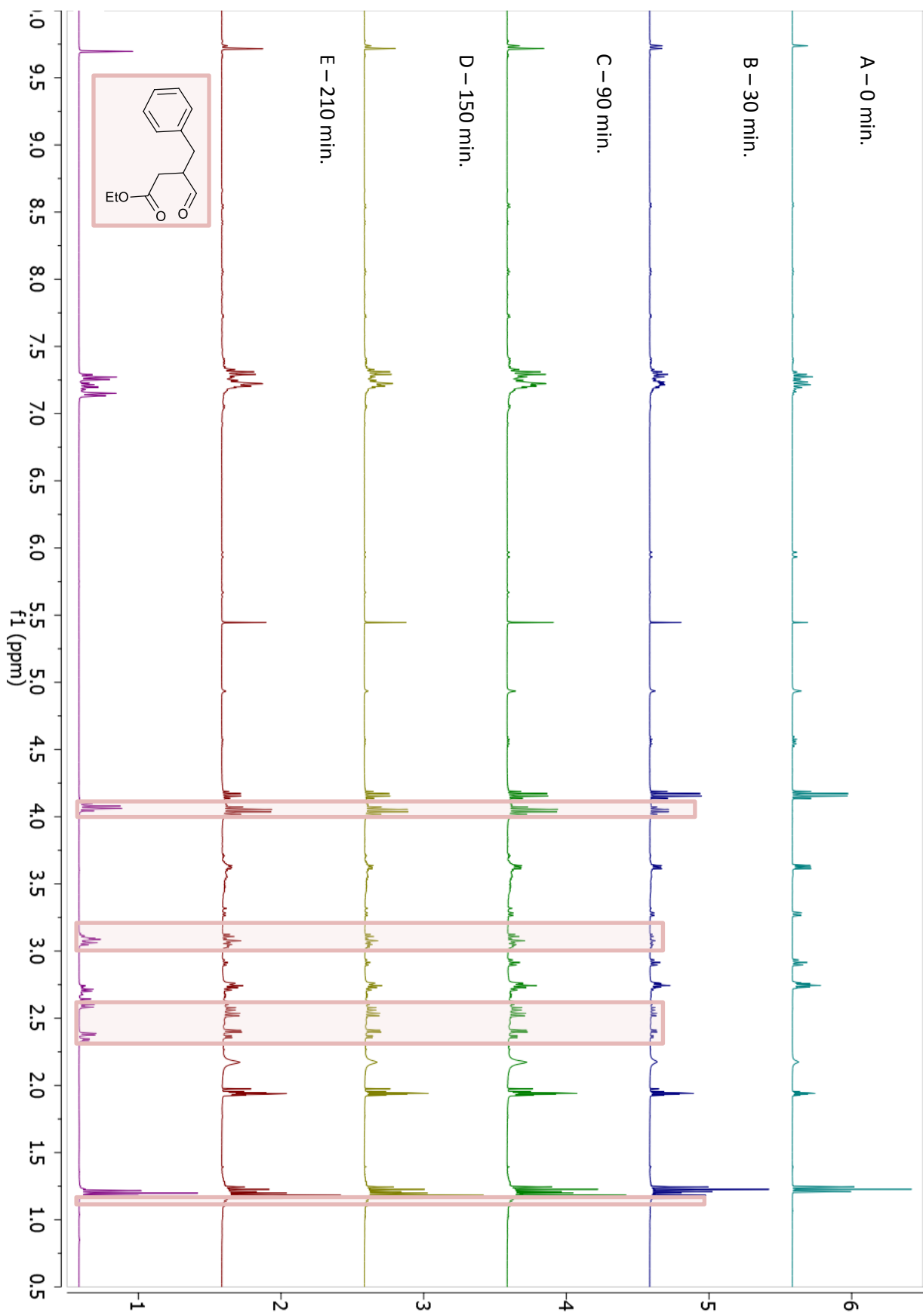
4.4. NMR studies



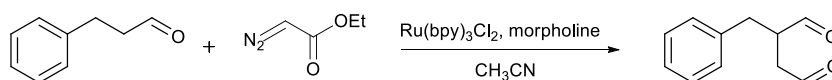
Reaction conditions: aldehyde (1 equiv., 1 mmol), morpholine (0.4 equiv., 0.4 mmol), EDA (1 equiv., 1 mmol), Ru(bpy)₃Cl₂ (2 mol%), CD₃CN. The progress of the reaction was followed by ¹H NMR spectroscopy. After 0, 30, 90, 150 and 210 min. of stirring under light irradiation (4xLED) NMR spectra (400 MHz) was recorded.

A - time - 0 min



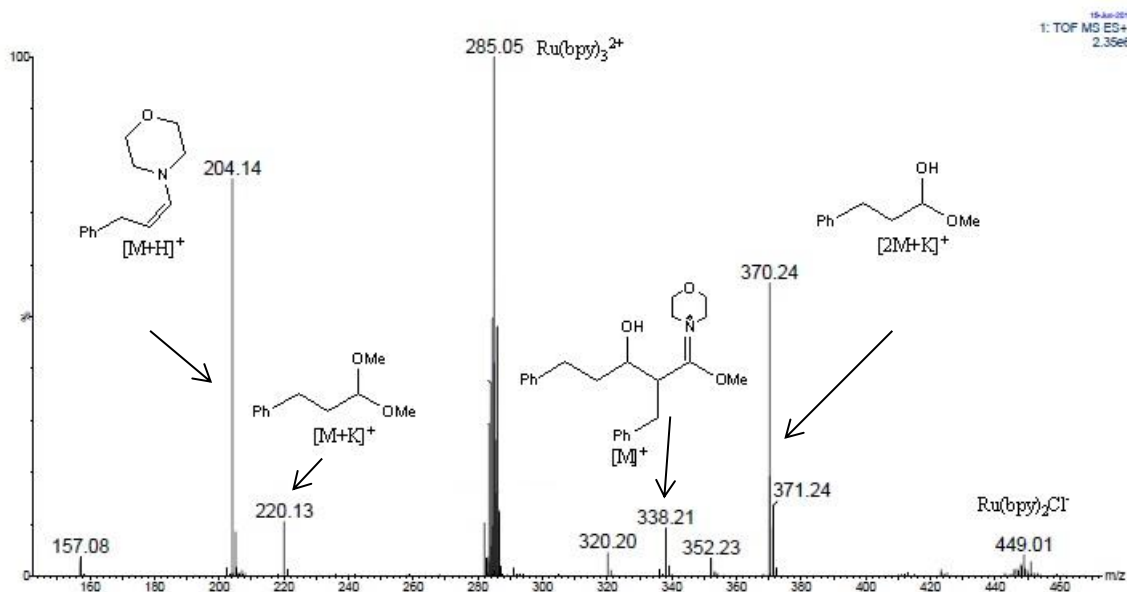


4.5. Mass spectrometry studies

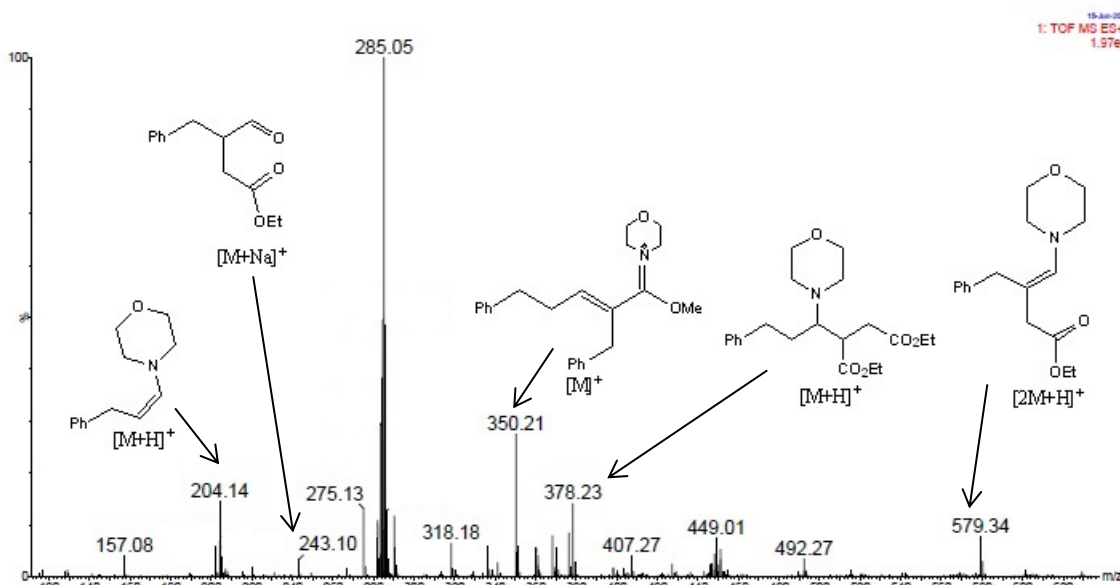


Reaction conditions: aldehyde (1 equiv., 1 mmol), morpholine (0.4 equiv., 0.4 mmol), EDA (1 equiv., 1 mmol), Ru(bpy)₃Cl₂ (2 mol%), CD₃CN. To support the proposed mechanism the progress of the reaction was also monitored by ESI-MS. After 0, 30, 90, 150 and 210 min. of stirring under light irradiation (4xLED) MS ESI spectra was recorded.

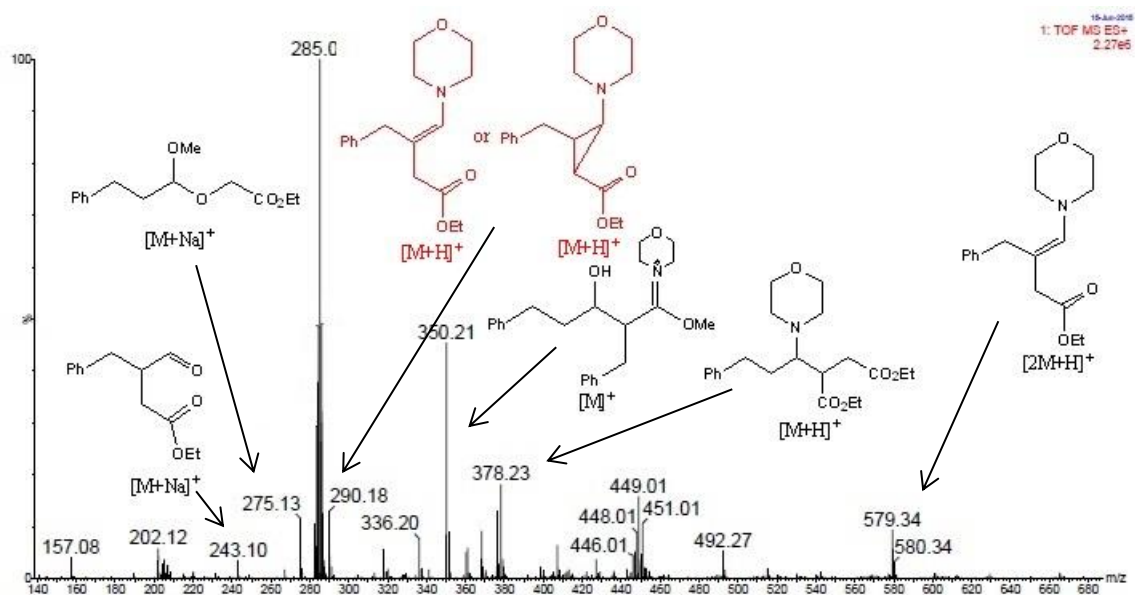
A – 0 min.:



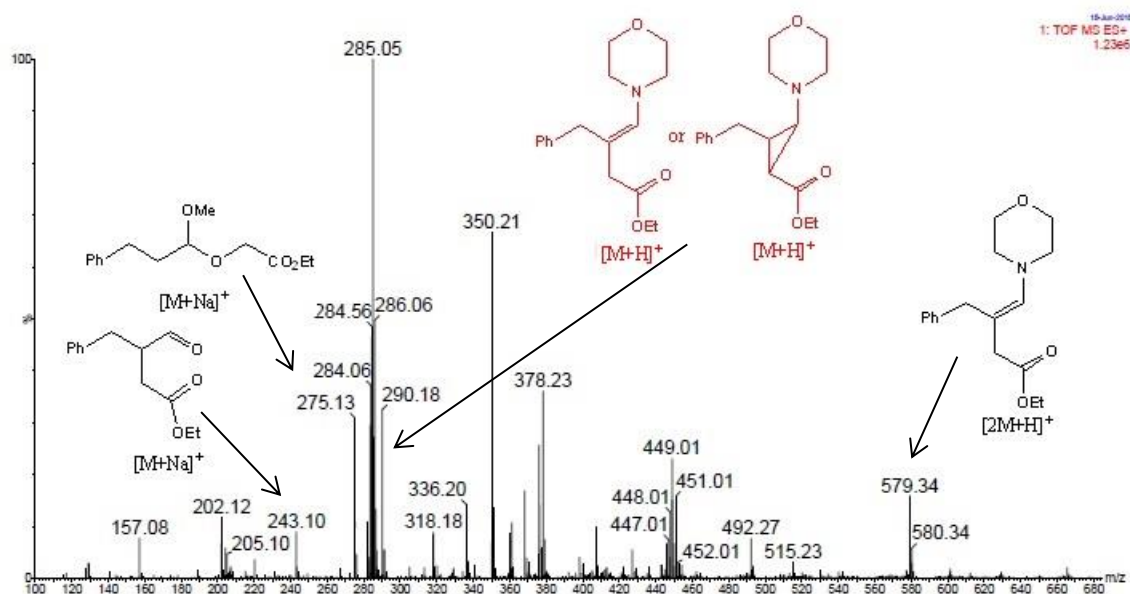
B – 30 min.:



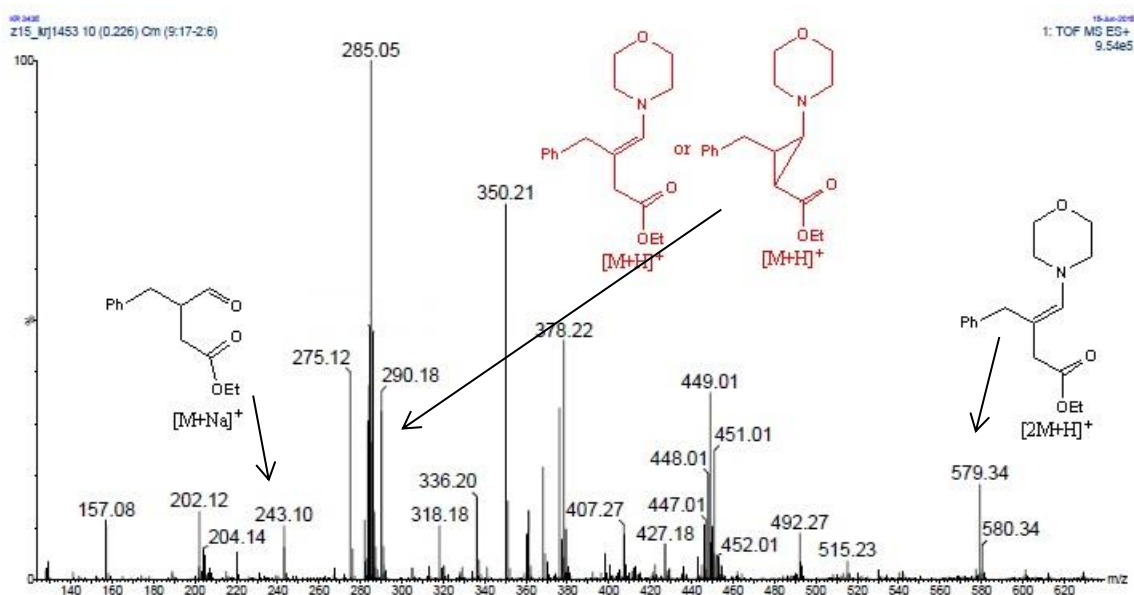
C – 90 min.:



D – 150 min.:



E - 210 min:

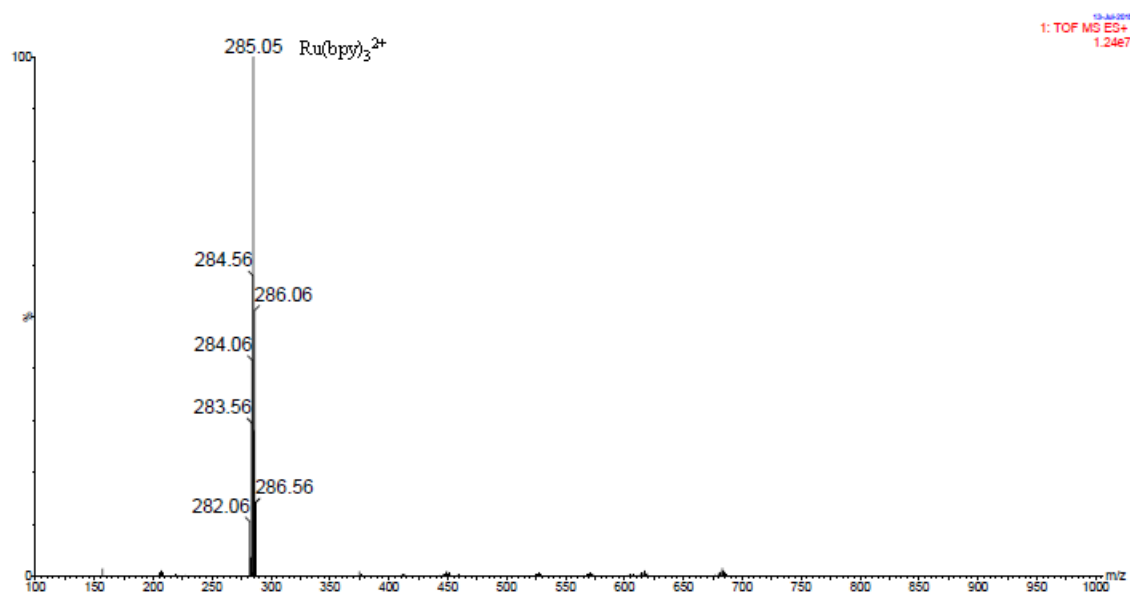


The ESI-MS analysis of the reaction shows a more complex mixture of products than NMR data. We assume that during the experiments subsequent reactions took place in the gas phase.

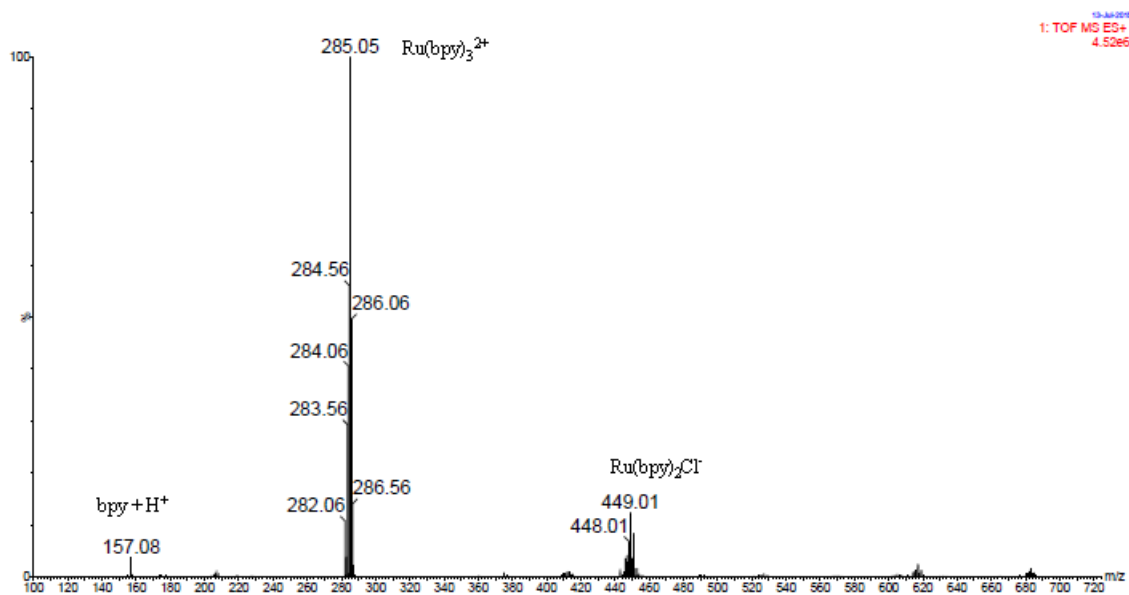
The control ESI-MS experiments of background's reactions were also performed:

1) Ru(bpy)₃Cl₂ in CH₃CN after:

a) 0 min. of stirring under light irradiation (4xLED):

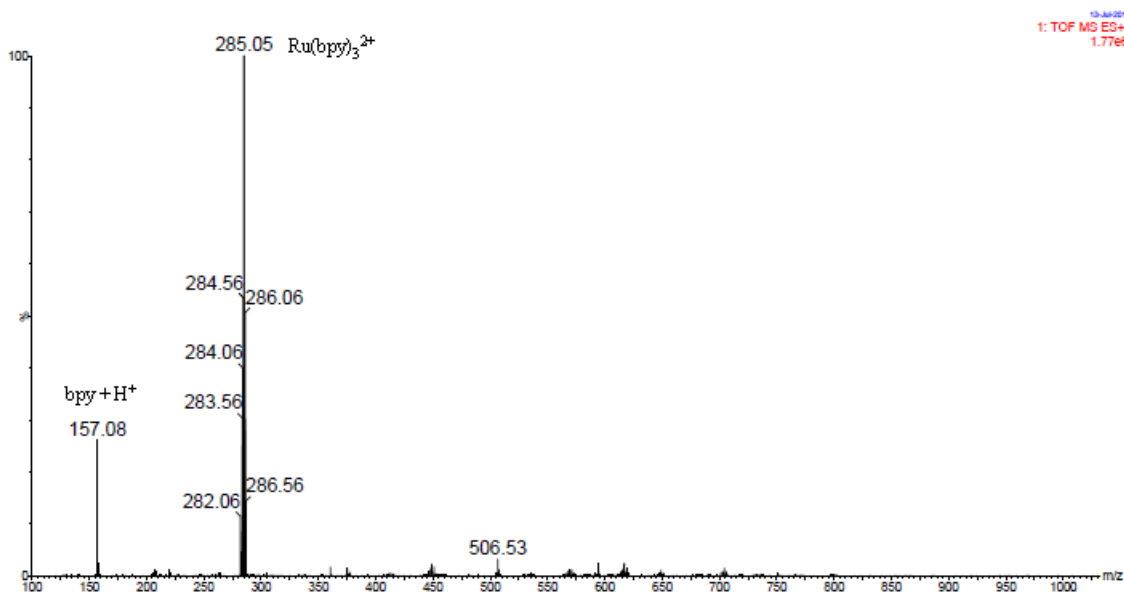


b) 30 min. of stirring under light irradiation (4xLED):

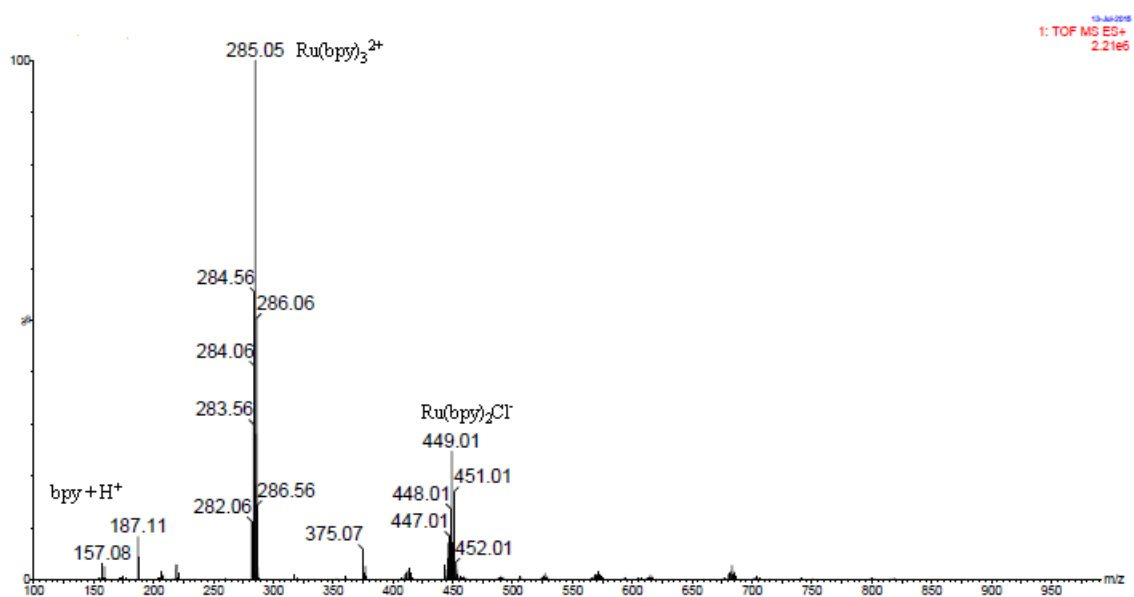


2) Ru(bpy)₃Cl₂ with morpholine in CH₃CN after:

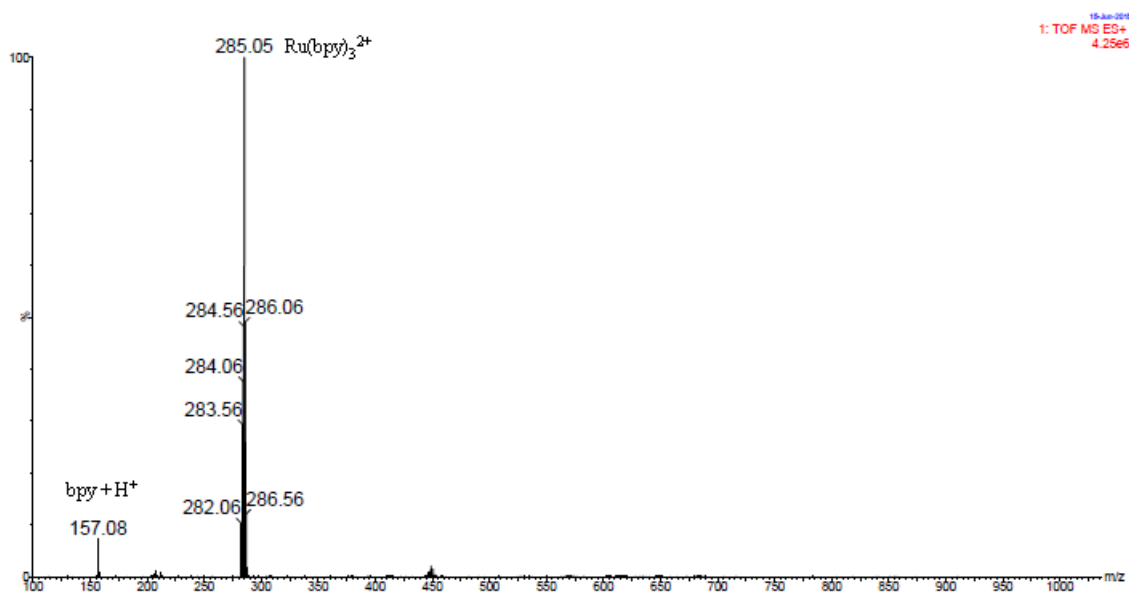
a) 0 min. of stirring under light irradiation (4xLED):



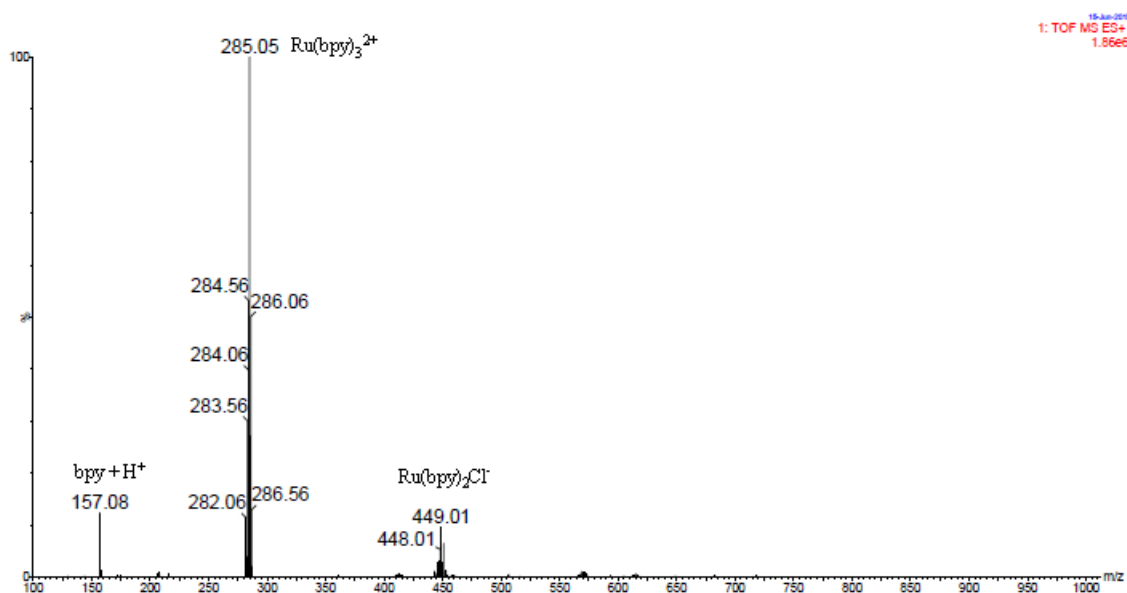
b) 30 min. of stirring under light irradiation (4xLED):



3) Ru(bpy)₃Cl₂ with EDA in CH₃CN after 30 min. of stirring under light irradiation (4xLED):

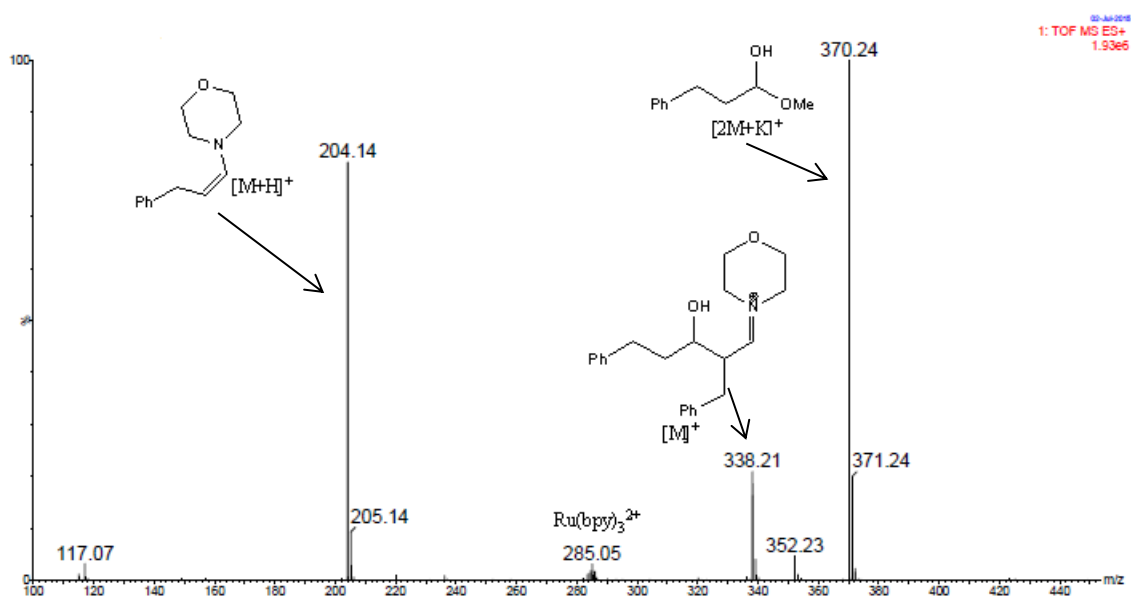


4) Ru(bpy)₃Cl₂ with EDA, morpholine in CH₃CN after 30 min. of stirring under light irradiation (4xLED):

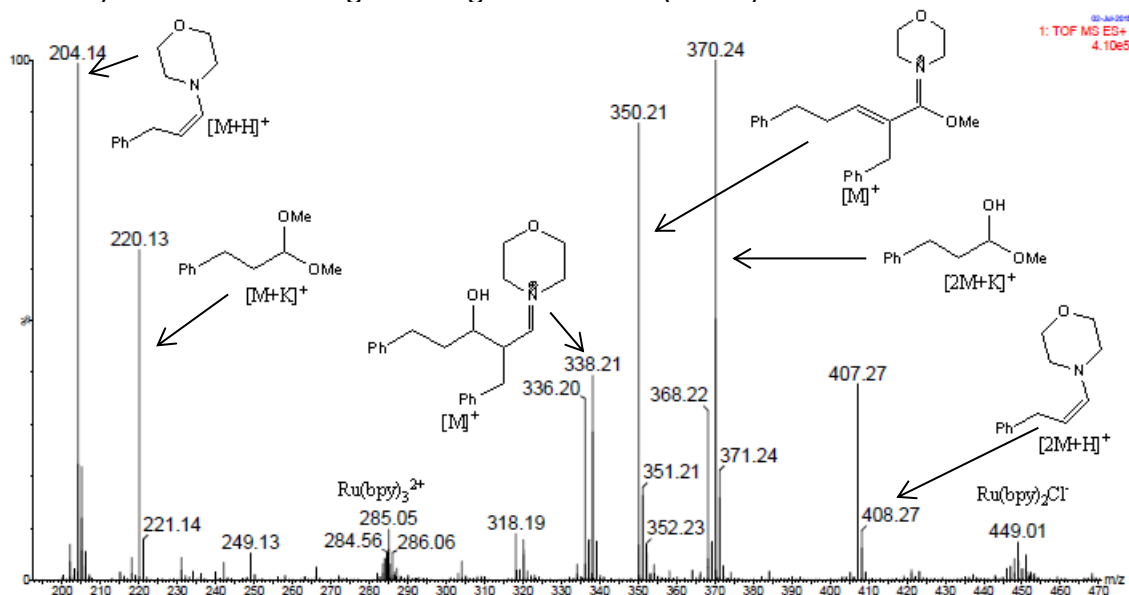


5) Ru(bpy)₃Cl₂ with 3-phenylpropanal, morpholine in CH₃CN after:

a) 0 min. of stirring under light irradiation (4xLED):

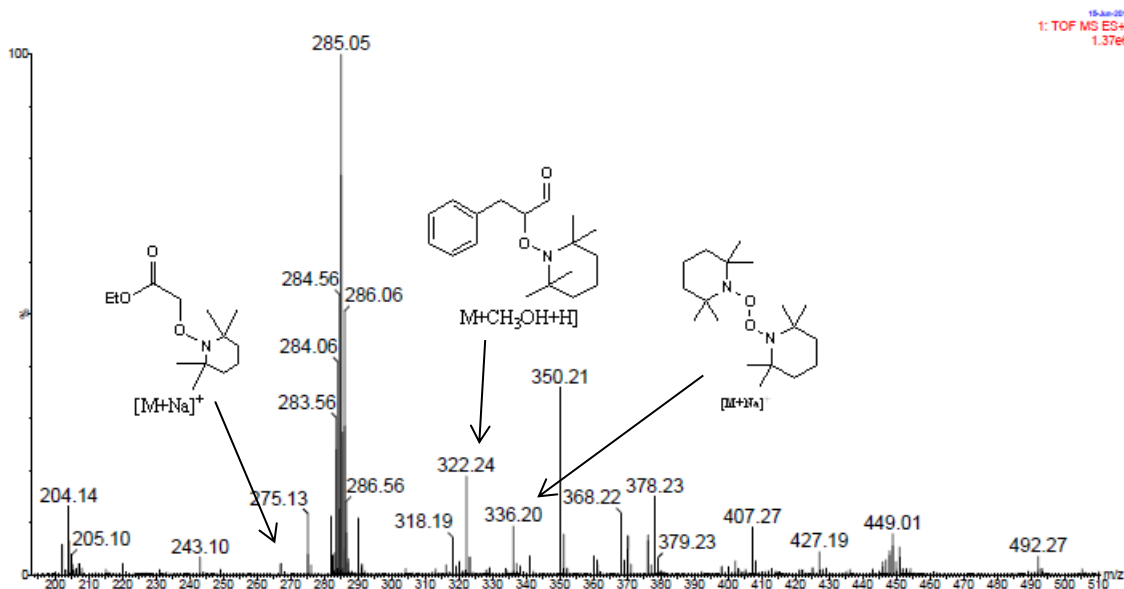


b) 30 min. of stirring under light irradiation (4xLED).



When no EDA was added to the reaction mixture the substantial formation of the aldol product was detected.

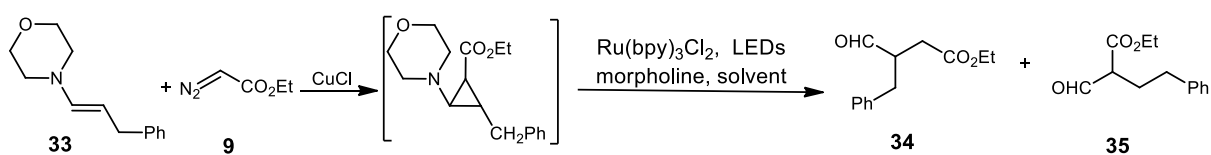
6) Ru(bpy)₃Cl₂ with aldehyde, morpholine and EDA in CH₃CN after 30 min. of stirring under light irradiation (4xLED) TEMPO as a radical scavenger was added, and after 30 min. of stirring under light irradiation (4xLED) MS spectra was recorded.



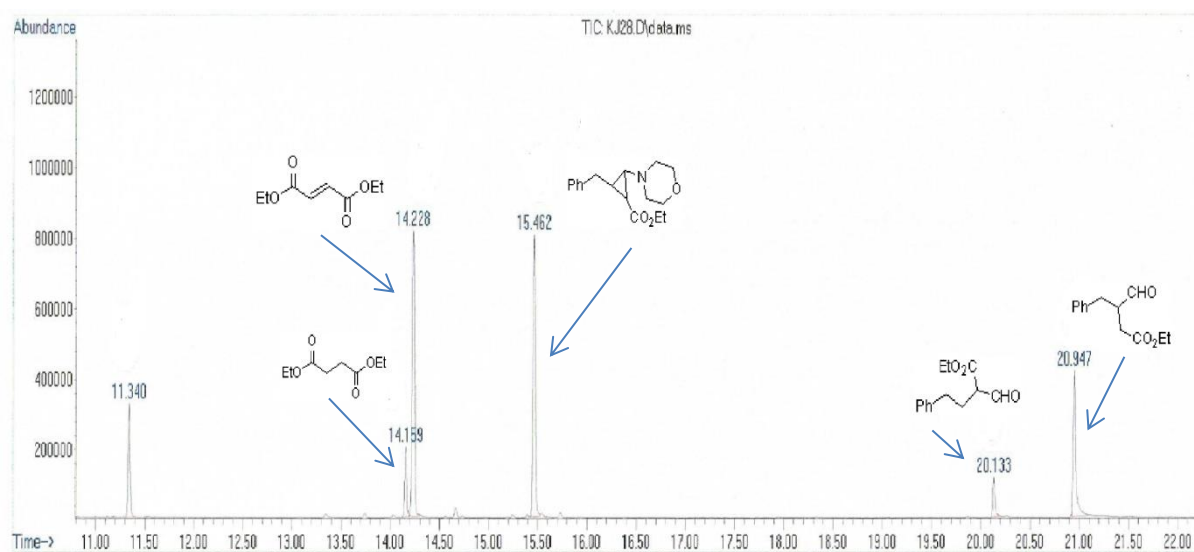
The experiment confirmed the formation of two compounds with TEMPO hence two radical species were present in the reaction mixture.

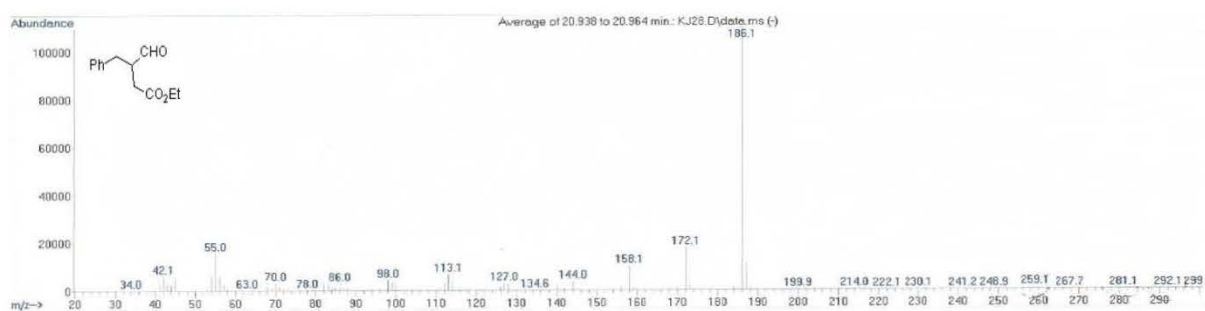
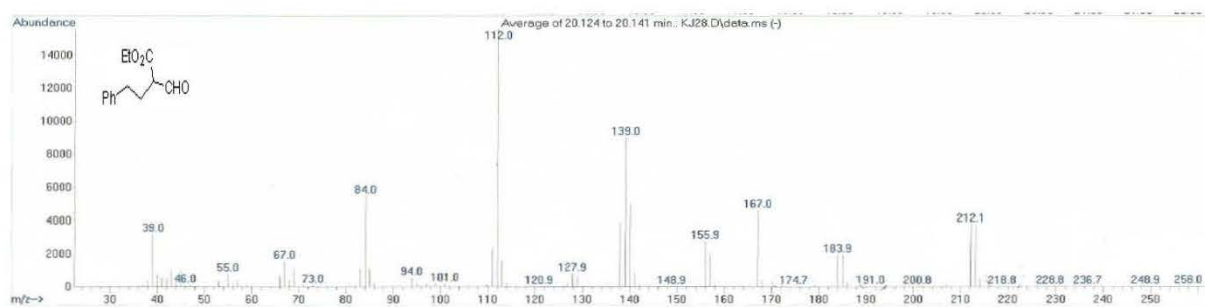
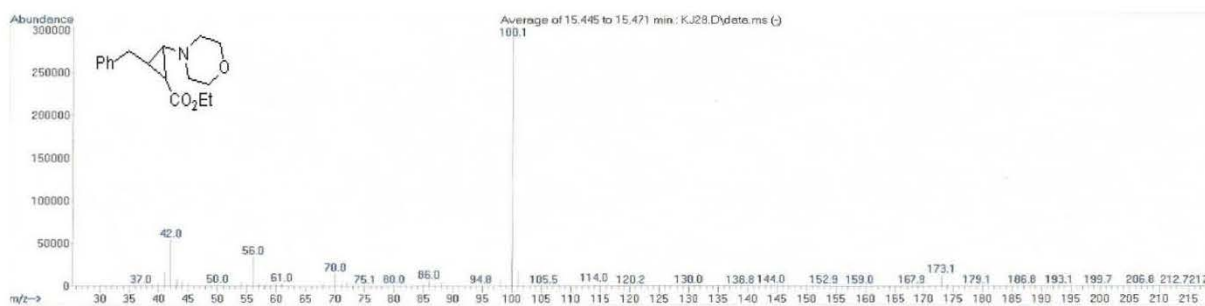
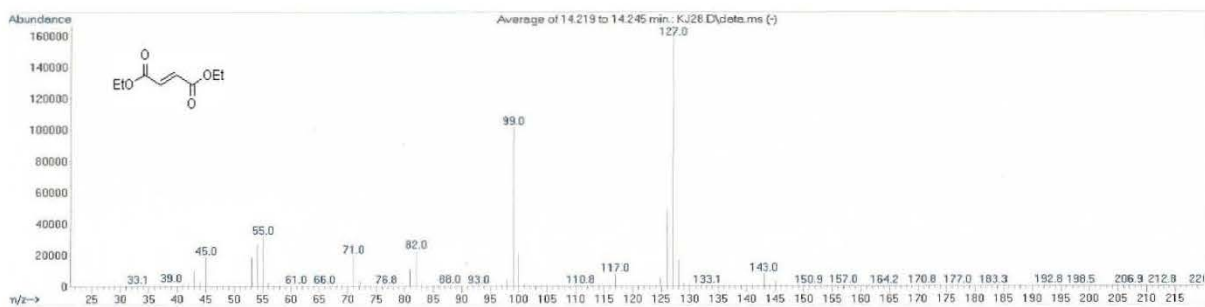
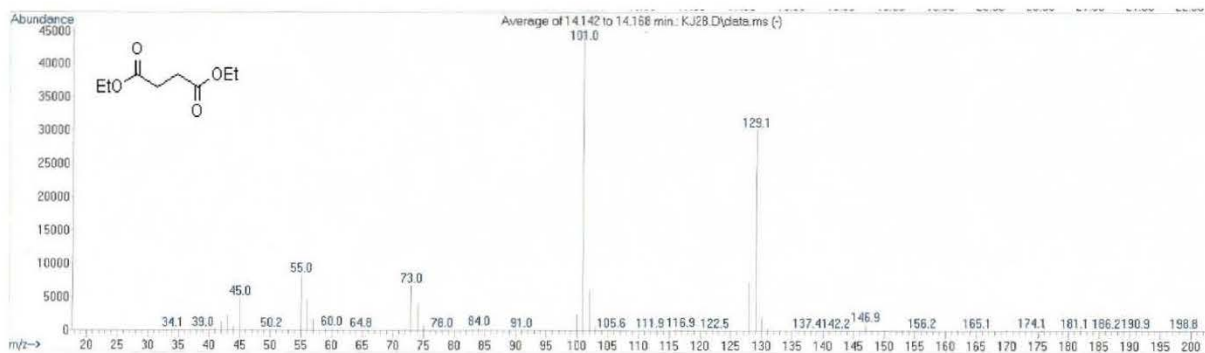
4.6. Verification of cyclopropane-intermediate mechanism

The prepared cyclopropylamine was subjected to the developed reaction conditions. Under light irradiation the expected ring cleavage occurred and the subsequent hydrolysis of the iminium moiety yielded α -functionalized product. GC-MS analysis revealed the presence of two regioisomeric derivatives **34** and **35**, hence the photocatalytic ring opening was not regioselective. As in our model reaction, only one product formed, we postulate that the described α -alkylation proceeds mainly via the radical pathway but to some extent cyclopropanation followed by ring opening may also operate.



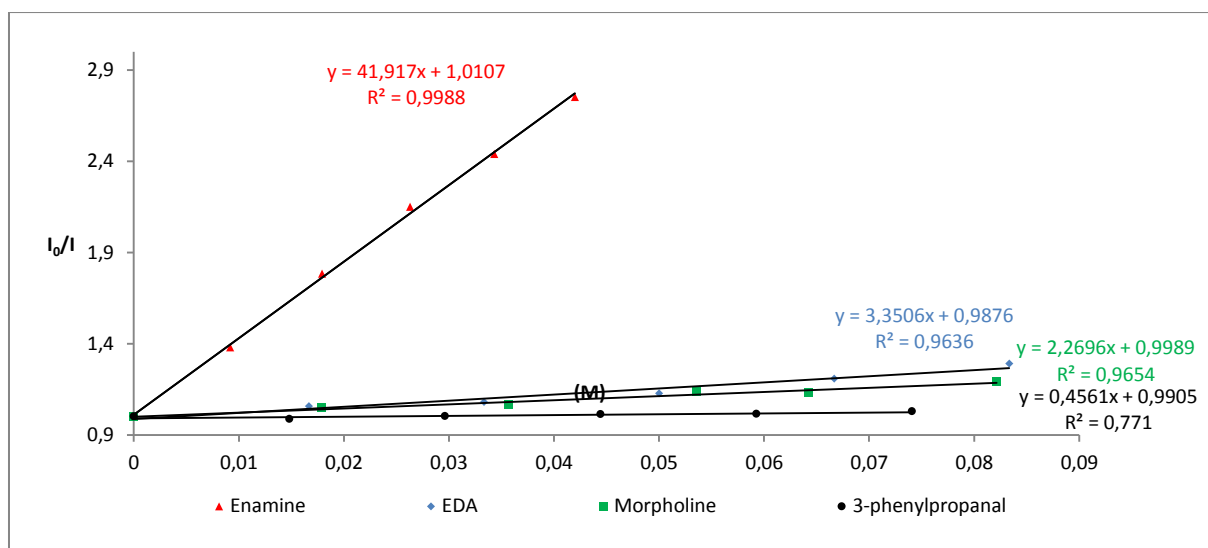
Reaction conditions: Cyclopropylamine (1 equiv., 1 mmol), $\text{Ru}(\text{bpy})_3\text{Cl}_2$ (2 mol%), DMSO (9 mL) and buffer pH=4 (1 mL) was stirring under light irradiation (4xLED) for 5 h and GC-MS spectra was recorded.



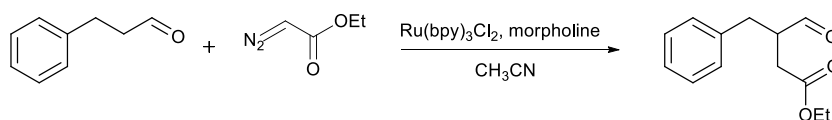


4.7. Stern–Volmer quenching experiment

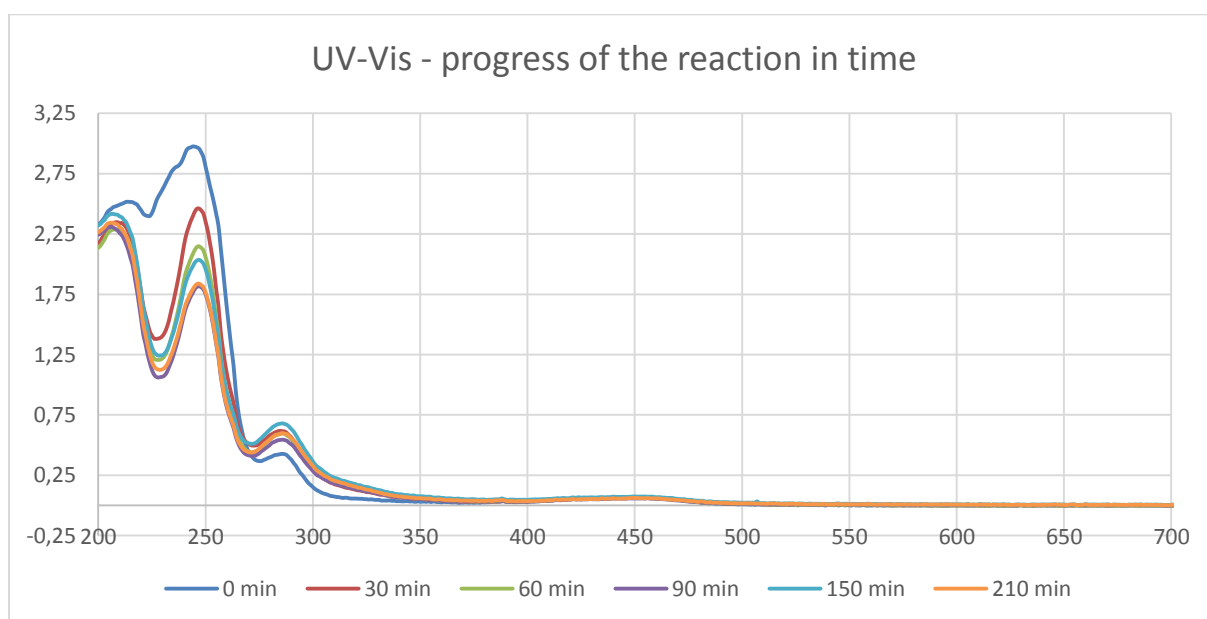
Stern-Volmer analyses for each of the reaction components clearly showed that for enamine **B** (see proposed mechanism) very strong, in comparison with EDA and morpholine, quenching of $[\text{Ru}^*(\text{bpy})_3\text{Cl}_2]^{3+}$ occurred thus confirming the proposed radical **C** being a reactive intermediate. In accord with the proposed mechanism aldehyde resulted in minute Stern-Volmer quenching. For 3-phenylpropanal, EDA, enamine **33**, morpholine and $\text{Ru}(\text{bpy})_3\text{Cl}_2$ samples were prepared by adding solutions of substrates to $\text{Ru}(\text{bpy})_3\text{Cl}_2$ solution in DMSO (total volume 2 mL) and degassed with Ar. The concentration of $\text{Ru}(\text{bpy})_3\text{Cl}_2$ in DMSO was $5.7 \cdot 10^{-4}$ M.



4.8. UV-Vis spectroscopy studies

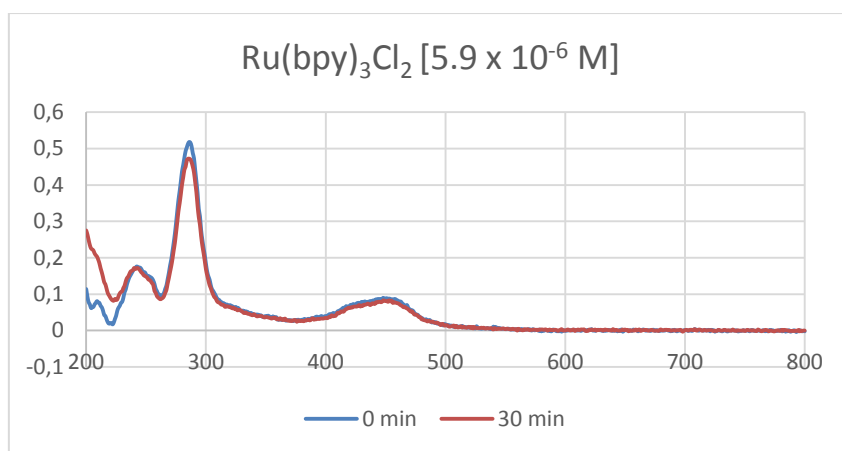
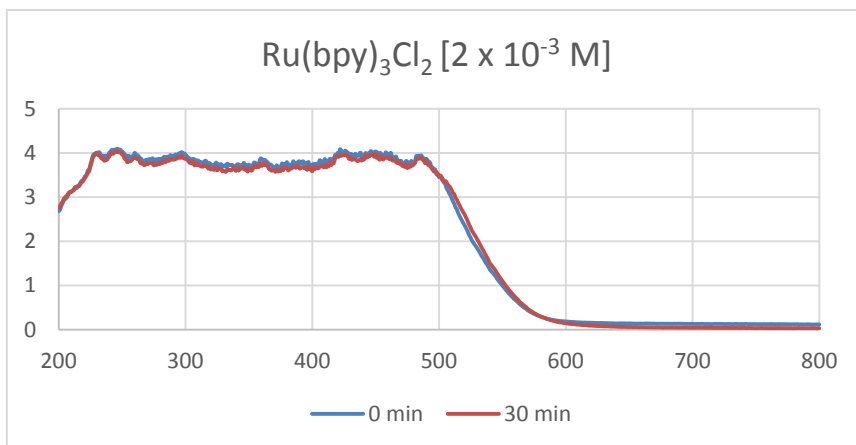


Reaction conditions: aldehyde (1 equiv., 0,5 mmol), morpholine (0.4 equiv., 0.2 mmol), EDA (1 equiv., 0,5 mmol), Ru(bpy)₃Cl₂ (2 mol%), CH₃CN. To support the proposed mechanism the progress of the reaction was also monitored by UV-Vis. After 0, 30, 90, 150 and 210 min. of stirring under light irradiation (4xLED) the sample of 15 μ l was taken from the reaction and it was diluted to 5,015 ml MeCN and UV-Vis spectra was recorded.

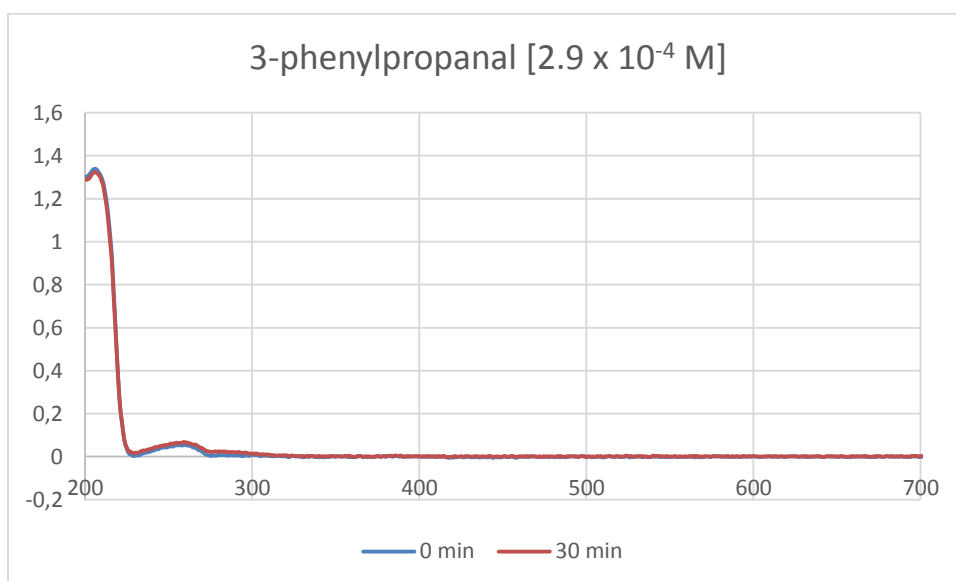


The control UV-Vis experiments of substrates and background's reactions were also performed:

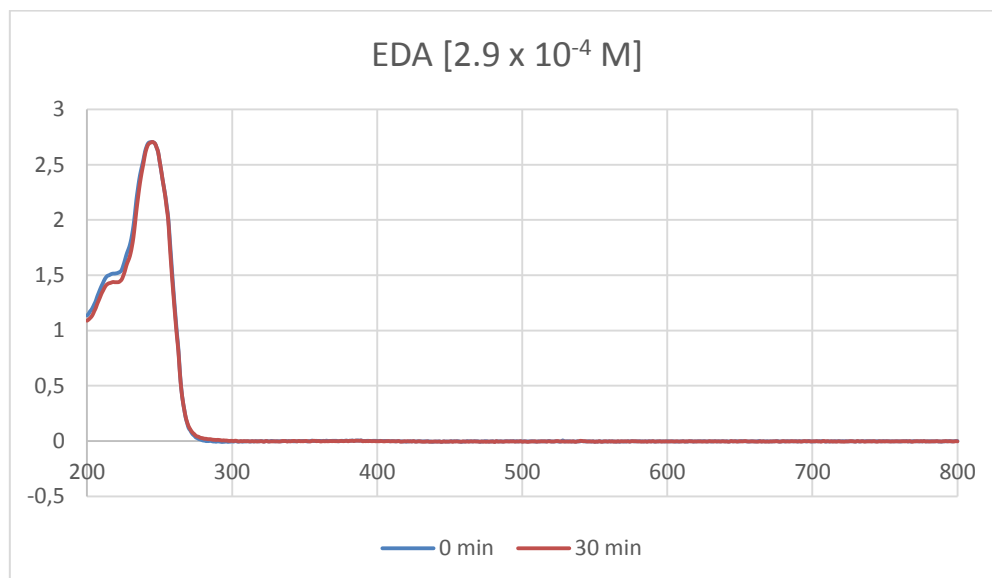
- 1) Ru(bpy)₃Cl₂ in CH₃CN after 0 min. of stirring under light irradiation (4xLED) and 30 min. of stirring under light irradiation (4xLED):



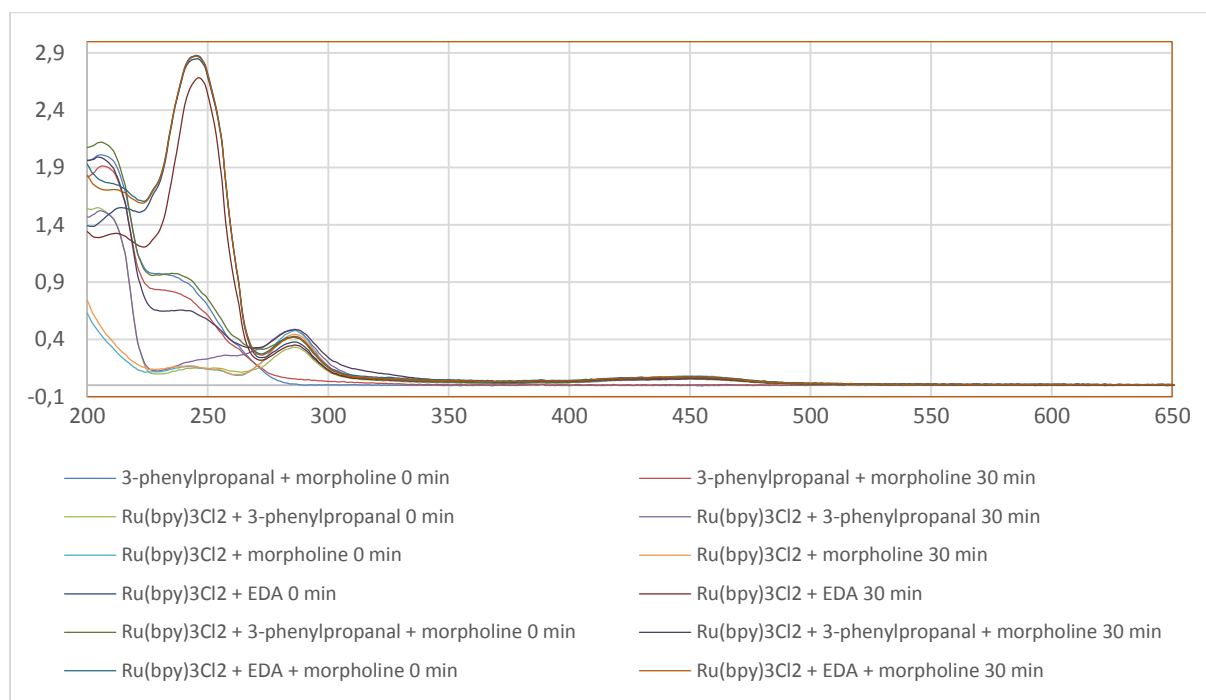
- 2) 3-phenylpropanal in CH_3CN after 0 min. of stirring under light irradiation (4xLED) and 30 min. of stirring under light irradiation (4xLED):



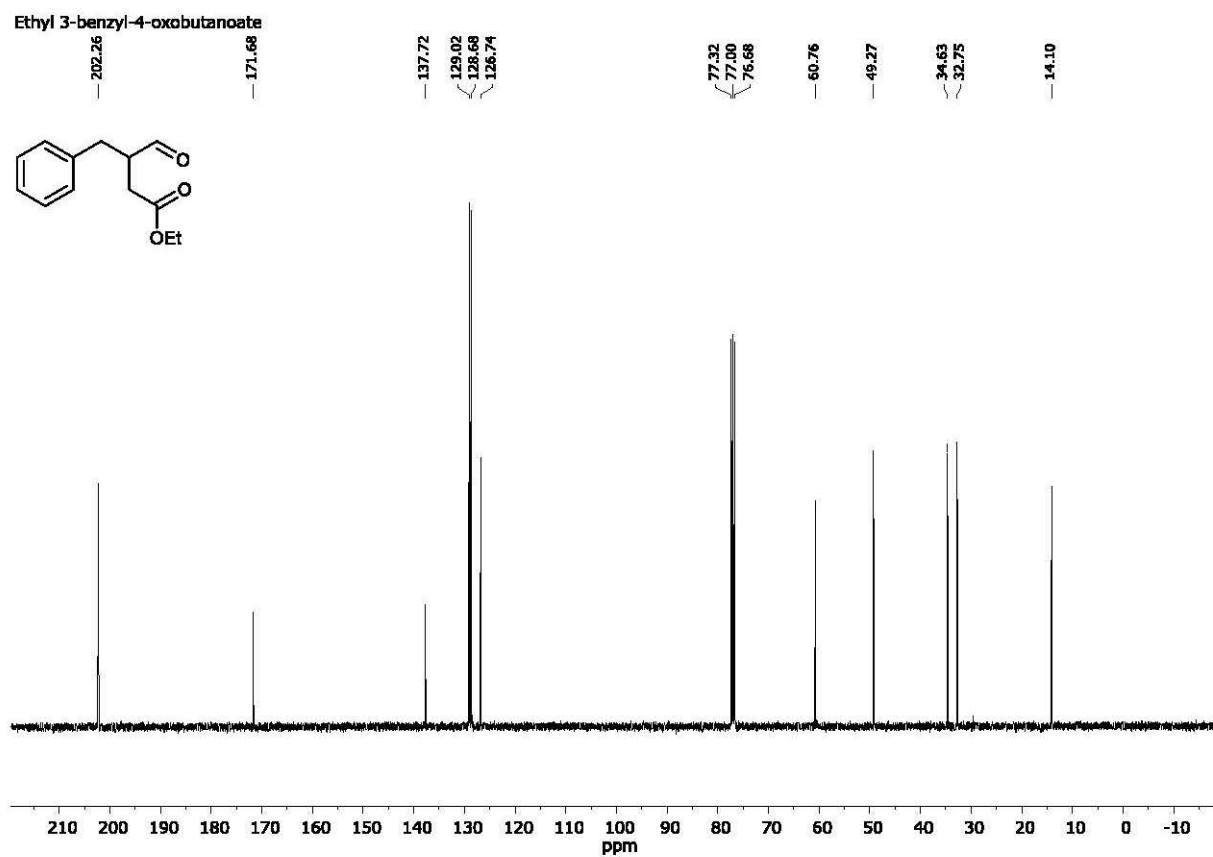
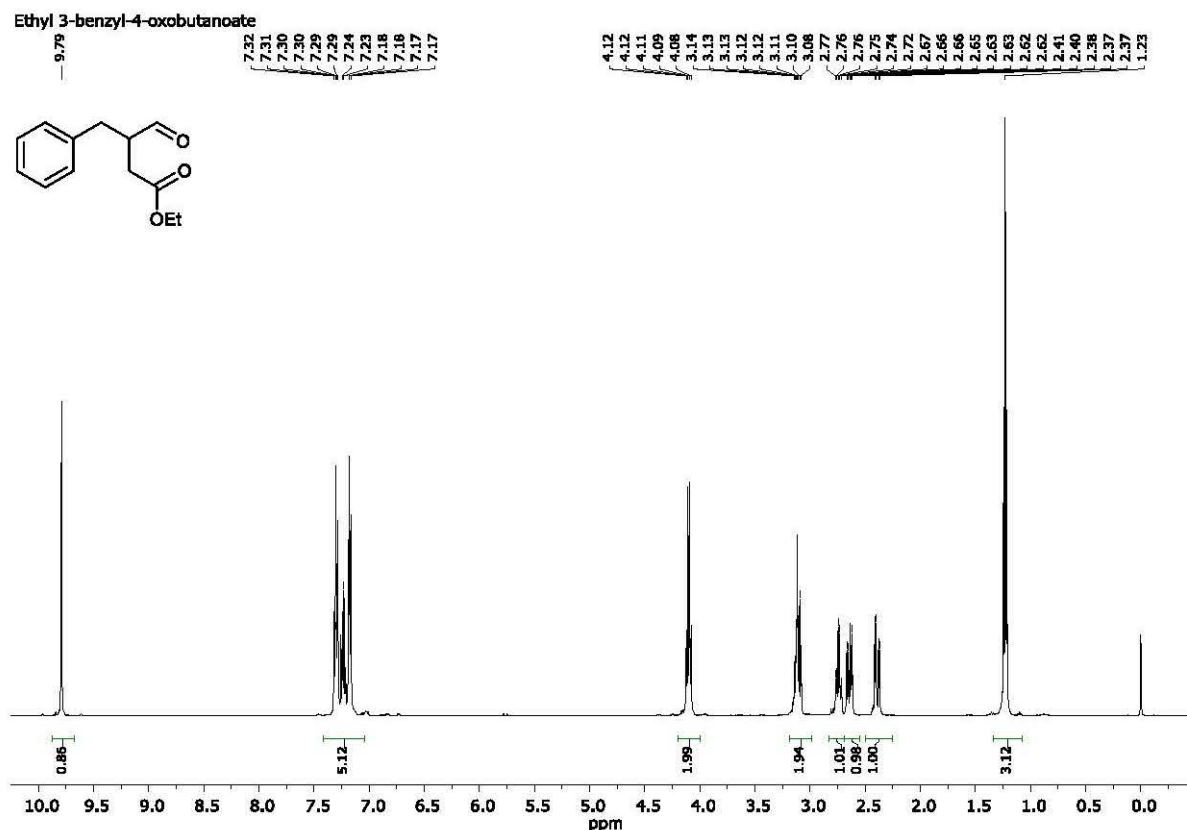
- 3) EDA in CH₃CN after 0 min. of stirring under light irradiation (4xLED) and 30 min. of stirring under light irradiation (4xLED):



- 4) Background's reaction in CH₃CN after 0 min. of stirring under light irradiation (4xLED) and 30 min. of stirring under light irradiation (4xLED):

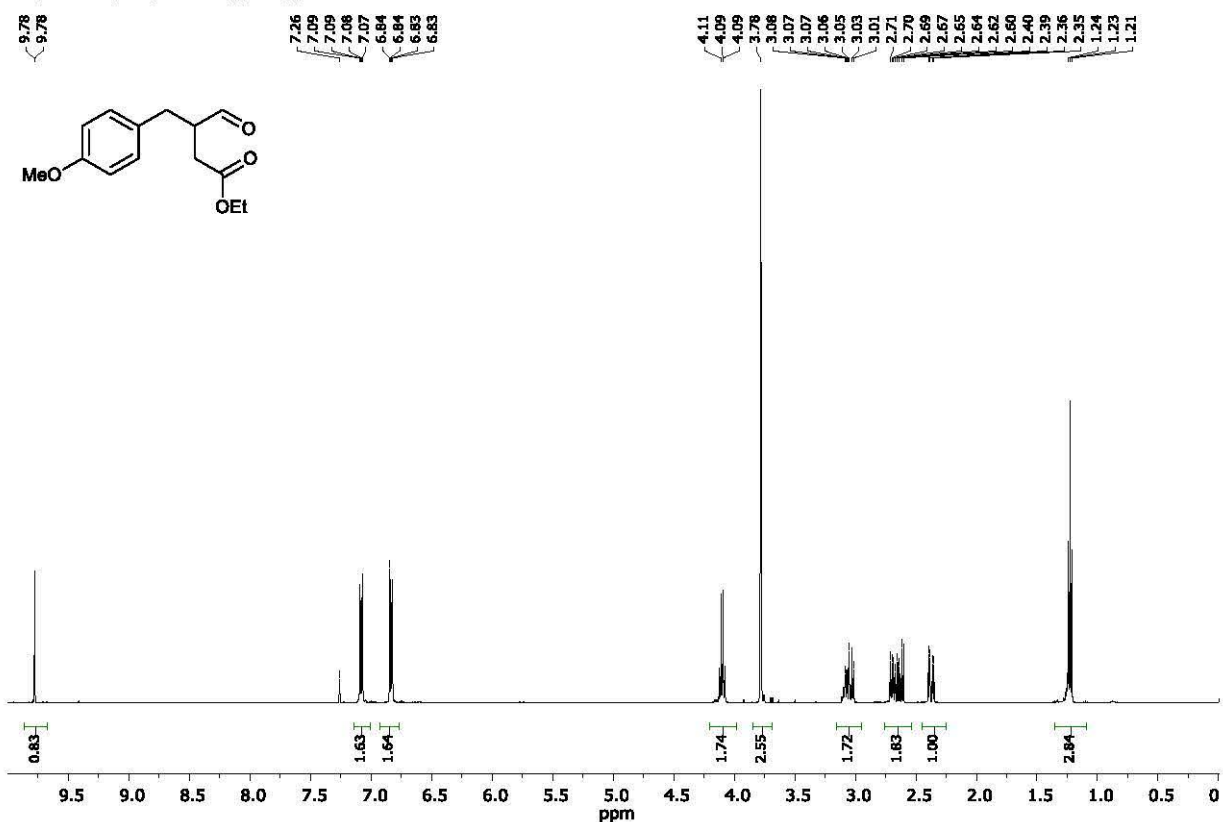


5. ^1H and ^{13}C NMR spectra
 a) Ethyl 3-benzyl-4-oxobutanoate (10)

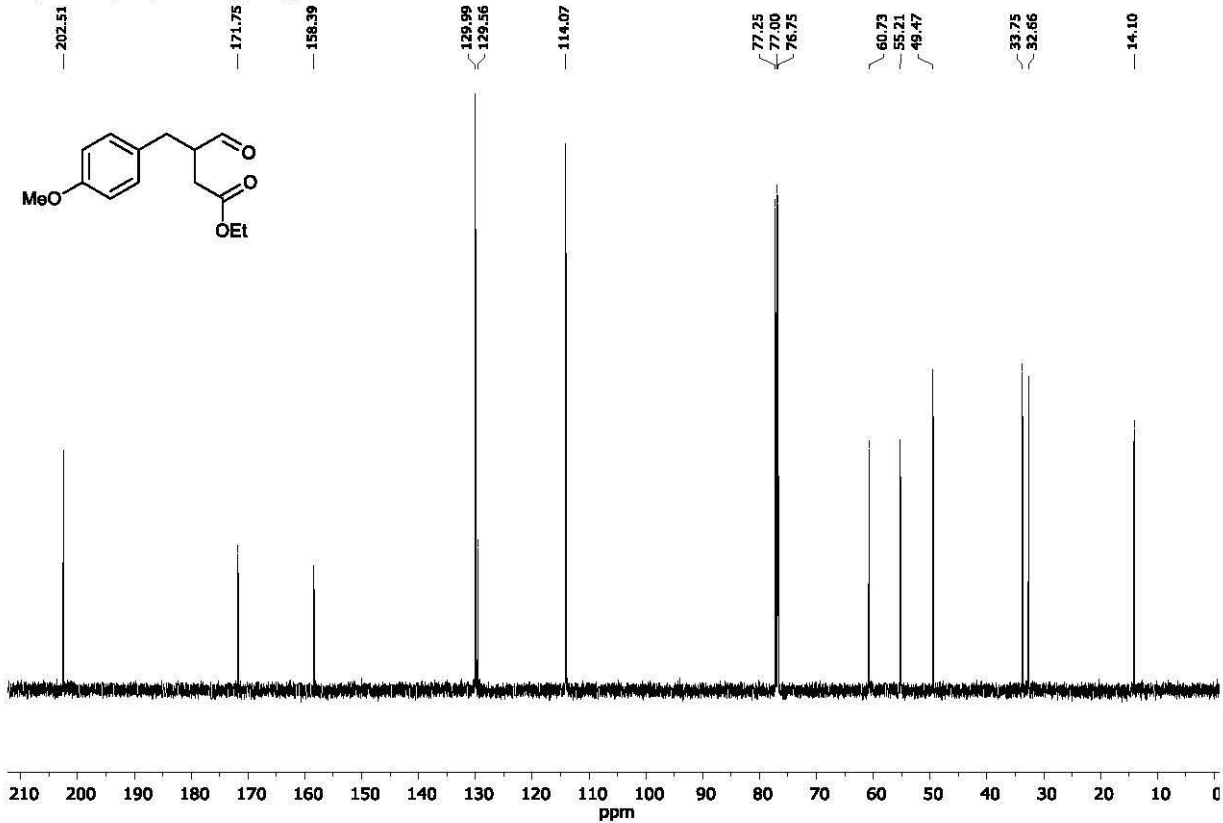


b) Ethyl 3-formyl-4-(4-methoxyphenyl)butanoate (22)

Ethyl 3-formyl-4-(4-methoxyphenyl)butanoate

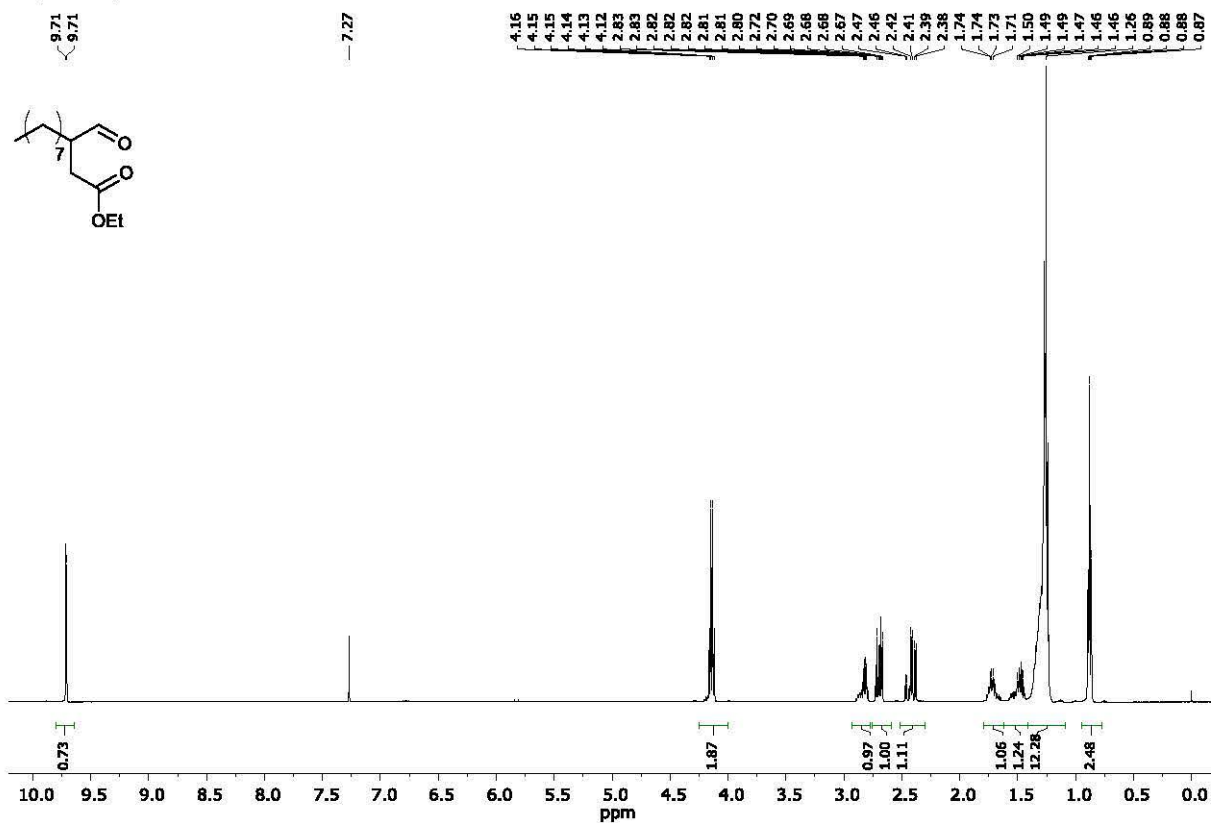


Ethyl 3-formyl-4-(4-methoxyphenyl)butanoate

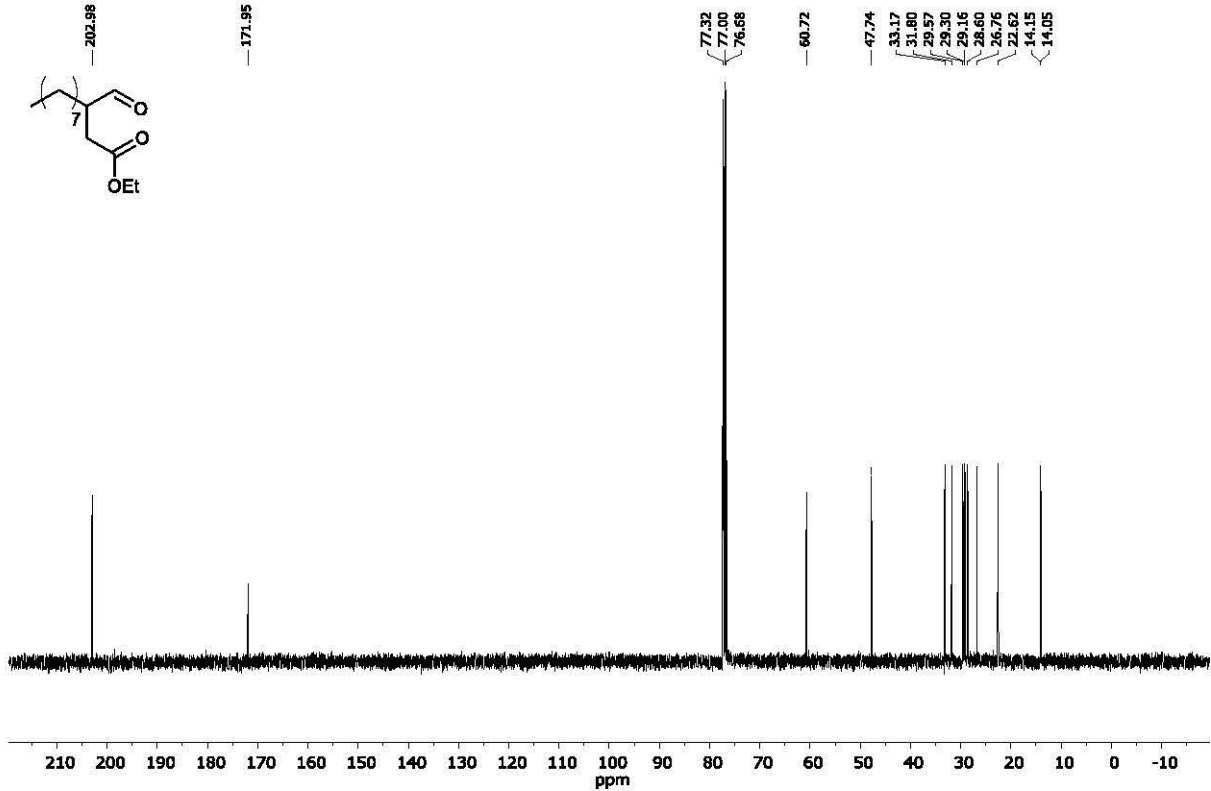


c) Ethyl 3-formylundecanoate (23)

Ethyl 3-formylundecanoate

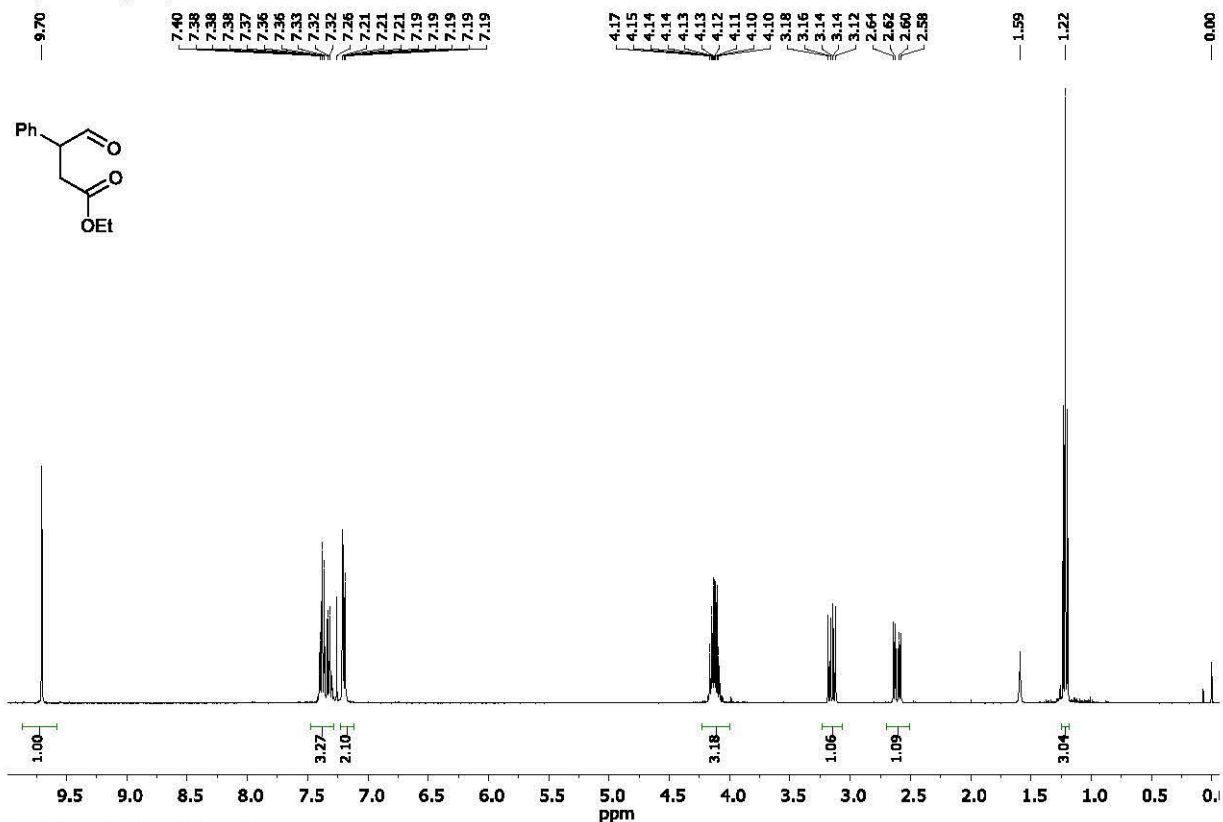


Ethyl 3-formylundecanoate

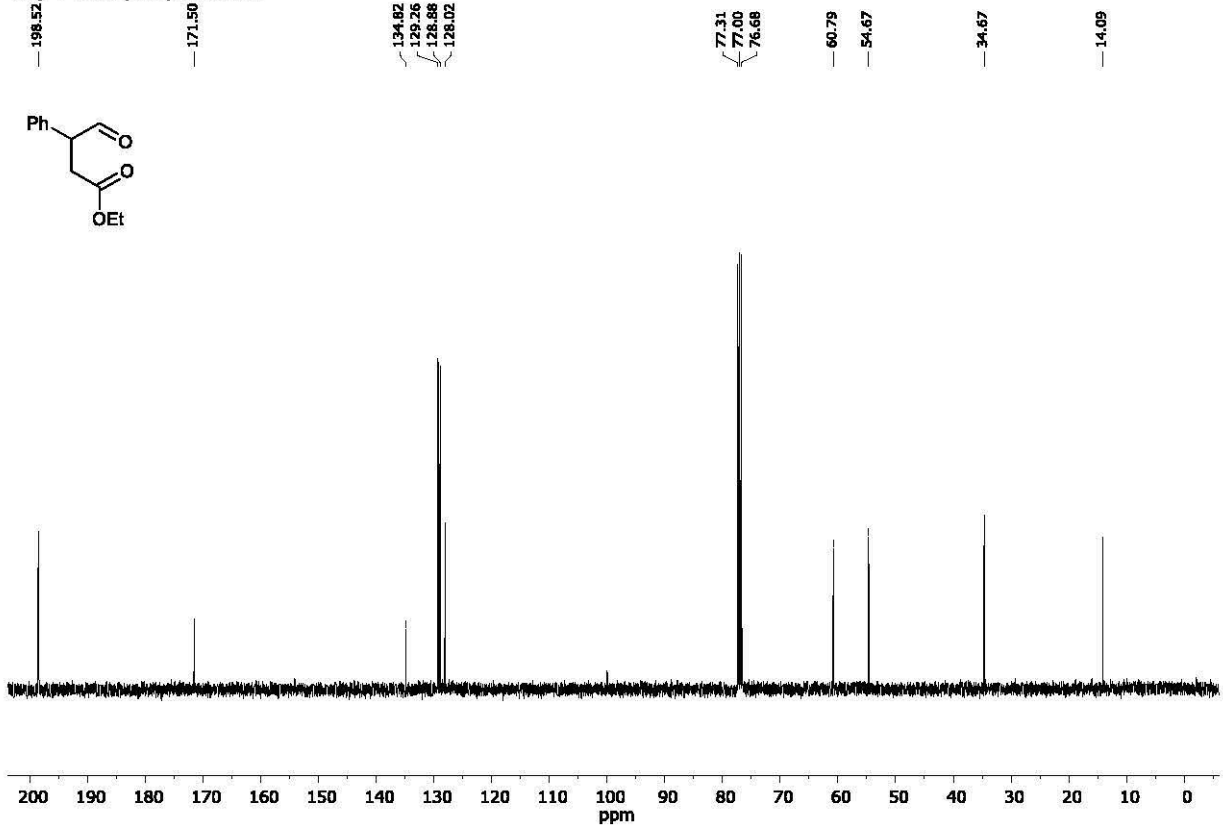


d) Ethyl 4-oxo-3-phenylbutanoate (24)

ethyl 4-oxo-3-phenylbutanoate

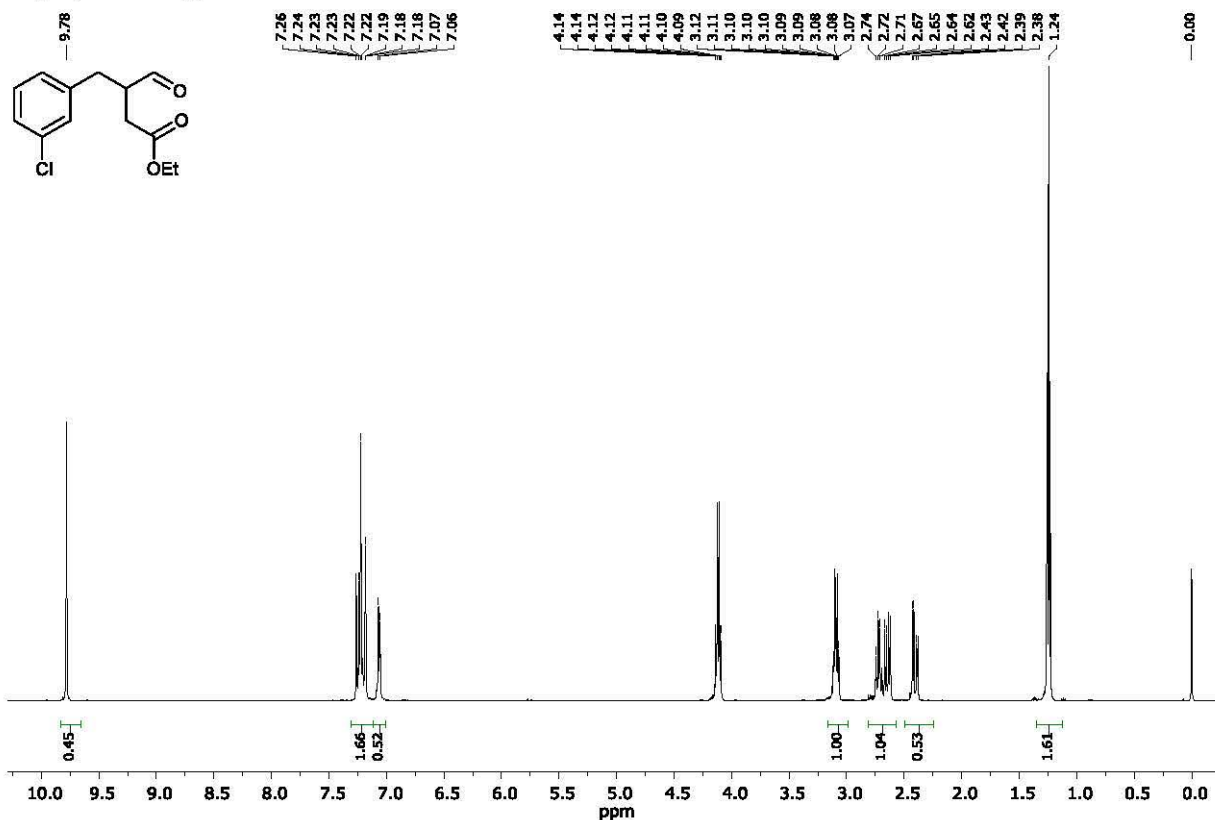


ethyl 4-oxo-3-phenylbutanoate

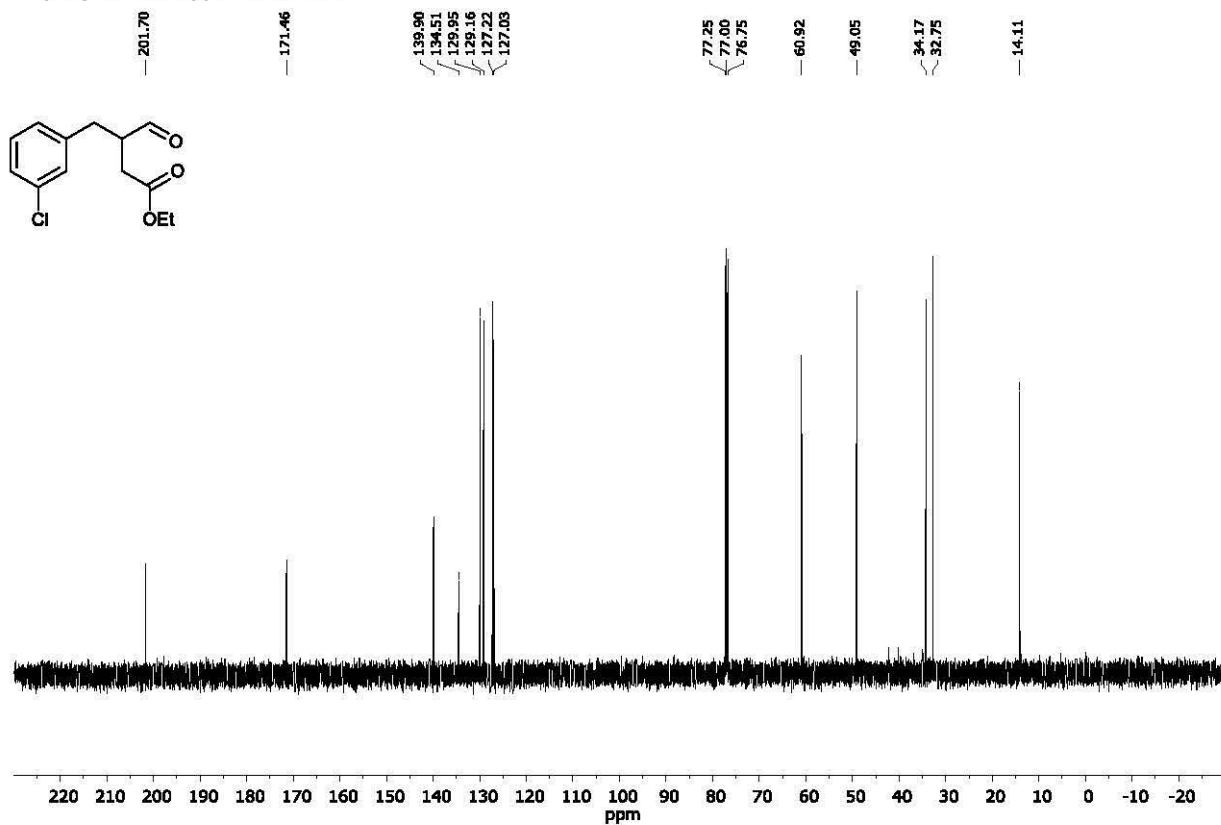


e) Ethyl 3-(3-chlorobenzyl)-4-oxobutanoate (25)

Ethyl 3-(3-chlorobenzyl)-4-oxobutanoate

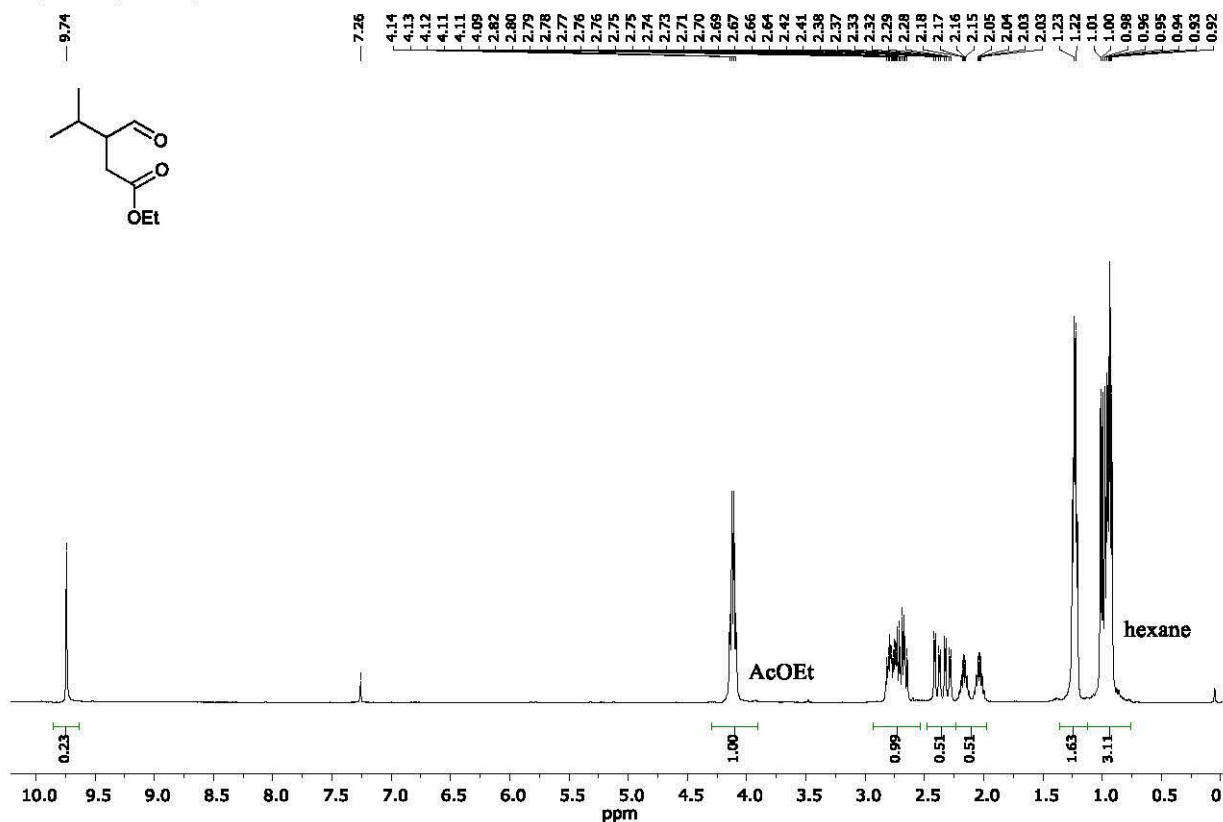


Ethyl 3-(3-chlorobenzyl)-4-oxobutanoate

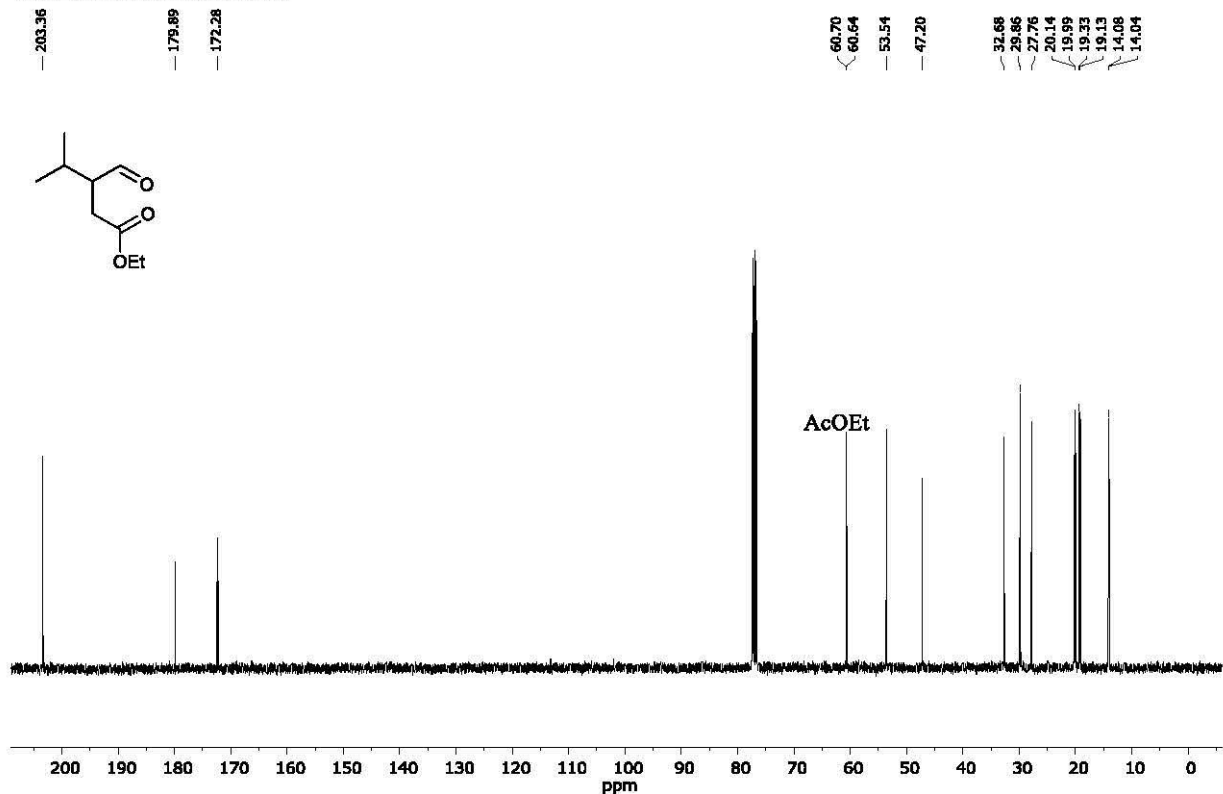


f) Ethyl 2-formyl-3-methylbutanoate (26)

Ethyl 2-formyl-3-methylbutanoate



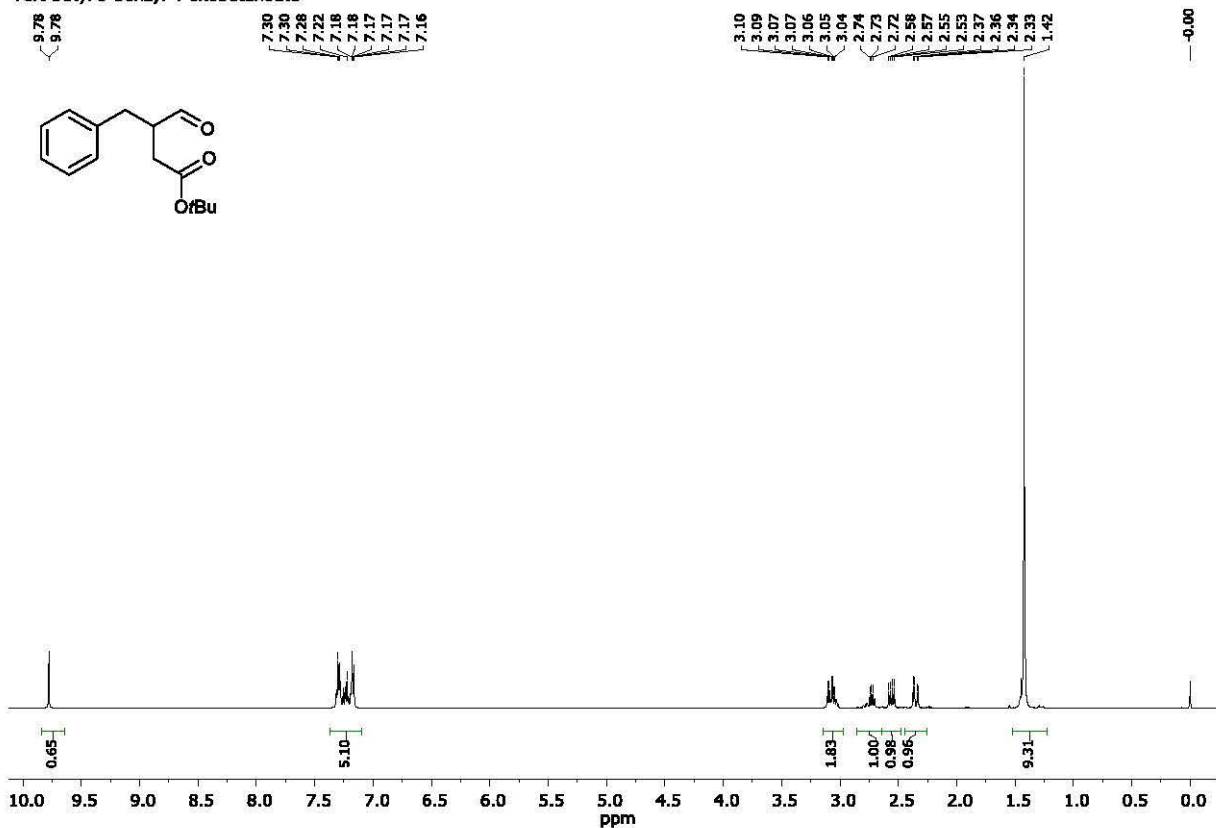
Ethyl 2-formyl-3-methylbutanoate



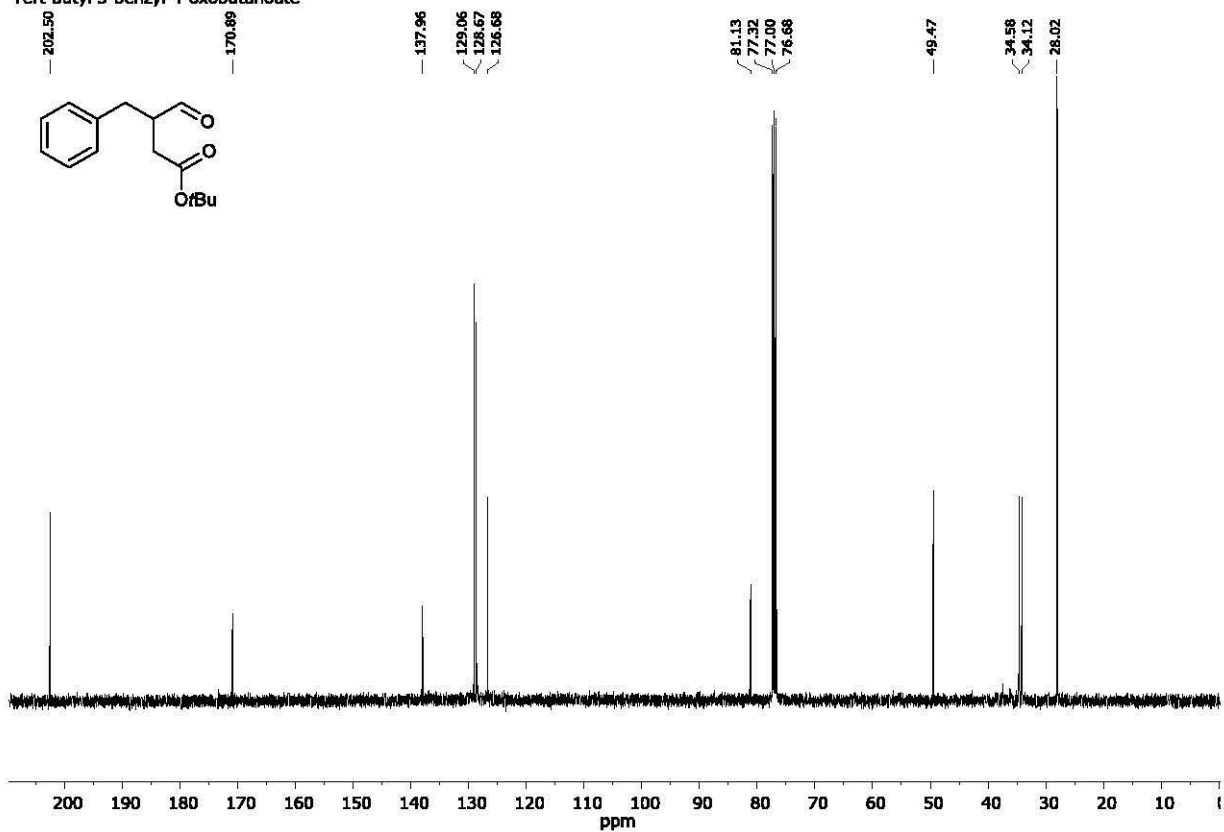
As the compound is very volatile signals corresponding to the solvents are present in both spectra

g) *tert*-Butyl 3-benzyl-4-oxobutanoate (29)

Tert-butyl 3-benzyl-4-oxobutanoate

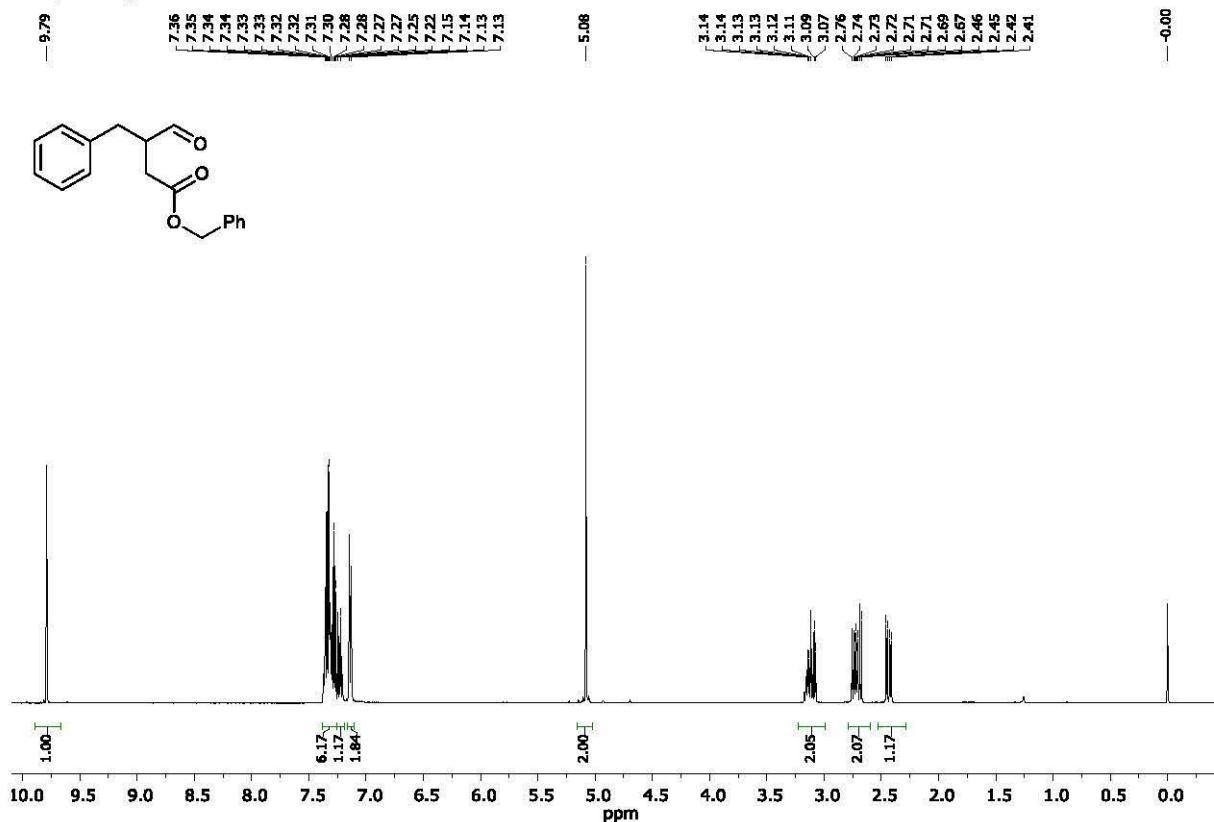


Tert-butyl 3-benzyl-4-oxobutanoate

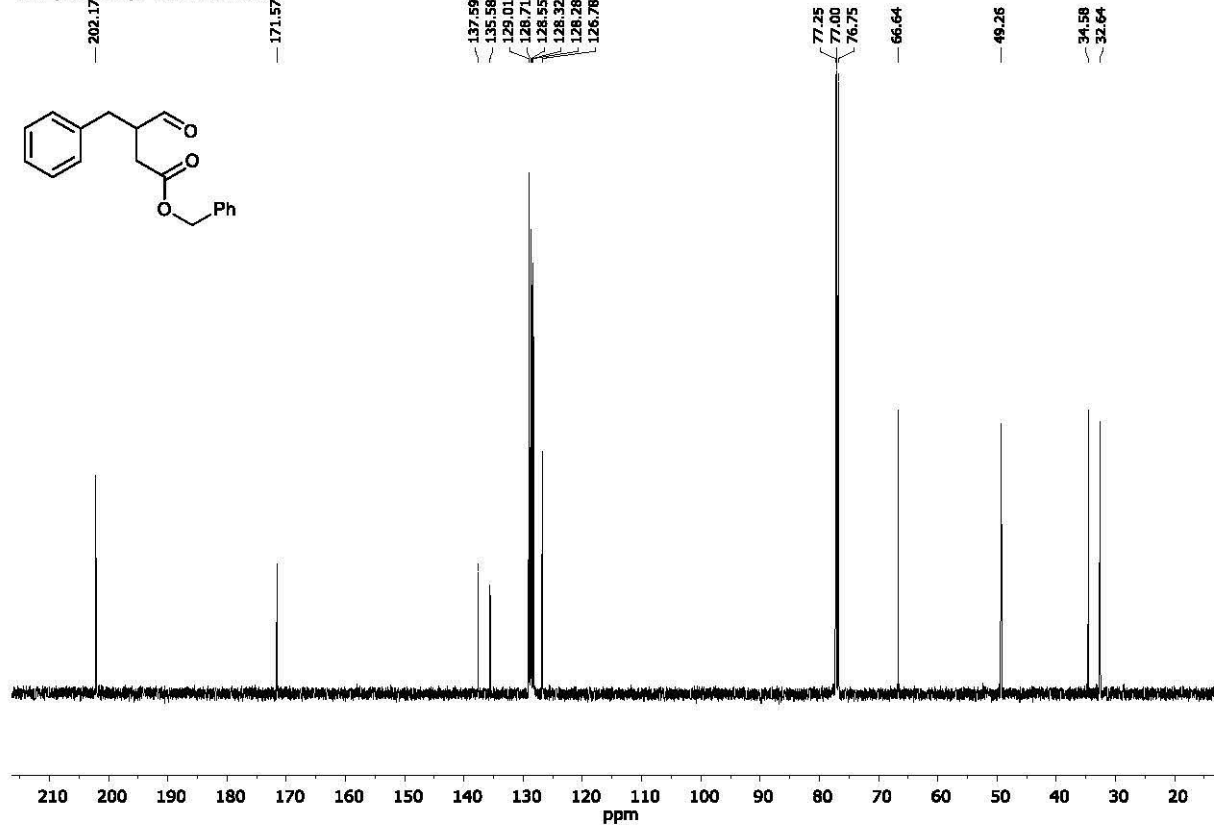


h) Benzyl 3-benzyl-4-oxobutanoate (30)

Benzyl 3-benzyl-4-oxobutanoate

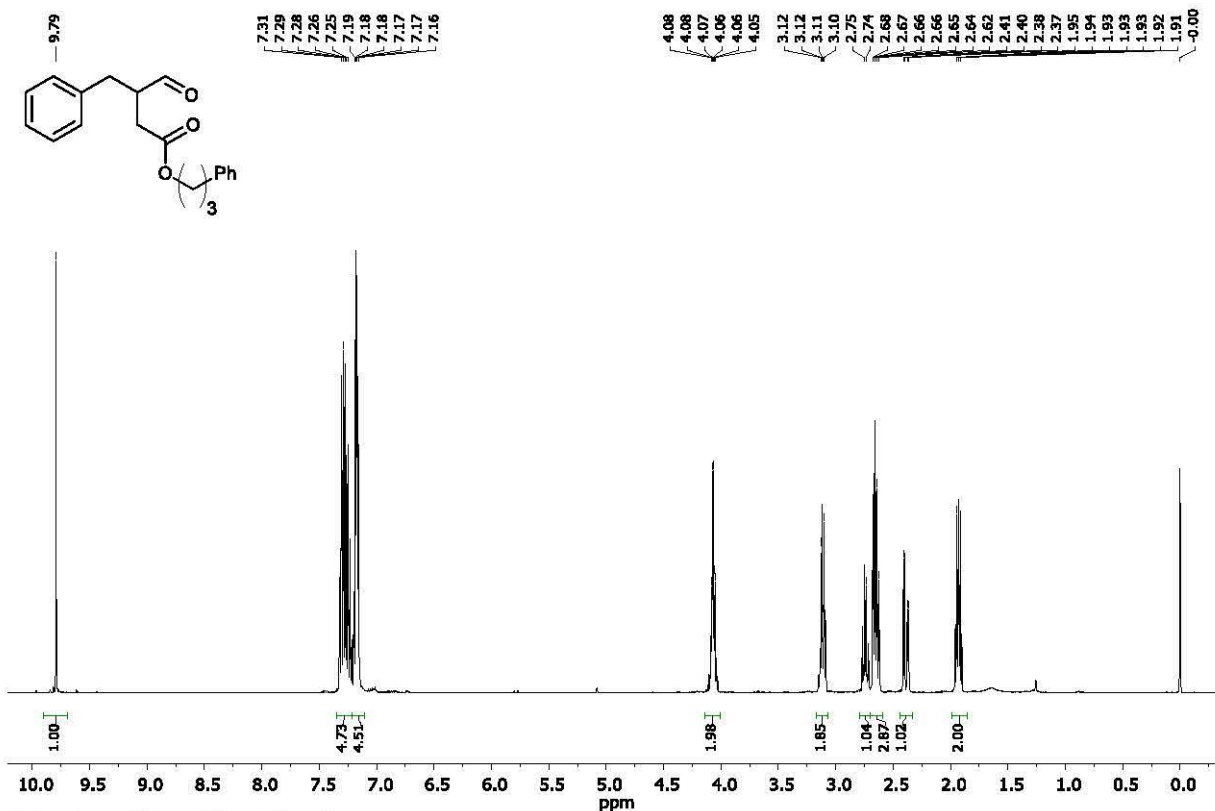


Benzyl 3-benzyl-4-oxobutanoate

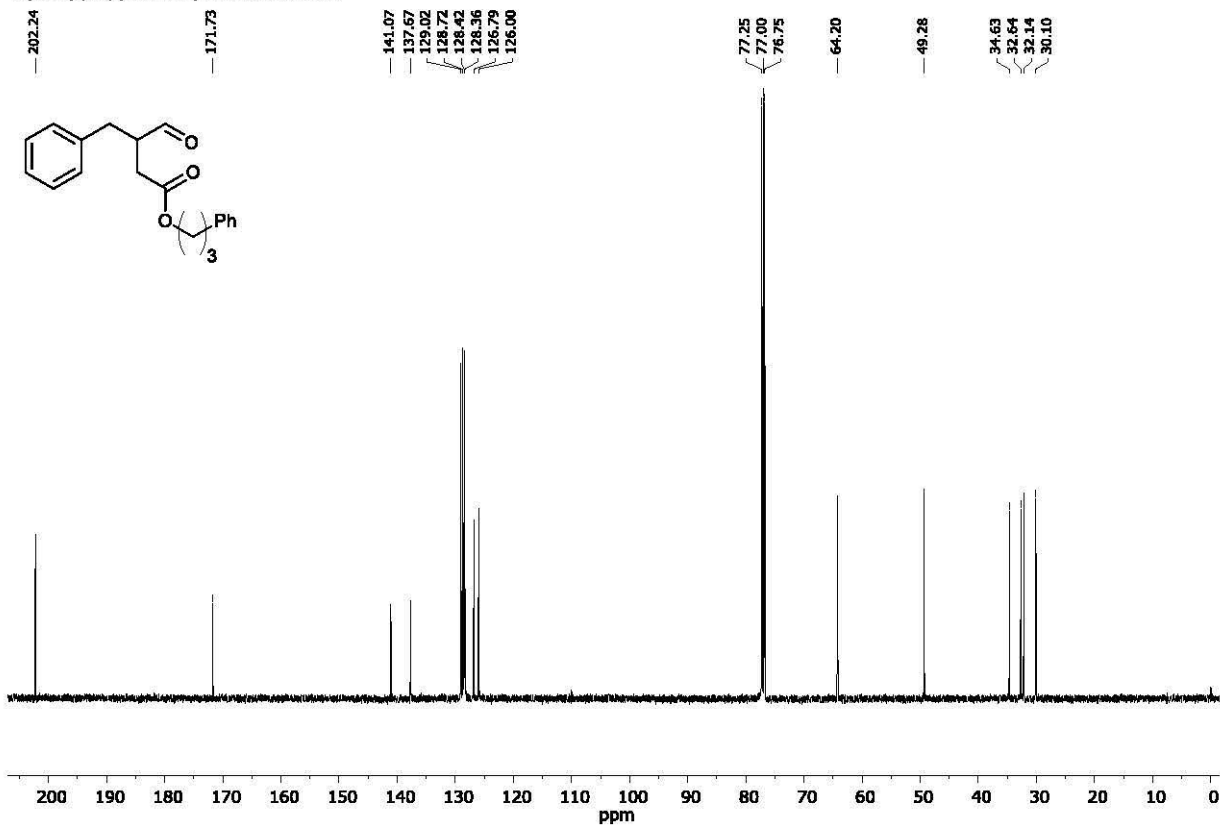


i) 3-Phenylpropyl 3-benzyl-4-oxobutanoate (31)

3-phenylpropyl 3-benzyl-4-oxobutanoate

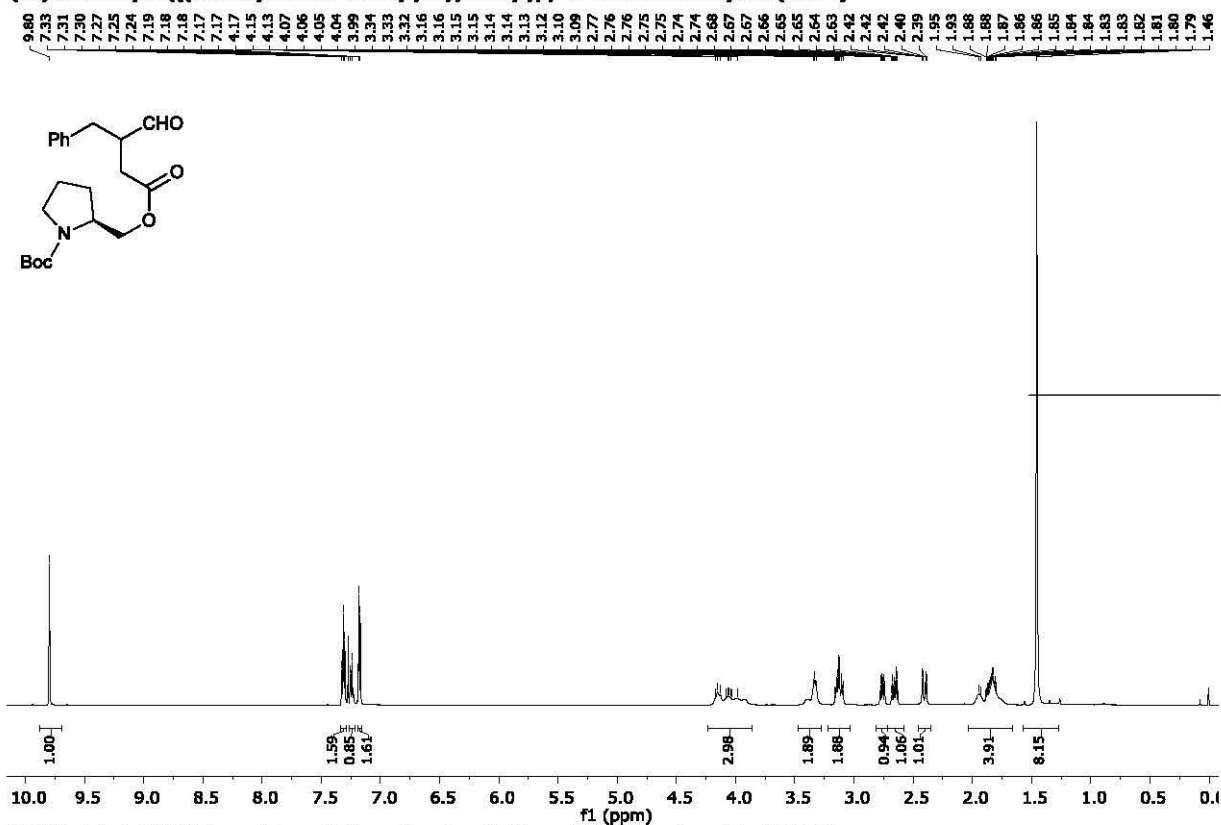


3-phenylpropyl 3-benzyl-4-oxobutanoate

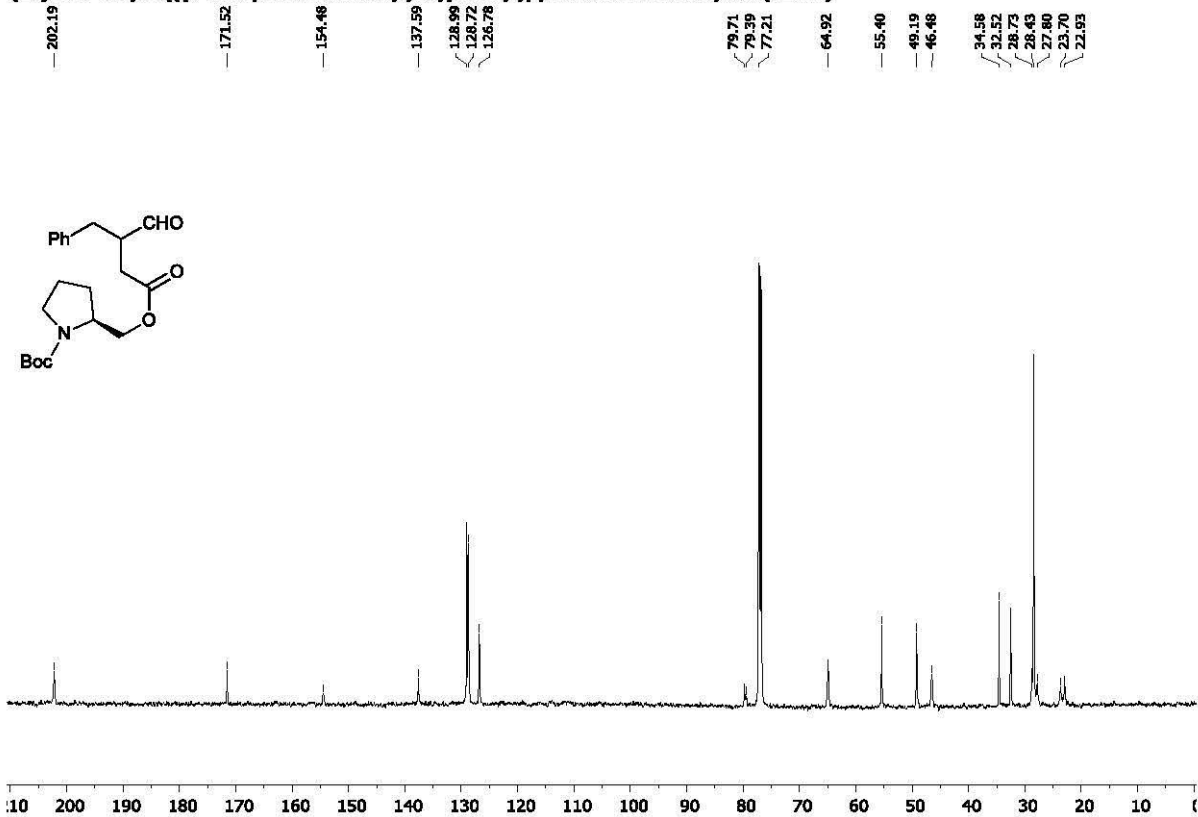


j) (2S)-tert-Butyl2-(((3-benzyl-4-oxobutanoyl)oxy)methyl)pyrrolidine-1-carboxylate (32)

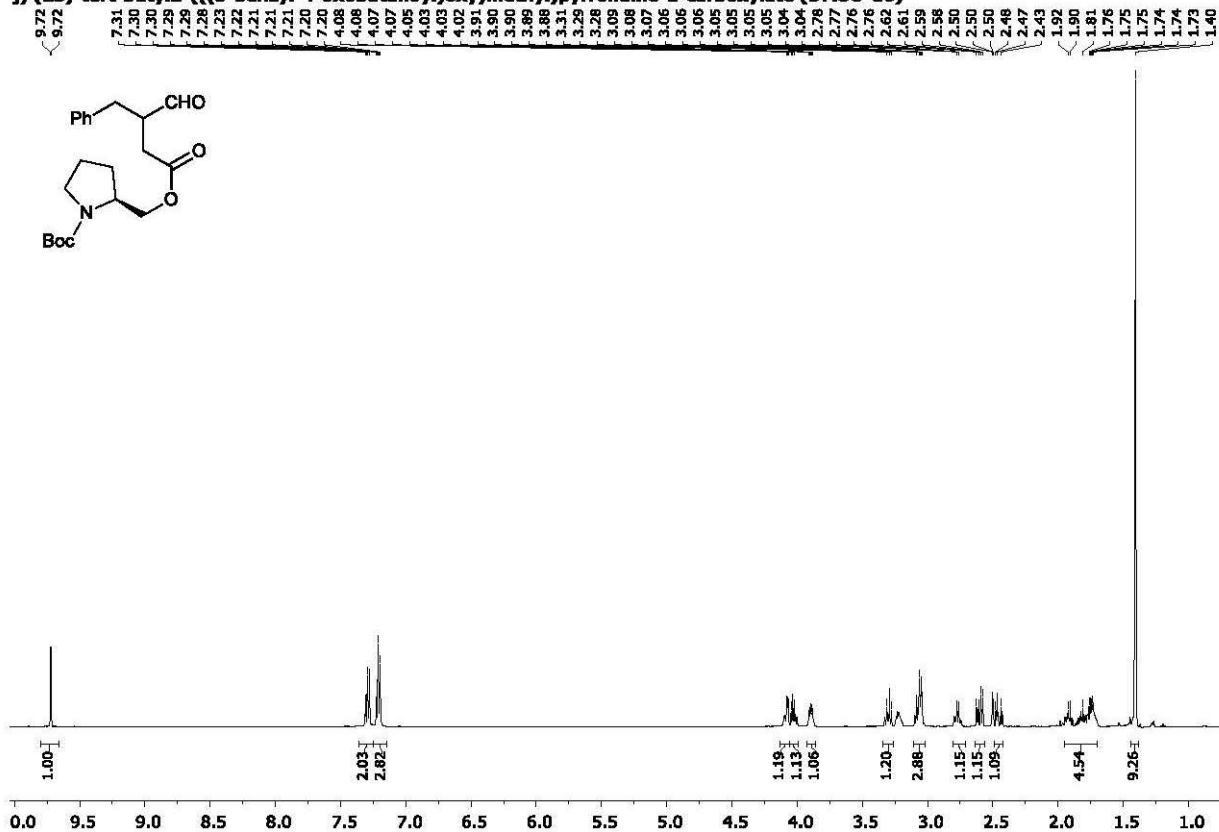
(2S)-tert-butyl2-(((3-benzyl-4-oxobutanoyl)oxy)methyl)pyrrolidine-1-carboxylate (CDCl₃)



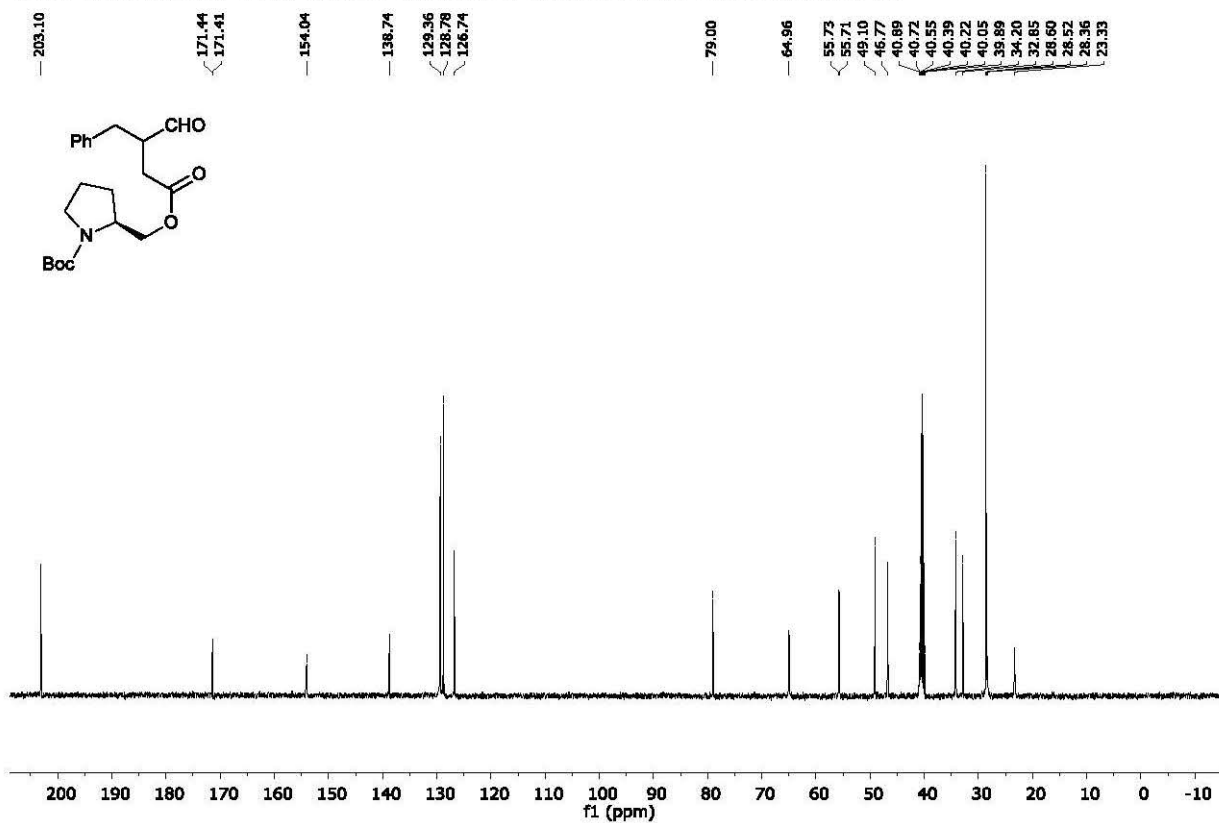
(2S)-tert-butyl2-(((3-benzyl-4-oxobutanoyl)oxy)methyl)pyrrolidine-1-carboxylate (CDCl₃)



j) (2S)-tert-butyl2-(((3-benzyl-4-oxobutanoyl)oxy)methyl)pyrrolidine-1-carboxylate (DMSO-d6)

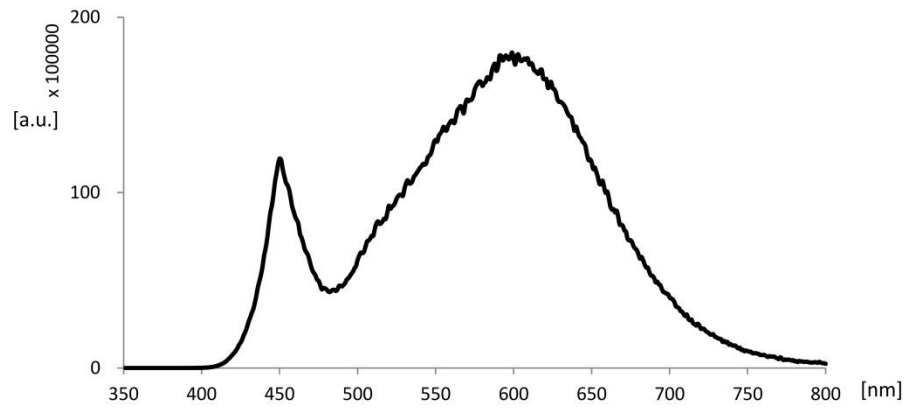


j) (2S)-tert-butyl2-(((3-benzyl-4-oxobutanoyl)oxy)methyl)pyrrolidine-1-carboxylate (DMSO-d6)

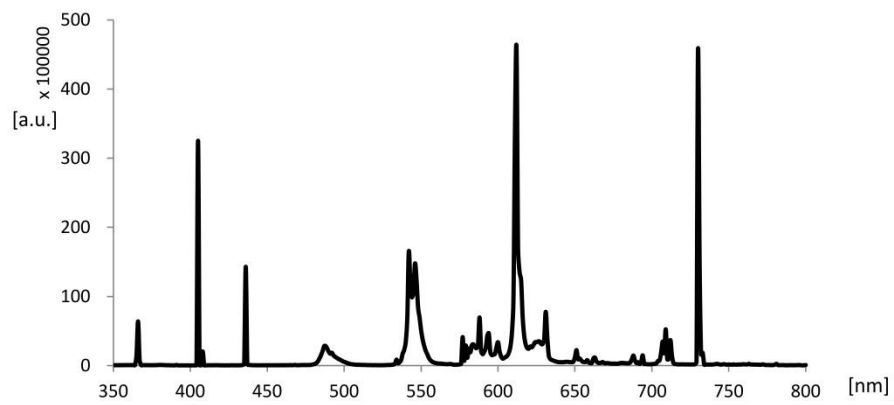


6. Emission spectra measurements:

a) 'household' LED



b) 'household' CFL bulb



7. Photoreactor



Porphyrins as Photoredox Catalysts: Experimental and Theoretical Studies

Katarzyna Rybicka-Jasińska,[†] Wenqian Shan,[‡] Katarzyna Zawada,^{*,§} Karl M. Kadish,^{*,‡} and Dorota Gryko^{*,†}

[†]Institute of Organic Chemistry, Polish Academy of Sciences, Kasprzaka 44/52, 01-224 Warsaw, Poland

[‡]University of Houston, Department of Chemistry, Houston, Texas 77204-5003, United States

[§]Medical University of Warsaw, Faculty of Pharmacy with the Laboratory Medicine Division, Department of Physical Chemistry, Banacha 1, 02-097 Warsaw, Poland

S Supporting Information

ABSTRACT: Metalloporphyrins not only are vital in biological systems but also are valuable catalysts in organic synthesis. On the other hand, catalytic properties of free base porphyrins have been less explored. They are mostly known as efficient photosensitizers for the generation of singlet oxygen via photoinduced energy transfer processes, but under light irradiation, they can also participate in electron transfer processes. Indeed, we have found that free base tetraphenylporphyrin (H₂TPP) is an efficient photoredox catalyst for the reaction of aldehydes with diazo compounds leading to α -alkylated derivatives. The performance of a porphyrin catalyst can be optimized by tailoring various substituents at the periphery of the macrocycle at both the β and *meso* positions. This allows for the fine tuning of their optical and electrochemical properties and hence their catalytic activity.



Supporting Information (SI)
for
**Porphyrins as Photoredox Catalysts - Experimental and
Theoretical studies**

Katarzyna Rybicka-Jasińska,¹ Wenqian Shan,² Katarzyna Zawada,^{3*} Karl Kadish,^{2*} Dorota Gryko^{1*}

¹ *Institute of Organic Chemistry Polish Academy of Sciences, Kasprzaka 44/52, 01-224 Warsaw, Poland*

² *University of Houston, Department of Chemistry, Houston, Texas 77024-5003, USA*

³ *Medical University of Warsaw, Faculty of Pharmacy with the Laboratory Medicine Division, Department of Physical Chemistry, Banacha 1, 02-097 Warsaw, Poland*

Table of Contents

1. General information	S4
2. General synthetic procedures	S4
3. Scope and limitations	S5
4. Optimization studies	S11
5. Mechanistic considerations	S15
5.1. Proposed mechanism	S15
5.2. EPR studies	S16
5.3. NMR studies	S24
5.4. Mass spectrometry studies	S27
5.5. Electrochemical studies	S29
5.7. Stern–Volmer quenching experiments	S35
5.6. UV-Vis measurement	S40
6. ¹ H and ¹³ C NMR spectra	S43
a) Ethyl 3-benzyl-4-oxobutanoate (3)	S43
b) Ethyl 3-formyl-4-phenylpentanoate (14)	S44
c) Ethyl 3-formyl-4-(4-methoxyphenyl)butanoate (15)	S45
d) Ethyl 3-(3-chlorobenzyl)-4-oxobutanoate (16)	S46
e) Ethyl 4-oxo-3-phenylbutanoate (17)	S47
f) Ethyl 3-formyl-4-methylpentanoate (20)	S48
g) Ethyl 3-formylundecanoate (21)	S49
h) <i>tert</i> -Butyl 3-benzyl-4-oxobutanoate (22)	S50
i) Benzyl 3-benzyl-4-oxobutanoate (23)	S51
j) 3-Phenylpropyl 3-benzyl-4-oxobutanoate (24)	S52
k) (2 <i>S</i>)- <i>tert</i> -Butyl-2-(((3-benzyl-4-oxobutanoyl)oxy)methyl)pyrrolidine-1-carboxylate (25) (CD ₃ Cl, rt)	S53
l) (2 <i>S</i>)- <i>tert</i> -Butyl-2-(((3-benzyl-4-oxobutanoyl)oxy)methyl)pyrrolidine-1-carboxylate (25) (DMSO- <i>d</i> ₆ , 80 °C)	S54
m) Ethyl 3-formyldodec-11-enoate (26)	S55
n) (<i>E</i>)-Ethyl 3-formylnon-7-enoate (27)	S56

o) (<i>Z</i>)-Ethyl 3-formyldec-7-enoate (28)	S57
p) (<i>E</i>)-Ethyl 3-formyldodec-9-enoate (29)	S58
7. Emission spectra measurements	S59
8. The photoreactor	S60
9. References	S60

1. General Information

All solvents and chemicals used in the syntheses were of reagent grade and were used without further purification. High resolution ESI mass spectra were recorded on a Mariner or SYNAPT spectrometer. ^1H and ^{13}C NMR spectra were recorded at rt on Bruker 400 or Varian 600 MHz instruments with TMS as an internal standard. EPR spectrum was recorded on Magnettech MS200 spectrometer. IR spectroscopy measurements were performed on FTIR Jasco 6200 instrument. Thin layer chromatography (TLC) was performed using Merck Silica Gel GF254, 0.20 mm thickness. GC measurements were made on Gas Chromatograph Perkin Elmer Clarus 500. Aldehydes were purified by flash column chromatography (hexane: AcOEt) if necessary.

Photo-induced reactions were performed using a homemade photoreactor equipped with four LED light bulbs (1200 Lm; warm light).

2. General synthetic procedures

General procedure for α -functionalization of aldehydes:

A photocatalyst (1 mol%) was placed in a reaction tube and dissolved in a mixture of DMSO and buffer pH = 4 (mixture 9:1, 10 mL) then an aldehyde (1 mmol), morpholine (0.4 equiv., 0.4 mmol), LiBF_4 (20 mol%), and EDA (1 equiv., 1 mmol) were added. The reaction mixture was stirred under light irradiation (4xLED, 1xLED = 300 lumens, 39 °C - generated by the light sources in the photoreactor) for 5 h. The light was turned off, the reaction mixture was diluted with AcOEt, and washed with 1N HCl. The aqueous phase was extracted with AcOEt three times. Combined organic phases were washed with saturated $\text{NaHCO}_{3\text{aq}}$, brine, dried over Na_2SO_4 , filtered, and concentrated. The crude product was purified by flash chromatography using silica gel (hexanes/AcOEt).

Scope and limitations

Ethyl 3-benzyl-4-oxobutanoate (3) (colorless oil, 198 mg, 90%)

^1H NMR (CDCl_3 , 500 MHz) δ 9.79 (s, 1H, CHO), 7.31-7.17 (m, 5H, Ph), 4.11 (q, $J = 7.1$ Hz, 2H COCH_2CH_3), 3.14-3.08 (m, 2H, CH_2), 2.77-2.71 (m, 1H, CH), 2.65 (dd, $J = 7.6$ Hz, 1H, CH), 1.40 (dd, $J = 4.8$ Hz, 1H, CH), 1.23 (t, $J = 7.0$ Hz, 3H, COCH_2CH_3) ppm.

^{13}C NMR (CDCl_3 , 100 MHz) δ 202.2, 171.6, 137.7, 129.0, 128.6, 126.7, 60.7, 49.2, 34.6, 32.7, 14.1 ppm.

IR film (cm^{-1}): 3029, 2982, 2934, 2725, 1733 (CO), 1496, 1454 (CHO), 1375, 1199, 1161, 1031, 750, 702.

HRMS ESI calcd. for $\text{C}_{13}\text{H}_{16}\text{O}_3$ $[\text{M}+\text{Na}]^+$ 243.0997; found: 243.0993.

Elemental analysis calcd (%) for $\text{C}_{13}\text{H}_{16}\text{O}_3$: C 70.89, H, 7.32; found: C 70.74, H, 7.40.

GC (mobile phase: hydrogen, flow rate: of 40 mL/min, the injector temperature: 220 °C, temperature range: 50 °C to 300 °C, time: 52 min) $t_R = 42.2$ min.

Ethyl 3-formyl-4-phenylpentanoate (14) (colorless oil, 119 mg, 51%, as a mixture of two diastereoisomers)

^1H NMR (CDCl_3 , 400 MHz) δ 9.86 (s, 1H, CHO), 9.69 (s, 1H, CHO), 7.32- 7.17 (m, 10H, 2 x Ph), 4.10- 4.02 (m, 4H, 2 x COCH_2CH_3), 3.26 (m, 1H, CH), 3.11- 3.07 (m, 3H, 3 x CH), 2.75- 2.68 (dd, $J = 8.0$ Hz, 1H, CH), 2.58- 2.53 (dd, $J = 8.0$ Hz, 1H, CH), 2.37-2.36 (dd, $J = 4.0$ Hz, 1H, CH), 2.32- 2.31 (dd, $J = 4.0$ Hz, 1H, CH), 2.27- 2.26 (dd, $J = 4.0$ Hz, 1H, CH), 2.23- 2.22 (dd, $J = 4.0$ Hz, 1H, CH), 1.38 (d, $J = 8.0$ Hz, 4H, CH_3), 1.31 (d, $J = 8.0$ Hz, 4H, CH_3), 1.25- 1.17 (m, 6H, 2 x CH_3) ppm.

^{13}C NMR (CDCl_3 , 100 MHz) δ 203.5, 202.8, 172.1, 171.9, 143.1, 142.8, 128.7, 128.7, 127.5, 127.4, 126.9, 126.9, 60.7, 53.8, 39.9, 38.9, 32.8, 30.6, 19.2, 17.5, 14.1 ppm.

IR film (cm^{-1}): 3086, 3061, 3029, 2977, 2833, 2730, 1732 (CO), 1603, 1495, 1454 (CHO), 1374, 1331, 1242, 1200, 1178, 1029, 767, 703.

HRMS ESI calcd. for $\text{C}_{14}\text{H}_{18}\text{O}_3$ $[\text{M}+\text{Na}]^+$ 257.1154; found: 257.1153

Elemental analysis calcd (%) for $\text{C}_{14}\text{H}_{18}\text{O}_3$: C 71.77, H 7.74; found: C 71.63, H 7.93.

Ethyl 3-formyl-4-(4-methoxyphenyl)butanoate (15) (colorless oil, 195 mg, 78%)

^1H NMR (CDCl_3 , 400 MHz) δ 9.78 (s, 1H, CHO), 7.09-7.07 (m, 2H, Ph), 6.84-6.83 (m, 2H, Ph), 4.10 (q, $J = 7.0$ Hz, 2H, COCH_2CH_3), 3.78 (s, 3H, OCH_3), 3.08-3.01 (m, 2H, CH_2), 2.71-2.60 (m, 2H, CH_2), 2.40 (dd, $J = 5.5$ Hz, 1H, CH), 1.23 (t, $J = 7.0$ Hz, 3H, COCH_2CH_3) ppm.

^{13}C NMR (CDCl_3 , 100 MHz) δ 202.5, 171.7, 158.3, 129.9, 129.5, 114.0, 60.7, 55.2, 49.4, 33.7, 32.6, 14.1 ppm.

IR film (cm^{-1}): 2982, 2958, 2935, 2837, 1731 (CO), 1612, 1514 (CHO), 1249 (OCH_3), 1179, 1034, 838.

HRMS ESI calcd. for $\text{C}_{14}\text{H}_{18}\text{O}_4$ [$\text{M}+\text{Na}$] $^+$ 273.11032; found: 273.1102

Elemental analysis calcd (%) for $\text{C}_{14}\text{H}_{18}\text{O}_4$: C 67.18, H 7.25; found: C 67.24, H 7.10.

Ethyl 3-(3-chlorobenzyl)-4-oxobutanoate (16) (colorless oil, 185 mg, 73%)

^1H NMR (CDCl_3 , 400 MHz) δ 9.78 (s, 1H, CHO), 7.26-7.18 (m, 3H, Ph), 7.07-7.06 (m, 1H, Ph), 4.12 (q, $J = 7.2$ Hz, 2H, COCH_2CH_3), 3.12-3.07 (m, 2H, CH_2), 2.74-2.69 (m, 1H, CH), 2.65 (dd, $J = 7.1$ Hz, 1H, CH), 2.40 (dd, $J = 5.1$ Hz, 1H, CH), 1.24 (t, $J = 7.1$ Hz, 3H, COCH_2CH_3) ppm.

^{13}C NMR (CDCl_3 , 100 MHz) δ 201.7, 171.4, 139.9, 134.5, 129.9, 129.1, 127.2, 127.0, 60.9, 49.0, 34.1, 32.7, 14.1 ppm.

IR film (cm^{-1}): 2982, 2934, 1730 (CO), 1598, 1574, 1476, 1374 (CHO), 1198, 1157, 1027, 878, 783, 703, 684, 443.

HRMS ESI calcd. for $\text{C}_{13}\text{H}_{15}\text{ClO}_3$ [$\text{M}+\text{CH}_3\text{OH}+\text{Na}$] $^+$ 309.0870; found: 309.0867.

Elemental analysis calcd (%) for $\text{C}_{13}\text{H}_{15}\text{ClO}_3$: C 61.30, H 5.94, Cl 13.9; found: C 61.27, H 5.91, Cl 13.86.

Ethyl 4-oxo-3-phenylbutanoate (17)¹ (colorless oil, 112 mg, 47%)

^1H NMR (CDCl_3 , 400 MHz) δ 9.70 (s, 1H, CHO), 7.40-7.32 (m, 3H, Ph), 7.21-7.19 (m, 2H, Ph), 4.17-4.10 (m, 3H, COCH_2CH_3 , CH), 3.14 (dd, $J = 8.0$ Hz, 1H, CH), 2.61 (dd, $J = 8.0$ Hz, 1H, CH), 1.22 (t, $J = 8.0$ Hz, 3H, COCH_2CH_3) ppm.

^{13}C NMR (CDCl_3 , 100 MHz) δ 198.5, 171.5, 134.8, 129.2, 128.8, 128.0, 60.7, 54.6, 34.6, 14.0 ppm.

Ethyl 3-formyl-4-methylpentanoate (20)² (colorless oil, 120 mg, 66%).

¹H NMR (CDCl₃, 400 MHz) δ 9.74 (s, 1H, CHO), 4.12 (q, *J* = 8.0 Hz, 2H, COCH₂CH₃), 2.81-2.64 (m, 2H, CH), 2.42-2.28 (ddd, *J* = 4.0 Hz, 1H, CH), 2.19-2.01 (m, 1H, CH), 1.25-1.21 (td, *J* = 8.0 Hz, *J* = 4.0 Hz, 3H, COCH₂CH₃), 1.01-0.92 (m, 6H, 2xCH₃) ppm.

¹³C NMR (CDCl₃, 100 MHz) δ 203.3, 179.8, 172.2, 60.7, 60.6, 53.5, 47.2, 32.6, 29.8, 27.7, 20.1, 19.9, 19.3, 19.1, 14.0, 14.0 ppm; residual peaks from AcOEt, hexane and CH₂Cl₂ – product is very volatile and we were not able to dry.

Ethyl 3-formylundecanoate (21) (colorless oil, 188 mg, 78%)

¹H NMR (CDCl₃, 400 MHz) δ 9.71 (s, 1H, CHO), 4.15 (q, *J* = 4.0 Hz, 2H, COCH₂CH₃), 2.83-2.79 (m, 1H, CH), 2.70-2.64 (m, 1H, CH), 3.39 (dd, *J* = 4.0 Hz, 1H, CH), 1.72-1.68 (m, 1H, CH), 1.49-1.43 (m, 1H, CH), 1.35-1.23 (m, 15H, CH₂), 0.87 (t, *J* = 4.0 Hz, 3H, CH₃) ppm.

¹³C NMR (CDCl₃, 100 MHz) δ 202.9, 171.9, 60.7, 47.7, 33.1, 31.8, 29.5, 29.3, 29.1, 28.6, 26.7, 22.6, 14.1, 14.0 ppm.

IR film (cm⁻¹): 2927, 2856, 1737 (CO), 1466 (CHO), 1374, 1185, 1032, 723.

HRMS ESI calcd. for C₁₄H₂₆O₃ [M+Na]⁺ 265.1780; found: 265.1779.

Elemental analysis calcd (%) for C₁₄H₂₆O₃: C 69.38, H 10.81; found: C 69.30, H 10.85.

tert-Butyl 3-benzyl-4-oxobutanoate (22) (colorless oil, 162 mg, 65%).

¹H NMR (CDCl₃, 500 MHz) δ 9.78 (s, 1H, CHO), 7.30-7.16 (m, 5H, Ph), 3.10-3.04 (m, 2H, CH₂), 2.74-2.2.72 (m, 1H, CH), 2.56 (dd, *J* = 7.6 Hz, 1H, CH), 2.35 (dd, *J* = 5.1 Hz, 1H, CH), 1.42 (s, 9H, *t*-Bu) ppm.

¹³C NMR (CDCl₃, 125 MHz) δ 202.5, 170.8, 137.9, 129.0, 128.6, 126.6, 81.1, 49.4, 34.5, 34.1, 28.0 ppm.

IR film (cm⁻¹): 2979, 2931, 1728 (CO), 1455, 1368 (CHO), 1255, 1150, 751, 701.

HRMS ESI calcd. for C₁₅H₂₀O₃ [M+CH₃OH+Na]⁺ 303.1572; found: 303.1562.

Elemental analysis calcd (%) for C₁₅H₂₀O₃: C 72.55; H 8.12; found: C 72.31, H 8.29.

Benzyl 3-benzyl-4-oxobutanoate (23) (colorless oil, 234 mg, 83%)

¹H NMR (CDCl₃, 500 MHz) δ 9.79 (s, 1H, CHO), 7.36-7.28 (m, 6H, Ph), 7.27-7.22 (m, 2H, Ph), 7.15-7.13 (m, 2H, Ph), 5.08 (s, 2H, CH₂Ph), 3.14-3.07 (m, 2H, CH₂), 2.76-2.67 (m, 2H, CH₂), 2.42 (dd, *J* = 4.0 Hz, 1H, CH) ppm.

^{13}C NMR (CDCl_3 , 125 MHz) δ 202.1, 171.5, 137.5, 135.5, 129.0, 128.7, 128.5, 128.3, 128.2, 126.7, 66.6, 49.2, 34.5, 32.6 ppm.

IR film (cm^{-1}): 3087, 3063, 3030, 2925, 2828, 2724, 1732 (CO), 1496, 1455, 1383 (CHO), 1352, 1189, 1160, 748, 700, 491

HRMS ESI calcd. for $\text{C}_{18}\text{H}_{18}\text{O}_3$ [$\text{M}+\text{CH}_3\text{OH}+\text{Na}$] $^+$ 337.1416; found: 337.1413.

Elemental analysis calcd (%) for $\text{C}_{18}\text{H}_{18}\text{O}_3$: C 76.57, H 6.43; found: C 76.48, H 6.24.

3-Phenylpropyl 3-benzyl-4-oxobutanoate (24) (colorless oil, 260 mg, 84%).

^1H NMR (CDCl_3 , 500 MHz) δ 9.79 (s, 1H, CHO), 7.31-7.25 (m, 5H, Ph), 7.19-7.16 (m, 5H, Ph), 4.06 (td, $J = 4.0$ Hz, 2H, CH_2), 3.12-3.10 (m, 2H, CH_2), 2.75 (d, $J = 4.0$ Hz, 1H, CH), 2.68-2.62 (m, 3H, $\text{CH}_2 + \text{CH}$), 2.39 (dd, $J = 4.0$ Hz, 1H, CH), 1.95-1.91 (m, 2H, CH_2) ppm.

^{13}C NMR (CDCl_3 , 125 MHz) δ 202.2, 171.7, 141.0, 137.6, 129.0, 128.7, 128.4, 128.3, 126.7, 126.0, 64.2, 49.2, 34.6, 32.6, 32.1, 30.1 ppm.

IR film (cm^{-1}): 3085, 3061, 3027, 2952, 2925, 2858, 1731 (CO), 1603, 1496, 1453 (CHO), 1192, 1163, 1030, 748, 701, 492.

HRMS ESI calcd. for $\text{C}_{20}\text{H}_{22}\text{O}_3$ [$\text{M}+\text{Na}$] $^+$ 333.1467; found: 333.1461.

Elemental analysis calcd. (%) for $\text{C}_{20}\text{H}_{22}\text{O}_3$: C 77.39, H 7.14; found: C, 77.36, H 7.01.

(2S)-tert-Butyl-2-(((3-benzyl-4-oxobutanoyl)oxy)methyl)pyrrolidine-1-carboxylate (25)

(colorless oil, 251 mg, 67%).

^1H NMR (CDCl_3 , 600 MHz) δ 9.78 (s, 1H, CHO), 7.33-7.30 (m, 2H, Ph), 7.27 (m, 1H, Ph), 7.19-7.17 (m, 2H, Ph), 4.17-3.99 (m, 3H, CH_2 , CH), 3.34-3.32 (m, 2H, CH_2), 3.16-3.09 (m, 2H, CH_2), 2.79-2.72 (m, 1H, CH), 2.69-2.61 (m, 1H, CH), 2.40 (dd, $J = 6.0$ Hz, 1H, CH), 2.01-1.70 (m, 4H, 2 x CH_2), 1.46 (s, 9H, *t*-Bu) ppm.

^{13}C NMR (CDCl_3 , 150 MHz) δ 202.1, 171.5, 154.4, 137.5, 129.9, 128.7, 126.7, 79.7, 79.3, 64.9, 55.4, 49.1, 46.4, 34.5, 32.5, 28.7, 28.4, 27.8, 23.7, 22.9 ppm.

^1H NMR ($\text{DMSO}-d_6$, 80 °C, 500 MHz) δ 9.70 (s, 1H, CHO), 7.31-7.27 (m, 2H, Ph), 7.23-7.18 (m, 3H, Ph), 4.11-4.06 (m, 1H, CH), 4.05-3.99 (m, 1H, CH), 3.92-3.86 (m, 1H, CH), 3.33-3.27 (m, 1H, CH), 3.10-3.02 (m, 3H, CH_2+CH), 2.80-2.73 (m, 1H, CH), 2.63-2.57 (dd, $J = 6.0$ Hz, 1H, CH), 2.49-2.41 (m, 1H, CH), 1.97-1.68 (m, 4H, 2 x CH_2), 1.41 (s, 9H, *t*-Bu) ppm.

^{13}C NMR (DMSO- d_6 , 80 °C, 125 MHz) δ 203.1, 171.4, 171.4, 154.0, 138.7, 129.3, 128.7, 126.7, 79.0, 64.9, 55.7, 55.7, 49.1, 46.7, 40.8, 40.7, 40.5, 40.3, 40.2, 40.0, 39.8, 34.2, 32.8, 28.6, 28.5, 28.3, 23.3 ppm.

IR film (cm^{-1}): 2975, 2932, 2880, 1736 (CO), 1693 (CO), 1394 (CHO), 1366, 1167, 1109, 702.

HRMS ESI calcd. for $\text{C}_{20}\text{H}_{29}\text{O}_5$ [$\text{M}+\text{CH}_3\text{OH}+\text{Na}$] $^+$ 430.2206; found: 430,2208.

Elemental analysis calcd. (%) for $\text{C}_{21}\text{H}_{29}\text{NO}_5$: C 67.18, H 7.79, N 3.73; found: C, 67.22, H 7.72, N 3.69.

Ethyl 3-formyldodec-11-enoate (26) (colorless oil, 148 mg, 58%)

^1H NMR (CDCl_3 , 400 MHz) δ 9.70 (s, 1H, CHO), 5.84-5.74 (m, 1H, CH=), 5.00-4.91 (dd, $J = 8\text{ Hz}$ 2H, $\text{CH}_2=\text{CH}$), 4.16-4.10 (q, 2H, $J = 8.0\text{ Hz}$, COCH_2CH_3), 2.80-2.78 (m, 1H, CH), 2.71-2.67 (dd, 1H, $J = 8.0\text{ Hz}$, CH), 2.41-2.36 (dd, $J = 4.0\text{ Hz}$, 1H, CH), 2.04-2.02 (m, 2H, CH_2), 1.79-1.66 (m, 1H, CH), 1.48-1.44 (m, 1H, CHH), 1.38-1.23 (m, 13H, CHH + 6 x CH_2) ppm.

^{13}C NMR (CDCl_3 , 100 MHz) δ 202.9, 171.9, 139.2, 114.2, 60.7, 47.7, 33.7, 33.2, 29.5, 29.2, 28.9, 28.8, 28.6, 26.7, 14.1 ppm.

IR film (cm^{-1}): 3076, 2976, 2927, 2855, 2717, 1736, 1640, 1463, 1415, 1394, 1373, 1348, 1300, 1254, 1184, 1097, 1033, 995, 910, 874.

HRMS ESI calcd. for $\text{C}_{15}\text{H}_{26}\text{O}_3$ [$\text{M}+\text{Na}$] $^+$ 277.1780; found: 277.1778.

Elemental analysis calcd (%) for $\text{C}_{15}\text{H}_{26}\text{O}_3$: C 70.83, H 10.30; found: C, 71.00, H 10.30.

(E)-Ethyl 3-formylnon-7-enoate (27) (colourless oil, 103 mg, 43%, as a mixture of two diastereoisomers)

^1H NMR (CDCl_3 , 400 MHz) δ 9.75 (s, 1H, CHO), 9.69 (s, 1H, CHO), 5.08-5.05 (m, 2H, CH=CH), 4.15-4.10 (q, $J = 8.0\text{ Hz}$, 4H, 2 x CH_2), 2.91-2.89 (m, 2H, CH), 2.77-2.66 (m, 2H, CH), 2.30-2.26 (m, 2H, CH), 2.02-1.99 (m, 5H, 3 x CH_2), 1.68 (d, $J = 4.0\text{ Hz}$, 6H, 2 x CH_3), 1.60 (d, $J = 4.0\text{ Hz}$, 6H, 2 x CH_3), 1.41-1.37 (m, 2H, CH), 1.33-1.22 (m, 9H, CH, CH_2), 1.25 (d, $J = 8.0\text{ Hz}$, 3H, CH_3), 0.97 (d, $J = 8.0\text{ Hz}$, 3H, CH_3) ppm.

^{13}C NMR (CDCl_3 , 100 MHz) δ 203.3, 203.1, 172.5, 172.42, 132.2, 132.1, 126.6, 123.5, 60.7, 52.86, 52.1, 34.5, 33.9, 32.8, 31.3, 30.4, 28.7, 25.7, 25.7 25.7, 25.6, 17.7, 17.0, 15.96, 14.12, 14.1 ppm.

IR film (cm^{-1}): 2965, 2925, 2875, 2857, 2720, 1736, 1459, 1376, 1344, 1299, 1244, 184, 1097, 1034, 341, 876, 829, 742, 565, 446.

HRMS ESI calcd. for $C_{14}H_{24}O_3$ $[M+Na]^+$ 263.1623; found: 263.1625.

Elemental analysis calcd (%) for $C_{14}H_{24}O_3$: C 69.96, H 10.07; found: C, 70.06, H 10.10.

(Z)-Ethyl 3-formyldec-7-enoate (28) (colorless oil, 160 mg, 70%)

1H NMR ($CDCl_3$, 400 MHz) δ 9.70 (d, J = 4.0 Hz, 1H, CHO), 5.37-5.35 (m, 1H, CH=), 5.28-5.25 (m, 1H, CH=), 4.15-4.12 (q, J = 8.0 Hz, 2H, $COCH_2CH_3$), 2.80-2.78 (m, 1H, CH), 2.71-2.65 (dd, J = 8.0 Hz, 1H, CH), 2.41-2.36 (dd, J = 4.0 Hz, 1H, CH), 2.01-1.99 (m, 4H, 2 x CH_2), 1.75-1.73 (m, 1H, CH), 1.43-1.39 (m, 3H, CH, CH_2), 1.24 (t, J = 8.0 Hz, 3H, CH_3), 0.94 (t, J = 8 Hz, 3H, CH_3) ppm.

^{13}C NMR ($CDCl_3$, 100 MHz) δ 202.8, 171.9, 132.53, 127.9, 60.7, 47.6, 33.1, 28.1, 26.9, 26.8, 20.5, 14.3, 14.1 ppm.

IR (cm^{-1}): 3001, 2963, 2933, 2861, 2719, 1735, 1461, 1373, 1302, 1256, 1187, 1096, 1070, 1031, 969, 902, 873, 757, 722, 581, 445.

HRMS ESI calcd. for $C_{13}H_{22}O_3$ $[M+Na]^+$ 249.1467; found: 249.1466.

Elemental analysis calcd (%) for $C_{13}H_{22}O_3$: C 68.99, H 9.80; found: C, 68.84, H 9.50.

(E)-Ethyl 3-formyldodec-9-enoate (29) (colorless oil, 200 mg, 78%)

1H NMR ($CDCl_3$, 400 MHz) δ 9.70 (s, 1H, CHO), 5.34-5.30 (m, 2H, CH=CH), 4.14-4.12 (q, J = 8.0 Hz, 2H, $COCH_2CH_3$), 2.80-2.78 (m, 1H, CH), 2.71-2.67 (dd, J = 8.0 Hz, 1H, CH), 2.41-2.36 (dd, J = 4.0 Hz, 1H, CH), 2.04-1.98 (m, 4H, 2 x CH_2), 1.73-1.69 (m, 1H, CH), 1.50-1.47 (m, 1H, CH), 1.45-1.33 (m, 6H, 3x CH_2), 1.26 (t, J = 4.0 Hz, 3H, CH_3), 0.94 (t, J = 8.0 Hz, 3H, CH_3) ppm.

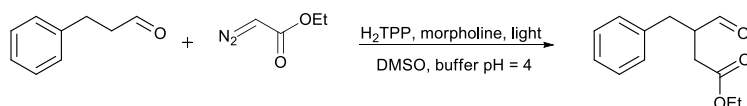
^{13}C NMR ($CDCl_3$, 100 MHz) δ 202.9, 171.9, 131.8, 128.9, 60.7, 47.7, 33.2, 29.41, 29.1, 28.5, 26.9, 26.7, 20.5, 14.3, 14.1 ppm.

IR (cm^{-1}): 2962, 2932, 2857, 2717, 1736, 1463, 1373, 1247, 1184, 1096, 1070, 1033, 873, 725, 585.

HRMS ESI calcd. for $C_{15}H_{26}O_3$ $[M+Na]^+$ 277.1780; found: 277.1776.

Elemental analysis calcd (%) for $C_{15}H_{26}O_3$: C 70.83, H 10.30; found: C, 70.73, H 10.20.

3. Optimization studies

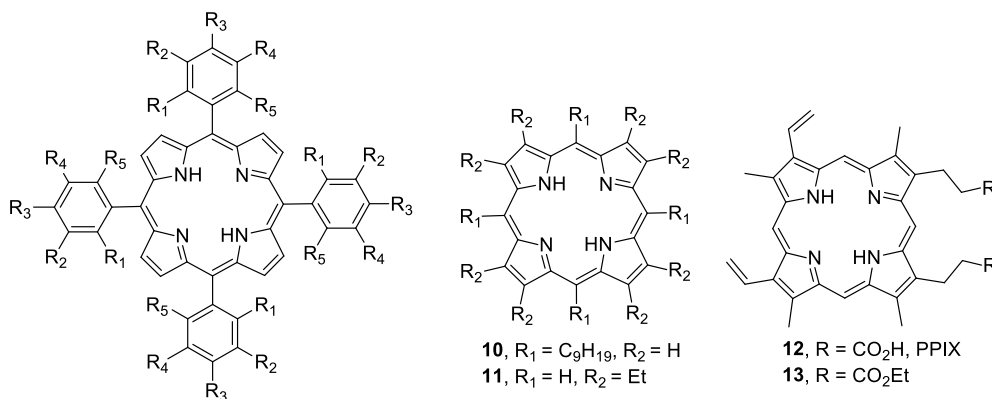


Background reactions:

entry	catalyst	amine	yield, (%) ^d
1 ^a	Eosin Y	morpholine	68
2 ^a	Methylene blue	morpholine	0
3 ^a	Fluorescein	morpholine	8
4 ^a	Rose bengal	morpholine	32
5 ^b	H_2TPP , 4	morpholine	84
6 ^b	ZnTPP, Zn-4	morpholine	88
7 ^b	no	morpholine	0
8 ^b	TPP, 4	no	0
9 ^c	TPP, 4	morpholine	0

^aReaction conditions: aldehyde **1** (0.5 mmol), morpholine (0.4 equiv.), catalyst (0.5 mol%), EDA (**2**, 1 equiv.), DMSO:buffer pH = 4 (5 mL, 9:1 mixture), 5 h. ^bAldehyde **1** (1 equiv., 0.5 mmol), morpholine (0.4 equiv.), catalyst (1 mol%), EDA (**2**, 1 equiv.), DMSO: buffer pH = 4 (5 mL, 9:1 mixture), 5 h. ^cNo light ^dYields were determined by GC.

Porphyrins tested in the alkylation reaction:



entry	catalyst	yYield/% ^b
1	TPP, 4	84
2	5	traces
3	6	44
4	7	14
5	8	10
6	9	60
7	10	8
8	11	15
9	PP-IX, 12	15
10	PP-IX diethyl ester, 13	54
11	ZnTPP, Zn- 4	88
12	Zn- 6	0
13	Zn- 7	54
14	Zn- 9	75

^aReaction conditions: aldehyde **1** (0.5 mmol), morpholine (0.4 equiv.), porphyrin (1 mol%), EDA (**2**, 1 equiv.), DMSO:buffer pH = 4 (5 mL, 9:1 mixture), 5 h. ^bYields were determined by GC.

Optimization of the catalyst loading:

entry	catalyst	loading/ mol%	yield/(%) ^b
1	H ₂ TPP, 4	1.5	73
2	H ₂ TPP, 4	1.0	84
3	H ₂ TPP, 4	0.7	63
4	H ₂ TPP, 4	0.4	65
5	H ₂ TPP, 4	0.1	61
6	ZnTPP, Zn- 4	2.0	84
7	ZnTPP, Zn- 4	1.5	90
8	ZnTPP, Zn- 4	1.0	88
9	ZnTPP, Zn- 4	0.8	86
10	ZnTPP, Zn- 4	0.6	84
11	ZnTPP, Zn- 4	0.4	86
12	ZnTPP, Zn- 4	0.2	82
13	ZnTPP, Zn- 4	0.1	80

^aReaction conditions: aldehyde **1** (1 equiv., 0.5 mmol), morpholine (0.4 equiv.), porphyrin (1 mol%), EDA (**2**, 1 equiv.), DMSO:buffer pH = 4 (5 mL, 9:1 mixture), 5 h. ^bYields were determined by GC.

The influence of an amine used:

entry	catalyst	amine	pK_b^3	yield/% ^b
1	H ₂ TPP, 4	pyrrolidine	2.89	57
2	H ₂ TPP, 4	piperidine	2.73	59
3	H ₂ TPP, 4	piperazine	4.19	26
4	H ₂ TPP, 4	<i>N</i> -methylpiperazine	4.87	24
5	H ₂ TPP, 4	morpholine	5.6	84
6	ZnTPP, Zn-4	pyrrolidine	2.89	68
7	ZnTPP, Zn-4	piperidine	2.73	83
8	ZnTPP, Zn-4	piperazine	4.19	79
9	ZnTPP, Zn-4	<i>N</i> -methylpiperazine	4.87	73
10	ZnTPP, Zn-4	morpholine	5.6	88

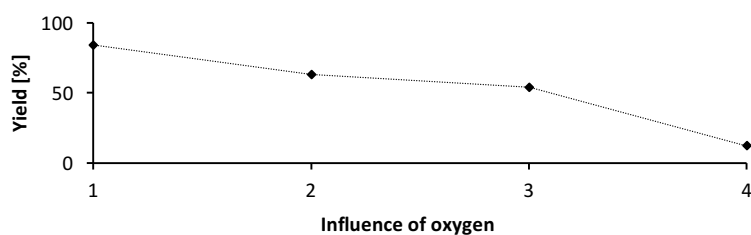
^aReaction conditions: aldehyde **1** (0.5 mmol), morpholine (0.4 equiv.), porphyrin (1 mol%), EDA (**2**, 1 equiv.), DMSO:buffer pH = 4 (5 mL, 9:1 mixture), 5 h. ^bYields were determined by GC.

The influence of pH buffer used in the reaction:

entry	catalyst	solvent	yield/% ^b
1	H ₂ TPP, 4	DMSO/buffer pH=6 9:1	66
2	H ₂ TPP, 4	DMSO/buffer pH=4,5 9:1	67
3	H ₂ TPP, 4	DMSO/buffer pH=4 9:1	84
4	H ₂ TPP, 4	DMSO/buffer pH=3,5 9:1	65
5	H ₂ TPP, 4	DMSO/buffer pH=3 9:1	66
1	ZnTPP, Zn-4	DMSO/buffer pH=6 9:1	83
2	ZnTPP, Zn-4	DMSO/buffer pH=4,5 9:1	82
3	ZnTPP, Zn-4	DMSO/buffer pH=4 9:1	88
4	ZnTPP, Zn-4	DMSO/buffer pH=3,5 9:1	66
5	ZnTPP, Zn-4	DMSO/buffer pH=3 9:1	63

^aAldehyde **1** (1 equiv., 0.5 mmol), morpholine (0.4 equiv.), H₂TPP, **4** (1 mol%), EDA (**2**, 1 equiv.), DMSO: buffer pH = 4 (5 mL, 9:1 mixture), 5 h. ^cYields were determined by GC.

The influence of oxygen on the yield of the reaction:



1 - degassed, under Ar 2 - only degassed 3 - open to air 4 - under O₂

^aReaction conditions: aldehyde **1** (0.5 mmol), morpholine (0.4 equiv.), H₂TPP (**4**, 1 mol%), EDA (**2**, 1 equiv.), DMSO:buffer pH = 4 (5 mL, 9:1 mixture), 5 h. Yields were determined by GC.

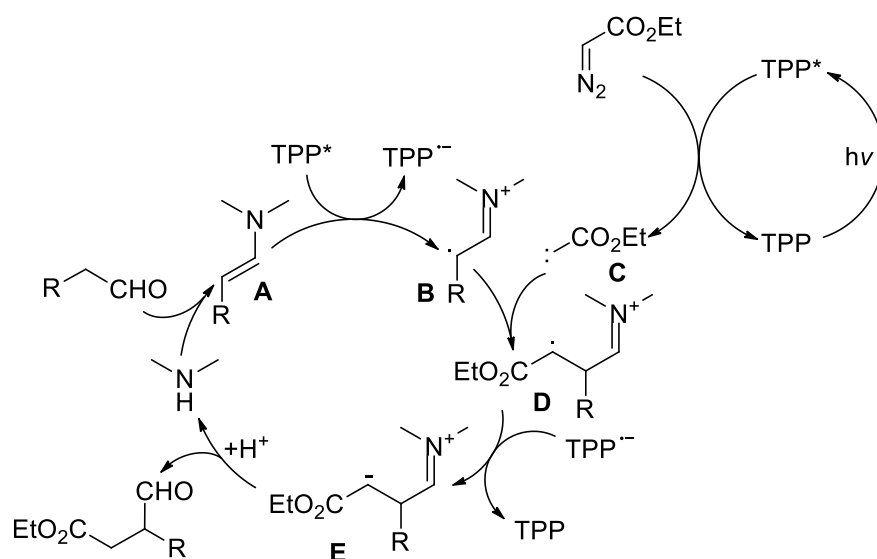
Co-catalyst effect:

entry	catalyst	co-catalyst	pK _a ⁴	yield/% ^c
1 ^a	H ₂ TPP, 4	PhCO ₂ H	4.20	32
2 ^a	H ₂ TPP, 4	4-methylbenzoic acid	4.37	47
3 ^a	H ₂ TPP, 4	4-hydroxybenzoic acid	4.54	44
4 ^a	H ₂ TPP, 4	AcOH	4.76	64
5 ^a	H ₂ TPP, 4	ascorbic acid	4.17; 11.60	21
6 ^a	H ₂ TPP, 4	H ₂ O	-	31
7 ^a	H ₂ TPP, 4	BF ₃ (OEt) ₂	-	17
8 ^a	H ₂ TPP, 4	Zn(OAc) ₂	-	64
9 ^a	H ₂ TPP, 4	LiBF ₄	-	76
10 ^b	H ₂ TPP, 4	LiBF ₄	-	90

^aReaction conditions: aldehyde **1** (0.5 mmol), morpholine (0.4 equiv.), H₂TPP (**4**, 1 mol%), EDA (**2**, 1 equiv.), DMSO (5 mL), 5 h. ^baldehyde **1** (0.5 mmol), morpholine (0.4 equiv.), H₂TPP (**4**, 1 mol%), EDA (**2**, 1 equiv.), DMSO:buffer pH = 4 (5 mL, 9:1 mixture), 5 h. ^cYields were determined by GC.

5. Mechanistic considerations:

5.1. Proposed Mechanism



A - confirmed by NMR and MS experiment – see pp. S24, S27

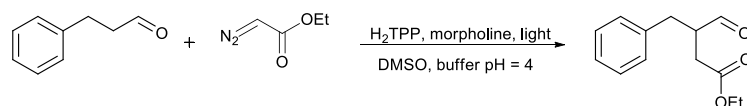
B – confirmed by EPR and MS experiment – see pp. S16, S27

C – confirmed by EPR and MS experiment – see pp. S16, S27

D – confirmed EPR and MS experiment – see pp. S16, S27

5.2. EPR spectroscopy – experimental and theoretical studies

spin trap:	<i>N-tert</i> -butyl- α -phenylnitrone (PBN) or 5,5-dimethyl-1-pyrroline <i>N</i> -oxide (DMPO)
central magnetic field:	333 mT;
sweep width:	7,9 mT;
modulation amplitude:	0,06 mT;
microwave strength:	6,3 mW;
sweep time:	30 s;
number of scans:	16
simulation	EasySpin package in Matlab



Reaction conditions: 3-phenyl-propanal (1 mmol), EDA (1 equiv., 1 mmol) morpholine (0.4 equiv., 0.4 mmol), H₂TPP (1 mol%), DMSO: buffer pH = 4 (10 mL, 9:1). After 10 min. of stirring under irradiation (4xLED) *N-tert*-butyl- α -phenylnitrone (BPN) or 5,5-dimethyl-1-pyrroline *N*-oxide (DMPO) was added and after next 10 min. of stirring under irradiation (4xLED) EPR spectra (9.3 GHz) was recorded.

In accordance with the proposed mechanism reactive radicals are formed. To confirm their presence, EPR spectroscopy experiments were performed. As the concentration of free radicals in the reaction mixture was too low to be detected directly, EPR measurements were performed with two spin traps *N-tert*butyl- α -phenylnitrone (PBN) (Figure S1) and 5,5-dimethyl-1-pyrroline *N*-oxide (DMPO) (Figure S3). Additionally, the spectra were simulated using EasySpin package in Matlab (Figure S2 and S4). EPR spectra of the reaction mixture were recorded after 10 min of irradiation. They show the same pattern but the total signals' intensity is significantly higher in the experiment with DMPO. Spectral simulations indicate the presence of three paramagnetic species with the intensity ratio of the two corresponding components being almost the same. A weak component (8% of total intensity, $a_N = 1.36$ mT, $a_{H\beta} = 0.73$ mT, $a_{H\alpha} = 0.17$ mT) can be tentatively ascribed to a peroxy radical adduct based on the literature data.⁵

Figure S1. EPR spectra of the reaction mixture with PBN

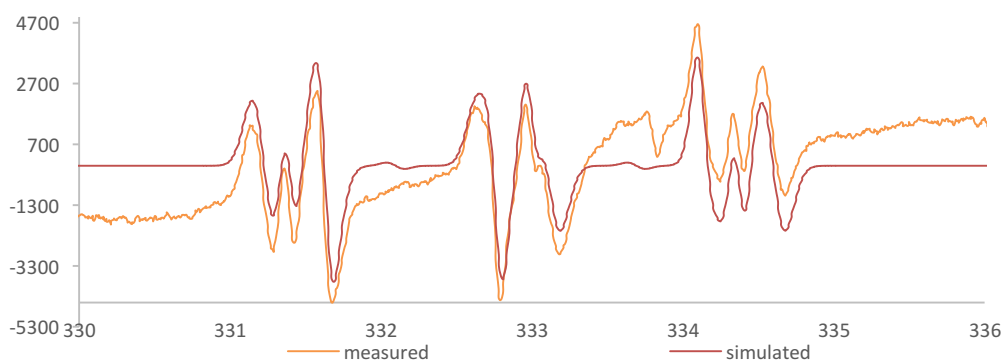


Figure S2. Simulated EPR spectra of the reaction mixture with PBN

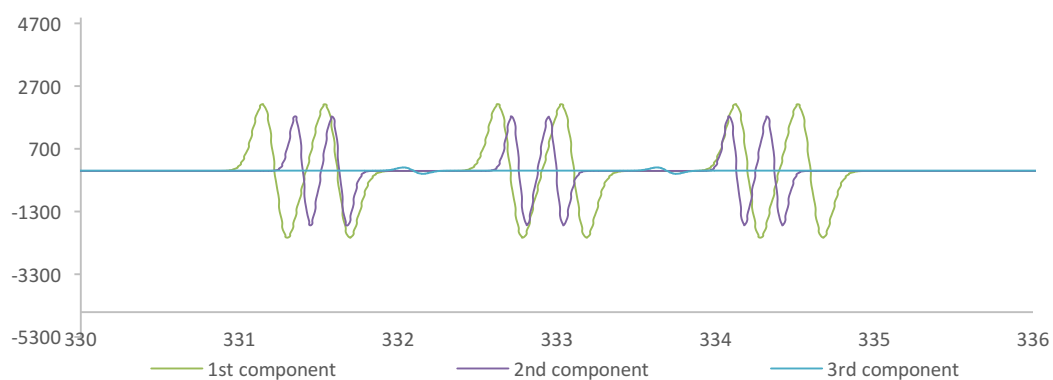


Figure S3. EPR spectra of the reaction mixture with DMPO

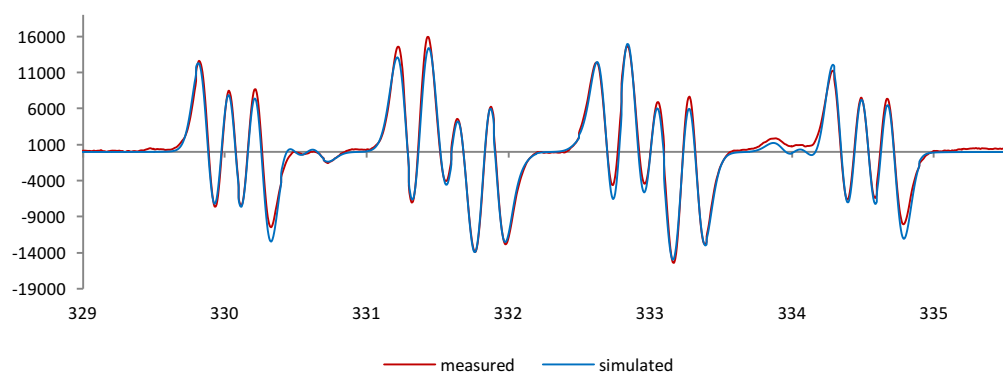
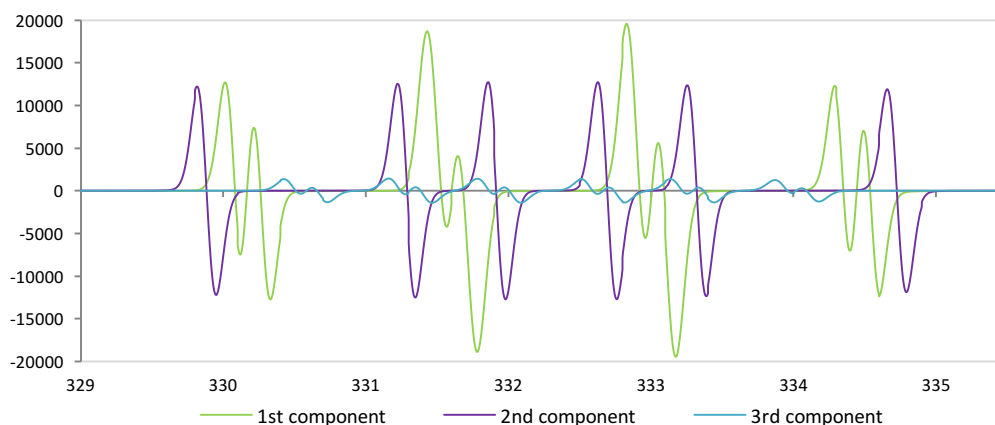


Figure S4. Simulated EPR spectra of the reaction mixture



a) EPR measurements of the background's reactions with *N-tert-butyl- α -phenylnitrone (BPN)* as a spin trap

1. H₂TPP in DMSO: buffer pH = 4 (10 mL, 9:1) was stirred under light irradiation (4xLED) for 10 minutes and then BPN was added and after next 10 min. of stirring under irradiation (4xLED) EPR spectra (9.3 GHz) was recorded.

No signals corresponding to radicals were detected.

2. H₂TPP with an 3-phenylpropanal and morpholine in DMSO: buffer pH = 4 (10 mL, 9:1) was stirred under light irradiation (4xLED) for 10 minutes and then BPN was added and after next 10 min. of stirring under irradiation (4xLED) EPR spectra (9.3 GHz) was recorded.

Figure S5. EPR spectra of the mixture of H₂TPP (4) with 3-phenylpropanal (1) and morpholine in DMSO: buffer pH = 4 (9:1) with PBN

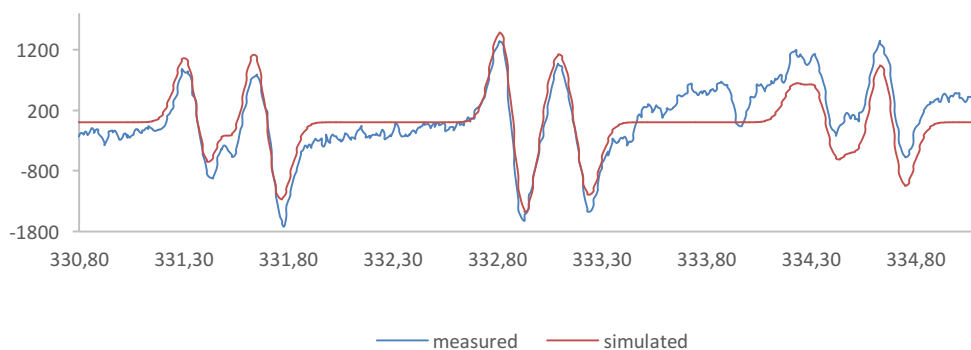
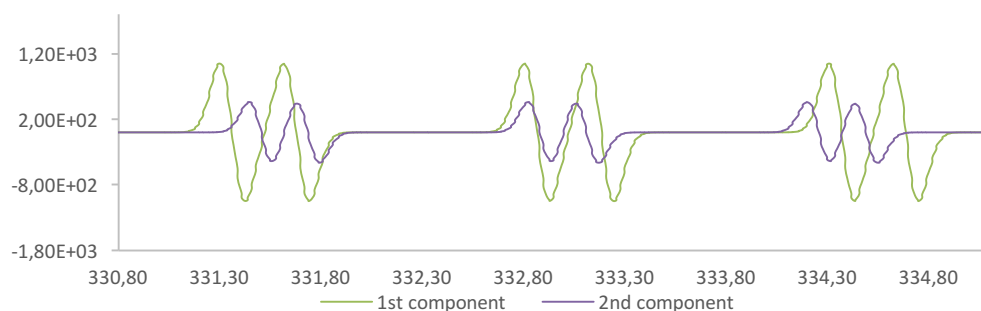


Figure S6. Simulated EPR spectra of the mixture of H₂TPP (**4**) with 3-phenylpropanal (**1**) and morpholine in DMSO: buffer pH = 4 (9:1) with PBN



In The EPR spectrum of H₂TPP (**4**), morpholine, and aldehyde (**1**) with no EDA added was registered in the presence of PBN after light irradiation (Figure S4, blue line). The simulated EPR spectrum shows two components (Figure S6) each as a six-line signal corresponding to PBN radical adducts. The signal (component 1) with the higher intensity (73% of total) is the triplet of doublets characterized by the hyperfine splitting constant with nitrogen $a_N = 1.50$ mT and the hyperfine splitting constant with β -hydrogen $a_H = 0.32$ mT. It can be assigned to a carbon-centered radical, most probably to the radical B, as the values obtained for these type of species are usually in the range of 1.55-1.6 mT for a_N and 0.3-0.35 for a_H . The second signal (27% of total intensity) relates to DMSO-derived radical (PBN-DMSO adduct), as its parameters $a_N = 1.37$ mT and $a_H = 0.23$ mT are the same as those given by Buettner.⁵

3. H₂TPP with EDA in DMSO: buffer pH=4 (9:1) was stirred under light irradiation (4xLED) for 10 minutes then BPN was added and after next 10 min. of stirring under irradiation (4xLED) EPR spectra (9.3 GHz) was recorded.

Figure S7. EPR spectra of the mixture of H₂TPP (**4**) EDA in DMSO: buffer pH = 4 (9:1) with PBN

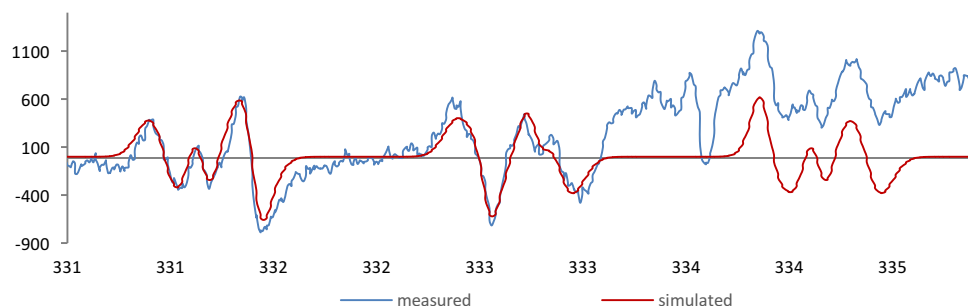
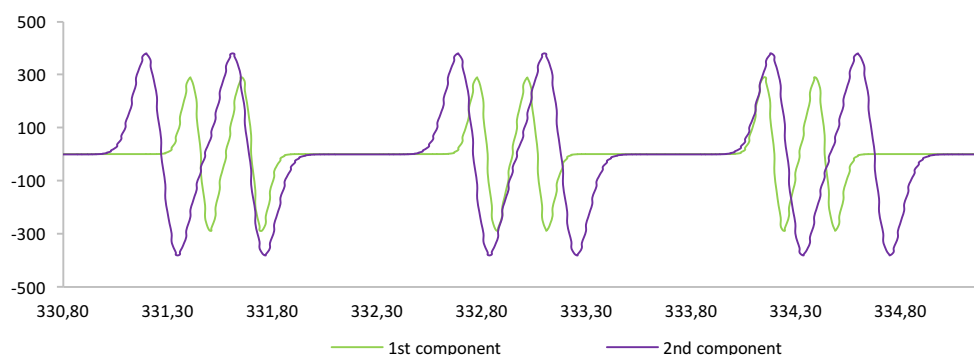


Figure S8. Simulated EPR spectra of the mixture of H₂TPP (**4**) EDA in DMSO: buffer pH = 4 (9:1) with PBN



Subsequently the EPR spectrum was measured for a mixture of H₂TPP (**4**) and EDA (**2**) in the presence of PBN (Figure S7). Two components are present in the simulated EPR spectrum (Figure S8). One of the components (23% of total intensity) is the same as observed previously and it corresponds to the DMSO-derived radical adduct. The second, more intensive is the six-line signal with nitrogen hyperfine splitting constant of 1.49 mT and hydrogen hyperfine splitting constant of 0.4 mT. It can be assigned to a carbon-centered radical adduct, as the a_H value is similar to that of the PBN-aliphatic radical adduct, and is larger than that for *O*-centered radical adducts with PBN. It is known that the thermal decomposition of diazo compounds leads to the formation of carbon-centered radicals that with PBN give adducts with $a_N = 1.54$ mT and $a_H = 0.4$ mT.⁶ Our measured parameters are very similar thus suggesting that the signal corresponds to a radical formed during photolysis of EDA (**2**), e.g. radical C. But its hyperfine splitting constants are also similar to those obtained for PBN-benzoyl radical adduct in DMSO solution ($a_N = 1.45$ mT and $a_H = 0.47$ mT), so its presence can be considered as an alternative.⁷

4. TPP with morpholine in DMSO: buffer pH = 4 (9:1) was stirred under light irradiation (4xLED) for 10 minutes and then PBN was added and after next 10 min. of stirring under irradiation (4xLED) EPR spectra (9.3 GHz) was recorded.

No signals corresponding to radicals were detected.

b) EPR measurements of the background's reactions with 5,5-dimethyl-1-pyrroline *N*-oxide (DMPO) as a spin trap

1. TPP (**4**) with 3-phenylpropanal (**1**) and morpholine in DMSO: buffer pH = 4 (9:1) was stirred under light irradiation (4xLED) for 10 minutes and then DMPO was added and after next 10 min. of stirring under irradiation (4xLED) EPR spectra (9.3 GHz) was recorded.

Figure S9. EPR spectra of the mixture of H₂TPP (**4**) with 3-phenylpropanal (**1**) and morpholine in DMSO: buffer pH = 4 (9:1) with DMPO

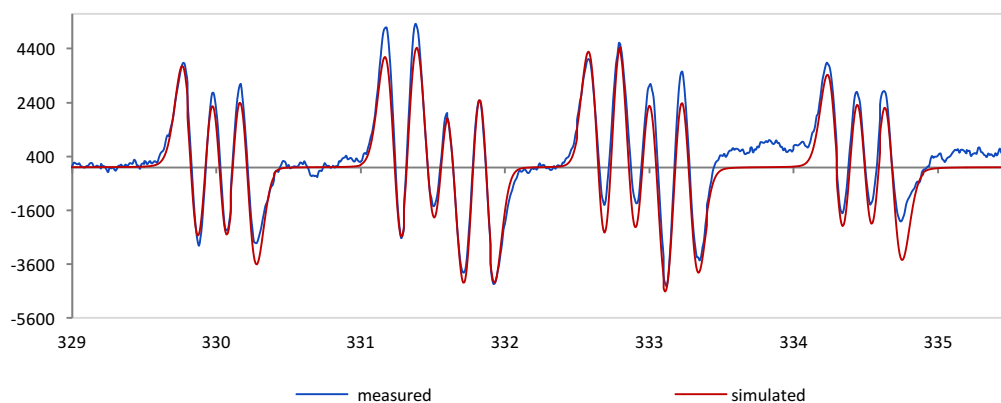
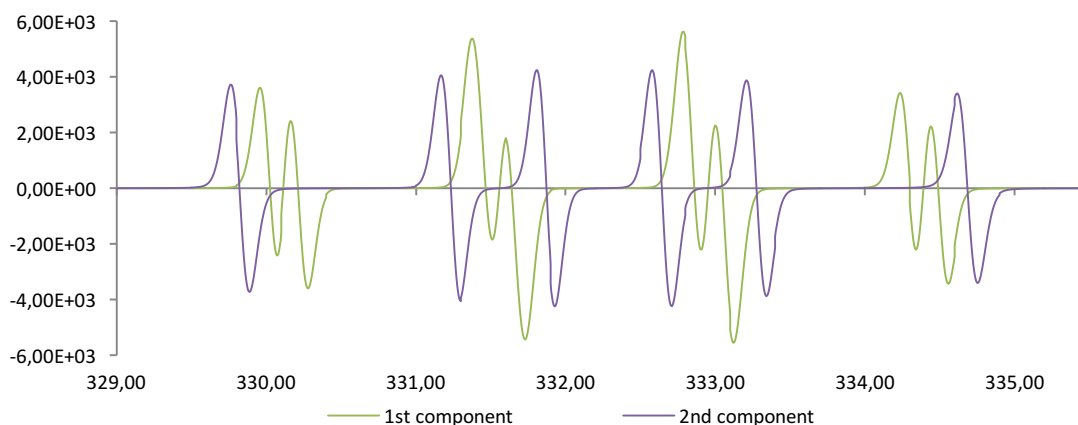


Figure S10. Simulated EPR spectra of the mixture of H₂TPP (**4**) with 3-phenylpropanal (**1**) and morpholine in DMSO: buffer pH = 4 (9:1) with DMPO



Additionally the EPR spectrum of the mixture of H₂TPP (**4**), morpholine and 3-phenylpropylaldehyde (**1**) was registered in the presence of 5,5-dimethyl-1-pyrroline *N*-oxide (DMPO spin trap) after light irradiation. When the DMPO spin trap was used, again two components can be seen in EPR spectrum (Figure S9). The first one, responsible for 63% of intensity ($a_N = 1.40$ mT, $a_{HB} = 1.47$ mT and $a_H = 0.20$ mT) corresponds to a carbon-centered radical adduct as indicated by the value of a_{HB} higher than a_N value and a small difference between them suggests the bulkiness of a radical (radical B) (Figure S10). The other component ($a_N = 1.41$ mT and $a_H = 2.05$ mT) corresponds to the DMSO-derived radical (DMPO-DMSO adduct), as a very similar radical

adduct was observed during UV irradiation of DMPO in DMSO solution.⁸ These experiments clearly suggest the formation of enamine radical B.

- H₂TPP (**4**) with EDA (**2**) in DMSO: buffer pH = 4 (9:1) was stirred under light irradiation (4xLED) for 10 minutes and then DMPO was added and after next 10 min. of stirring under irradiation (4xLED) EPR spectra (9.3 GHz) was recorded.

Figure S11. EPR spectra of the mixture of H₂TPP (**4**) with EDA (**2**) in DMSO: buffer pH = 4 (9:1) with DMPO

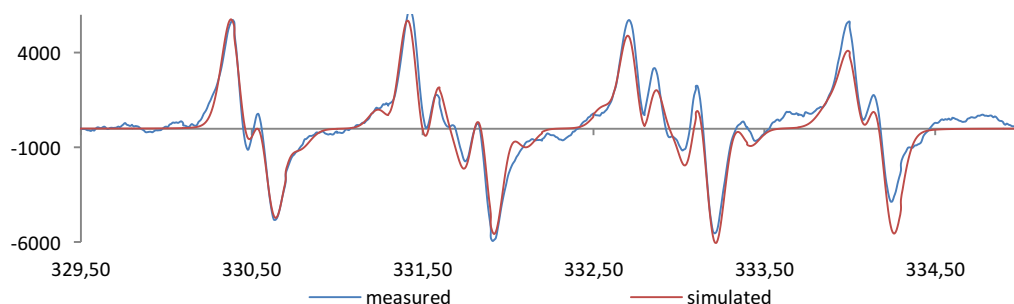
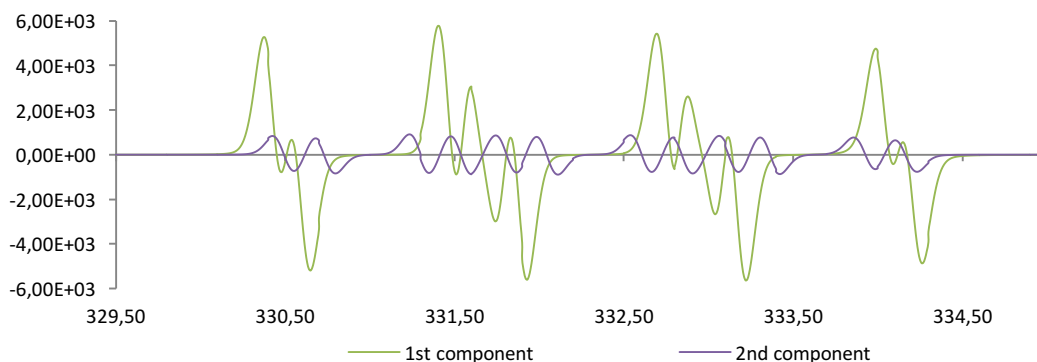


Figure S12. Simulated EPR spectra of the mixture of TPP (**4**) with EDA (**2**) in DMSO: buffer pH = 4 (9:1) with DMPO



When a mixture of H₂TPP (**4**) and EDA (**2**) was irradiated in the presence of DMPO, simulated EPR spectrum showed again two components (Figure S11). The spectrum is dominated (86% of intensity) by a signal with parameters as follows: $a_N = 1.29$ mT, $a_{H\beta} = 1.04$ mT and $a_{H\gamma} = 0.15$ mT. This signal can be tentatively ascribed to a peroxy radical, as it is similar to the DMPO $\cdot\text{-OOH}$ adduct signal in DMSO ($a_N = 1.27$ mT, $a_{H\beta} = 1.03$ mT, no $a_{H\gamma}$ given) (Figure S12). The second component comes from a radical adduct with $a_N = 1.32$ mT, $a_{H\beta} = 0.80$ mT and $a_{H\gamma} = 0.25$ mT. These parameters suggest an oxygen-centered radical. As it is known that PBN adduct with oxygen-centered radicals are not stable, contrary to the DMPO adducts, it is possible that at this stage of reaction oxygen-centered radicals

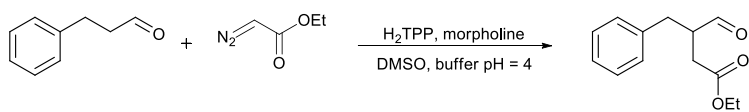
and radical adducts are formed, and then in case of PBN spin trap they react with a solvent to form secondary carbon-centered products. Parameters for the second component suggest an oxygen-centered radical. So this spin-trap is not suitable for the detection of radical C. Contrary to the experiment with BPN as a spin trap in the presence of DMPO no signal from DMSO-derived radical adduct could be seen.

Concluding, when the recorded EPR spectrum of the reaction mixture in the presence of PBN is very similar to the one simulated for a mixture of H₂TPP (4) and EDA (2) with no aldehyde added (Figure S8), while in the presence of DMPO to the one simulated for a mixture of H₂TPP (4), morpholine and aldehyde (1) (Figure S4 and Figure S7). Hence the use of two different spin-traps in the EPR experiments proved beneficial allowing the detection of two paramagnetic species B and C thus supporting the proposed mechanism. However, it should be clearly stated that we were not able to detect the radical D using this technique.

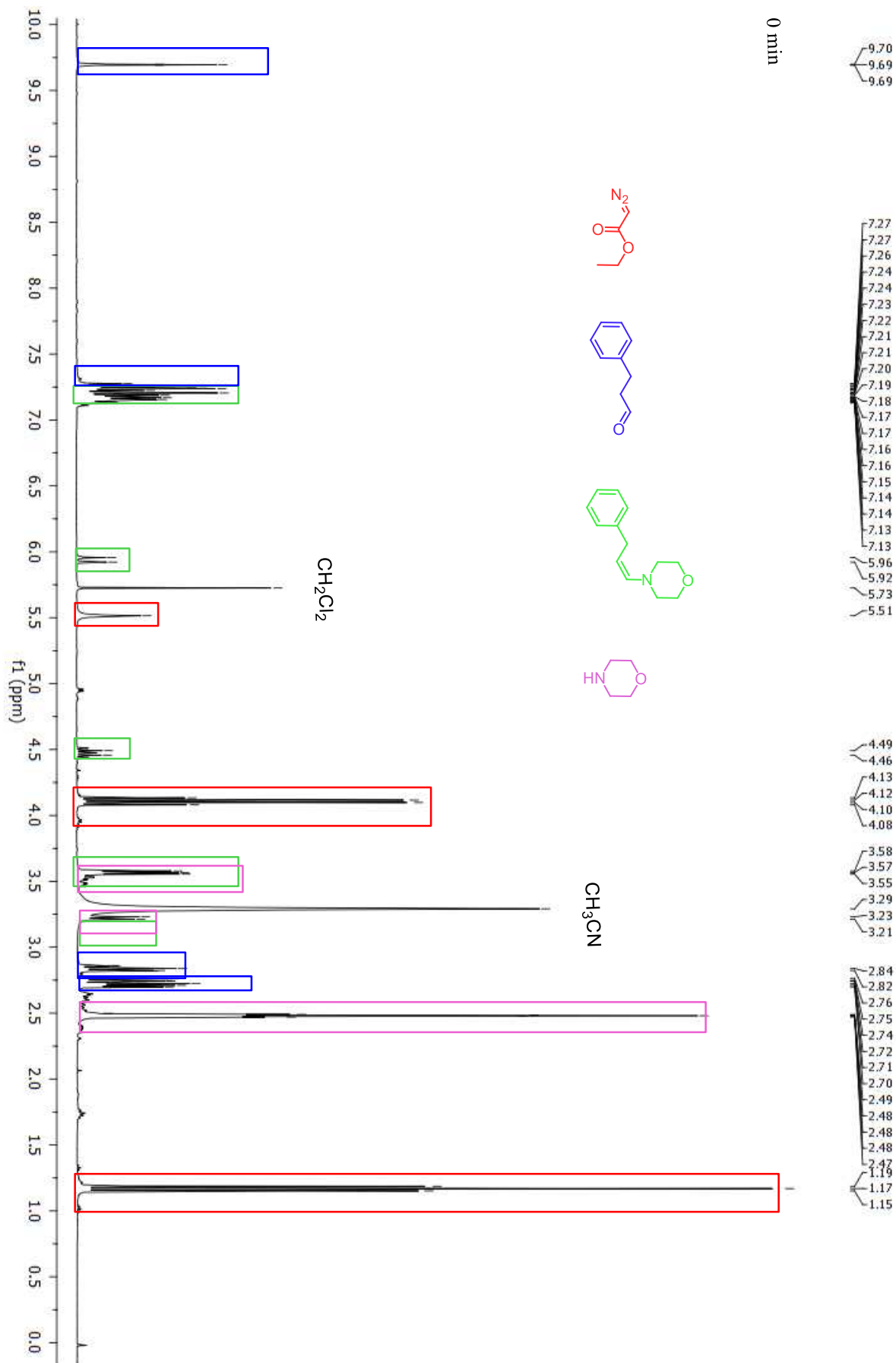
Simulated hyperfine splitting constants of spin adducts:

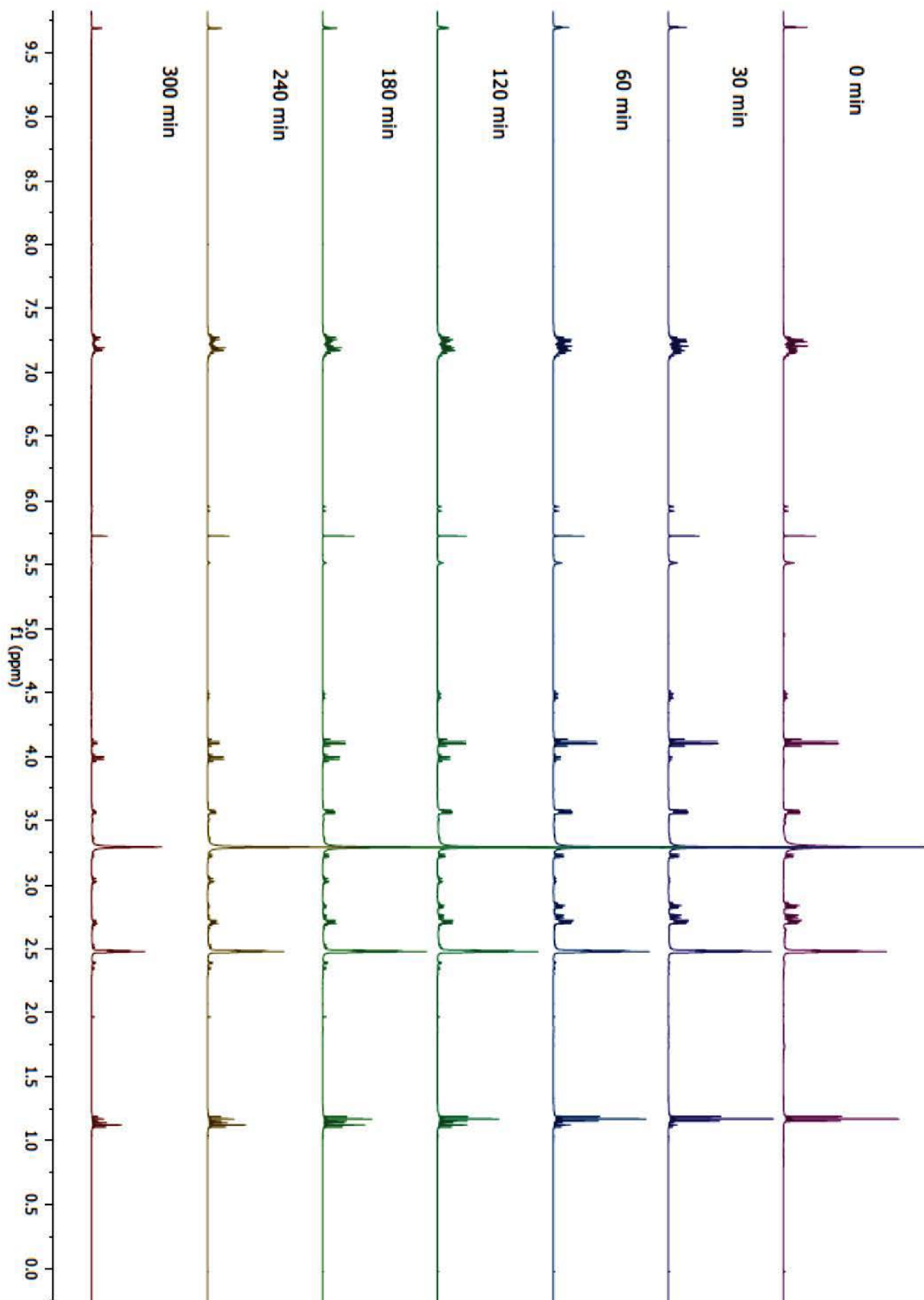
	Component	PBN			DMPO			
		a _N	a _H	% I	a _N	a _{Hβ}	a _{Hγ}	% I
3-phenylpropanal + morpholine	1	1.50	0.32	73	1.40	1.47	0.20	63
	2	1.37	0.23	27	1.41	2.05	-	37
EDA	1	1.49	0.40	76	1.29	1.04	0.15	86
	2	1.37	0.23	24	1.32	0.80	0.24	14
Reaction	1	1.49	0.40	77	1.40	1.48	0.19	62
	2	1.37	0.23	23	1.41	2.04	-	30
	3				1.36	0.73	0.17	8

5.3. NMR studies

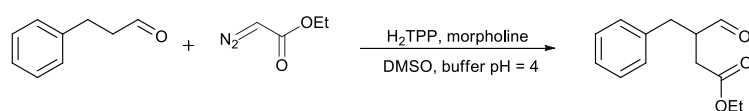


Reaction conditions: aldehyde (**1**) (0.5 mmol), morpholine (0.4 equiv., 0.2 mmol), EDA (**2**, 1 equiv., 0.5 mmol), H₂TPP (**4**, 1 mol%), DMSO-d₆ (5 mL). The progress of the reaction was followed by ¹H NMR spectroscopy. After 0, 30, 60, 120, 180, 240 and 300 min. of stirring under light irradiation (4xLED) NMR spectra (400 MHz) was recorded.

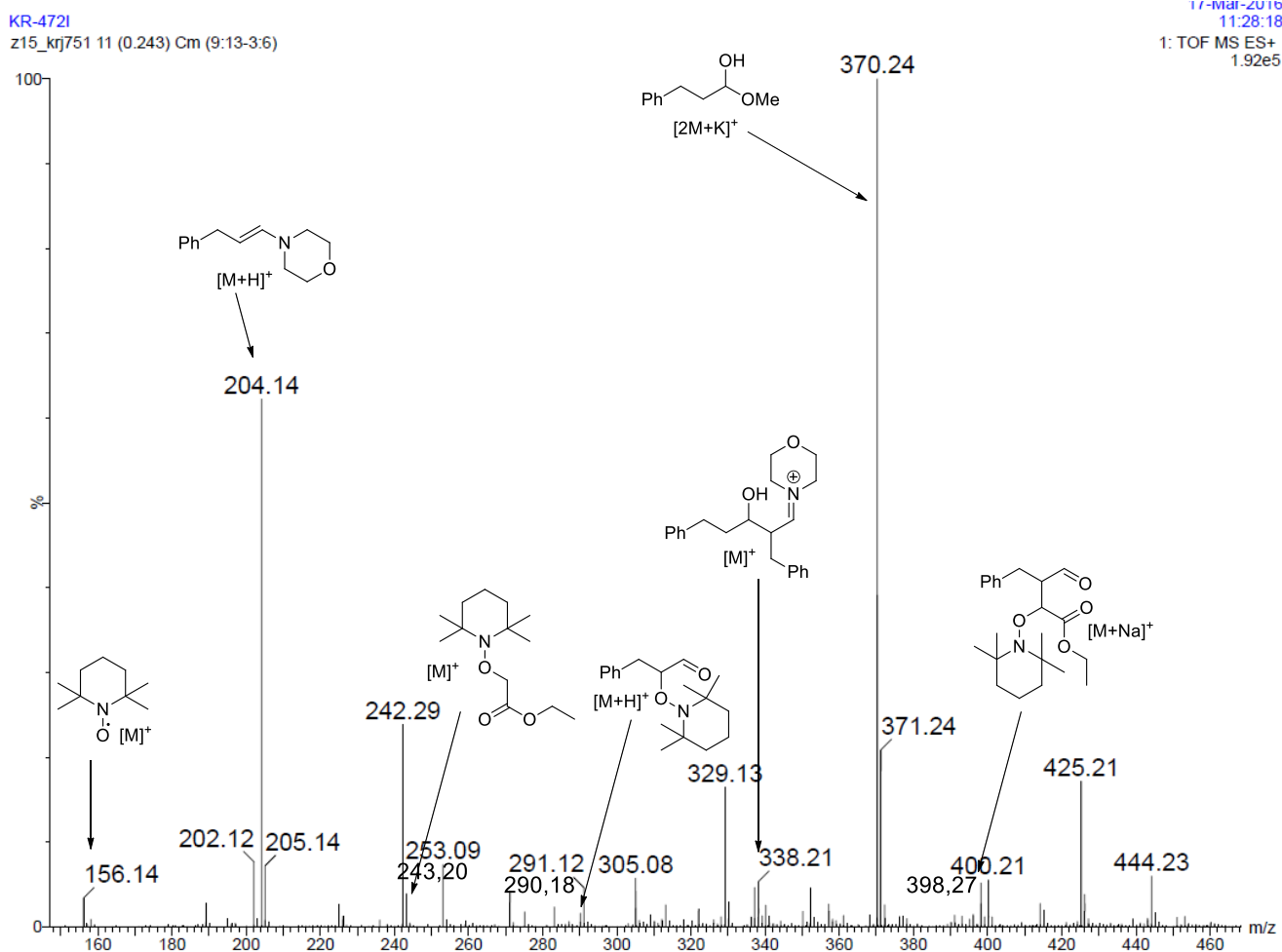




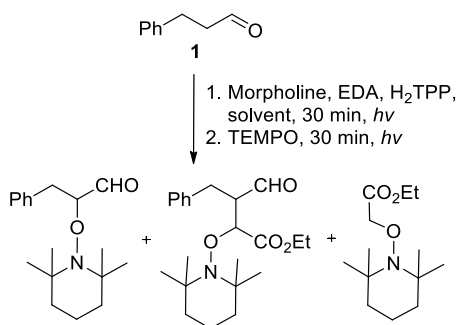
5.4. Mass spectrometry studies



Reaction conditions: aldehyde (**1**, 1 mmol), morpholine (0.4 equiv., 0.4 mmol), EDA (**2**, 1 equiv., 1 mmol), H₂TPP (**4**, 1 mol%), DMSO: buffer pH = 4 (10 mL, 9:1) after 30 min. of stirring under light irradiation (4xLED) TEMPO as a radical scavenger was added, and after 30 min. of stirring under light irradiation (4xLED) MS spectra was recorded.



The experiment confirmed the formation of three compounds with TEMPO hence three radical species were presents in the reaction mixture.



5.5. Electrochemical studies

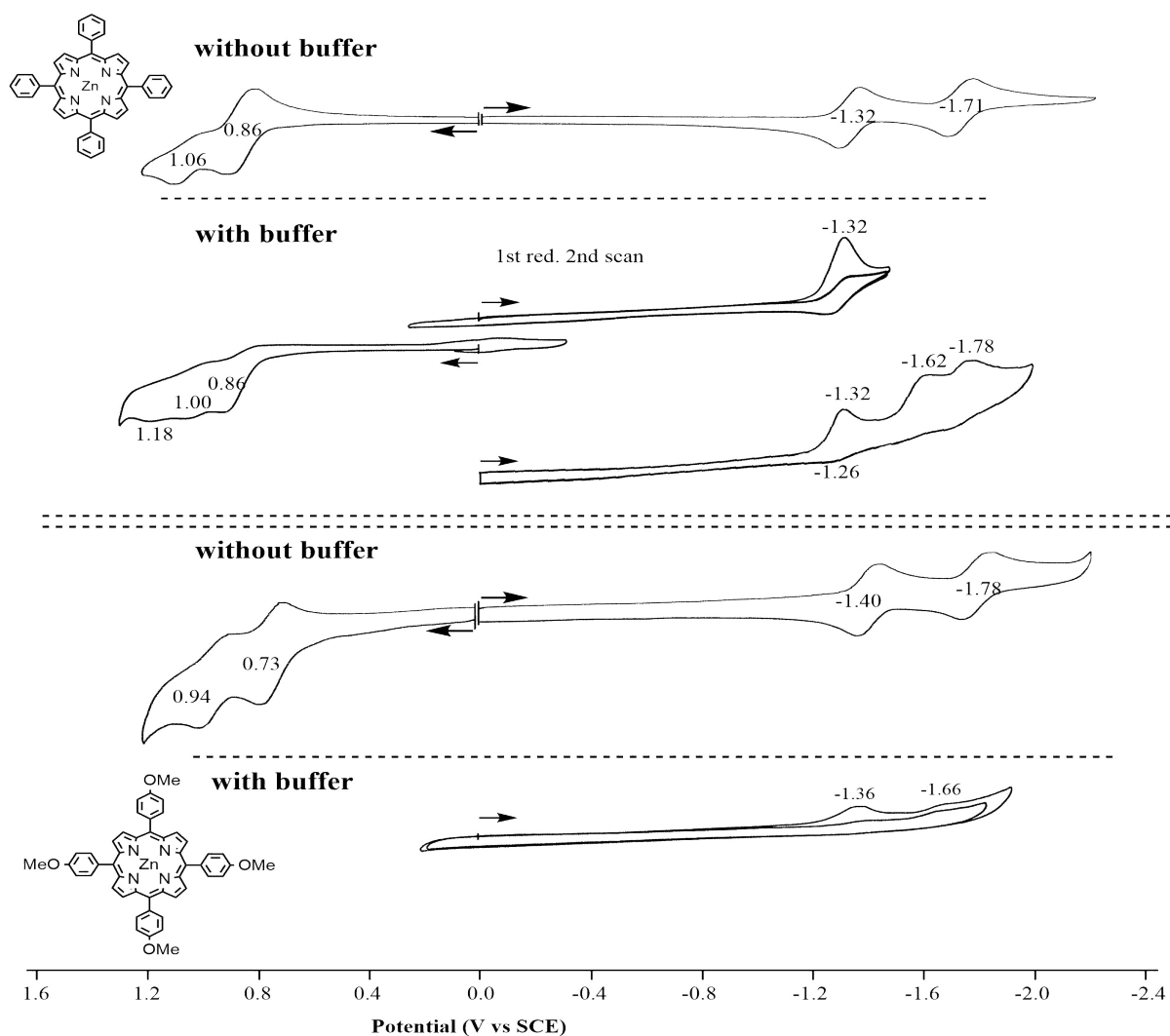
Materials:

CH₃COONa (s), CH₃COOH (l), distilled water, DMSO, TBAP (as a supporting electrolyte).

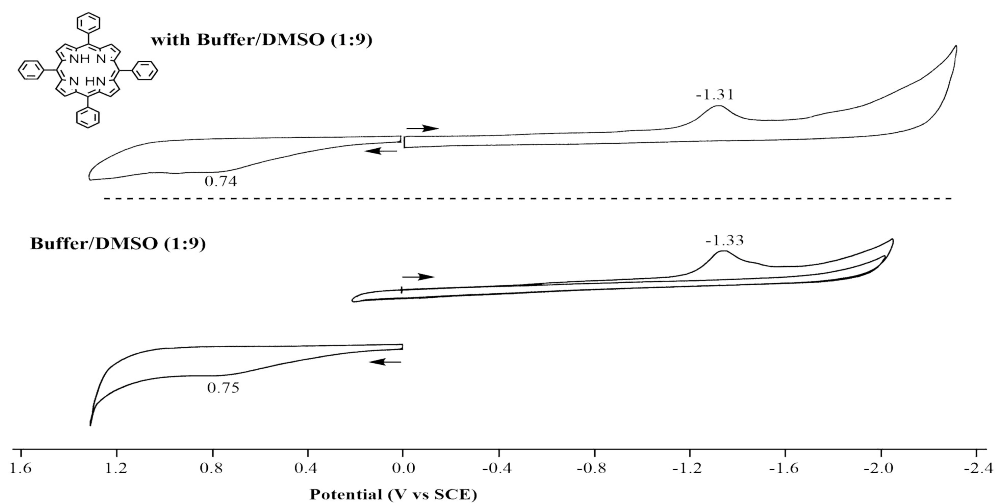
Experimental:

All the cyclic voltammetry experiments were performed under nitrogen and without bench light. Three-electrode system in home-made cell was used. Glass Carbon electrode was the working electrode, while Pt wire served as the counter electrode. Saturated calomel electrode was used as a reference.

- I) Cyclic voltammograms of two Zn porphyrins with and without buffer added to the DMSO solutions containing 0.1 M TBAP:

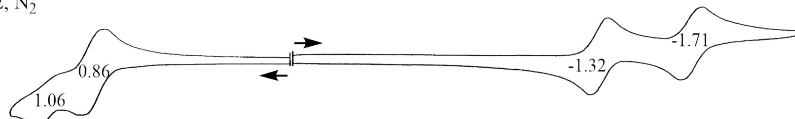


II) The comparison of Cyclic voltammograms of H₂TPP (**4**) with buffer and only buffer in DMSO, containing 0.1 M TBAP:

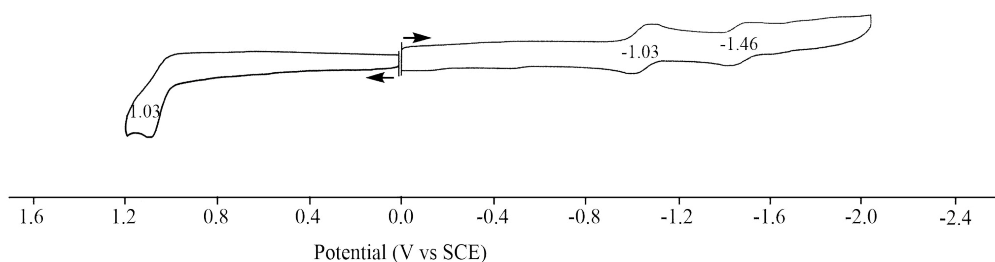


The reduction of ZnTPP (**Zn-4**) is located at $E_{1/2} = -1.32$ and -1.71 V and the oxidation at $E_{1/2} = 0.86$ V and 1.06 V. The reduction of H₂TPP (**4**) is at $E_{1/2} = -1.03$ and -1.46 V and the oxidation at 1.03 in DMSO, 0.1 M TBAP. A second oxidation is beyond the positive potential limit of the solvent.

a) ZnTPP in DMSO, 0.1 M TBAP
0.74mg/1.0ml, 100mV/s, 10 μ A/inch,
GCE vs SCE, N₂

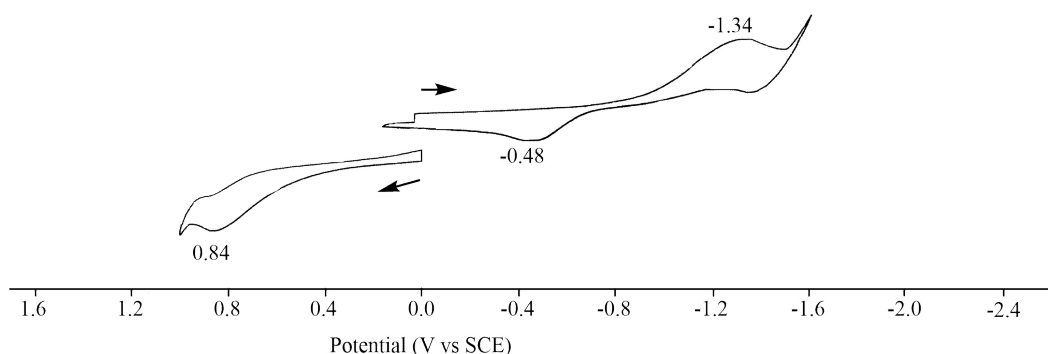


b) H₂TPP in DMSO, 0.1 M TBAP
0.70mg/1.5ml, 100mV/s, 2 μ A/inch
(not completely dissolved), GCE vs SCE, N₂

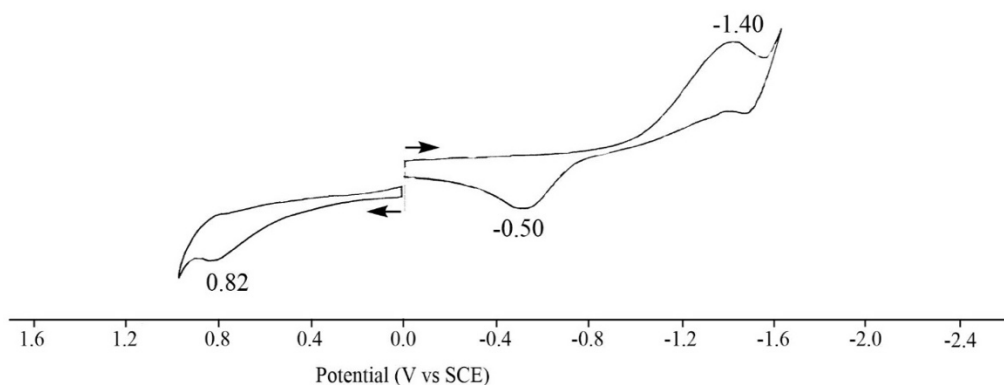


porphyrin	solution	electrode	cell	red.(V)	ox.(V)
ZnTPP	DMSO	GCE	regular	-1.32, -1.71	0.86, 1.06
ZnTPP	DMSO	Pt	thin-layer	-1.31, -1.70, (ox.-0.61)	0.85
ZnTPP	DMSO	Pt	regular	-1.33, -1.72, (ox. -0.54)	0.85

The cyclic voltammogram of DMSO:buffer pH = 4 (9:1) mixture shows one broad irreversible reduction at a peak potential between -1.20 and -1.36 V. There is also a re-oxidation peak at around $E_p = -0.50$ V (see CV below). We think the reduction results from protons in the buffer solution.



The CV of ZnTPP (**Zn-4**) or H₂TPP (**4**) in the DMSO:buffer pH = 4 (9:1) (0.1 M TBAP) is almost the same as the CV of the buffer in DMSO alone with 0.1 M TBAP. This is because the current for reduction of protons in the buffer is higher than that of the porphyrin when added to the buffer solution. Thus, it was not possible to observe the reduction of the porphyrin in the buffer solution.



Summary of selected measured potentials

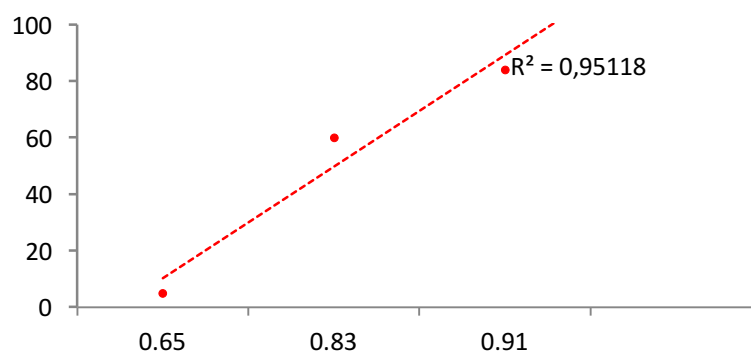
No	Porphyrin	Solution	electrode	cell	red.(V)	ox.(V)
1	none	DMSO	GCE	regular	range: 0.0 ~ -2.3	range: 0.0 ~ 1.3
2	ZnTPP, Zn-4	DMSO	GCE	regular	-1.32, -1.71	0.86, 1.06
3	H ₂ TPP, 4	DMSO	GCE	regular	-1.03, -1.45	1.03
9	none	DMSO	Pt	regular	range: 0.0 ~ -2.0	range: 0.0 ~ 1.1
10	ZnTPP, Zn-4	DMSO	Pt	regular	-1.33, -1.72,	0.85
11	H ₂ TPP, 4	DMSO	Pt	regular	-1.04, -1.46	--

Electrochemical data for porphyrins 4, 5, 9

Porphyrin	E_{ox}	E_{red}	E_{ox}^{*s}	E_{ox}^{*t}	E_{red}^{*s}	E_{red}^{*t}	E_{00}^s	E_{00}^t
TPP	1.03	-1.03; -1.43	-0.91	-0.42	0.91	0.42	1.90	1.45 ⁹
T(<i>p</i> -OMeP)P	0.91	-1.07; -1.46	-0.99	-0.54	0.83	0.38	1.90 ¹⁰	1.45 ¹⁰
T(F ₅ P)P	0.89; 1.23 ¹¹	-1.28; -1.71 ¹¹	-1.04	-0.78	0.65	0.39	1.93 ¹²	1.67 ¹²

E_{red}/E_{ox} vs SCE

The dependence of the reaction yield on reduction potentials of porphyrins



Energetics - considerations

Because of the irreversible electrochemical oxidation of the enamines, and solvents used (DMSO:buffer), we do not have exact values for the potentials for their oxidation. For acetonitrile, the voltammograms show peak potentials between about 0.3 and 0.6 V vs. SCE for oxidation of enamines.¹³ For irreversible oxidation the inflection points, rather than the peak potential, are representative for the standard reduction potentials.¹⁴ Therefore, we can assume that the reduction potentials for oxidation of enamines ranges between about 0.2 and 0.6 V vs. SCE. Furthermore, an increase in the media polarity causes negative shifts in the potentials of oxidation, making the enamines better electron donors; there are also positive shifts in the potentials of reduction, making the porphyrins better electron acceptors.¹⁵ Therefore, for PET initiated from the singlet-excited state of the porphyrins, ΔG most likely assumes negative values of a tens of electronvolts (estimated -0.39 V), making it thermodynamically favorable. Conversely, the triplet excited states of the sensitizers lie about half an electron volt below their singlet states, which may or may not results in positive values for the $\Delta G_{\text{PET}}^{(0)}$ estimates. Therefore, we cannot necessarily claim a triplet manifold for PET.

For estimating the driving force, $-\Delta G_{\text{PET}}^{(0)}$, of photoinduced electron transfer (PET) from the enamine to the photoexcited porphyrin, we use Rehm-Weller equation:

$$\Delta G_{\text{PET}}^{(0)} = F \left(E_{\text{D}^{+}/\text{D}}^{(0)} - E_{\text{A}/\text{A}^{\cdot-}}^{(0)} \right) - \mathcal{E}_{00} + \Delta G_{\text{S}} + W$$

Where $E_{\text{D}^{+}/\text{D}}^{(0)}$ (E_{ox}) is the reduction potential for oxidation of the donor (the enamine); $E_{\text{A}/\text{A}^{\cdot-}}^{(0)}$ (E_{red}) is the reduction potential for reduction of the acceptor (the porphyrin), F is the Faraday constant ($F = 1 \text{ e}$ for calculating the energy in eV), E_{00} is the zero-to-zero energy for PET from the singlet excited state, and the triplet energy for PET from the triplet excited state, ΔG_{S} is the Born solvation energy (accounting for the interaction energy between the generated ions and the solvent environment), and W is the Coulomb work term (accounting electrostatic interaction energy between the generated ions).

If the reduction potentials and E_{00} are measured for the same solvent media, $\Delta G_{\text{S}} = 0$.

$$E_{\text{ox}} = \text{estimated } \sim +0.6 \text{ V vs. SCE in } \text{CH}_3\text{CN}^{13}$$

$$E_{\text{red}}(\text{TPP}) = -1.03 \text{ V vs. SCE}$$

$$E_{00} = 1.94 \text{ eV}$$

$$W = -e^2 / 4 \pi \epsilon_0 \epsilon R_{\text{DA}}$$

Where the dielectric permittivity of vacuum is, $\epsilon_0 = 8.854 \times 10^{-12} \text{ F m}^{-1} = 5.526 \times 10^{-3} \text{ e V}^{-1} \text{ \AA}^{-1}$

For the center-to-center donor-acceptor distance, R_{DA} , we can use the sum of the van der Waals radii of the donor and the acceptor, assuming that the PET occurs during contact (collision) between them (i.e., inner sphere ET). For the dielectric constant, we used the dielectric constant of DMSO, $\epsilon = 47$.

$$W = -0.061 \text{ eV for } R_{DA} = 5 \text{ \AA}$$

$$W = -0.077 \text{ eV for } R_{DA} = 4 \text{ \AA}$$

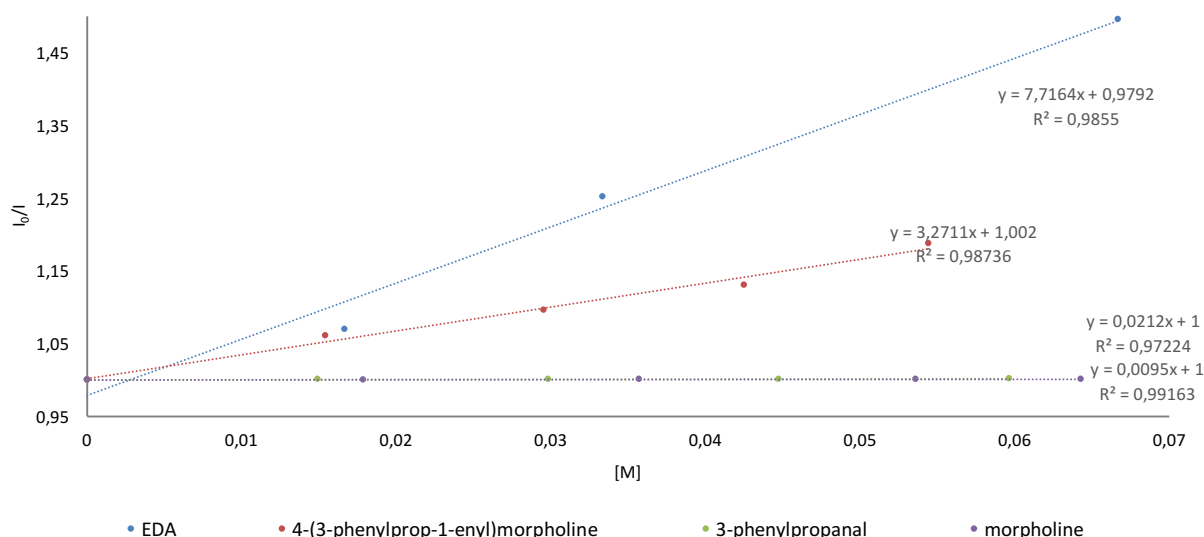
$$W = -0.102 \text{ eV for } R_{DA} = 3 \text{ \AA}$$

Making $\Delta G_{\text{PET}}^{(0)}$ acquire negative value (-0.39 V), implying that PET is thermodynamically possible.

5.6. Stern–Volmer quenching experiment

a. H₂TPP (4)

Stern-Volmer analyses for each of the reaction components clearly showed that enamine and EDA (2) strong, in comparison with morpholine and 3-phenylpropanal (1), quenching of H₂TPP (4) occurred. For 3-phenylpropanal, EDA, 4-(3-phenylprop-1-enyl)morpholine, morpholine and H₂TPP (4) samples were prepared by adding solutions of substrates to H₂TPP (4) solution in DMSO (total volume 2 mL) and degassed with Ar. The concentration of H₂TPP (4) in DMSO was 3.6 × 10⁻⁵ M. Samples were irradiated at 420 nm, and emission was detected at 651 nm.



Stern–Volmer quenching rate data:

Rates of quenching (k_q) were determined using Stern–Volmer kinetics:

$$\frac{I_0}{I} = 1 + k_q \cdot \tau \cdot [\text{quencher}]$$

Where I_0 - the luminescence intensity without the quencher,

I - the intensity with the quencher,

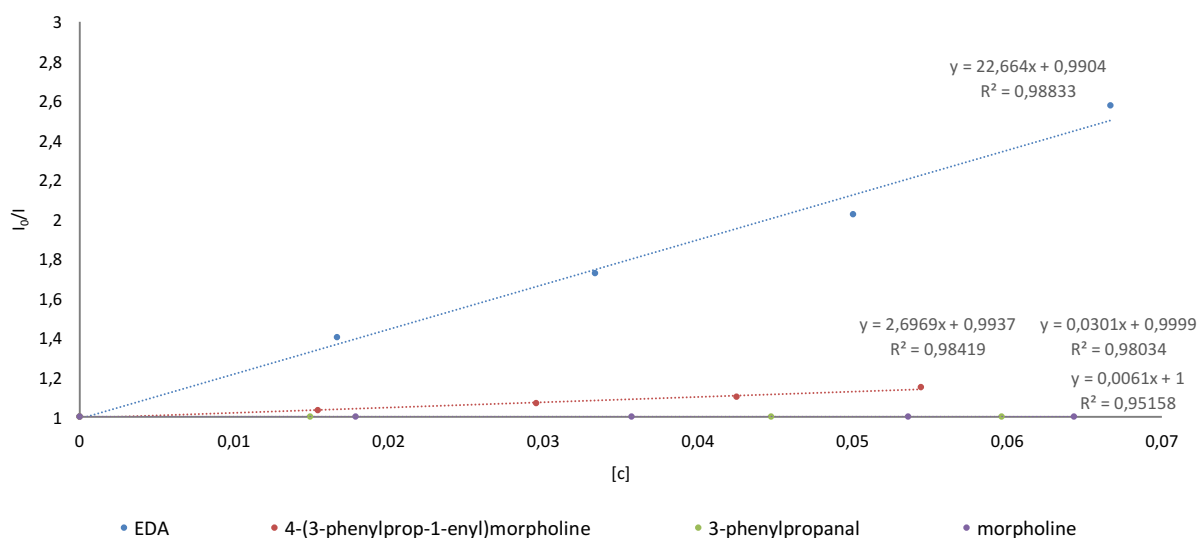
τ - the lifetime of the photocatalyst (for TPP is 9.95 ns)¹⁶

a) EDA: $k_q = 7.3 \cdot 10^8 [M^{-1}s^{-1}]$

b) 4-(3-phenylprop-1-enyl)morpholine : $k_q = 3.3 \cdot 10^8 [M^{-1}s^{-1}]$

b. Porphyrin 9

Stern-Volmer analyses for each of the reaction components clearly showed that enamine and EDA (**2**) strong, in comparison with morpholine and 3-phenylpropanal (**1**), quenching of porphyrin **9** occurred. For 3-phenylpropanal, EDA (**2**), 4-(3-phenylprop-1-enyl)morpholine, morpholine and porphyrin **9** samples were prepared by adding solutions of substrates to TPP solution in DMSO (total volume 2 mL) and degassed with Ar. The concentration of porphyrin **9** in DMSO was 3.4×10^{-5} M. Samples were irradiated at 420 nm, and emission was detected at 651 nm.



Stern–Volmer quenching rate data:

Rates of quenching (k_q) were determined using Stern–Volmer kinetics:

$$\frac{I_0}{I} = 1 + k_q \cdot \tau \cdot [\text{quencher}]$$

Where I_0 - the luminescence intensity without the quencher,

I - the intensity with the quencher,

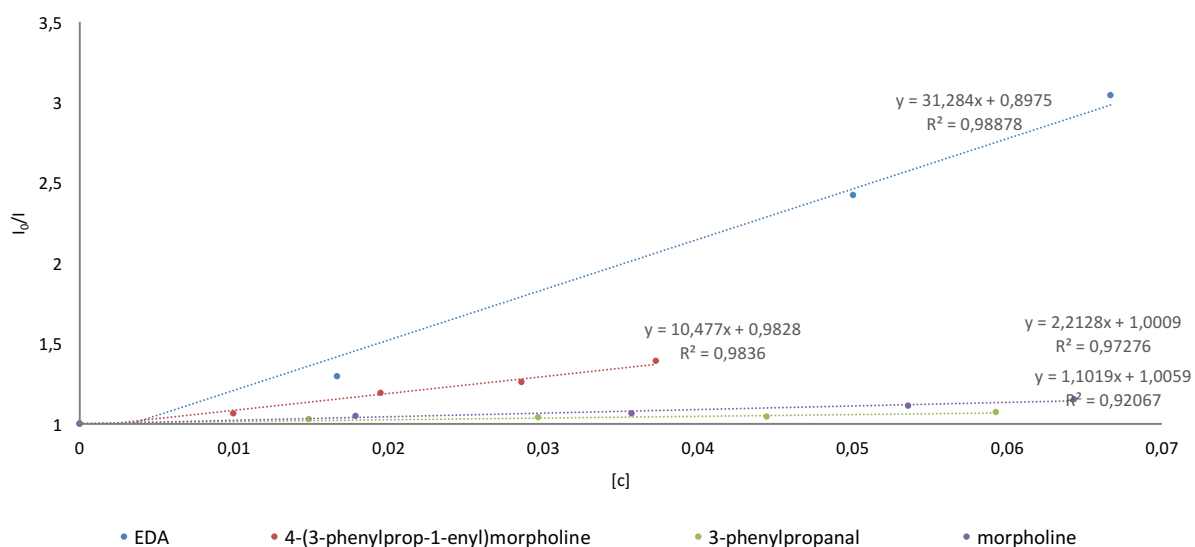
τ - the lifetime of the photocatalyst (for porphyrin **9** is 8.6 ns)¹⁷

a) EDA: $k_q = 2.6 \cdot 10^9 [M^{-1}s^{-1}]$

b) 4-(3-phenylprop-1-enyl)morpholine: $k_q = 2.9 \cdot 10^8 [M^{-1}s^{-1}]$

c. Porphyrin 5:

Stern-Volmer analyses for each of the reaction components clearly showed that enamine and EDA (**2**) strong, in comparison with morpholine and 3-phenylpropanal (**1**), quenching of porphyrin **5** occurred. For 3-phenylpropanal, EDA (**2**), 4-(3-phenylprop-1-enyl)morpholine, morpholine and porphyrin **5** samples were prepared by adding solutions of substrates to porphyrin **5** solution in DMSO (total volume 2 mL) and degassed with Ar. The concentration of porphyrin **5** in DMSO was 3.8×10^{-5} M. Samples were irradiated at 411 nm, and emission was detected at 636 nm.



Stern–Volmer quenching rate data:

Rates of quenching (k_q) were determined using Stern–Volmer kinetics (E1):

$$\frac{I_0}{I} = 1 + k_q \cdot \tau \cdot [\text{quencher}]$$

Where I_0 - the luminescence intensity without the quencher,

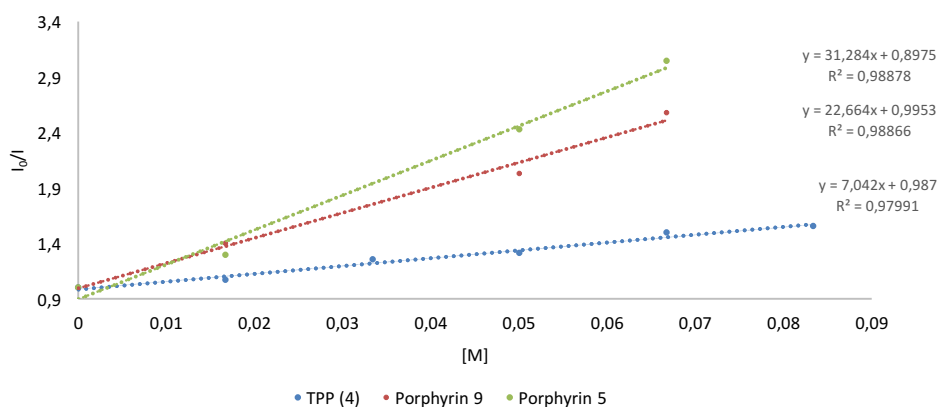
I - the intensity with the quencher,

τ - the lifetime of the photocatalyst (for porphyrin **5** is 10.1 ns)¹⁸

a) EDA: $k_q = 2.9 \cdot 10^9 [M^{-1}s^{-1}]$

b) 4-(3-phenylprop-1-enyl)morpholine : $k_q = 1.0 \cdot 10^8 [M^{-1}s^{-1}]$

d. Stern–Volmer quenching experiment for EDA – comparison of catalysts used:



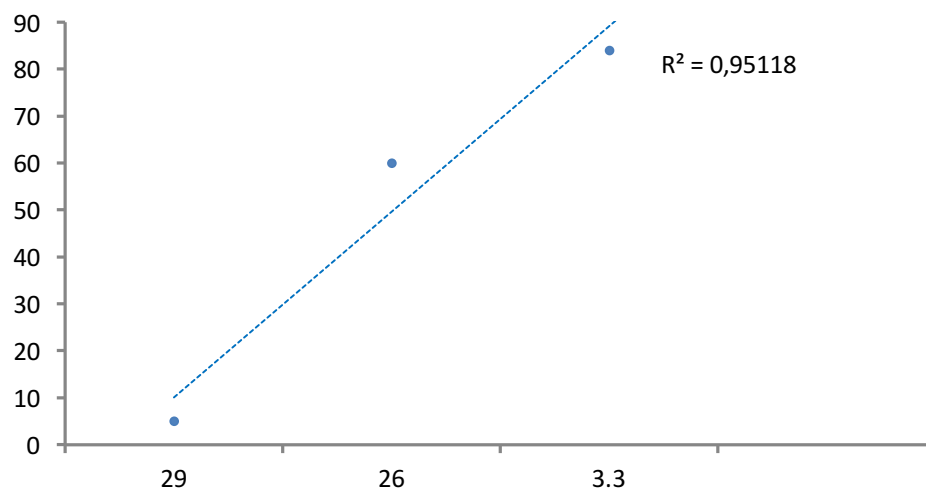
e. Photophysical properties of H₂TPP and ZnTPP

dye	ϕ_f	τ_f [ns]	k_f [s ⁻¹]	k_{isc} [s ⁻¹]	ϕ_T	τ_T [μs]	k_T [s ⁻¹]	$E_{00} S_1$ [eV]	$E_{00} T_1$ [eV]
H ₂ TPP	0.13 ¹⁹	13.6 ¹⁹	8.7 ¹⁹	4.7 × 10 ⁷ ¹⁹	0.82 ¹⁹			1.94 ⁹	1.45 ⁹
ZnTPP	0.04 ¹⁹	2.7 ¹⁹	1.7 × 10 ⁷ ¹⁹	3.6 × 10 ⁶ ¹⁹	0.88 ¹⁹		0.38 × 10 ² ¹⁹	2.04 ¹⁰	1.59 ¹⁰
Ru(bpy) ₃		890			0.04 ²⁰	0.6 ²⁰		2.12 ²⁰	

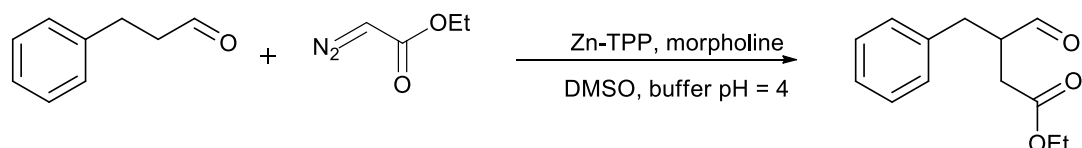
f. Photophysical data for porphyrins 4, 5, 9

	H ₂ T(<i>p</i> -OMeP)P	H ₂ TPP	H ₂ T(F ₅ P)P
reaction yield	60	84	traces
τ_0	8.6 ns	9.95 ns	10.1 ns
k_q enamine	2.9 · 10 ⁸ [M ⁻¹ s ⁻¹]	3.3 · 10 ⁸ [M ⁻¹ s ⁻¹]	1.0 · 10 ⁹ [M ⁻¹ s ⁻¹]
k_q EDA	2.6 · 10 ⁹ [M ⁻¹ s ⁻¹]	7.3 · 10 ⁸ [M ⁻¹ s ⁻¹]	2.9 · 10 ⁹ [M ⁻¹ s ⁻¹]
$E_{red}P^*$	0.83 V	0.91 V	0.65 V

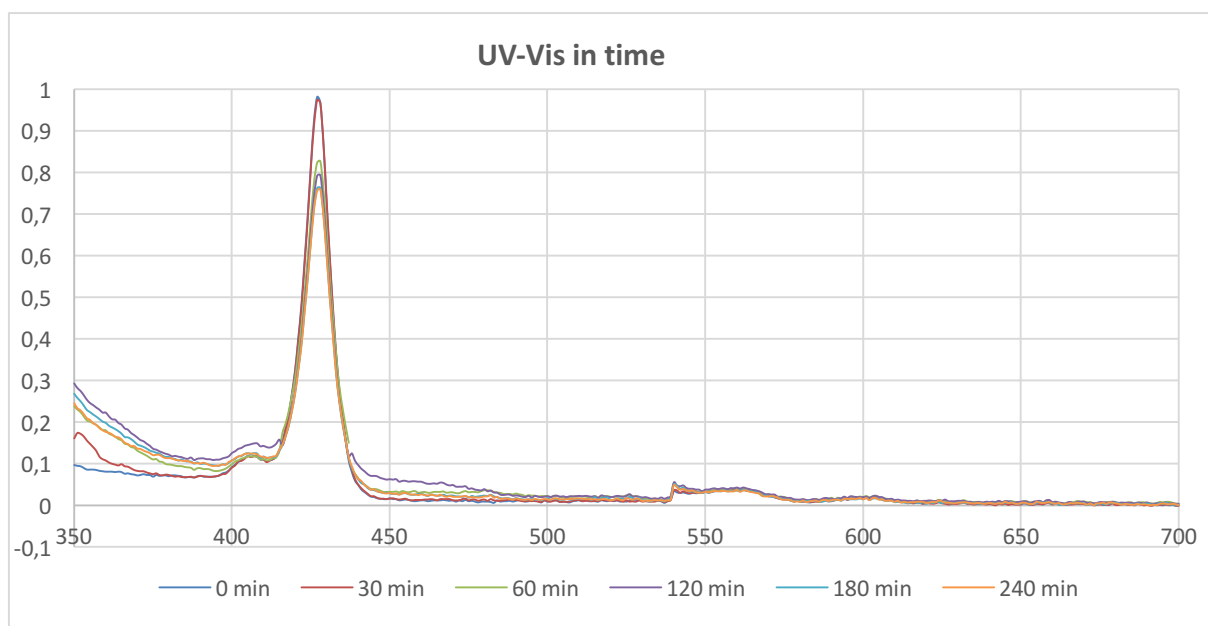
g. The dependence of the reaction yield on the luminescence quenching rate by enamine



5.7. UV-Vis spectroscopy studies



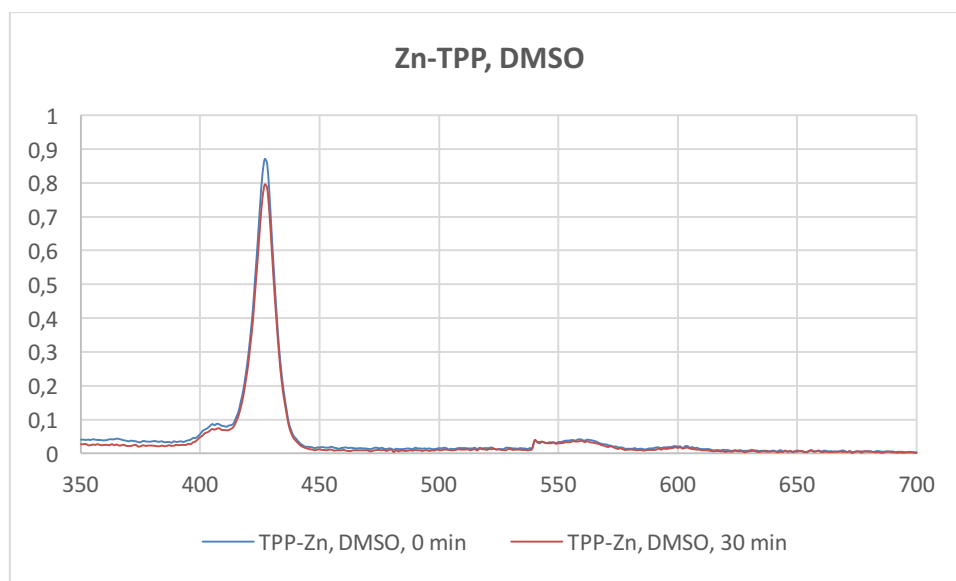
Reaction conditions: aldehyde (**1**, 0.5 mmol), morpholine (0.4 equiv., 0.2 mmol), EDA (**2**, 1 equiv., 0.5 mmol), Zn-TPP (0.2 mol%), CH₃CN (5mL). To support the proposed mechanism the progress of the reaction was also monitored by UV-Vis. After 0, 30, 60, 120, 180 and 240 min. of stirring under light irradiation (4xLED) the sample of 200 μ L was taken from the reaction and it was diluted with DMSO to 10.2 mL and UV-Vis spectra was recorded.



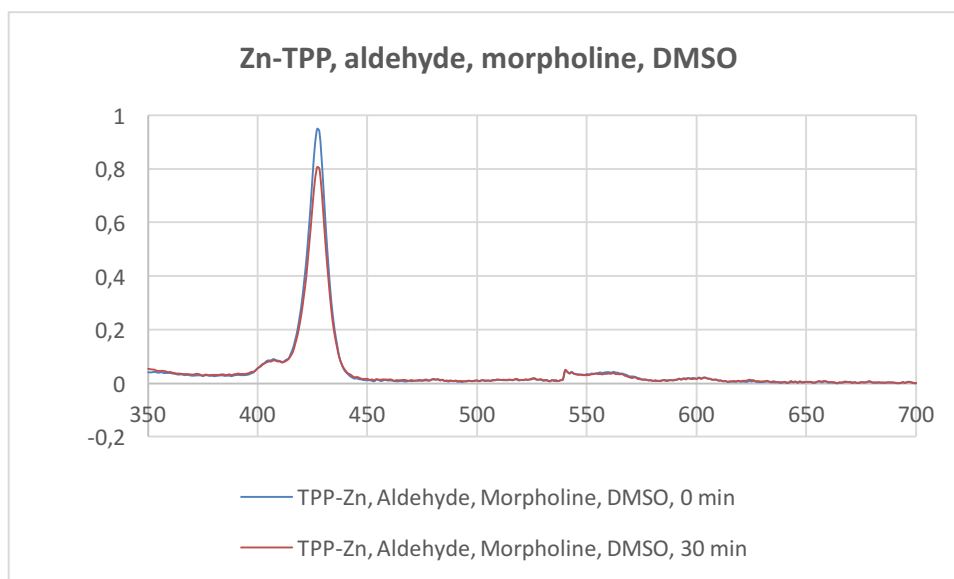
The experiment shows that to the end of the photochemical reaction porphyrin is still present in the reaction mixture but its concentration slightly decreases.

The control UV-Vis experiments of substrates and background's reactions were also performed:

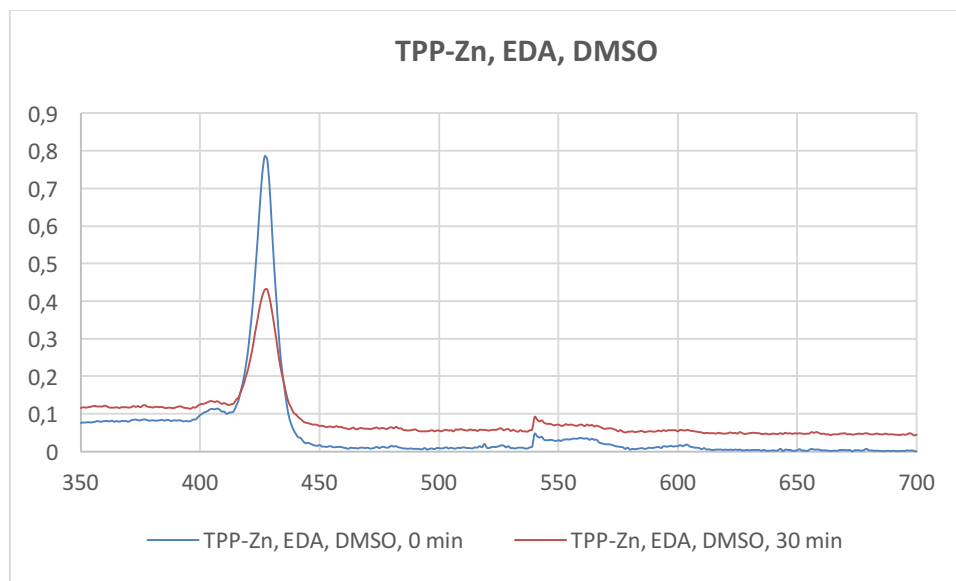
- 1) Zn-TPP after 0 min. of stirring under light irradiation (4xLED) and 30 min. of stirring under light irradiation (4xLED):



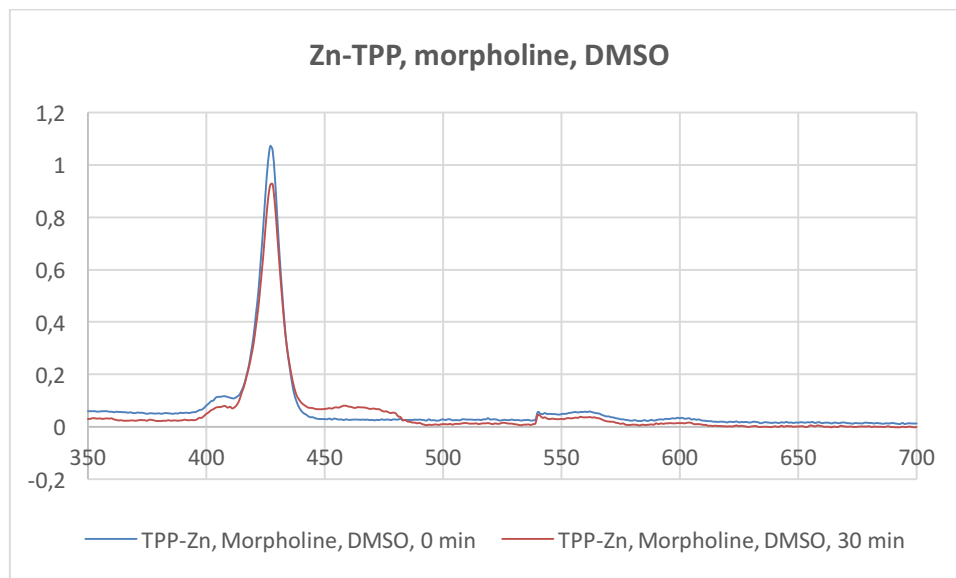
- 2) Zn-TPP, 3-phenylpropanal and morpholine in DMSO after 0 min. of stirring under light irradiation (4xLED) and 30 min. of stirring under light irradiation (4xLED):



- 3) Zn-TPP and EDA in DMSO after 0 min. of stirring under light irradiation (4xLED) and 30 min. of stirring under light irradiation (4xLED):

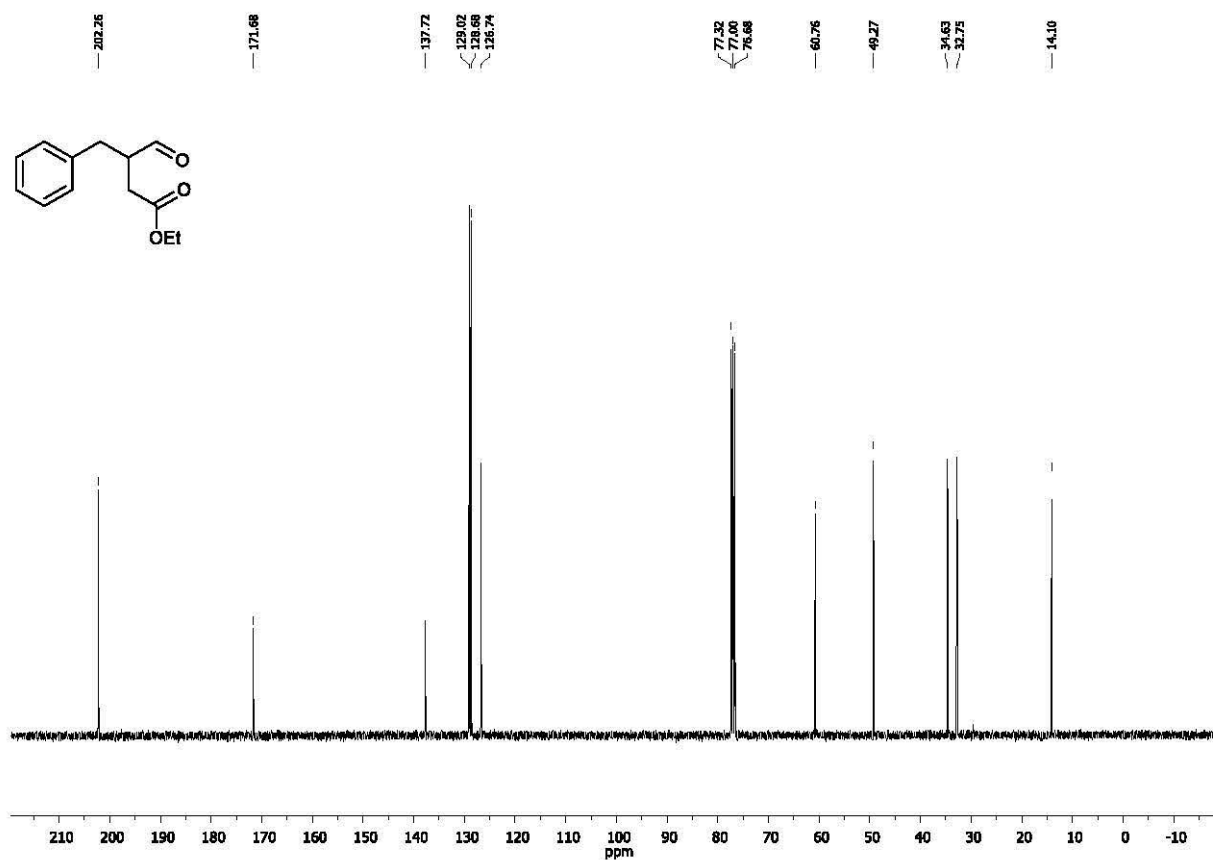
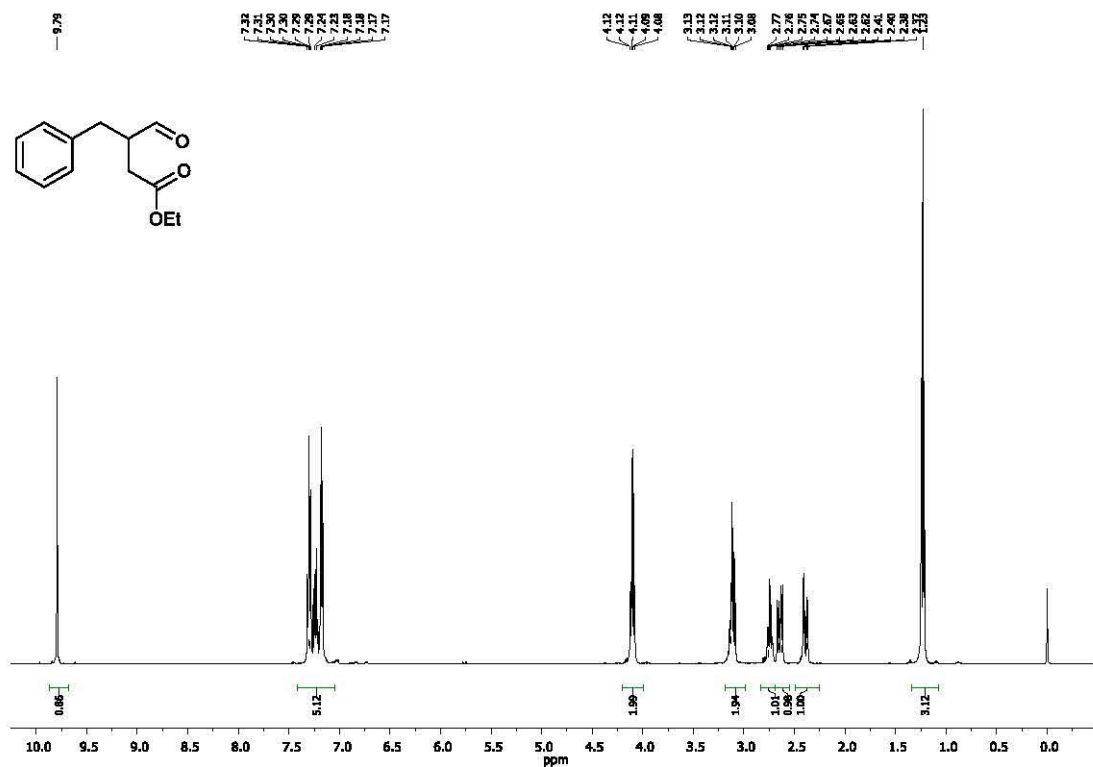


- 4) Zn-TPP and morpholine in DMSO after 0 min. of stirring under light irradiation (4xLED) and 30 min. of stirring under light irradiation (4xLED):

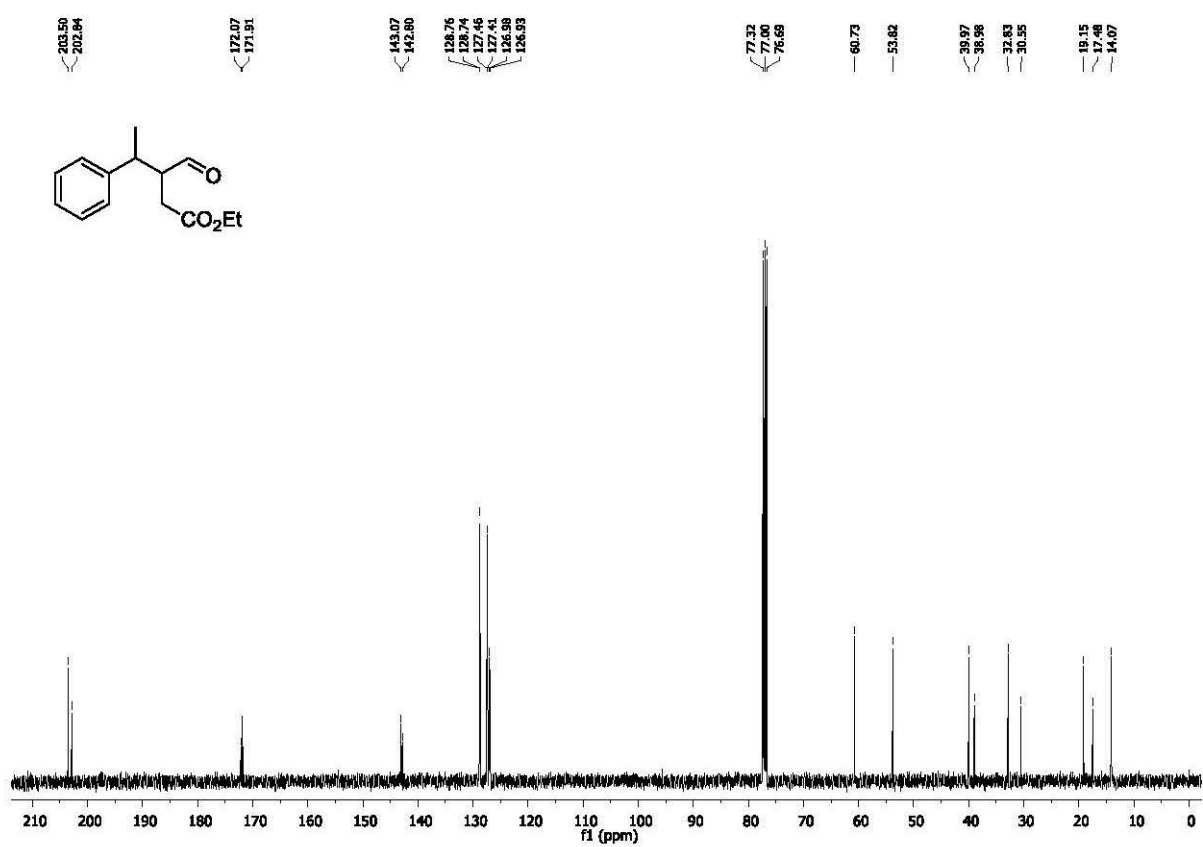
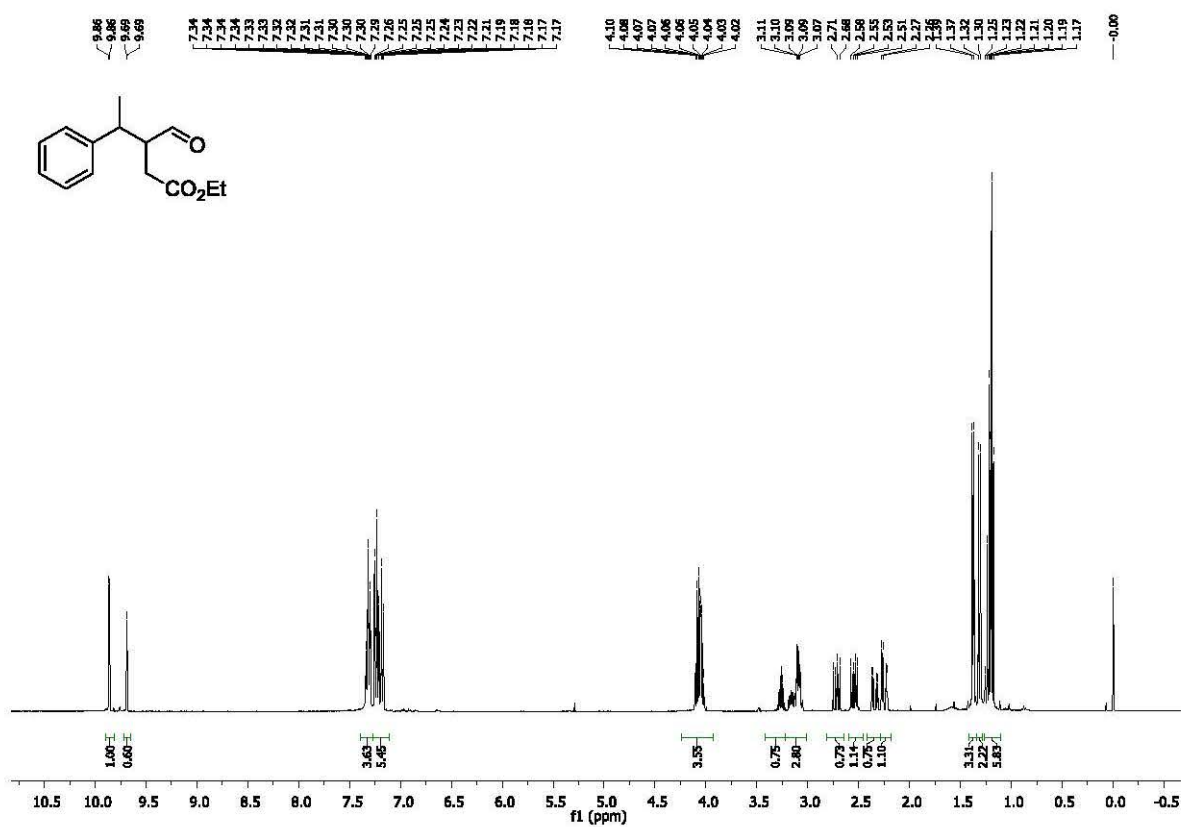


The background experiments showed that in the presence of EDA porphyrin decomposes.

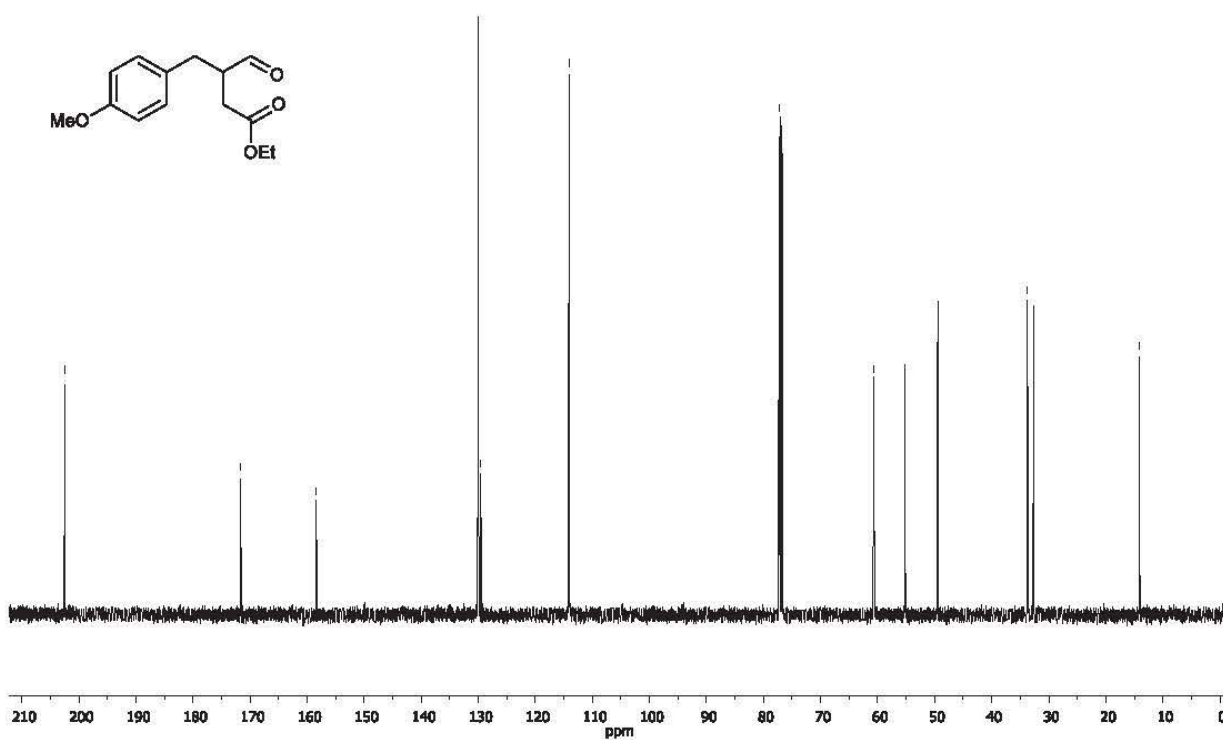
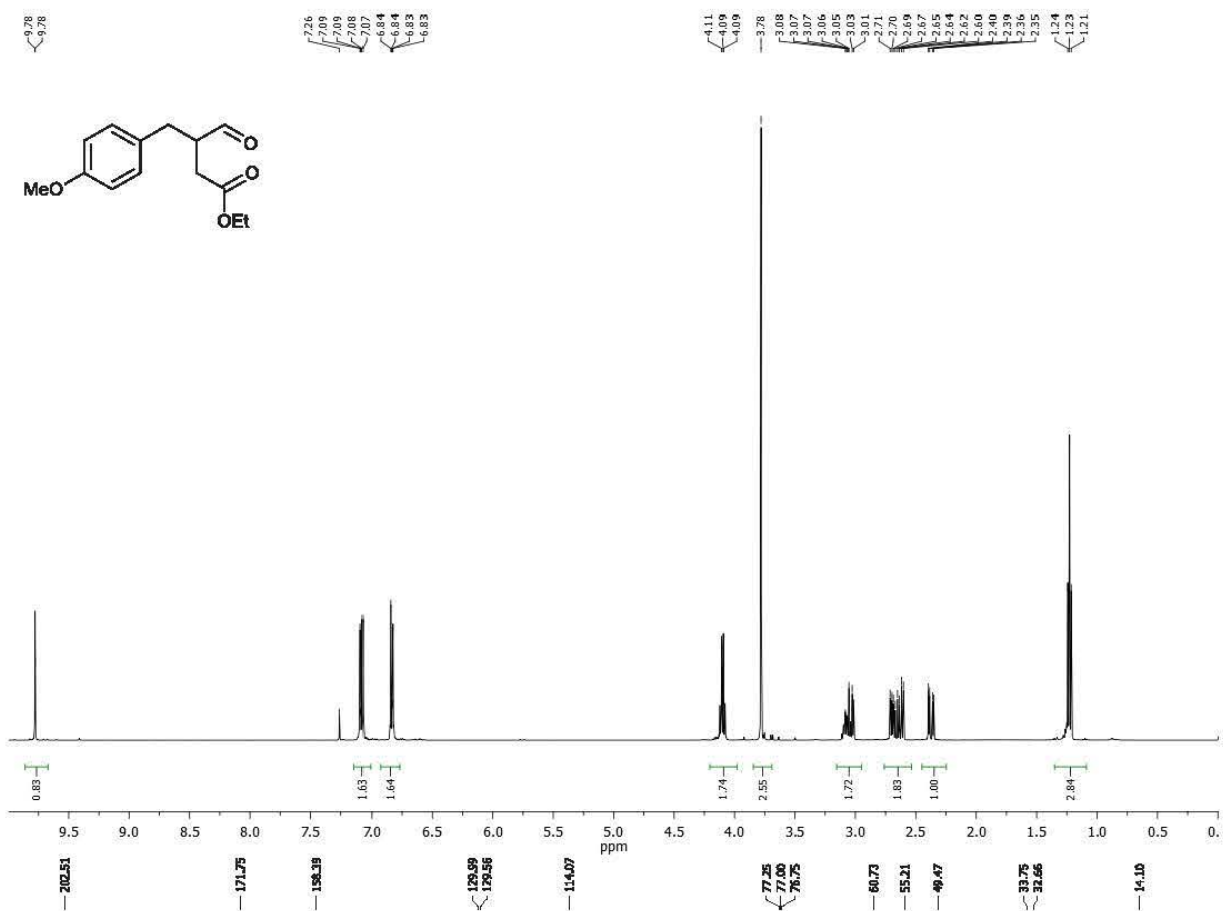
6. ^1H and ^{13}C NMR spectra
 a) Ethyl 3-benzyl-4-oxobutanoate (3)



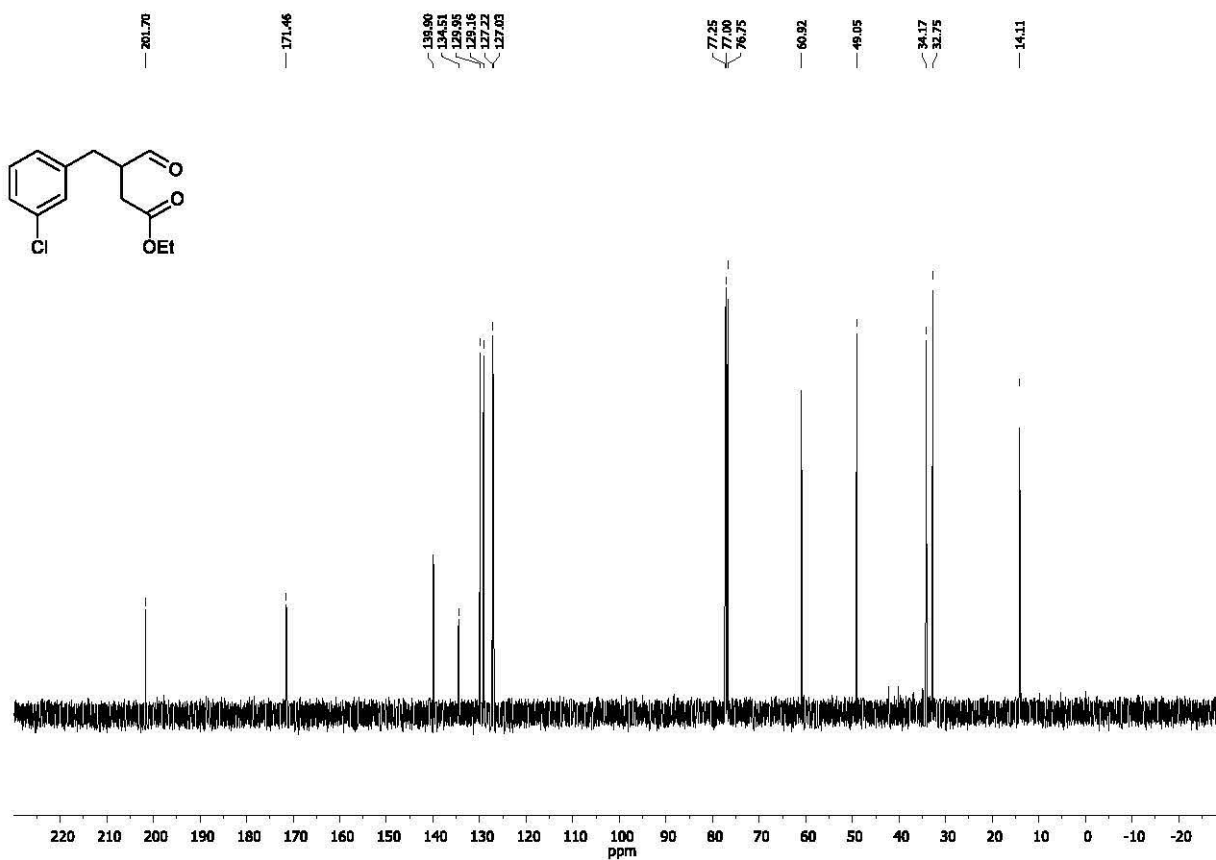
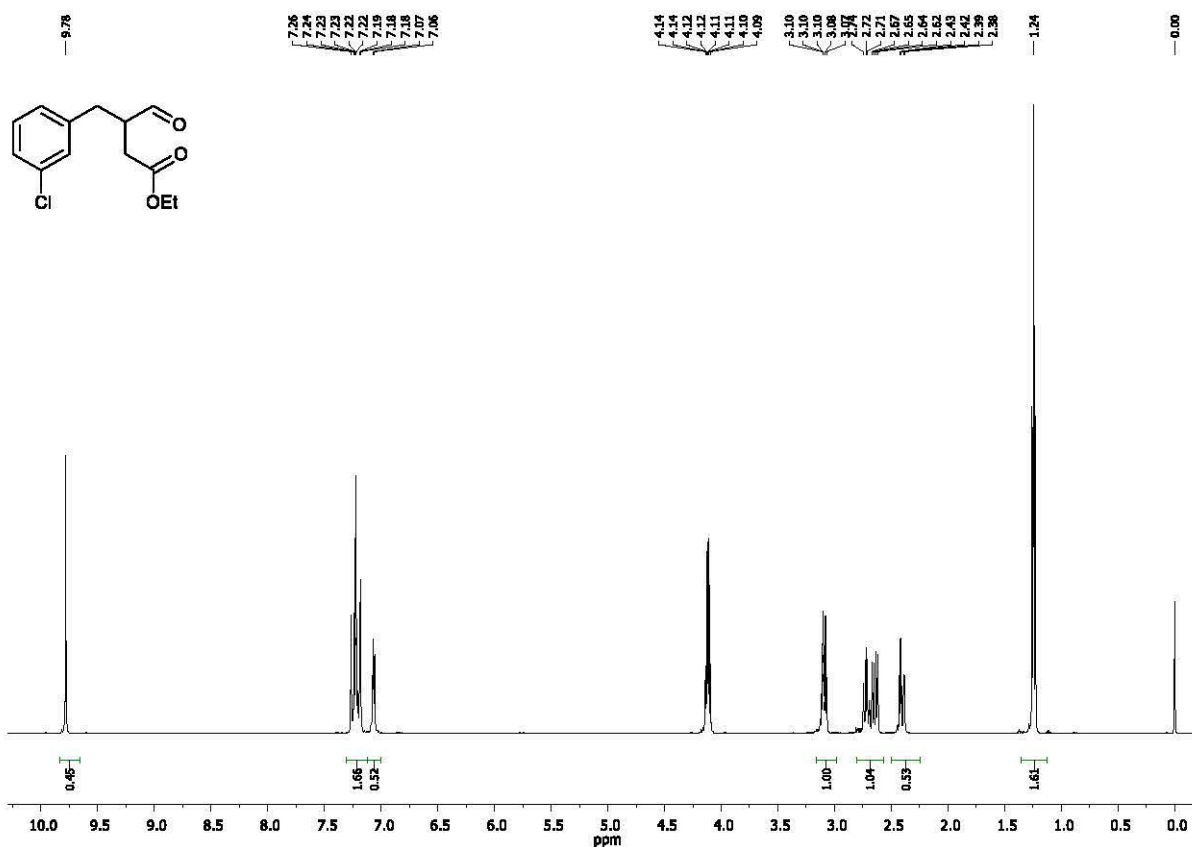
b) Ethyl 3-formyl-4-phenylpentanoate (14)



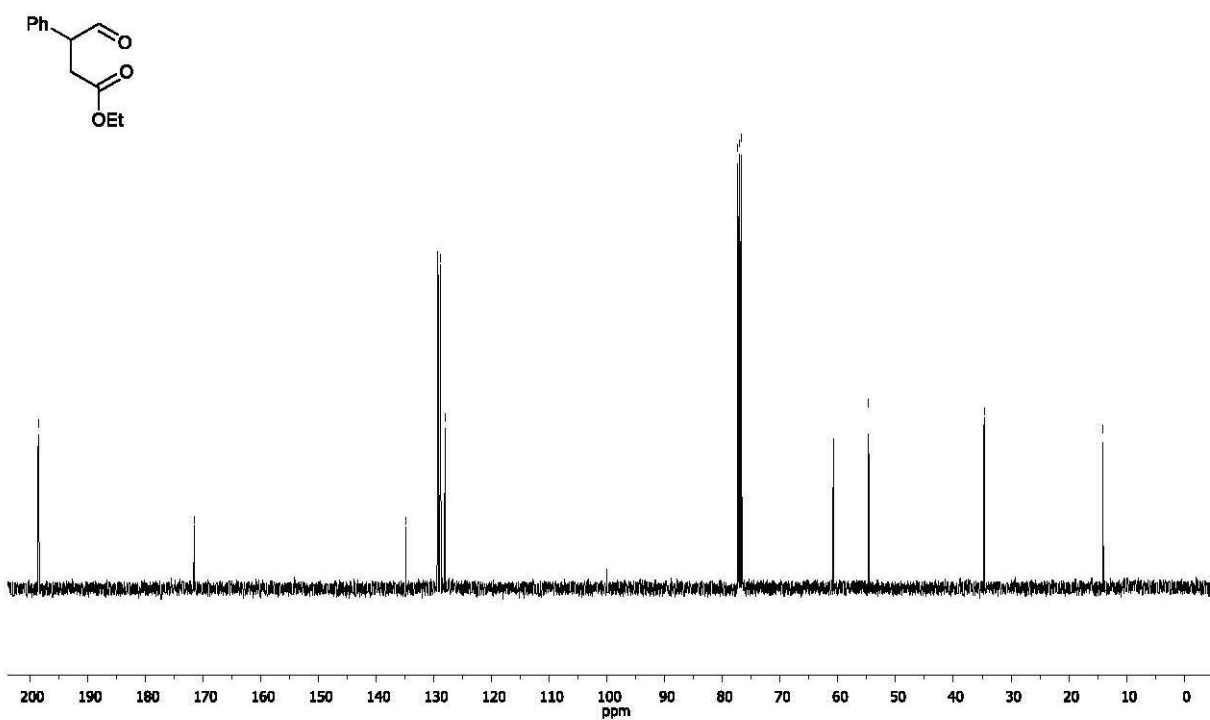
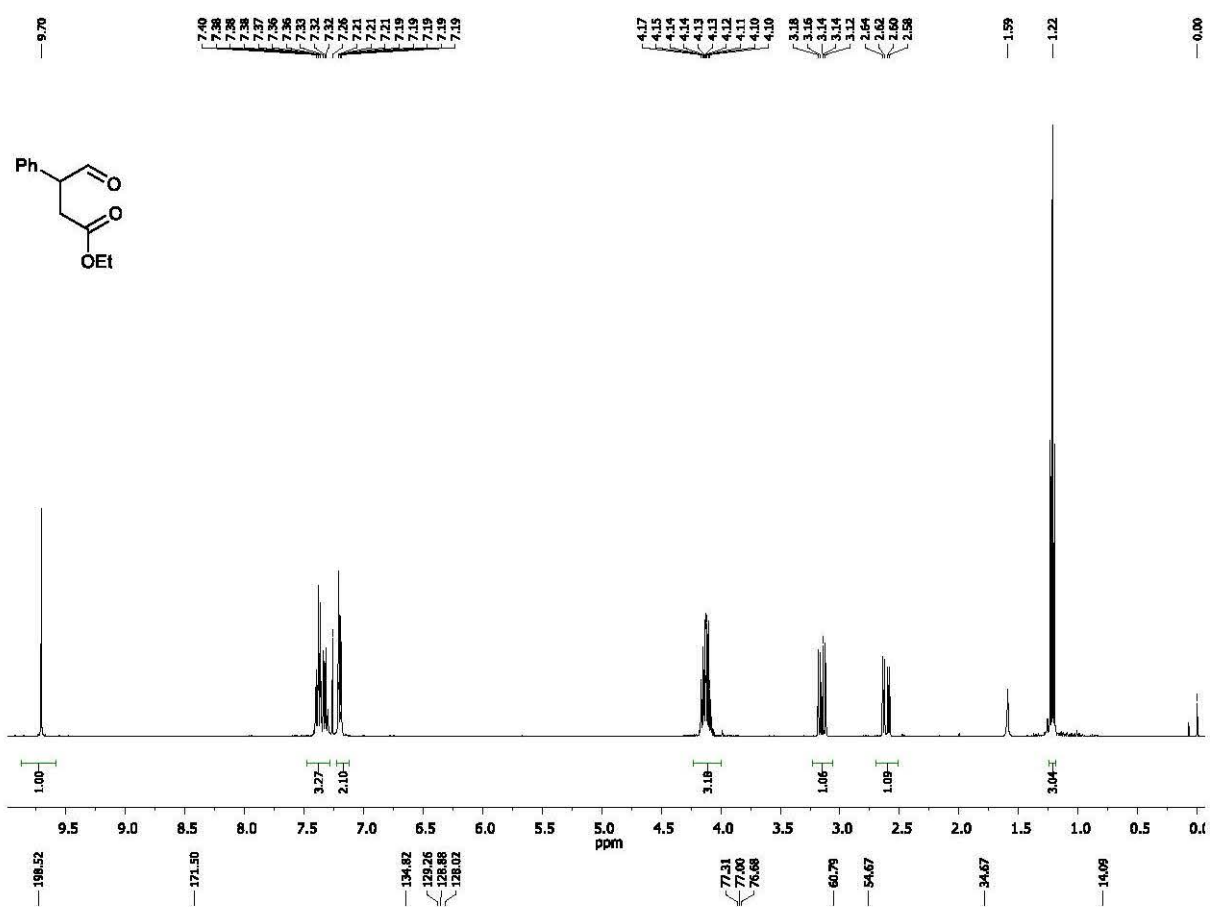
c) Ethyl 3-formyl-4-(4-methoxyphenyl)butanoate (15)



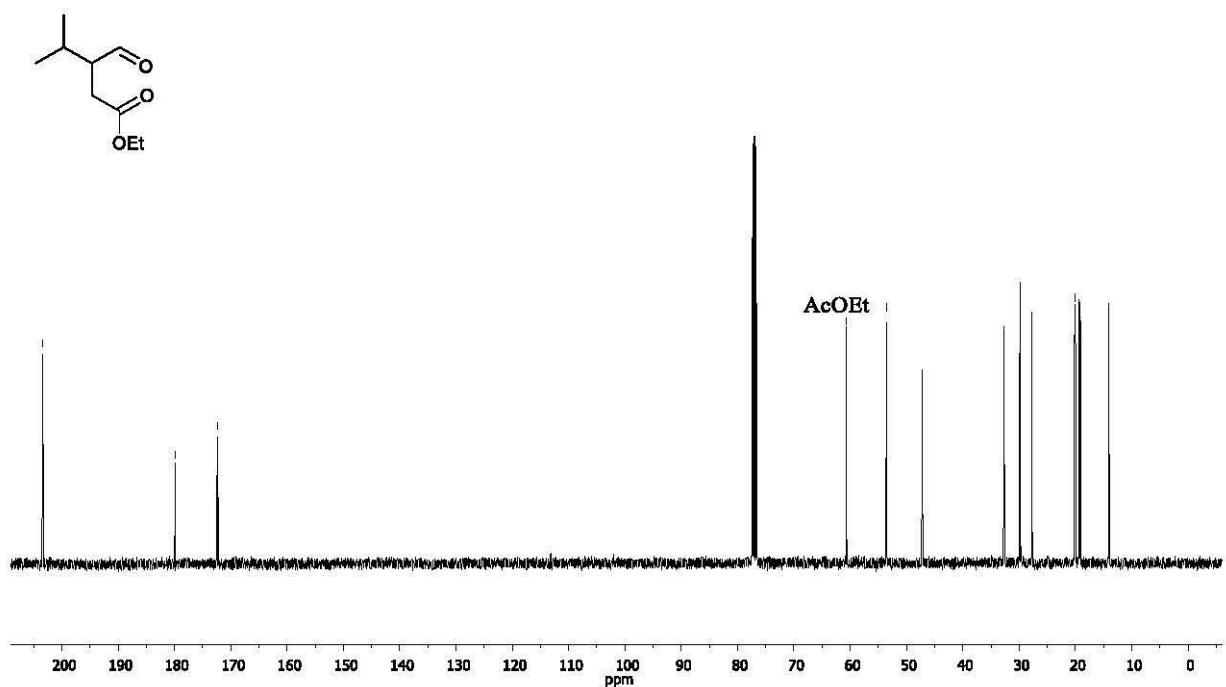
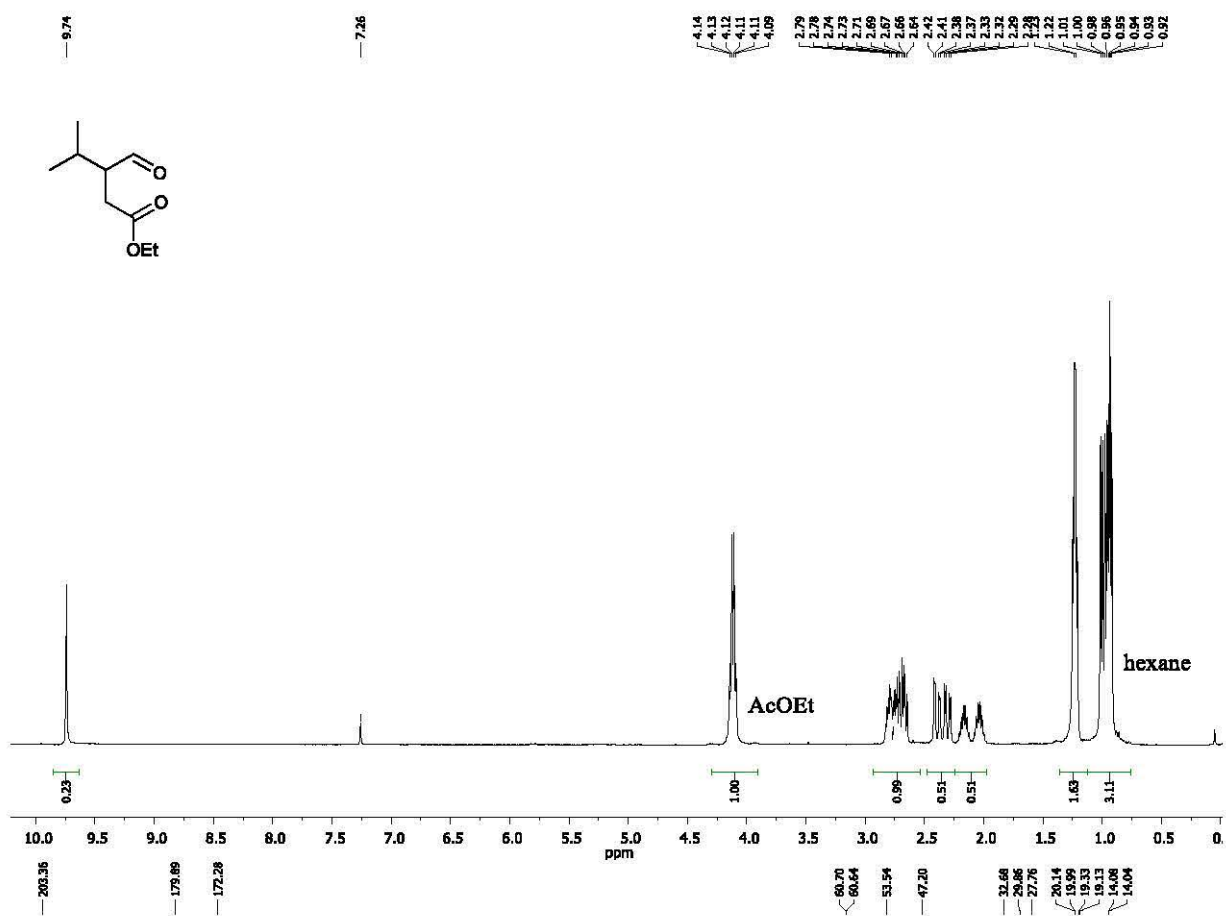
d) Ethyl 3-(3-chlorobenzyl)-4-oxobutanoate (16)



e) Ethyl 4-oxo-3-phenylbutanoate (17)

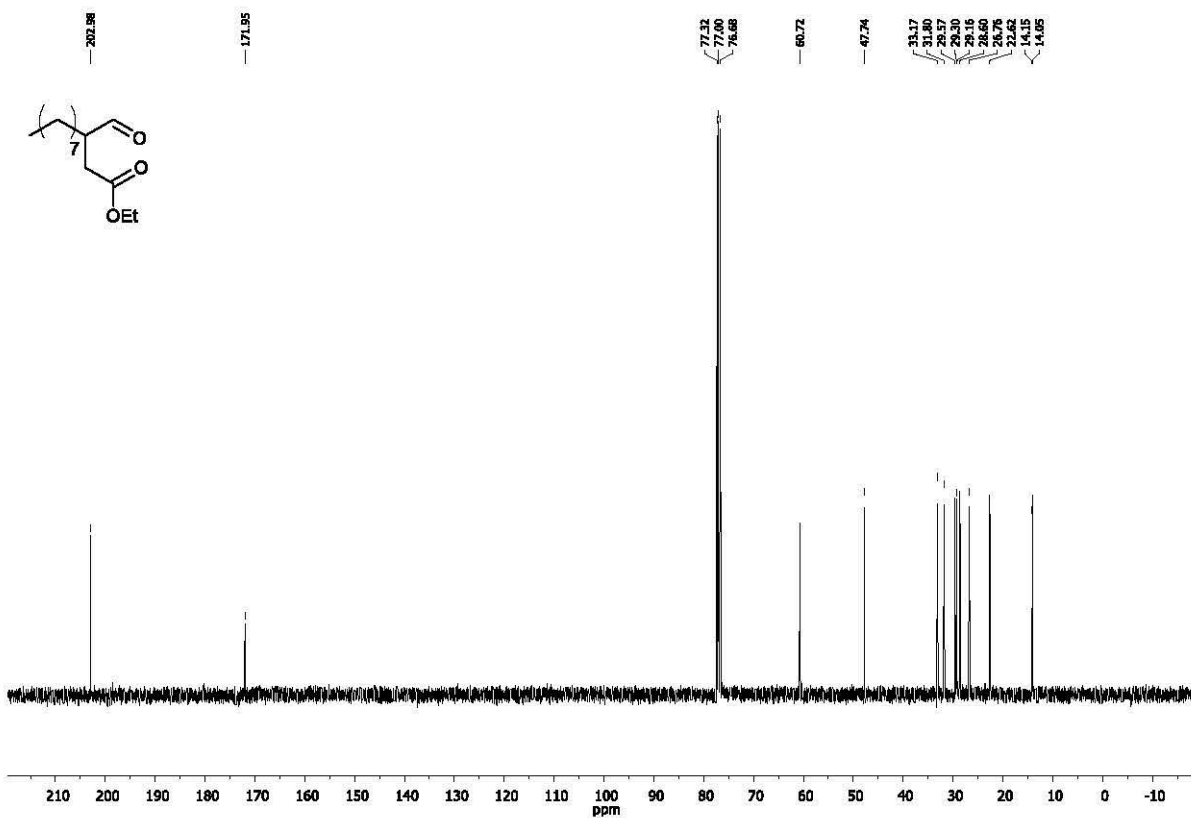
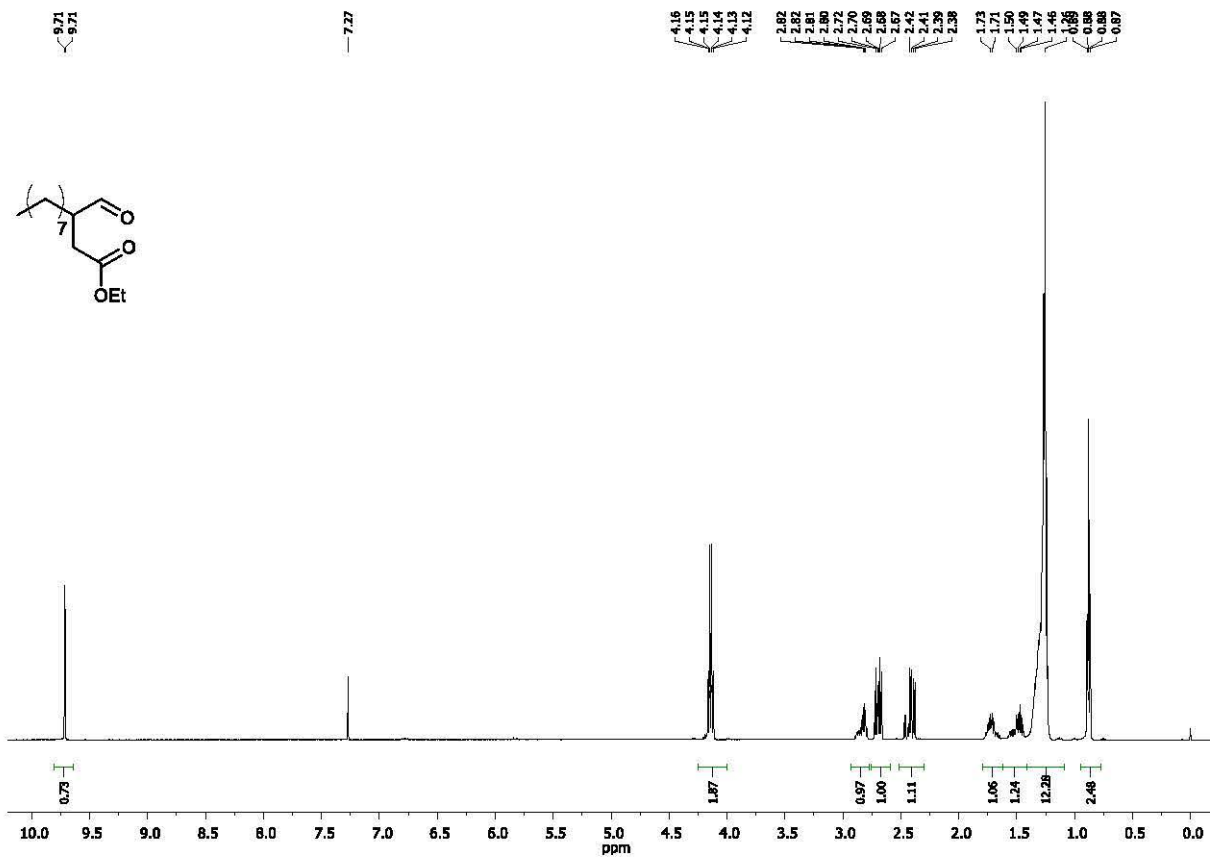


f) Ethyl 3-formyl-4-methylpentanoate (20)



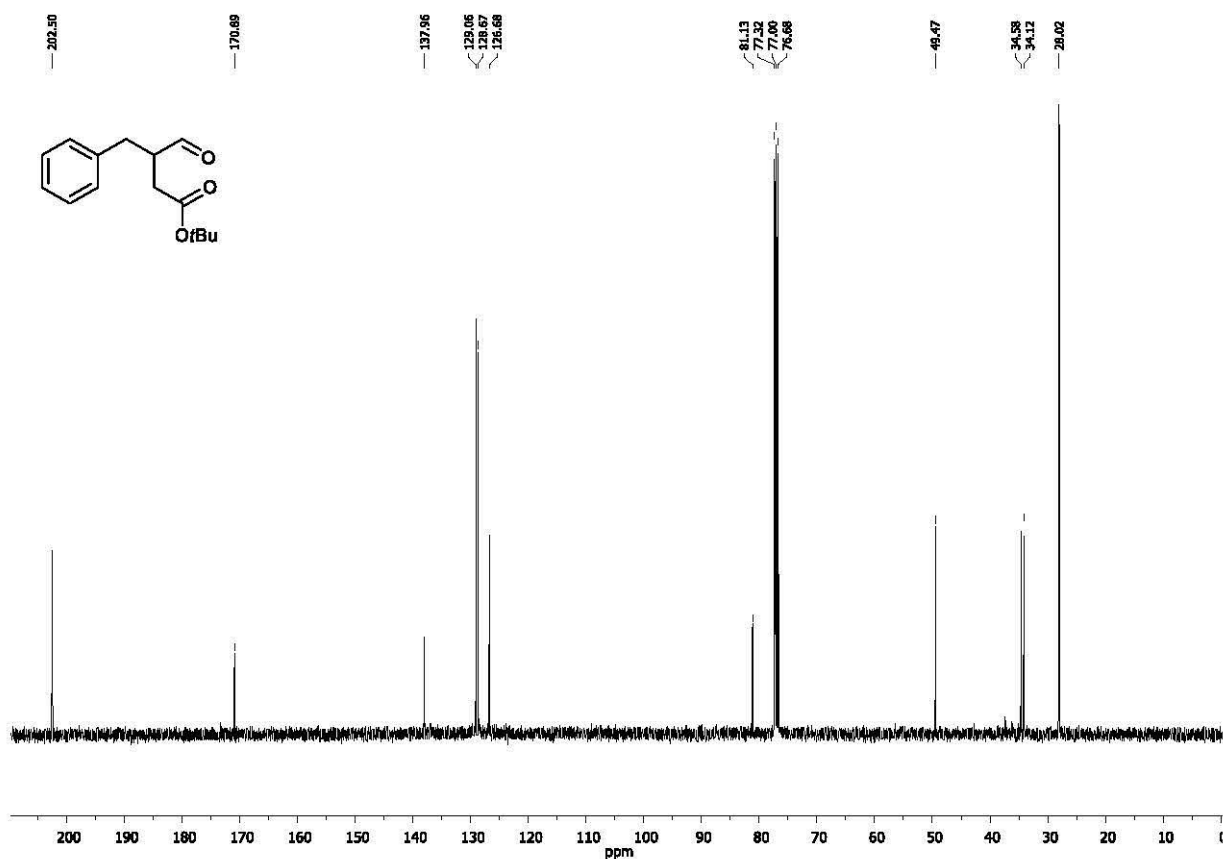
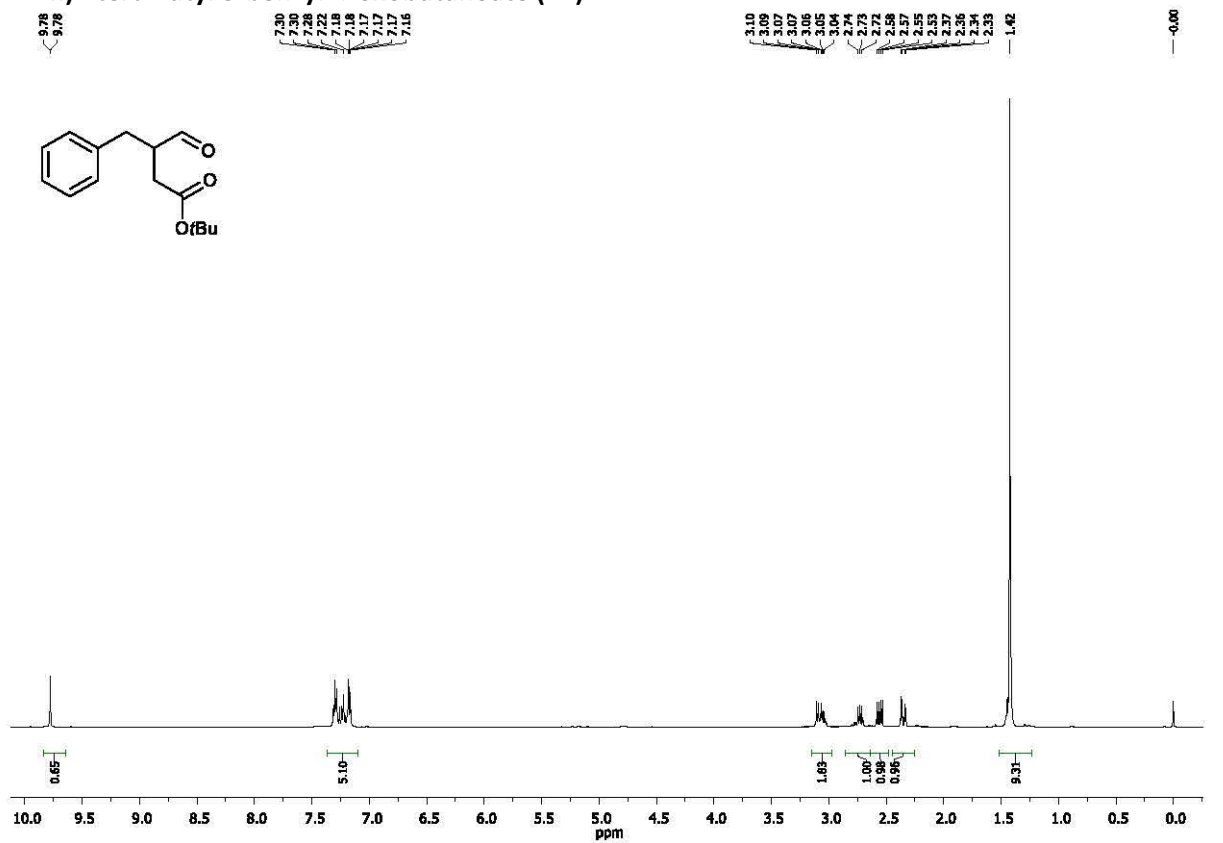
As the compound is very volatile signals corresponding to the solvents are present in both spectra

g) Ethyl 3-formylundecanoate (21)

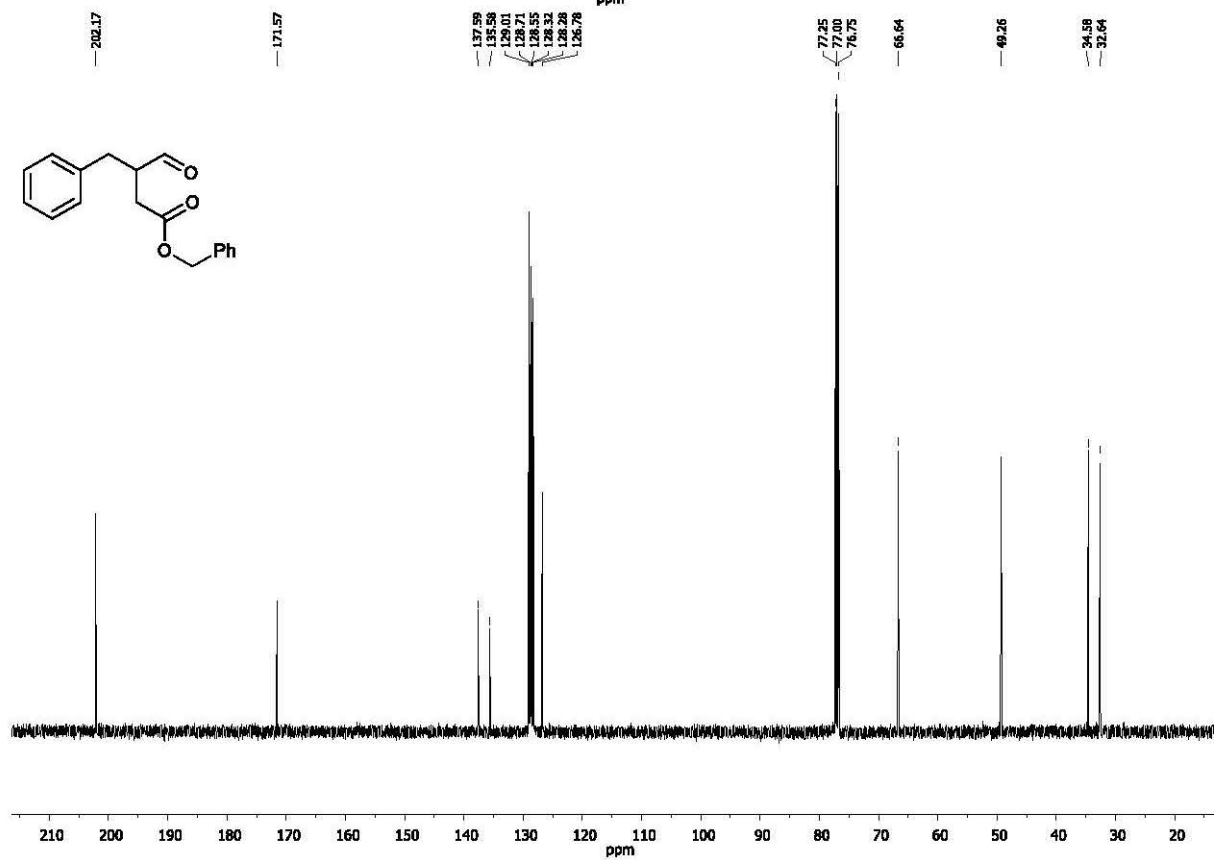
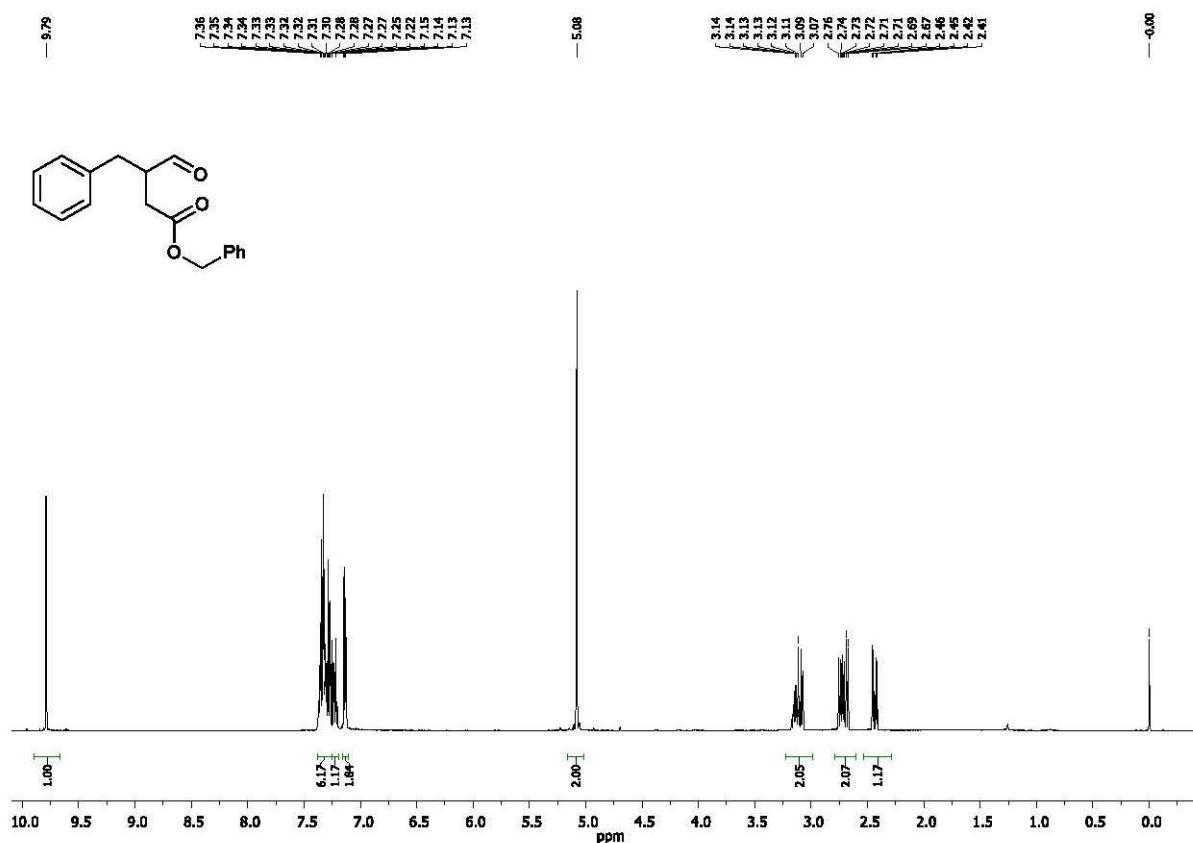


S49

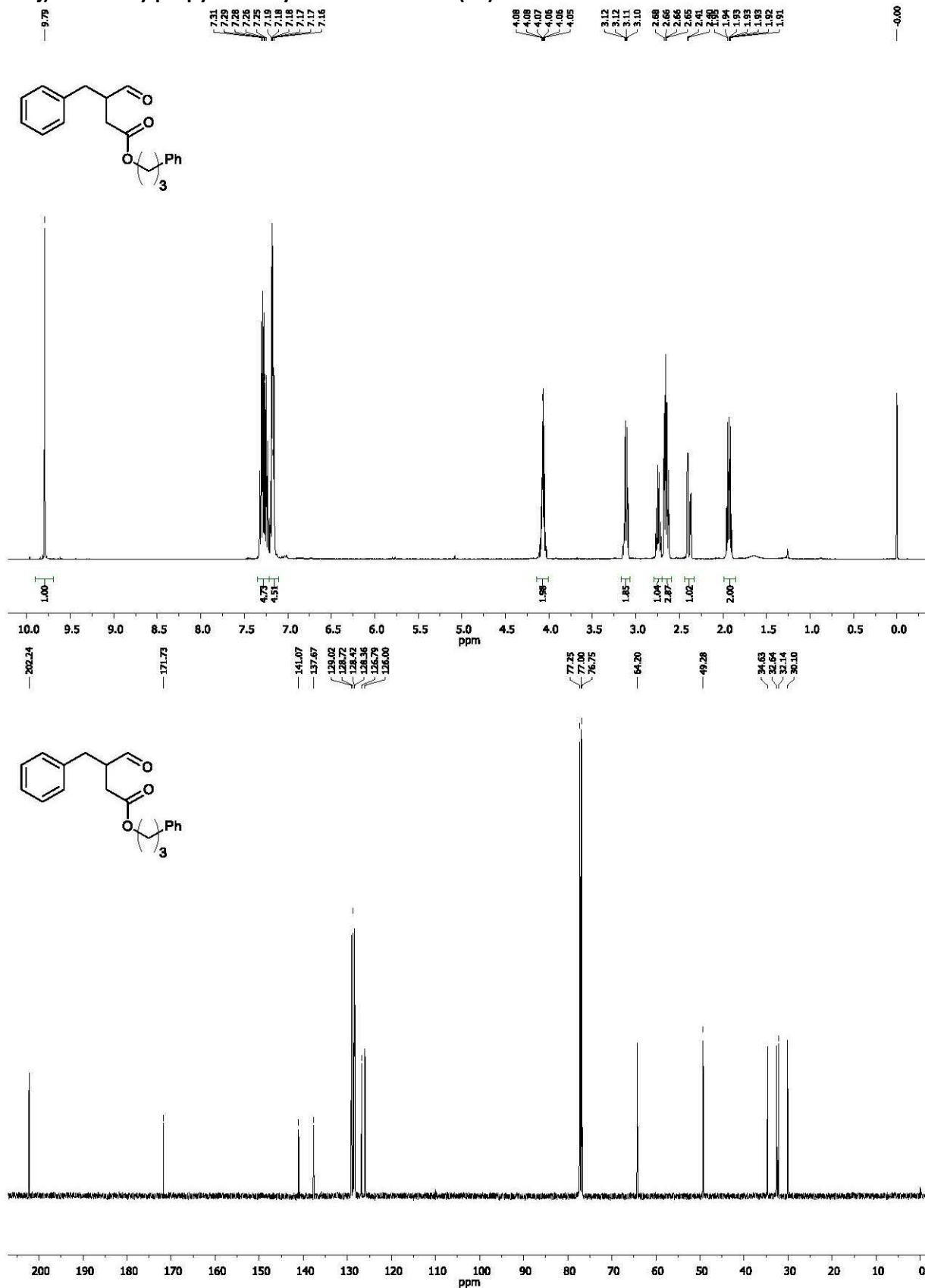
h) *tert*-Butyl 3-benzyl-4-oxobutanoate (22)



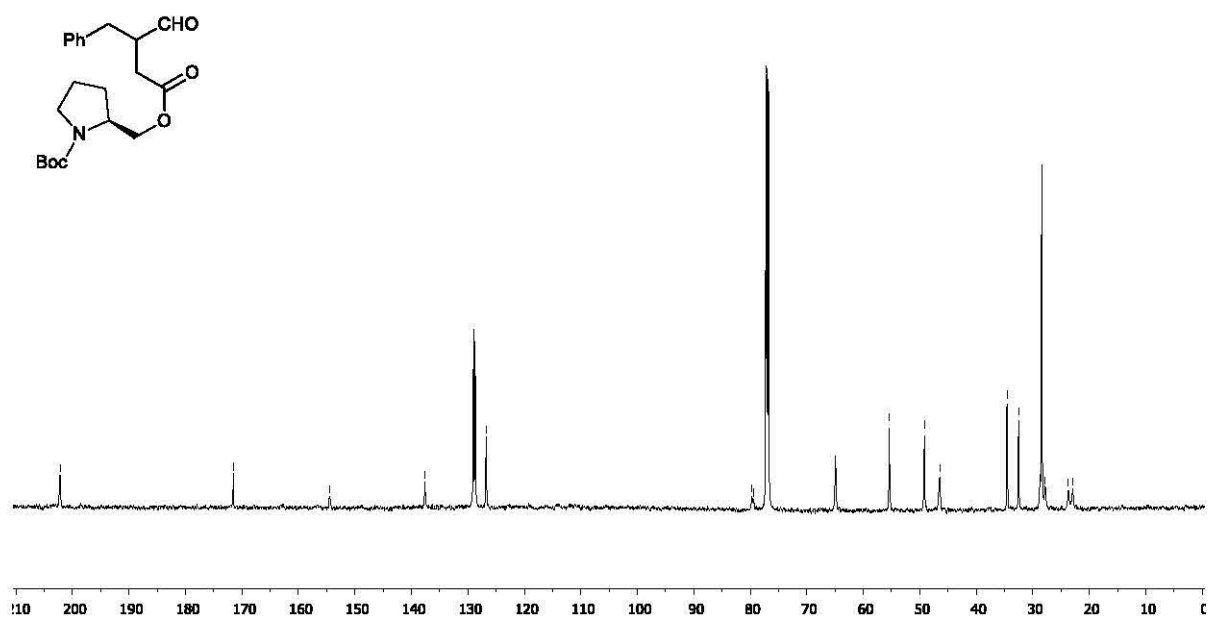
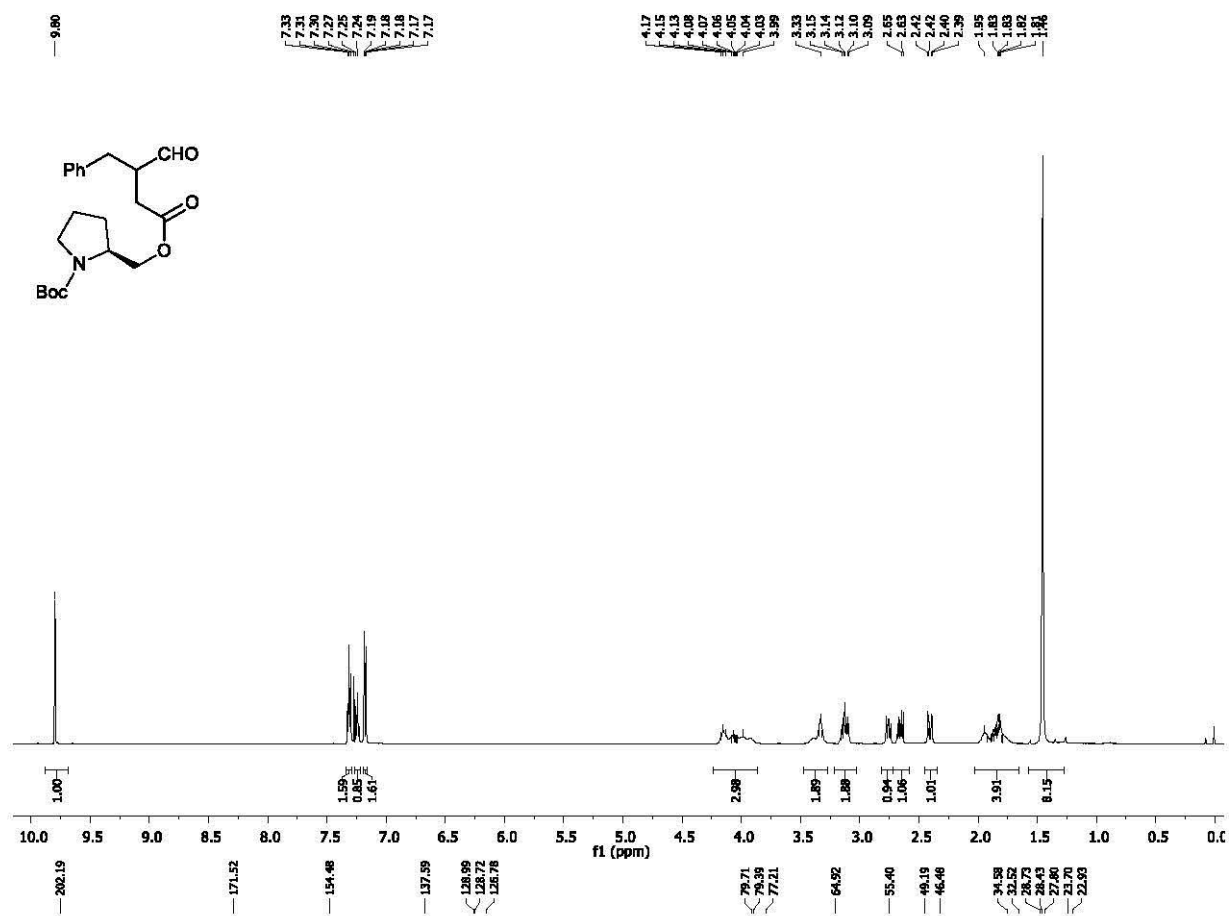
i) Benzyl 3-benzyl-4-oxobutanoate (23)

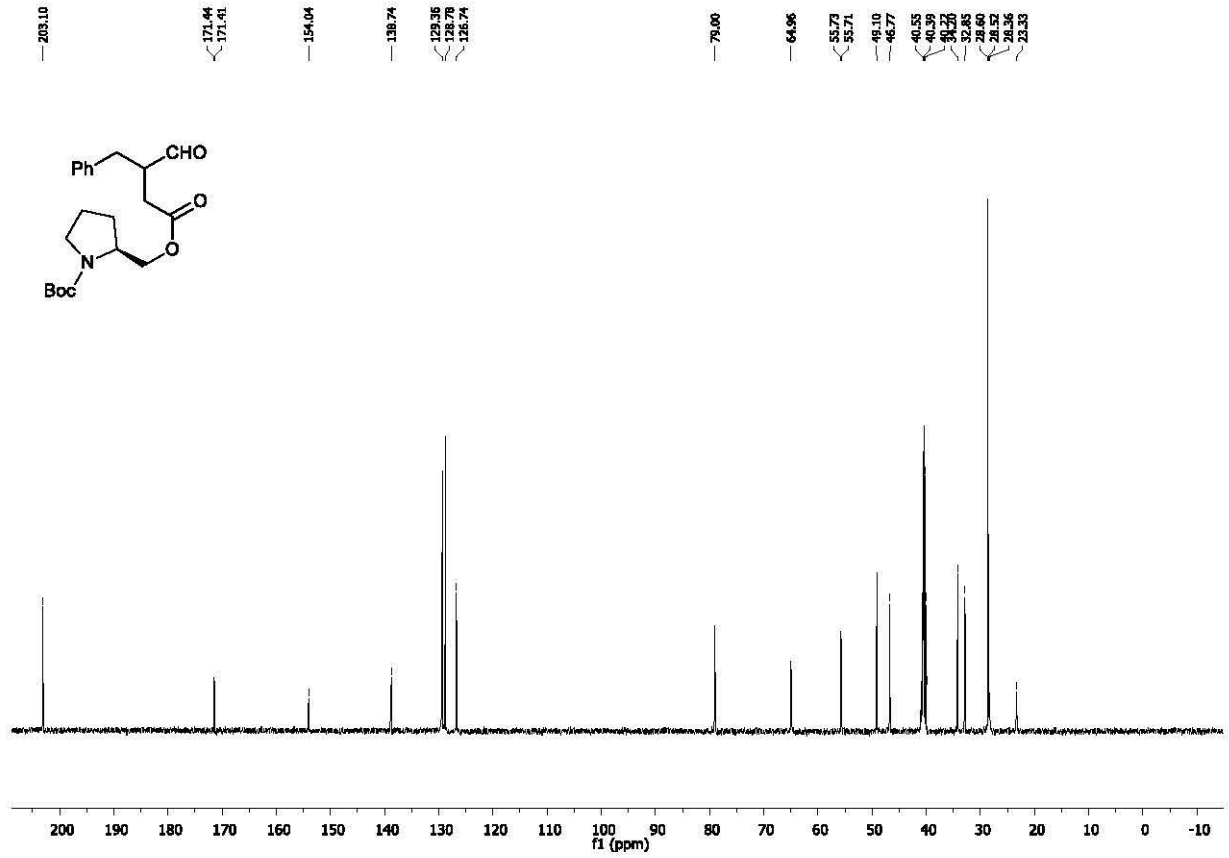
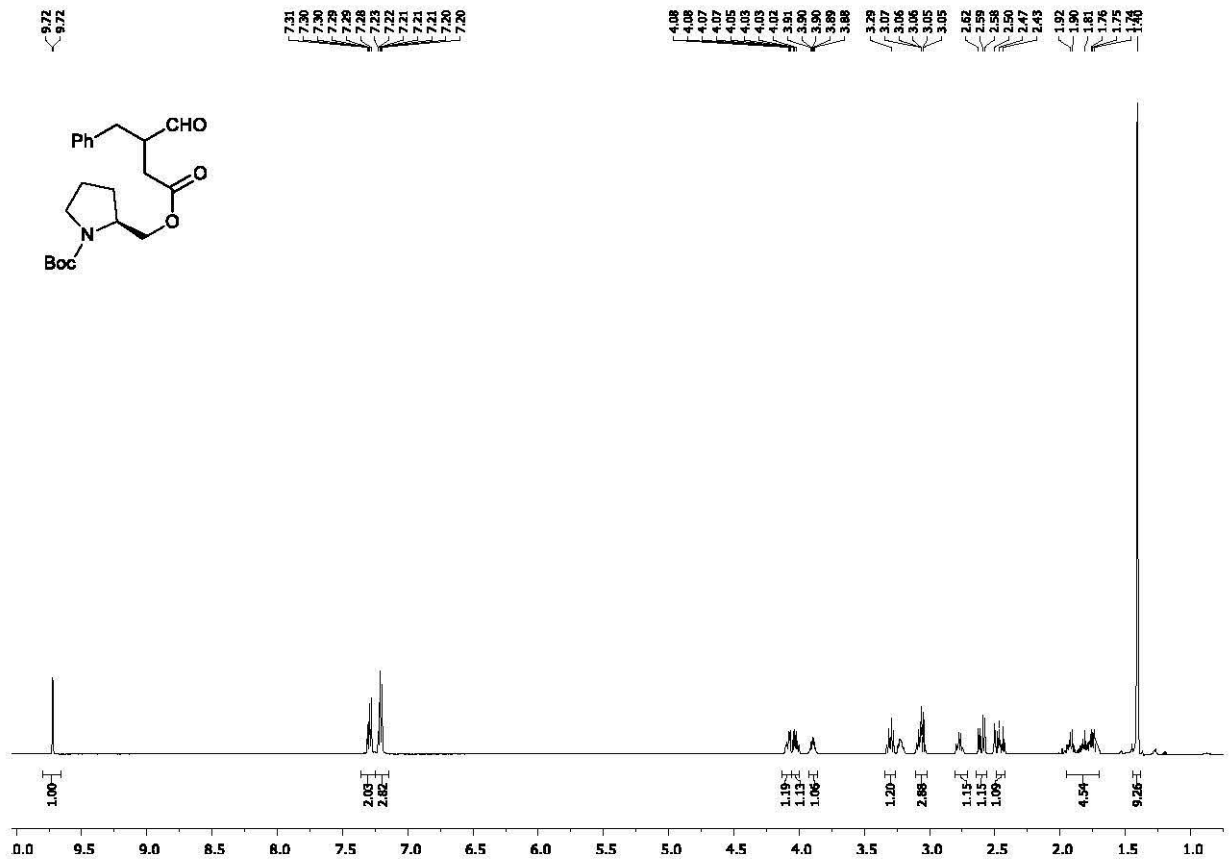


j) 3-Phenylpropyl 3-benzyl-4-oxobutanoate (24)

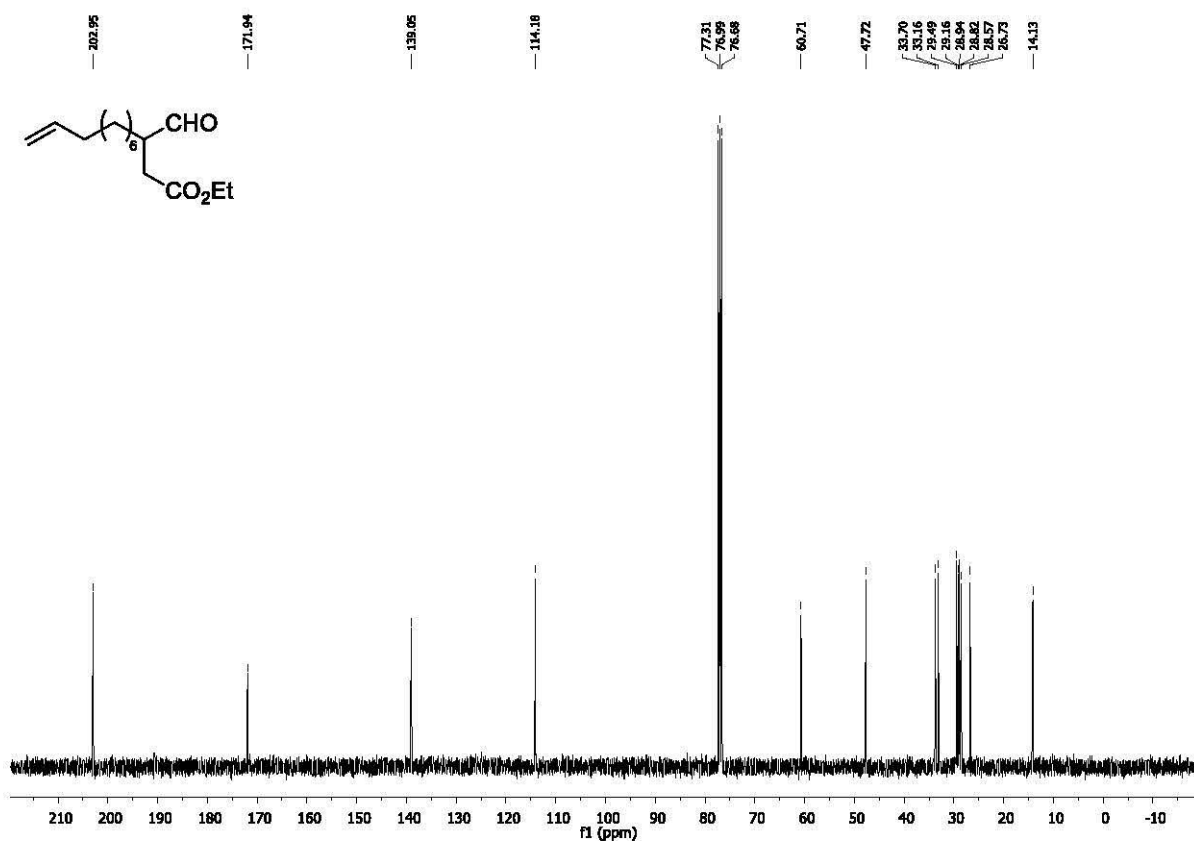
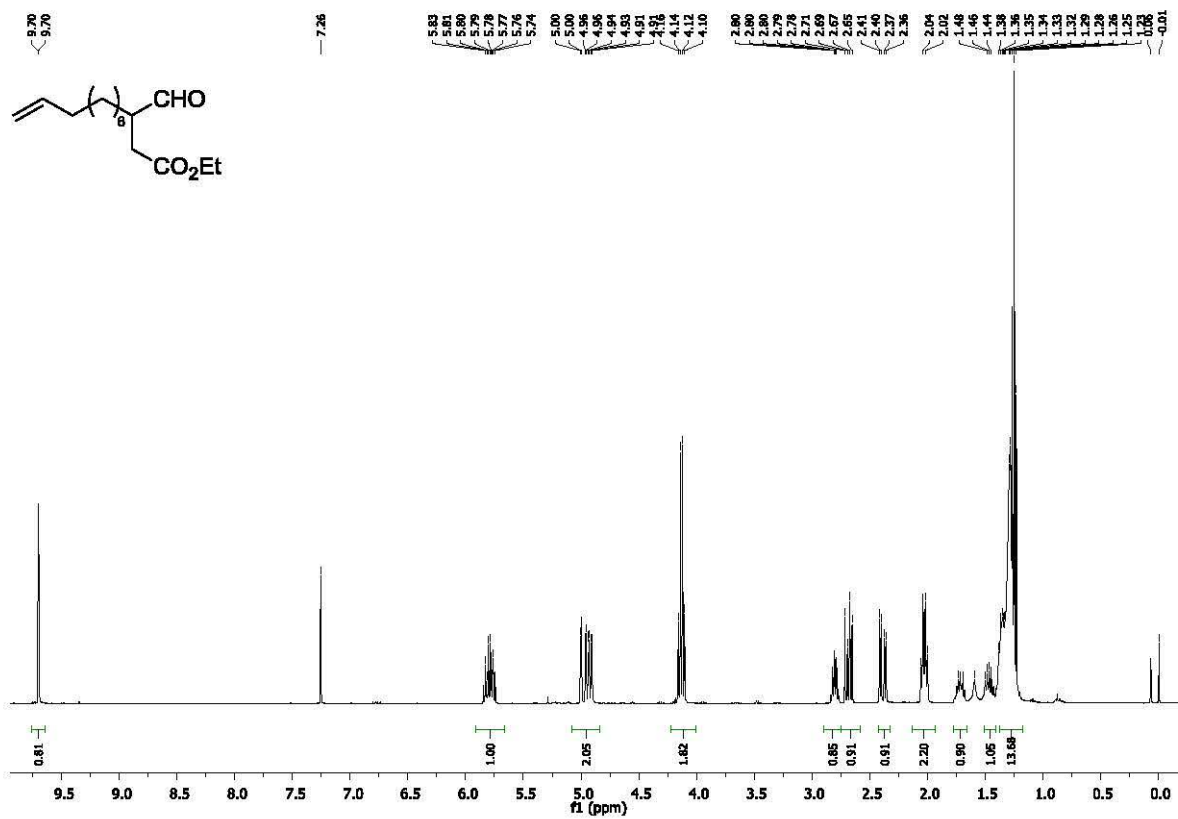


k) (2S)-tert-Butyl2-(((3-benzyl-4-oxobutanoyl)oxy)methyl)pyrrolidine-1-carboxylate (25)

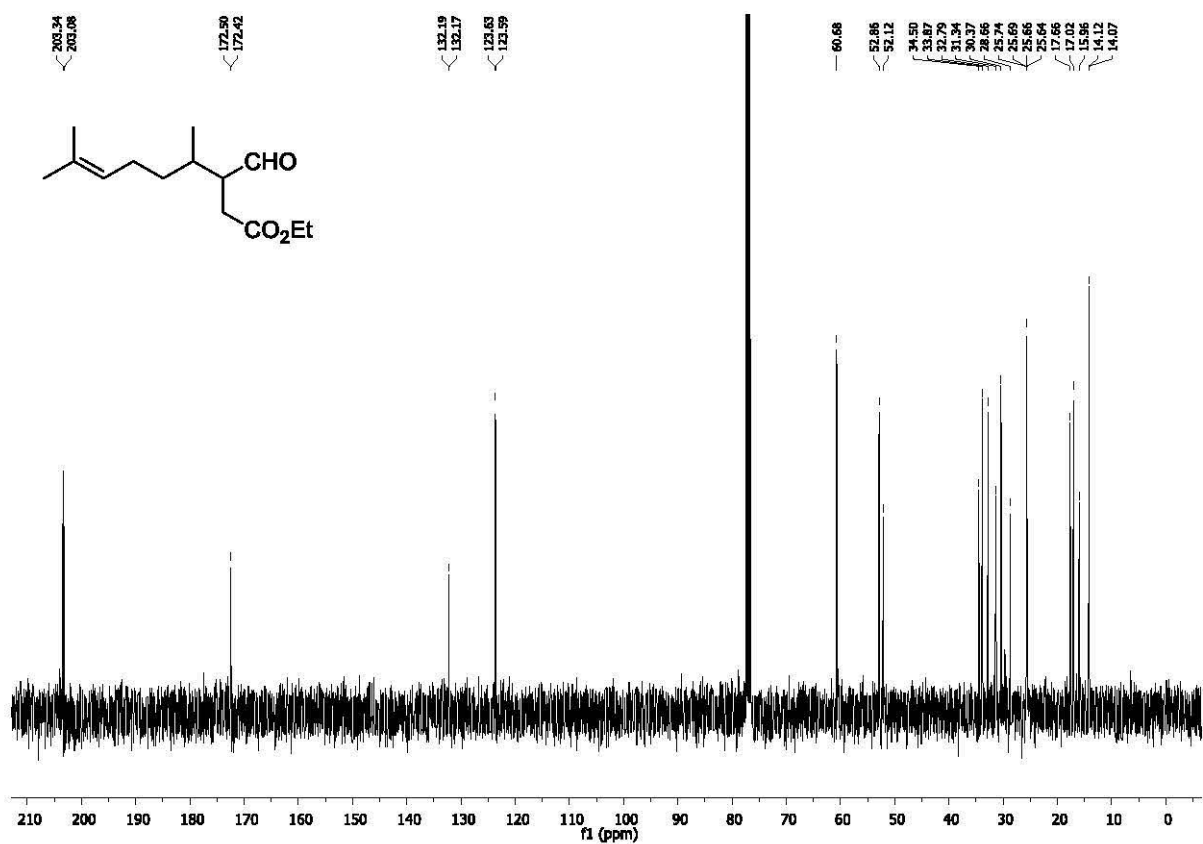
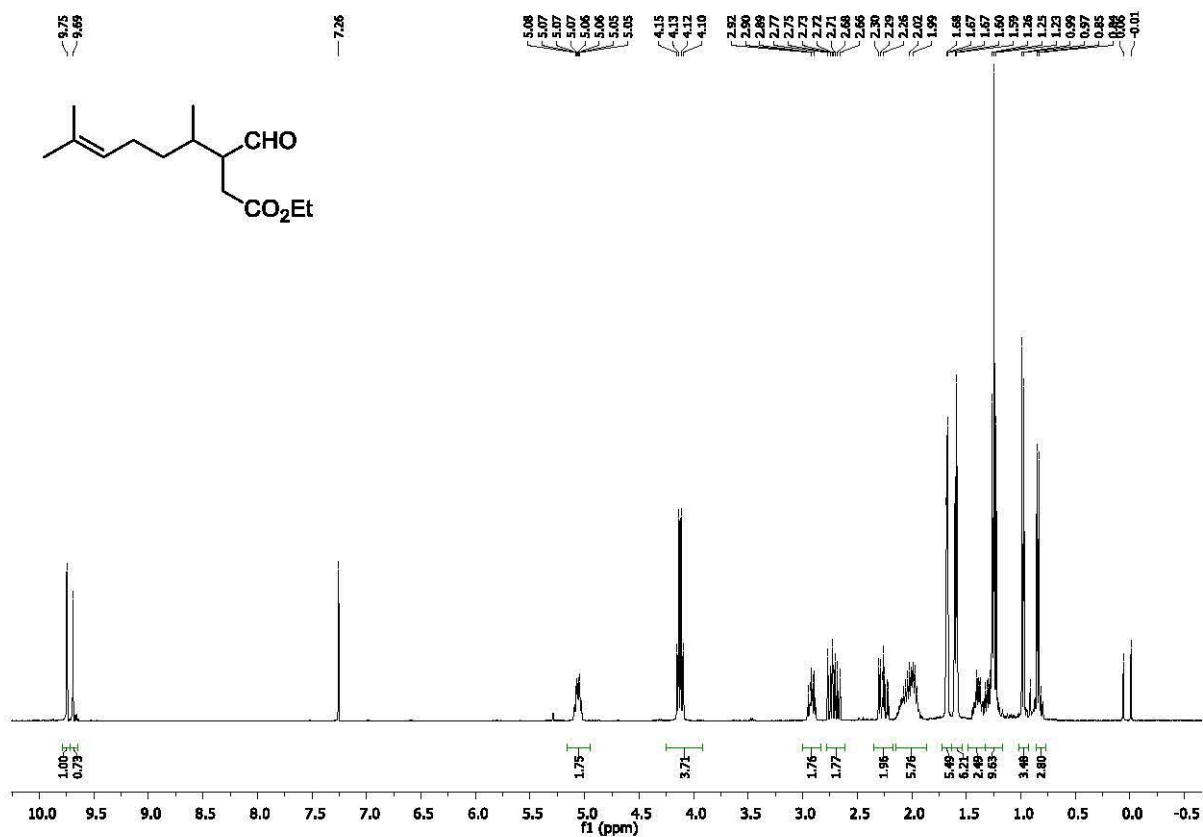




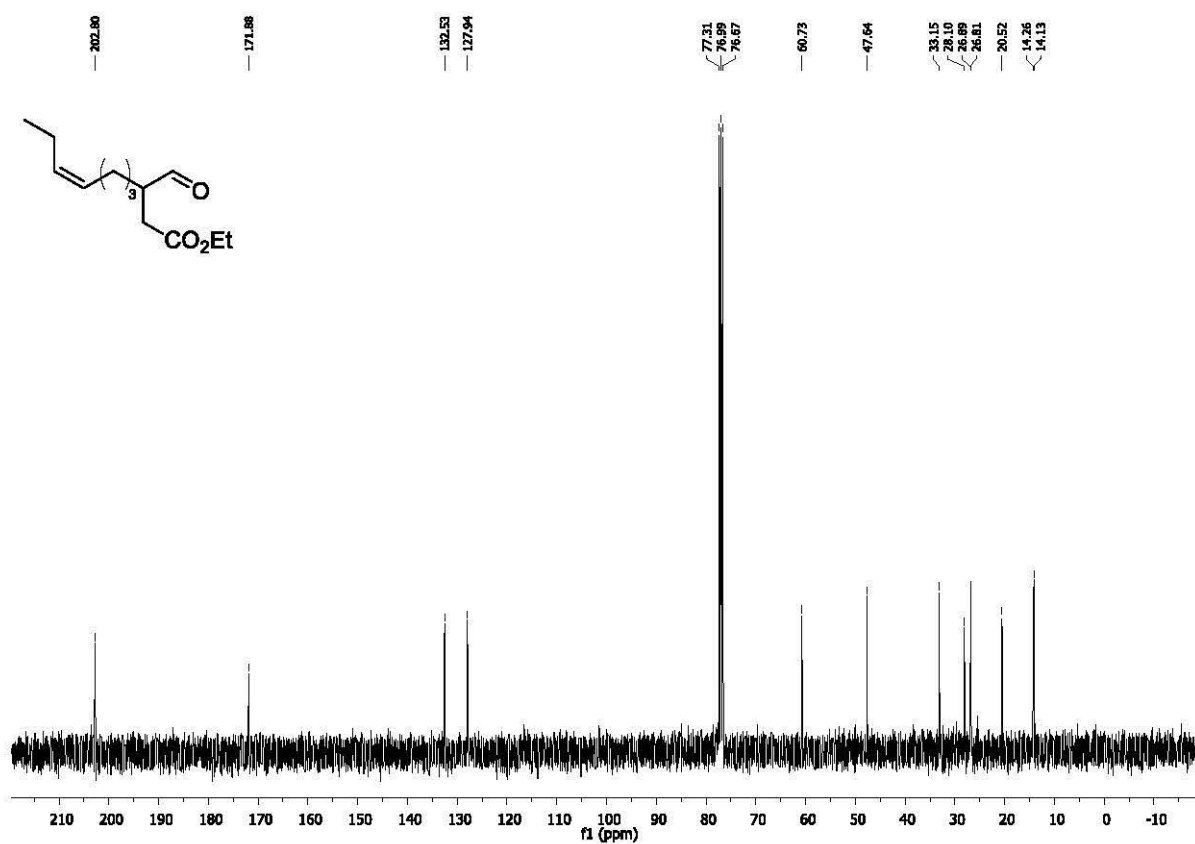
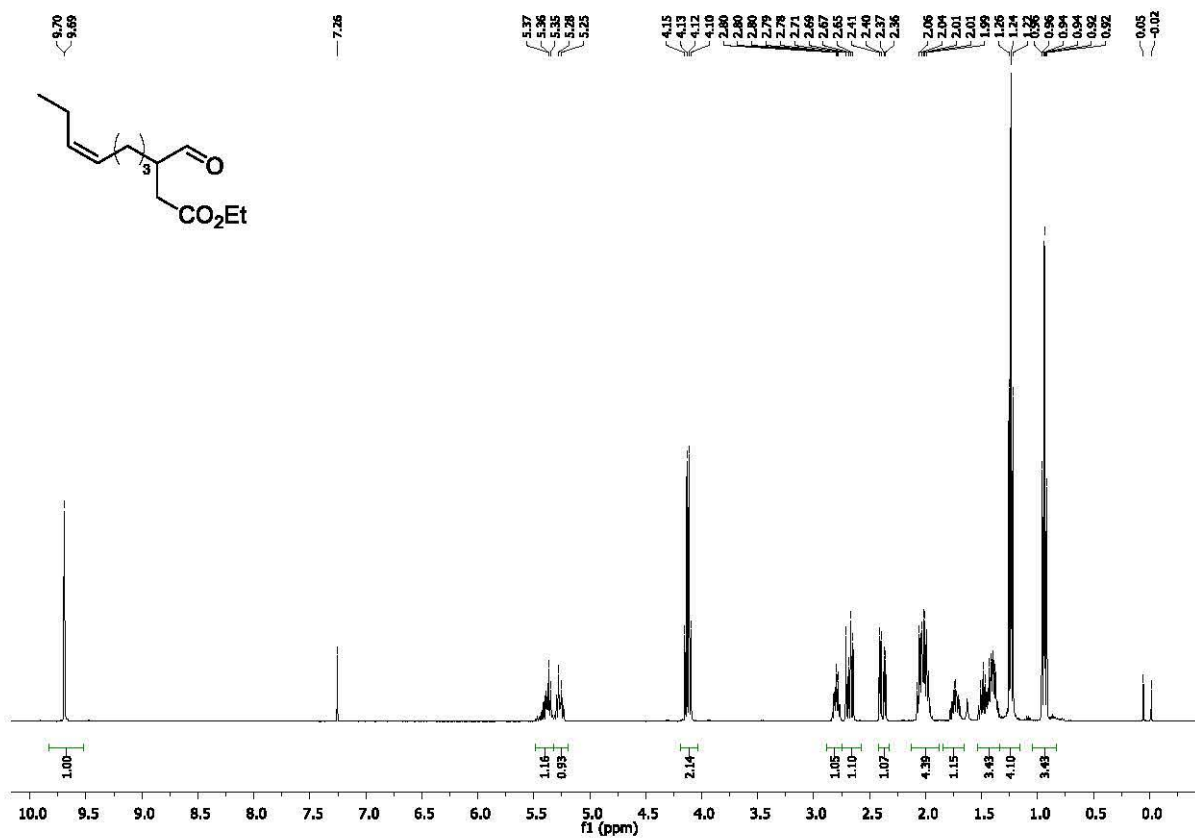
I) Ethyl 3-formyldodec-11-enoate (26)



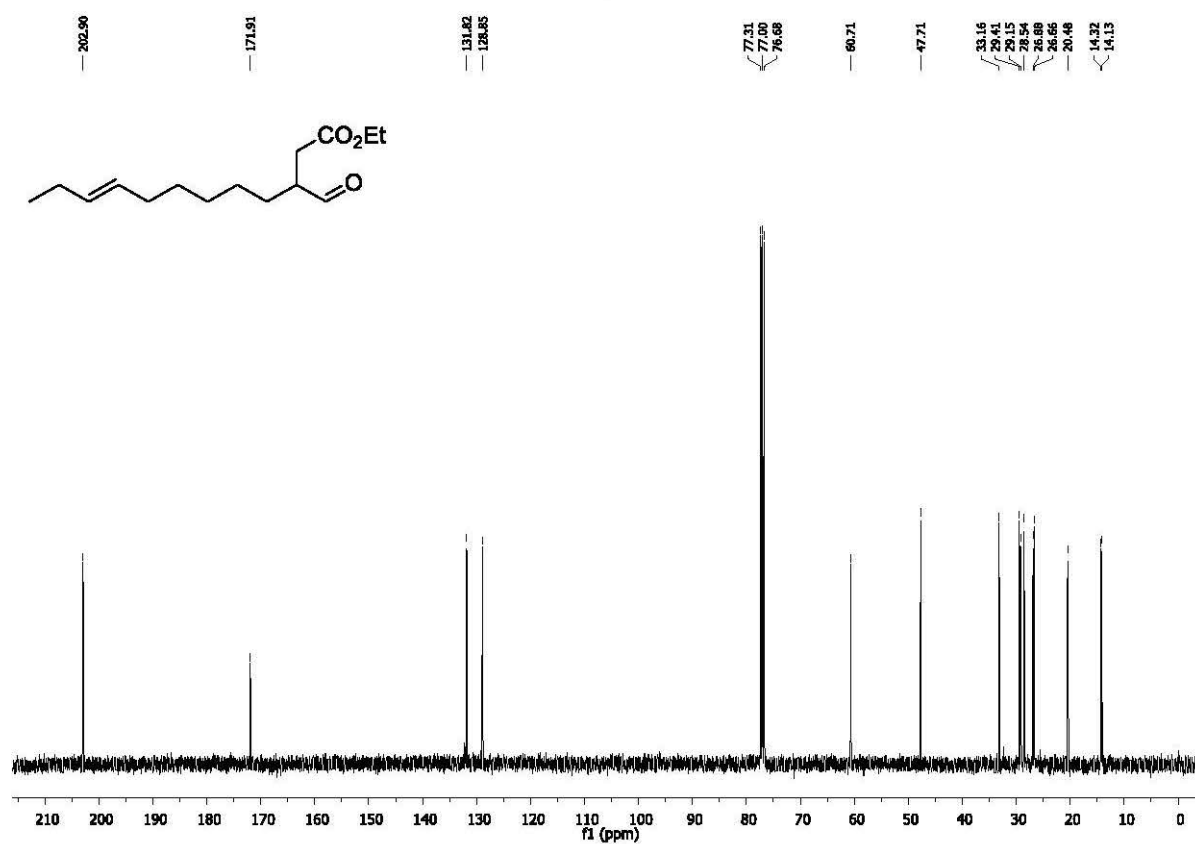
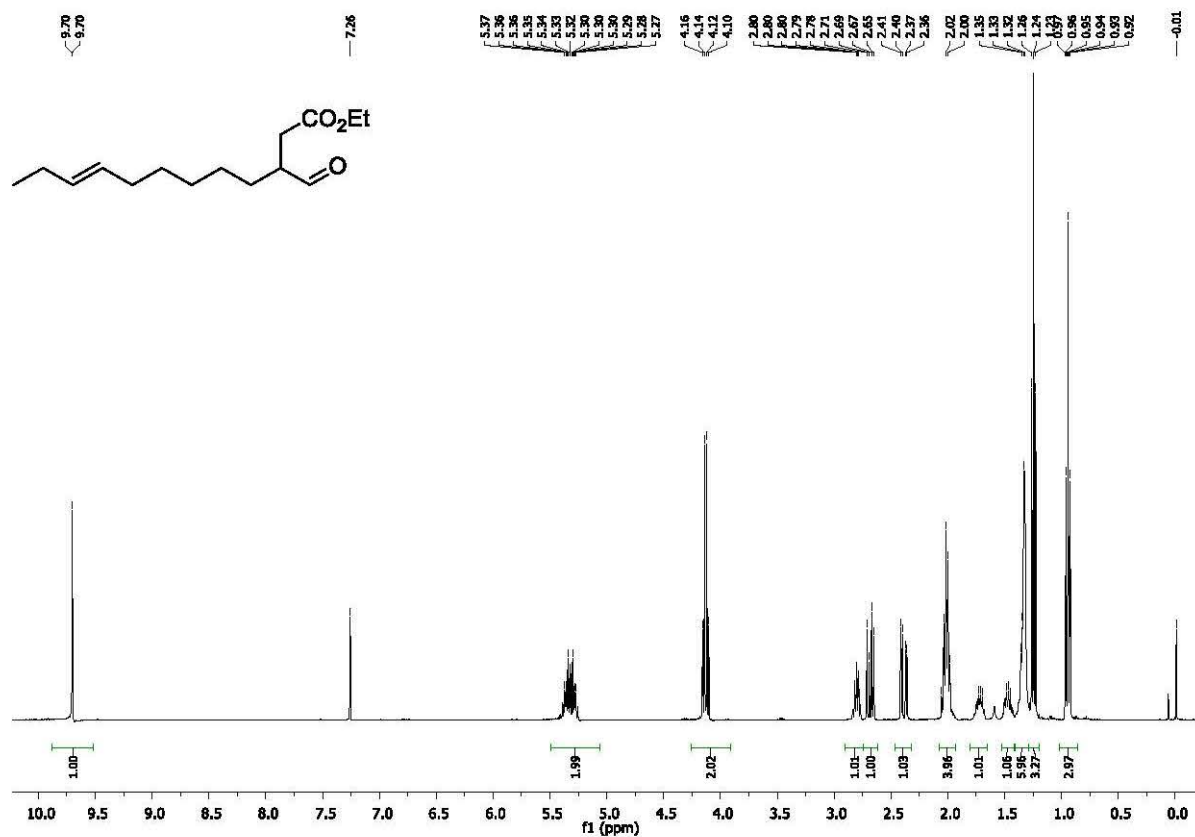
m) (*E*)-Ethyl 3-formylnon-7-enoate (27)



n) (Z)-Ethyl 3-formyldec-7-enoate (28)

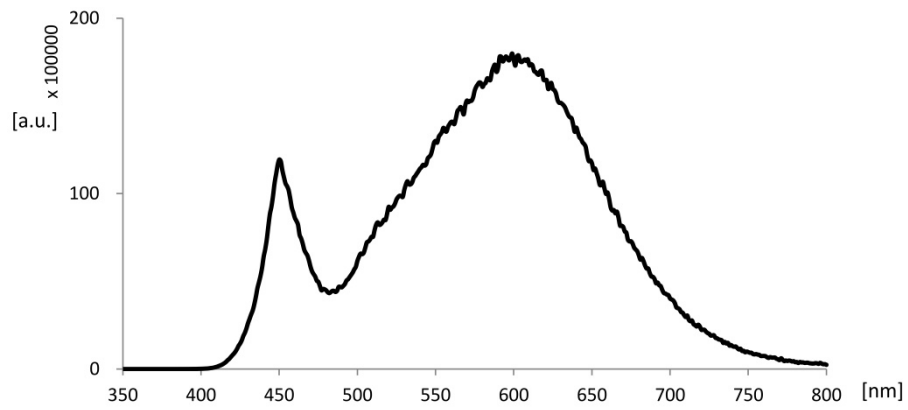


o) (*E*)-Ethyl 3-formyldodec-9-enoate (29)

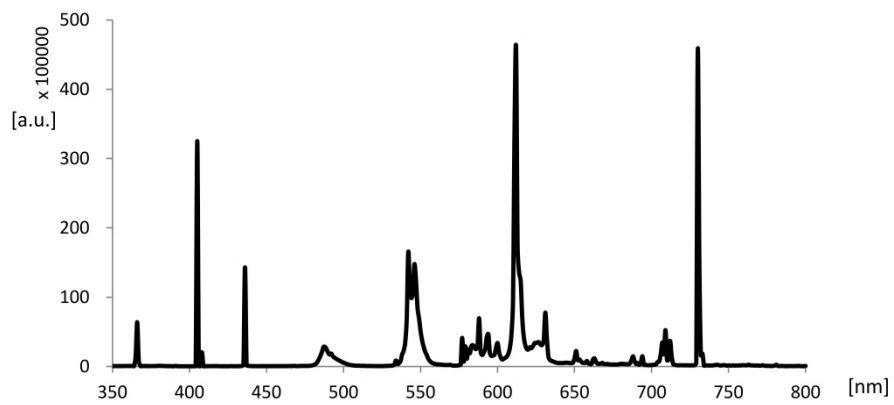


7. Emission spectra measurements:

a) 'household' LED



b) 'household' CFL bulb



8. Photoreactor



9. References

1. Carman, L. D.; Kwart, T. Hulicky, *Synth. Commun.* **1986**, *16*, 169.
2. Deslongchamps, P. A.; Bélanger, D. J. F.; Berney, H.-J.; Borschberg, R.; Brousseau, A.; Doutheau, R.; Durand, H. Katayama, R.; Lapalme, Leturc, D. M., Liao, C.-C.; MacLachlan, F. N.; Maffrand, J.-P.; Marazza, F.; Martino, R.; Moreau, C.; Ruest, L.; Saint-Laurent, L.; Saintonge, R.; Soucy, P. *Can. J. Chem.* **1990**, *68*, 127.
3. Mukherjee, S.; Yang, J. W.; Hoffmann, S.; List, B. *Chem. Rev.* **2007**, *107*, 5471.
4. Ramirez, F.; Marecek, J. F. *Pure Appl. Chem.* **1980**, *52*, 1021.
5. Buettner, G.R *Free Radic. Biol. Med.* **1987**, *3*, 259.
6. Hiramoto, K.; Johkoh, H.; Sako, K.; Kikugawa, K. *Free Radic. Res Commun.* **1993**, *19*, 323.
7. Janzen, E.G.; Coulter, G.A.; Oehler, U.M.; Bergsma, J.P. *Can. J. Chem.* **1982**, *60*, 2725.
8. Dvoranová, D.; Barbieriková, Z.; Dorotíková, S.; Malček, M.; Brincko, A.; Rišpanová, L.; Bučinský, L.; Staško, A.; Brezová V.; Rapta P. *J. Solid State Electrochem.* **2015**, *19*, 2633.
9. Seely, G. R. *Photochemistry and Photobiology* **1978**, *27*, 639.
10. Quimby, D. J.; Longo, F. R. *J. Am. Chem. Soc.* **1974**, *97*, 5111.
11. Vicente, M. G. H.; Neves M. G. P. M. S.; Cavaleiro, J. A. S.; Hombrecher, H. K.; Koll, *D.Tetrahedron Letter*, **1996**, *37*, 261.
12. Kumar, P. H.; Venkatesh, Y.; Siva, D.; Ramakrishna, B., Bangal, P. R. *J. Phys. Chem. A* **2015**, *119*, 1267.

13. Schoeller, W. W.; Niemann, J.; Rademacher, P. *J. Chem. Soc. Perkin Trans 2* **1988**, 369.
14. a) Espinoza, E. M.; Larsen, J. M.; Vullev, V. L. *J. Phys. Lett.* **2016**, *7*, 758; b) Larsen, J. M.; Espinoza, E. M.; Hartman, J. D.; Lin, Ch-K.; Wurch, M.; Maheshwari, P.; Kaushal, R. K.; Marsella, M. J.; Beran, G. J. O.; Vullev, V. L. *Pure Appl. Chem.* **2015**, *87*, 779.
15. a) Bao D.; Ramu, S.; Contreras, A.; Upadhyayula, S.; Vasquez, J. M.; Beran, G.; Vullev, V. *J. Phys. Chem. B* **2010**, *114*, 14467; b) Bao D.; Millare, B.; Xia, W.; Steyer, B. G.; Gerasimenko, A. A.; Ferreira, A.; Contreras, A.; Vullev, V. I. *J. Phys. Chem. A* **2009**, *113*, 1259.
16. Yao, D.; Zhang, X.; Mongin, O.; Paul, F.; Paul-Roth, C. O. *Chem. Eur. J.* **2016**, *22*, 5583.
17. Cho, S.; Lee, Y.; Han, H. S.; Lee, H. K.; Jeon, S. *J. Phys. Chem. A* **2014**, *118*, 4995.
18. Weinkauff, J. R.; Cooper, S. W.; Schweiger, A.; Wamser, C. C. *J. Phys. Chem. A* **2003**, *107*, 3486.
19. a) Harriman, A. *J. Chem. Soc., Faraday Trans. 1*, **1980**, *76*, 1978. b) Harriman, A. *J. Chem. Soc., Faraday Trans. 2*, **1981**, *77*, 1281. c) Harriman, A. *J. Chem. Soc., Faraday Trans. 1*, **1981**, *77*, 369; d) Harriman, A.; Hosie, J. *J. Chem. Soc. Faraday Trans. 2*, **1981**, *77*, 1695.
20. Kalyanasundaram, K. *Coord. Chem. Rev.* **1982**, *46*, 159.



Accepted Article

Title: Why Cyclopropanation is not involved in Photoinduced α -Alkylation of Ketones with Diazo Compounds?

Authors: Dorota Gryko, Katarzyna Rybicka-Jasińska, Katarzyna Orłowska, Maksymilian Karczewski, and Katarzyna Zawada

This manuscript has been accepted after peer review and appears as an Accepted Article online prior to editing, proofing, and formal publication of the final Version of Record (VoR). This work is currently citable by using the Digital Object Identifier (DOI) given below. The VoR will be published online in Early View as soon as possible and may be different to this Accepted Article as a result of editing. Readers should obtain the VoR from the journal website shown below when it is published to ensure accuracy of information. The authors are responsible for the content of this Accepted Article.

To be cited as: *Eur. J. Org. Chem.* 10.1002/ejoc.201800542

Link to VoR: <http://dx.doi.org/10.1002/ejoc.201800542>

WILEY-VCH

Accepted Manuscript

Supporting Information (SI)

for

Why Cyclopropanation is not involved in Photoinduced α -Alkylation of Ketones with Diazo Compounds?

Katarzyna Rybicka-Jasińska,^a Katarzyna Orłowska,^a Maksymilian Karczewski,^a Katarzyna Zawada,^{b} Dorota Gryko^{a*}*

^aInstitute of Organic Chemistry, Polish Academy of Sciences, Kasprzaka 44/52, 01-224 Warsaw, Poland

^bMedical University of Warsaw, Faculty of Pharmacy with the Laboratory Medicine Division, Department of Physical Chemistry, Banacha 1, 02-097 Warsaw, Poland

Table of Contents

1.	General information	S3
2.	General synthetic procedures	S3
3.	Scope and limitations	S5
4.	Optimization studies	S15
5.	Mechanistic considerations	S20
5.1.	Proposed mechanism	S20
5.2.	Electrochemical data for porphyrins	S20
5.3.	EPR	S21
5.4.	TEMPO trapping	S30
5.5.	Experiment with deuterated reagents (CD ₃ CN)	S31
5.6.	Verification of cyclopropane-intermediate mechanism	S32
5.7.	UV-Vis	S33
5.8.	Stern–Volmer quenching experiments	S37
5.9.	NMR studies	S38
5.10.	Oxygen dependence	S42
5.11.	Quantum yield measurements	S42
5.13.	Energetics consideration	S45
5.12.	Theoretical calculations	S46
6.	¹ H and ¹³ C NMR spectra	S49
7.	References	S68

1. General information

All solvents and chemicals used in the syntheses were of a reagent grade and were used without further purification. High resolution ESI mass spectra were recorded on a Mariner or SYNAPT spectrometer. ^1H and ^{13}C NMR spectra were recorded at rt on Bruker 400 instrument with TMS as an internal standard. EPR spectrum was recorded on Magnettech MS200 spectrometer. IR spectroscopy measurements were performed on FTIR Jasco 6200 instrument. Thin layer chromatography (TLC) was performed using Merck Silica Gel GF254, 0.20 mm thickness. GC measurements were made on Gas Chromatograph Shimadzu GC-2010Plus with Zebron ZB-5MSi 30 m 0.25 μm /0.25 mm column. Ketones were purified by flash column chromatography (hexane : Et₂O) if necessary.

Photo-induced reactions were performed using a homemade photoreactors equipped with: LED_{green} – single diode or LED_{green} stripes.

2. General synthetic procedures

General procedure for α -mono-alkylation of ketones in the presence of porphyrin – **method A**:

To a 10 mL vial equipped with a stir bar a porphyrin (1 mol %) was added and dissolved in a mixture of DMSO and buffer pH 4 (mixture 9:1, 5 mL). The vial was sealed and solvents were purged with argon for 5 min. Then a ketone (0.5 mmol), pyrrolidine (0.2 equiv., 0.1 mmol) and a diazo ester (1.2 equiv., 0.6 mmol) were added. The reaction mixture was stirred under light irradiation (LED_{525nm}, 25 °C) for 5 h. The light was turned off, the reaction mixture was diluted with Et₂O, and washed with 1N HCl. The aqueous phase was extracted with Et₂O three times. Combined organic phases were washed with saturated NaHCO₃aq, brine, dried over MgSO₄, filtered, and concentrated. The crude product was purified by flash chromatography using silica gel (hexane/Et₂O).

General procedure for α -mono-alkylation of ketones with no porphyrin added – **method A'**:

To a 10 mL vial equipped with a stir bar a mixture of DMSO and buffer pH 4 (mixture 9:1, 5 mL) were added than a ketone (0.5 mmol), pyrrolidine (0.2 equiv., 0.1 mmol) and a diazo ester (1.2 equiv., 0.6 mmol) were added without purging with argon. The reaction mixture was stirred under light irradiation (LED_{525nm}, 25 °C) for 5 h. The light was turned off; the reaction mixture was diluted with Et₂O, and washed with 1N HCl. The aqueous phase was extracted with Et₂O three times. Combined organic phases were washed with saturated NaHCO₃aq, brine, dried over MgSO₄, filtered, and concentrated. The crude product was purified by flash chromatography using silica gel (hexane/Et₂O).

General procedure for α -bis-alkylation of ketones in the presence of porphyrin – method B:

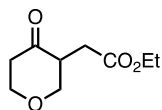
To a 10 mL vial equipped with a stir bar a photocatalyst (1 mol %) was added and dissolved in a mixture of DMSO and buffer pH 4 (mixture 9:1, 5 mL). The vial was sealed and solvent were purged with argon for 5 min. Then a ketone (1 equiv., 0.25 mmol), pyrrolidine (0.4 equiv., 0.1 mmol) and a diazo ester (3 equiv., 0.75 mmol) were added. The reaction mixture was stirred under light irradiation (LED_{525nm}, 25 °C) for 5 h. The light was turned off, the reaction mixture was diluted with Et₂O, and washed with 1N HCl. The aqueous phase was extracted with Et₂O three times. Combined organic phases were washed with saturated NaHCO₃aq, brine, dried over MgSO₄, filtered, and concentrated. The crude product was purified by flash chromatography using silica gel (hexane/Et₂O).

General procedure for α -bis-alkylation of ketones with no porphyrin added – method B':

To a 10 mL vial equipped with a stir bar a mixture of DMSO and buffer pH 4 (mixture 9:1, 5 mL) were added a ketone (1 equiv., 0.25 mmol), pyrrolidine (0.4 equiv., 0.1 mmol) and a diazo ester (3 equiv., 0.75 mmol) were added without purging with argon. The reaction mixture was stirred under light irradiation (LED_{525nm}, 25 °C) for 5 h. The light was turned off; the reaction mixture was diluted with Et₂O, and washed with 1N HCl. The aqueous phase was extracted with Et₂O three times. Combined organic phases were washed with saturated NaHCO₃aq, brine, dried over MgSO₄, filtered, and concentrated. The crude product was purified by flash chromatography using silica gel (hexane/Et₂O).

3. Scope and limitations

- 1) **ethyl 2-(4-oxotetrahydro-2H-pyran-3-yl)acetate (10h)** (colorless oil, Method A: 74 mg, 80% with porphyrin, 51 mg, 55% - no catalyst)



^1H NMR (400 MHz, CDCl_3 , 25°C): δ = 4.30-4.23 (m, 2 H, CH_2CO), 4.16-4.10 (m, 2 H, CH_2CH_3), 3.72-3.66 (td, 1 H, $^3J_{\text{H,H}} = 2.9, 11.7$ Hz, CHH), 3.40 (t, 1 H, $^3J_{\text{H,H}} = 11$ Hz, CHH), 3.13-3.05 (m, 1 H, CH), 2.74-2.69 (m, 2 H, CHH), 2.41-2.37 (dq, 1 H, $^3J_{\text{H,H}} = 1.7, 14.3$ Hz, CHH), 2.18-2.12 (dd, 1 H, $^3J_{\text{H,H}} = 6.52, 16.88$ Hz, CHH), 1.25 (t, 3 H, $^3J_{\text{H,H}} = 7.2$ Hz, CH_2CH_3) ppm.

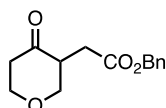
^{13}C NMR (100 MHz, CDCl_3 , 25°C): δ = 206.1, 171.5, 72.1, 68.6, 60.7, 47.7, 42.4, 29.9, 14.1 ppm.

IR film ν = 3630, 3536, 3418, 2979, 2936, 2856, 2759, 2726, 1734, 1716, 1475, 1447, 1415, 1371, 1352, 1306, 1254, 1213, 1181, 1152, 1100, 1028, 976, 945, 891, 865, 776, 751, 703, 526, 480, 426 cm^{-1} .

HRMS (ESI) calcd. for $\text{C}_9\text{H}_{14}\text{O}_4\text{Na}$ $[\text{M}+\text{Na}]^+$: 209.0790; found: 209.0784.

Elemental analysis calcd. (%) for $\text{C}_9\text{H}_{14}\text{O}_4$: C, 58.05, H, 7.58; found: C, 57.92, H, 7.75.

- 2) **benzyl 2-(4-oxotetrahydro-2H-pyran-3-yl)acetate (10a)** (colorless oil, Method A: 103 mg, 83% with porphyrin, 79 mg, 64% - no catalyst)



^1H NMR (400 MHz, CDCl_3 , 25°C): δ = 7.38-7.32 (m, 5 H, Ph), 5.13 (brs, 2 H, CH_2), 4.30-4.23 (m, 2 H, CH_2), 3.71-3.64 (td, 1 H, $^3J_{\text{H,H}} = 2.8, 11.7$ Hz, CHH), 3.40 (t, 1 H, $^3J_{\text{H,H}} = 11.1$ Hz, CHH), 3.14-3.09 (m, 1 H, CH), 2.82-2.74 (dd, 1 H, $^3J_{\text{H,H}} = 6.3, 16.9$ Hz, CHH), 2.73-2.67 (m, 1 H, CHH), 2.43-2.38 (dq, 1 H, $^3J_{\text{H,H}} = 1.7, 14.2$ Hz, CHH), 2.25-2.20 (dd, 1 H, $^3J_{\text{H,H}} = 6.4, 16.9$ Hz, CHH) ppm.

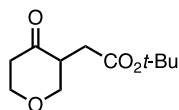
^{13}C NMR (100 MHz, CDCl_3 , 25°C): δ = 206.0, 171.4, 135.7, 128.6, 128.3, 128.2, 72.1, 68.6, 66.6, 47.6, 42.4, 29.9 ppm.

IR film ν = 3088, 3064, 3033, 2966, 2921, 2854, 1961, 1736, 1715, 1606, 1585, 1497, 1456, 1415, 1385, 1355, 1311, 1253, 1226, 1213, 1171, 1150, 1102, 1050, 971, 891, 868, 749, 699, 579, 504, 463, 403 cm^{-1} .

HRMS ESI calcd. for $\text{C}_{14}\text{H}_{16}\text{O}_4\text{Na}$ $[\text{M}+\text{Na}]^+$ 271.0946; found: 271.0939.

Elemental analysis calcd. (%) for $\text{C}_{14}\text{H}_{16}\text{O}_4$: C, 67.73, H, 6.50; found: C, 67.52, H, 6.54.

- 3) **tert-butyl 2-(4-oxotetrahydro-2H-pyran-3-yl)acetate (10i)** (colorless oil, Method A: 67 mg, 63% with porphyrin, 11 mg, 10% - no catalyst)



^1H NMR (400 MHz, CDCl_3 , 25°C): δ = 4.29-4.21 (m, 2 H, CH_2), 3.72-3.65 (td, 1 H, $^3J_{\text{H,H}} = 2.9, 11.6$ Hz, **CHH**), 3.40 (t, 1 H, $^3J_{\text{H,H}} = 10.9$ Hz, **CHH**), 3.07-3.02 (m, 1 H, CH), 2.73-2.67 (m, 1 H, **CHH**), 2.67-2.60 (dd, 1 H, $^3J_{\text{H,H}} = 6.3, 16.8$ Hz, **CHH**), 2.42-2.37 (dq, 1 H, $^3J_{\text{H,H}} = 1.96, 14.3$ Hz, **CHH**), 2.11-2.06 (dd, 1 H, $^3J_{\text{H,H}} = 6.6, 16.7$ Hz, **CHH**), 1.43 (brs, 9 H, $\text{C}(\text{CH}_3)_3$) ppm.

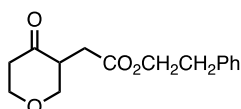
^{13}C NMR (100 MHz, CDCl_3 , 25°C): δ = 206.3, 170.7, 80.9, 72.2, 68.6, 47.9, 42.4, 31.2, 28.0 ppm.

IR film ν = 2977, 2930, 2852, 1722, 1475, 1415, 1367, 1255, 1221, 1156, 1102, 977, 947, 890, 850, 759, 702 cm^{-1} .

HRMS ESI calcd. for $\text{C}_{11}\text{H}_{18}\text{O}_4\text{Na}$ $[\text{M}+\text{Na}]^+$ 237.1103; found: 237.1092.

Elemental analysis calcd. (%) for $\text{C}_{11}\text{H}_{18}\text{O}_4$: C, 61.66, H, 8.47; found: C, 61.70, H, 8.51.

- 4) **phenethyl 2-(4-oxotetrahydro-2H-pyran-3-yl)acetate (10j)** (colorless oil, Method A: 82 mg, 54% with porphyrin, 68 mg, 42% - no catalyst)



^1H NMR (400 MHz, CDCl_3 , 25°C): δ = 7.32-7.20 (m, 5 H, Ph), 4.33-4.17 (m, 4 H, 2 x CH_2), 3.70-3.63 (td, 1 H, $^3J_{\text{H,H}} = 2.8, 11.3$ Hz, **CHH**), 3.36 (t, 1 H, $^3J_{\text{H,H}} = 10.9$ Hz, **CHH**), 3.09-3.06 (m, 1 H, CH), 2.93 (t, 2 H, $^3J_{\text{H,H}} = 7.0$, **CHH**), 2.74-2.66 (m, 2 H, CH_2), 2.41-2.36 (dq, 1 H, $^3J_{\text{H,H}} = 1.8, 14.3$ Hz, **CHH**), 2.18-2.12 (dd, 1 H, $^3J_{\text{H,H}} = 6.6, 16.9$ Hz, **CHH**) ppm.

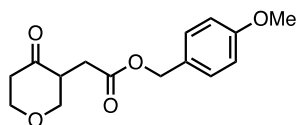
^{13}C NMR (100 MHz, CDCl_3 , 25°C): δ = 206.1, 171.4, 137.7, 128.9, 128.5, 126.6, 72.1, 68.6, 65.2, 47.6, 42.4, 35.0, 29.9 ppm.

IR film ν = 3061, 3030, 2964, 2921, 2855, 1734, 1716, 1604, 1497, 1455, 1415, 1386, 1356, 1310, 1253, 1212, 1174, 1151, 1102, 1051, 973, 890, 751, 701, 569, 494, 419 cm^{-1} .

HRMS ESI calcd. for $\text{C}_{15}\text{H}_{18}\text{O}_4\text{Na}$ $[\text{M}+\text{Na}]^+$ 285.1103; found: 285.1096.

Elemental analysis calcd. (%) for $\text{C}_{15}\text{H}_{18}\text{O}_4$: C, 68.68, H, 6.92; found: C, 68.40, H, 6.98.

- 5) **4-methoxybenzyl 2-(4-oxotetrahydro-2H-pyran-3-yl)acetate (10k)** (colorless oil, Method A: 87 mg, 63% with porphyrin, 72 mg, 52% - no catalyst)



^1H NMR (400 MHz, CDCl_3 , 25°C): δ = 7.29-7.27 (m, 2 H, Ph), 6.90-6.86 (m, 2 H, Ph), 5.06 (brs, 2 H, CH_2), 4.30-4.21 (m, 2 H, CH_2), 3.80 (s, 3 H, OCH_3), 3.70-3.63 (td, 1 H, $^3J_{\text{H,H}} = 2.9, 11.4$ Hz, **CHH**), 3.42-3.37 (t, 1 H, $^3J_{\text{H,H}} = 11$ Hz, **CHH**), 3.12-3.08 (m, 1 H, CH), 2.78-2.66 (m, 2 H, 2 x **CHH**), 2.42-2.37 (dq, 1 H, $^3J_{\text{H,H}} = 1.8, 14.0$ Hz, **CHH**), 2.22-2.16 (dd, 1 H, $^3J_{\text{H,H}} = 6.5, 17.0$ Hz, **CHH**) ppm.

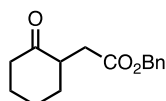
^{13}C NMR (100 MHz, CDCl_3 , 25°C): δ = 206.1, 171.4, 159.7, 130.1, 127.8, 114.0, 72.1, 68.6, 66.4, 55.3, 47.6, 42.4, 30.0 ppm.

IR film ν = 2963, 2839, 1733, 1715, 1613, 1586, 1516, 1461, 1417, 1385, 1354, 1304, 1250, 1171, 1150, 1102, 1033, 969, 891, 822, 752, 705, 560, 523 cm^{-1} .

HRMS ESI calcd. for $\text{C}_{15}\text{H}_{18}\text{O}_5\text{Na}$ [$\text{M}+\text{Na}$] $^+$ 301.1052; found: 301.1046.

Elemental analysis calcd. (%) for $\text{C}_{15}\text{H}_{18}\text{O}_5$: C, 64.74, H, 6.52; found: C, 64.71, H, 6.60.

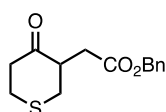
- 6) **benzyl 2-(2-oxocyclohexyl)acetate (10b)** (colorless oil, Method A: 59 mg, 48% with porphyrin, 12 mg, 10% - no catalyst)¹



^1H NMR (400 MHz, CDCl_3 , 25°C): δ = 7.36-7.25 (m, 5 H, Ph), 5.12 (brs, 2 H, CH_2), 2.90-2.80 (m, 2 H, **CHH**), 2.44-2.34 (m, 2 H, **CHH**), 2.22-2.06 (m, 3 H, CH, CH_2), 1.90-1.82 (m, 1 H, CH), 1.73-1.59 (m, 2 H, **CHH**), 1.46-1.37 (m, 1 H, **CHH**) ppm.

^{13}C NMR (100 MHz, CDCl_3 , 25°C): δ = 210.8, 172.4, 136.0, 128.5, 128.1, 128.1, 66.3, 47.1, 41.8, 34.4, 33.9, 27.7, 25.2 ppm.

- 7) **benzyl 2-(4-oxotetrahydro-2H-thiopyran-3-yl)acetate (10d)** (colorless oil, Method A: 46 mg, 35% with porphyrin, 24 mg, 20% - no catalyst)



^1H NMR (400 MHz, CDCl_3 , 25°C): δ = 7.36-7.25 (m, 5 H, **Ph**), 5.12 (brs, 2 H, **CH₂**), 3.26-3.15 (m,

1 H, **CH**), 2.98-2.90 (m, 3 H, **CHH**, **CH₂**) 2.90-2.83 (dd, 1 H, $^3J_{H,H} = 6.96, 16.8$ Hz, **CHH**), 2.80-2.73 (m, 3 H, **CHH**, **CH₂**), 2.39-2.33 (dd, 1 H, $^3J_{H,H} = 6.24, 16.8$ Hz, **CHH**) ppm.

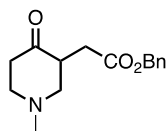
^{13}C NMR (100 MHz, CDCl_3 , 25°C): $\delta = 207.9, 171.5, 135.8, 128.6, 128.3, 128.2, 66.5, 49.4, 44.1, 35.5, 34.2, 30.8$ ppm.

IR film $\nu = 3065, 3032, 2954, 2915, 2836, 1734, 1711, 1497, 1455, 1425, 1386, 1342, 1319, 1297, 1276, 1216, 1186, 1158, 1116, 970, 810, 742, 699, 583, 477$ cm^{-1} .

HRMS ESI calcd. for $\text{C}_{14}\text{H}_{16}\text{O}_3\text{SNa}$ $[\text{M}+\text{Na}]^+$ 287.0718; found: 287.0708.

Elemental analysis calcd. (%) for $\text{C}_{14}\text{H}_{16}\text{O}_3\text{S}$: C, 63.61, H, 6.10, S, 12.13; found: C, 63.45, H, 6.29, S, 12.38.

8) benzyl 2-(N-methyl-4-oxopiperidin-3-yl)acetate (10e) (colorless oil, Method A: 20 mg, 15% with porphyrin, 30 mg, 23% - no catalyst)



^1H NMR (400 MHz, CDCl_3 , 25°C): $\delta = 7.35-7.30$ (m, 5 H, Ph), 5.12 (brs, 2 H, CH_2), 3.13-3.07 (m, 3 H, **CHH**, **CH₂**), 2.83-2.78 (dd, 1 H, $^3J_{H,H} = 6.24, 16.76$ Hz, **CHH**), 2.72-2.63 (m, 1 H, CH), 2.39-2.32 (m, 5 H, N- CH_3 , **CHH**), 2.24-2.18 (dd, 1 H, $^3J_{H,H} = 6.48, 16.76$ Hz, **CHH**), 2.17-2.07 (m, 1 H, **CHH**) ppm.

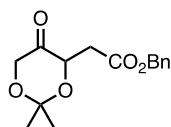
^{13}C NMR (100 MHz, CDCl_3 , 25°C): $\delta = 208.0, 171.8, 135.9, 128.5, 128.2, 128.2, 66.4, 60.8, 55.9, 45.9, 45.1, 40.7, 31.8$ ppm.

IR film $\nu = 3033, 2945, 2850, 2789, 1736, 1716, 1497, 1454, 1416, 1379, 1352, 1313, 1277, 1232, 1163, 1146, 1118, 1064, 982, 879, 806, 748, 699, 579, 461, 411$ cm^{-1} .

HRMS ESI calcd. for $\text{C}_{15}\text{H}_{20}\text{NO}_3$ $[\text{M}+\text{H}]^+$ 262.1443; found: 262.1443.

Elemental analysis calcd. (%) for $\text{C}_{15}\text{H}_{19}\text{NO}_3$: C, 68.94, H, 7.33, N, 5.36; found: C, 68.87, H, 7.32, N, 5.23.

9) benzyl 2-(2,2-dimethyl-5-oxo-1,3-dioxan-4-yl)acetate (10g) (colorless oil, Method A: 42 mg, 30% with porphyrin, 21 mg, 15% - no catalyst)



^1H NMR (400 MHz, CDCl_3 , 25°C): $\delta = 7.37-7.32$ (m, 5 H, Ph), 5.16 (brs, 2 H, CH_2), 4.73-4.70 (m, 1 H, CH), 4.32-4.27 (dd, 1 H, $^3J_{H,H} = 1.52, 17.08$ Hz, **CHH**), 4.04-4.00 (d, 1 H, $^3J_{H,H} = 17.04$, **CHH**),

2.97-2.91 (dd, 1 H, $^3J_{\text{H,H}} = 4.12, 16.72$, CHH), 2.69-2.63 (dd, 1 H, $^3J_{\text{H,H}} = 7.84, 16.8$ Hz, CHH), 1.43-1.40 (d, 6 H, $^3J_{\text{H,H}} = 14.76$, 2 x CH₃) ppm.

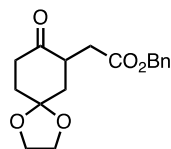
¹³C NMR (100 MHz, CDCl₃, 25°C): $\delta = 207.9, 170.1, 135.6, 128.5, 128.3, 128.3, 101.2, 71.6, 66.7, 66.5, 34.3, 23.7, 23.5$ ppm.

IR film $\nu = 3475, 3066, 3033, 2989, 2939, 2887, 1746, 1498, 1456, 1422, 1376, 1327, 1288, 1255, 1222, 1168, 1106, 1080, 1034, 969, 906, 835, 753, 699, 579, 516, 462$ cm⁻¹.

HRMS ESI calcd. for C₁₅H₁₈O₅Na [M+Na]⁺ 301.1052; found: 301.1045.

Elemental analysis calcd. (%) for C₁₅H₁₈O₅: C, 64.74, H, 6.52; found: C, 64.59, H, 6.57.

10) benzyl 2-(8-oxo-1,4-dioxaspiro[4.5]decan-7-yl)acetate (10f) (colorless oil, Method A: 70 mg, 46% with porphyrin, 8 mg, 5% - no catalyst)



¹H NMR (400 MHz, CDCl₃, 25°C): $\delta = 7.37-7.29$ (m, 5 H, Ph), 5.15-5.07 (m, 2 H, CH₂), 4.03-3.94 (m, 4 H, 2 x CH₂), 3.23-3.18 (m, 1 H, CHH), 2.81-2.75 (dd, 1 H, $^3J_{\text{H,H}} = 6.88, 16.72$ Hz, CHH), 2.74-2.65 (m, 1 H, CHH), 2.41-2.35 (ddd, 1 H, $^3J_{\text{H,H}} = 2.76, 5.04, 14.44$ Hz, CH), 2.27-2.21 (dd, 1 H, $^3J_{\text{H,H}} = 6.16, 16.72$ Hz, CHH), 2.11-1.92 (m, 3 H, CHH, CH₂), 1.79 (t, 1 H, $^3J_{\text{H,H}} = 13.16$ Hz, CHH) ppm.

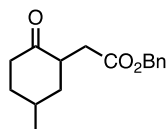
¹³C NMR (100 MHz, CDCl₃, 25°C): $\delta = 209.4, 171.8, 136.0, 128.8, 128.1, 128.1, 107.1, 66.3, 64.8, 64.6, 43.1, 40.1, 37.8, 34.6, 34.0$ ppm.

IR film $\nu = 3066, 3032, 2960, 2892, 1735, 1716, 1497, 1455, 1438, 1389, 1346, 1308, 1280, 1233, 1169, 1144, 1056, 999, 948, 930, 822, 743, 699, 579, 479, 454, 421$ cm⁻¹.

HRMS ESI calcd. for C₁₇H₂₀O₅Na [M+Na]⁺ 327.1208; found: 327.1204.

Elemental analysis calcd. (%) for C₁₇H₂₀O₅: C, 67.09, H, 6.62; found: C, 67.05, H, 6.67.

11) benzyl 2-(5-methyl-2-oxocyclohexyl)acetate (10c) (colorless oil, Method A: 39 mg, 30% with porphyrin, traces - no catalyst)



¹H NMR (400 MHz, CDCl₃, 25°C): two diastereoisomers (D1:D2 = 2 : 1) $\delta = 7.36-7.29$ (m, 2 x 5 H, Ph), 5.12 (s, 2 x 2 H, CH₂), 3.09-3.00 (m, 1 H, CH), [2.95-2.87 (m, 1 H, CH)], 2.84-2.77 (m, 2 x 1 H, 2 x CH), 2.55-2.46 (m, 1 H, CH), 2.45-2.37 (m, 1 H, CH), 2.34-2.26 (m, 2 x 1 H, 2 x CH), 2.25-2.14

(m, 2 x 1 H, 2 x CH), 2.13-1.197 (m, 3 H, CH, CH₂), 1.95-1.74 (m, 2 x 2 H, 2 x CH₂), 1.72-1.63 (m, 2 x 1 H, 2 x CH), 1.43-1.33 (m, 1 H, CH), 1.99 (d, 3 H, ³J_{H,H} = 7.08 Hz, CH₃), [0.97 (d, 3 H, ³J_{H,H} = 6.24 Hz, CH₃)] ppm.¹

¹³C NMR (100 MHz, CDCl₃, 25°C): two diastereoisomers δ = 211.5, [211.0], [172.4], 172.2, [136.0], 136.0, 128.5, 128.2, 128.1, 66.3, [66.3], [46.1], 42.5, [41.8], [41.0], 39.1, 37.3, [35.7], 34.7, [34.3], 33.1, [31.9], 26.9, [21.1], 18.1 ppm.

IR film ν = 3064, 3033, 2956, 2927, 2869, 1737, 1712, 1497, 1456, 1384, 1348, 1325, 1264, 1226, 1158, 1132, 1095, 1001, 913, 846, 744, 699, 580, 546, 504, 461 cm⁻¹.

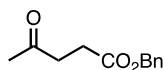
HRMS ESI calcd. for C₁₆H₂₀O₃Na [M+Na]⁺ 283.1310; found: 283.1305.

Elemental analysis calcd. (%) for C₁₆H₂₀O₃: C, 73.82, H, 7.74; found: C, 73.58, H, 8.00.

dr = 67:33 (GC; t₁ = 15.38 min, t₂ = 15.28 min, injection temp: 300; column flow: 1.50; split ratio: 20; purge flow: 3; temperature: 100-340°C, time of analysis: 30 min)

12) benzyl 4-oxopentanoate (10m) (colorless oil, Method A: 36 mg, 36% with porphyrin

Method B: 27 mg, 53% with porphyrin, 0% - no catalyst)²

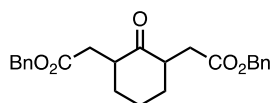


¹H NMR (400 MHz, CDCl₃, 25°C): δ = 7.37-7.29 (m, 5 H, Ph), 5.12 (brs, 2 H, CH₂), 2.76 (t, 2 H, ³J_{H,H} = 6.56 Hz CH₂), 2.63 (t, 2 H, ³J_{H,H} = 6.80 Hz, CH₂), 2.17 (s, 3 H, CH₃) ppm.

¹³C NMR (100 MHz, CDCl₃, 25°C): δ = 206.4, 172.5, 135.9, 128.5, 128.2, 128.1, 66.5, 37.9, 29.8, 28.0 ppm.

13) dibenzyl 2,2'-(2-oxocyclohexane-1,3-diyl)diacetate (10bb) + diastereoisomer (8: 2,

colorless oil, Method B: 79 mg, 80% with porphyrin, traces - no catalyst)



¹H NMR (400 MHz, CDCl₃, 25°C): δ = 7.38-7.29 (m, 10 H, 2 x Ph), 5.12 (brs, 4 H, 2 x CH₂), 2.97-2.91 (m, 2 H, 2 x CHH), 2.87-2.82 (dd, 2 H, ³J_{H,H} = 6.84, 16.56 Hz, 2 x CHH), 2.26-2.19 (dd, 2 H, ³J_{H,H} = 6.36, 16.6 Hz, 2 x CHH), 2.19-2.14 (m, 2 H, 2 x CH), 1.87-1.79 (m, 2 H, 2 x CHH), 1.43-1.39 (m, 2 H, CH₂) ppm.

¹³C NMR (100 MHz, CDCl₃, 25°C): δ = 209.9, 172.2, 136.0, 128.5, 128.1, 128.1, 66.3, 47.0, 34.4, 34.3, 25.0 ppm.

¹ [] – concerns second diastereoisomer

IR film $\nu = 3064, 3033, 2935, 2859, 1736, 1712, 1497, 1455, 1413, 1388, 1346, 1276, 1166, 1117, 1000, 911, 864, 751, 698, 580, 457 \text{ cm}^{-1}$.

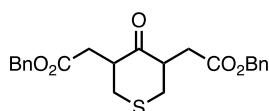
HRMS ESI calcd. for $\text{C}_{24}\text{H}_{26}\text{O}_5\text{Na} [\text{M}+\text{Na}]^+$ 417.1678; found: 417.1671.

Elemental analysis calcd. (%) for $\text{C}_{24}\text{H}_{26}\text{O}_5$: C, 73.08, H, 6.64; found: C, 72.76, H, 6.72.

$dr = 82:18$ (GC) (GC; $t_1 = 15.1 \text{ min}$, $t_2 = 14.7 \text{ min}$, injection temp: 300; column flow: 1.50; split ratio: 20; purge flow: 3; temperature: 100-340°C, time of analysis: 30 min)

14) dibenzyl 2,2'-(4-oxotetrahydro-2H-thiopyran-3,5-diyl)diacetate (10dd) + diastereoisomer

(8 : 2, colorless oil, Method B: 80 mg, 77% with porphyrin, traces - no catalyst)



^1H NMR (400 MHz, CDCl_3 , 25°C): $\delta = 7.38\text{-}7.29$ (m, 10 H, 2 x Ph), 5.12 (brs, 4 H, 2 x CH_2), 3.35-3.29 (m, 2 H, 2 x CH), 2.98-2.96 (m, 2 H, 2 x **CHH**), 2.88-2.84 (dd, 2 H, $^3J_{\text{H,H}} = 6.72, 16.84 \text{ Hz}$, 2 x **CHH**), 2.80-2.73 (m, 2 H, 2 x **CHH**), 2.36-2.30 (dd, 2 H, $^3J_{\text{H,H}} = 6.52, 16.88 \text{ Hz}$, 2 x **CHH**) ppm.

^{13}C NMR (100 MHz, CDCl_3 , 25°C): $\delta = 207.8, 171.3, 135.8, 128.6, 128.3, 128.2, 66.5, 49.8, 36.3, 34.2 \text{ ppm}$.

IR film $\nu = 3089, 3064, 3033, 2955, 2837, 1736, 1712, 1607, 1586, 1497, 1455, 1428, 1410, 1386, 1342, 1298, 1168, 1108, 1002, 923, 876, 751, 698, 580, 505, 456 \text{ cm}^{-1}$.

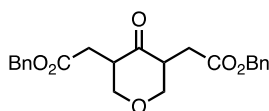
HRMS ESI calcd. for $\text{C}_{23}\text{H}_{24}\text{O}_5\text{SNa} [\text{M}+\text{Na}]^+$ 435.1242; found: 435.1232.

Elemental analysis calcd. (%) for $\text{C}_{23}\text{H}_{24}\text{O}_5\text{S}$: C, 66.97, H, 5.86, S, 7.77; found: C, 67.13, H, 6.14, S, 7.74.

$dr = 77:33$ (GC) (GC; $t_1 = 22.3 \text{ min}$, $t_2 = 22.1 \text{ min}$, injection temp: 300; column flow: 1.50; split ratio: 20; purge flow: 3; temperature: 100-340°C, time of analysis: 30 min)

15) dibenzyl 2,2'-(4-oxotetrahydro-2H-pyran-3,5-diyl)diacetate (10aa) + diastereoisomer (7 :

3, colorless oil, Method B: 74 mg, 75% with porphyrin, traces - no catalyst)



^1H NMR (400 MHz, CDCl_3 , 25°C): $\delta = 7.37\text{-}7.31$ (m, 10 H, 2 x Ph), 5.12 (brs, 4 H, 2 x CH_2), 4.32-4.28 (m, 2 H, 2 x CH), 3.38 (t, 2 H, $^3J_{\text{H,H}} = 11.28, 2 \times \text{CHH}$), 3.24-3.21 (m, 2 H, 2 x **CHH**), 2.88-2.77 (dd, 2 H, $^3J_{\text{H,H}} = 6.20, 17.04 \text{ Hz}$, 2 x **CHH**), 2.21-2.16 (dd, 2 H, $^3J_{\text{H,H}} = 6.52, 16.96 \text{ Hz}$, 2 x

CHH) ppm.

^{13}C NMR (100 MHz, CDCl_3 , 25°C): $\delta = 205.8, 171.3, 135.7, 128.6, 128.3, 128.2, 72.8, 66.6, 47.2, 29.7$ ppm.

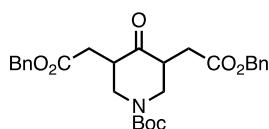
IR film $\nu = 3089, 3064, 3033, 2959, 2845, 1736, 1716, 1586, 1497, 1456, 1413, 1383, 1355, 1254, 1219, 1172, 1133, 1081, 1059, 946, 868, 752, 698, 580, 498, 470$ cm^{-1} .

HRMS ESI calcd. for $\text{C}_{23}\text{H}_{24}\text{O}_6\text{Na}$ $[\text{M}+\text{Na}]^+$ 419.1471; found: 419.146.3

Elemental analysis calcd. (%) for $\text{C}_{23}\text{H}_{24}\text{O}_6$: C, 69.68, H, 6.10; found: C, 69.58, H, 6.05.

$dr = 72:28$ (GC) (GC; $t_1 = 22.2$ min, $t_2 = 21.8$ min, injection temp: 300; column flow: 1.50; split ratio: 20; purge flow: 3; temperature: 100-340 $^\circ\text{C}$, time of analysis: 30 min)

16) dibenzyl 2,2'-(1-(*tert*-butoxycarbonyl)-4-oxopiperidine-3,5-diyl)diacetate (10oo) + diastereoisomer (8 : 2) colorless oil, Method B: 103 mg, 83% with porphyrin, traces - no catalyst)



^1H NMR (400 MHz, CDCl_3 , 25°C): $\delta = 7.37\text{-}7.31$ (m, 10 H, 2 x Ph), 5.12 (brs, 4 H, 2 x CH_2), 4.56-4.35 (m, 2 H, 2 x CH), 3.06-3.00 (m, 2 H, 2 x **CHH**), 2.83-2.77 (m, 4 H, 2 x CH_2), 2.31-2.26 (m, 2 H, 2 x **CHH**), 1.48 (s, 9 H, $\text{C}(\text{CH}_3)_3$) ppm.

^{13}C NMR (100 MHz, CDCl_3 , 25°C): $\delta = 206.8, 171.8, 154.1, 135.8, 128.5, 128.2, 128.2, 80.9, 66.6, 46.2, 31.2, 28.3, 28.0$ ppm.

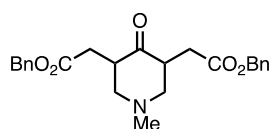
IR film $\nu = 3628, 3449, 3090, 3065, 3033, 3005, 2976, 2931, 1806, 1738, 1717, 1696, 1608, 1497, 1475, 1454, 1420, 1392, 1366, 1305, 1278, 1241, 1166, 1119, 1048, 1030, 971, 889, 827, 750, 699, 580, 500, 460$ cm^{-1} .

HRMS ESI calcd. for $\text{C}_{28}\text{H}_{33}\text{NO}_7\text{Na}$ $[\text{M}+\text{Na}]^+$ 518.2155; found: 518.2154.

Elemental analysis calcd. (%) for $\text{C}_{28}\text{H}_{33}\text{NO}_7$: C, 67.86, H, 6.71, N, 2.83; found: C, 68.05, H, 6.90, N, 2.75.

$dr = 76:24$ (GC) (GC; $t_1 = 14.5$ min, $t_2 = 13.8$ min, injection temp: 300; column flow: 1.50; split ratio: 20; purge flow: 3; temperature: 170-340 $^\circ\text{C}$, time of analysis: 30 min)

17) dibenzyl 2,2'-(1-methyl-4-oxopiperidine-3,5-diyl)diacetate (10ee) + diastereoisomer (7 : 3, colorless oil, Method B: 55 mg, 54% with porphyrin, traces - no catalyst)



^1H NMR (400 MHz, CDCl_3 , 25°C): δ = 7.37-7.25 (m, 10 H, 2 x Ph), 5.11 (brs, 4 H, 2 x CH_2), 3.26-3.21 (m, 2 H, 2 x **CH**), 3.17-3.12 (m, 2 H, 2 x **CHH**), 2.85-2.79 (dd, 2 H, $^3J_{\text{H,H}} = 6.2$, 16.76 Hz, 2 x **CHH**), 2.35 (s, 3 H, CH_3), 2.21-2.11 (m, 4 H, 2 x CH_2) ppm.

^{13}C NMR (100 MHz, CDCl_3 , 25°C): δ = 207.6, 171.7, 135.9, 128.5, 128.2, 128.2, 66.4, 61.3, 45.4, 44.8, 31.6 ppm.

IR film ν = 3064, 3033, 2945, 2850, 2785, 1737, 1717, 1607, 1497, 1454, 1413, 1380, 1355, 1281, 1235, 1171, 1121, 1059, 975, 950, 911, 862, 825, 750, 699, 580, 467 cm^{-1} .

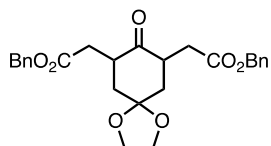
HRMS ESI calcd. for $\text{C}_{24}\text{H}_{28}\text{NO}_5$ $[\text{M}+\text{H}]^+$ 410.1967; found: 410.1960.

Elemental analysis calcd. (%) for $\text{C}_{24}\text{H}_{27}\text{NO}_5$: C, 70.40, H, 6.65, N, 3.42; found: C, 70.50, H, 6.90, N, 3.47.

dr = 73:27 (GC) (GC; t_1 = 13.3 min, t_2 = 12.5 min, injection temp: 300; column flow: 1.50; split ratio: 20; purge flow: 3; temperature: 100-340 $^\circ\text{C}$, time of analysis: 30 min)

18) dibenzyl 2,2'-(8-oxo-1,4-dioxaspiro[4.5]decane-7,9-diyl)diacetate (10ff) + diastereoisomer

(7 : 3, colorless solid, Method B: 67 mg, **59%** with porphyrin, traces - no catalyst)



^1H NMR (400 MHz, CDCl_3 , 25°C): δ = 7.36-7.25 (m, 10 H, 2 x Ph), 5.12 (2 x brs, 4 H, 2 x CH_2), 4.02-3.93 (m, 4 H, 2 x CH_2), 2.83-2.77 (dd, 2 H, $^3J_{\text{H,H}} = 6.44$, 13.48 Hz, 2 x **CHH**), 2.27-2.21 (dd, 2 H, $^3J_{\text{H,H}} = 6.48$, 16.76 Hz, 2 x **CHH**), 2.13-2.08 (m, 2 H, 2 x CH), 1.78 (t, 2 H, $^3J_{\text{H,H}} = 18.88$ Hz, 2 x CH) ppm.

^{13}C NMR (100 MHz, CDCl_3 , 25°C): δ = 208.8, 171.7, 135.9, 128.5, 128.2, 128.2, 106.6, 66.3, 64.8, 64.7, 42.9, 40.8, 33.9 ppm.

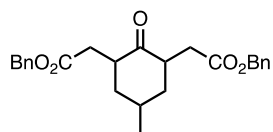
IR film ν = 3065, 3033, 2956, 2891, 1736, 1718, 1497, 1455, 1389, 1350, 1291, 1234, 1170, 1119, 1096, 1057, 1031, 998, 950, 793, 752, 698, 580, 459, 434 cm^{-1} .

HRMS ESI calcd. for $\text{C}_{26}\text{H}_{29}\text{O}_7$ $[\text{M}+\text{H}]^+$ 475.1733; found: 475.1720.

Elemental analysis calcd. (%) for $\text{C}_{26}\text{H}_{28}\text{O}_7$: C, 69.01, H, 6.24; found: C, 69.07, H, 25.

dr = 71:28 (GC) (GC; t_1 = 18.1 min, t_2 = 17.7 min, injection temp: 300; column flow: 1.50; split ratio: 20; purge flow: 3; temperature: 100-340 $^\circ\text{C}$, time of analysis: 30 min)

19) dibenzyl 2,2'-(5-methyl-2-oxocyclohexane-1,3-diyl)diacetate (10cc) + diastereoisomer (8 : 2, colorless oil, Method A: 41 mg, 20% with porphyrin, traces - no catalyst)



^1H NMR (400 MHz, CDCl_3 , 25°C): two diastereoisomers: $\delta = 7.36\text{-}7.25$ (m, 10 H, 2 x Ph + diastereoisomer m, 10 H, 2 x Ph), 5.12 (brs, 4 H, 2 x CH_2), [5.13 (brs, 4 H, 2 x CH_2)], 3.20-3.08 (m, 2 H, 2 x CH), [3.05-2.80 (m, 2 H, 2 x CH)], 2.87-2.81 (dd, 2 H, $^3J_{\text{H,H}} = 6.84, 16.64$ Hz, 2 x CHH), [2.76-2.56 (m, 2 H, 2 x CH)], 2.28-2.06 (m, 4 H, 4 x CHH + diastereoisomer m, 4 H, 4 x CHH), 1.95-1.90 (m, 2 H, 2 x CHH + diastereoisomer m, 2 H, 2 x CHH), 1.69-1.63 (m, 1 H, CHH + diastereoisomer m, 1 H, 4 x CHH), 1.28 (d, 3 H, $^3J_{\text{H,H}} = 7.20$ Hz, CH_3), [0.96-0.94 (d, 3 H, $^3J_{\text{H,H}} = 6.28$ Hz, CH_3)]² ppm

^{13}C NMR (100 MHz, CDCl_3 , 25°C): $\delta = 210.4, 172.2, 136.0, 128.5, 128.3, 128.1, 66.3, 42.0, 40.1, 34.3, 27.1, 17.8$ ppm.

IR film $\nu = 3064, 3033, 2957, 2925, 1737, 1712, 1607, 1497, 1456, 1413, 1386, 1348, 1229, 1170, 1119, 1001, 970, 924, 750, 699, 580, 467$ cm^{-1} .

HRMS ESI calcd. for $\text{C}_{25}\text{H}_{29}\text{O}_5$ $[\text{M}+\text{H}]^+$ 431.1834; found: 431.1830.

Elemental analysis calcd. (%) for $\text{C}_{25}\text{H}_{28}\text{O}_5$: C, 73.51, H, 6.91; found: C, 73.48, H, 7.00.

$dr = 79:21$ (GC) (GC; $t_1 = 22.1$ min, $t_2 = 21.9$ min, injection temp: 300; column flow: 1.50; split ratio: 20; purge flow: 3; temperature: 100-340°C, time of analysis: 30 min)

² [] – concerns second diastereoisomer

4. Optimization studies

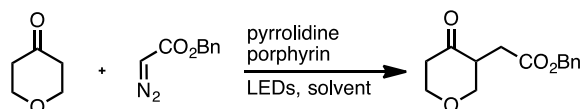


Table S1. Background reactions^a

Entry	Amine	Light	Temp	Photocatalyst	Additive	Yield [%] [*]
1	pyrrolidine	LED _{525nm}	rt	H ₂ T(<i>p</i> -CO ₂ MeP)P	-	68
2	pyrrolidine	LED _{525nm}	rt	-	-	51
3 ^b	pyrrolidine	LED _{525nm}	rt	-	-	25
4	pyrrolidine	-	rt	H ₂ T(<i>p</i> -CO ₂ MeP)P	-	3
5	pyrrolidine	-	45°C	H ₂ T(<i>p</i> -CO ₂ MeP)P	-	traces
6	-	LED _{525nm}	rt	H ₂ T(<i>p</i> -CO ₂ MeP)P	-	0
7	NEt ₃	LED _{525nm}	rt	H ₂ T(<i>p</i> -CO ₂ MeP)P	-	0
8	pyrrolidine	UV	rt	benzophenone	-	20
9	pyrrolidine	LED _{525nm}	rt	H ₂ T(<i>p</i> -CO ₂ MeP)P	benzochinone ^{**}	0
10	pyrrolidine	LED _{525nm}	rt	-	benzochinone ^{**}	0
11	pyrrolidine	LED _{525nm}	rt	H ₂ T(<i>p</i> -CO ₂ MeP)P	1,3-cycloheksadien ^{***}	0
12	pyrrolidine	LED _{525nm}	rt	-	1,3-cycloheksadien ^{***}	traces
13	pyrrolidine	LED _{525nm}	rt	-	CAN	0
14	pyrrolidine	LED _{525nm}	rt	-	nitrobenzene	0
15	pyrrolidine	LED _{525nm}	rt	-	K ₂ S ₂ O ₈	25

Reaction conditions: ^aketone (0.5 mmol), diazo ester (0.5 mmol), photocatalyst: H₂T(*p*-CO₂MeP)P (1.0 mol%) or benzophenone (20 mol%), amine (20 mol%), DMSO/buffer pH 4.0 = 9:1 (V/V, 5 mL), 8 h. ^bketone (0.5 mmol), diazo ester (0.5 mmol), photocatalyst: H₂T(*p*-CO₂MeP)P (1.0 mol%) or benzophenone (20 mol%), amine (20 mol%), DMSO (5 mL), 8 h, LED_{525nm}. ^{*}Isolated yields ^{**}Quencher of triplet excited states ^{***}Quencher of singlet and triplet excited states⁴.

Table S2. Light^a

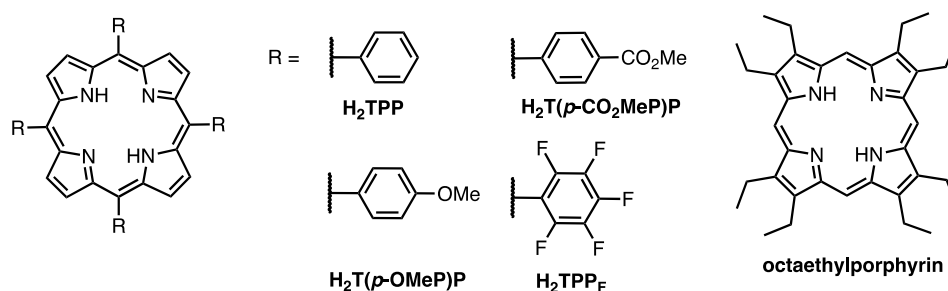
Entry	Photocatalyst	Light	Yield [%] ^b
1	H ₂ T(<i>p</i> -CO ₂ MeP)P	LED _{525nm}	61
2	-	LED _{525nm}	53
3	H ₂ T(<i>p</i> -CO ₂ MeP)P	LED _{454nm}	55
4	-	LED _{454nm}	30
5	H ₂ T(<i>p</i> -CO ₂ MeP)P	LED _{525nm} - stripes	68
6	-	LED _{525nm} - stripes	51
7	H ₂ T(<i>p</i> -CO ₂ MeP)P	LED _{454nm} - stripes	50
8	-	LED _{454nm} - stripes	32

Reaction conditions: ^aketone (0.5 mmol), diazo ester (0.5 mmol), photocatalyst (1.0 mol%), pyrrolidine (20 mol%), DMSO/buffer pH 4.0 = 9:1 (V/V, 5 mL), 8 h, LED_{525nm}. ^bIsolated yields.

Table S3. Time^a

Entry	Time [h]	Yield [%] ^b
1	4	60
2	6	61
3	7	71
4	8	68
5	9	68
6	10	58
7	12	47

Reaction conditions: ^aketone (0.5 mmol), diazo ester (0.5 mmol), H₂T(*p*-CO₂MeP)P (1.0 mol%), pyrrolidine (20 mol%), DMSO/buffer pH 4.0 = 9:1 (V/V, 5 mL), X h, LED_{525nm}. ^bIsolated yields

Table S4. Photocatalyst^a

Entry	Photocatalyst	Yield [%]*
1	H ₂ T(<i>p</i> -CO ₂ MeP)P	71
2	H ₂ T(<i>p</i> -CO ₂ MeP)P-Zn	65
3	H ₂ TPP	44
4	H ₂ TPP _F	14
5	H ₂ T(<i>p</i> -OMeP)P	65
6	octaethylporphyrin	45

Reaction conditions: ^aketone (0.5 mmol), diazo ester (0.5 mmol), photocatalyst (1.0 mol%), pyrrolidine (20 mol%), DMSO/buffer pH 4.0 = 9:1 (V/V) 5 mL, 7 h, LED_{525nm}. *Isolated yields

Table S5. Solvent^a

Entry	Solvent	Yield [%] ^b
1	DMSO/buffer pH = 4	71
2	DMSO	22
2	DMSO/H ₂ O	59
3	DMF/buffer pH = 4	24
4	DMF	27
5	MeCN	30
6	MeCN/buffer pH = 4	traces
7	MeOH	24
8	MeOH/buffer pH = 4	0
9	MTBE	0
10	DCM	0
11	Toluene	0
12	EtOH	0
13	EtOH/buffer pH = 4	0
14	1,1,1,3,3,3-hexafluoroisopropanol	0

Reaction conditions: ^aketone (0.5 mmol), diazo ester (0.5 mmol), H₂T(*p*-CO₂MeP)P (1.0 mol%), pyrrolidine (20 mol%), solvent (5 mL) or solvent/buffer pH 4.0 = 9:1 (V/V, 5 mL), 7 h, LED_{525nm}. ^bIsolated yields

Table S6. pH of buffer^a

Entry	Solvent	Yield [%] ^b
1	DMSO/buffer pH = 3.0	56
2	DMSO/buffer pH = 4.0	71
2	DMSO/buffer pH = 5.0	50
3	DMSO/buffer pH = 7.0	59
4	DMSO/buffer pH = 8.0	33

Reaction conditions: ^aketone (0.5 mmol), diazo ester (0.5 mmol), H₂T(*p*-CO₂MeP)P (1.0 mol%), pyrrolidine (20 mol%), DMSO/buffer pH = X, 9:1 (V/V, 5 mL), 7 h, LED_{525nm}. ^bIsolated yield

Table S7. Amine^a

Entry	Amine	pK _b	Yield [%]b
1	pyrrolidine	2.89	71
2	morpholine	5.60	21
2	piperazine	4.19	21
4	dicyclohexylamine	3.60	0

Reaction conditions: ^aketone (0.5 mmol), diazo ester (0.5 mmol), H₂T(*p*-CO₂MeP)P (1.0 mol%), amine (20 mol%), DMSO/buffer pH = 4, 9:1 (V/V, 5 mL), 7 h, LED_{525nm}. ^bIsolated yields

Table S8. Light vs. time^a

Entry	Light	Time	Yield [%]b
1	LED _{525nm} - stripes	7	71
2	LED _{525nm}	4	48
3	LED _{525nm}	5	74
4	LED _{525nm}	6	71

Reaction conditions: ^aketone (0.5 mmol), diazo ester (0.5 mmol), H₂T(*p*-CO₂MeP)P (1.0 mol%), pyrrolidine (20 mol%), DMSO/buffer pH 4 = 9:1 (V/V, 5 mL), X h, LED_{525nm}. ^bIsolated yields

Table S9. Amine – amount^a

Entry	Pyrrolidine [mol%]	Yield [%]b
1	30	75
2	20	74
3	15	65
4	10	55

Reaction conditions: ^aketone (0.5 mmol), diazo ester (0.5 mmol), H₂T(*p*-CO₂MeP)P (1.0 mol%), pyrrolidine (X mol%), DMSO/buffer pH = 4, 9:1 (V/V, 5 mL), 5 h, LED_{525nm}. ^bIsolated yields

Table S10. Additives^a

Entry	Solvent	Additive	pK _a	Yield [%]b
1	DMSO/buffer pH 4	LiBF ₄	-	47
2	DMSO	H ₂ O	15.7	42
3	DMSO	PhCOOH	6.60	18
4	DMSO	AcOH	4.73	14
5	DMSO/	2,3-lutidine	4.17	traces
6	DMSO	<i>p</i> -TSA·H ₂ O	-2.80	9

Reaction conditions: ^aketone (0.5 mmol), diazo ester (0.5 mmol), H₂T(*p*-CO₂MeP)P (1.0 mol%), pyrrolidine (20 mol%), DMSO/buffer pH = 4, 9:1 (V/V, 5 mL), additive (20 mol%), 5 h, LED_{525nm}. ^bIsolated yields

Table S11. Catalyst loading^a

Entry	Catalyst loading [mol%]	Yield [%]b
1	1.5	58
2	1.0	74
3	0.5	68

Reaction conditions: ^aketone (0.5 mmol), diazo ester (0.5 mmol), H₂T(*p*-CO₂MeP)P (X mol%), pyrrolidine (20 mol%), DMSO/buffer pH = 4, 9:1 (V/V, 5 mL), 5 h, LED_{525nm}. ^bIsolated yields

Table S12. Ketone: diazoester ratio [equiv. : equiv.]^a

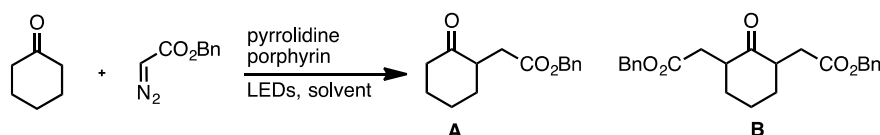
Entry	Ketone: Diazo compound [equiv.]	Yield [%] ^b
1	1:1.2	83
2	1:1	74
3	1.2:1	65

Reaction conditions: ^aketone (X mmol), diazo ester (X mmol), H₂T(*p*-CO₂MeP)P (1 mol%), pyrrolidine (20 mol%), DMSO/buffer pH = 4, 9:1 (V/V, 5 mL), 5 h, LED_{525nm}. ^bIsolated yields

Table S13. Solvent: buffer ratio [V/V]^a

Entry	Solvent : buffer pH = 4 [V/V]	Yield [%] ^b
1	8.5 : 1.5	30
2	9.0 : 1.0	83
3	9.5 : 0.5	65

Reaction conditions: ^aketone (0.5 mmol), diazo ester (0.5 mmol), H₂T(*p*-CO₂MeP)P (1 mol%), pyrrolidine (20 mol%), DMSO/buffer pH = 4, X:X (V/V, 5 mL), 5 h, LED_{525nm}. ^bIsolated yields

**Table S14. Background reactions^a**

Entry	Amine	Light	Temp	Photocatalyst	Yield A [%] ^c	Yield B [%] ^c
1	pyrrolidine	-	rt	H ₂ T(<i>p</i> -CO ₂ MeP)P	traces	traces
2	pyrrolidine	LED _{525nm}	rt	-	10	3
3 ^b	pyrrolidine	LED _{525nm}	rt	H ₂ T(<i>p</i> -CO ₂ MeP)P	30	30

Reaction conditions: ^aketone (0.5 mmol), diazo ester (0.5 mmol), H₂T(*p*-CO₂MeP)P (1.0 mol%), amine (20 mol%), DMSO/buffer pH 4.0 = 9:1 (V/V, 5 mL), 5 h, LED_{525nm}. ^bModel conditions for 4-oxotetrahydropyran: ketone (0.5 mmol), diazoester (0.6 mmol), photocatalyst: H₂T(*p*-CO₂MeP)P (1.0 mol%), amine (20 mol%), DMSO/buffer pH 4.0 = 9:1 (V/V, 5 mL), 5 h, LED_{525nm}. ^cIsolated yields.

Table S15. Optimization – mono product (A)

Entry	Ketone [equiv.]	BDA [equiv.]	Temp.	Yield A [%] ^c	Yield B [%] ^c
1	1	1.2	rt	30	30
2 ^b	1	1.2	rt	33	28
3 ^b	1	1	rt	48	20
4 ^b	1	1	15 °C	14	31
5	2	1	rt	20	26

Reaction conditions: ^aketone (0.5 mmol), diazo ester (X mmol), H₂T(*p*-CO₂MeP)P (1.0 mol%), amine (20 mol%), DMSO/buffer pH 4.0 = 9:1 (V/V, 5 mL), 5 h, LED_{525nm}. ^bketone (0.5 mmol), diazo ester (X mmol), H₂T(*p*-CO₂MeP)P (1.0 mol%), amine (20 mol%), DMSO/buffer pH 4.0 = 9:1 (V/V, 10 mL), 5 h, LED_{525nm}. ^cIsolated yields

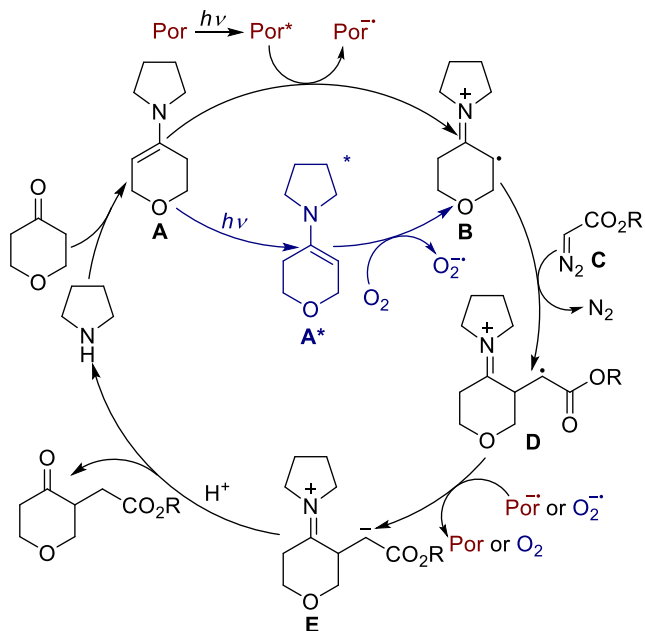
Table S16. Optimization – bis product (B)

Entry	BDA [equiv.]	Amine [mol%]	Temp	Yield A [%] ^b	Yield B [%] ^b
1	1.2	20	rt	30	30
2	3	20	rt	20	65
3	3	20	39°C	18	56
4	3	40	rt	10	80
5	1.5 + 1.5	20	rt	19	66
6	4	20	rt	20	67

Reaction conditions: ^aketone (0.5 mmol, 1 equiv.), diazoester (X mmol), H₂T(*p*-CO₂MeP) (1.0 mol%), amine (X mol%), DMSO/buffer pH = 4.0, 9:1 (V/V, 5 mL), 5 h, LED_{525nm}. ^bIsolated yields.

5. Mechanistic considerations

5.1. Proposed mechanism



5.2. Electrochemical data for porphyrins

Porphyrin	E_{ox}	E_{red}	E_{ox}^{*s}	E_{red}^{*s}	E_{00}^s	Solvent
H ₂ TPP	1.03	-1.04, -1.46	-0.91	0.91	1.90	DMSO
H ₂ T(<i>p</i> -OMeP)P	0.91	-1.07, -1.46	-0.99	0.83	1.90 ⁵	DMSO
H ₂ T(F ₅ P)P	0.89, 1.23 ⁶	-1.28, -1.71	-1.04	0.65	1.93 ⁷	DMSO
H ₂ T(<i>p</i> -CO ₂ MeP)P	1.14 ⁸	-0.92, -1.33 ⁹	-0.81	1.03	1.95	CH ₂ Cl ₂
octaethylporphyrin	0.46, 0.95	-1.34, -1.79	-1.52	0.64	1.98 ¹⁰	CH ₂ Cl ₂

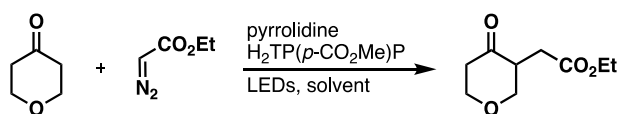
E_{red}/E_{ox} vs SCE

5.3. EPR – experimental and theoretical studies

spin trap:	<i>N-tert</i> -butyl- α -phenylnitron (PBN) or 5,5-dimethyl-1-pyrroline <i>N</i> -oxide (DMPO)
central magnetic field:	333 mT;
sweep width:	7,9 mT;
modulation amplitude:	0,06 mT;
microwave strength:	6,3 mW;
sweep time:	30 s;
number of scans:	16
simulation	EasySpin package in Matlab

System with porphyrin

Conditions: Ketone (0.5 mmol), EDA (1 equiv., 0.5 mmol), pyrrolidine (0.2 equiv., 0.1 mmol), H₂T(*p*-CO₂MeP)P (1 mol%), DMSO : buffer pH 4 (5 mL, 9:1). After 10 min. of stirring under irradiation (LED_{525nm} stripes) *N-tert*-butyl- α -phenylnitron (BPN) was added and after next 10 min. of stirring under irradiation (LED_{525nm} stripes) EPR spectra (9.3 GHz) were recorded.



The EPR spectrum obtained for the whole reaction (4-oxotetrahydro-2H-pyran, pyrrolidine, EDA, H₂T(*p*-CO₂Me)P in the presence of PBN (Figure S1) is the superposition of two very similar components (triplets of doublets with hyperfine splitting constants: $a_N = 1.49$ mT, $a_{H\beta} = 0.44$ mT and $a_N = 1.51$ mT, $a_{H\beta} = 0.41$ mT, relative intensity 53 and 47%, respectively). Their hyperfine splitting constants suggest the presence of carbon-centered radicals where the carbon with an unpaired electron is near a carbonyl group, as they are similar to values obtained for PBN-benzoyl radical adduct in DMSO solution ($a_N = 1.45$ mT and $a_H = 0.47$ mT).¹¹ When the reaction has been conducted in the presence of DMPO (Figure S2) two components are present, the dominating one (90% of total intensity) with hyperfine splitting constants of 1.47 mT (a_N) and 2.16 mT ($a_{H\beta}$) and a second one with $a_N = 1.60$ mT and $a_H = 2.46$ mT. Both components indicate the formation of carbon-centered radicals, as the value of $a_{H\beta}$ is higher than this of a_N .¹²

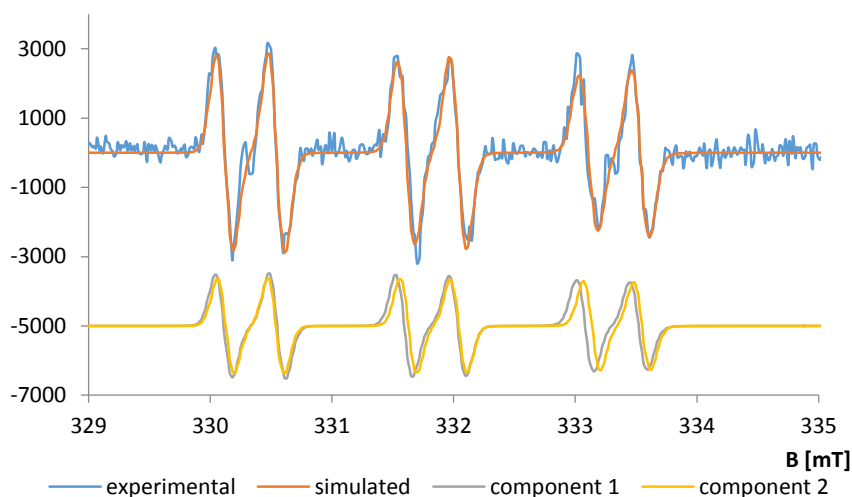


Figure S1. EPR spectra of the reaction mixture with PBN Conditions: 4-oxotetrahydropyran (0.5 mmol), EDA (1 equiv., 0.5 mmol), pyrrolidine (0.2 equiv., 0.1 mmol), H₂T(*p*-CO₂MeP)P (1 mol%), DMSO : buffer pH 4 (5 mL, 9:1). After 10 min. of stirring under irradiation (LED_{525nm} stripes) *N*-*tert*-butyl- α -phenylnitron (BPN) was added and after next 10 min. of stirring under irradiation (LED_{525nm} stripes) EPR spectra (9.3 GHz) was recorded.

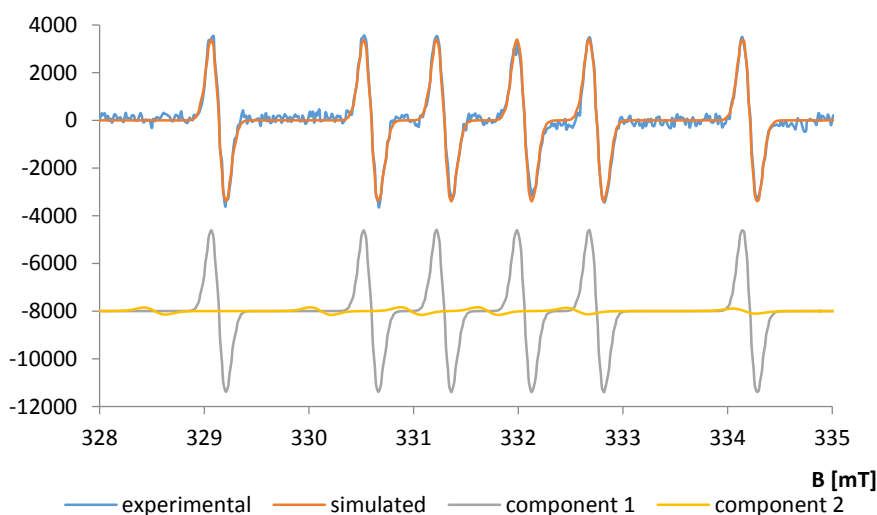


Figure S2. EPR spectra of the reaction mixture with DMPO Conditions: 4-oxotetrahydropyran (0.5 mmol), EDA (1 equiv., 0.5 mmol), pyrrolidine (0.2 equiv., 0.1 mmol), H₂T(*p*-CO₂MeP)P (1 mol%), DMSO : buffer pH 4 (5 mL, 9:1). After 10 min. of stirring under irradiation (LED_{525nm} stripes) 5,5-dimethyl-1-pyrroline *N*-oxide (DMPO) was added and after next 10 min. of stirring under irradiation (LED_{525nm} stripes) EPR spectra (9.3 GHz) was recorded.

In the EPR spectrum registered after the visible light irradiation of the mixture of H₂T(*p*-CO₂MeP)P, pyrrolidine and 4-oxotetrahydropyran in the presence of PBN spin trap a triplet of doublets has been observed (Figure 3). The best fit was obtained for two very similar components (hyperfine splitting constants: $a_N = 1.51$ mT, $a_{H\beta} = 0.33$ mT and $a_N = 1.50$ mT, $a_{H\beta} = 0.35$ mT). These values are in a range typical for a carbon-centered radicals (1.50-1.6 mT for a_N and 0.3-0.35 for $a_{H\beta}$). When DMPO spin trap was used in this system (Figure S4) the spectrum was very similar to the one of the whole

reaction, differing only by a lower intensity. The dominating component was the same, the second component was impossible to simulate due to a very low signal intensity.

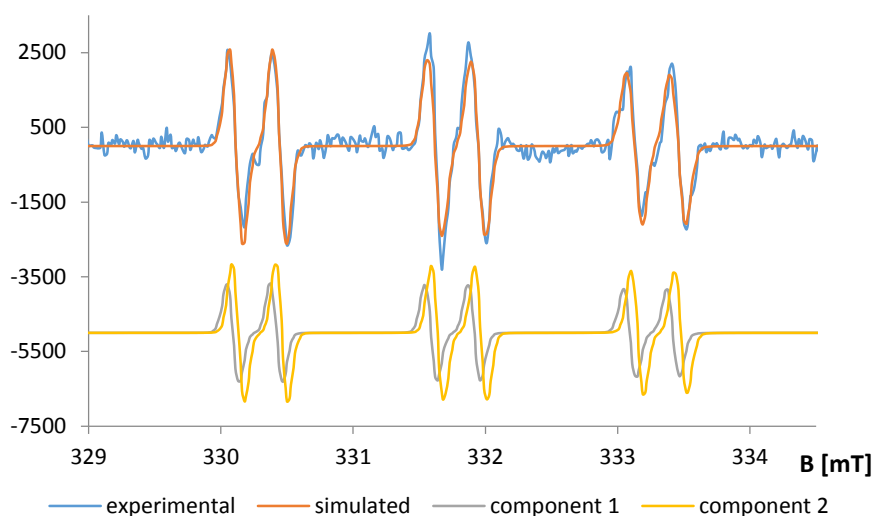


Figure S3. EPR spectra of the mixture of $H_2T(p-CO_2MeP)P$ with 4-oxotetrahydropyran and pyrrolidine with PBN Conditions: 4-oxotetrahydropyran (0.5 mmol), pyrrolidine (0.2 equiv., 0.1 mmol), $H_2T(p-CO_2MeP)P$ (1 mol%), DMSO : buffer pH 4 (5 mL, 9:1). After 10 min. of stirring under irradiation (LED_{525nm} stripes) *N-tert-butyl- α -phenylnitron* (PBN) was added and after next 10 min. of stirring under irradiation (LED_{525nm} stripes) EPR spectra (9.3 GHz) was recorded.

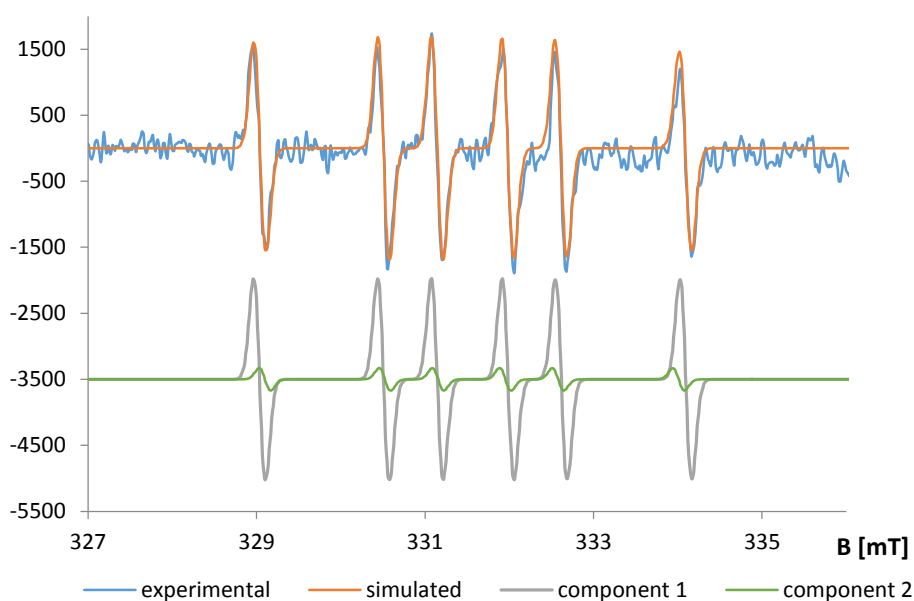


Figure S4. EPR spectra of the mixture of $H_2T(p-CO_2MeP)P$ with 4-oxotetrahydropyran and pyrrolidine with DMPO Conditions: 4-oxotetrahydropyran (0.5 mmol), pyrrolidine (0.2 equiv., 0.1 mmol), $H_2T(p-CO_2MeP)P$ (1 mol%), DMSO : buffer pH 4 (5 mL, 9:1). After 10 min. of stirring under irradiation (LED_{525nm} stripes) 5,5-dimethyl-1-pyrroline *N*-oxide (DMPO) was added and after next 10 min. of stirring under irradiation (LED_{525nm} stripes) EPR spectra (9.3 GHz) was recorded.

When only porphyrin and EDA were present in the system in the presence of PBN, a triplet with $a_N = 1.63$ mT has been observed, and the intensity of a spectrum has been very low. The same

spectral pattern has been obtained for EDA alone in the presence of PBN. It could be due to an oxygen-centered radical adduct with a very small hydrogen splitting constant, which could not be seen in the spectrum due to the low signal/noise ratio.

System without porphyrin

Conditions: Ketone (0.5 mmol), EDA (1 equiv., 0.5 mmol), pyrrolidine (0.2 equiv., 0.1 mmol), DMSO : buffer pH 4 (5 mL, 9:1). After 10 min. of stirring under irradiation (LED_{525nm} stripes) *N-tert-butyl- α -phenylnitron* (BPN) was added and after next 10 min. of stirring under irradiation (LED_{525nm} stripes) EPR spectra (9.3 GHz) was recorded.

When the mixture of 4-oxotetrahydropyran, EDA and pyrrolidine was irradiated with a green light in the presence of PBN, two-component EPR spectrum was observed ($a_N = 1.51$ mT, $a_{H\beta} = 0.40$ mT, $I = 62\%$ and $a_N = 1.38$ mT, $a_{H\beta} = 0.24$ mT, $I = 38\%$, Figure S5). The first component is the same as one of the components in the EPR spectrum of a whole reaction (Figure S1) and corresponds to a carbon-centered radical. The second one is not present in spectra registered in the presence of porphyrin. Thus, it indicates the alternative path of reaction as compared with that in the presence of porphyrin. This component can be seen in the EPR spectrum obtained for Fenton reaction (hydrogen peroxide and ferrous sulfate) in the DMSO:buffer solvent, and could be due to a PBN-CH₃ or PBN-OH adduct. It should be noted, however, that the latter adduct could be a result of a decomposition of superoxide anion radical adduct which could be formed in the reaction with molecular oxygen. When DMPO was used as a spin trap when the mixture of 4-oxotetrahydropyran, EDA and pyrrolidine was irradiated with a green light (Figure S6), the dominating component (90% of total intensity) was the same as in the presence of porphyrin ($a_N = 1.47$ mT, $a_{H\beta} = 2.16$ mT), arising from the carbon-centered radical. However, the minor component (10%, $a_N = 1.56$ mT, $a_{H\beta} = 1.81$ mT, $a_{H\gamma} = 0.51$ mT) is a new one. It also corresponds to a carbon-centered radical adduct, but it is not a DMPO-CH₃ adduct derived from DMSO as the parameters for such adduct are $a_N = 1.58$ mT and $a_{H\beta} = 2.26$ mT.

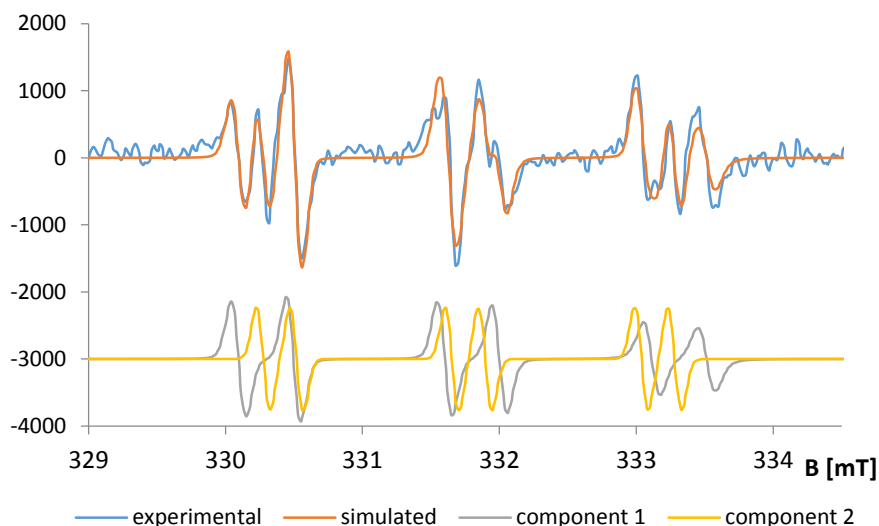


Figure S5. EPR spectra of the mixture of 4-oxotetrahydropyran, pyrrolidine and EDA with PBN Conditions: 4-oxotetrahydropyran (0.5 mmol), EDA (1 equiv., 0.5 mmol), pyrrolidine (0.2 equiv., 0.1 mmol), DMSO : buffer pH 4 (5 mL, 9:1). After 10 min. of stirring under irradiation (LED_{525nm} stripes) *N-tert-butyl- α -phenylnitron* (PBN) was added and after next 10 min. of stirring under irradiation (LED_{525nm} stripes) EPR spectra (9.3 GHz) was recorded.

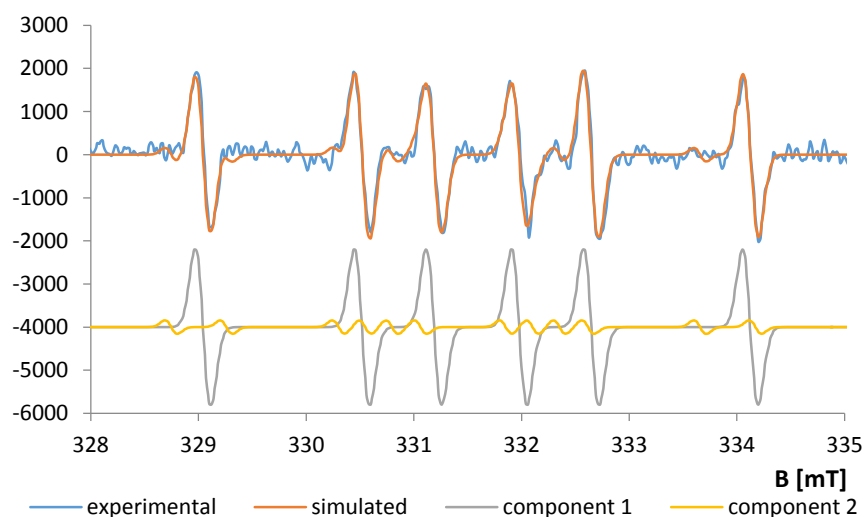


Figure S6. EPR spectra of the mixture of 4-oxotetrahydropyran, pyrrolidine and EDA with DMPO Conditions: 4-oxotetrahydropyran (0.5 mmol), EDA (1 equiv., 0.5 mmol), pyrrolidine (0.2 equiv., 0.1 mmol), DMSO : buffer pH 4 (5 mL, 9:1). After 10 min. of stirring under irradiation (LED_{525nm} stripes) 5,5-dimethyl-1-pyrroline *N*-oxide (DMPO) was added and after next 10 min. of stirring under irradiation (LED_{525nm} stripes) EPR spectra (9.3 GHz) was recorded.

The same pattern, but with a significantly lower total intensity, was observed in the absence of EDA. Thus, to check this hypothesis, a reaction of 4-oxotetrahydropyran and pyrrolidine was conducted in aerated conditions, under green light irradiation. In these conditions only one component could be seen in the EPR spectrum, with $a_N = 1.39$ mT and $a_{H\beta} = 0.23$ mT – which was observed as a minor one in the spectrum of 4-oxotetrahydropyran, pyrrolidine and EDA system in degassed solvent. These two components could be assigned to radical cation formed from enamine **B** and radical **D**.

When tetrahydro-4*H*-thiopyran-4-one (Figure S7), cyclohexanone (Figure S8) or *N*-Boc-4-piperidone (Figure S9) was used instead of 4-oxotetrahydropyran, two components could be again seen in the EPR spectrum in the presence of EDA. The one with a higher relative intensity ($a_N = 1.39$ mT, $a_{H\beta} = 0.24$ mT) is the same as one of the components observed when 4-oxotetrahydropyran was used, which could be ascribed to PBN-OH radical adduct. The second one ($a_N = 1.52$ mT, $a_{H\beta} = 0.33$ mT in case of tetrahydro-4*H*-thiopyran-4-one and cyclohexanone, 0.36 mT in case of *N*-Boc-4-piperidone) is very similar to the one dominating in the spectrum of porphyrin, 4-oxotetrahydropyran and pyrrolidine system (carbon-centered radical adduct). The only difference between systems with tetrahydro-4*H*-thiopyran-4-one and cyclohexanone is the ratio of both components: 60:40 in case of tetrahydro-4*H*-thiopyran-4-one and 90:10 in case of cyclohexanone.

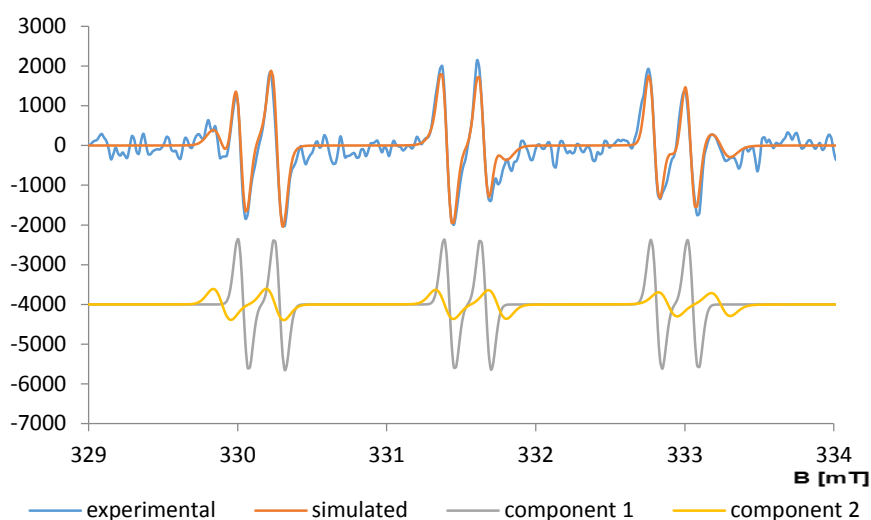


Figure S7. EPR spectra of the mixture of tetrahydro-4*H*-thiopyran-4-one, pyrrolidine, and EDA in DMSO : buffer pH = 4 (9:1) with PBN Conditions: tetrahydro-4*H*-thiopyran-4-one (0.5 mmol), EDA (1 equiv., 0.5 mmol), pyrrolidine (0.2 equiv., 0.1 mmol), DMSO : buffer pH 4 (5 mL, 9:1). After 10 min. of stirring under irradiation (LED_{525nm} stripes) *N*-*tert*-butyl- α -phenylnitronone (BPN) was added and after next 10 min. of stirring under irradiation (LED_{525nm} stripes) EPR spectra (9.3 GHz) was recorded.

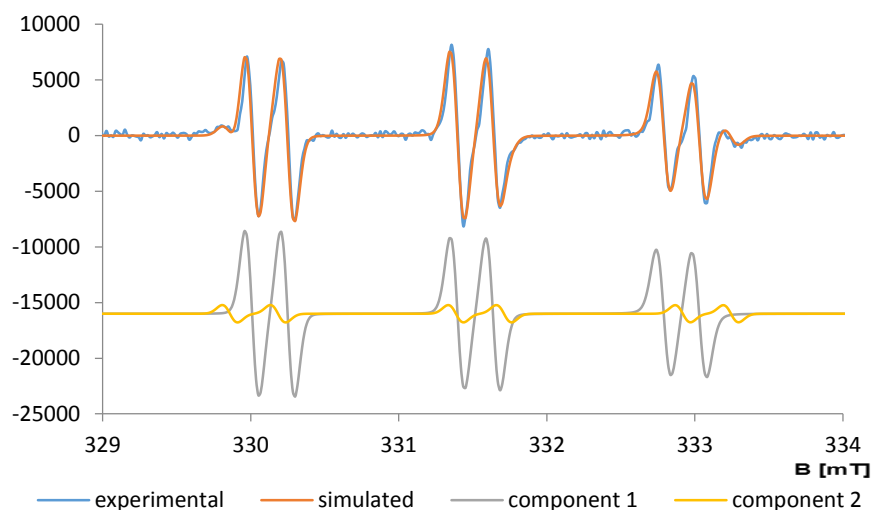


Figure S8. EPR spectra of the mixture of cyclohexanone, pyrrolidine, and EDA in DMSO : buffer pH = 4 (9:1) with PBN
 Conditions: cyclohexanone (0.5 mmol), EDA (1 equiv., 0.5 mmol), pyrrolidine (0.2 equiv., 0.1 mmol), DMSO : buffer pH 4 (5 mL, 9:1). After 10 min. of stirring under irradiation (LED_{525nm} stripes) *N-tert*-butyl- α -phenylnitron (BPN) was added and after next 10 min. of stirring under irradiation (LED_{525nm} stripes) EPR spectra (9.3 GHz) was recorded.

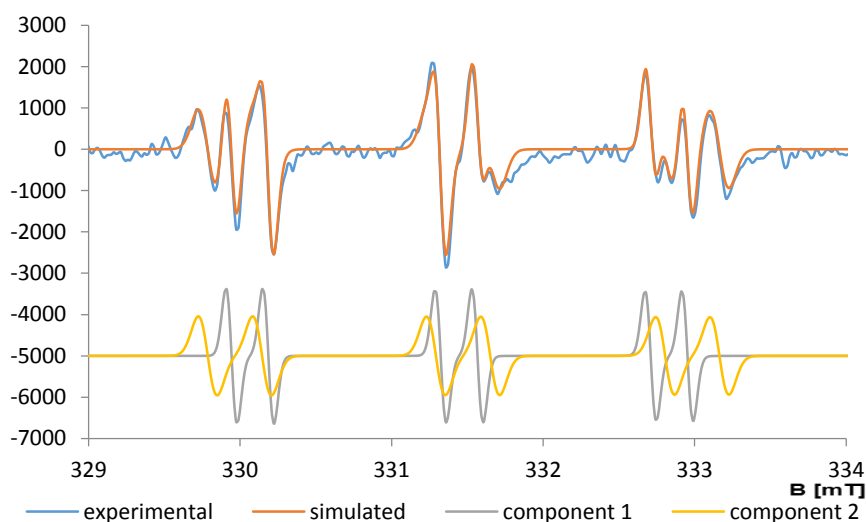


Figure S9. EPR spectra of the mixture of *N*-Boc-4-piperidone, pyrrolidine and EDA in DMSO : buffer pH = 4 (9:1) with PBN
 Conditions: *N*-Boc-4-piperidone (0.5 mmol), EDA (1 equiv., 0.5 mmol), pyrrolidine (0.2 equiv., 0.1 mmol), DMSO : buffer pH 4 (5 mL, 9:1). After 10 min. of stirring under irradiation (LED_{525nm} stripes) *N-tert*-butyl- α -phenylnitron (BPN) was added and after next 10 min. of stirring under irradiation (LED_{525nm} stripes) EPR spectra (9.3 GHz) was recorded.

In the absence of EDA, for tetrahydro-4*H*-thiopyran-4-one (Figure S10) and *N*-Boc-4-piperidone (Figure S11) the EPR spectrum pattern was identical with this obtained in the presence of EDA, while for cyclohexanone no signal was obtained.

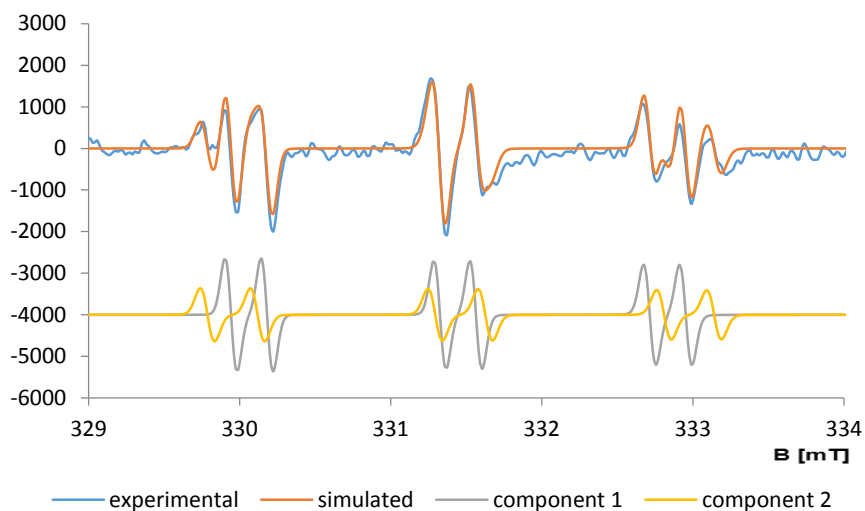


Figure S10. EPR spectra of the mixture of tetrahydro-4*H*-thiopyran-4-one, pyrrolidine in DMSO : buffer pH = 4 (9:1) with PBN Conditions: tetrahydro-4*H*-thiopyran-4-one (0.5 mmol), pyrrolidine (0.2 equiv., 0.1 mmol), DMSO : buffer pH 4 (5 mL, 9:1). After 10 min. of stirring under irradiation (LED_{525nm} stripes) *N-tert*-butyl- α -phenylnitron (BPN) was added and after next 10 min. of stirring under irradiation (LED_{525nm} stripes) EPR spectra (9.3 GHz) was recorded.

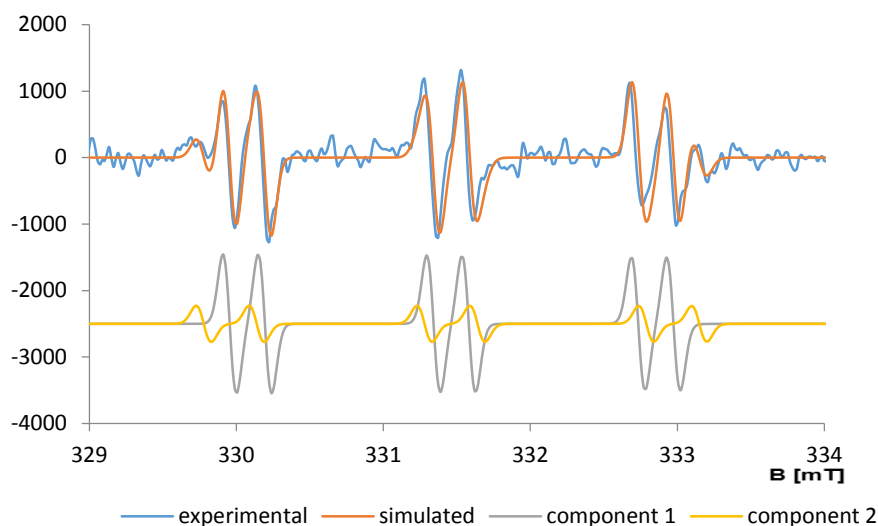


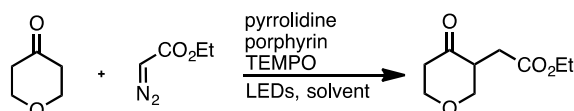
Figure S11. EPR spectra of the mixture of *N*-Boc-4-piperidone, pyrrolidine in DMSO:buffer pH = 4 (9:1) with PBN Conditions: *N*-Boc-4-piperidone (0.5 mmol), pyrrolidine (0.2 equiv., 0.1 mmol), DMSO : buffer pH 4 (5 mL, 9:1). After 10 min. of stirring under irradiation (LED_{525nm} stripes) *N-tert*-butyl- α -phenylnitron (BPN) was added and after next 10 min. of stirring under irradiation (LED_{525nm} stripes) EPR spectra (9.3 GHz) was recorded.

Table S17. Simulated hyperfine splitting constants of spin adducts - comparison

No	Experiment	Component	PBN		
			a _N [mT]	a _H [mT]	I [%]
1	4-oxotetrahydropyran + pyrrolidine + EDA + H ₂ T(<i>p</i> -CO ₂ MeP)P	1	1.49	0.44	53
		2	1.51	0.41	47
2	4-oxotetrahydropyran + pyrrolidine + EDA	1	1.51	0.40	62
		2	1.38	0.24	38
3	4-oxotetrahydropyran + pyrrolidine + H ₂ T(<i>p</i> -CO ₂ MeP)P	1	1.51	0.33	59
		2	1.50	0.35	41
4	4-oxotetrahydropyran + pyrrolidine	1	1.39	0.23	-
		2	-	-	-
5	oxotetrahydropyran + pyrrolidine + EDA + H ₂ T(<i>p</i> -CO ₂ MeP)P	1	1.49	0.45	62
		2	1.53	0.37	38
6	4-oxotetrahydropyran + pyrrolidine + EDA	1	1.39	0.25	60
		2	1.50	0.36	40
7	4-oxotetrahydropyran + pyrrolidine	1	1.39	0.24	60
		2	1.52	0.33	40
8	cyclohexanone + pyrrolidine + EDA + H ₂ T(<i>p</i> -CO ₂ MeP)P	1	1.50	0.43	72
		2	1.55	0.39	28
9	cyclohexanone + pyrrolidine + EDA	1	1.39	0.24	90
		2	1.53	0.33	10
10	<i>N</i> -Boc-4-piperidone + pyrrolidine + EDA	1	1.39	0.24	38
		2	1.51	0.36	62
11	<i>N</i> -Boc-4-piperidone + pyrrolidine	1	1.39	0.24	76
		2	1.51	0.36	24

In accordance with the proposed mechanism reactive radicals are formed. EPR measurements proved creating two different carbon-centered radicals, which after analyzing simulated hyperfine splitting constants of spin adducts can be assigned to radical cation **B** and radical cation **D**. Additionally, no signal from carbene radical was found in the reaction mixture or background reactions.

5.4. TEMPO trapping



a) Addition TEMPO (1.5 equiv.) at the beginning:

Reaction conditions: ketone (0.5 mmol), pyrrolidine (0.2 equiv., 0.1 mmol), EDA (1 equiv., 0.5 mmol), H₂T(*p*-CO₂MeP)P (1 mol%), TEMPO (1.5 equiv.), DMSO: buffer pH = 4 (5 mL, 9:1) after 5h of stirring under light irradiation (LED_{green}) reaction was checked by TLC – no product was observed – reaction was halted completely.

a) Addition TEMPO (1.5 equiv.) after 2h

Reaction conditions: ketone (0.5 mmol), pyrrolidine (0.2 equiv., 0.1 mmol), EDA (1 equiv., 0.5 mmol), H₂T(*p*-CO₂MeP)P (1 mol%), DMSO: buffer pH = 4 5 mL, 9:1) after 120 min of stirring under light irradiation (LED_{green}) TEMPO as a radical scavenger was added, and after 30 min. of stirring under light irradiation (LED_{green}) MS spectra was recorded.

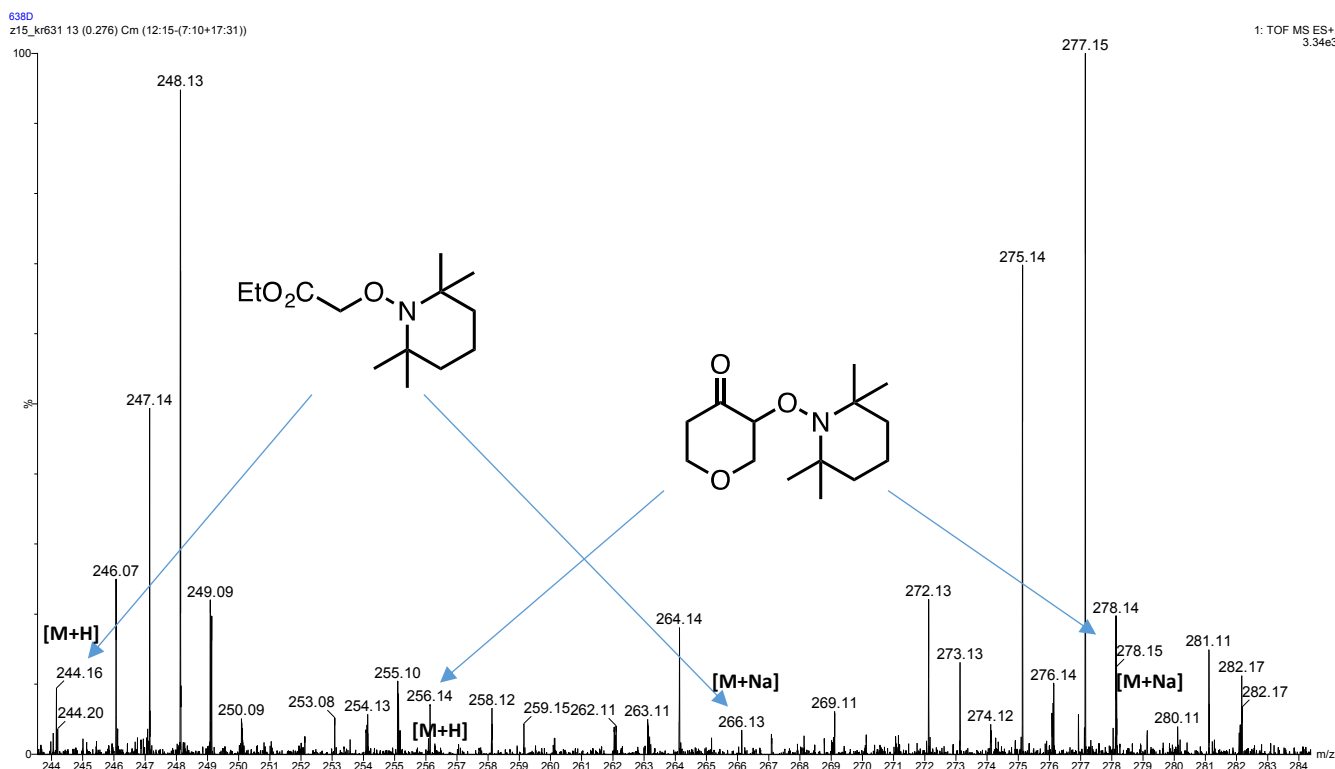
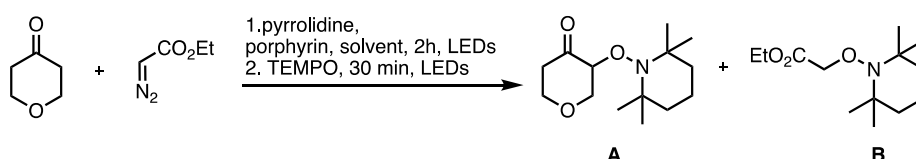


Figure S12. MS LR spectra of a reaction mixture after TEMPO trapping

The experiment confirmed the formation of two compounds with TEMPO hence two radical species were present in the reaction mixture.



Adduct **B** can form as a result of EDA photolysis but current data suggest that it is rather not involved in C-C bond forming reaction.

5.5. Experiment with deuterated reagents (CD₃CN)

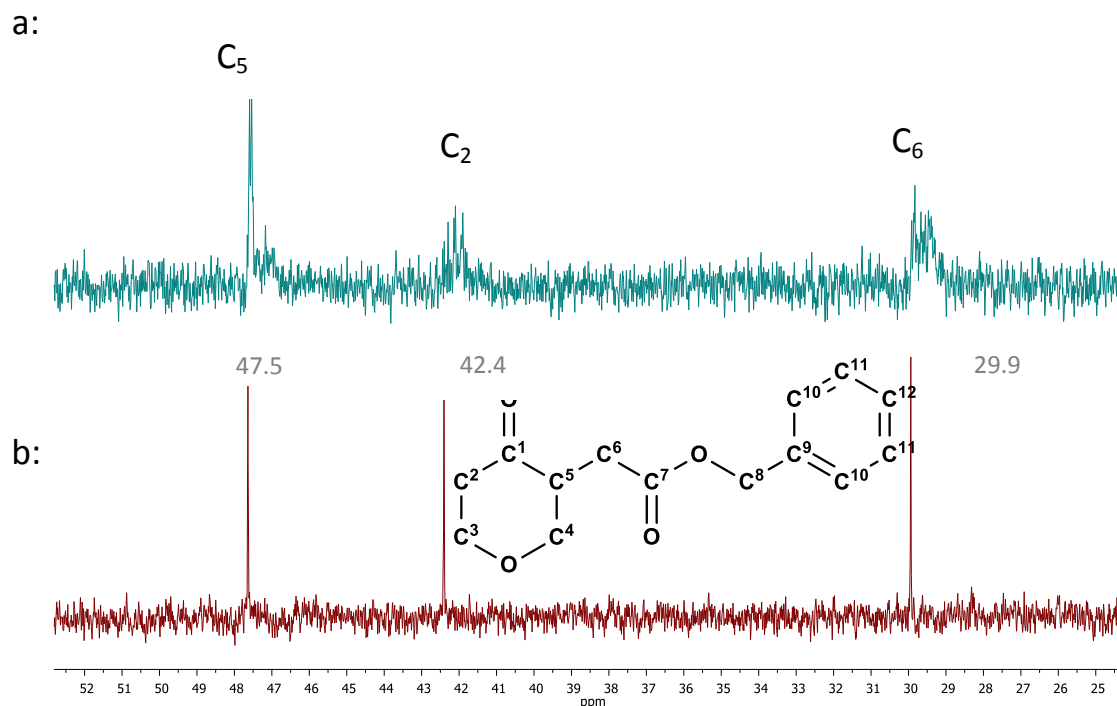


Figure S13. ¹³C NMR spectra a) product of reaction in CD₃CN, b) product of a reaction in DMSO/buffer pH 4 9:1 mixture [V/V].

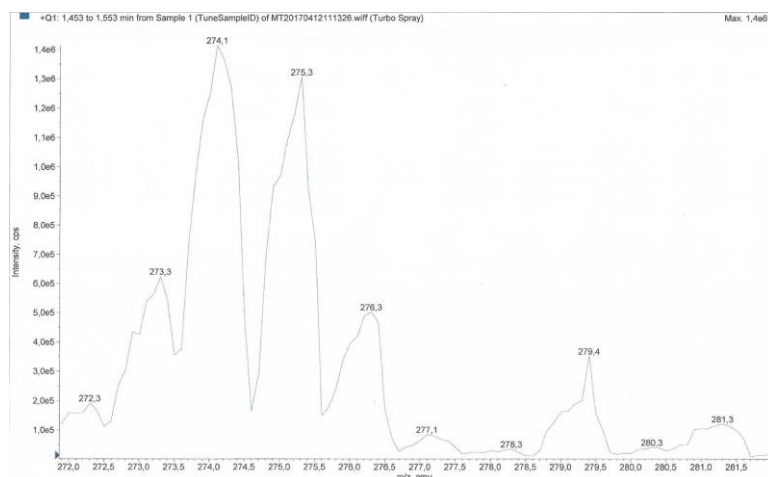


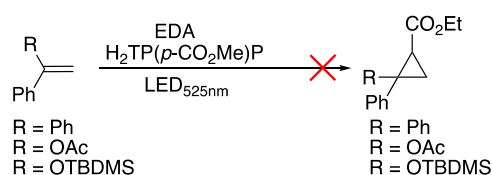
Figure S14. MS LR spectra of a product of reaction in CD₃CN

To prove the hypothesis of the external proton incorporation in the α -position to the ester group, the experiment in CD₃CN was performed. ¹H, ¹³C NMR and MS spectra suggested that after the reaction in CD₃CN, a mixture of deuterated products formed. In ¹³C NMR spectrum signals 47.5, 42.4 and 29.9 suggested the presence of the deuterated products (Chart 2). Also MS LR (MD+Na 272.3, MD₂+Na 273.3, MD₃+Na 274.1, MD₄+Na 275.3, MD₅+Na 276.3 Da) corresponds to mono-, di-, tri-,

tetra-, and pentadeuterated products (Chart 3). In ^1H NMR spectrum signals corresponding to the deuterated product are too weak to determine the ratio of products.

5.6. Verification of cyclopropane-intermediate mechanism

Olefins, common substrates for cyclopropanation were subjected to our model, porphyrin-catalyzed reaction conditions. No conversion was observed (substrates species were recovered), thus excluding cyclopropane intermediate pathway from the considered reaction mechanism.



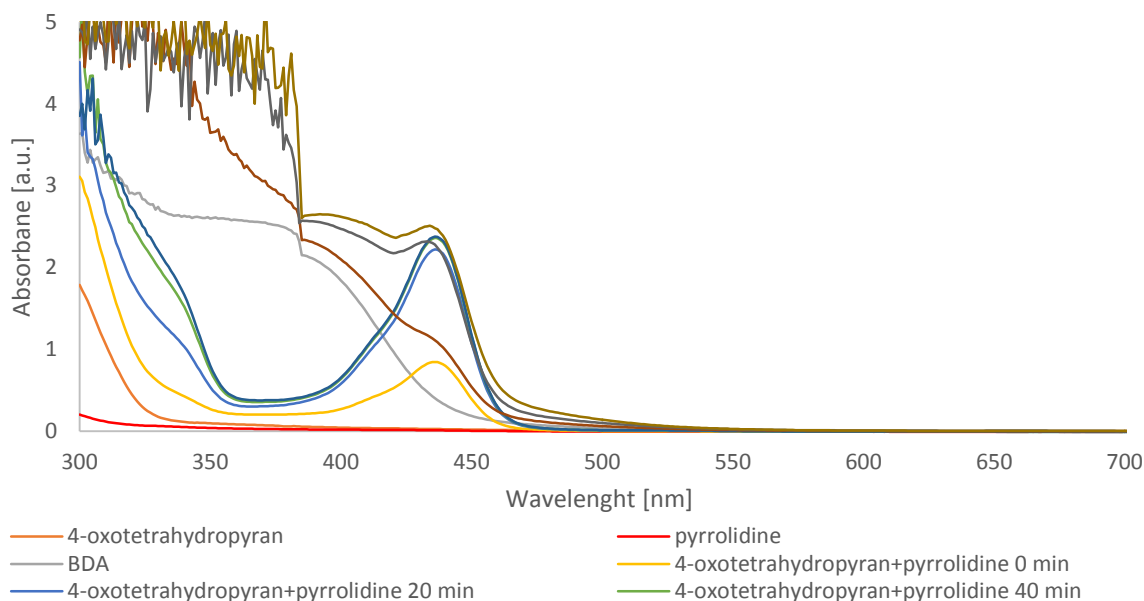
Reaction conditions: olefin (0.5 mmol), EDA (1 equiv., 0.5 mmol), $\text{H}_2\text{T}(p\text{-CO}_2\text{Me})\text{P}$ (1 mol%), DMSO: buffer pH = 4 (5 mL, 9:1) after 5h of stirring under light irradiation ($\text{LED}_{\text{green}}$) reaction was checked by TLC and GC – no product was observed.

5.7. UV-Vis experiments

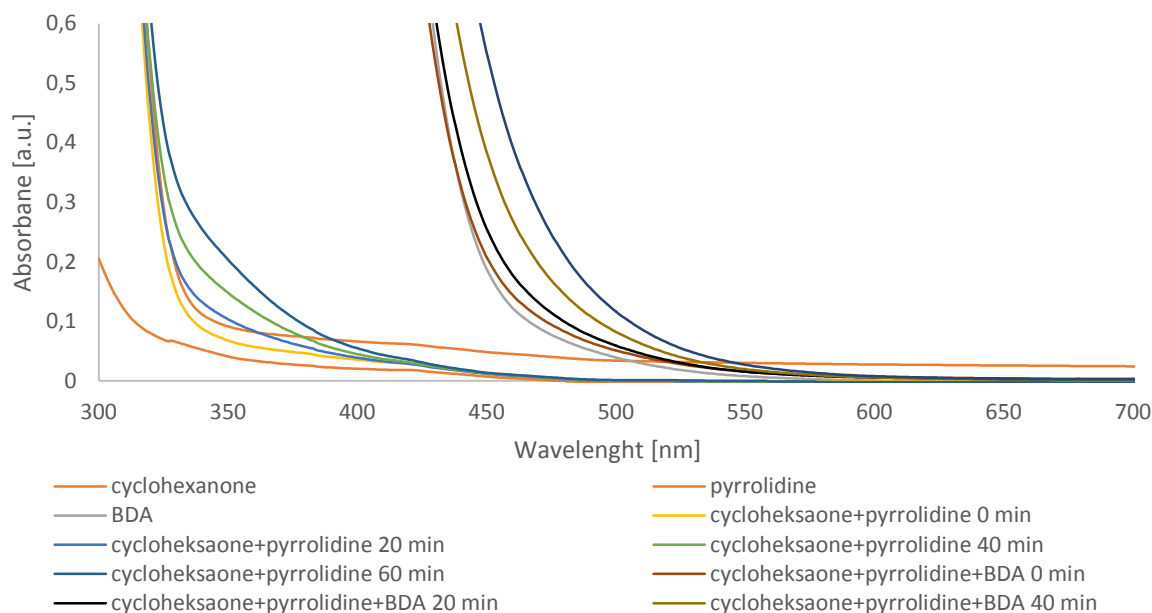
5.7.1. Control experiments

The control UV-Vis experiments of substrates and background reactions were performed. Conditions: ketone (0.25 mmol), BDA (1 equiv., 0.25 mmol), pyrrolidine (0.25 mmol), DMSO : buffer pH 4 (9:1, 2.5 mL,) after stirring 0, 20, 40 min under light irradiation (LED_{green}) UV-Vis spectra was recorded.

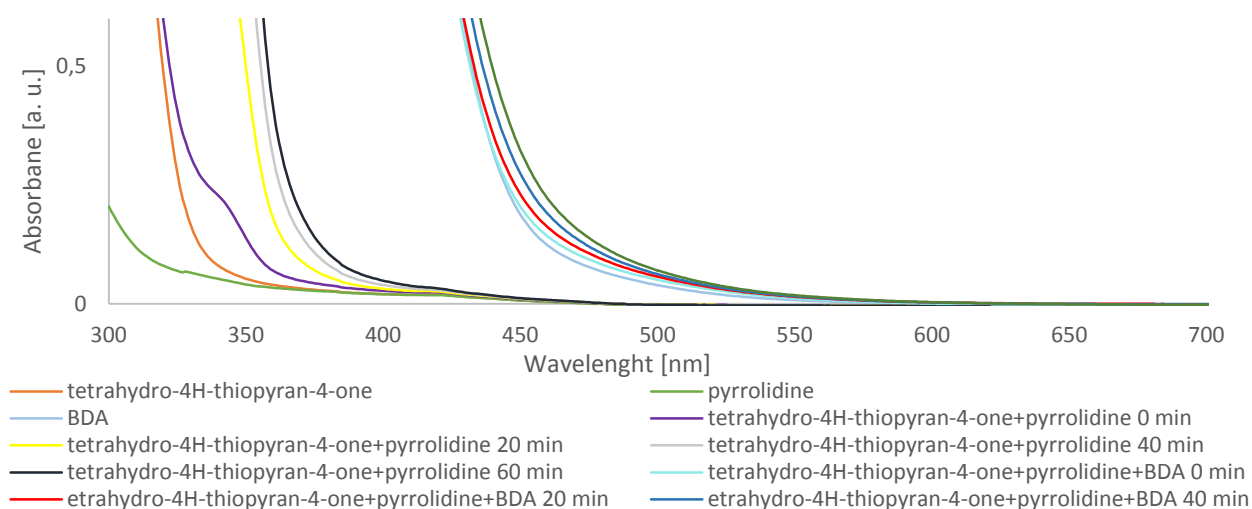
a) 4-oxotetrahydropyran:



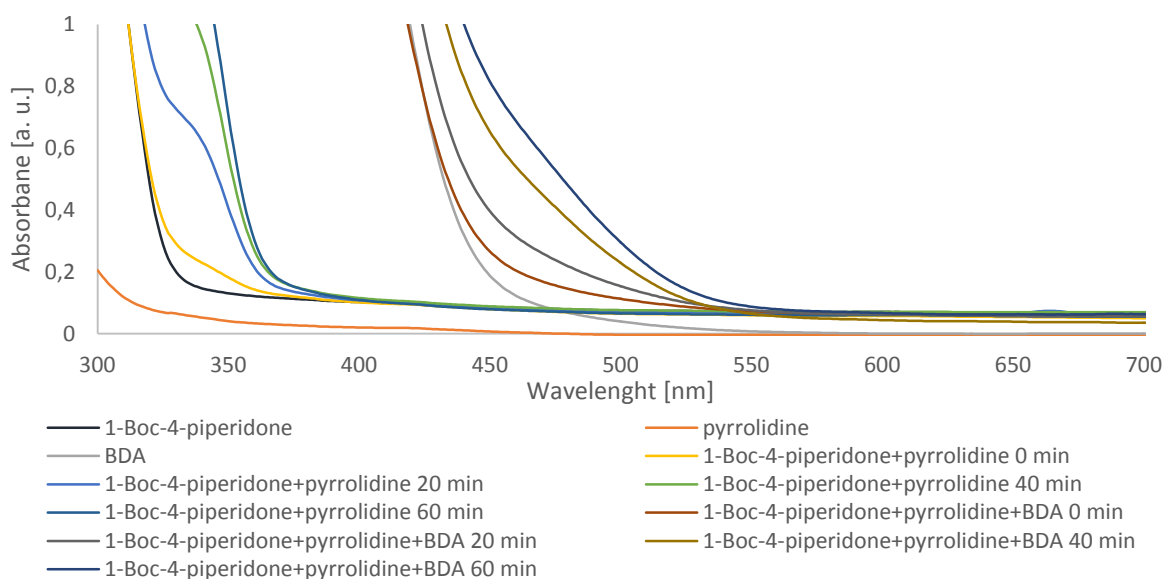
b) cyclohexanone:



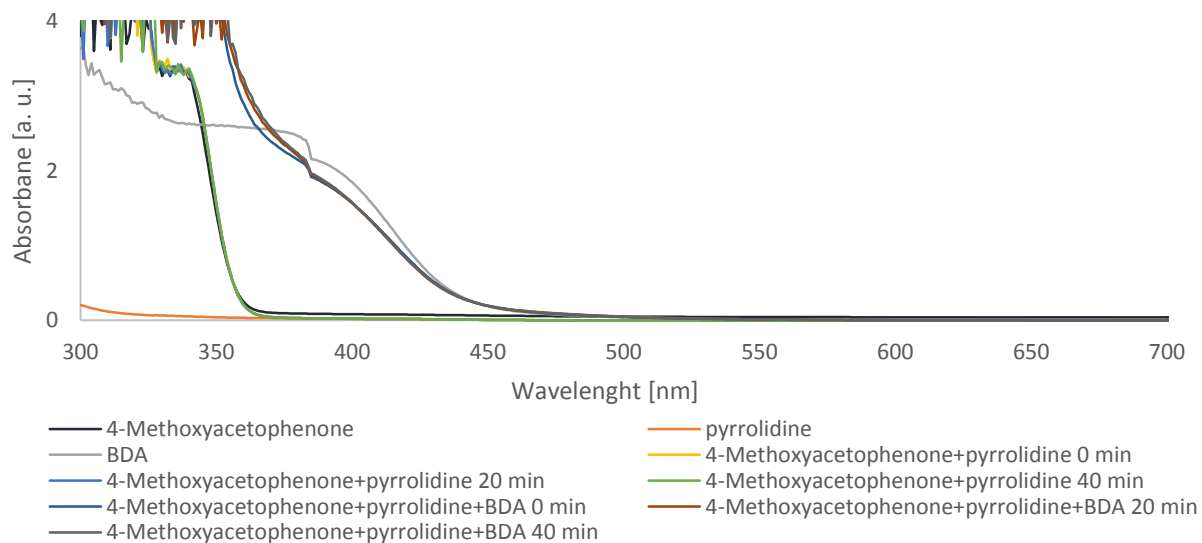
c) tetrahydro-4*H*-thiopyran-4-one:



d) *N*-Boc-piperidinone:



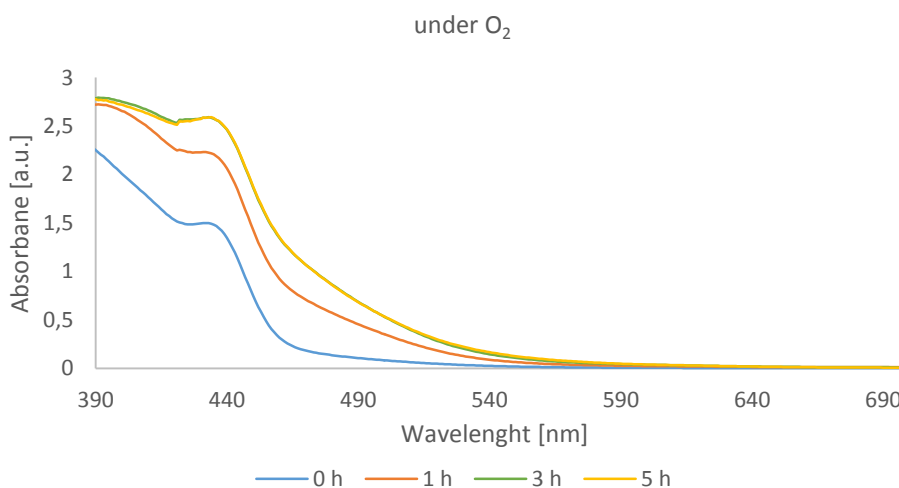
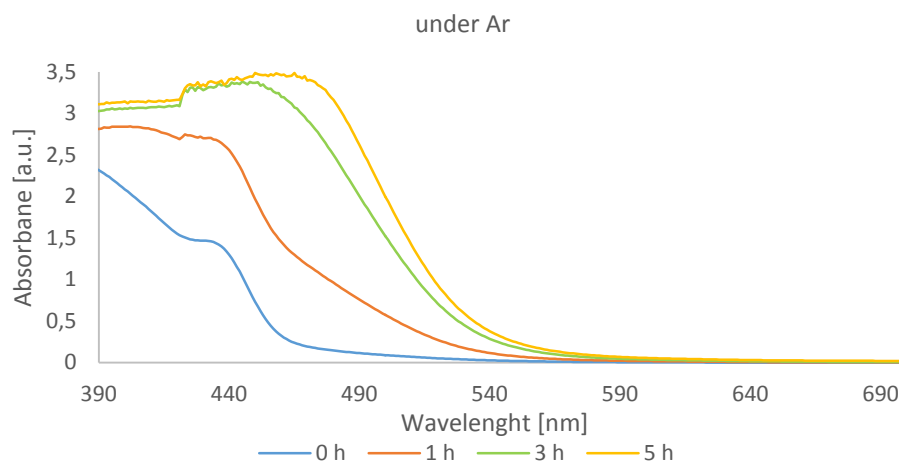
e) 4-methoxyacetophenone:



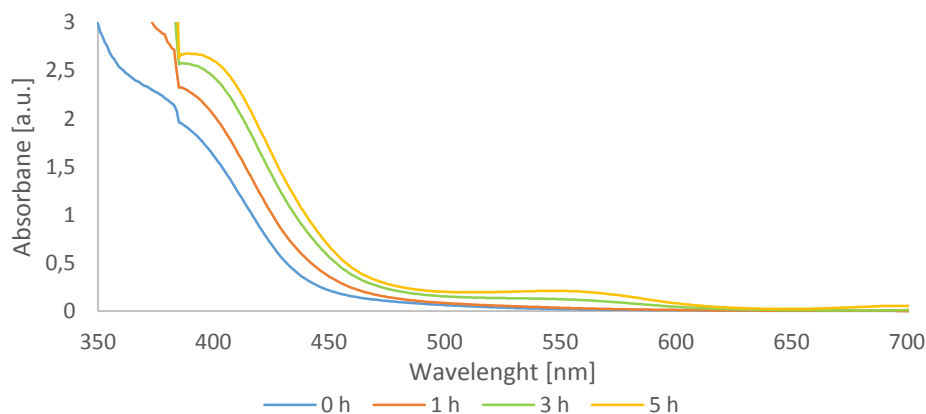
5.7.2. Reaction in time

Reaction conditions: ketone (0.25 mmol), BDA (1 equiv., 0.25 mmol) pyrrolidine (0.2 equiv.), DMSO : buffer pH = 4 (2.5 mL, 9:1). After 0, 60, 180, 300 min. of stirring under irradiation (LED_{525nm} stripes) UV-Vis spectra were recorded.

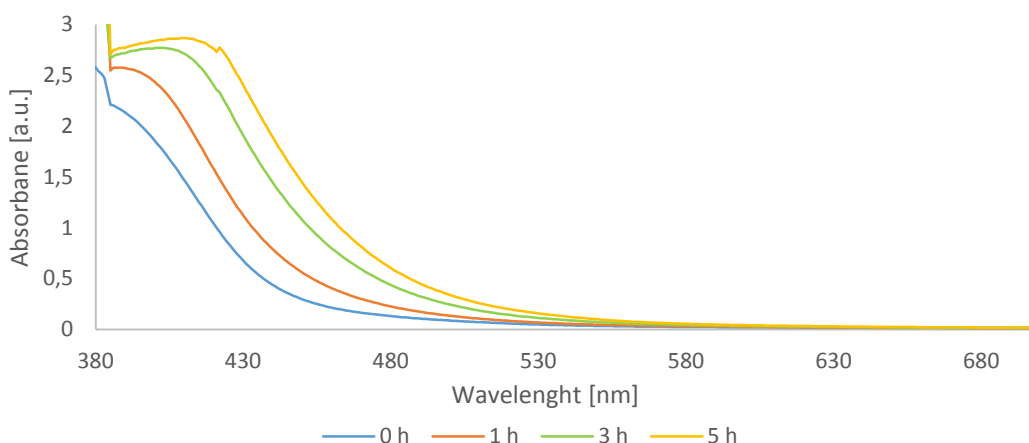
a) 4-oxotetrahydropyran



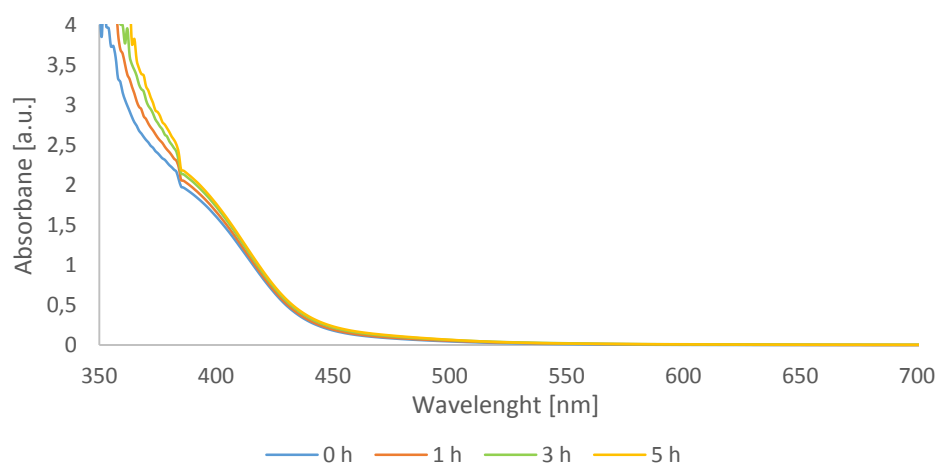
b) tetrahydro-4*H*-thiopyran-4-one



c) cyclohexanone



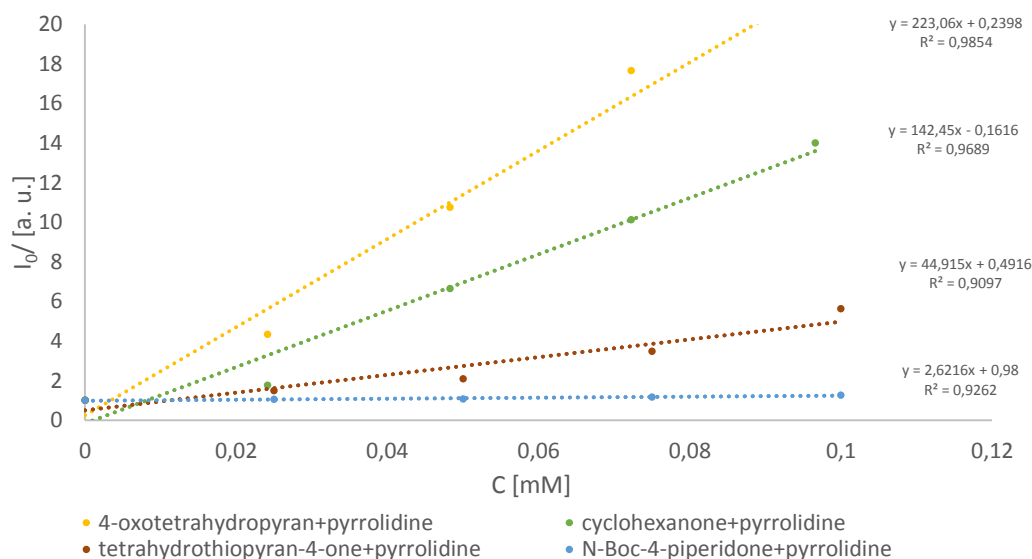
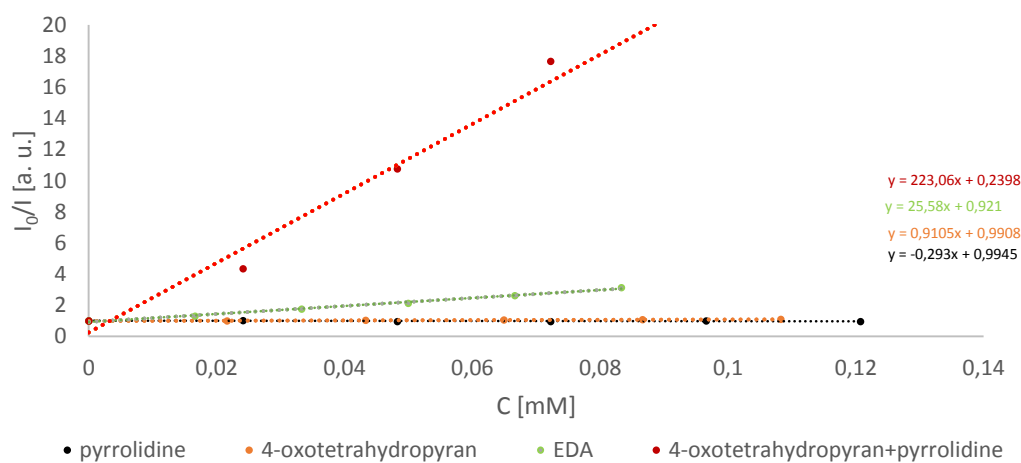
d) 4-methoxyacetophenone



For ketones which are reactive under no-catalyst conditions we can observe that the enamine generated in situ from ketone (4-oxotetrahydropyran, tetrahydro-4*H*-thiopyran-4-one) and pyrrolidine absorbs visible light at the maximum in visible region and its absorption increases over time. In the case of less reactive (cyclohexanone) and unreactive (e.g. 4-methoxyacetophenone, acetone) enamines the new absorption band is not present and as a result they afford products only in the porphyrin-catalyzed reaction. Hence, **the absorption of visible light by enamine is crucial in reactions with no porphyrin added.**

5.8. Stern-Volmer quenching experiment

Stern–Volmer analyses for the reaction components shows strong quenching of the porphyrin by formed in situ (from 4-oxotetrahydropyran and pyrrolidine) enamine ($k_q = 4.1 \times 10^{10} \text{ [M}^{-1}\text{s}^{-1}]$) while quenching rates are much smaller for EDA ($k_q = 4.5 \times 10^9 \text{ [M}^{-1}\text{s}^{-1}]$), 4-oxotetrahydropyran ($k_q = 1.2 \times 10^8 \text{ [M}^{-1}\text{s}^{-1}]$) and pyrrolidine ($k_q \sim 8.2 \times 10^7 \text{ [M}^{-1}\text{s}^{-1}]$)¹³ (Figure 1). Samples were prepared by adding solutions of substrates to $\text{H}_2\text{T}(p\text{-CO}_2\text{MeP})\text{P}$ solution in DMSO (total volume 2 mL) and degassed with Ar. The concentration of $\text{H}_2\text{T}(p\text{-CO}_2\text{MeP})\text{P}$ in DMSO was $7.2 \times 10^{-7} \text{ mol/dm}^3$.



Quenching rates for enamines formed in situ from:

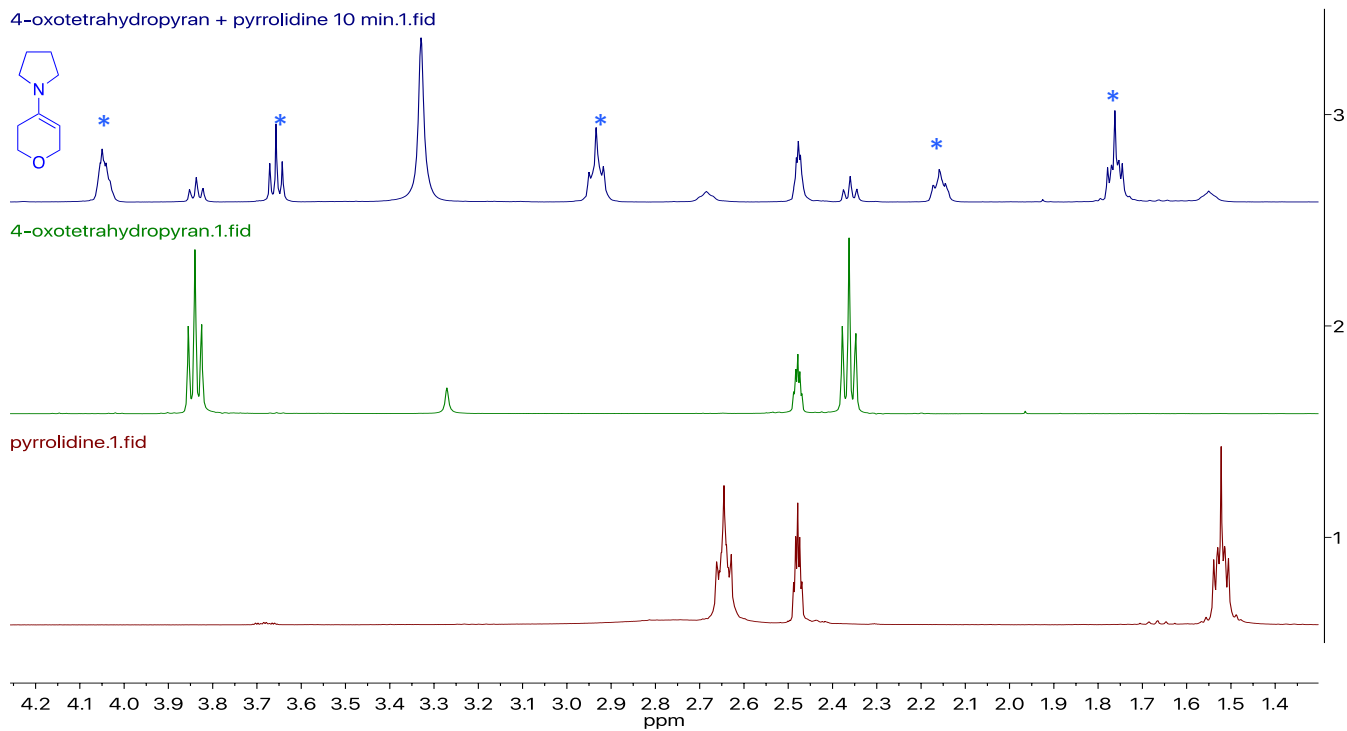
1. 4-oxotetrahydropyran + pyrrolidine $k_q = 4.1 \times 10^{10} \text{ [M}^{-1}\text{s}^{-1}]$
2. cyclohexanone + pyrrolidine $k_q = 2.2 \times 10^{10} \text{ [M}^{-1}\text{s}^{-1}]$
3. tetrahydro-4*H*-thiopyran-4-one + pyrrolidine $k_q = 6.1 \times 10^9 \text{ [M}^{-1}\text{s}^{-1}]$
4. *N*-Boc-4-piperidone + pyrrolidine $k_q = 4.0 \times 10^8 \text{ [M}^{-1}\text{s}^{-1}]$

5.9. NMR time-resolved

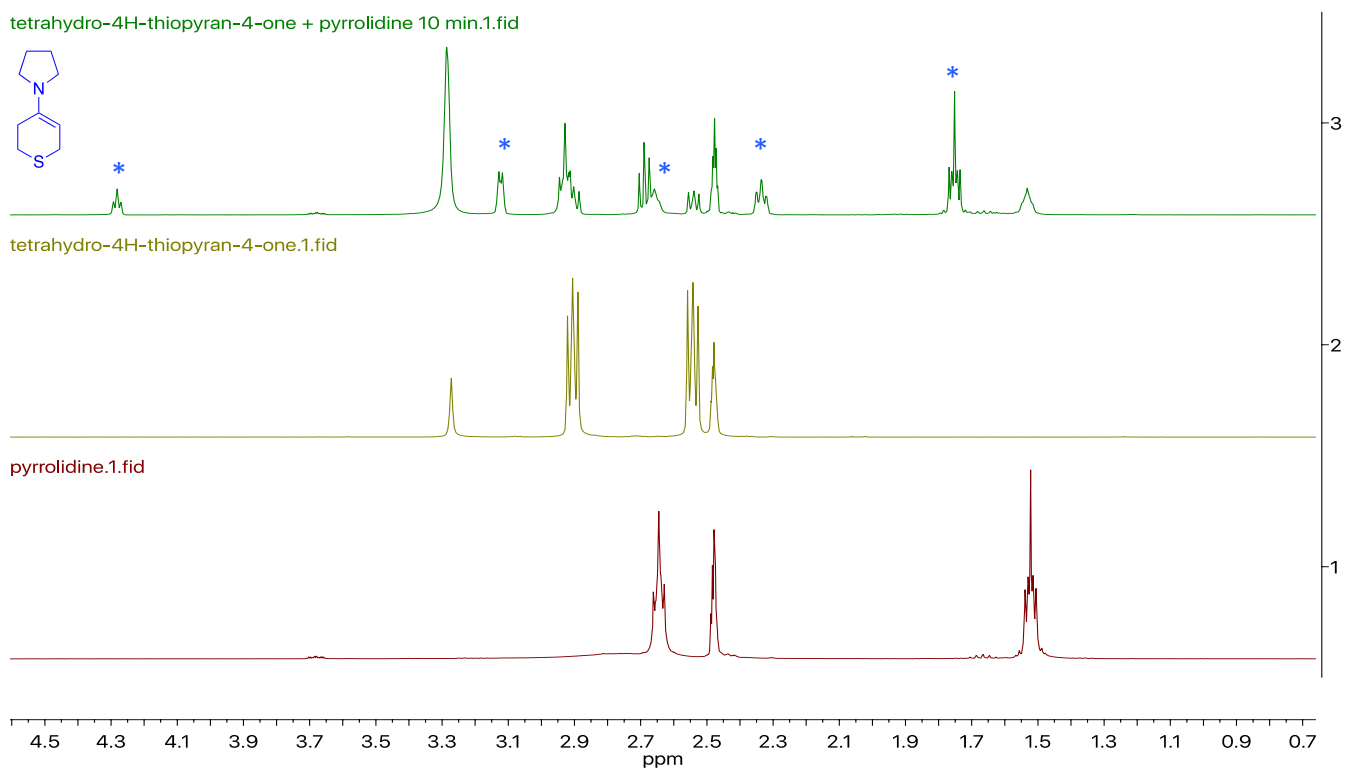
5.9.1. Background

Reaction conditions: ketone (0.25 mmol), pyrrolidine (20 mol%), DMSO-d₆ (0.5 mL). After 0, 60, 180, 300 min. of stirring under irradiation (LED_{525nm} stripes) in NMR tubes NMR spectra (400 MHz) were recorded.

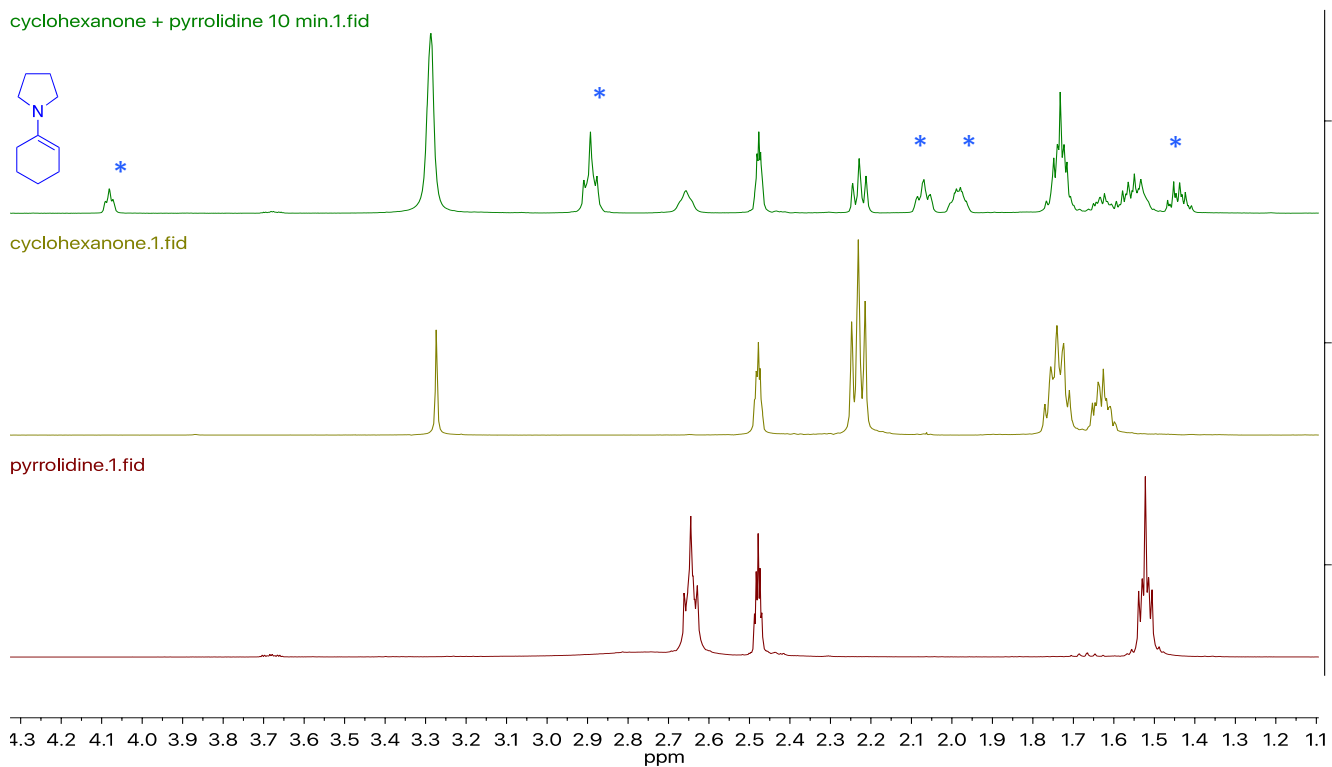
a) 4-oxotetrahydropyran (10 min):



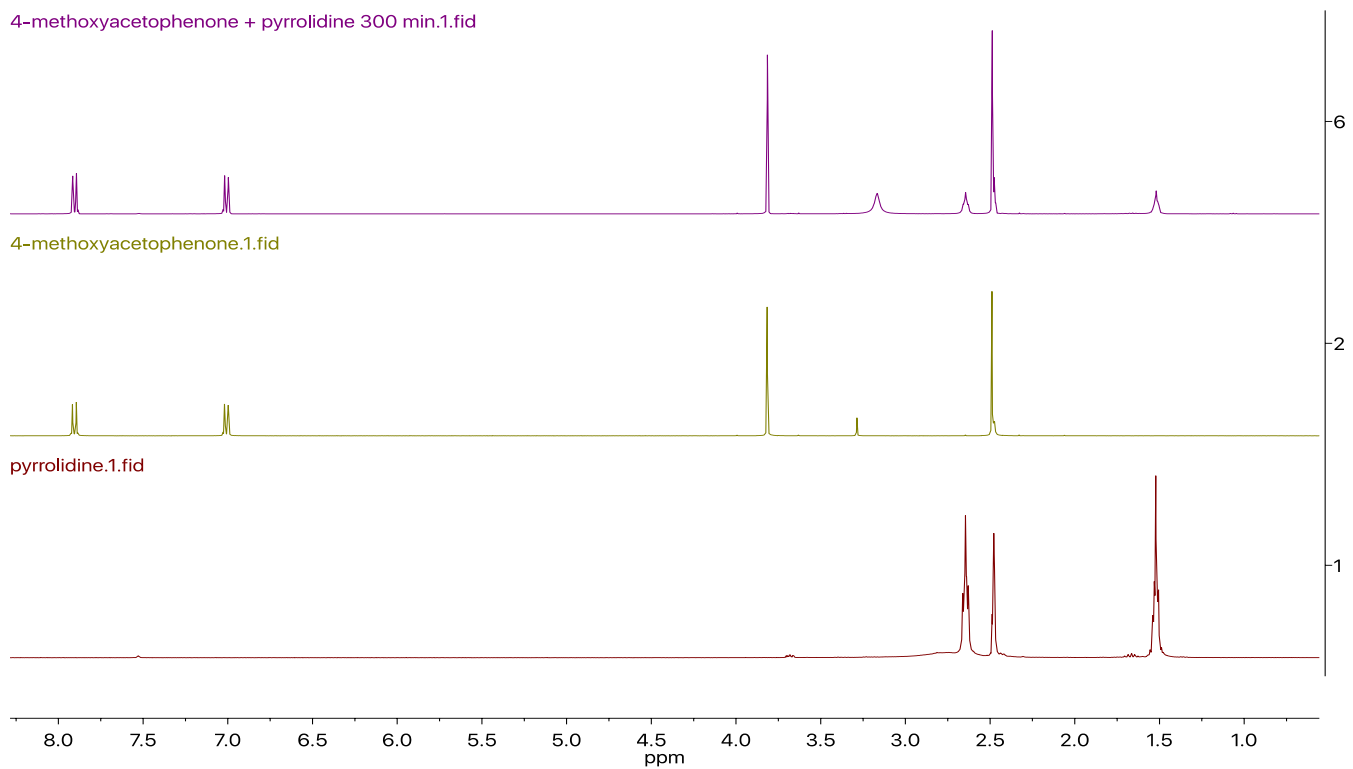
b) tetrahydro-4H-thiopyran-4-one (10 min):



c) **cyclohexanone** (10 min):



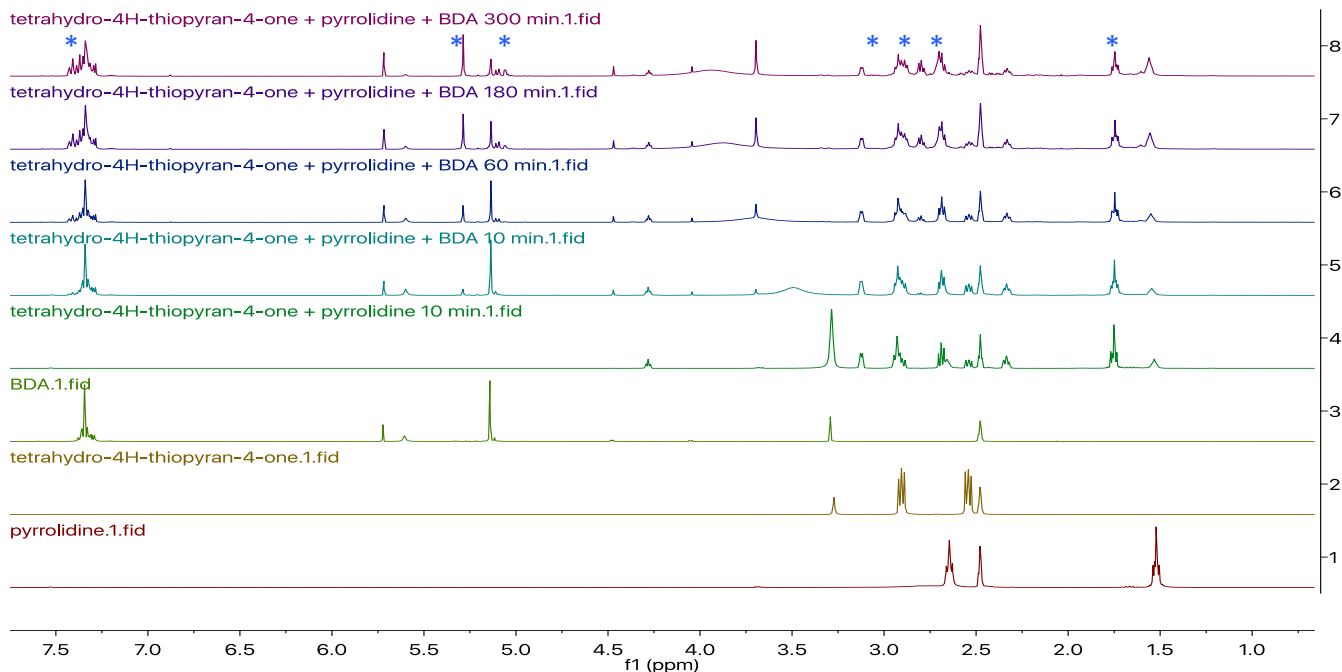
d) **4-methoxyacetophenone** (300 min):



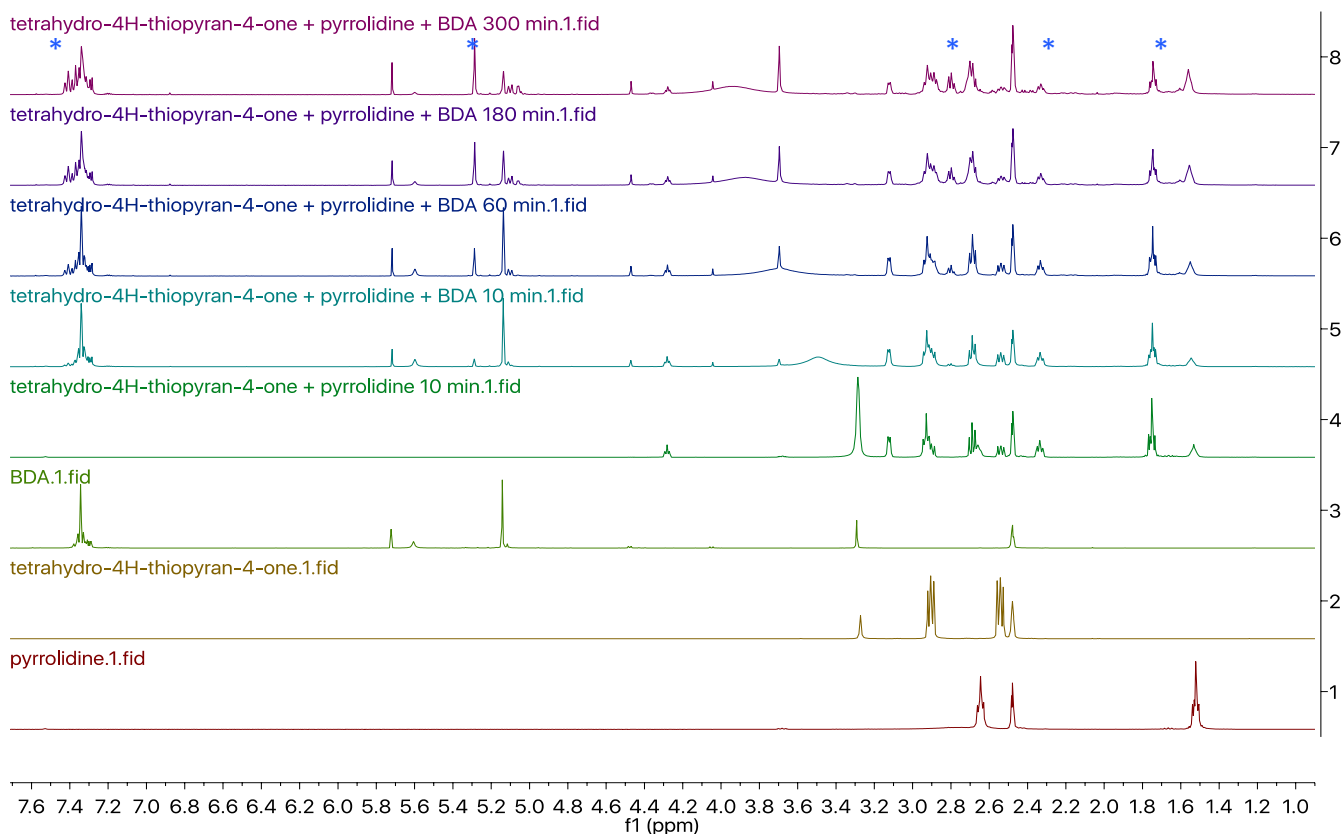
5.9.2. Reaction in time

Reaction conditions: ketone (0.25 mmol), BDA (0.25 mmol) pyrrolidine (20 mol%), DMSO-d₆ (0.5 mL). After 0, 60, 180, 300 min. of stirring under irradiation (LED_{525nm} stripes) in NMR tubes NMR spectra were recorded. [* - products]

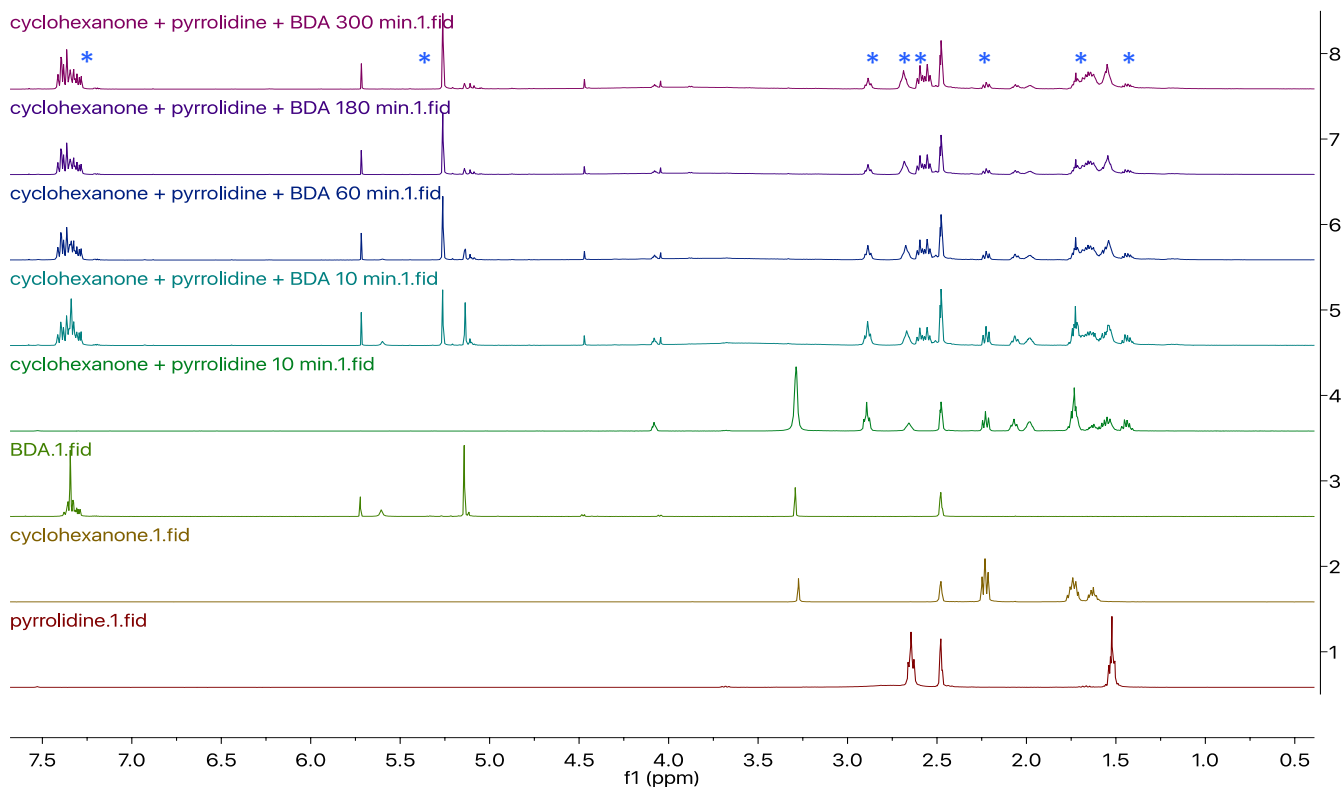
a) 4-oxotetrahydropyran (10 min, 60 min, 180 min, 300 min):



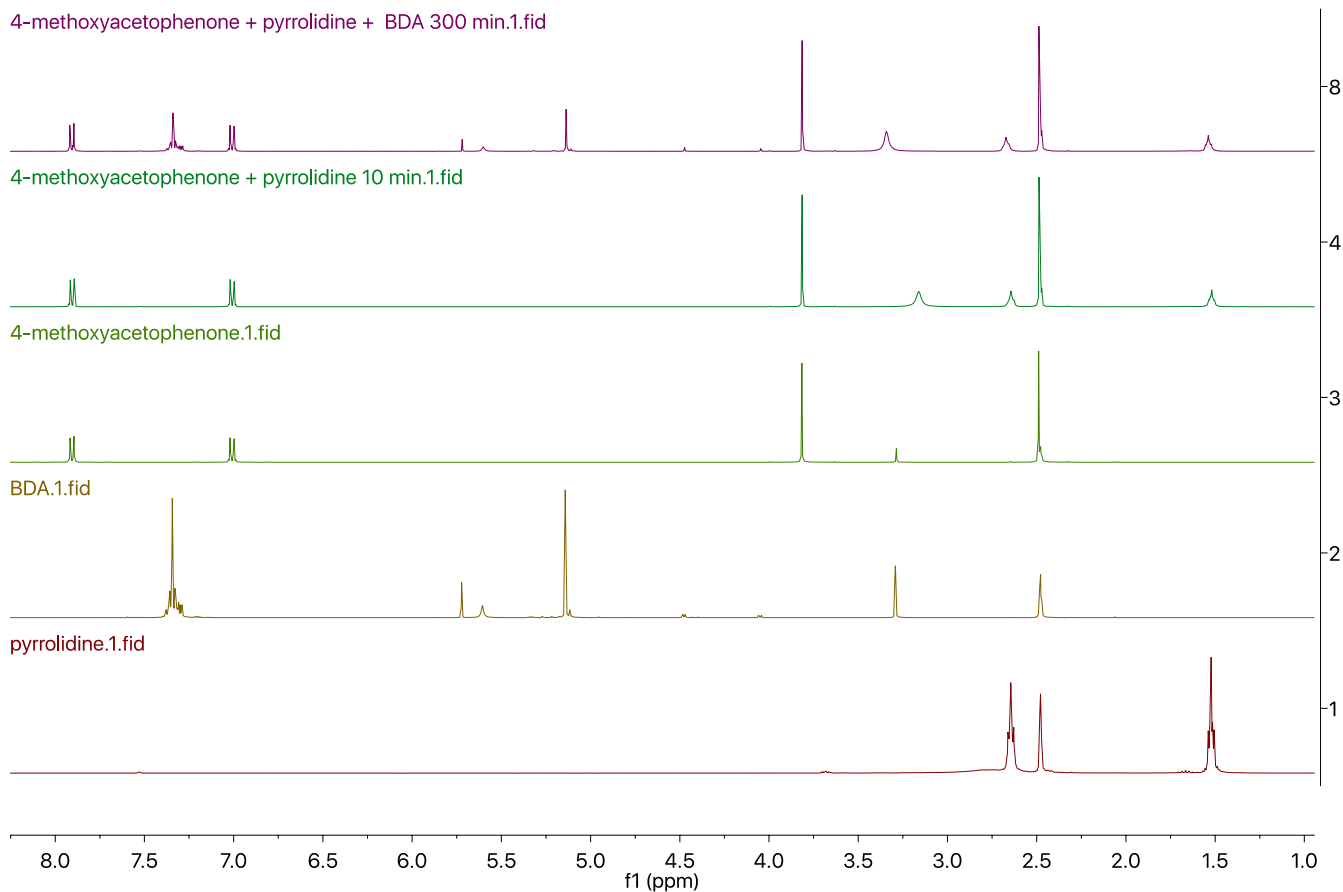
b) tetrahydro-4H-thiopyran-4-one (10 min, 60 min, 180 min, 300 min):



c) cyclohexanone (10 min, 60 min, 180 min, 300 min):

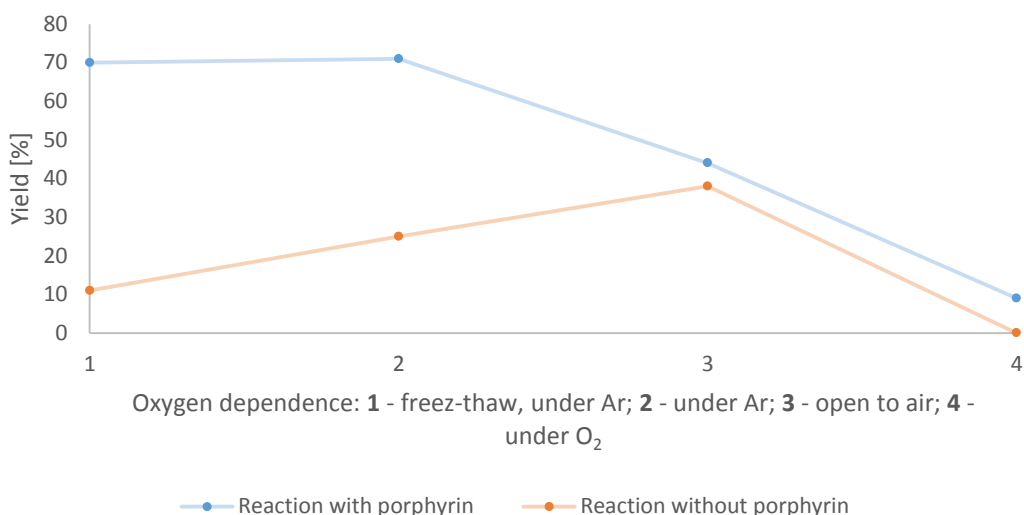


d) 4-methoxyacetophenone (10 min, 300 min):



5.10. Oxygen dependence

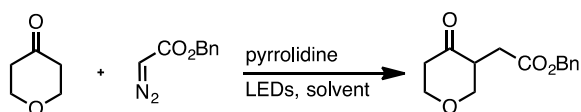
Reaction conditions: (blue) 4-oxotetrahydropyran (**15**, 0.5 mmol), pyrrolidine (**18**, 20 mol %), H₂T(*p*-CO₂MeP)P (**19**, 1 mol %), BDA (**16**, 1 equiv.), DMSO/buffer pH = 4 (5 mL, 9/1 mixture), LED_{525nm}, 5 h. (orange) 4-oxotetrahydropyran (**15**, 0.5 mmol), pyrrolidine (**18**, 20 mol %), BDA (**2**, 1 equiv.), DMSO/buffer pH 4 (5 mL, 9/1 mixture), LED_{525nm}, 5 h. Isolated yields.



5.11. Quantum yield measurements

The quantum yield was measured with a quantum yield determination setup: translation stages (horizontal and vertical): Thorlabs DT 25/M or DT S25/M; photographic lens with $f = 50$ mm; magnetic stirrer: Faulhaber motor (1524B024S R) with 14:1 gear (15A); PS19Q power sensor from Coherent; PowerMax software; adjustable power supply “Basetech BT-153 0–15 V/DC 0–3 A 45 W”¹⁴

b.1. without porphyrin



A typical reaction mixture of 4-oxotetrahydropyran (0.2 mmol, 2 equiv.), benzyl diazoacetate (**X**) (0.2 mmol, 1 equiv.), pyrrolidine (0.04 mmol, 0.2 equiv.), DMSO (1.8 mL), buffer pH = 4 (0.2 mL) in a 10 mm Hellma^R quartz fluorescence cuvette with a stirring bar was used. The measurement of quantum yield was accomplished in covered apparatus to minimize the influence of the ambient light. The cuvette with solvent (DMSO : buffer pH = 4, mixture 9:1 [V/V] 2.0 mL) and a stir bar was placed in the beam of a 528 nm LED and the transmitted power ($P_{\text{ref}} = 17,64$ mW) was measured by a calibrated photodiode horizontal to the cuvette. The content of the cuvette was changed to the reaction mixture and the transmitted power was measured analogously to the blank solution. The

sample was further irradiated and the transmitted power as well as the respective yield of photocatalytic product (measured by quantitative GC using dodecane as internal standard) were recorded after different times (Table 1). The quantum yield was calculated from equation E1:

$$6. \quad \Phi = \frac{N_{product}}{N_{ph}} = \frac{N_A \cdot n_{product}}{\frac{E_{light}}{E_{ph}}} = \frac{N_A \cdot n_{product}}{\frac{P_{absorbed} \cdot t}{\frac{h \cdot c}{\lambda}}} = \frac{h \cdot c \cdot N_A \cdot n_{product}}{\lambda \cdot (P_{ref} - P_{sample}) \cdot t}$$

where Φ - the quantum yield,

$N_{product}$ - the number of molecules created

N_{ph} - the number of photons absorbed

N_A - Avogadro's constant [mol^{-1}],

$n_{product}$ - is the molar amount of molecules created [mol],

E_{light} - the energy of light absorbed [J],

E_{ph} - the energy of a single photon [J],

$P_{absorbed}$ - the radiant power absorbed [W],

t - the irradiation time [s],

h - the Planck's constant in [$\text{J}\cdot\text{s}$],

c - the speed of light in [ms^{-1}],

λ - the wavelength of irradiation source (420 nm) [m],

P_{ref} - the radiant power transmitted by a blank vial [W],

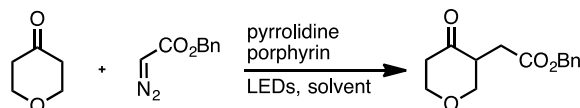
P_{sample} - the radiant power transmitted by the vial with reaction mixture [W].

Table S18. Calculation of the quantum yield Φ after different irradiation times.

Entry	Irradiation time [min]	P_{sample} [mW]	Yield [%]	Φ [%]
1	300	9.64	36	5
2	180	11.2	32	7.4
3	60	0.194	15	10.4

The mean value for the quantum yield was calculated to be $\Phi = 7.6 \pm \%$

b.2. with porphyrin



A typical reaction mixture of 4-oxotetrahydropyran (0.2 mmol, 1 equiv.), benzyl diazoacetate (**X**) (0.2 mmol, 1 equiv.), pyrrolidine (0.04 mmol, 0.2 equiv.), $\text{H}_2\text{T}(p\text{-CO}_2\text{MeP})\text{P}$ (**X**) (1 mol%), DMSO (1.8 mL), buffer pH = 4 (0.2 mL) in a 10 mm Hellma^R quartz fluorescence cuvette with a stirring bar was used. The measurement of quantum yield was accomplished in covered apparatus to minimize the ambient light. The cuvette with solvent (DMSO : buffer pH = 4, mixture 9:1 [V/V] 2.0 mL) and a

stir bar was placed in the beam of a 528 nm LED and the transmitted power ($P_{ref} = 17,74$ mW) was measured by a calibrated photodiode horizontal to the cuvette. The content of the cuvette was changed to the reaction mixture and the transmitted power was measured analogously to the blank solution. The sample was further irradiated and the transmitted power as well as the respective yield of photocatalytic product (measured by quantitative GC using dodecane as internal standard) were recorded after different times (Table 1). The quantum yield was calculated from equation E1:

$$7. \phi = \frac{N_{product}}{N_{ph}} = \frac{N_A \cdot n_{product}}{\frac{E_{light}}{E_{ph}}} = \frac{N_A \cdot n_{product}}{\frac{P_{absorbed} \cdot t}{\frac{h \cdot c}{\lambda}}} = \frac{h \cdot c \cdot N_A \cdot n_{product}}{\lambda \cdot (P_{ref} - P_{sample}) \cdot t}$$

where Φ - the quantum yield,

$N_{product}$ - the number of molecules created

N_{ph} - the number of photons absorbed

N_A - Avogadro's constant [mol^{-1}],

$n_{product}$ - is the molar amount of molecules created [mol],

E_{light} - the energy of light absorbed [J],

E_{ph} - the energy of a single photon [J],

$P_{absorbed}$ - the radiant power absorbed [W],

t - the irradiation time [s],

h - the Planck's constant in [$\text{J}\cdot\text{s}$],

c - the speed of light in [$\text{m}\cdot\text{s}^{-1}$],

λ - the wavelength of irradiation source (420 nm) [m],

P_{ref} - the radiant power transmitted by a blank vial [W],

P_{sample} - the radiant power transmitted by the vial with reaction mixture [W].

Table S19. Calculation of the quantum yield Φ after different irradiation times.

Entry	Irradiation time [min]	P_{sample} [mW]	Yield [%]	Φ [%]
1	300	9.75	60	17.6
2	180	10.08	46	23.8
3	60	5.51	21	20.6

The mean value for the quantum yield was calculated to be $\Phi = 20.6$ %

5.13. Energetics consideration

For estimating the driving force, $G_{\text{PET}}^{(0)}$, of photoinduced electron transfer (PET) from the enamine to the photoexcited porphyrin, we use Rehm-Weller equation:

$$G_{\text{PET}}^{(0)} = F \left(E_{\text{D}^{+}/\text{D}}^{(0)} - E_{\text{A}/\text{A}^{\cdot-}}^{(0)} \right) \epsilon_{00} + G_{\text{S}} + W$$

Where:

$E_{\text{D}^{+}/\text{D}}^{(0)}$ (E_{ox}) - the reduction potential for oxidation of the donor (the enamine);

$E_{\text{A}/\text{A}^{\cdot-}}^{(0)}$ (E_{red}) - the reduction potential for reduction of the acceptor (the porphyrin),

F - the Faraday constant ($F = 1 \text{ e}$ for calculating the energy in eV),

E_{00} - the zero-to-zero energy for PET from the singlet excited state, and the triplet energy for PET from the triplet excited state,

ΔG_{S} - the Born solvation energy (accounting for the interaction energy between the generated ions and the solvent environment), if the reduction potentials and E_{00} are measured for the same solvent media, $\Delta G_{\text{S}} = 0$

W - the Coulomb work term (accounting electrostatic interaction energy between the generated ions).

$E_{\text{ox}} = \sim 0.5 \text{ V}$ vs. SCE in CH_3CN

$E_{\text{red}}(\text{H}_2\text{T}(p\text{-CO}_2\text{MeP})\text{P}) = -0.92 \text{ V}$ vs. SCE

$E_{00} = 1.99 \text{ eV}$

$W = -e^2 / 4 \pi \epsilon_0 \epsilon R_{\text{DA}}$

Where the dielectric permittivity of vacuum is, $\epsilon_0 = 8.854 \times 10^{-12} \text{ F m}^{-1} = 5.526 \times 10^{-3} \text{ e V}^{-1} \text{ \AA}^{-1}$

For the center-to-center donor-acceptor distance, R_{DA} , we can use the sum of the van der Waals radii of the donor and the acceptor, assuming that the PET occurs during contact (collision) between them (i.e., inner sphere ET). For the dielectric constant, we used the dielectric constant of DMSO, $\epsilon = 47$.

$W = -0.061 \text{ eV}$ for $R_{\text{DA}} = 5 \text{ \AA}$

$W = -0.077 \text{ eV}$ for $R_{\text{DA}} = 4 \text{ \AA}$

$W = -0.102 \text{ eV}$ for $R_{\text{DA}} = 3 \text{ \AA}$

Making $G_{\text{PET}}^{(0)}$ acquire negative value (-0.64 V), implying that PET is thermodynamically possible.

Therefore, for PET initiated from the singlet-excited state of the porphyrins, ΔG most likely assumes negative values of a tens of electronvolts (estimated -0.64 V), making it thermodynamically favorable.

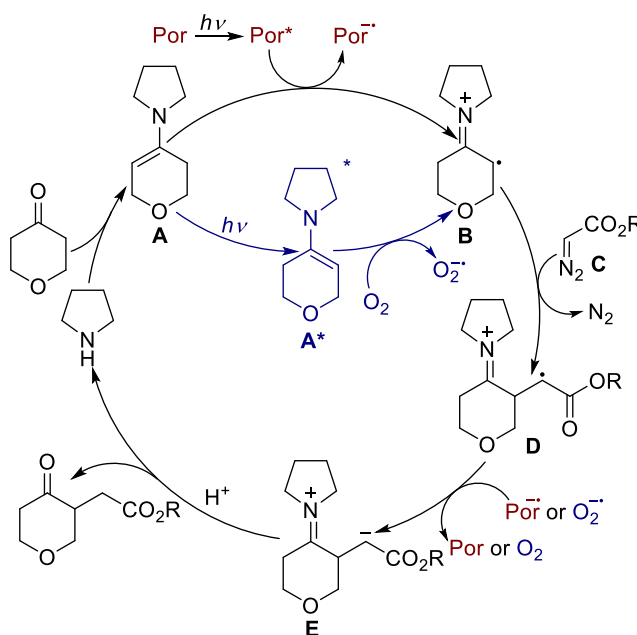
5.14. Theoretical calculations

Experimental

The thermochemistry calculations were performed with Gaussian 09 software.¹⁵ Geometry optimizations and frequency calculations have been carried out with the B3LYP and M06-2X density functionals with the 6-311++G(2d,2p) basis set for all molecules aside from porphyrin. For porphyrin, only the porphyrin core has been taken into account, and the calculations have been performed at the B3LYP/6-31G and M06-2X/6-31G levels of theory. To assess the thermochemistry of all reactions with porphyrin as a reagent, the geometry and frequencies have been calculated for all reagents at the B3LYP/6-31G¹⁶ and M06-2X/6-31G¹⁷ levels of theory as well. The geometry was optimized first in the gas phase and then reoptimized in DMSO using the PCM model of the solvent. For the calculation of the excited state geometries and frequencies TDDFT was applied with the same functional and basis set combinations as for the ground state. To assess the thermodynamic probability of a given reaction, ΔG has been calculated as a difference between the calculated free enthalpies of products and free enthalpies of substrates of this reaction.

Results

Mechanistic proposal:



For steps including porphyrin in the excited state we have been able to conduct only calculations using only a very small basis set (B3LYP/6-31G and M06-2X/6-31G). Thus, for all reactions including porphyrin as a catalyst the data obtained from small basis set calculations are taken into account while for the reactions with no porphyrin added the values obtained with the 6-311++G(2d,2p) basis set are used.

The oxidation of enamine **A** by $^3\text{O}_2$ seems to be not allowed thermodynamically ($\Delta G_{\text{B3LYP/6-311++G(2d,2p), DMSO}} = +27.02$ kcal/mol, $\Delta G_{\text{M06-2X/6-311++G(2d,2p), DMSO}} = +35.40$ kcal/mol). On the other hand, for $^1\text{O}_2$ the obtained Gibbs energies tentatively indicated the spontaneity of enamine oxidation, although the values are close to zero ($\Delta G_{\text{B3LYP/6-311++G(2d,2p), DMSO}} = -11.72$ kcal/mol, $\Delta G_{\text{M06-2X/6-311++G(2d,2p), DMSO}} = -2.30$ kcal/mol).

Although in the presence of water and acetic acid enamine **A** is present in a protonated form (Figure S16), as confirmed by the calculated absorbance spectrum, the positive value of Gibbs energy of the oxidation of protonated enamine **A** to radical cation **B** by both $^3\text{O}_2$ and $^1\text{O}_2$ ($\Delta G_{\text{B3LYP/6-311++G(2d,2p), DMSO}} = +309.73$ kcal/mol, $\Delta G_{\text{M06-2X/6-311++G(2d,2p), DMSO}} = +315.24$ kcal/mol and $\Delta G_{\text{B3LYP/6-311++G(2d,2p), DMSO}} = +271.99$ kcal/mol, $\Delta G_{\text{M06-2X/6-311++G(2d,2p), DMSO}} = +277.54$ kcal/mol, respectively) suggests that the most probable path involves the oxidation of non-protonated enamine **A** by singlet oxygen.

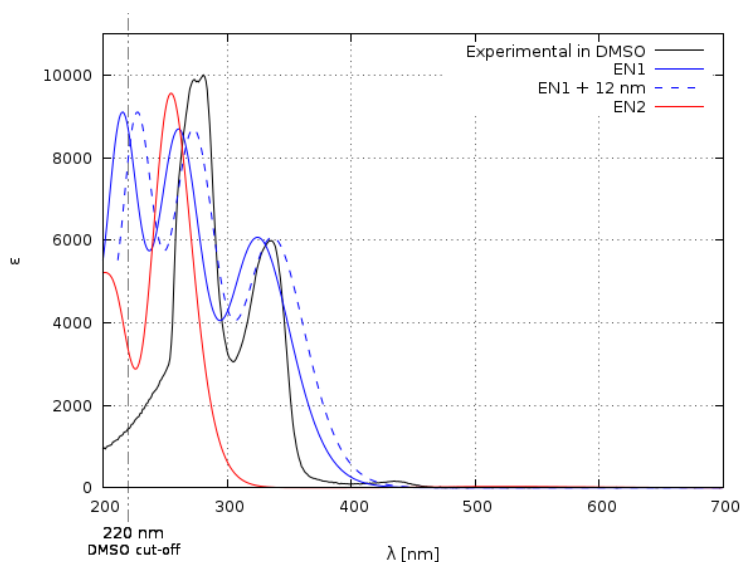


Figure S16. Computed and experimental UV-Vis spectra of enamine formed in situ from 4-oxotetrahydropyran and pyrrolidine

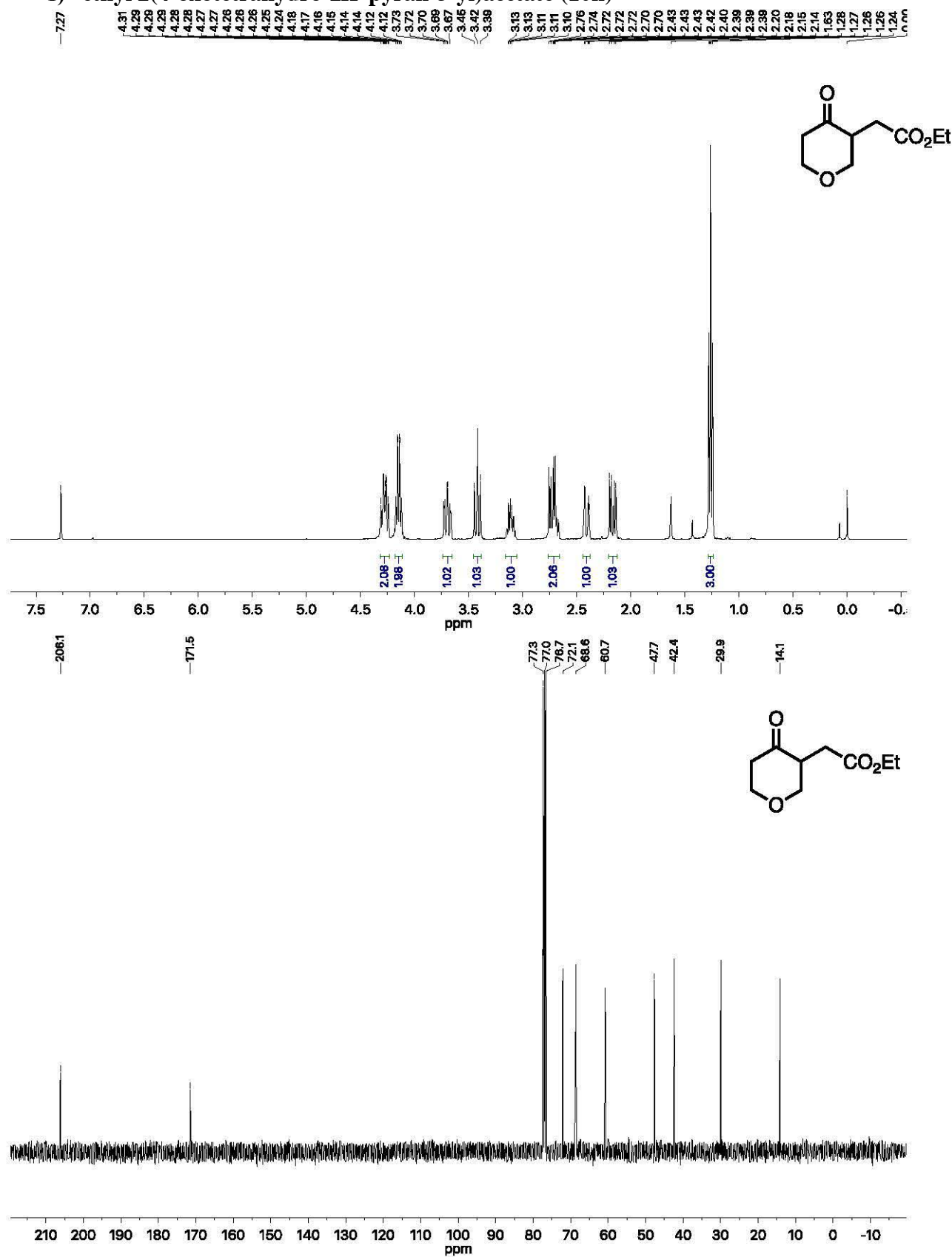
Even more preferred would be – according to the calculated Gibbs energy values – the oxidation of non-protonated enamine in the excited state **A***, as these values are negative for both triplet ($\Delta G_{\text{B3LYP/6-311++G(2d,2p), DMSO}} = -60.32$ kcal/mol, $\Delta G_{\text{M06-2X/6-311++G(2d,2p), DMSO}} = -60.29$ kcal/mol) and singlet ($\Delta G_{\text{B3LYP/6-311++G(2d,2p), DMSO}} = -99.06$ kcal/mol, $\Delta G_{\text{M06-2X/6-311++G(2d,2p), DMSO}} = -97.99$ kcal/mol) oxygen. For the protonated enamine in the excited state the positive Gibbs energies were obtained ($\Delta G_{\text{B3LYP/6-311++G(2d,2p), DMSO}} = 224.28$ kcal/mol, $\Delta G_{\text{M06-2X/6-311++G(2d,2p), DMSO}} = 203.99$ kcal/mol for the reaction with triplet oxygen, $\Delta G_{\text{B3LYP/6-311++G(2d,2p), DMSO}} = 185.54$ kcal/mol, $\Delta G_{\text{M06-2X/6-311++G(2d,2p), DMSO}} = 166.28$ kcal/mol for reaction with singlet oxygen).

For the reaction of porphyrin in the excited state with an enamine **A** the values of Gibbs energy were negative, but very close to zero ($\Delta G_{\text{B3LYP/6-31G, DMSO}} = -9.29$ kcal/mol, $\Delta G_{\text{M06-2X/6-31G, DMSO}} = -7.55$ kcal/mol). For the protonated form of enamine positive values of Gibbs energy were obtained ($\Delta G_{\text{B3LYP/6-31G, DMSO}} = 41.5$ kcal/mol, $\Delta G_{\text{M06-2X/6-31G, DMSO}} = 220.9$ kcal/mol), indicating that - as in the reaction with oxygen - also in the presence of porphyrin the reaction of neutral form of enamine is favored thermodynamically.

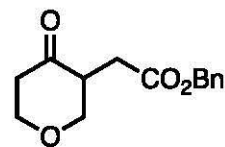
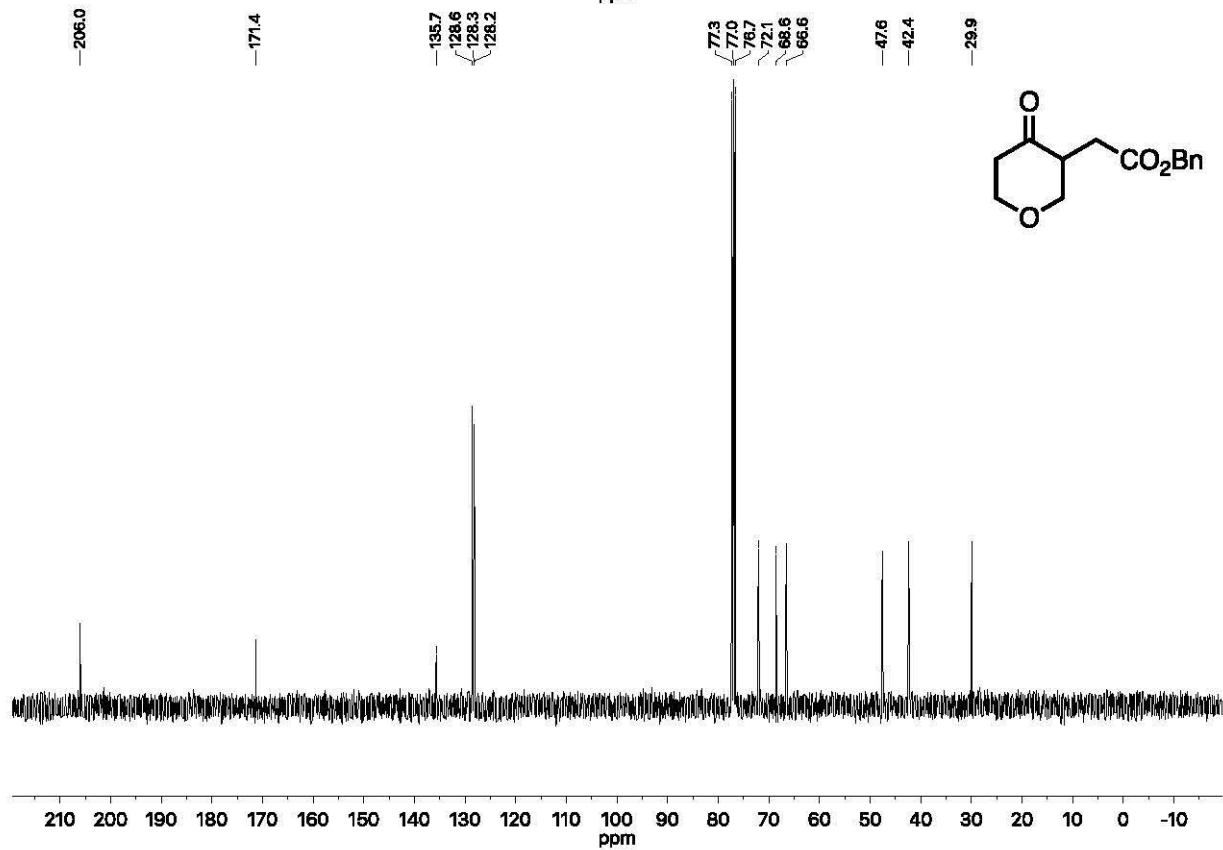
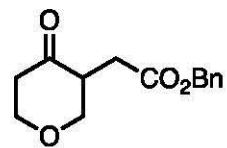
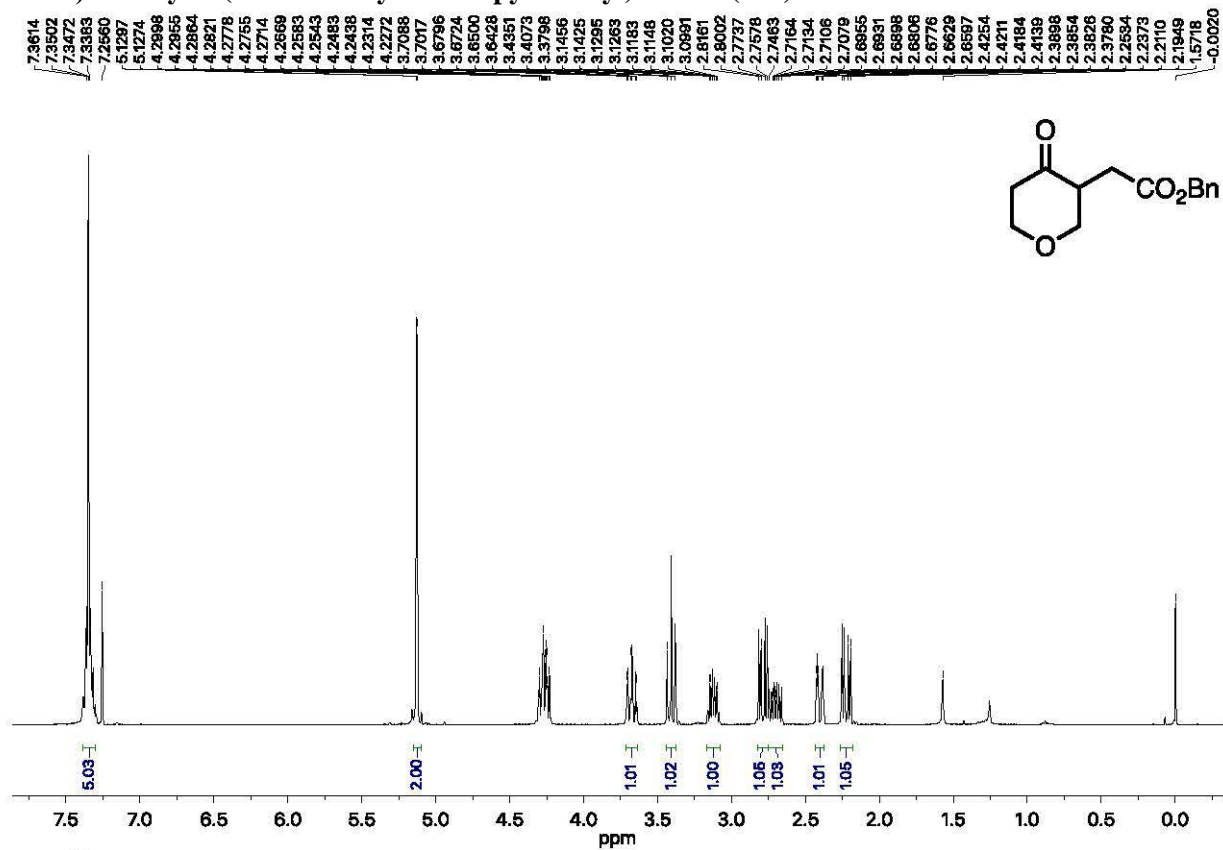
The formation of radical adduct **D** after the reaction of radical cation **B** with EDA with simultaneous extrusion of nitrogen is more favorable than formation of the covalent adduct of EDA to radical cation **B**, as such process would require insane energy of more than 300 kcal mol⁻¹ (see Figure S15), what made us discard such a process in mechanistic considerations. The consequent reduction of radical adduct **D** by porphyrin radical anion Por^{•-} is also favorable ($\Delta G_{\text{B3LYP/6-31G, DMSO}} = -28.83$ kcal/mol). When superoxide radical anion takes place of porphyrin both B3LYP and M06-2X functional give negative value of free enthalpy ($\Delta G_{\text{B3LYP/6-31G, DMSO}} = -20.26$ kcal/mol, $\Delta G_{\text{M06-2X/6-31G, DMSO}} = -22.93$ kcal/mol). However, when a larger basis set was taken for calculations (6-311++(2d,2p)), for M06-2X potential a positive value was obtained: $\Delta G_{\text{M06-2X/6-311++G(2d,2p), DMSO}} = +8.95$ kcal/mol). This indicates that in the absence of porphyrin this step is less favorable thermodynamically.

6. ^1H and ^{13}C NMR spectra measured in CDCl_3

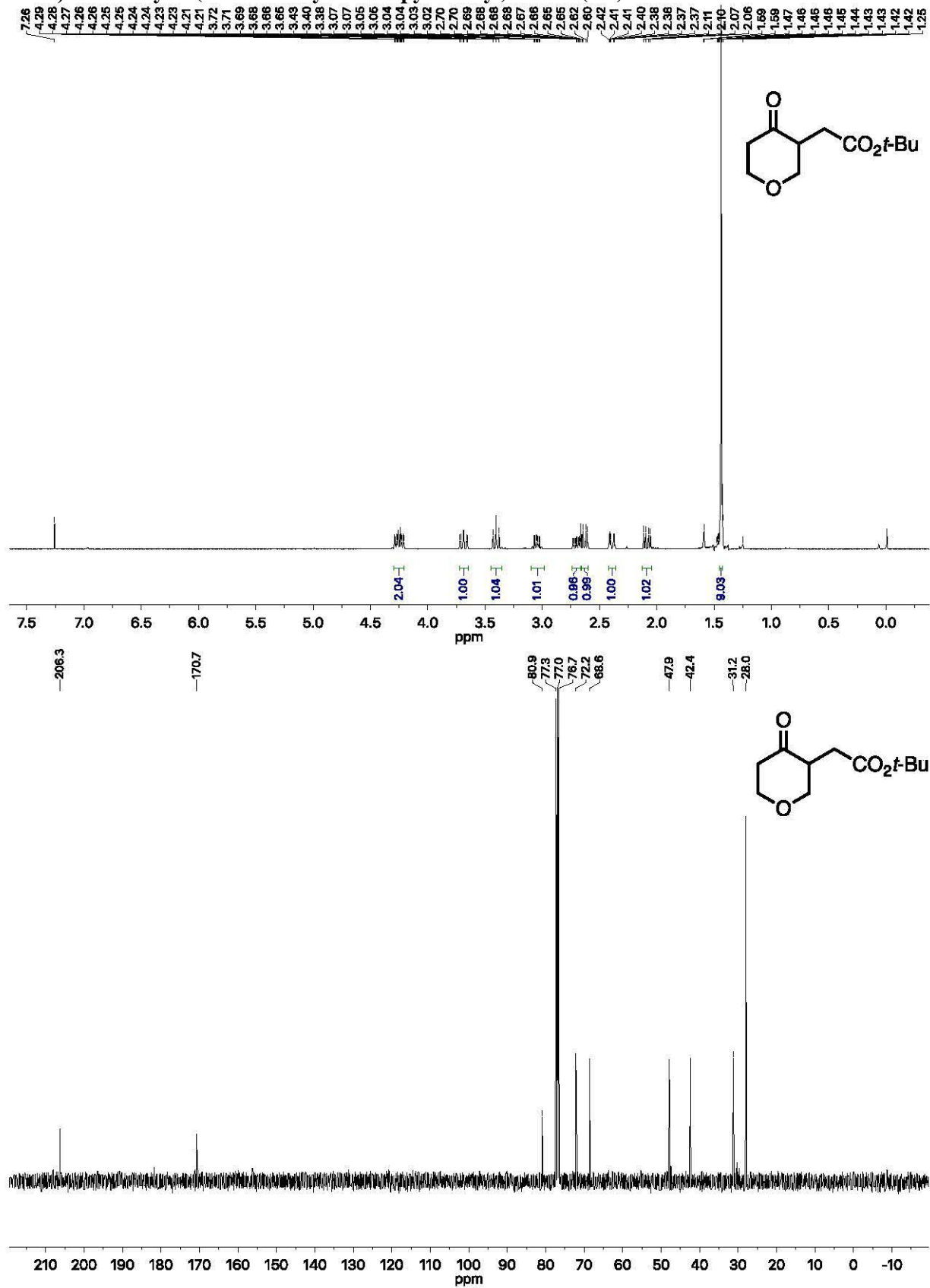
1) ethyl 2(4-oxotetrahydro-2H-pyran-3-yl)acetate (10h)



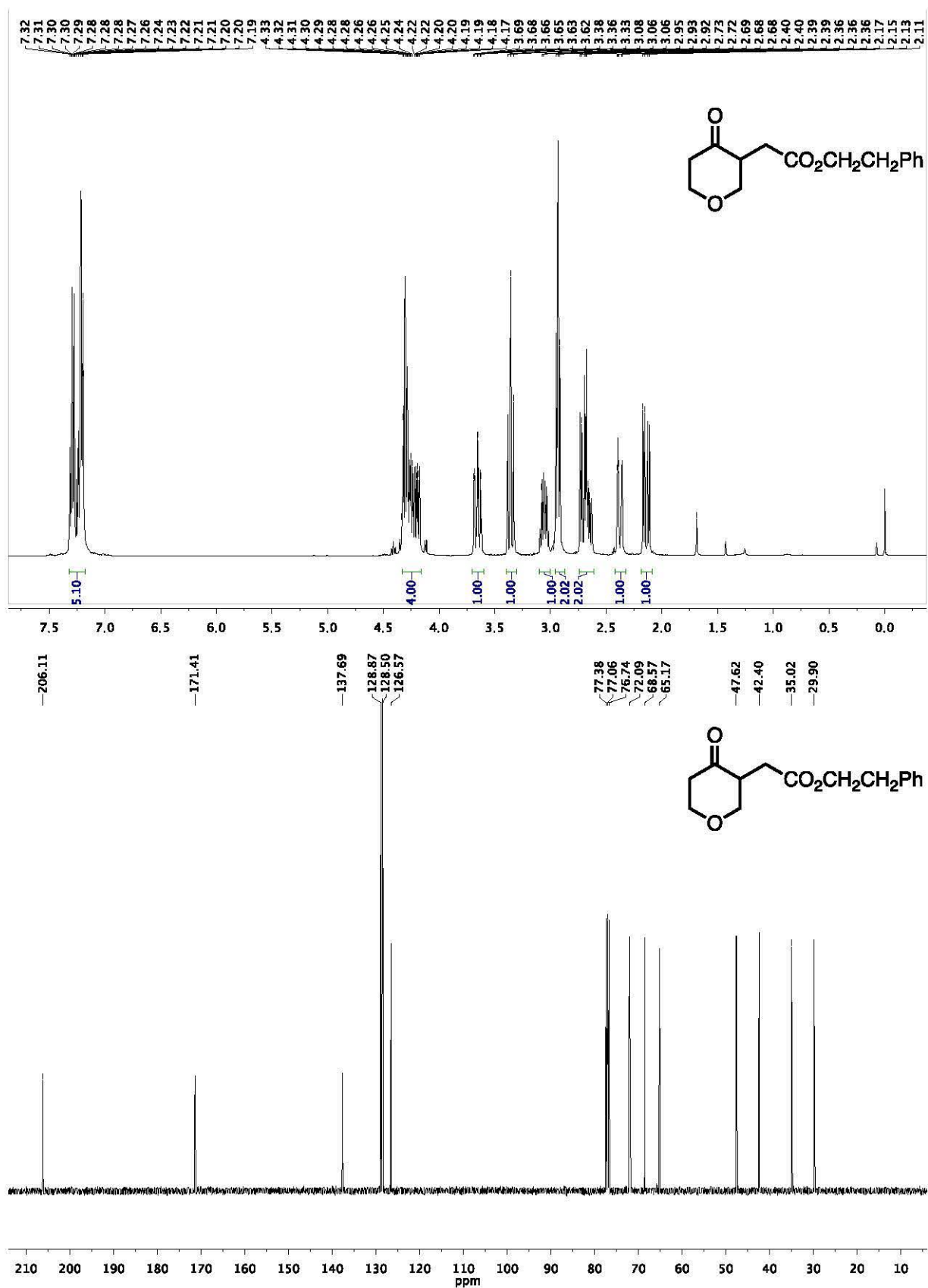
2) benzyl 2-(4-oxotetrahydro-2H-pyran-3-yl)acetate (10a)



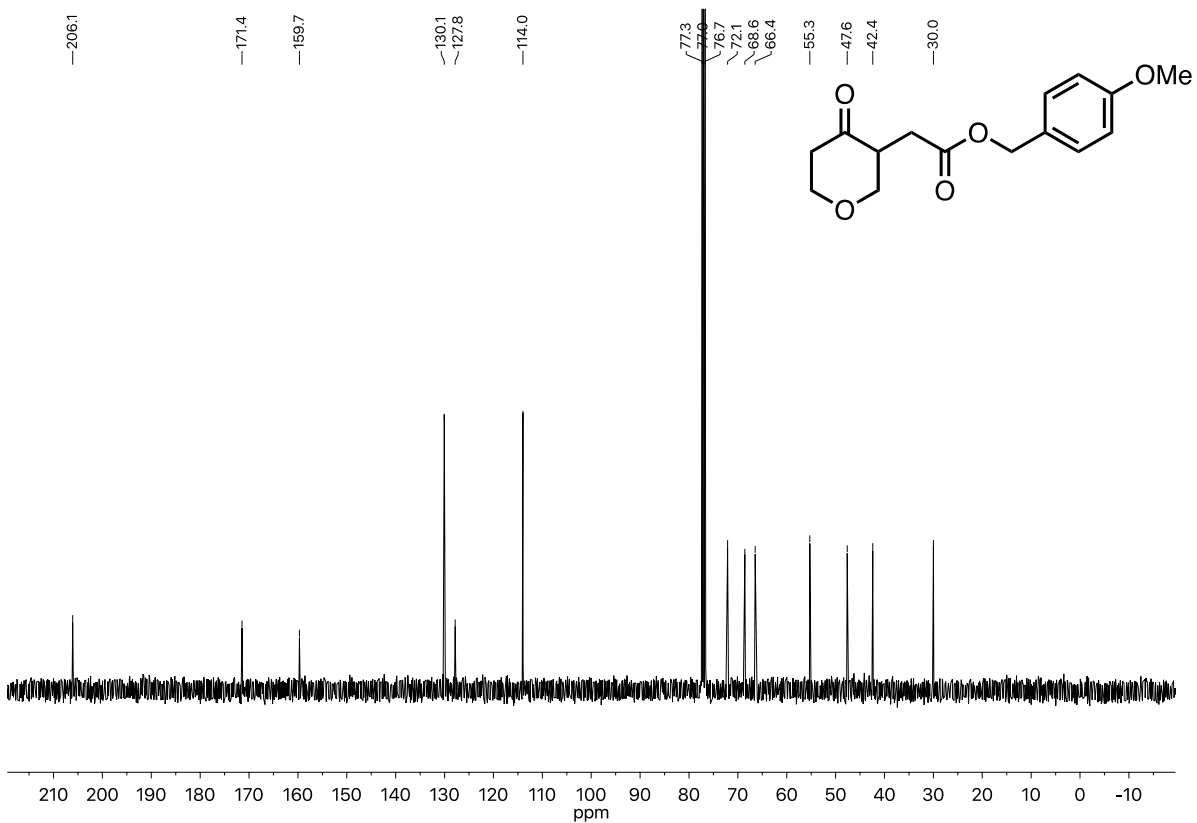
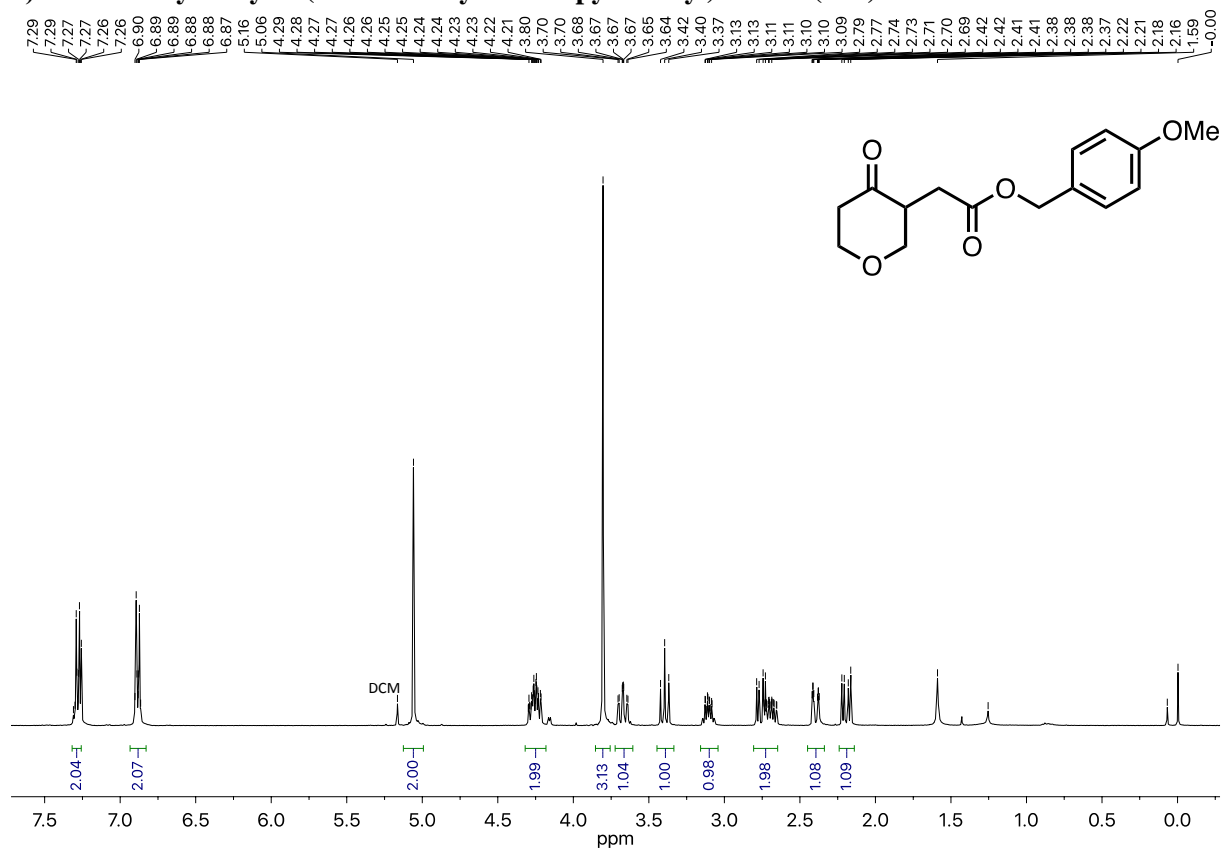
3) *tert*-butyl 2-(4-oxotetrahydro-2*H*-pyran-3-yl)acetate (10i)



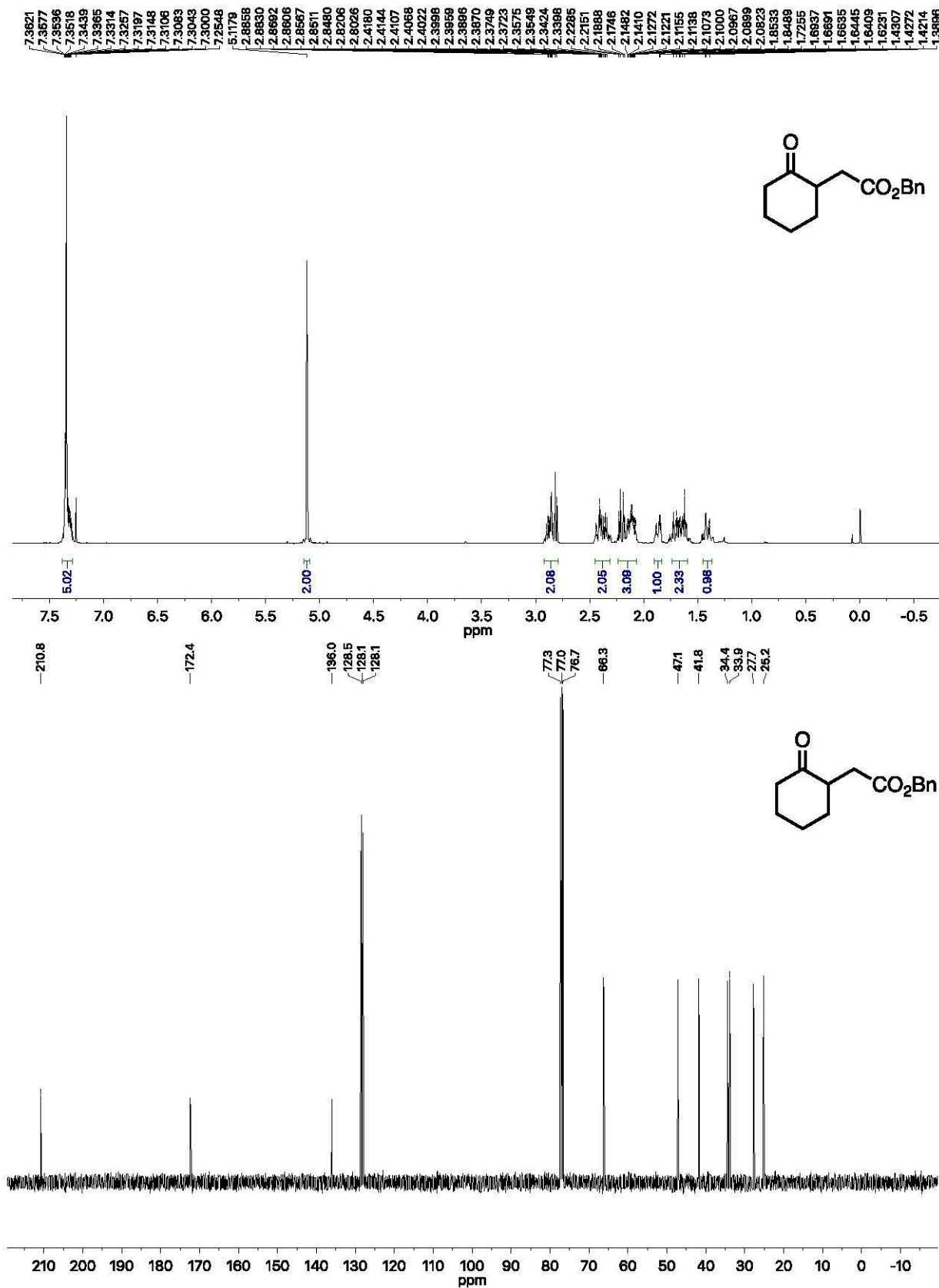
4) phenethyl 2(4-oxotetrahydro-2H-pyran-3-yl)acetate (10j)



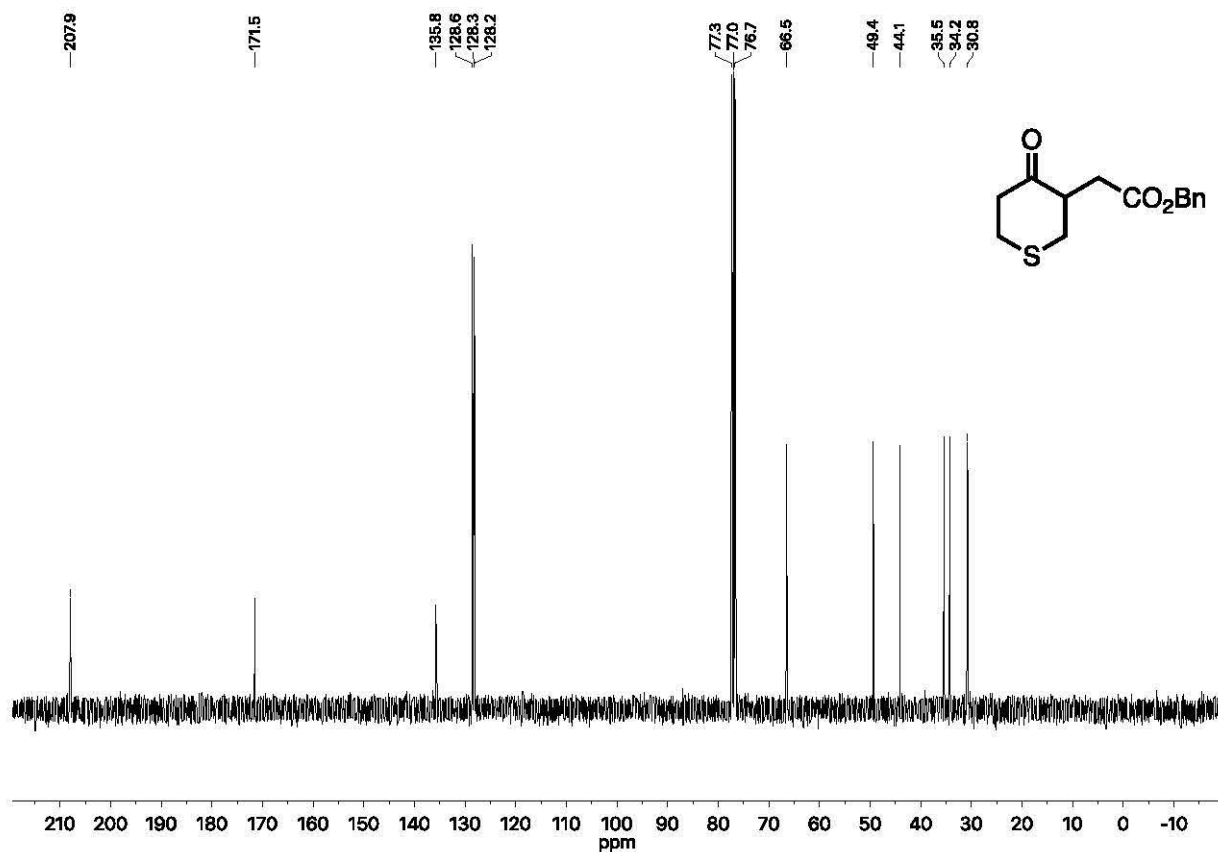
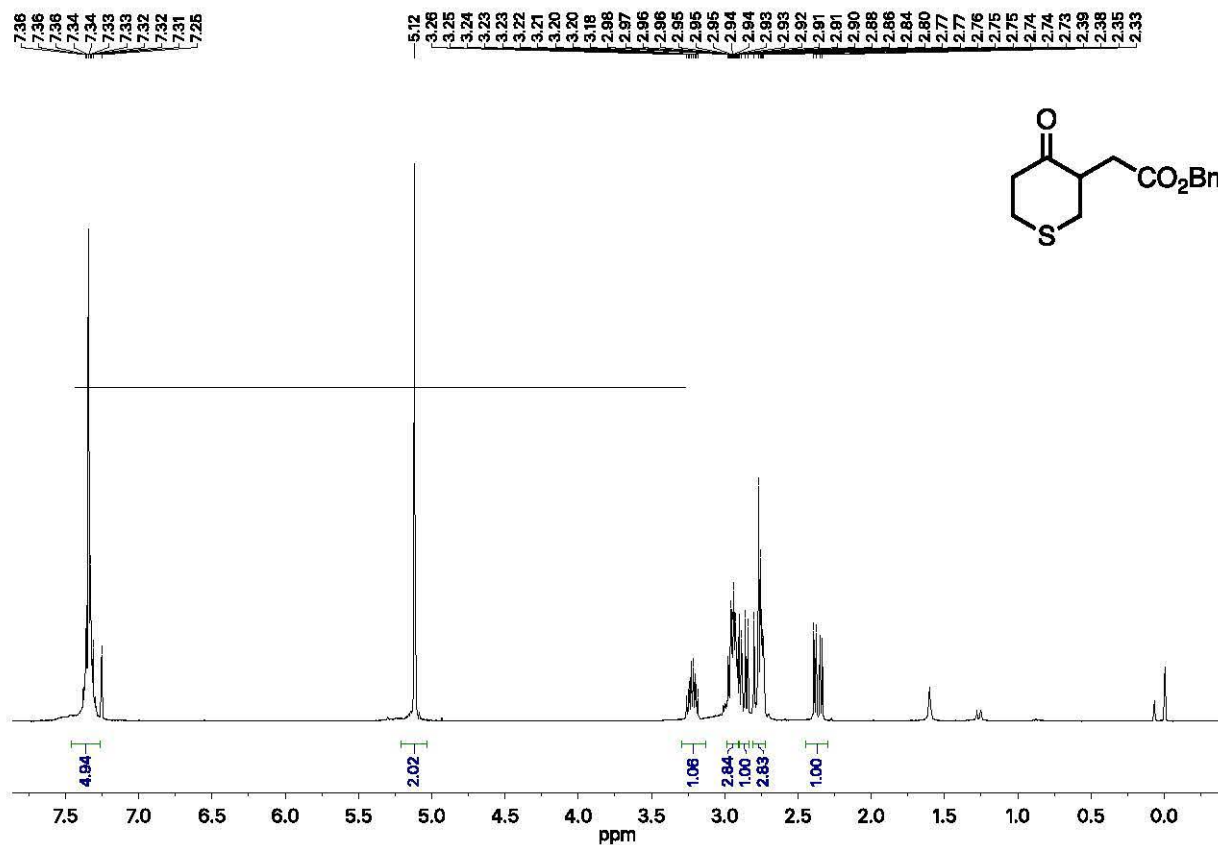
5) 4-methoxybenzyl 2-(4-oxotetrahydro-2H-pyran-3-yl)acetate (10k)



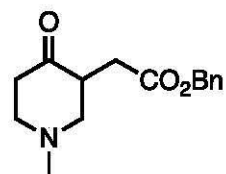
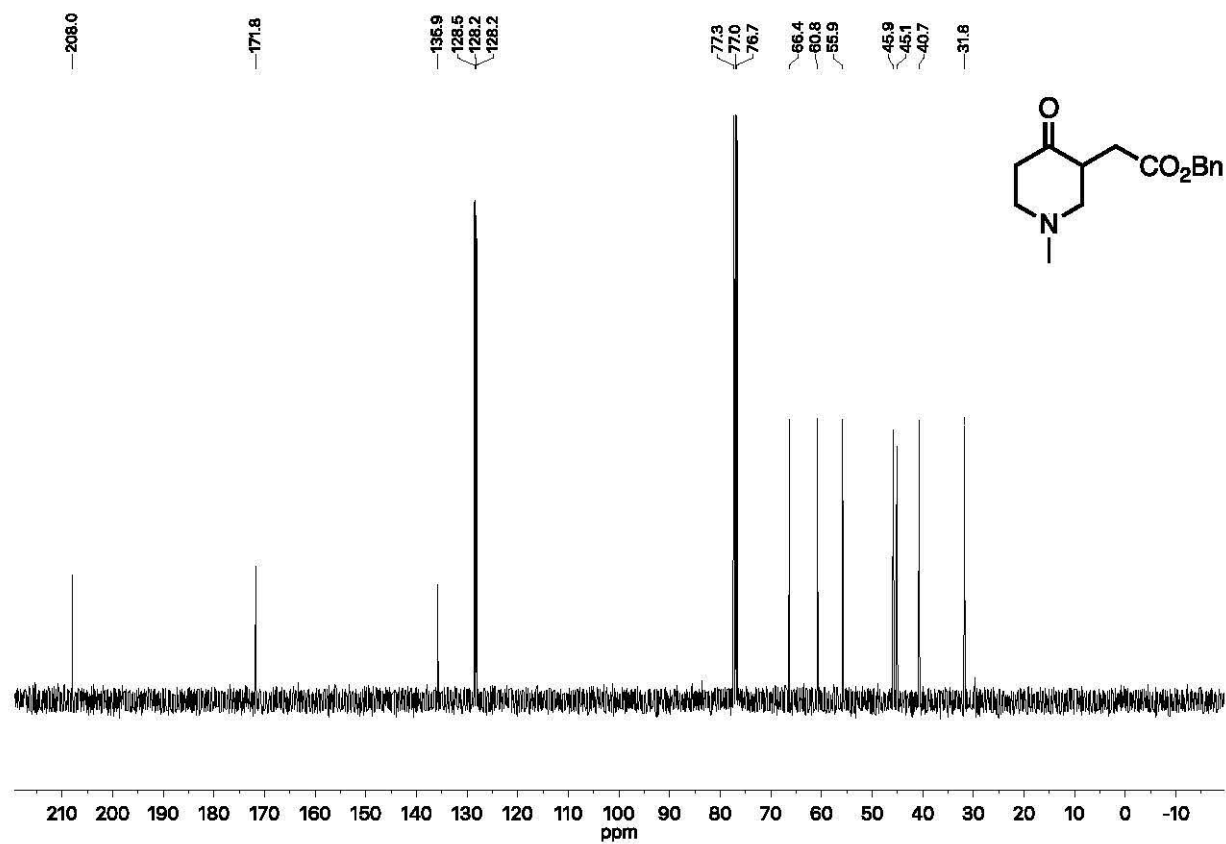
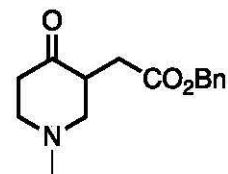
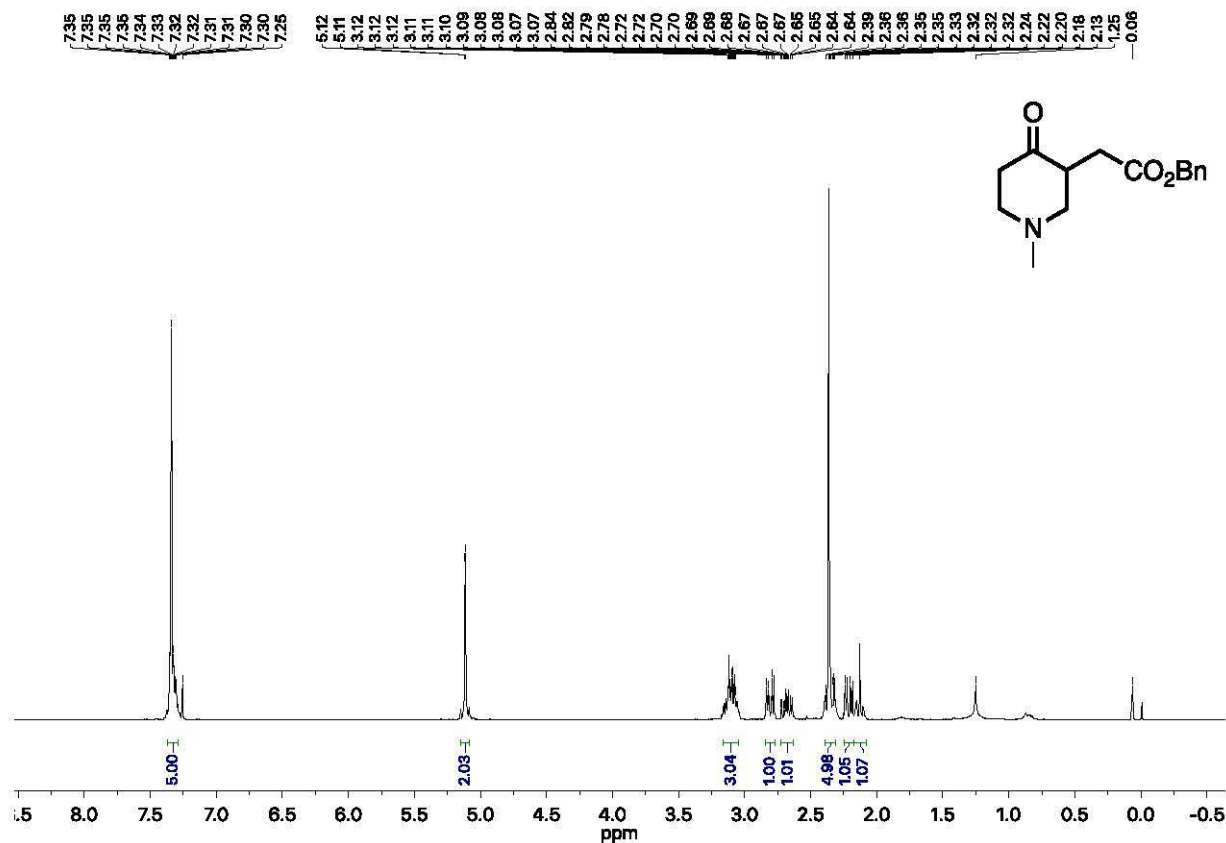
6) benzyl 2-(2-oxocyclohexyl)acetate (10b)



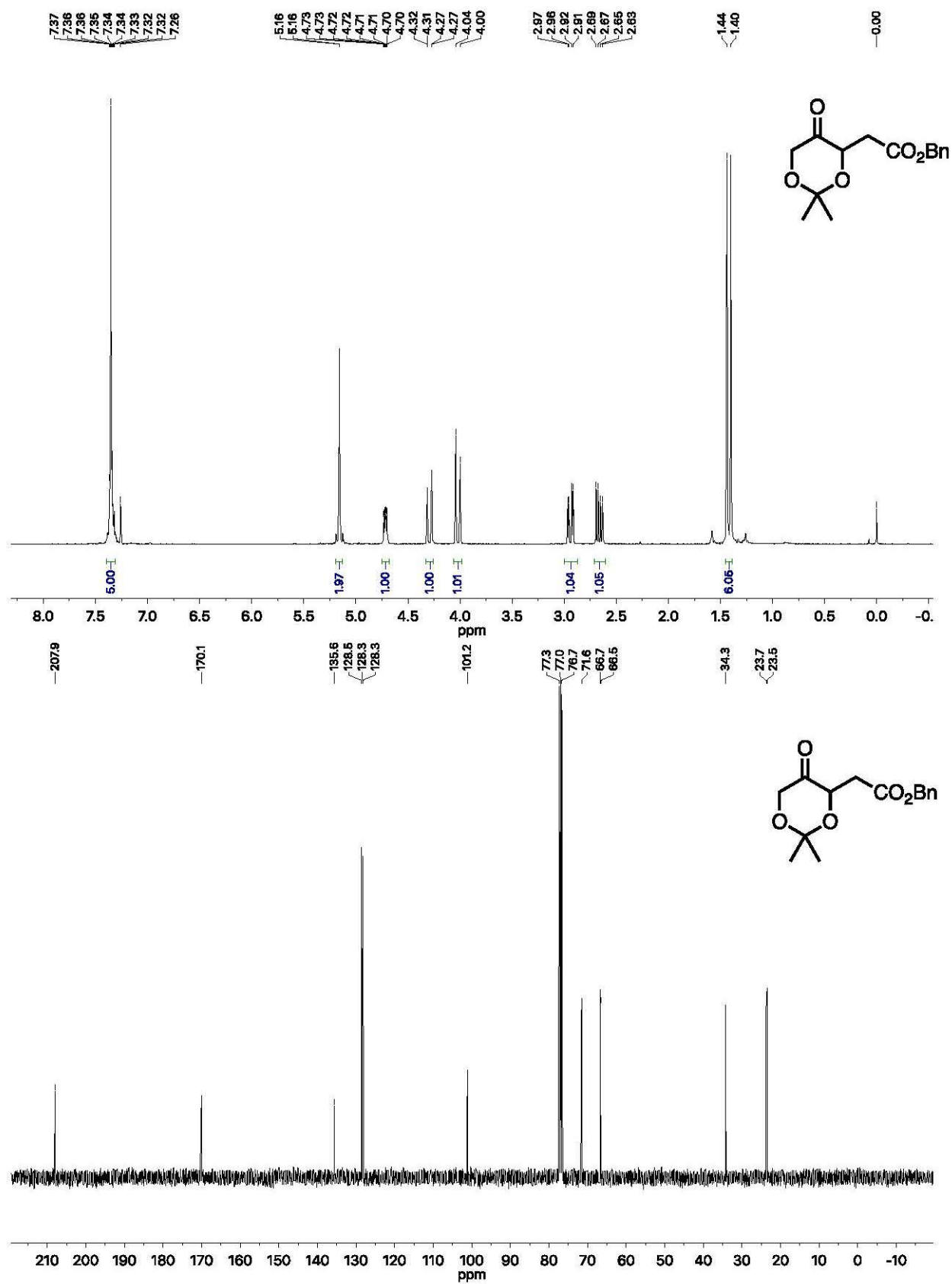
7) benzyl 2-(4-oxotetrahydro-2H-thiopyran-3-yl)acetate (10d)



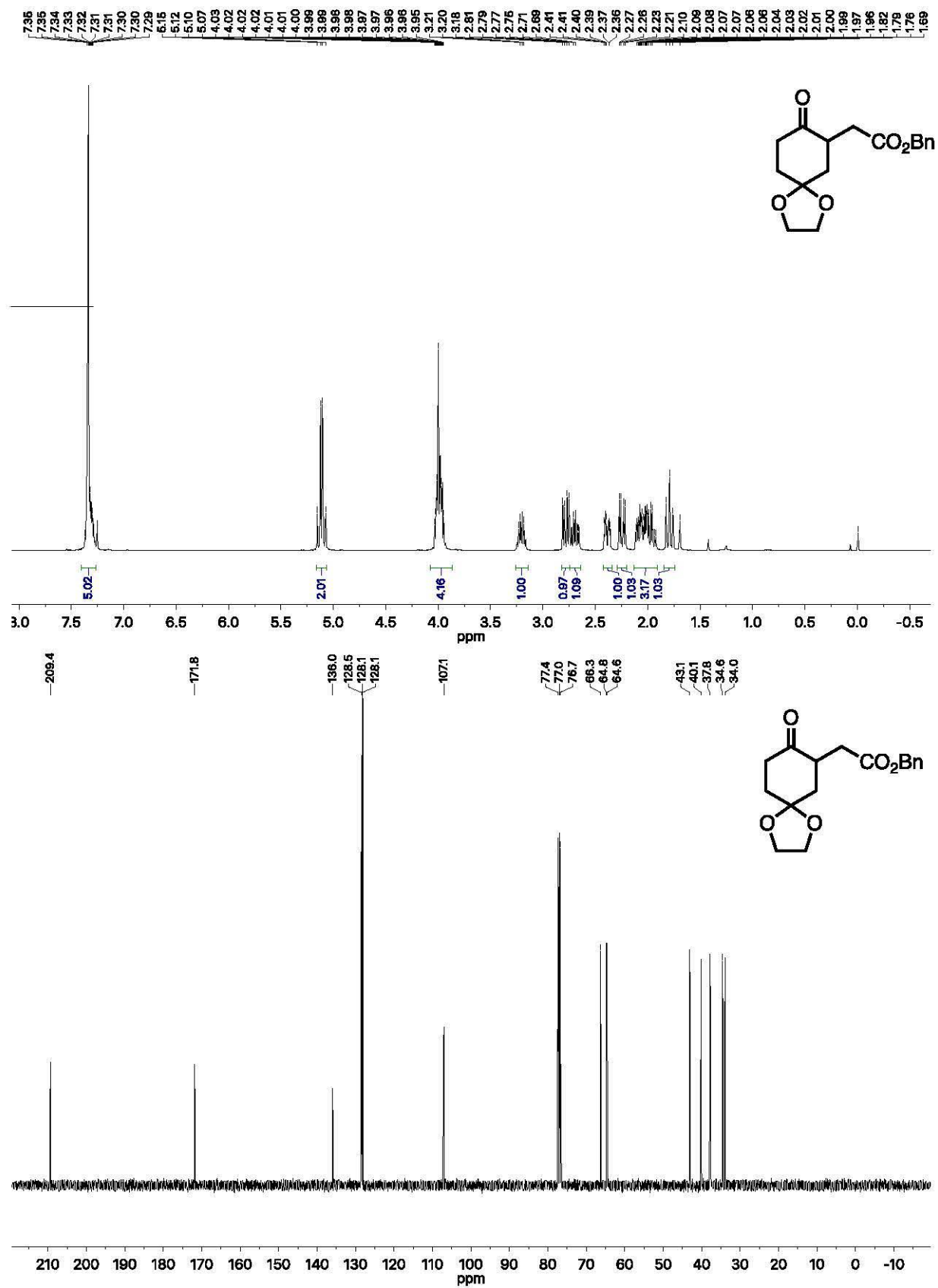
8) benzyl 2-(*N*-methyl-4-oxopiperidin-3-yl)acetate (10e)



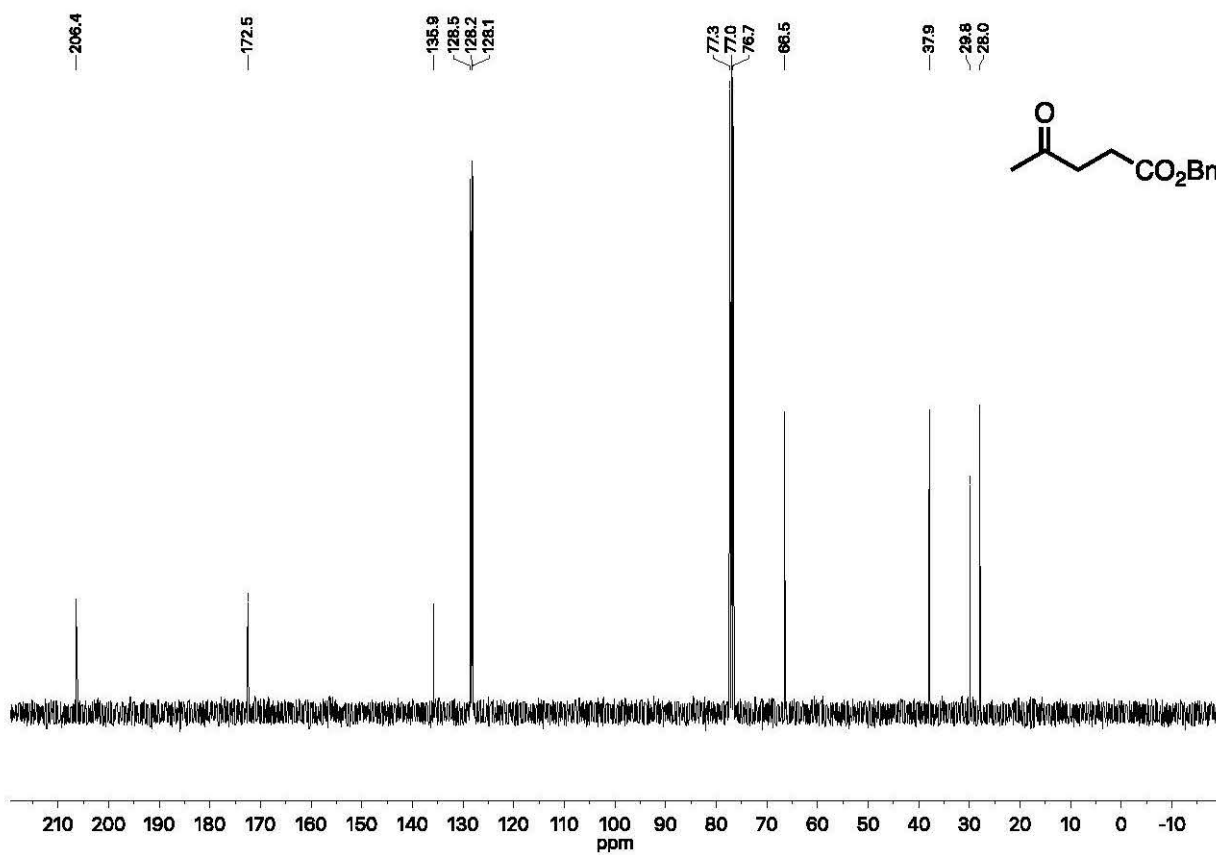
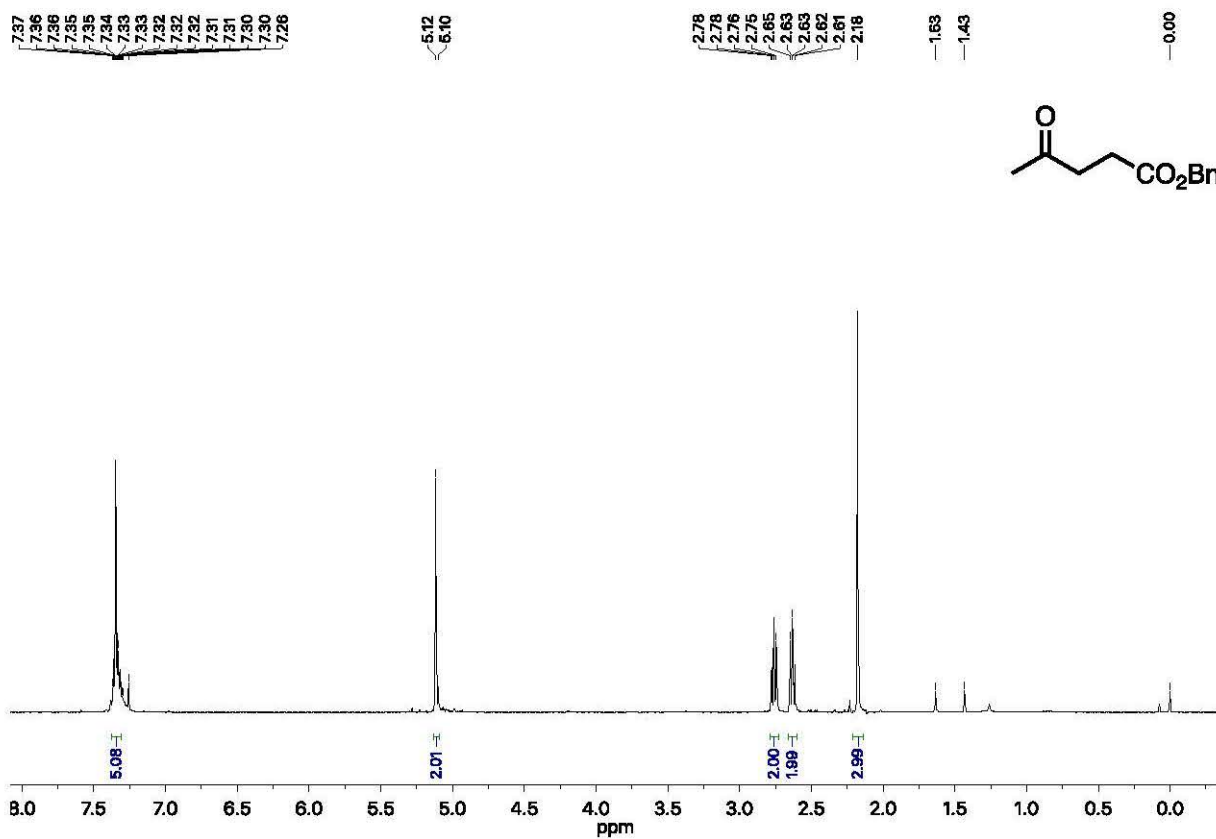
9) benzyl 2-(2,2-dimethyl-5-oxo-1,3-dioxan-4-yl)acetate (10g)



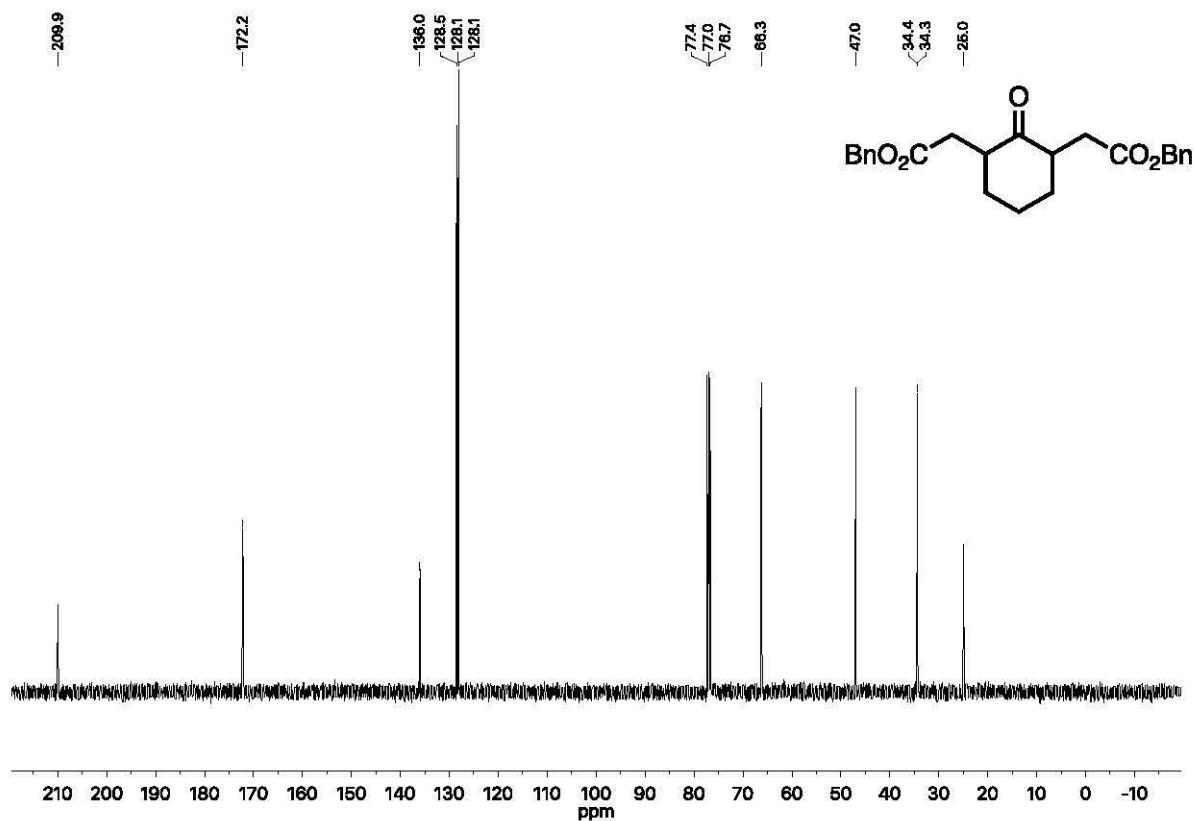
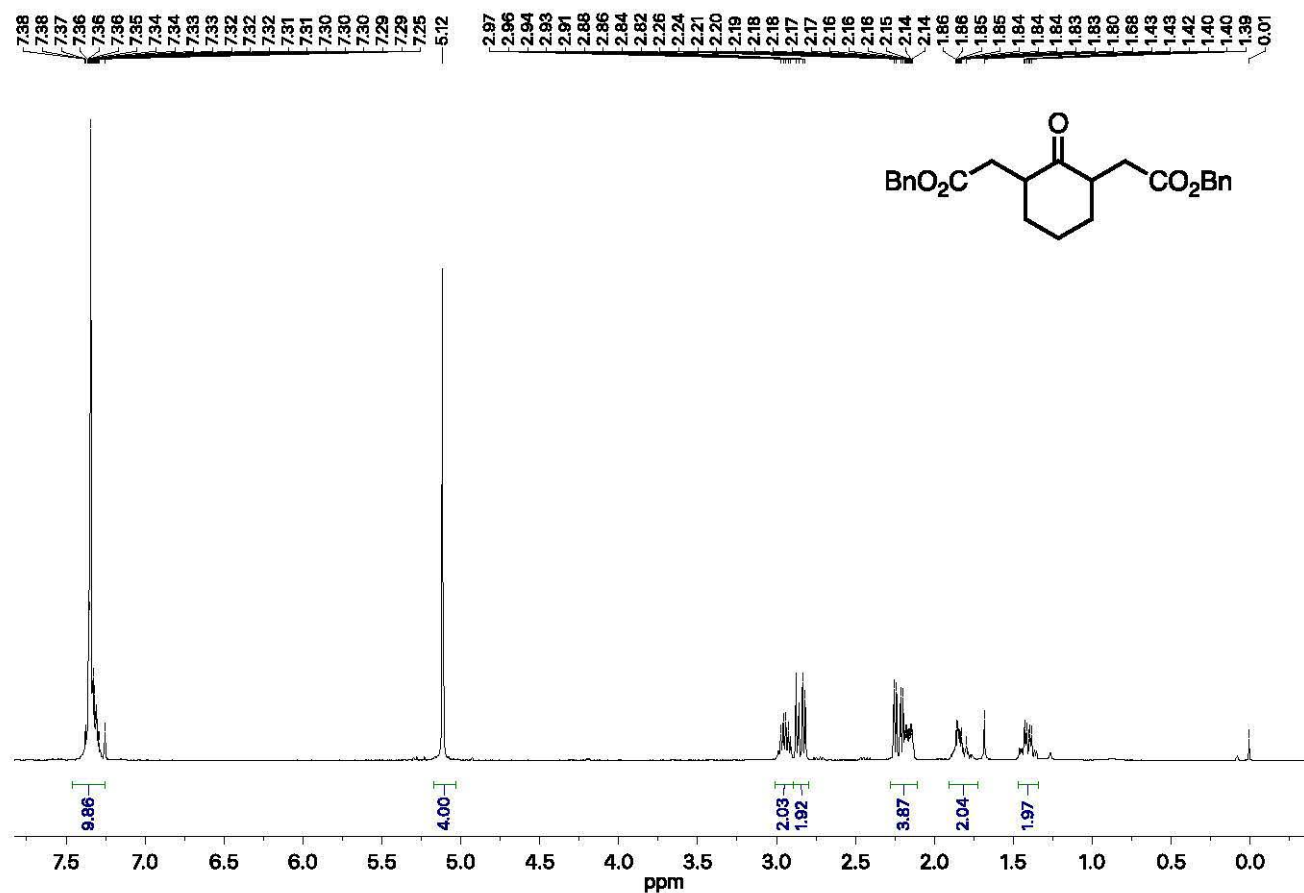
10) benzyl 2-(8-oxo-1,4-dioxaspiro[4.5]decan-7-yl)acetate (10f)



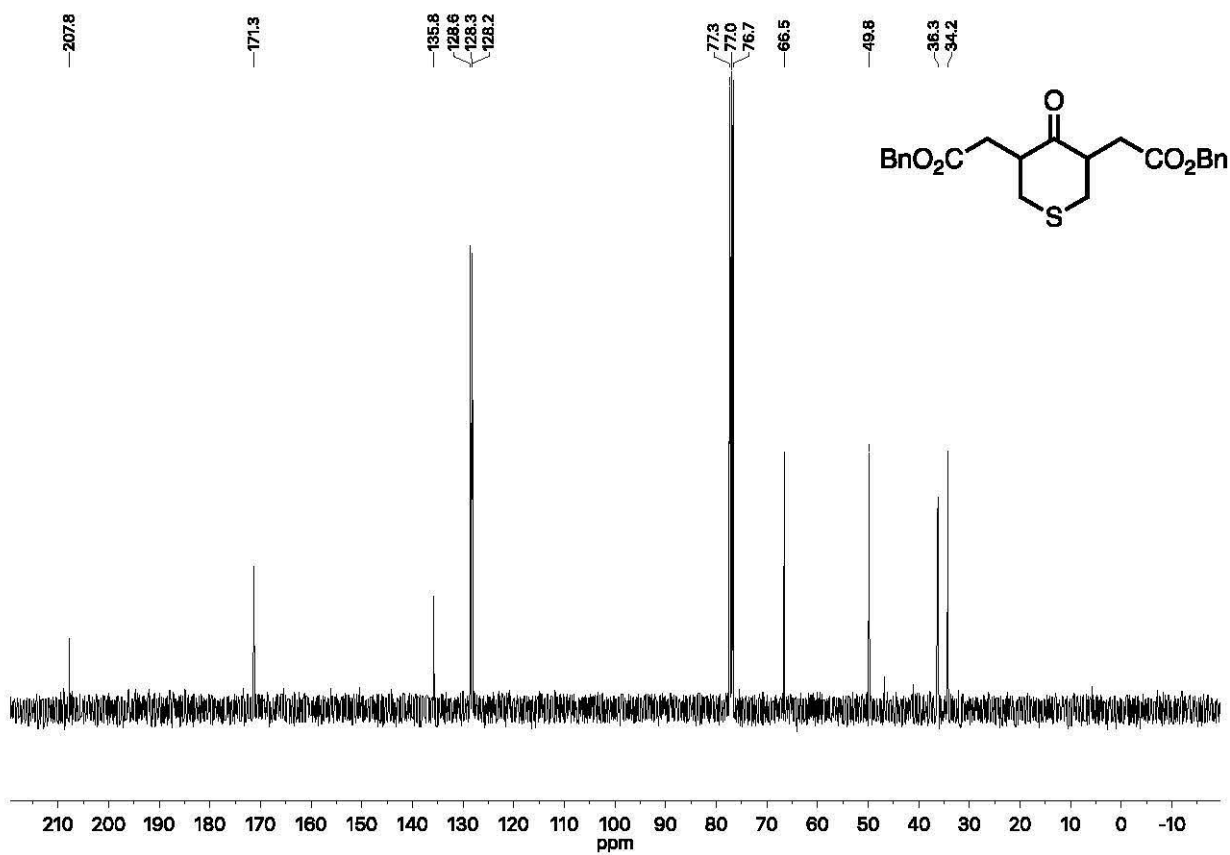
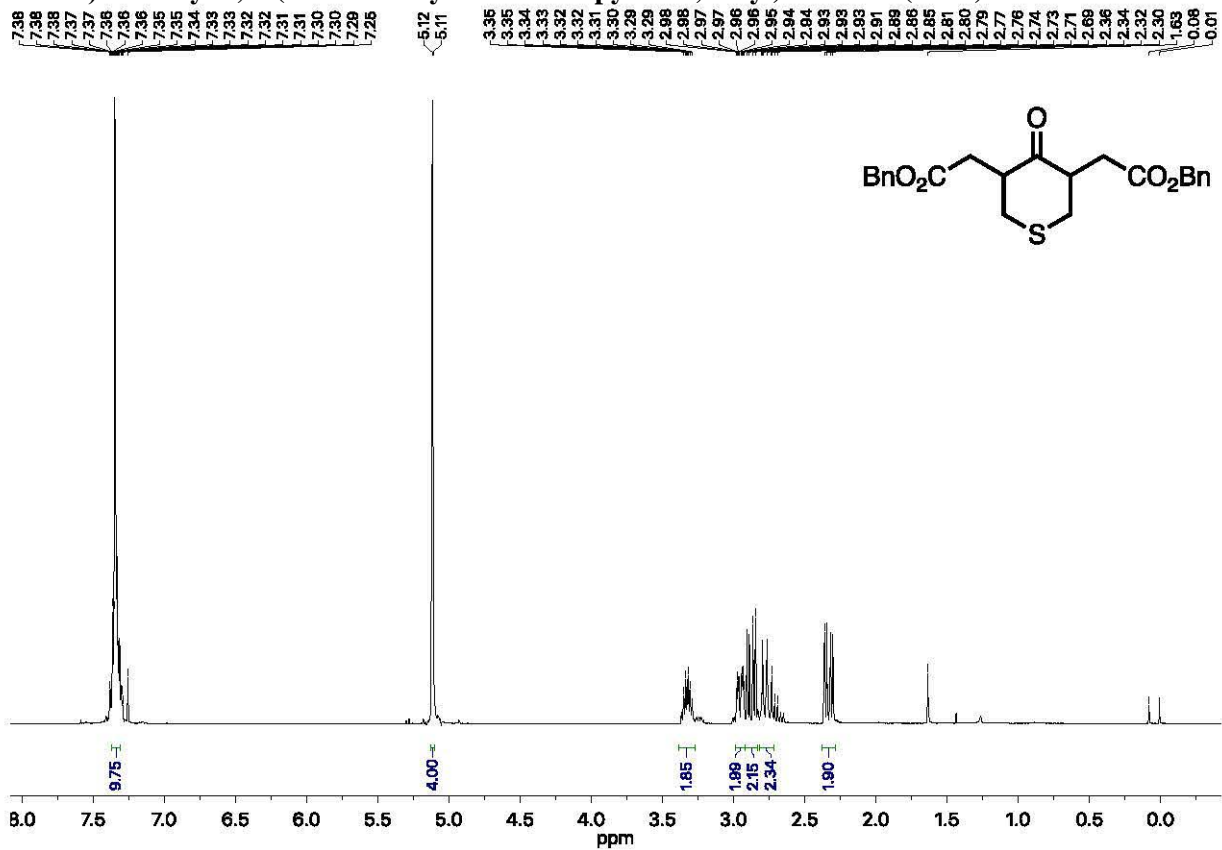
12) benzyl 4-oxopentanoate (10m)



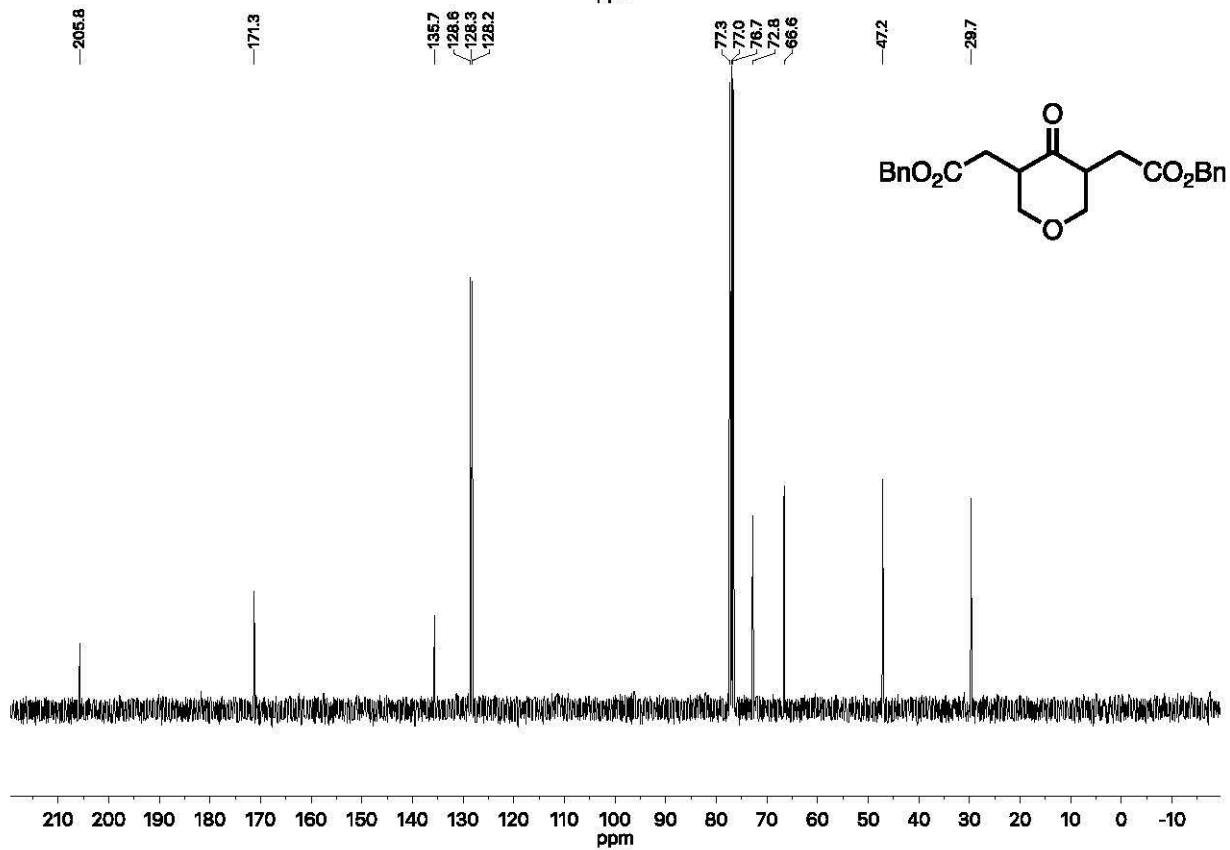
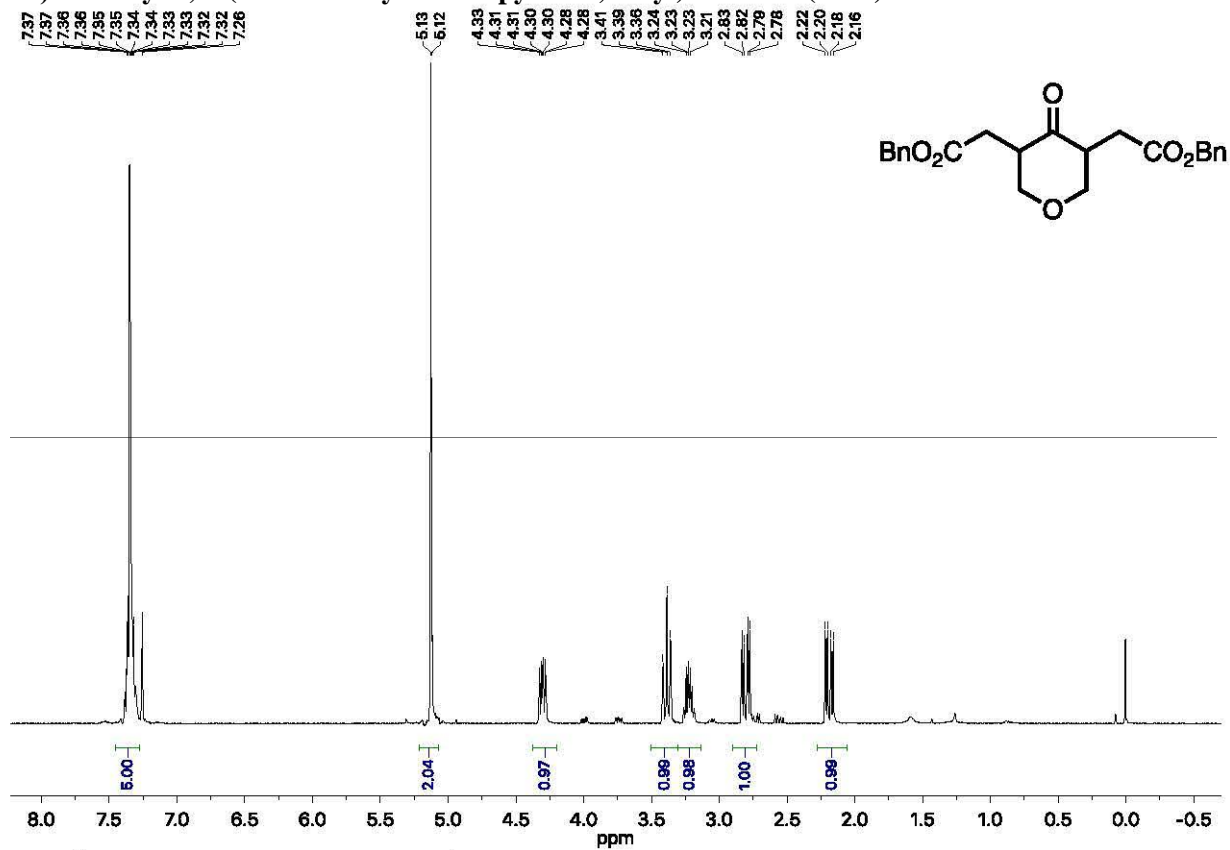
13) dibenzyl 2,2'-(2-oxocyclohexane-1,3-diyl)diacetate (10bb) + *diastereoisomer*



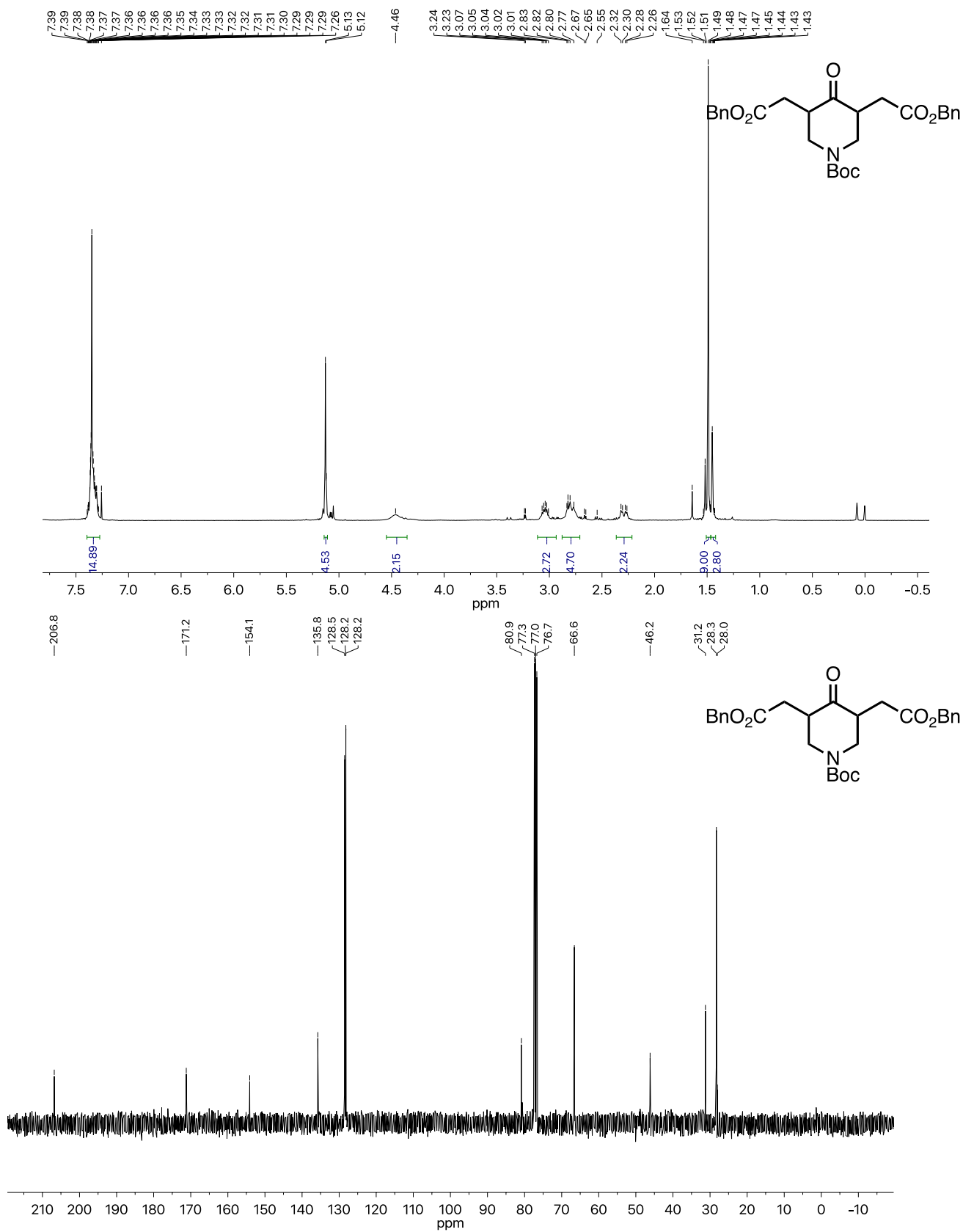
14) dibenzyl 2,2'-(4-oxotetrahydro-2H-thiopyran-3,5-diyl)diacetate (10dd) + diastereoisomer



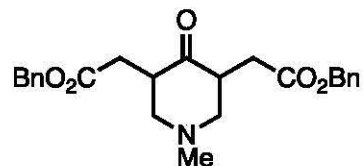
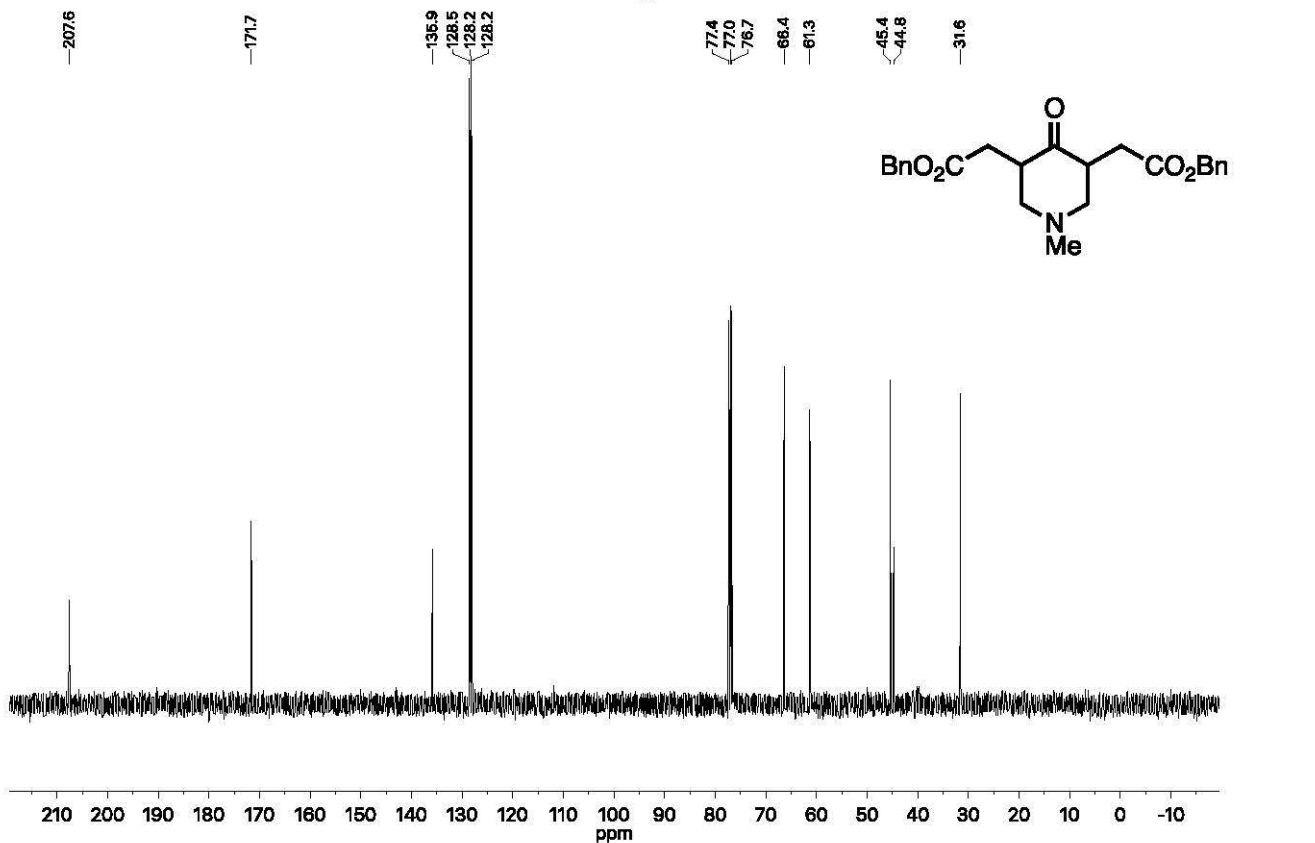
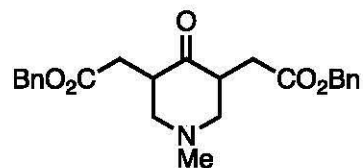
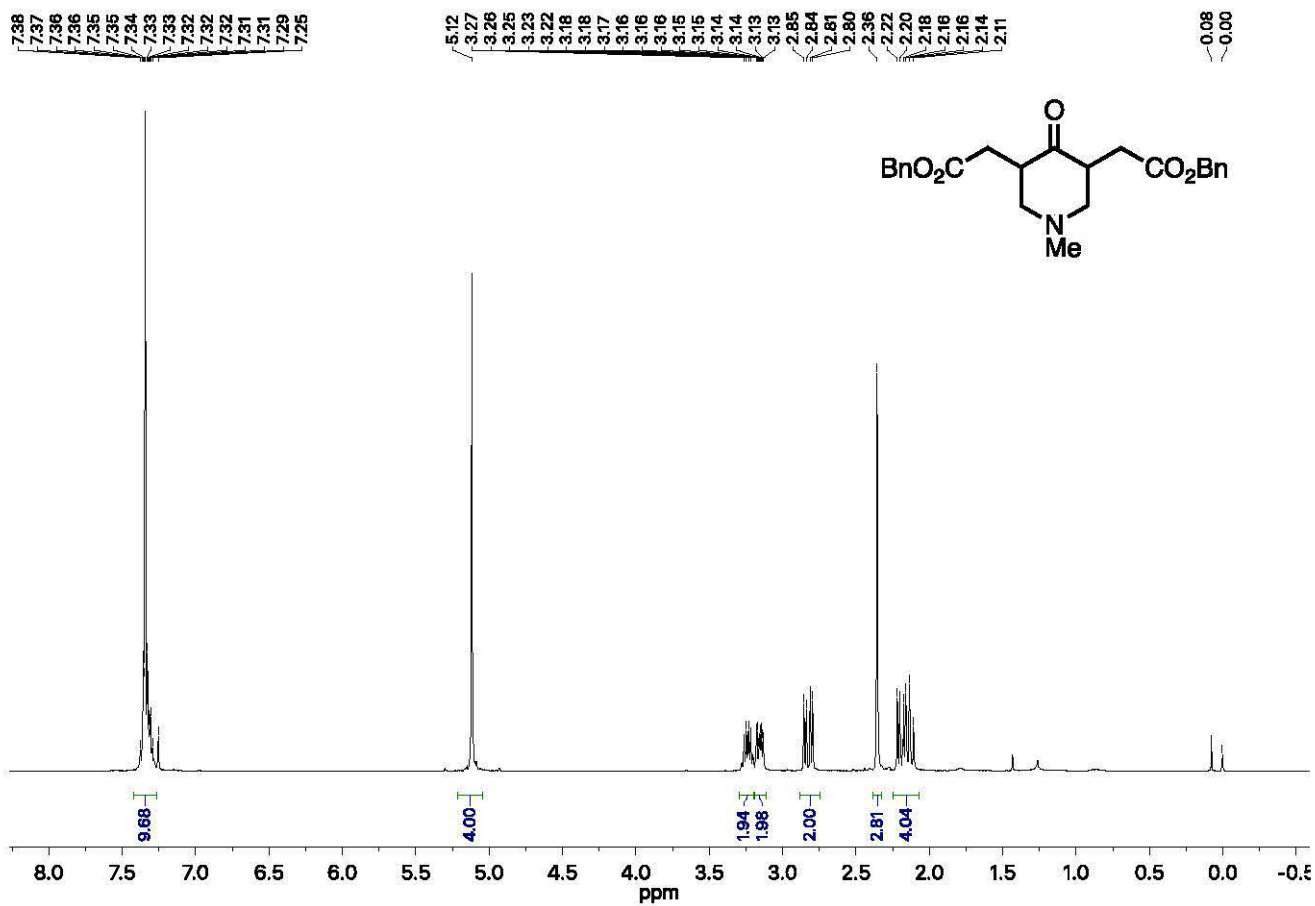
15) dibenzyl 2,2'-(4-oxotetrahydro-2H-pyran-3,5-diyl)diacetate (10aa) + diastereoisomer



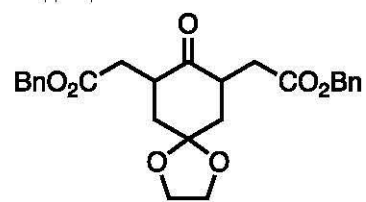
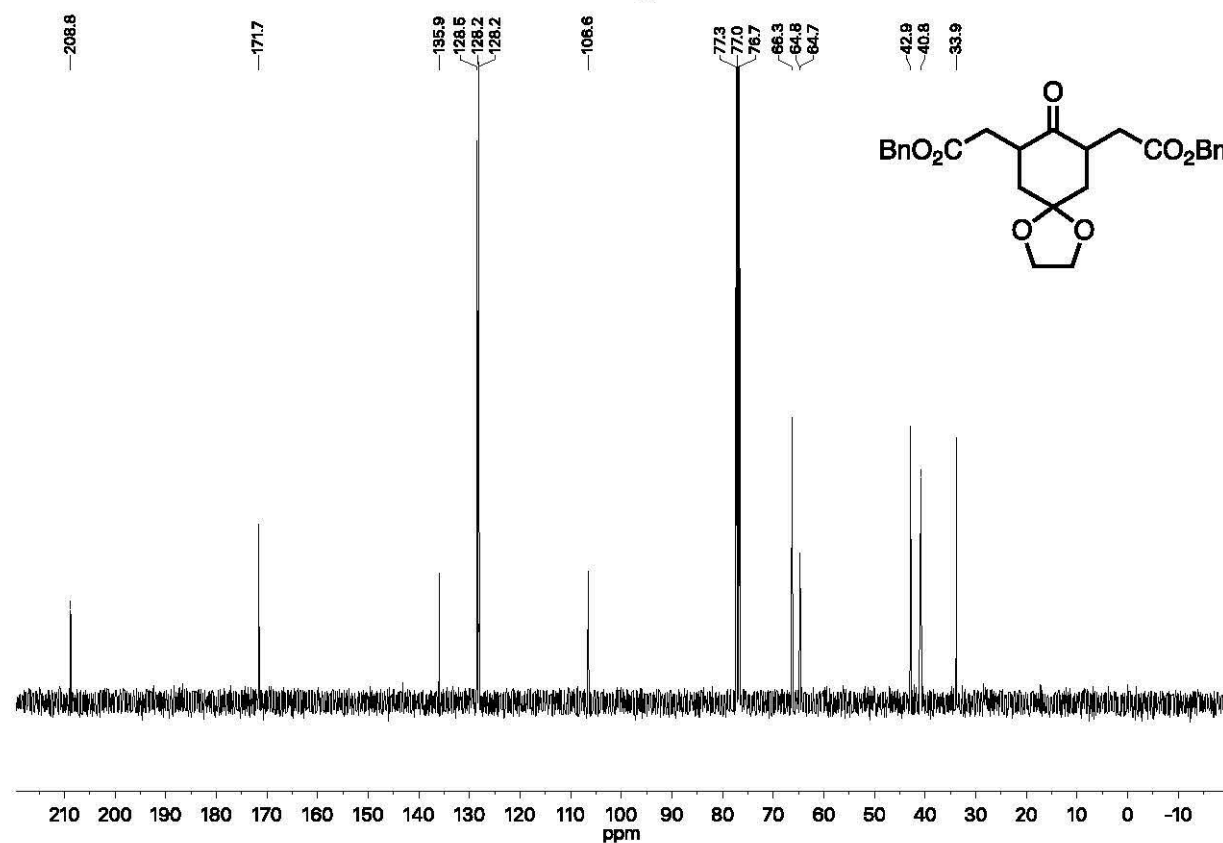
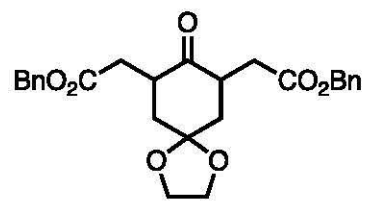
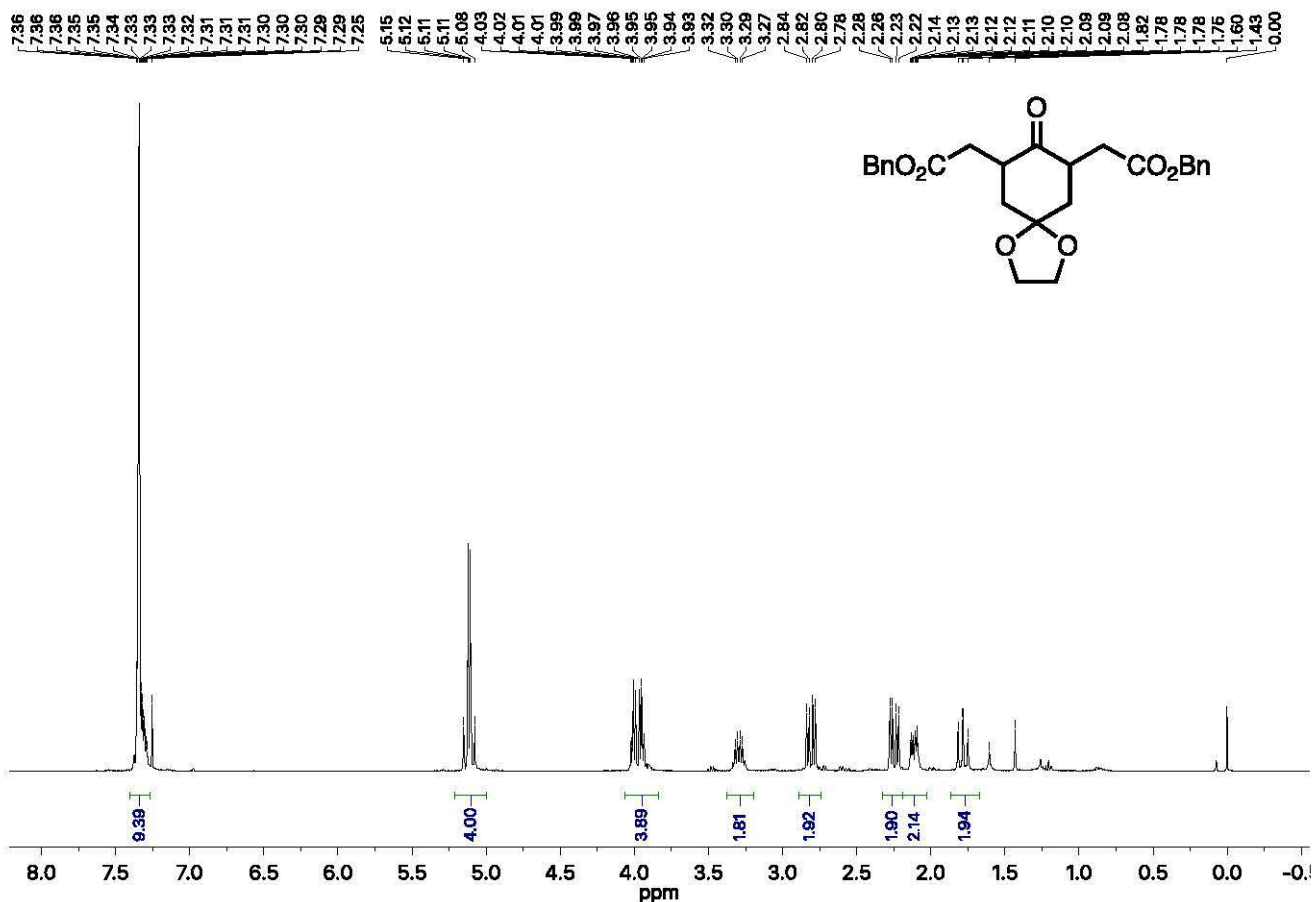
16) dibenzyl 2,2'-(1-(*tert*-butoxycarbonyl)-4-oxopiperidine-3,5-diyl)diacetate (10oo) + diastereoisomer



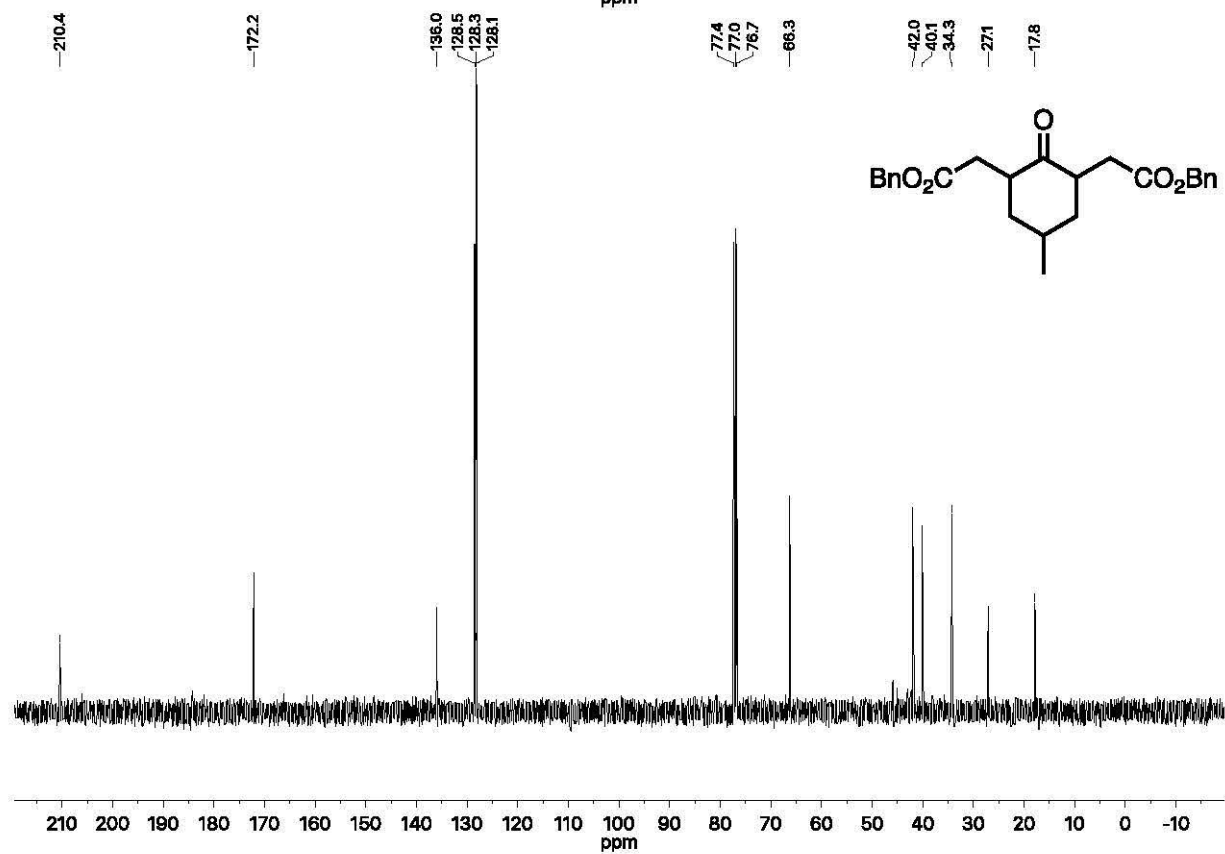
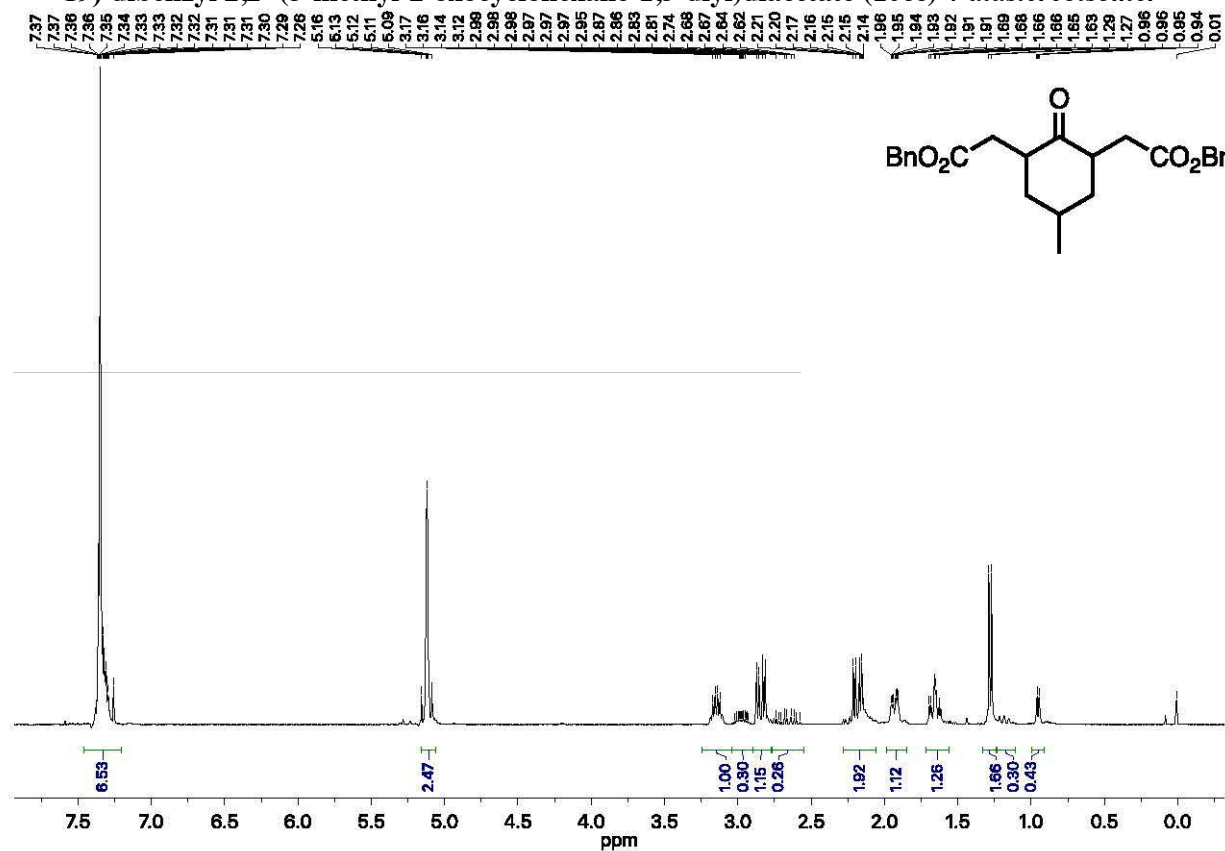
17) dibenzyl 2,2'-(1-methyl-4-oxopiperidine-3,5-diyl)diacetate (10ee)



18) dibenzyl 2,2'-(8-oxo-1,4-dioxaspiro[4.5]decane-7,9-diyl)diacetate (10ff) + diastereoisomer



19) dibenzyl 2,2'-(5-methyl-2-oxocyclohexane-1,3-diyl)diacetate (10c) + diastereoisomer



7. References

- ¹Turrini, N. G.; Cioc, R. C. Van der Niet, D. J. H.; Ruijter, E.; Orru, R. V. A.; Hall, M.; Faber, K. *Green Chem.* **2017**, *19*, 511.
- ²Esumi, N.; Suzuki, K., Nishimoto, Y.; Yasuda, M. *Org. Lett.* **2016**, *18*, 5704.
- ³ Osuka, A.; Maruyama, K. *J. Chem. Res.* **1987**, 2401.
- ⁴ Tomioka, H.; Itoh, M.; Yamakawa, S.; Izawa, Y. *J. Chem. Soc., Perkin Trans. 2*, **1980**, 603.
- ⁵Quimby, D. J.; Longo, F. R. *J. Am. Chem. Soc.* **1975**, *97*, 5111.
- ⁶ Vicente, M. G. H.; Neves, M. G. P. M. S.; Cavaleiro, J. A. S.; Hombrecher, H. K.; Koll, D. *Tetrahedron Letter*, **1996**, *37*, 261.
- ⁷ Kumar, P. H.; Venkatesh, Y.; Siva, D.; Ramakrishna, B., Bangal, P. R. *J. Phys. Chem. A* **2015**, *119*, 1267.
- ⁸ Ransdell, R. A., Wamser, C. C. *J. Phys. Chem.* **1992**, *96*, 10572.
- ⁹ Solvent and Substituent Effects on the Redox Potentials of Several Substituted Tetraphenylporphyrins Robert Arthur Ransdell *Portland State University* Follow this and additional works at: http://pdxscholar.library.pdx.edu/open_access_etds
- ¹⁰ A. Singh, A.; Johnson, L. W. *Spectrochim. Acta Part A* **2003**, *59*, 905.
- ¹¹ Buettner, G.R. *Free Radic. Biol. Med.* **1987**, *4*, 259.
- ¹² Dvoranová, D.; Barbieriková, Z.; Dorotíková, S.; Malček M.; Brincko A.; Rišpanová L.; Bučinský L.; Staško A.; Brezová V.; Rapta P. *J Solid State Electrochem* **2015**, *19*, 633.
- ¹³ Estimation because of low quality of graph.
- ¹⁴ Megerle, U.; Lechner, R.; König, B.; Riedle, E. *Photochem. Photobiol. Sci.* **2010**, *9*, 1400-1406.
- ¹⁵ Frisch M. J.; Trucks, G. W.; Schlegel, H. B.; Scuseria, G. E.; Robb, M. A.; Cheeseman, J. R.; Scalmani, G.; Barone, V.; Mennucci, B.; Petersson, G. A.; Nakatsuji, H.; Caricato, M.; Li, X.; Hratchian, H. P.; Izmaylov, A. F.; Bloino, J.; Zheng, G.; Sonnenberg, J. L.; Hada, M.; Ehara, M.; Toyota, K.; Fukuda, R.; Hasegawa, J.; Ishida, M.; Nakajima, T.; Honda, Y.; Kitao, O.; Nakai, H.; Vreven, T.; Montgomery, J. A.; Peralta, J. E.; Ogliaro, F.; Bearpark, M.; Heyd, J. J.; Brothers, E.; Kudin, K. N.; Staroverov, V. N.; Keith, T.; Kobayashi, R.; Normand, J.; Raghavachari, K.; Rendell, A.; Burant, J. C.; Iyengar, S. S.; Tomasi, J.; Cossi, M.; Rega, N.; Millam, J. M.; Klene, M.; Knox, J. E.; Cross, J. B.; Bakken, V.; Adamo, C.; Jaramillo, J.; Gomperts, R.; Stratmann, R. E.; Yazyev, O.; Austin, A. J.; Cammi, R.; Pomelli, C.; Ochterski, J. W.; Martin, R. L.; Morokuma, K.; Zakrzewski, V. G.; Voth, G. A.; Salvador, P.; Dannenberg, J. J.; Dapprich, S.; Daniels, A. D.; Farkas, O.; Foresman, J. B.; Ortiz, J. V.; Cioslowski, J.; Fox, D. J.; Gaussian, Inc., "Gaussian 09, Revision D.01", Wallingford CT, **2013**.
- ¹⁶ (a) Lee, C.; Yang, W.; Parr, R. G. *Phys. Rev. B: Condens. Matter Mater. Phys.* **1988**, *37*, 785. (b) Becke, A. D. *J. Chem. Phys.* **1993**, *98*, 5648.
- ¹⁷ Zhao Y.; Truhlar D.G. *Theor. Chem. Acc.* **2008**, *120*, 215.

Photocatalysis

Porphyrin-Catalyzed Photochemical C–H Arylation of Heteroarenes

Katarzyna Rybicka-Jasińska,^[a] Burkhard König,^[b] and Dorota Gryko^{*[a]}*Dedicated to the memory of Professor Teodor Silviu Balaban*

Abstract: Organic dyes are a promising class of photoredox catalysts and offer a meaningful alternative to broadly applied Ru and Ir complexes. We found that porphyrins with tuned physicochemical properties, by tailoring various substituents at the periphery of the macrocycle, are effective in catalyzing the

light-induced direct arylation of heteroarenes and coumarins with diazonium salts. Mechanistic studies confirmed that the reaction operates by an oxidative quenching pathway of the porphyrin.

DOI: 10.1002/ejoc.201601518

SUPPORTING INFORMATION

DOI: 10.1002/ejoc.201601518

Title: Porphyrin-Catalyzed Photochemical C–H Arylation of Heteroarenes

Author(s): Katarzyna Rybicka-Jasińska, Burkhard König, Dorota Gryko*

Table of Contents

1. General information	S3
2. General synthetic procedures	S3
3. Scope and limitations	S5
4. Optimization studies	S7
5. Mechanistic considerations	S9
5.1. Proposed mechanism	S9
5.2. Mass spectrometry studies	S9
5.3. Electrochemical data for porphyrins	S10
5.4. Stern–Volmer quenching experiments	S11
5.5. Quantum yield measurements	S16
6. ^1H and ^{13}C NMR spectra	S18
a) 2-(4-bromophenyl)furan (3)	S18
b) 2-(3-bromophenyl)furan (14)	S19
c) 2-(2-bromophenyl)furan (15)	S20
d) 2-(4-chlorophenyl)furan (16)	S21
e) 2-(4-iodophenyl)furan (17)	S22
f) 2-(4-nitrophenyl)furan (18)	S23
g) 2-(4-methoxyphenyl)furan (19)	S24
h) 2-(4-bromophenyl)thiophene (20)	S25
i) 2-(4-nitrophenyl)thiophene (21)	S26
j) <i>N-tert</i> -butoxycarbonyl-2-(4-nitrophenyl)-1H-pyrrole (24)	S27
k) 3-(4-bromophenyl)-2H-chromen-2-one (26)	S28
l) 3-(4-methoxyphenyl)-2H-chromen-2-one (27)	S39
7. References	S30

1. General Information

All solvents and chemicals used were of reagent grade and were used without further purification. High resolution ESI mass spectra were recorded on a Mariner or SYNAPT spectrometer. ^1H and ^{13}C NMR spectra were recorded at rt on Bruker 400 or Varian 600 MHz instruments with TMS as an internal standard. Thin layer chromatography (TLC) was performed using Merck Silica Gel GF254, 0.20 mm thickness. GC measurements were made on Gas Chromatograph Perkin Elmer Clarus 500.

Photo-induced reactions were performed using a photoreactor (blue LED, 455 nm).

2. General synthetic procedures

General procedure for arylation of furan:

A photocatalyst (1 mol%), diazonium salt (0.25 mmol, 1 equiv.) were placed in a vial with a septum, dissolved in dry DMSO, degassed followed by the addition of furan (10 equiv.). The reaction mixture was stirred under light irradiation for 3 h under argon atmosphere. The light was turned off, the reaction mixture was diluted with AcOEt and washed with water. The aqueous phase was extracted with AcOEt three times. Combined organic phases were washed with water and brine, dried over Na_2SO_4 , filtered, and concentrated. The crude product was purified by flash chromatography using silica gel (hexane/DCM).

General procedure for arylation of thiophene:

A photocatalyst (1 mol%), diazonium salt (0.25 mmol, 1 equiv.) were placed in a vial with a septum, dissolved in dry DMSO, degassed followed by the addition of thiophene (5 equiv.). The reaction mixture was stirred under light irradiation for 6 h under argon atmosphere. The light was turned off, the reaction mixture was diluted with AcOEt and washed with water. The aqueous phase was extracted with AcOEt three times. Combined organic phases were washed with water and brine, dried over Na_2SO_4 , filtered, and concentrated. The crude product was purified by flash chromatography using silica gel (hexane/DCM).

General procedure for arylation of coumarine and pyrrole derivatives:

A photocatalyst (1 mol%), diazonium salt (0.25 mmol, 1 equiv.) were placed in a vial with a septum, dissolved in dry DMSO, degassed followed by the addition of coumarine (5 equiv.) or pyrrole derivative (2 equiv.). The reaction mixture was stirred under light irradiation for 17 h under argon atmosphere. The light was turned off, the reaction mixture was diluted with AcOEt and washed with water. The aqueous phase was extracted with AcOEt three times. Combined organic phases were

washed with water and brine, dried over Na_2SO_4 , filtered, and concentrated. The crude product was purified by flash chromatography using silica gel (hexane/DCM).

3. Scope and limitations

Analytical data for compounds **3**¹, **14**², **15**³, **16**¹, **17**¹, **18**¹, **19**¹, **20**⁴, **21**⁴, **24**⁵, **26**⁶ and **27**⁶ are in agreement with the literature data.

a) **2-(4-bromophenyl)furan (3)** (white solid, 45 mg, 0.20 mmol, 81%)¹

¹H NMR (CDCl₃, 400 MHz) δ = 7.54-7.46 (m, 5H), 6.65-6.64 (dd, J = 3.4 Hz, J = 0.8 Hz, 1H), 6.47-6.46 (dd, J = 3.4 Hz, J = 1.8 Hz, 1H) ppm.

¹³C NMR (CDCl₃, 100 MHz) δ = 153.0, 142.4, 131.8, 129.8, 125.3, 124.1, 111.8, 105.5 ppm

b) **2-(3-bromophenyl)furan (14)** (white solid, 32 mg, 0.14 mmol, 58%)²

¹H NMR (CDCl₃, 400 MHz) δ = 7.83-7.82 (t, J = 1.8 Hz, 1H), 7.60-7.57 (m, 1H), 7.48-7.47 (dd, J = 1.8 Hz, J = 0.7 Hz, 1H), 7.48-7.47 (dq, J = 7.8 Hz, J = 1.1 Hz, 1H), 7.39-7.36 (dq, J = 7.9 Hz, J = 1.0 Hz, 1H), 7.24 (t, J = 7.8 Hz, 1H), 6.67-6.66 (dd, J = 3.4 Hz, J = 0.7 Hz, 1H), 6.48-6.47 (dd, J = 3.4 Hz, J = 1.8 Hz, 1H) ppm.

¹³C NMR (CDCl₃, 100 MHz) δ = 152.4, 142.6, 132.8, 130.2, 130.1, 126.7, 122.9, 122.3, 111.8, 106.1 ppm

c) **2-(2-bromophenyl)furan (15)** (white solid, 41 mg, 0.18 mmol, 73%)³

¹H NMR (CDCl₃, 400 MHz) δ = 7.81-7.78 (dd, J = 7.9 Hz, J = 1.6 Hz, 1H), 7.66-7.63 (dd, J = 8.0 Hz, J = 1.2, 1H), 7.53-7.52 (dd, J = 1.8 Hz, J = 0.7), 7.37-7.34 (ddd, J = 7.9 Hz, J = 7.4 Hz, J = 1.2, 1H), 7.17-7.10 (m, 2H), 6.53-6.52 (dd, J = 3.4 Hz, J = 1.8 Hz, 1H) ppm

¹³C NMR (CDCl₃, 100 MHz) δ = 151.4, 142.2, 134.1, 131.3, 128.2, 128.4, 127.4, 119.7, 111.4, 110.6, ppm.

d) **2-(4-chlorophenyl)furan (16)** (white solid, 32 mg, 0.17 mmol, 71%)¹

¹H NMR (CDCl₃, 400 MHz) δ = 7.60-7.58 (m, 2H), 7.47-7.46 (dd, J = 1.8 Hz, J = 0.7 Hz, 1H), 7.36-7.33 (m, 2H), 6.64-6.63 (dd, J = 3.4, J = 0.7 Hz, 1H), 6.47-6.46 (dd, J = 3.4 Hz, J = 1.8 Hz, 1H) ppm.

¹³C NMR (CDCl₃, 100 MHz) δ = 152.9, 142.3, 132.9, 129.4, 128.9, 125.0, 111.8, 105.4 ppm.

e) **2-(4-iodophenyl)furan (17)** (white solid, 42 mg, 0.16 mmol, 62%)¹

¹H NMR (CDCl₃, 400 MHz) δ = 7.72-7.69 (m, 2H), 7.47 (dd, J = 1.8 Hz, J = 0.7 Hz, 1H), 7.42-.39 (m, 2H), 6.66-6.65 (dd, J = 3.4 Hz, J = 0.7 Hz, 1H), 6.48-6.46 (dd, J = 3.4 Hz, J = 1.8 Hz, 1H) ppm.

¹³C NMR (CDCl₃, 100 MHz) δ = 153.0, 142.4, 137.7, 130.3, 125.5, 111.8, 105.7, 92.4 ppm.

f) **2-(4-nitrophenyl)furan (18)** (pale yellow solid, 37 mg, 0.20 mmol, 78%)¹

¹H NMR (CDCl₃, 400 MHz) δ = 8.25-8.22 (m, 2H), 7.80-7.76 (m, 2H), 7.57-7.56 (dd, J = 1.8 Hz, J = 0.6 Hz, 1H), 6.87-6.86 (dd, J = 3.5 Hz, J = 0.6 Hz, 1H), 6.55-6.54 (dd, J = 3.5 Hz, J = 1.8 Hz, 1H) ppm.

¹³C NMR (CDCl₃, 100 MHz) δ = 151.7, 146.4, 144.1, 134.4, 124.3, 123.9, 112.4, 108.9 ppm.

g) **2-(4-methoxyphenyl)furan (19)** (white solid, 18 mg, 0.1 mmol, 40%)¹

¹H NMR (CDCl₃, 400 MHz) δ = 7.61-7.59 (m, 2H), 7.42 (dd, J = 1.8 Hz, J = 0.8 Hz, 1H), 6.93-6.90 (m, 2H), 6.51-6.50 (dd, J = 3.3 Hz, J = 0.8 Hz, 1H), 6.44-6.43 (dd, J = 3.3, J = 1.8 Hz, 1H), 3.83 (s, 3H) ppm.

^{13}C NMR (CDCl_3 , 100 MHz) δ = 159.4, 154.1, 141.4, 125.2, 124.1, 114.1, 111.5, 103.4, 55.3 ppm.

h) **2-(4-bromophenyl)thiophene (20)** (white solid, 23 mg, 0.1 mmol, 38%)⁴

^1H NMR (CDCl_3 , 400 MHz) δ = 7.49-7.48 (m, 4H), 7.30-7.29 (m, 2H), 7.09-7.06 (m, 1H) ppm.

^{13}C NMR (CDCl_3 , 100 MHz) δ = 143.1, 133.4, 131.9, 128.2, 127.4, 125.2, 12.49, 121.3 ppm.

i) **2-(4-nitrophenyl)thiophene (21)** (pale yellow solid, 31 mg, 0.15 mmol, 60%)⁴

^1H NMR (CDCl_3 , 400 MHz) δ = 8.25-8.22 (m, 2H), 7.75-7.72 (m, 2H), 7.48-7.43 (m, 2H), 7.16-7.14 (dd, J = 3.7 Hz, J = 1.4 Hz, 1H) ppm.

^{13}C NMR (CDCl_3 , 100 MHz) δ = 141.6, 140.6, 128.7, 127.6, 126.8, 126.0, 125.7, 124.4 ppm.

j) ***N*-tert-butoxycarbonyl-2-(4-nitrophenyl)-1H-pyrrole (24)** (pale yellow solid, 21 mg, 29%)⁵

^1H NMR (CDCl_3 , 400 MHz) δ = 8.22-8.20 (m, 2H), 7.52-7.50 (m, 2H), 7.41-7.39 (dd, J = 3.3 Hz, J = 1.8 Hz, 1H), 6.32-6.31 (dd, J = 3.4 Hz, J = 1.8 Hz, 1H), 6.28-6.26 (app t, J = 3.3 Hz, 1H), 1.43 (s, 9H) ppm.

^{13}C NMR (CDCl_3 , 100 MHz) δ = 148.6, 146.3, 140.7, 132.8, 129.6, 124.3, 122.9, 116.5, 111.1, 84.5, 27.7 ppm.

k) **3-(4-bromophenyl)-2H-chromen-2-one (26)** (white solid, 55 mg, 0.18 mmol, 73%)⁶

^1H NMR (CDCl_3 , 400 MHz) δ = 7.81 (s, 1H), 7.61-7.52 (m, 6H), 7.37-7.26 (m, 2H) ppm.

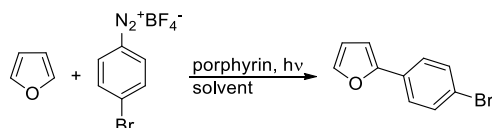
^{13}C NMR (CDCl_3 , 100 MHz) δ = 160.2, 153.6, 139.9, 133.6, 131.7, 131.7, 130.1, 127.9, 127.2, 124.6, 123.2, 119.5, 116.5 ppm.

l) **3-(4-methoxyphenyl)-2H-chromen-2-one (27)** (white solid, 45 mg, 0.17 mmol, 71%)⁵

^1H NMR (CDCl_3 , 400 MHz) δ = 7.76 (s, 1H), 7.69-7.67 (m, 2H), 7.54-7.49 (m, 2H), 7.37-7.27 (m, 2H), 6.99-6.69 (m, 2H), 3.85 (s, 3H) ppm.

^{13}C NMR (CDCl_3 , 100 MHz) δ = 160.5, 160.0, 153.5, 138.4, 130.9, 130.3, 129.8, 127.7, 127.1, 124.4, 119.9, 116.4, 113.9, 55.4 ppm.

4. Optimization studies



Background reactions:^[a]

No.	Furan [equiv.]	Solvent	Light	Time [h]	Photocatalyst	Catalyst loading [mol%]	Yield [%] ^[b]
1	10	DMSO_{dry}	+	3	H₂TPP (4)	1.0	80
2	10	DMSO _{dry}	-	16	-	-	5
3	10	DMSO _{dry}	+	3	-	-	8
4	10	DMSO _{dry}	+	16	-	-	23
5	10	DMSO _{dry}	-	16	H₂TPP (4)	1.0	6

[a] Reaction conditions: diazonium salt (**2**, 0.25 mmol, 1 equiv.), furan (**1**, 2.5 mmol, 10 equiv.), DMSO (2 mL), porphyrin (**4**, 1 mol%), blue LED (455 nm). [b] Yield determined by GC.

Time:^[a]

No.	Solvent	Time [h]	Photocatalyst	Catalyst loading [mol%]	Yield [%] ^a
1	DMSO _{dry}	4	H₂TPP (4)	1.0	78
2	DMSO_{dry}	3	H₂TPP (4)	1.0	80
3	DMSO _{dry}	2	H₂TPP (4)	1.0	79
4	DMSO _{dry}	1	H₂TPP (4)	1.0	74

[a] Reaction conditions: diazonium salt (**2**, 0.25 mmol, 1 equiv.), furan (**1**, 2.5 mmol, 10 equiv.), DMSO (2 mL), porphyrin (**4**, 1 mol%), blue LED (455 nm). [b] Yield determined by GC.

Photocatalyst:^[a]

No.	Solvent	Time [h]	Photocatalyst	Catalyst loading [mol%]	Yield [%] ^[b]
1	DMSO _{dry}	3	H ₂ T(<i>p</i> -OMeP)P (6)	1.0	41
2	DMSO _{dry}	3	H ₂ TPP (4)	1.0	80(80)
3	DMSO _{dry}	3	H ₂ T(<i>p</i> -COOMeP)P (7)	1.0	74
4	DMSO_{dry}	3	H₂T(F₅P)P (8)	1.0	86(81)
5	DMSO _{dry}	3	Octaethylporphyrin (9)	1.0	(72)

[a] Reaction conditions: diazonium salt (**2**, 0.25 mmol, 1 equiv.), furan (**1**, 2.5 mmol, 10 equiv.), DMSO (2 mL), porphyrin (1 mol%), blue LED (455 nm), 3h. [b] Yield determined by GC. () Isolated yield

Catalyst loading:^[a]

No.	Solvent	Time [h]	Photocatalyst	Catalyst loading [mol%]	Yield [%] ^[b]
1	DMSO _{dry}	3	H ₂ T(F ₅ P)P (8)	2.0	77
2	DMSO _{dry}	3	H ₂ T(F ₅ P)P (8)	1.5	78
3	DMSO _{dry}	3	H ₂ T(F ₅ P)P (8)	1.0	80
4	DMSO _{dry}	3	H ₂ T(F ₅ P)P (8)	0.8	71
5	DMSO _{dry}	3	H ₂ T(F ₅ P)P (8)	0.6	47
6	DMSO _{dry}	3	H ₂ T(F ₅ P)P (8)	0.1	42

[a] Reaction conditions: diazonium salt (**2**, 0.25 mmol, 1 equiv.), furan (**1**, 2.5 mmol, 10 equiv.), DMSO (2 mL), porphyrin (**8**, 0.1 – 2.0 mol%), blue LED (455 nm), 3h. [b] Yield determined by GC.

Solvent:^[a]

No.	Solvent	Time [h]	Photocatalyst	Catalyst loading [mol%]	Yield [%] ^[b]
1	DMSO _{dry}	3h	H ₂ T(F ₅ P)P (8)	1.0	86(81)
2	DMSO	3h	H ₂ T(F ₅ P)P (8)	1.0	76
3	DMF _{dry}	3h	H ₂ T(F ₅ P)P (8)	1.0	39
4	DMF	3h	H ₂ T(F ₅ P)P (8)	1.0	36
5	DCM _{dry}	3h	H ₂ T(F ₅ P)P (8)	1.0	3
6	MeOH _{dry}	3h	H ₂ T(F ₅ P)P (8)	1.0	47

[a] Reaction conditions: diazonium salt (**2**, 0.25 mmol, 1 equiv.), furan (**1**, 2.5 mmol, 10 equiv.), DMSO (2 mL), porphyrin (1 mol%), blue LED (455 nm), 3h. [b] Yield determined by GC. () Isolated yield

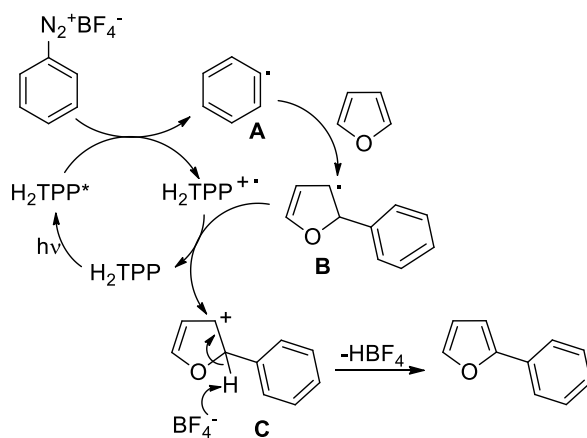
Furan equiv:^[a]

No.	Furan [equiv.]	Solvent	Time [h]	Photocatalyst	Catalyst loading [mol%]	Yield [%] ^[b]
1	15	DMSO _{dry}	3h	H ₂ T(F ₅ P)P (8)	1.0	71
2	10	DMSO _{dry}	3h	H ₂ T(F ₅ P)P (8)	1.0	80
3	5	DMSO _{dry}	3h	H ₂ T(F ₅ P)P (8)	1.0	76
4	2.5	DMSO _{dry}	3h	H ₂ T(F ₅ P)P (8)	1.0	40

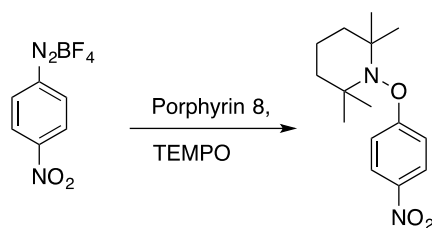
[a] Reaction conditions: diazonium salt (**2**, 0.25 mmol, 1equiv.), furan (**1**, 2.5 mmol, 10 equiv.), DMSO (2 mL), porphyrin (**8**, 1 mol%), blue LED (455 nm), 3h. [b] Isolated yield.

5. Mechanistic considerations:

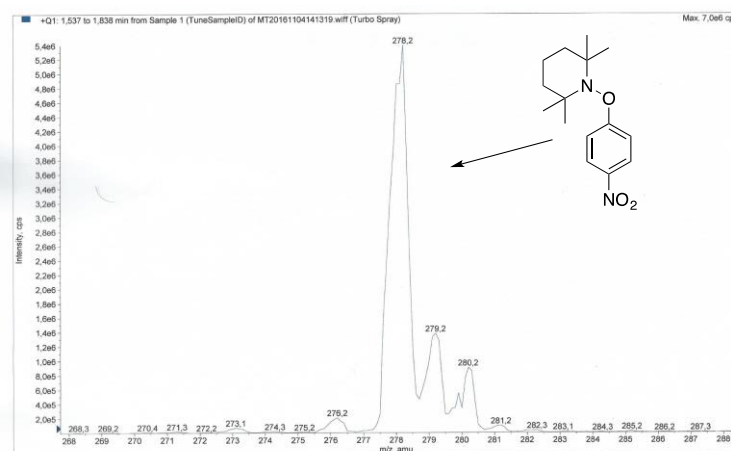
5.1. Proposed Mechanism



5.2. Mass spectrometry studies



Reaction conditions: diazonium salt (**2**, 0.25 mmol), DMSO (2 mL), H₂T(F₅)P (**8**, 1 mol%), blue LED (455 nm), after 60 min. of stirring under light irradiation (blue LED, 455 nm), TEMPO as a radical scavenger was added. After another 30 min. of stirring under light irradiation (blue LED, 455 nm) MS spectra was recorded.



5.3. Electrochemical data for porphyrins

Summary of selected measured potentials

No	Porphyrin	Solution	electrode	cell	red.(V)	ox.(V)
1	none	DMSO	GCE	regular	range: 0.0 ~ -2.3	range: 0.0 ~ 1.3
2	H ₂ TPP, 4	DMSO	GCE	regular	-1.03, -1.45	1.03
3	none	DMSO	Pt	regular	range: 0.0 ~ -2.0	range: 0.0 ~ 1.1
4	H ₂ TPP, 4	DMSO	Pt	regular	-1.04, -1.46	--

m) Electrochemical data for porphyrins

Porphyrin	E_{ox}	E_{red}	E_{ox}^{*s}	E_{ox}^{*t}	E_{red}^{*s}	E_{red}^{*t}	E_{00}^s	E_{00}^t
H₂TPP	1.03	-1.03; -1.43	-0.91	-0.42	0.91	0.42	1.90	1.45 ⁷
H₂T(<i>p</i>-OMeP)P	0.91	-1.07; -1.46	-0.99	-0.54	0.83	0.38	1.90 ⁸	1.45 ⁸
H₂T(F₅P)P	0.89; 1.23 ⁹	-1.28; -1.71 ⁹	-1.04	-0.78	0.65	0.39	1.93 ¹⁰	1.67

E_{red}/E_{ox} vs SCE

5.4. Stern–Volmer quenching experiments

a) Porphyrin 4

Stern–Volmer analyses clearly showed that 4-bromobenzenediazonium tetrafluoroborate (**2**) strongly quenched the luminescence of H₂TPP (**4**) in comparison with furan (**1**). For furan (**1**) and 4-bromobenzenediazonium (**2**) and H₂TPP (**4**) samples were prepared by adding solutions of substrates to H₂TPP (**4**) solution in DMSO (total volume 2 mL) and degassed with N₂. The concentration of H₂TPP (**4**) in DMSO was $7.2 \cdot 10^{-5}$ M. Samples were irradiated at 420 nm, and emission of porphyrin **4** was detected at 651 nm.

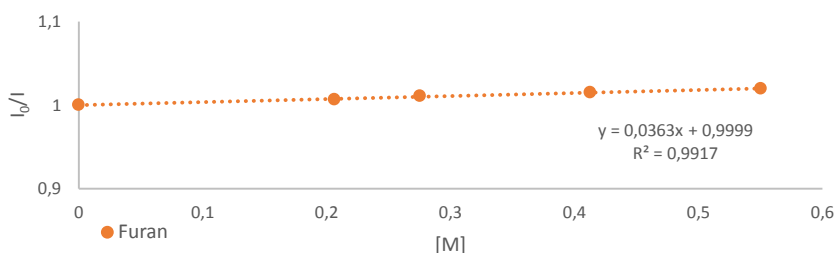


Fig. 1. Stern–Volmer quenching experiment for furan (**1**).

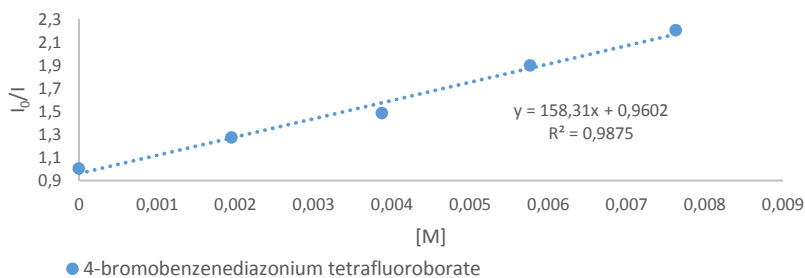


Fig. 2. Stern–Volmer quenching experiment for 4-bromobenzenediazonium tetrafluoroborate (**2**).

Stern–Volmer quenching rate data:

Rates of quenching (k_q) were determined using Stern–Volmer kinetics:

$$\frac{I_0}{I} = 1 + k_q \cdot \tau_0 \cdot [\text{quencher}]$$

Where I_0 - the luminescence intensity without the quencher,

I - the intensity with the quencher,

τ_0 - the lifetime of the photocatalyst (for TPP is 9,95 ns)

4-bromobenzenediazonium tetrafluoroborate (**2**): $k_q = 1,5 \cdot 10^{10} [M^{-1}s^{-1}]$

b) Porphyrin 8

Stern-Volmer analyses clearly showed that 4-bromobenzenediazonium tetrafluoroborate (**2**) strongly quenched the luminescence of porphyrin **8** in comparison with furan (**1**). For furan (**1**), 4-bromobenzenediazonium and porphyrin **8** samples were prepared by adding solutions of substrates to porphyrin **8** solution in DMSO (total volume 2 mL) and degassed with N₂. The concentration of porphyrin **8** in DMSO was $7.2 \cdot 10^{-5}$ M. Samples were irradiated at 411 nm, and emission of porphyrin **8** was detected at 636 nm.

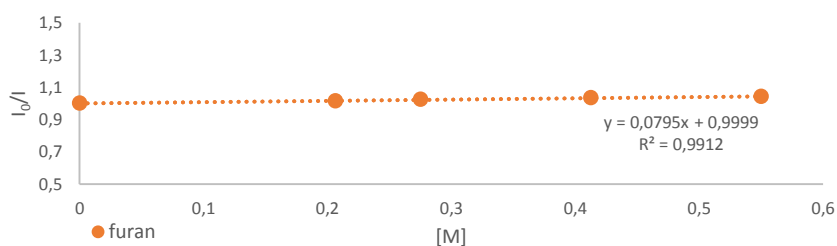


Fig. 3. Stern–Volmer quenching experiment for furan (**1**).

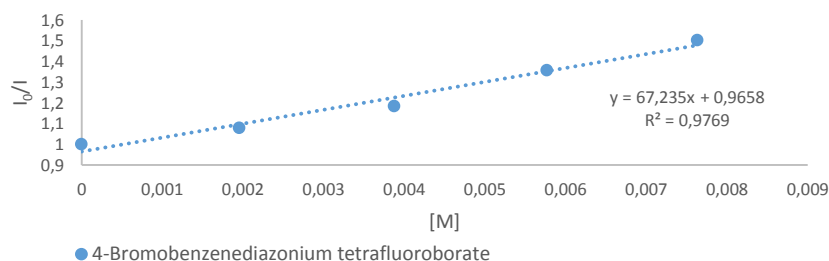


Fig. 4. Stern–Volmer quenching experiment for 4-bromobenzenediazonium tetrafluoroborate (**2**).

Stern–Volmer quenching rate data:

Rates of quenching (k_q) were determined using Stern–Volmer kinetics:

$$\frac{I_0}{I} = 1 + k_q \cdot \tau_0 \cdot [\text{quencher}]$$

Where I_0 - the luminescence intensity without the quencher,

I - the intensity with the quencher,

τ_0 - the lifetime of the photocatalyst (for porphyrin **8** is 8.6 ns)

4-bromobenzenediazonium tetrafluoroborate (**2**): $k_q = 7.02 \cdot 10^9 [M^{-1}s^{-1}]$

c) Porphyrin 6

Stern-Volmer analyses clearly showed that 4-bromobenzenediazonium tetrafluoroborate (**2**) strongly quenched the luminescence of porphyrin **6** in comparison with furan (**1**). For furan (**1**), 4-bromobenzenediazonium (**2**) and porphyrin **6** samples were prepared by adding solutions of substrates to porphyrin **6** solution in DMSO (total volume 2 mL) and degassed with N₂. The concentration of porphyrin **6** in DMSO was $7.2 \cdot 10^{-5}$ M. Samples were irradiated at 420 nm, and emission of porphyrin **6** was detected at 651 nm.

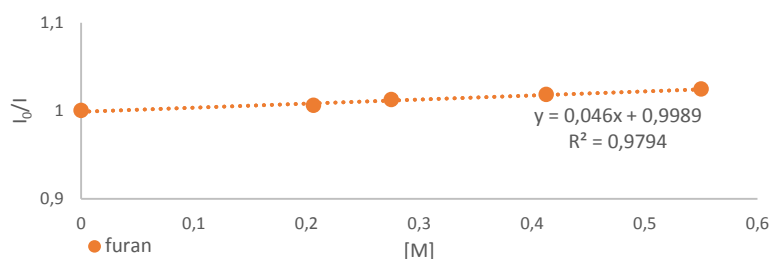


Fig. 1. Stern–Volmer quenching experiment for furan (**1**)

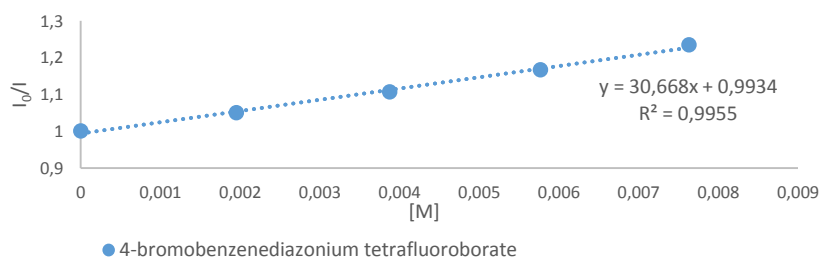


Fig. 2. Stern–Volmer quenching experiment for 4-bromobenzenediazonium tetrafluoroborate (**2**)

Stern–Volmer quenching rate data:

Rates of quenching (k_q) were determined using Stern–Volmer kinetics:

$$\frac{I_0}{I} = 1 + k_q \cdot \tau_0 \cdot [\text{quencher}]$$

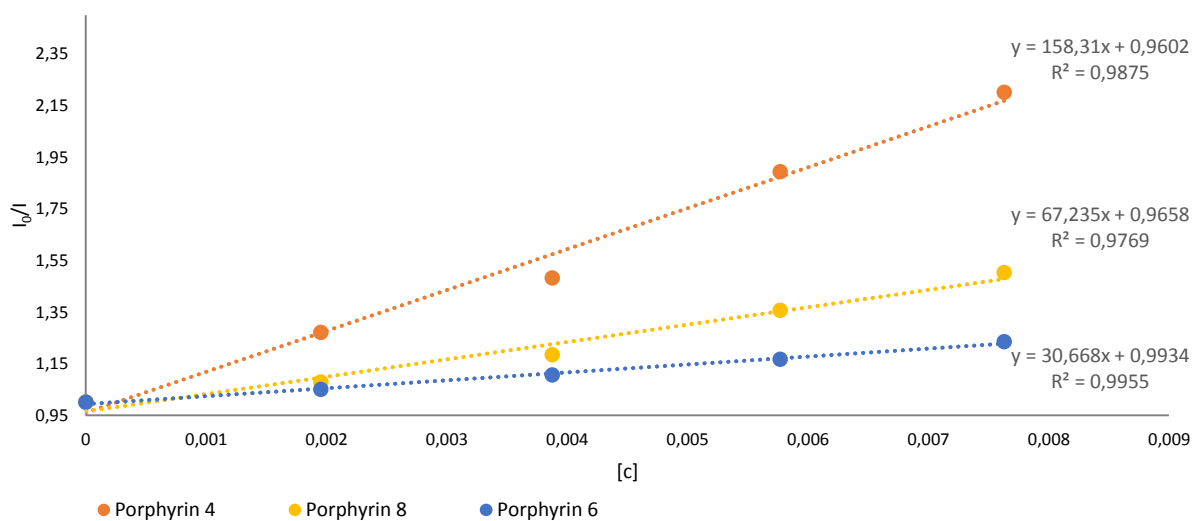
Where I_0 - the luminescence intensity without the quencher,

I - the intensity with the quencher,

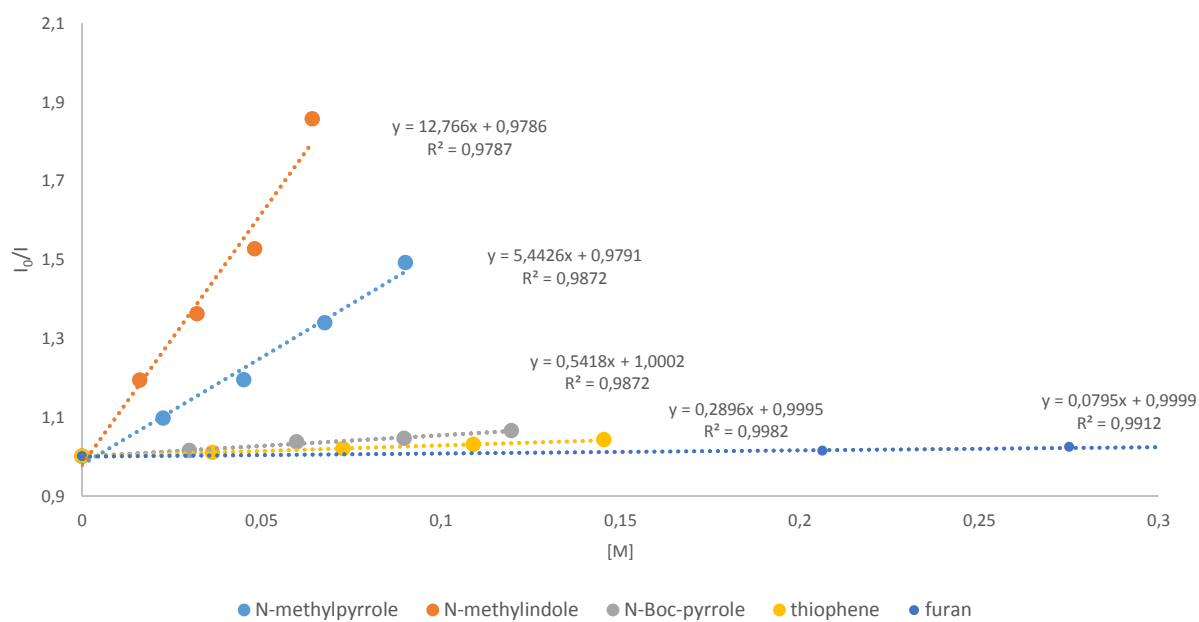
τ_0 - the lifetime of the photocatalyst (for porphyrin **6** is 10.1 ns)

4-bromobenzenediazonium tetrafluoroborate (**2**): $k_q = 2.9 \cdot 10^9 [M^{-1}s^{-1}]$

d) Stern–Volmer quenching experiments for diazonium salt 2 – comparison of catalysts used:



e) Stern–Volmer quenching experiments for porphyrin 8 – comparison of heteroarenes used:



Stern–Volmer quenching rate data:

Rates of quenching (k_q) were determined using Stern–Volmer kinetics:

$$\frac{I_0}{I} = 1 + k_q \cdot \tau_0 \cdot [\text{quencher}]$$

Where I_0 - the luminescence intensity without the quencher,

I - the intensity with the quencher,

τ_0 - the lifetime of the photocatalyst (for porphyrin **8** is 8.6 ns)

N-Methylpyrrole (**11**): $k_q = 9.8 \cdot 10^8 [M^{-1}s^{-1}]$

N-Methylindole (**12**): $k_q = 1.4 \cdot 10^8 [M^{-1}s^{-1}]$

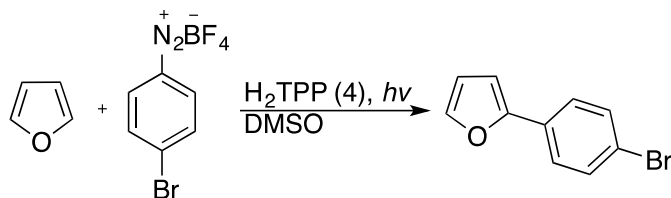
N-Boc-pyrrole (**13**): $k_q = 6.8 \cdot 10^7 [M^{-1}s^{-1}]$

Thiophene (**10**): $k_q = 2.2 \cdot 10^7 [M^{-1}s^{-1}]$

Furan (**1**): $k_q = 6.9 \cdot 10^6 [M^{-1}s^{-1}]$

5.5. Quantum yield measurements

The quantum yield was measured with a quantum yield determination setup: translation stages (horizontal and vertical): Thorlabs DT 25/M or DT S25/M; photographic lens with $f = 50$ mm; magnetic stirrer: Faulhaber motor (1524B024S R) with 14:1 gear (15A); PS19Q power sensor from Coherent; PowerMax software; adjustable power supply "Basetech BT-153 0–15 V/DC 0–3 A 45 W"¹¹



A typical reaction mixture of diazonium salt (**2**) (0.2 mmol, 1 equiv.), furane (**1**, 2 mmol, 10 equiv.), H₂TPP (**4**) (1 mol%), DMSO (2.0 mL) in a 10 mm Hellma^R quartz fluorescence cuvette with a stirring bar was used. The measurement of quantum yield was accomplished in covered apparatus to minimize the ambient light. The cuvette with solvent (DMSO, 2.0 mL) and a stirring bar was placed in the beam of a 420 nm LED and the transmitted power ($P_{ref} = 18,46$ mW) was measured by a calibrated photodiode horizontal to the cuvette. The content of the cuvette was changed to the reaction mixture and the transmitted power was measured analogously to the blank solution. The sample was further irradiated and the transmitted power as well as the respective yield of photocatalytic product (measured by quantitative GC using dodekane as internal standard) were recorded after different times (Table 1).

The quantum yield was calculated from equation E1:

$$\Phi\Phi\phi = \frac{N_{product}}{N_{ph}} = \frac{N_A \cdot n_{product}}{\frac{E_{light}}{E_{ph}}} = \frac{N_A \cdot n_{product}}{\frac{P_{absorbed} \cdot t}{\frac{h \cdot c}{\lambda}}} = \frac{h \cdot c \cdot N_A \cdot n_{product}}{\lambda \cdot (P_{ref} - P_{sample}) \cdot t}$$

where Φ - the quantum yield,

$N_{product}$ - the number of molecules created

N_{ph} - the number of photons absorber

N_A - Avogadro's constant [mol^{-1}],

$n_{product}$ - is the molar amount of molecules created [mol],

E_{light} - the energy of light absorbed [J],

E_{ph} - the energy of a single photon [J],

$P_{absorbed}$ - the radiant power absorbed [W],

t - the irradiation time [s],

h - the Planck's constant in [Jxs],

c - the speed of light in [ms^{-1}],

λ - the wavelength of irradiation source (420 nm) [m],

P_{ref} - the radiant power transmitted by a blank vial [W],

P_{sample} - the radiant power transmitted by the vial with reaction mixture [W].

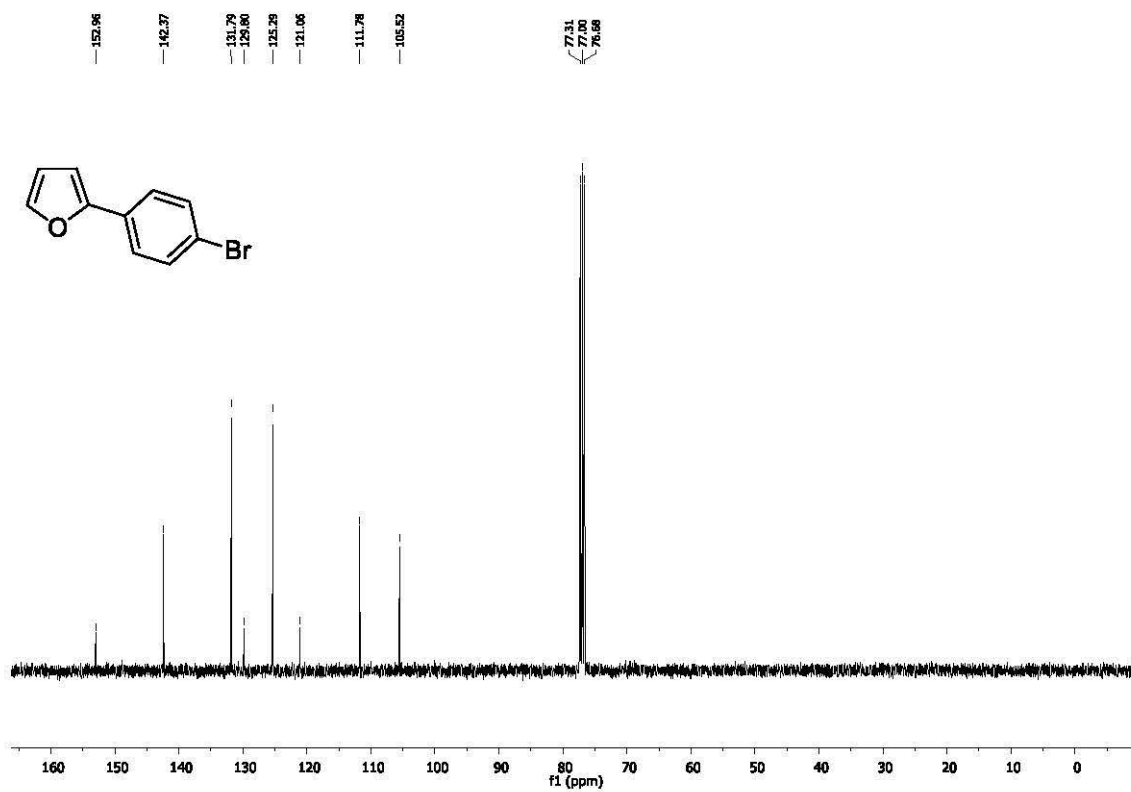
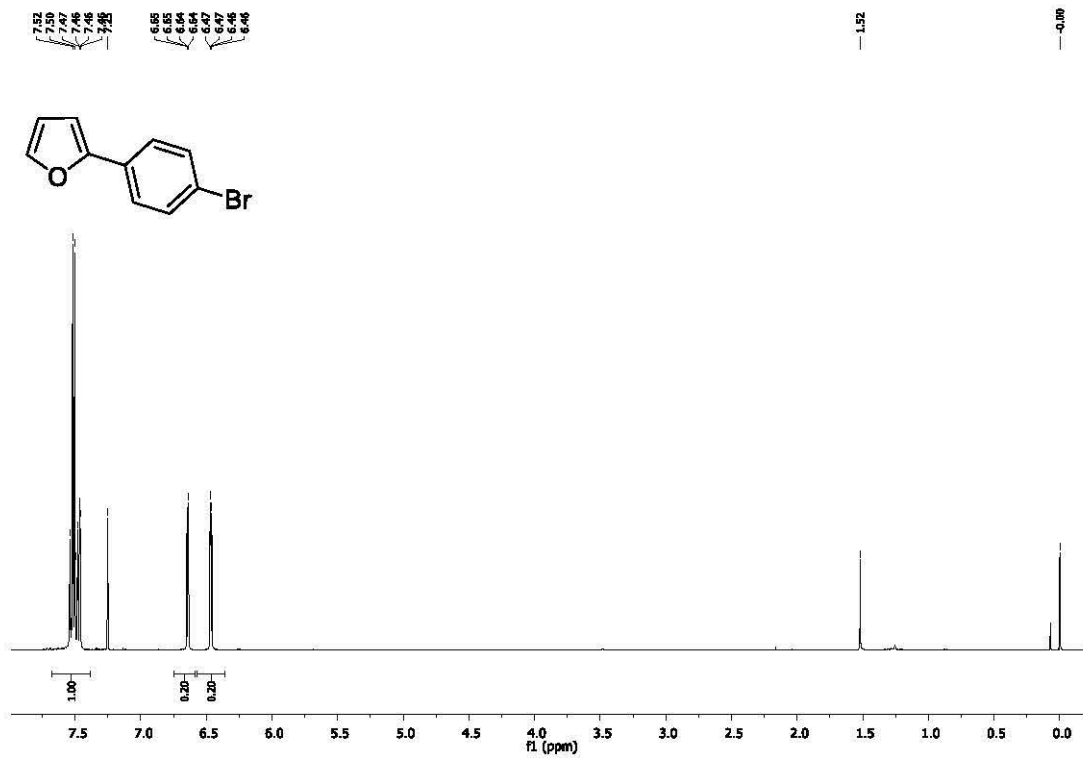
Table 1: Calculation of the quantum yield Φ after different irradiation times.

Entry	Irradiation time [min]	P_{sample} [μW]	Yield [%]	Φ [%]
1	150	7.56	88	0.6
2	60	6.90	79	1.4
3	30	6.89	67	2.3

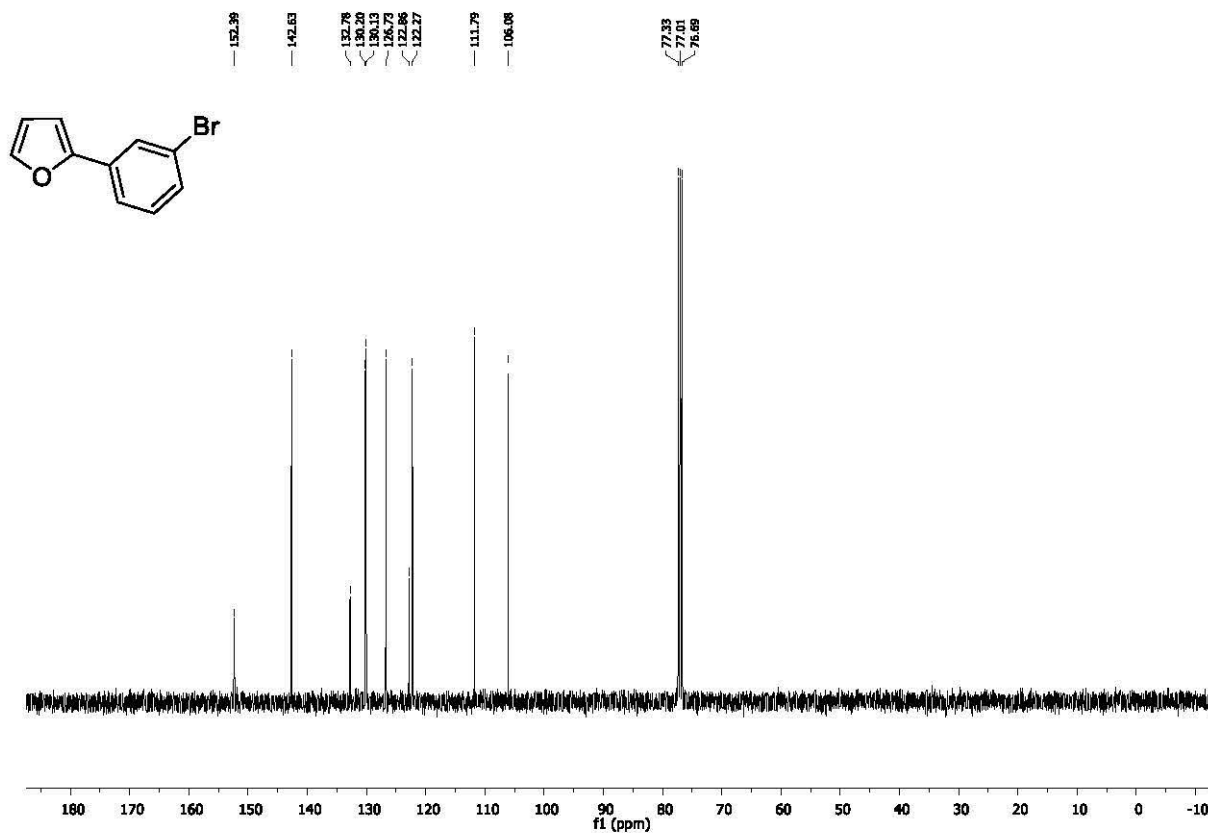
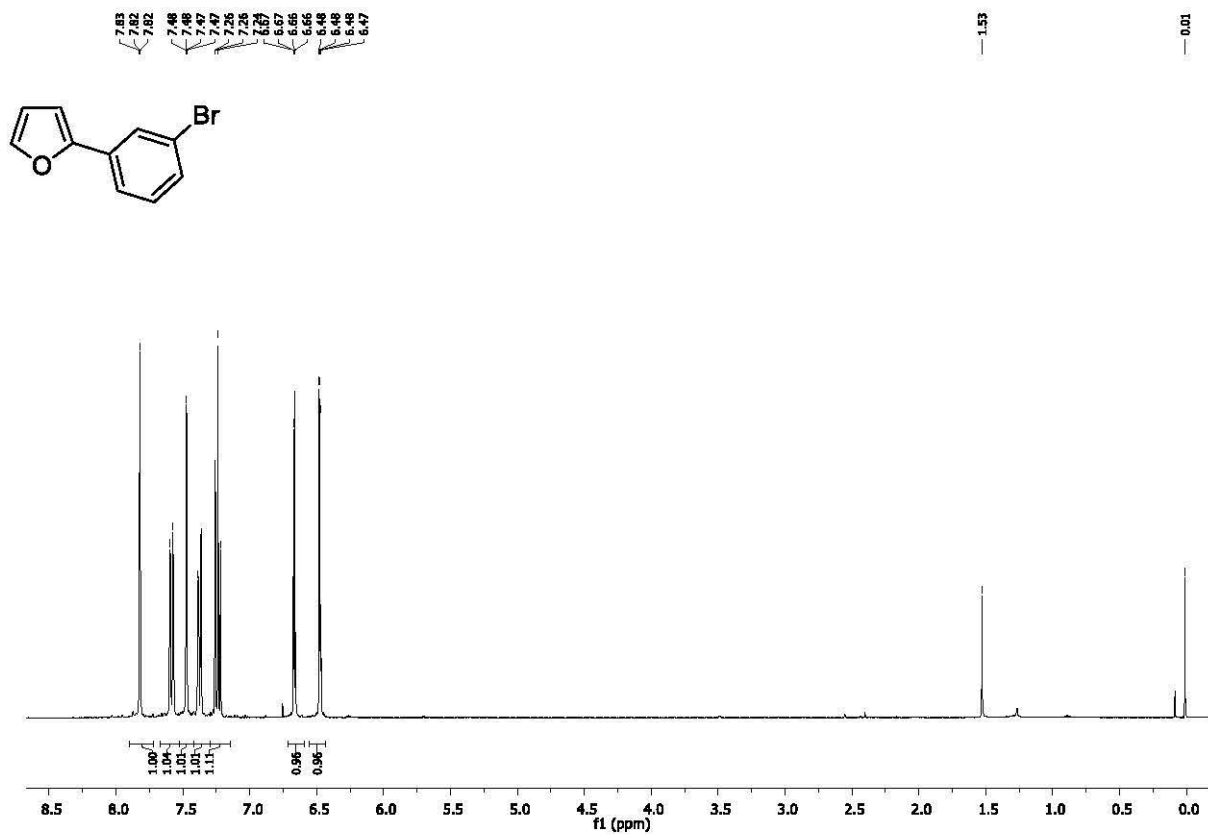
The mean value for the quantum yield was calculated to be $\Phi = 1.4 \pm 0.8 \%$

6. ^1H and ^{13}C NMR spectra

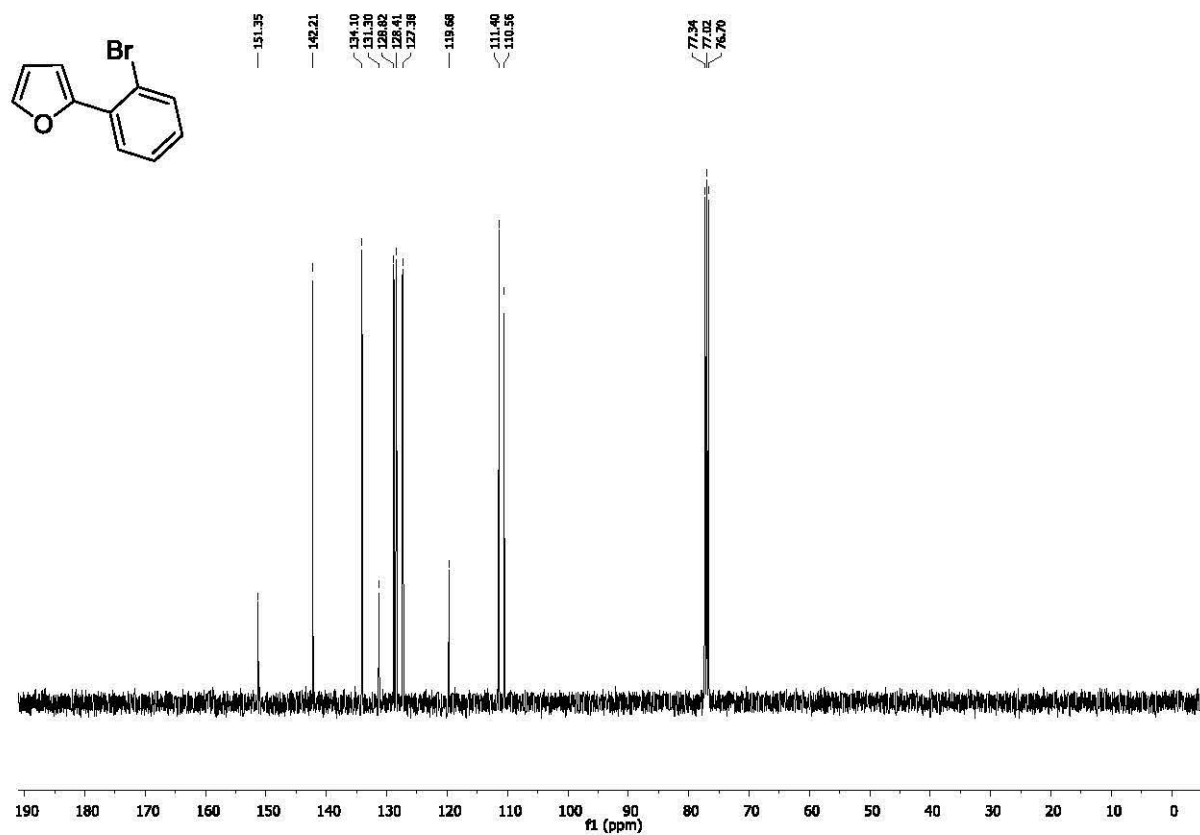
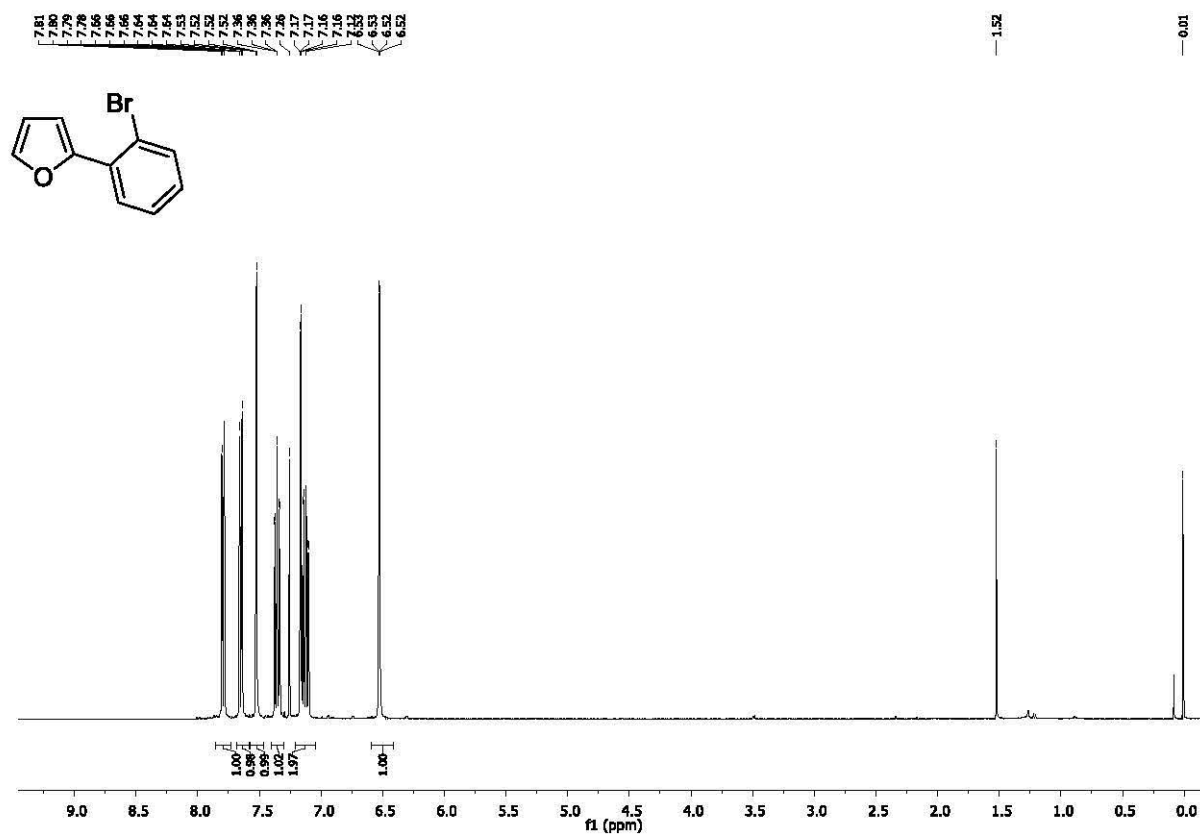
a) 2-(4-bromophenyl)furan (3)



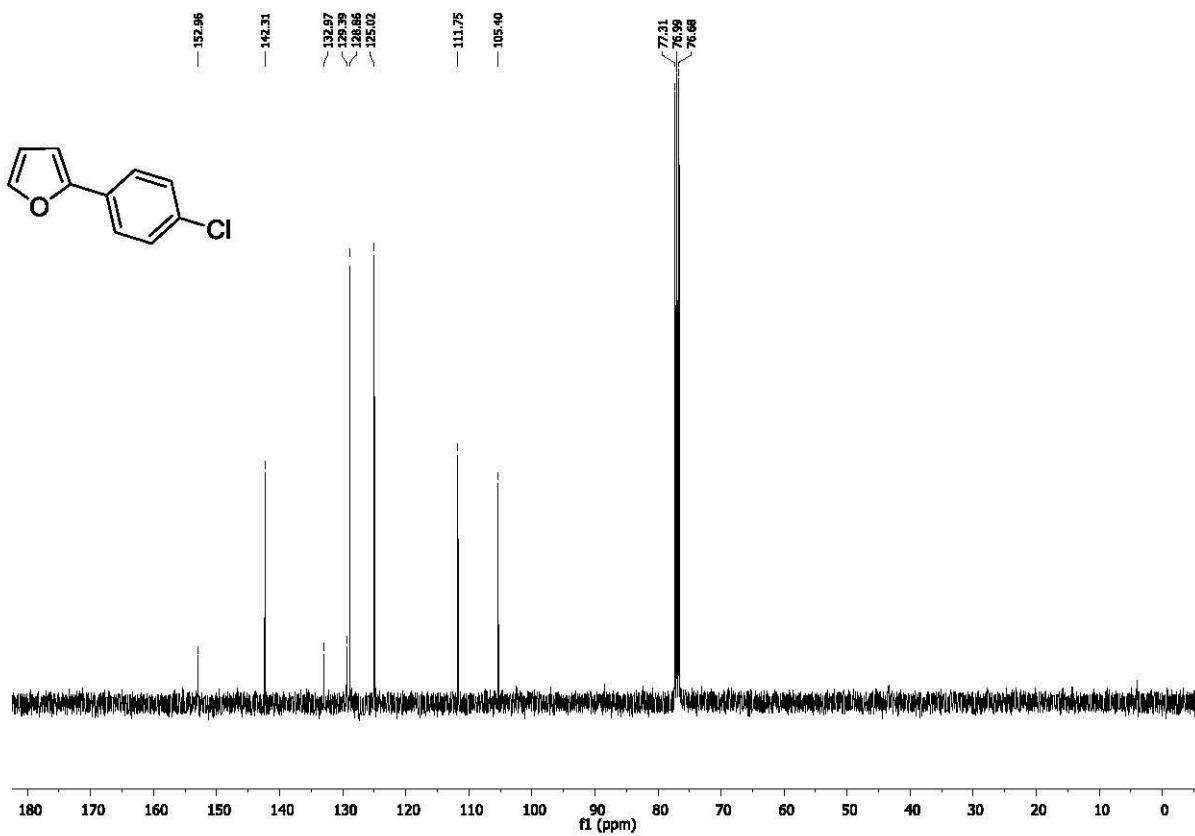
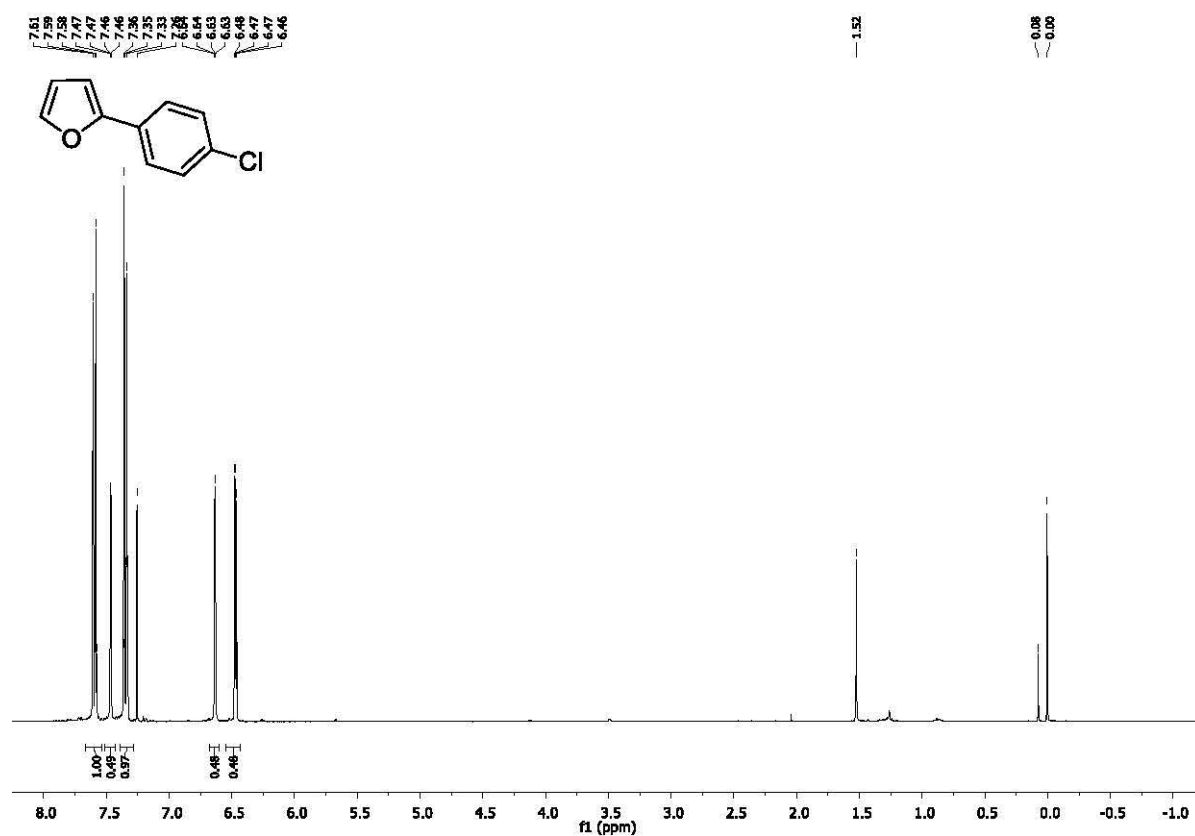
b) 2-(3-bromophenyl)furan (14)



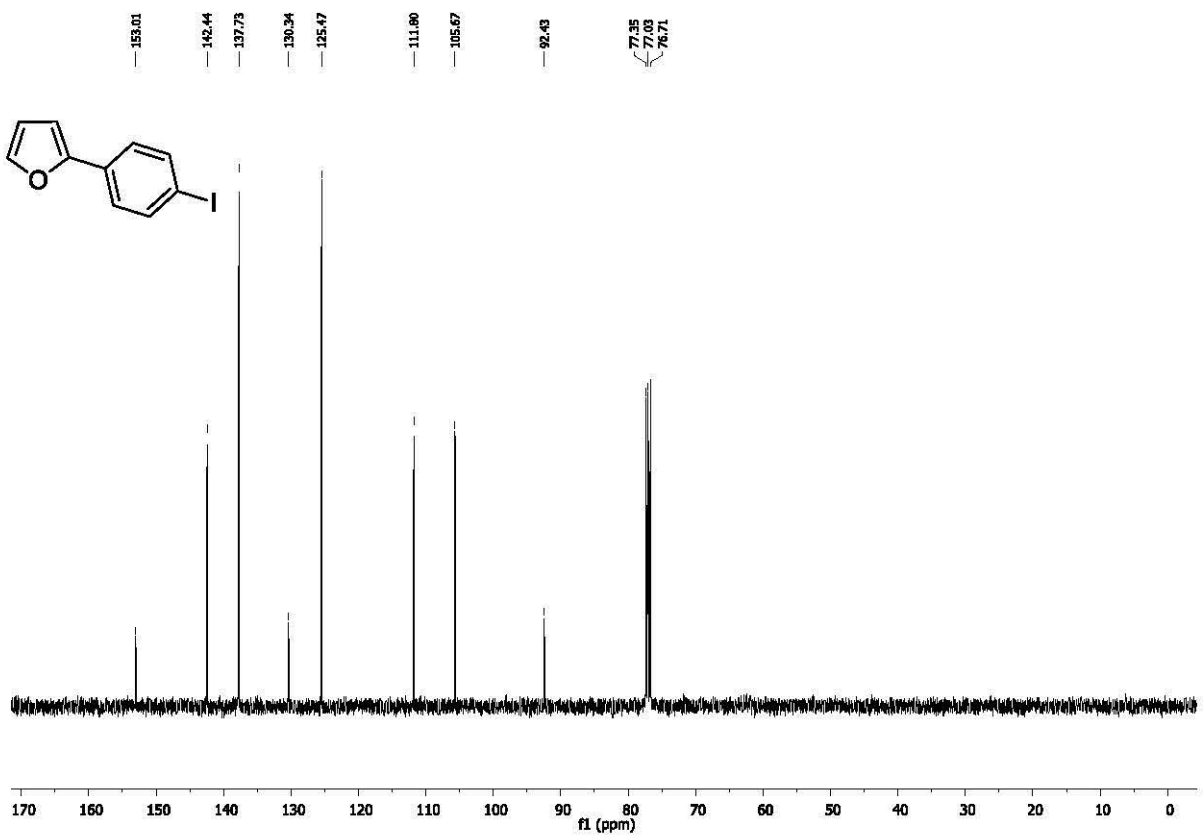
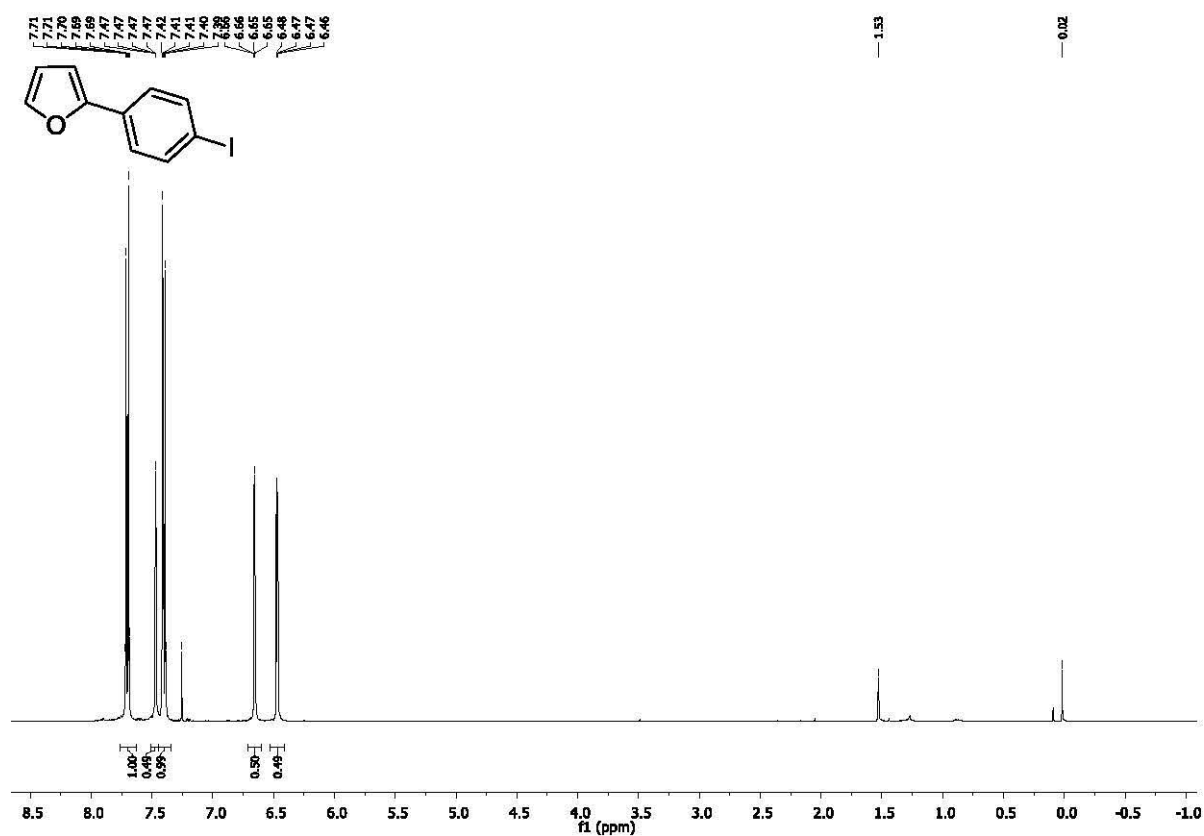
c) 2-(2-bromophenyl)furan (15)



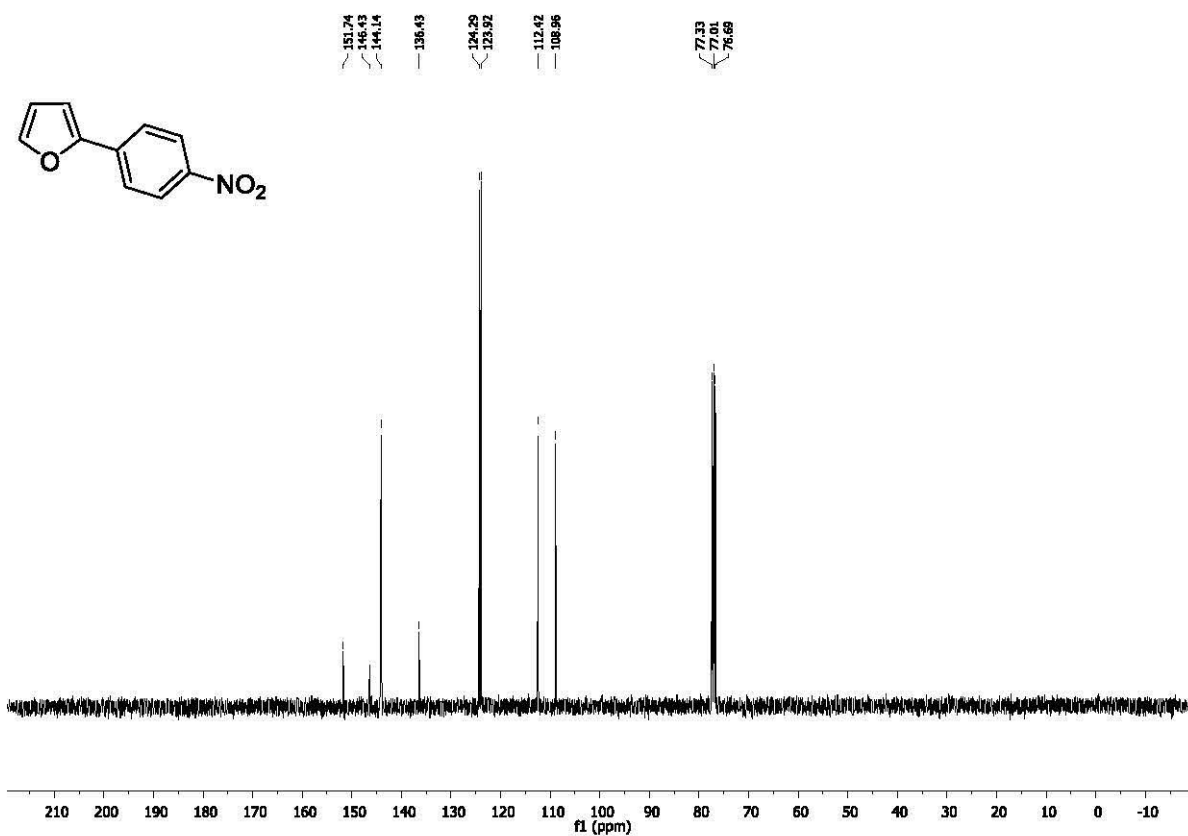
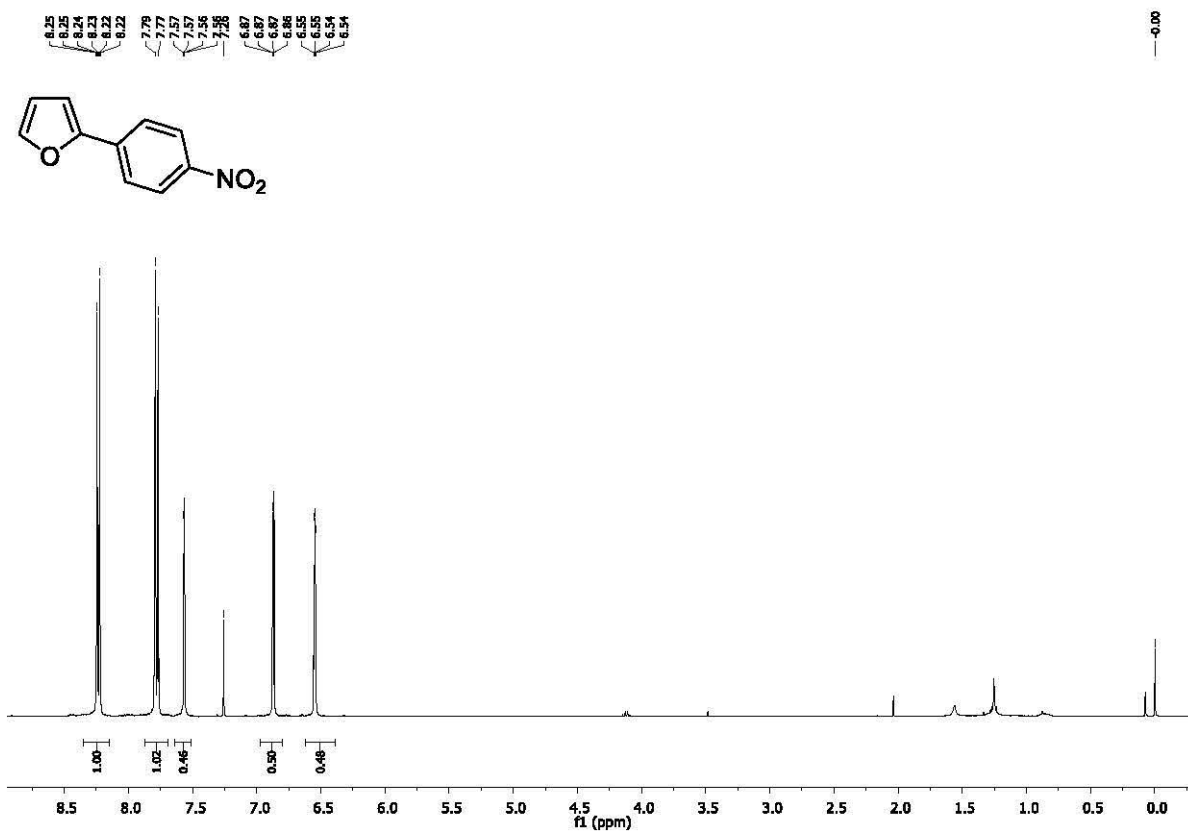
d) 2-(4-chlorophenyl)furan (16)



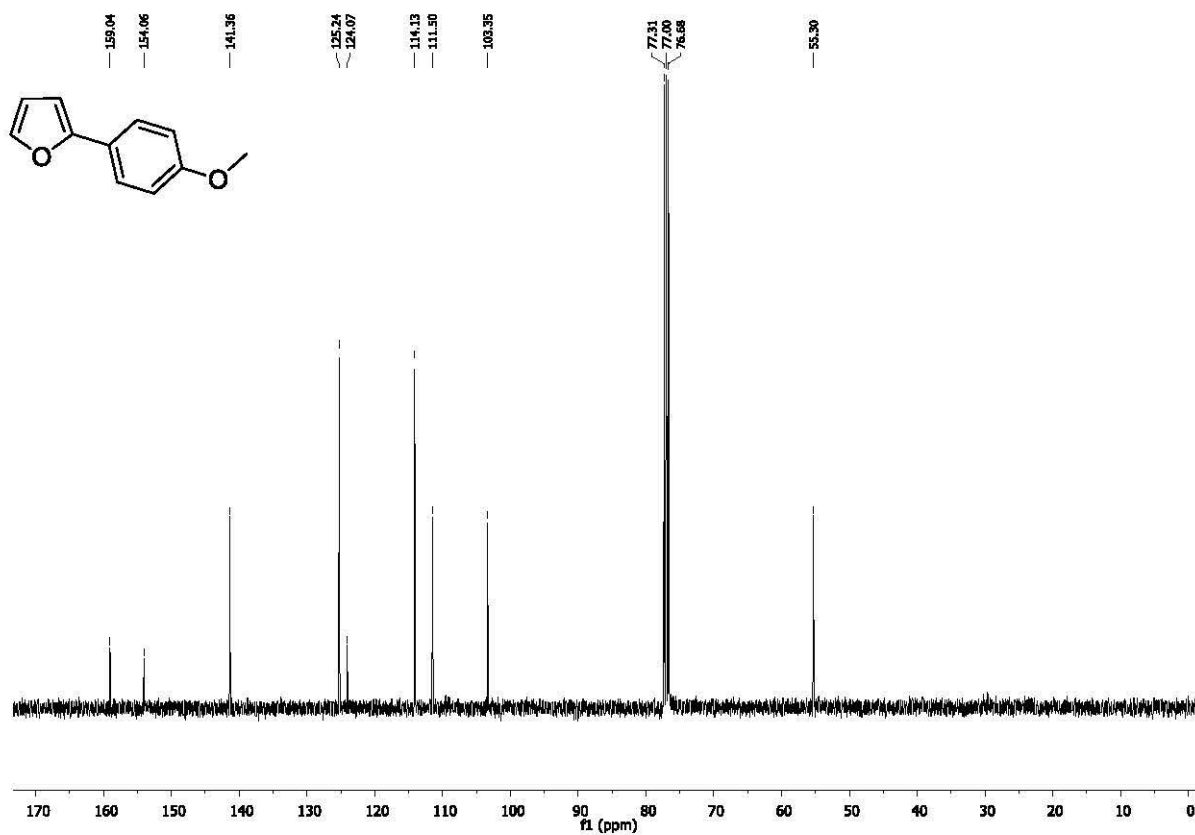
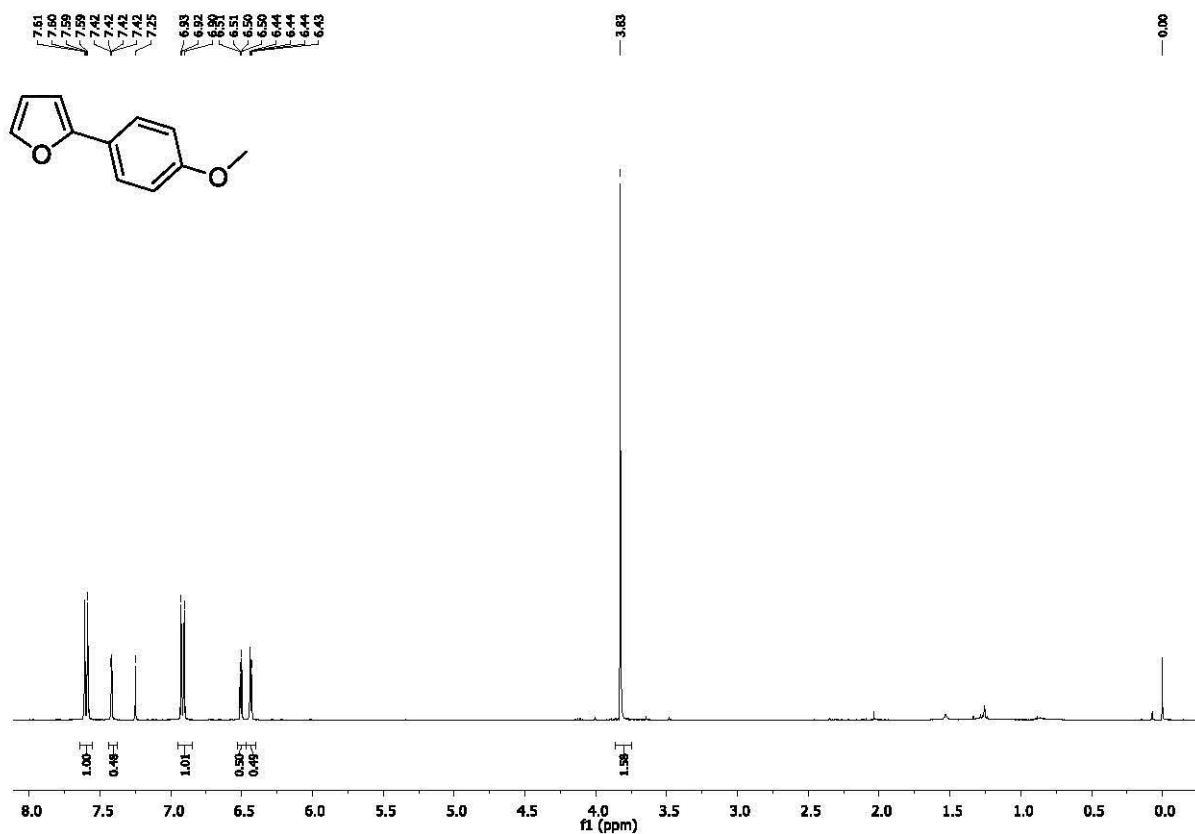
e) 2-(4-iodophenyl)furan (17)



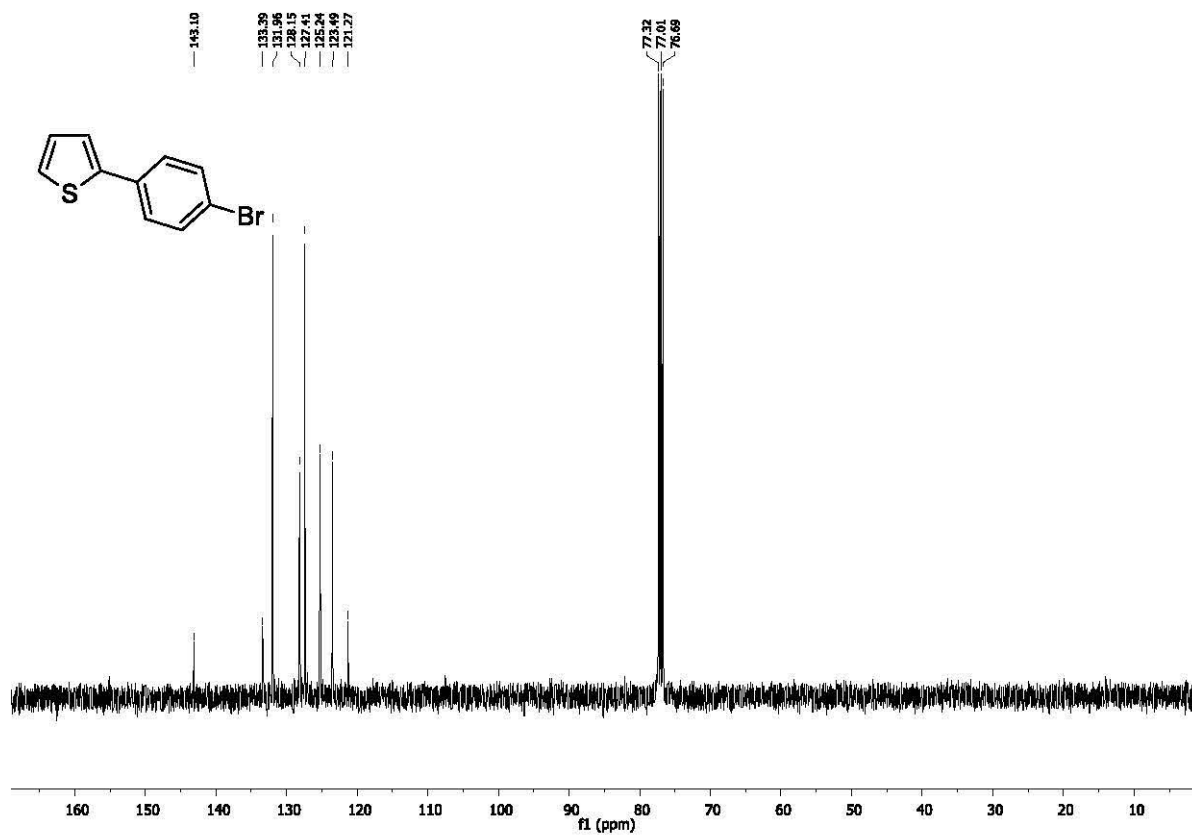
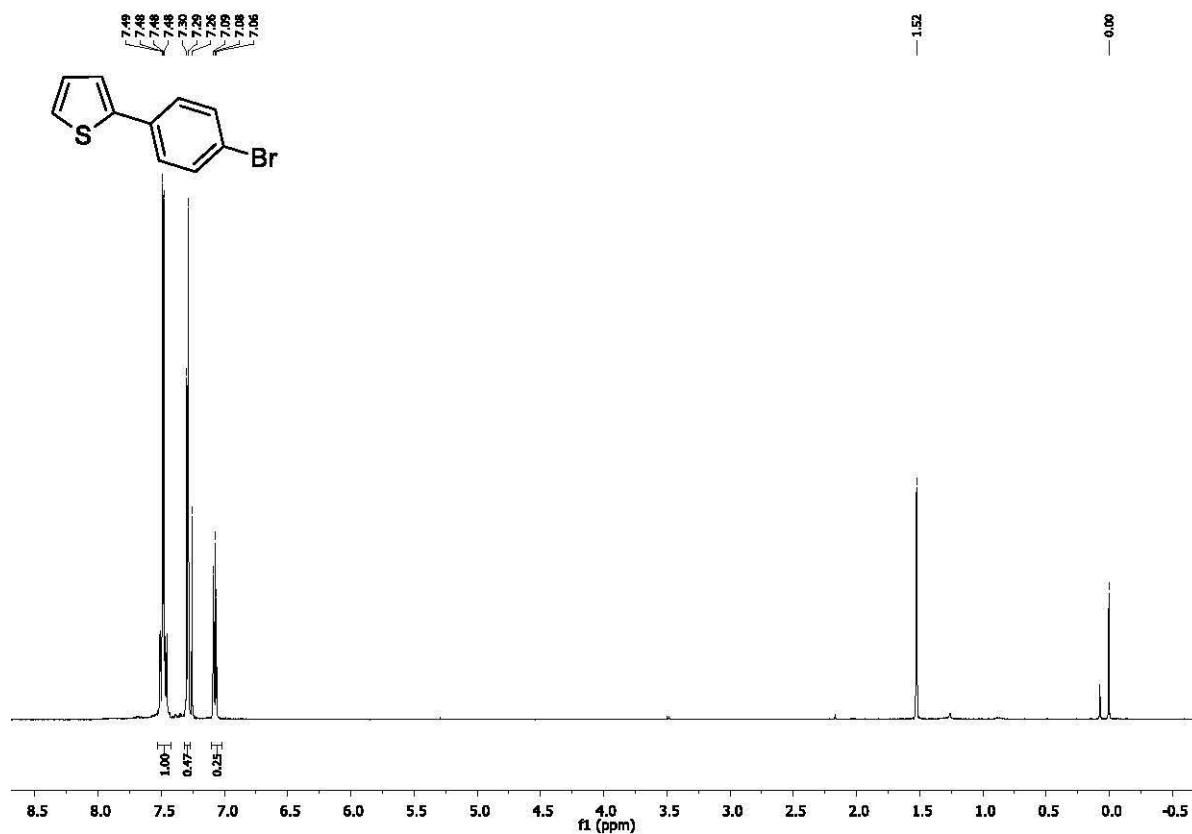
f) 2-(4-nitrophenyl)furan (18)



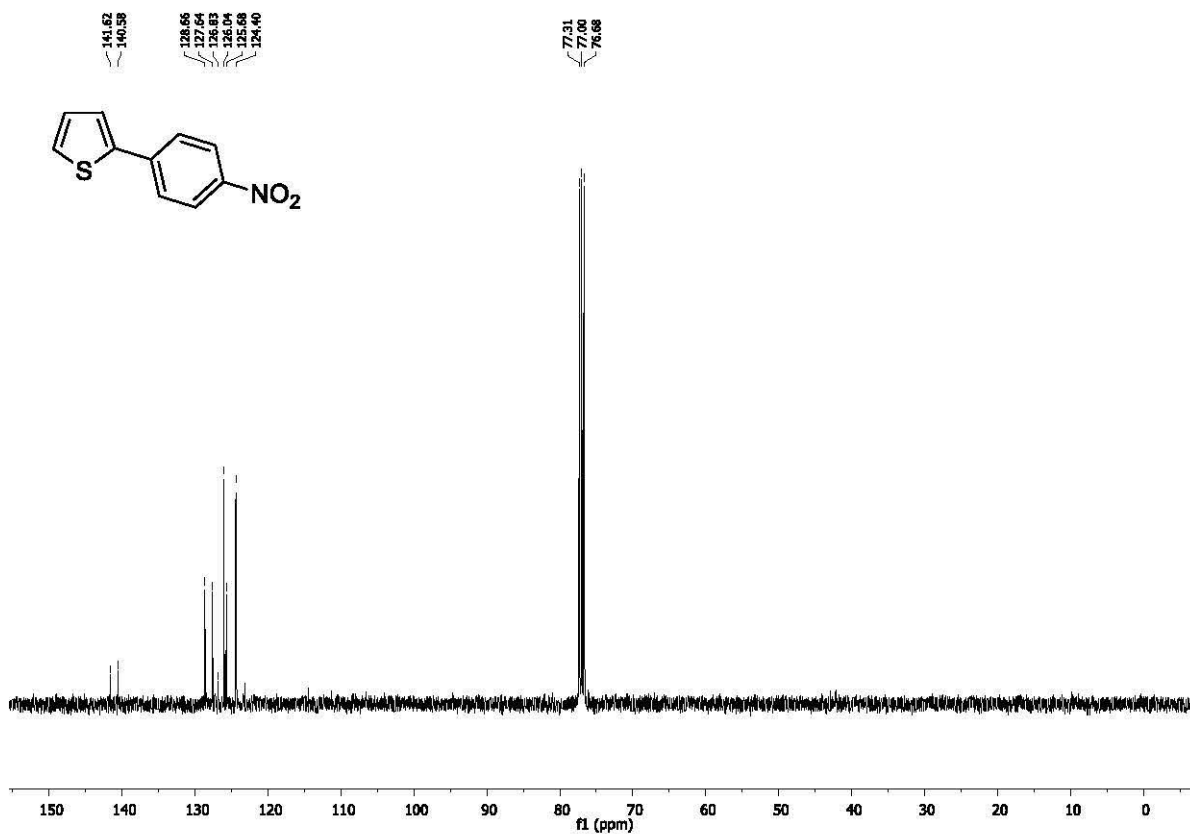
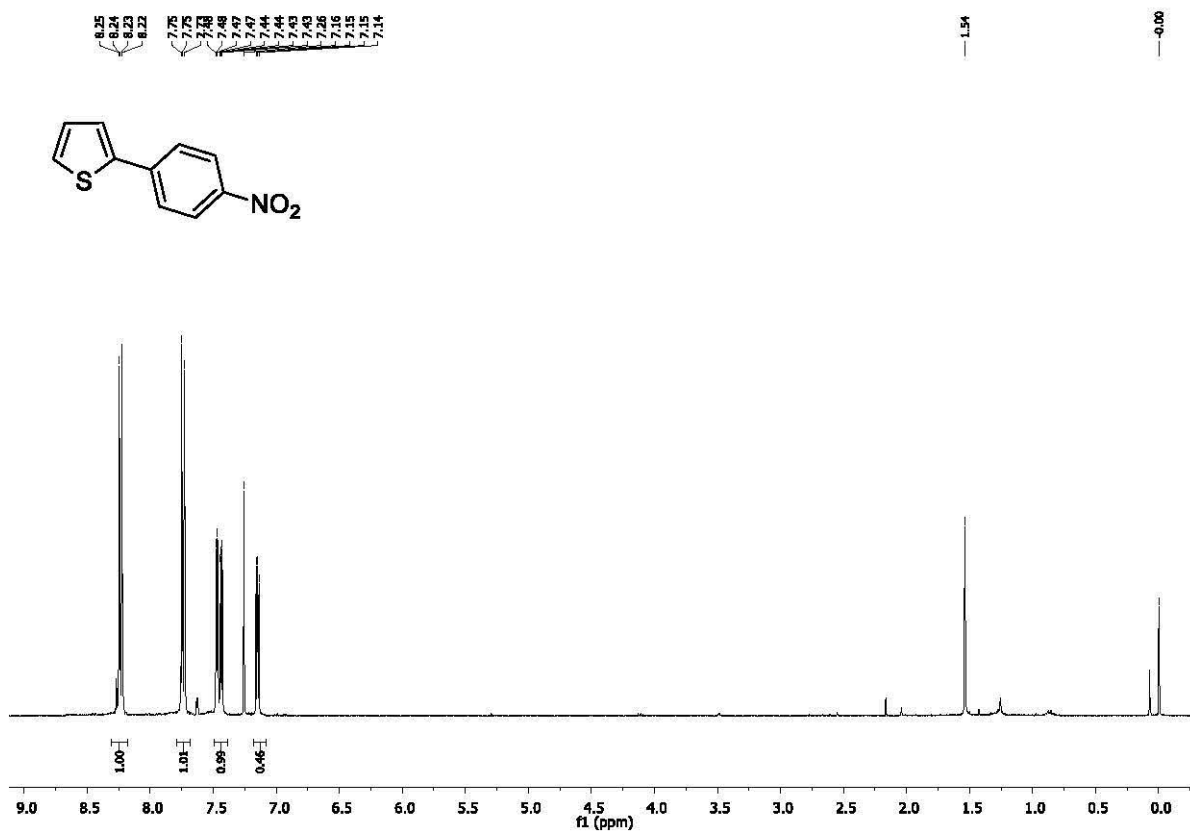
g) 2-(4-methoxyphenyl)furan (19)



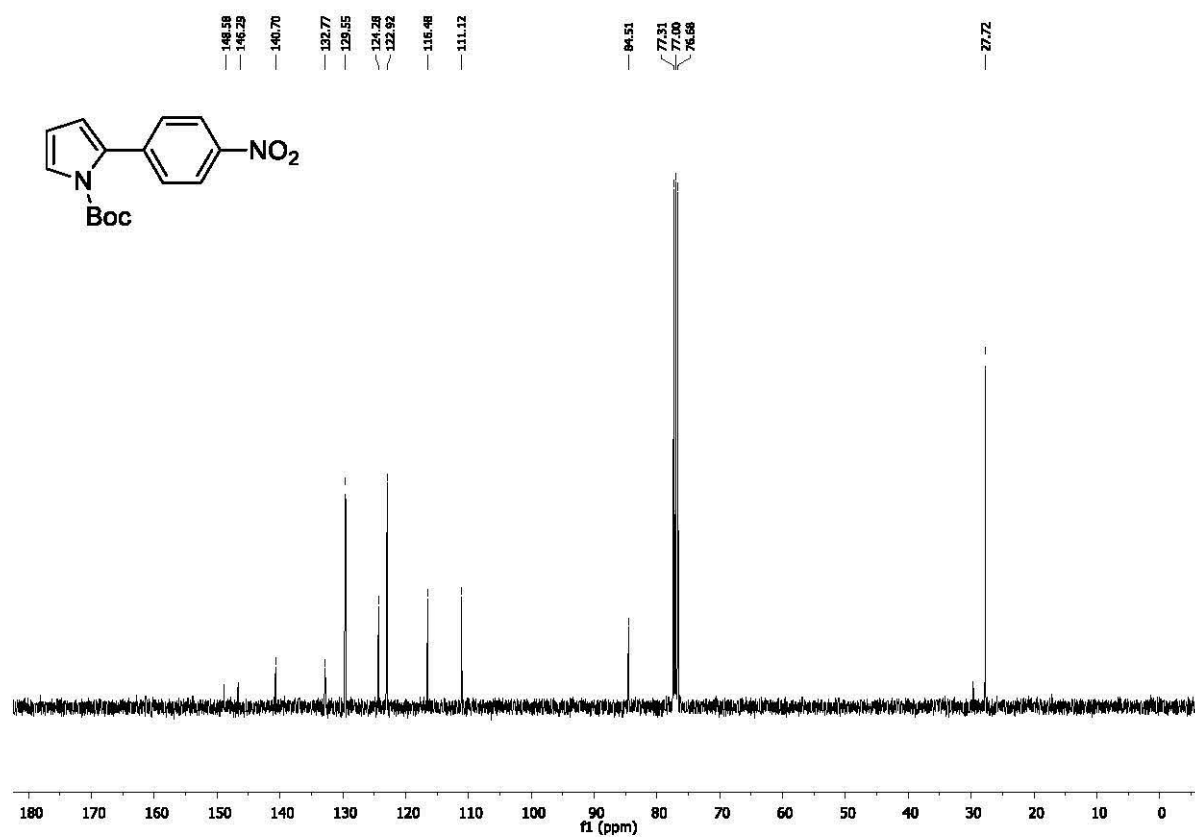
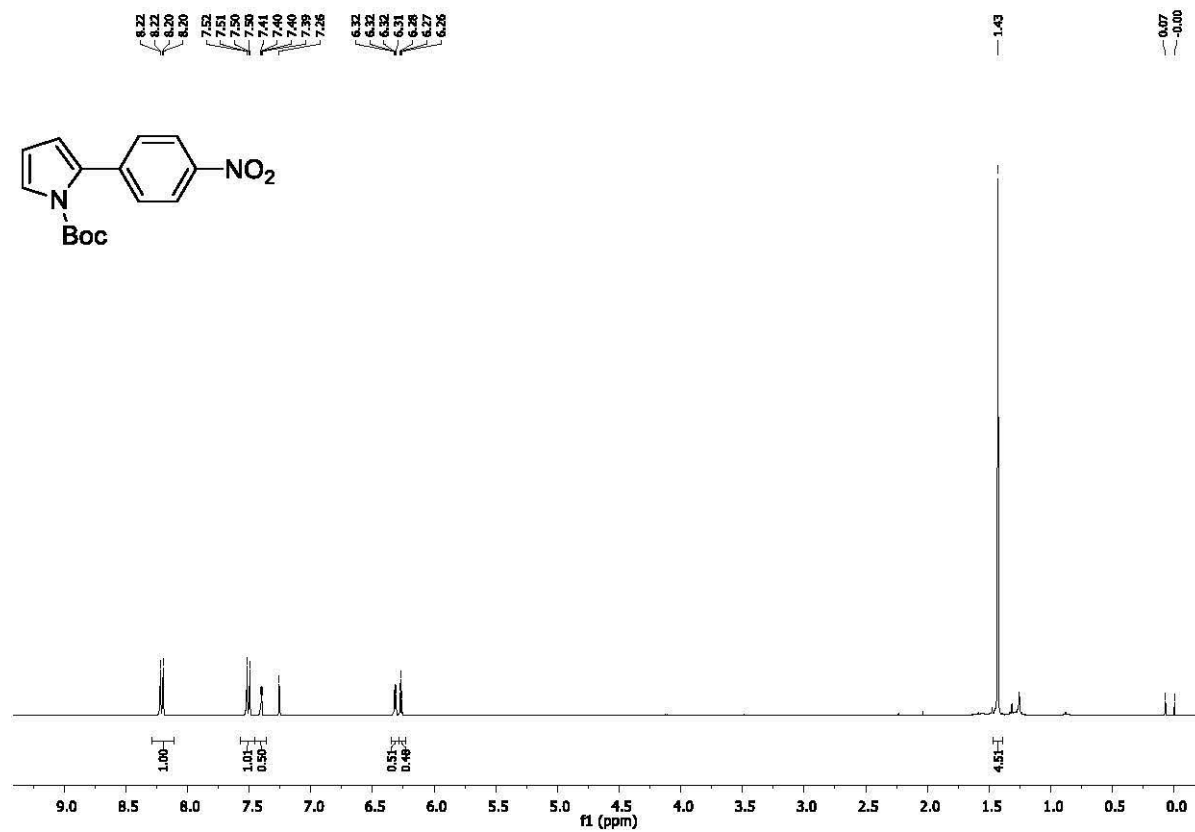
h) 2-(4-bromophenyl)thiophene (20)



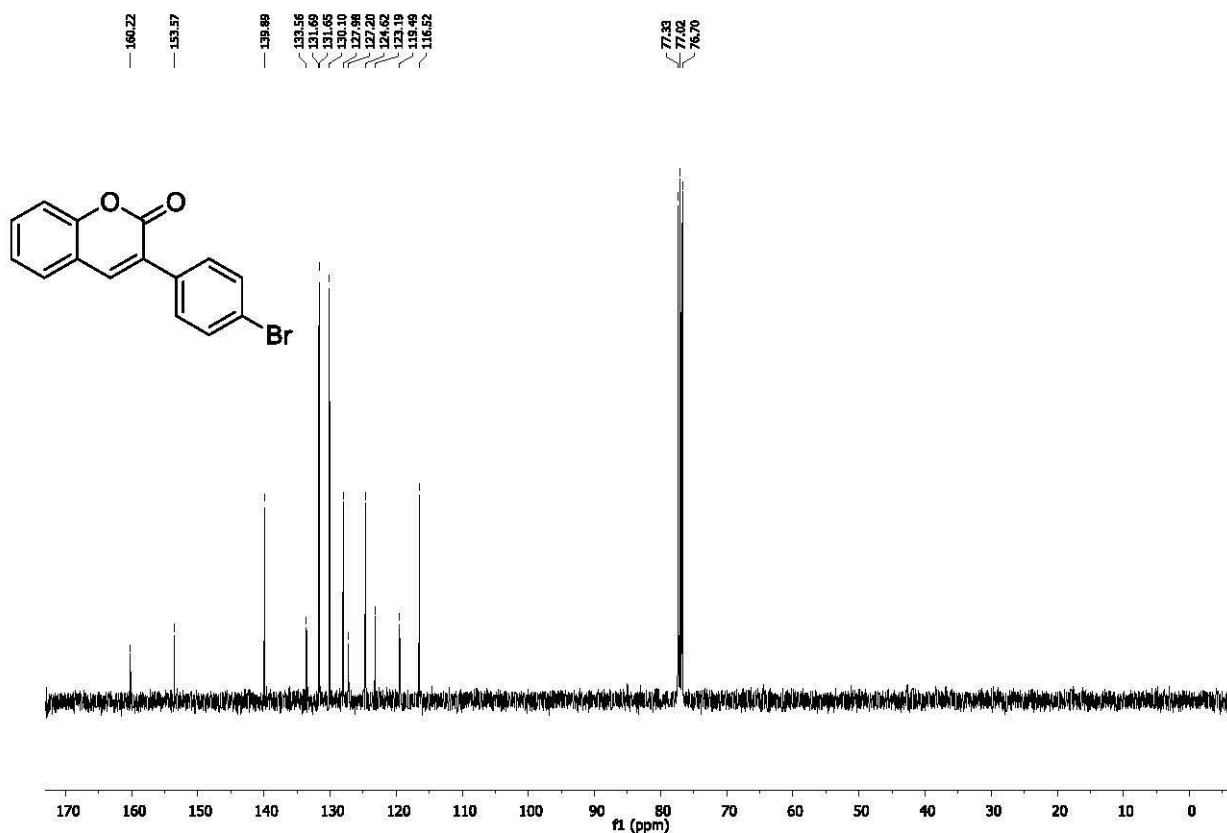
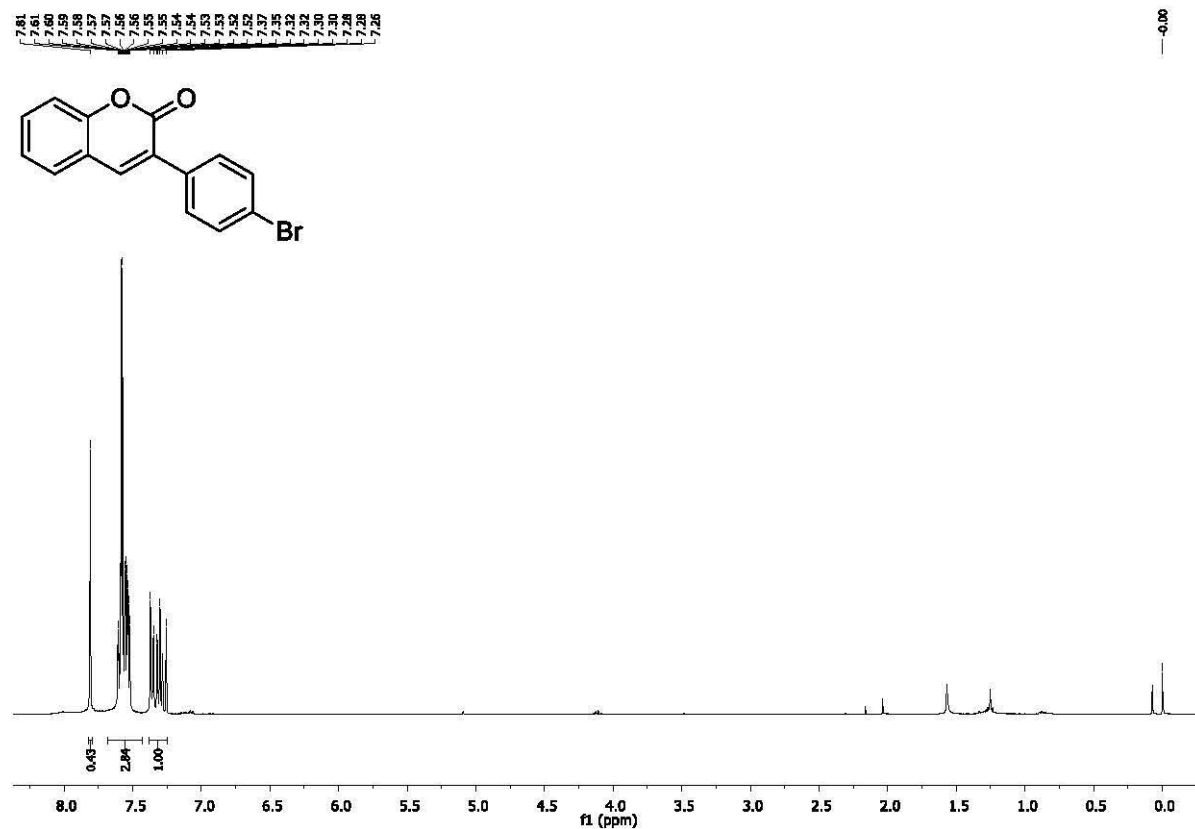
i) 2-(4-nitrophenyl)thiophene (21)



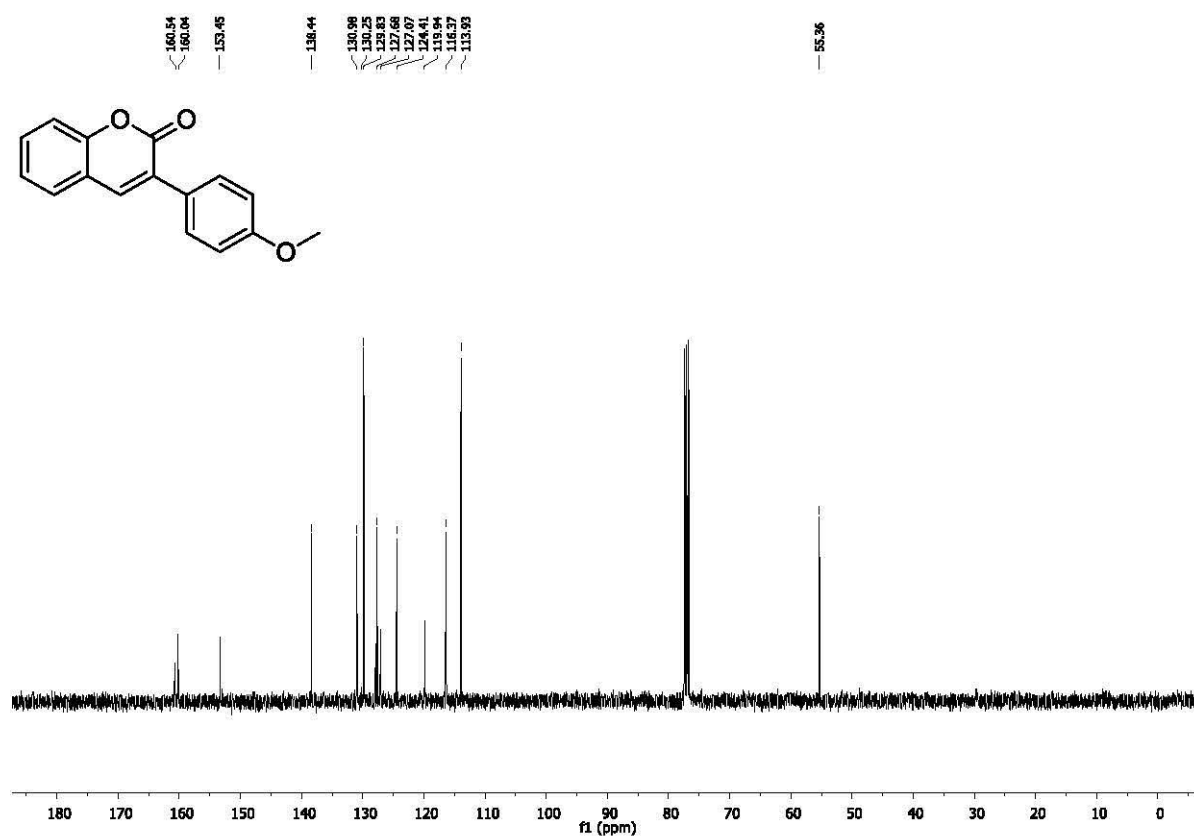
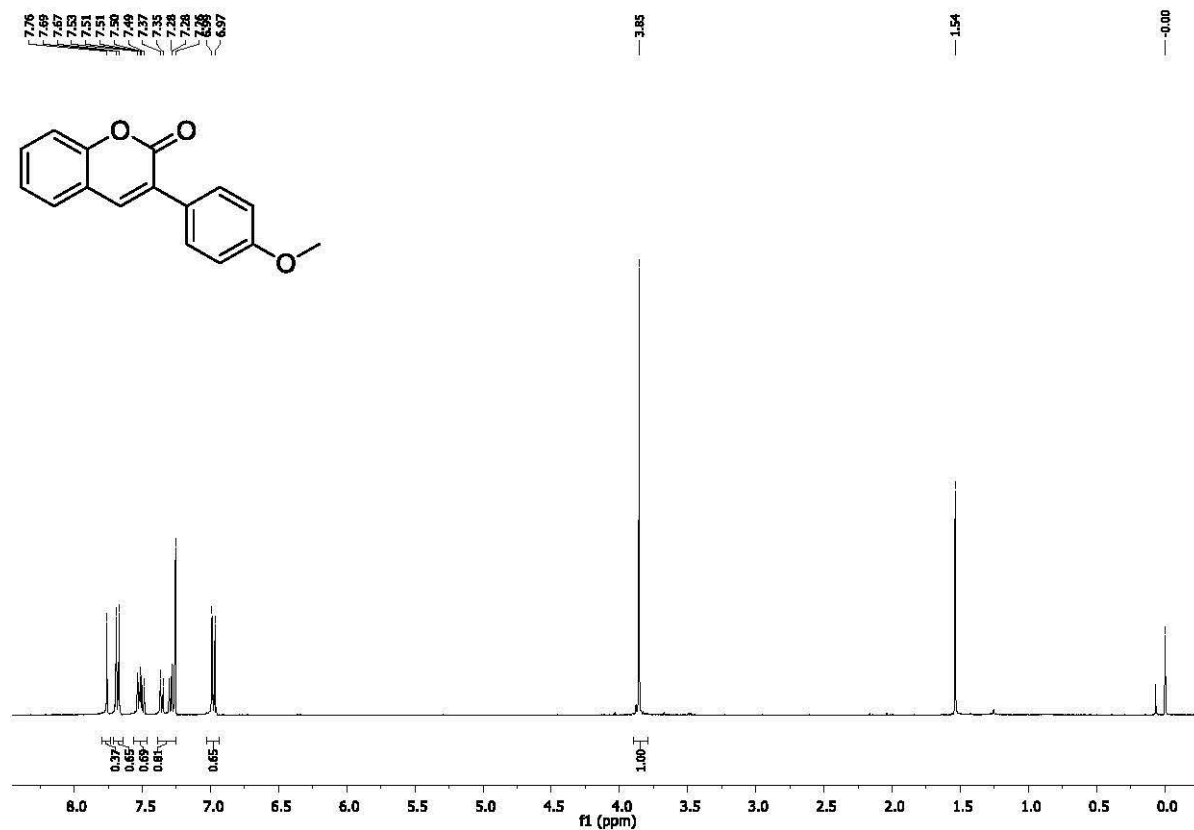
j) *N*-*tert*-butoxycarbonyl-2-(4-nitrophenyl)-1H-pyrrole (24)



k) 3-(4-bromophenyl)-2H-chromen-2-one (26)



l) 3-(4-methoxyphenyl)-2H-chromen-2-one (27)



7. References

-
- ¹ D. P. Hari, P. Schroll, B. König, *J. Am. Chem. Soc.* **2012**, *134*, 2958-2961.
- ² T. Lokman, B. K. Madras, P. C. Meltzer, *Bioorganic and Medicinal Chemistry* **2012**, *20*, 2776-2772.
- ³ S. Gowrisankar, J. Seayad, *Chem. Eur. J.* **2014**, *20*, 12754-12758.
- ⁴ L. Zhi, H. Zhang, Z. Yang, W. Liu, B. Wang, *Chem. Commun.* **2016**, *52*, 6431-6434.
- ⁵ A. Honraedt, M.-A. Raux, E. Le Grogneq, D. Jacquemin, F.-X. Felpin, *Chem. Commun.* **2014**, *50*, 5236-5238.
- ⁶ J.-W. Yuan, L.-R. Yang, Q.-Y. Yin, P. Mao, L.-B. Qu, *RSC Adv.* **2016**, *6*, 35936-35944.
- ⁷ G. R. Seely, *Photochemistry and Photobiology* **1978**, *27*, 639-654.
- ⁸ D. J. Quimby, F. R. Longo, *J. Am. Chem. Soc.* **1974**, *97*, 5111-5117.
- ⁹ M. G. H. Vicente, M. G. P. M. S. Neves, J. A. S. Cavaleiro, H. K. Hombrecher, D. Koll, *Tetrahedron Letter*, **1996**, *37*, 261-262.
- ¹⁰ Kumar, P. H.; Venkatesh, Y.; Siva, D.; Ramakrishna, B., Bangal, P. R. *J. Phys. Chem. A* **2015**, *119*, 1267-1278.
- ¹¹ U. Megerle, R. Lechner, B. König, E. Riedle, *Photochem. Photobiol. Sci.* **2010**, *9*, 1400-1406.

9. Oświadczenia autorów publikacji

Katarzyna Rybicka-Jasińska, mgr

Oświadczam, że mój wkład w powstanie poniższych pracy polegał na:

1. K. Rybicka-Jasińska, K. Orłowska, M. Karczewski, K. Zawada, D. Gryko *Eur. J. Org. Chem.* DOI: 10.1002/ejoc.201800542 *Why Cyclopropanation is not involved in Photoinduced α -Alkylation of Ketones with Diazo Compounds?*

Współpracowałam koncepcję badań oraz brałam udział w procesie optymalizacji reakcji, przeprowadziłam część reakcji mających na celu zbadanie zakresu stosowalności i ograniczeń metody; konkretnie wydzieliłam i oczyściłam związki **10c-g**, **10m**. Wykonałam również większą część badań eksperymentalnych mających na celu wyjaśnienie mechanizmu badanej reakcji (Analiza Sterna-Volmera, Eksperymenty UV-Vis, NMR i MS). Brałam udział w interpretacji wyników oraz uczestniczyłam także w przygotowaniu manuskryptu.

2. K. Rybicka-Jasińska, B. König, D. Gryko *Eur. J. Org. Chem.* **2017**, 2104-2107

Współpracowałam koncepcję badań, przeprowadziłam optymalizację reakcji oraz wszystkie reakcje mające na celu zbadanie zakresu stosowalności i ograniczeń metody; konkretnie wydzieliłam i oczyściłam związki **3**, **14-27**. Wykonałam również wszystkie badania eksperymentalne mające na celu wyjaśnienie mechanizmu badanej reakcji (Analiza Sterna-Volmera, badanie wydajności badanych reakcji i eksperymenty MS). Brałam udział w interpretacji wyników oraz uczestniczyłam także w przygotowaniu manuskryptu.

3. K. Rybicka-Jasińska, W. Shan, K. Zawada, K. M. Kadish, D. Gryko *J. Am. Chem. Soc.* **2016**, *138*, 15451-15458

Współpracowałam koncepcję badań, przeprowadziłam optymalizację reakcji oraz wszystkie reakcje mające na celu zbadanie zakresu stosowalności i ograniczeń metody; konkretnie wydzieliłam i oczyściłam związki **3**, **14-29**. Wykonałam również większą część badań eksperymentalnych mających na celu wyjaśnienie mechanizmu badanej reakcji (Analiza Sterna-Volmera, Eksperymenty UV-Vis, NMR i MS oraz uczestniczyłam w pomiarach EPR). Brałam udział w interpretacji wyników oraz uczestniczyłam także w przygotowaniu manuskryptu.

4. K. Rybicka-Jasińska, E. W. Ciszewski, D. Gryko *J. Porphyrins Phthalocyanines* **2016**, *20*, 76-95

Zgromadziłam i dokładnie zapoznałam się z aktualną literaturą naukową dotyczącą opisywanego zagadnienia. Brałam także czynny udział w pisaniu manuskryptu.

5. K. Rybicka-Jasińska, Ł. W. Ciszewski, D. Gryko *Adv. Synth. Catal.* **2016**, *358*, 1671-1678

Współpracowałam koncepcję badań oraz brałam udział w procesie optymalizacji reakcji, przeprowadziłam część reakcji mających na celu zbadanie zakresu stosowności i ograniczeń metody; konkretnie wydzieliłam i oczyściłam związki **10 - 21, 23, 24, 27 - 32**. Wykonałam również większą część badań eksperymentalnych mających na celu wyjaśnienie mechanizmu badanej reakcji (Analiza Sterna-Volmera, Eksperymenty UV-Vis, NMR i MS oraz uczestniczyłam w pomiarach EPR). Brałam udział w interpretacji wyników oraz uczestniczyłam także w przygotowaniu manuskryptu.

Katarzyna Rybicka-Jasińska

Dorota Gryko, prof.

Oświadczam, że mój wkład w powstanie poniższych pracy polegał na:

1. K. Rybicka-Jasińska, K. Orłowska, M. Karczewski, K. Zawada, D. Gryko *Eur. J. Org. Chem.* **2018** Why Cyclopropanation is not involved in Photoinduced α -Alkylation of Ketones with Diazo Compounds?

Współpracowałam koncepcję badań, interpretowałam ich wyniki, a także pisałam manuskrypt.

2. K. Rybicka-Jasińska, B. König, D. Gryko *Eur. J. Org. Chem.* **2017**, 2104-2107

Współpracowałam koncepcję badań, interpretowałam ich wyniki, a także pisałam manuskrypt.

3. K. Rybicka-Jasińska, W. Shan, K. Zawada, K. M. Kadish, D. Gryko *J. Am. Chem. Soc.* **2016**, *138*, 15451-15458

Współpracowałam koncepcję badań, uczestniczyłam w planowaniu eksperymentów i interpretacji wyników, a także pisaniu manuskryptu.

4. K. Rybicka-Jasińska, Ł. W. Ciszewski, D. Gryko *J. Porphyrins Phthalocyanines* **2016**, *20*, 76-95

Opracowałam koncepcję przeglądu i uczestniczyłam w jego pisaniu.

5. K. Rybicka-Jasińska, Ł. W. Ciszewski, D. Gryko *Adv. Synth. Catal.* **2016**, *358*, 1671-1678

Współpracowałam koncepcję badań, interpretowałam ich wyniki, a także pisałam manuskrypt.

Z poważaniem,



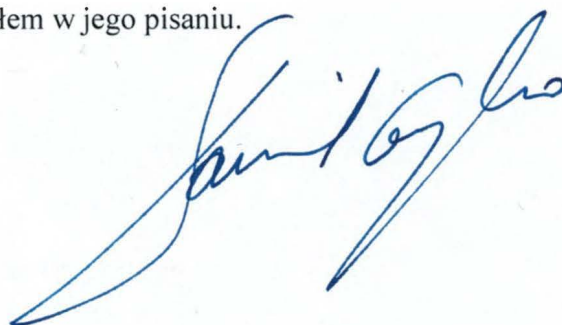
Prof. dr hab. Dorota Gryko

Prof. Daniel T. Gryko

Oświadczam, że mój wkład w powstanie poniższych pracy polegał na:

1. K. Rybicka-Jasińska, Ł. W. Ciszewski, D. T. Gryko, D. Gryko *J. Porphyrins Phthalocyanines* **2016**, 20, 76-95

Współpracowałem koncepcję przeglądu i uczestniczyłem w jego pisaniu.





Universität Regensburg

Universität Regensburg · D-93040 Regensburg

Prof. Dorota Gryko
Institute of Organic Chemistry
Polish Academy of Sciences
Kasprzaka 44/52,
01-224 Warsaw
Poland

FAKULTÄT
CHEMIE UND PHARMAZIE

Lehrstuhl für Organische Chemie

Prof. Dr. Burkhard König
Telefon +49 941 943-4576
Telefax +49 941 943-1717
Sekretariat:
Telefon +49 941 943-4575
Telefax +49 941 943-1717
Universitätsstraße 31
D-93053 Regensburg

burkhard.koenig@chemie.uni-regensburg.de
www.uni-regensburg.de

February 27th 2018

Confirmation of contribution

I hereby declare that my contribution to below mentioned publication is as follows:

K. Rybicka-Jasińska, B. König, D. Gryko *Eur. J. Org. Chem.* **2017**, [2104-2107](#)

I supervised quantum yield measurements and I was also involved in correcting manuscript.

Sincerely,

Burkhard König

Katarzyna Zawada, dr

Oświadczam, że mój wkład w powstanie poniższych prac polegał na:

1. K. Rybicka-Jasińska, K. Orłowska, M. Karczewski, K. Zawada, D. Gryko *Eur. J. Org. Chem.* Why Cyclopropanation is not involved in Photoinduced α -Alkylation of Ketones with Diazo Compounds?

Przeprowadziłam pomiary EPR oraz obliczenia potrzebne do interpretacji wyników EPR, a także obliczenia kwantowo-mechaniczne (obliczenia entalpii swobodnej). Dokonałam również analizy i interpretacji otrzymanych danych. Przygotowałam również część manuskryptu dotycząca badań obliczeniowych oraz badań EPR.

2. K. Rybicka-Jasińska, W. Shan, K. Zawada, K. M. Kadish, D. Gryko *J. Am. Chem. Soc.* **2016**, *138*, 15451-15458

Przeprowadziłam pomiary EPR oraz obliczenia potrzebne do ich interpretacji. Dokonałam analizy i interpretacji otrzymanych danych. Przygotowałam również część manuskryptu dotyczącą badań EPR.

KZawada



U N I V E R S I T Y *of* H O U S T O N

Department of Chemistry
Karl M. Kadish
Hugh Roy and Lillie Cranz
Distinguished University Professor

4800 Calhoun Rd. 77204-5003
phone: (713) 743-2740
fax: (713) 743-2745
e-mail: KKADISH@UH.EDU

Dr. Dorota Gryko
Institute of Organic Chemistry
Polish Academy of Sciences
Kasprzaka 44/52
01-224 Warsaw Poland
(dgryko@gmail.com)

April 23, 2018

Dear Dr Gryko:

I hearby declare that my contribution to the below-mentioned publication was to assist Wenquian Shan in performing cyclic voltammetry measurements and measuring redox potentials which were important to know when analyzing the chemistry described in the manuscript.

K. Rybicka-Jasińska, W. Shan, K. Zawada, K. M. Kadish, D. Gryko, "Porphyrins as Photoredox Catalysts: Experimental and Theoretical Studies," J. Am. Chem. Soc. **2016**, 138, 15451-15458

Sincerely,

Karl M. Kadish
Hugh Roy and Lillie Cranz
Distinguished University Professor



U N I V E R S I T Y *of* H O U S T O N

4800 Calhoun Rd. 77204-5003
phone: (713) 743-2740
fax: (713) 743-2745
e-mail: KKADISH@UH.EDU

Dr. Dorota Gryko
Institute of Organic Chemistry
Polish Academy of Sciences
Kasprzaka 44/52
01-224 Warsaw Poland
(dgryko@gmail.com)

March 20, 2018

Dear Dr Gryko:

I hereby declare that my contribution to the below-mentioned publication was to perform cyclic voltammetry measurements and measure redox potentials which were important to know when analyzing the chemistry described in the manuscript.

K. Rybicka-Jasińska, W. Shan, K. Zawada, K. M. Kadish, D. Gryko, "Porphyrins as Photoredox Catalysts: Experimental and Theoretical Studies," *J. Am. Chem. Soc.* **2016**, *138*, 15451-15458

Sincerely,

Wenqian Shan
Graduate Student

Maksymilian Karczewski, dr

Oświadczam, że mój wkład w powstanie poniższych pracy polegał na:

1. K. Rybicka-Jasińska, K. Orłowska, M. Karczewski, K. Zawada, D. Gryko *Eur. J. Org. Chem.* DOI: 10.1002/ejoc.201800542 *Why Cyclopropanation is not involved in Photoinduced α -Alkylation of Ketones with Diazo Compounds?*

Przeprowadziłem obliczenia kwantowo-mechaniczne oraz dokonałem analizy i interpretacji otrzymanych danych. Przygotowałem również część manuskryptu dotyczącą badań obliczeniowych.



Katarzyna Orłowska, mgr inż.

Oświadczam, że mój wkład w powstanie poniższych pracy polegał na:

1. K. Rybicka-Jasińska, K. Orłowska, M. Karczewski, K. Zawada, D. Gryko *Eur. J. Org. Chem.* DOI: 10.1002/ejoc.201800542 *Why Cyclopropanation is not Involved in Photoinduced α -Alkylation of Ketones with Diazo Compounds?*

Brałam udział w procesie optymalizacji reakcji, przeprowadziłam część reakcji mających na celu zbadanie zakresu stosowalności i ograniczeń metody; konkretnie wydzieliłam i oczyściłam związki **10a**, **10b**, **10h**, **10i** oraz **10k**. Uczestniczyłam także w przygotowaniu manuskryptu.

Katarzyna Orłowska

Lukasz Ciszewski, mgr inż.

Oświadczam, że mój wkład w powstanie poniższych pracy polegał na:

1. K. Rybicka-Jasińska, Ł. W. Ciszewski, D. T. Gryko, D. Gryko *J. Porphyrins Phthalocyanines* **2016**, *20*, 76-95

Zgromadziłem aktualną literaturę dotyczącą opisywanego zagadnienia oraz uczestniczyłem w pisaniu przeglądu.

2. K. Rybicka-Jasińska, Ł. W. Ciszewski, D. Gryko *Adv. Synth. Catal.* **2016**, *358*, 1671-1678

Brałem udział w procesie optymalizacji reakcji, przeprowadziłem część eksperymentów mających na celu zbadanie zakresu stosowalności i ograniczeń metody; otrzymałem, wydzieliłem i oczyściłem związki **22**, **25**, **26**. Uczestniczyłem także w przygotowaniu manuskryptu.

Lukasz Ciszewski

Biblioteka Instytutu Chemii Organicznej PAN

O-B.399/18



10000000101568